The Dissertation Committee for Anders Mikal Eliasen Certifies that this is the approved version of the following dissertation:

Total Synthesis and Chemical Modification of Small Molecules: A Study of Axonal Regeneration and Aryl Oxidation

Committee:

Grant Willson, Supervisor

Dionicio Siegel, Co-Supervisor

Eric Anslyn

Adrian Keatinge-Clay

Hung-Wen Liu

Jonathan Sessler

Total Synthesis and Chemical Modification of Small Molecules: A Study of Axonal Regeneration and Aryl Oxidation

by

Anders Mikal Eliasen, A. B.

Dissertation

Presented to the Faculty of the Graduate School of

The University of Texas at Austin

in Partial Fulfillment

of the Requirements

for the Degree of

Doctor of Philosophy

The University of Texas at Austin

May 2015

Dedication

To my teachers

Acknowledgements

I would like to extend my deepest gratitude to Professor Dionicio Siegel. Dio had the courage to allow me to learn by doing—my development and maturation as a scientist is due to his leadership and mentorship. Dio pushed me to do my best work, and I will always be enormously proud to consider myself a member of the Siegel group. I will forever be thankful to Professor Donald Deardorff for being one of the best teachers I have ever had and for encouraging me to pursue graduate school. Professor emeritus Tatsuo Otsuki and Professor Linda Lasater are acknowledged for making organic chemistry fun. I would like to thank the members of my doctoral committee for agreeing to serve on my defense. Particular thanks to Professor Grant Willson for agreeing to serve as my UT supervisor—you have always been an unwavering advocate for our group. I would like to thank Vince Lynch for help with crystallography, and solving multiple crystal structures for me. My thanks to Steve Sorey, Angela Spangenberg and Ben Shoulders for endless patience and help with NMR analysis. I am indebted to Betsy Hamblen and Penny Kile for constant guidance and support. I thank all of my undergraduate co-workers I collaborated with: Alex Schuppe, Karin Claussen, Paxton Thedford, and Mitchell Christy. I consider it a great privilege and honor to have been in the trenches with an amazing family of scientists in the Siegel group, past and present. Special thanks to Katie and Matt, who had to put up with me for the longest. None of this would have been possible without the unwavering love and support from my family, Mark, Debbie, Morgan and Kimi (Scout too!). It has been an incredible journey.

Total Synthesis and Chemical Modification of Small Molecules: A Study of Axonal Regeneration and Aryl Oxidation

Anders Mikal Eliasen, Ph.D.

The University of Texas at Austin, 2015

Supervisor: Grant Willson

Co-Supervisor: Dionicio Siegel

Injuries to the central nervous system are irreversible and debilitating due to the limited regrowth of damaged or severed neurons. Two small molecules, xanthofulvin and vinaxanthone, isolated from *P. vinaceum* and *P. glabrum* promote spinal cord regeneration in animal models. It is speculated that these natural products inhibit semaphorin 3A, a chemorepellent that mitigates axonal growth-cone formation. In addition to promoting axonal growth, rats treated with vinaxanthone and xanthofulvin following complete spinal cord transection experienced greater remyelination, increased angiogenesis, attenuated apoptosis, and depressed scaring of the lesion site. The only prior synthesis of vinaxanthone speculated that the xanthone core is constructed *via* enzyme-catalyzed intermolecular Diels-Alder reaction. We have demonstrated, however, that warming a functionalized acetoacetyl chromone in water, furnishes vinaxanthone in good yield, providing an alternative biosynthetic pathway. With a robust syntheses of both natural products, we

determined the protein target of the observed regeneration: succinate receptor 1, providing a new therapeutic target to promote neuronal regeneration.

Among the various methods of incorporating oxygen into aryl rings, the direct conversion of a C-H bond into a C-OH bond is ideal. The metal-free hydroxylation of arenes developed in our laboratory, utilizing phthaloyl peroxide, marks the first disclosure of this transformation using mild conditions. Computational and experimental evidence obtained thus far has supported a mechanism involving a diradical intermediate. The reactivity of phthaloyl peroxide was increased by the incorporation of two chlorine atoms onto the ring. To minimize the accumulation of large quantities of peroxide, the optimization of the preparation of the peroxide in flow has been developed. This protocol immediately consumes the peroxide as it is generated. Finally, a new dearomatization reaction has been optimized. This reaction forms two carbon-oxygen bonds and dearomatizes the ring system.

Table of Contents

List of Tables

List of Figures

Abbreviations

Å	angstrom
2D-NMR	two dimensional nuclear magnetic resonance
AAD	acute axonal degeneration
Ac	acetyl
AcCl	acetyl chloride
AcOH	acetic acid
Ar	aryl
atm	atmosphere
BDNF	brain-derived neurotrophic factor
BHT	butylated hydroxytoluene
Bn	benzyl
Boc_2O	di-*tert*-butyl dicarbonate
B.P.	boiling point
BPO	benzoyl peroxide
BPR	back pressure regulator
calcd.	calculated
CAM	ceric ammonium molybdate
cAMP	cyclic adenosine monophosphate
CI	chemical ionization
cis	*L*., same side
cm	centimeter
CNTF	ciliary neurotrophic factor
CNS	central nervous system

CoA	coenzyme A
COSY	correlation spectroscopy
CSPGs	chondroitin sulphate proteoglycans
DBU	1,8-diazabicycloundec-7-ene
DCC	N,N'-dicyclohexylcarbodiimide
DCE	dichloroethane
DCM	methylene chloride
DEPT	distortionless enhancement by polarization transfer
DFT	density functional theory
DMAP	4-dimethylaminopyridine
DME	dimethoxyethane
DMF	dimethylformamide
DMFDMA	dimethylformamide dimethylacetal
DMSO	dimethyl sulfoxide
DRG	dorsal root ganglion
DSC	differential scanning calorimetry
E	energy
EAS	electrophilic aromatic substitution
EC_{50}	half maximal effective concentration
EDCI	1-ethyl-3-(3-dimethylaminopropyl) carbodiimide
equiv.	equivalent
ESI	electrospray ionization
Et	ethyl
EtOAC	ethyl acetate

EtOH	ethanol
eV	electron volts
EVE	ethyl vinyl ether
FDA	food and drug administration
FG	functional group
FGF	fibroblast growth factor
g	gram
GDNF	glial cell line-derived neurotrophic factor
GDP	guanosine diphosphate
GFP	green fluorescent protein
GPCR	G protein-coupled receptor
GPR91	succinate receptor 1
GTP	guanosine triphosphate
h	hour
HBTU	N,N,N',N'-tetramethyl-O-(1H-benzotriazol-1-yl)uranium hexafluorophosphate
HFIP	1,1,1,3,3,3,-hexafluoro-2-propanol
HMBC	heteronuclear multiple bond correlation
HOMO	highest occupied molecular orbital
HRMS	high resolution mass spectrometry
HSQC	heteronuclear single quantum coherence
Hz	hertz
IC_{50}	half maximal inhibitory concentration
IGF	insulin-like growth factor

i-Pr	isopropyl
IR	infrared spectroscopy
J	coupling constant
Kcal	kilocalorie
L	liter
LUMO	lowest unoccupied molecular orbital
M	molar
MAG	myelin-associated glycoprotein
m-CPBA	*meta*-chloroperoxybenzoic acid
Me	methyl
MeCN	acetonitrile
MeOAc	methyl acetate
MeOH	methanol
mg	milligram
MHz	megahertz
min	minute
mL	milliliter
mmol	millimole
mol	mole
MOM	methoxymethyl
MOMCl	chloromethyl methyl ether
M.P.	melting point
MS	mass spectrometry
MS-4Å	4 angstrom molecular sieves

n-Bu	normal butyl
NGF	nerve growth factor
nM	nanomolar
NMR	nuclear magnetic resonance
NOE	nuclear Overhauser effect
N.R.	no reaction
NRP1	neuropilin-1
NSAID	nonsteroidal anti-inflammatory drug
NT-3	neurotrophin-3
Nu	nucleophile
obs.	observed
OMgp	oligodendrocyte-myelin glycoprotein
P	para
PDC	pyridinium dichromate
PDGF	platelet-derived growth factor
Ph	phenyl
PhH	benzene
PhMe	toluene
Pin	pinacol
Piv	pivaloyl
Plex 1	plexin 1
PNS	peripheral nervous system
ppm	parts per million
PPO	phthaloyl peroxide

PPTS	pyridinium *para*-toluenesulfonate
psi	pounds per square inch
pyr.	pyridine
Q	coenzyme Q
R	alkyl group
R_f	retention factor
RPM	rotations per minute
SCI	spinal cord injury
Sema3A	semaphorin 3A
SET	single electron transfer
SOMO	singly occupied molecular orbital
SUCNR1	succinate receptor 1
TBS	*tert*-butyldimethylsilyl
t-Bu	tertiary butyl
TEMPO	(2,2,6,6-tetramethyl-piperidin-1-yl)oxyl
Tf	trifluoromethanesulfonyl
TFA	trifluoroacetic acid
TFE	2,2,2-trifluoroethanol
TFT	trifluorotoluene
TGA	thermogravimetric analysis
THF	tetrahydrofuran
TLC	thin layer chromatography
TMS	trimethylsilyl
trans	*L*., across

TS	transition state
Ts	4-toluenesulfonyl
UV/Vis	ultraviolet-visible spectroscopy
VEGF	vascular endothelial growth factor
VX	vinaxanthone
XF	xanthofulvin

Chapter 1. Oxidation of Arenes

Peroxides are characterized by a relatively weak oxygen-oxygen bond. They are found in a variety of substances, from natural products to bleaching agents. One important subset of peroxides is organoperoxides, which contain at least one carbon-oxygen bond. Figure 1.1 lists commonly encountered peroxides including (a.) organo and hydroperoxides (b.) acyl peroxides and (c.) diacyl peroxides. Of particular interest are cyclic peroxides such as **1.13**, as these are a source of diradicals.

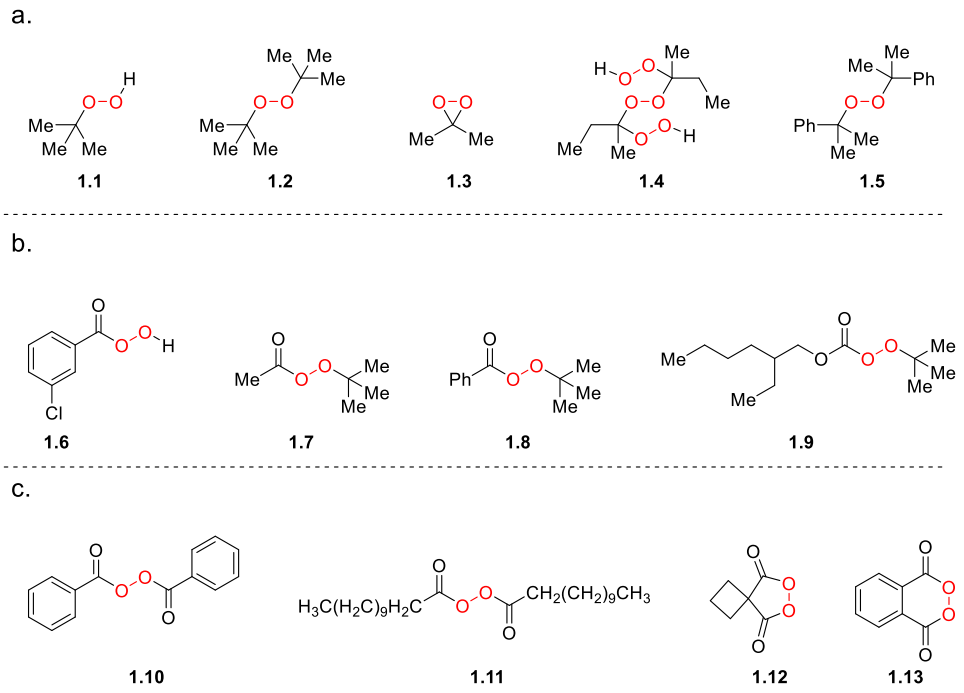

Figure 1.1. Examples of organic peroxides. (a.) alkyl peroxides. (b.) acyl peroxides. (c.) diacyl peroxides.

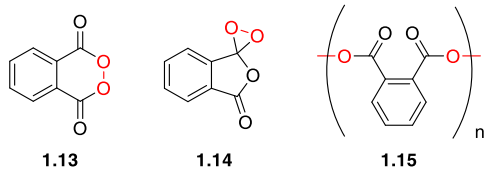

Figure 1.2. Proposed structures of phthaloyl peroxide.

Pechmann and Vanino were the first to disclose the cyclic diacyl peroxide phthaloyl peroxide in 1894 (Figure 1.2).[1] This protocol calls for shaking neat phthaloyl chloride in aqueous sodium peroxide. The diacyl or orthoester peroxide (**1.13** or **1.14**) were proposed as possible structures for the material they synthesized.[2] However, limits to 19th century spectroscopic techniques could not differentiate the two structures. Seven years following this disclosure, Adolf von Baeyer and Victor Villiger reassigned Pechmann and Vanino's proposed structures to the polymeric structure (**1.15**) as the material prepared following Pechmann and Vanino was insoluble in many common organic solvents.[3]

Almost half a century later, Kleinfelle, Rastadter[4] and Russell[5] disclosed a method to prepare monomeric phthaloyl peroxide. The motivation for synthesizing monomeric phthaloyl peroxide was to make a more effective radical initiator, as the polymeric peroxide (**1.15**) behaves like a source of monoradical. By buffering aqueous sodium peroxide with sodium phosphate, and diluting phthaloyl chloride, they successfully prepared phthaloyl peroxide in the monomeric form (**1.13**), which was soluble in halogenated and hydrocarbon solvents. Russell monitored the decomposition of phthaloyl peroxide in toluene and xylene, which occurred at a rate of 9-26% per hour, depending on the temperature. The presence of oxygen in these experiments was found to reduce the amount of decomposition, a phenomenon also observed with benzoyl peroxide.[6] In addition to observing the decomposition of phthaloyl peroxide in solvent, Russell interrogated its ability to initiate polymerization of methyl methacrylate and styrene. While 90% of styrene was consumed in 5 minutes, phthaloyl peroxide was inefficient at forming long chain polymers, due to

competitive decomposition of the peroxide. In fact, the rate of polymerization of styrene in the presence of phthaloyl peroxide was only slightly greater than the background polymerization of styrene itself. It was speculated that thermolysis of the peroxide leads to a diradical which undergoes self-termination after the addition of only a few monomers.

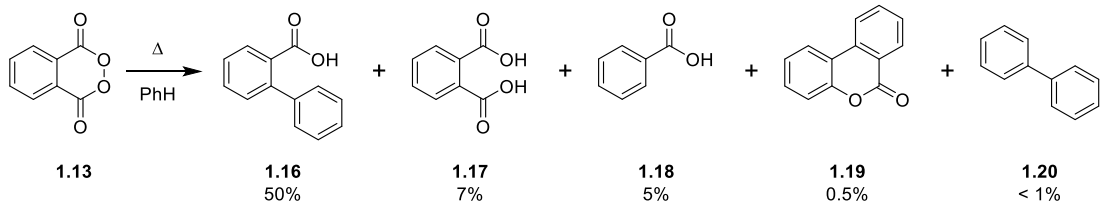

Figure 1.3. Decomposition studies of phthaloyl peroxide (**1.13**) in benzene.

Following Russell's study of the synthesis and decomposition of phthaloyl peroxide, Frederick Greene assigned the symmetric structure (**1.13**) as the most likely atom connectivity of phthaloyl peroxide using UV/Vis.[7] Studying the thermal decomposition of phthaloyl peroxide in benzene, Greene identified products that arose from this decomposition (Figure 1.3). Several products were the result of decarboxylation (**1.16**, **1.18**, **1.19**, **1.20**). Two conditions were found to inhibit decomposition: oxygen and carbon tetrachloride solvent. Taken together with Russell's observations, it was hypothesized that decomposition occurred *via* radical formation and subsequent decarboxylation. The resulting aryl radical could then recombine with other species in solution, giving rise to the product distribution observed.

While phthaloyl peroxide (**1.13**) and benzoyl peroxide (**1.10**) share similarities in atom connectivity, both exhibit unique characteristics. The dihedral angle for hydrogen peroxide is 95° which attenuates the electrostatic repulsion for the non-bonding electron pair on the peroxy-oxygen atoms. The dihedral angle for the peroxy-oxygen bond of benzoyl peroxide is 91.3° and has an O-O bond length of 1.46 Å.[8] The electrostatic repulsion is only slightly reduced for phthaloyl peroxide, due to its cyclic structure, with a

dihedral angle of 11.4°.[9] Additionally, the O-O bond length of phthaloyl peroxide is 1.47 Å, similar in length to benzoyl peroxide.

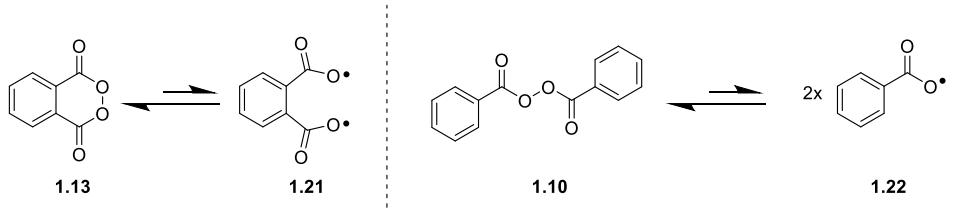

Figure 1.4. Homolysis of phthaloyl peroxide (**1.13**) and benzoyl peroxide (**1.10**).

Despite the increased strain of phthaloyl peroxide (**1.13**), the molecule exhibits heightened thermal stability when compared to other acyclic peroxides (Figure 1.4). Benzoyl peroxide (**1.10**) decomposes 87 times more readily than phthaloyl peroxide, and yet bond homolysis is only 2.1 times greater than that of phthaloyl peroxide.[10] Thus the thermal stability of phthaloyl peroxide results from the ease by which the radical recycles, calculated as being 1.5 kcal/ mol lower in energy than decomposition (*via* decarboxylation). To date, phthaloyl peroxide is the only acyl peroxide for which ^{18}O scrambling occurs faster than decomposition.[10] For the case of the benzoyl peroxide, the decomposition pathway predominates over the return pathway as a result of diffusion and solvent caging of the benzoyloxy radical (**1.22**).

What phthaloyl peroxide (**1.13**) lacked as an efficient polymerization initiator made it a suitable reagent for small molecule functionalization. As was previously observed by Russell, phthaloyl peroxide (**1.13**) readily reacts with styrene.[5] In addition to styrene, Greene found that stilbene was even more reactive (Figure 1.5a). The resulting adducts were characterized as the double ester (**1.24**) and lactonic orthoester (**1.25**).[11] The combined yield for both isomers was near quantitative in carbon tetrachloride solvent.

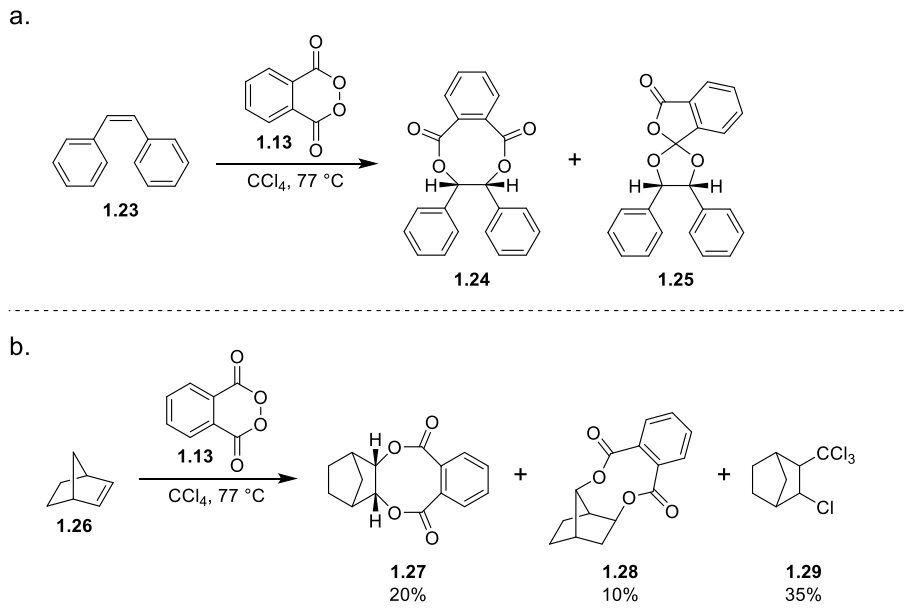

Figure 1.5. Previous reactivity utilizing phthaloyl peroxide (**1.13**). (a.) Dihydroxylation of stilbene. (b.) Dihydroxylation of norbornylene.

Phthaloyl peroxide's (**1.13**) reactivity was not confined to aryl-substituted olefins—in select cases, aliphatic olefins also underwent oxidation (Figure 1.5b). When norbornylene (**1.26**) was exposed to phthaloyl peroxide, a product mixture was obtained.[12] Regioisomeric product **1.28** arises from phthaloyl peroxide addition into the olefin, followed by bond migration. In addition to the work of Russell and Greene, others have developed reactivity including oxidative dearomatization of anthracene[13], oxidation and subsequent rearrangement of benzofuran[14], and oxidative addition into platinum complexes[15]. If the starting material possesses allylic hydrogens, the major product is the allylic half-acid ester.

There is ambiguity surrounding the mechanism of incorporation of phthaloyl peroxide (**1.13**) into olefins. The reaction was found to be first order in olefin and peroxide (second order overall).[16] Greene postulated that phthaloyl peroxide's reactivity with olefins was electrophilic in nature. Hammett plot analysis provided a reaction constant, ρ, equal to

-1.65, with σ^+ affording a stronger correlation than σ, which could be indicative of an ionic mechanism.[16] However, Greene also acknowledges that the slight polarization observed does not preclude a diradical mechanism. Additionally, in the case of the reaction of phthaloyl peroxide with norbornylene in carbon tetrachloride, adduct (**1.29**) produced in 35% yield is indicative of radicals present in the reaction medium. Interestingly, the carbon tetrachloride adduct (**1.29**) was also isolated when using benzoyl peroxide (**1.10**) in place of phthaloyl peroxide. Subsequent studies supported a single electron transfer mechanism, using nanosecond laser spectroscopy, which identified odd-electron intermediates.[14] The-rate limiting step for this pathway is the transfer of one electron from the olefin to the peroxide. More recent studies utilizing ^{18}O-encorporated phthaloyl peroxide found that scrambling was rapid, supporting the diradical mechanism.[17]

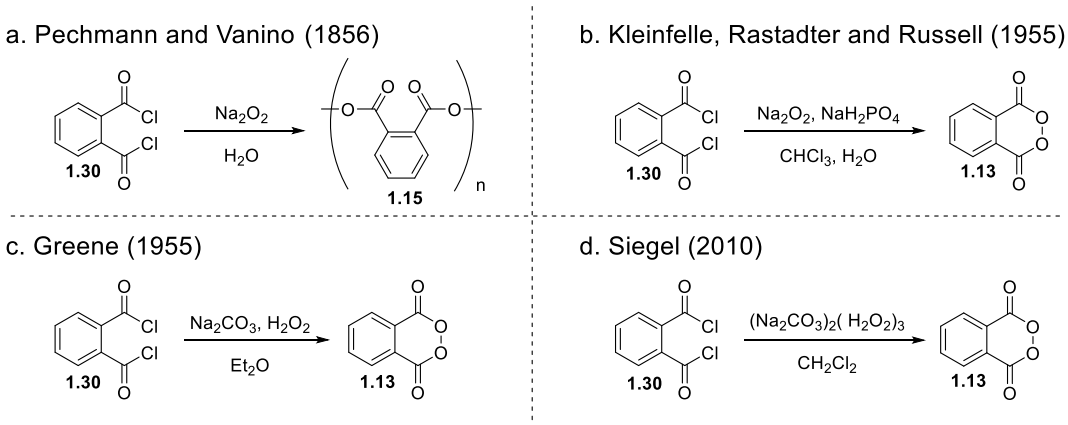

Figure 1.6. Preparation of phthaloyl peroxide (**1.13**).

Following the preparation of Russell[5], Greene[7] noted that phthaloyl peroxide (**1.13**) was sensitive to shock. Indeed, material prepared following Russell's protocol can detonate upon standard isolation techniques (Figure 1.6b). However, it is hypothesized that this instability is the result of the formation of oligomeric peroxide byproducts and does not necessarily suggest that phthaloyl peroxide itself is exceptionally unstable. Additionally,

the requirement of concentrated hydrogen peroxide should be avoided as it is no longer commercially available and is unsafe. Also, using ether as solvent in the presence of concentrated hydrogen peroxide has the potential to produce explosive low-molecular weight organoperoxides.

With this in mind, a safer preparation was developed using phthaloyl chloride (**1.30**) and sodium percarbonate in methylene chloride at ambient temperature (Figure 1.6d).[18] Sodium percarbonate as a source of hydrogen peroxide is advantageous for several reasons. It is produced on the ton scale, is the active oxidant in Oxiclean® and is present in many toothpastes and household cleaning supplies.[19] It is even less expensive than the desiccant sodium sulfate. The use of this salt results in a heterogeneous reaction medium, with the excess salts and byproducts removed *via* filtration. Finally, the sodium carbonate neutralizes HCl liberated during the course of the reaction. To date, following the implementation of the described protocol, no accidental detonation has occurred.

The role of water in this reaction proved critical to satisfactory generation of phthaloyl peroxide (**1.13**). Sodium percarbonate leaches hydrogen peroxide even in non-aqueous solvent. However, trace water present in the solvent increases the amount of hydrogen peroxide liberated. In the case of methylene chloride, non-anhydrous solvent contains six times the amount of dissolved hydrogen peroxide.[19,20] Simply washing reagent-grade methylene chloride with water provides a solution of “wet” solvent. Karl Fischer titration revealed that methylene chloride prepared in this manner contains 1420 ppm of water, much higher than solvent left untreated (62 ppm).

Filtration of the salts and evaporation of the solvent yields crude phthaloyl peroxide (**1.13**). Precipitation from warm benzene and pentane yields highly pure phthaloyl peroxide which can be stored for weeks at -20 °C without any noticeable loss in purity. A slight depression in yield is observed for larger scale reactions (53-62% for 2 g reactions, 45-51% for 10 g reactions).

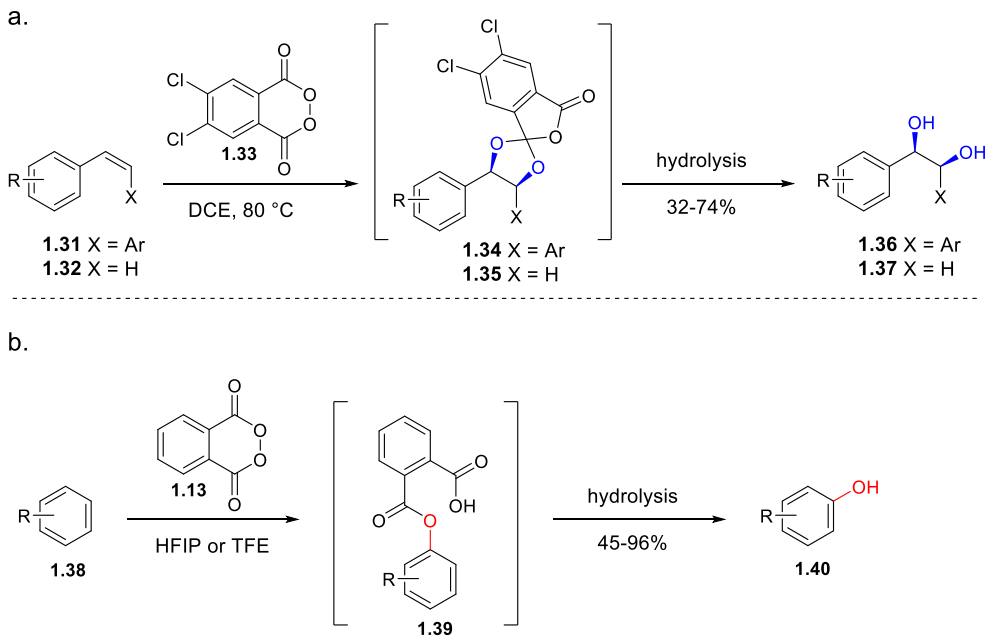

Figure 1.7. Previous reactivity discovered in our laboratory.

Following Greene's disclosure of the reactivity of phthaloyl peroxide (**1.13**) with stilbenes, a screen of new variants of phthaloyl peroxide was undertaken in an attempt to optimize the dioxygenation of olefins.[21] In this study, 4,5-dichlorophthaloyl peroxide (**1.33**) was identified as being more reactive than phthaloyl peroxide, hydroxylating *trans*-stilbene in 72% yield with high levels of selectivity (Figure 1.7a). Cyclic olefins could be hydroxylated as well. Intuitively, addition of electron withdrawing groups on the arene increase the polarization of the incipient diradical. For example, halogenated derivatives of benzoyl peroxide (i.e. fluorinated or chlorinated) demonstrate higher rates of hydrogen

abstraction than benzoyl peroxide (**1.10**) alone.[22] On the other hand, *para*-methoxy benzoyl peroxide is less reactive, due to conjugative electron delocalization of the ether.

In the course of understanding the reactivity of phthaloyl peroxide (**1.13**), it was found that this reagent readily oxidizes arenes, providing phenols after hydrolysis of mixed phthalate ester **1.39** (Figure 1.7b).[23] Phenols are found in a wide variety of chemical applications, including pharmaceuticals, agrochemicals, and materials. A major limitation of previous protocols developed for arene hydroxylation was that the resulting phenol was more reactive than the starting material, leading to over-oxidized products. Strong Brønsted/ Lewis acids have been effective at hydroxylating arenes. The acid has the dual role of activating the oxidant towards electrophilic substitution while also deactivating the resulting phenol towards subsequent oxidation. However the necessity of strong acids diminishes the broad utilization of this method. In addition to strong acids, transition metal complexes have been developed for this transformation.[24-27] The cost of using precious metals, and incompatibility with select functionality (like halogens, for instance) may limit this approach.

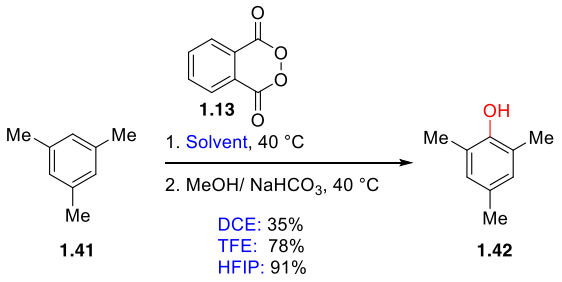

Figure 1.8. Solvents for hydroxylation reaction of mesitylene (**1.41**).

This procedure marks the first instance of a method that directly transforms aryl C-H bonds into C-OH bonds.[23] Hexafluoroisopropanol (HFIP) and trifluoroethanol (TFE) proved to be optimal solvents for the hydroxylation reaction (Figure 1.8). This trend agrees with the previous observation that the rate of reaction of radical reactions are often solvent

dependent.[28] Others have commented on the stabilization afforded by polar solvents[29-31], and fluorinated solvents[32,33] in particular, of radical intermediates.

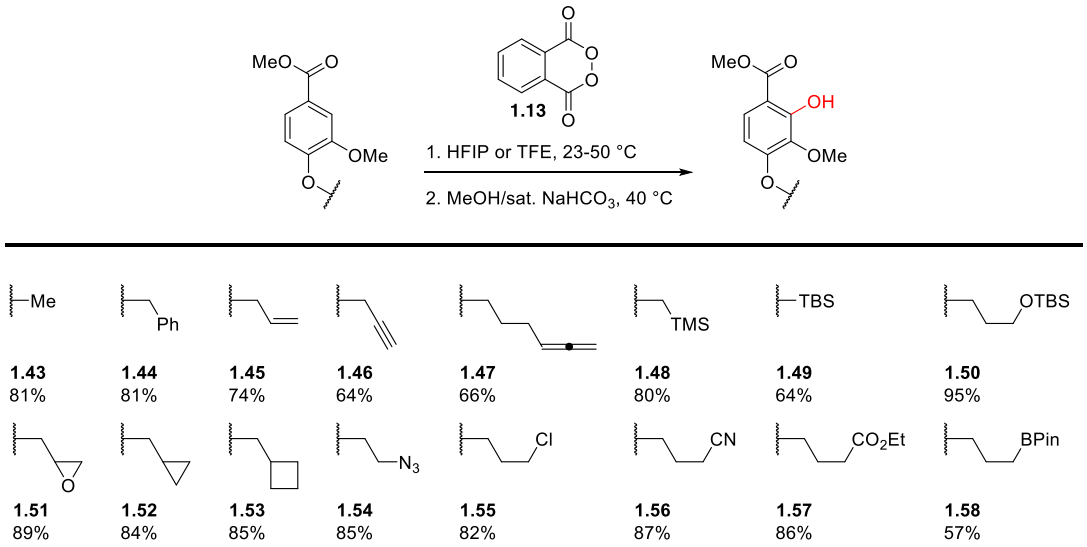

Figure 1.9. Broad functional group compatibility of the hydroxylation reaction.

To probe the functional group compatibility, a variety of vanillate derivatives were prepared and subjected to the hydroxylation reaction (Figure 1.9).[23] A wide variety of substituents are tolerated. Methyl vanillate provides the corresponding phenol (**1.43**) in 81% yield. Benzyl (**1.44**), allyl (**1.45**), alkynyl (**1.46**), and allenyl (**1.47**) functionality undergo aryl hydroxylation in good yields. In the case of benzyl groups, the reaction is selective for the more electron rich vanillate arene. Silicon-based protecting groups including trimethylsilane (**1.48**), and *tert*-butyldimethylsilane (**1.49** and **1.50**) are compatible with this reaction, with no evidence of protodesilylation. Strained ring systems including cyclopropyl (**1.52**) and cyclobutyl (**1.53**) remain intact and do not undergo ring opening. Surprisingly, the pinicol boronic ester (**1.58**) hydroxylated in acceptable yields, which provides a synthetic handle for further carbon-carbon bond forming reactions. Phthaloyl peroxide hydroxylates substrates containing azides (**1.54**), nitriles (**1.56**) and halogens (**1.55**), providing handles for further chemical manipulation.

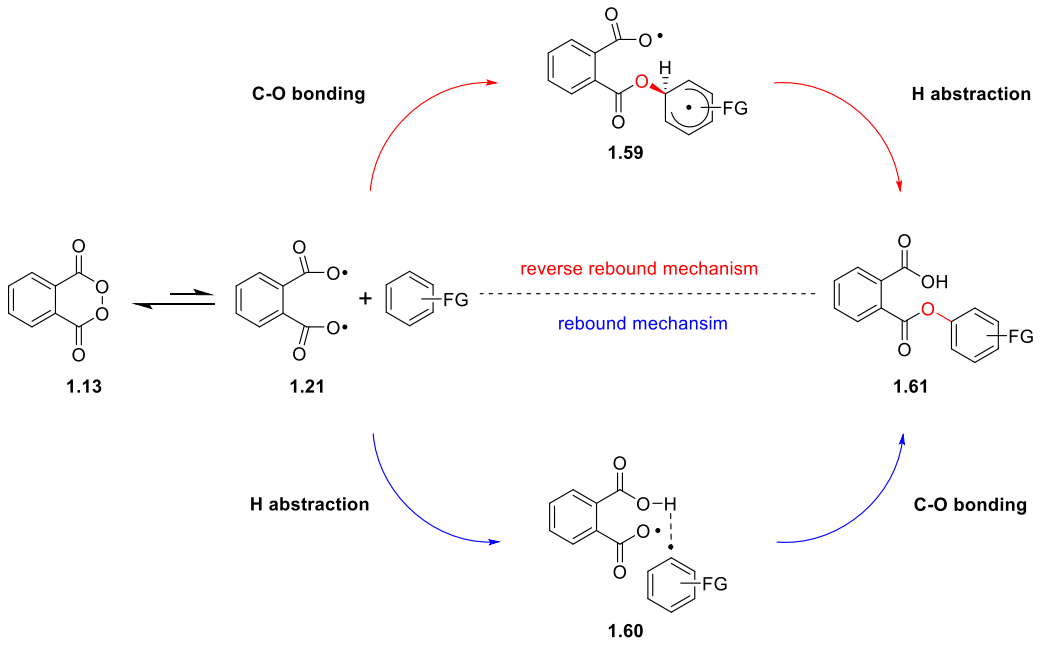

Figure 1.10. Mechanisms employing phthaloyl peroxide diradical (**1.21**).

The possibility of several mechanistic pathways was envisioned for this transformation (Figure 1.10). The relative ease by which homolysis of the peroxide bond occurs led to the examination of mechanisms proceeding through the phthaloyl diradical (**1.21**).[17] The phthaloyloxy radical (**1.21**) can add into the arene and form a carbon-oxygen bond, creating a stabilized cyclohexadienyl radical (**1.59**). Hydrogen abstraction re-aromatizes the arene. This pathway is termed the reverse rebound mechanism. Monooxygenases such as cytochrome P450 are thought to insert oxygen *via* the rebound mechanism.[34-36] In this pathway, C-O bonding is preceded by hydrogen abstraction, creating an aryl radical intermediate (**1.60**). The aryl radical then undergoes carbon-oxygen bond formation, providing the mixed phthalate ester (**1.61**).

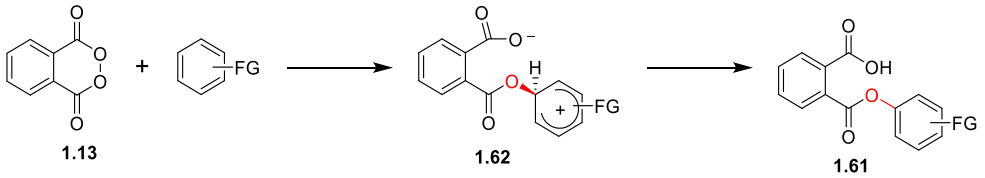

Figure 1.11. Electrophilic aromatic substitution mechanism.

An electrophilic aromatic substitution mechanism was also considered (Figure 1.11). Attack of the arene on the phthaloyl peroxy-oxygen bond would result in a conjugated carbocation (**1.62**). Elimination of a proton would give the aromatized mixed phthalate ester (**1.61**). This reaction pathway is analogous to the classical Friedel-Crafts acylation mechanism for the insertion of activated carboxylates.

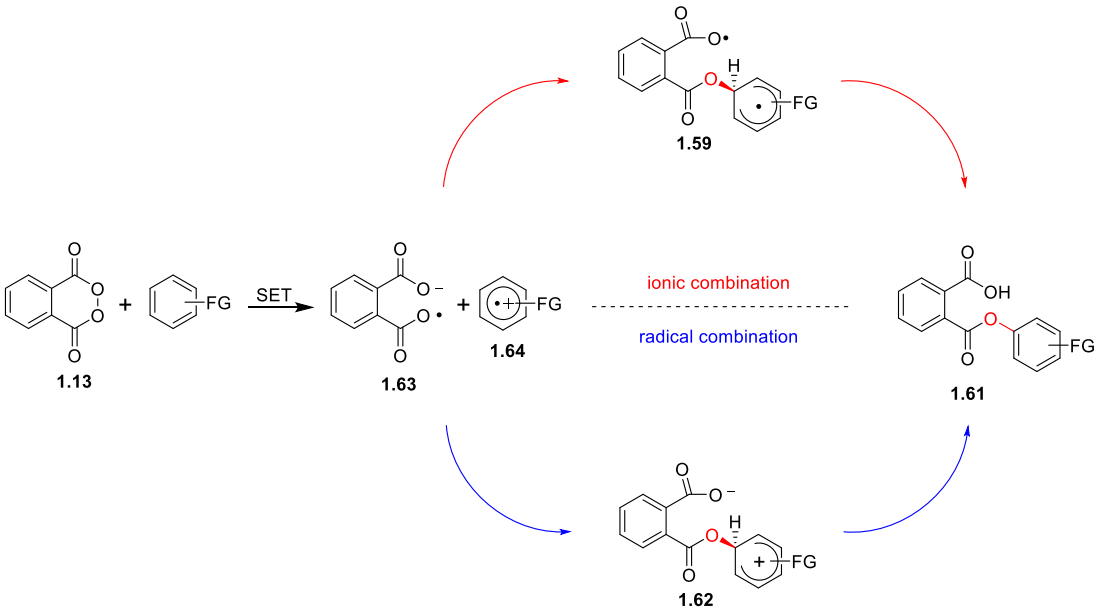

Figure 1.12. Single electron transfer mechanism.

Finally, the possibility of a single electron transfer (SET) pathway was examined (Figure 1.12). After electron transfer from the arene to phthaloyl peroxide, an aryl radical cation would be produced (**1.64**). Recombination could either occur *via* ionic or radical means. Carbon-oxygen bond formation could occur *via* nucleophilic addition of the carboxylate on the aryl radical cation, providing a cyclohexadienyl radical (**1.59**), the same intermediate in the reverse rebound mechanism (Figure 1.10). Hydrogen abstraction by the resulting phthaloyl radical would yield the phthalic ester (**1.61**). Alternatively, the phthaloyl radical could combine with the aryl radical, yielding a cyclohexadienyl carbocation **1.62**. Elimination of the proton would yield phthalic ester **1.61**.

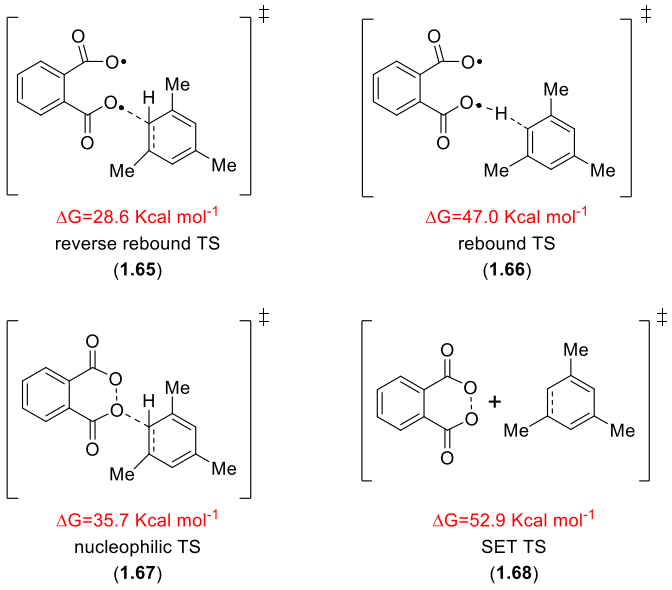

Figure 1.13. Calculated energetics of reaction transition states.

To determine the feasibility of each proposed mechanisms, the energetics of the transition states were calculated by Houk and co-workers (Figure 1.13).[23] The (U)B3LYP/6-31+G(d) methodology, which has been previously utilized in peroxide calculations was used in DFT and *ab initio* calculations.[37] Through these calculations, the single electron transfer (SET) pathway was calculated to possess the highest energy

transition state (**1.68**). This conflicts with the single electron transfer mechanism proposed for the dioxygenation of olefins found previously.[14] Direct hydrogen abstraction *via* rebound (**1.66**) is also unfavorable, with a calculated energy barrier of 47.0 kcal mol^{-1}. The reverse rebound mechanism transition state (**1.65**) has the lowest energy barrier (28.6 kcal mol^{-1}), 7 kcal mol^{-1} lower than nucleophilic addition (**1.67**).

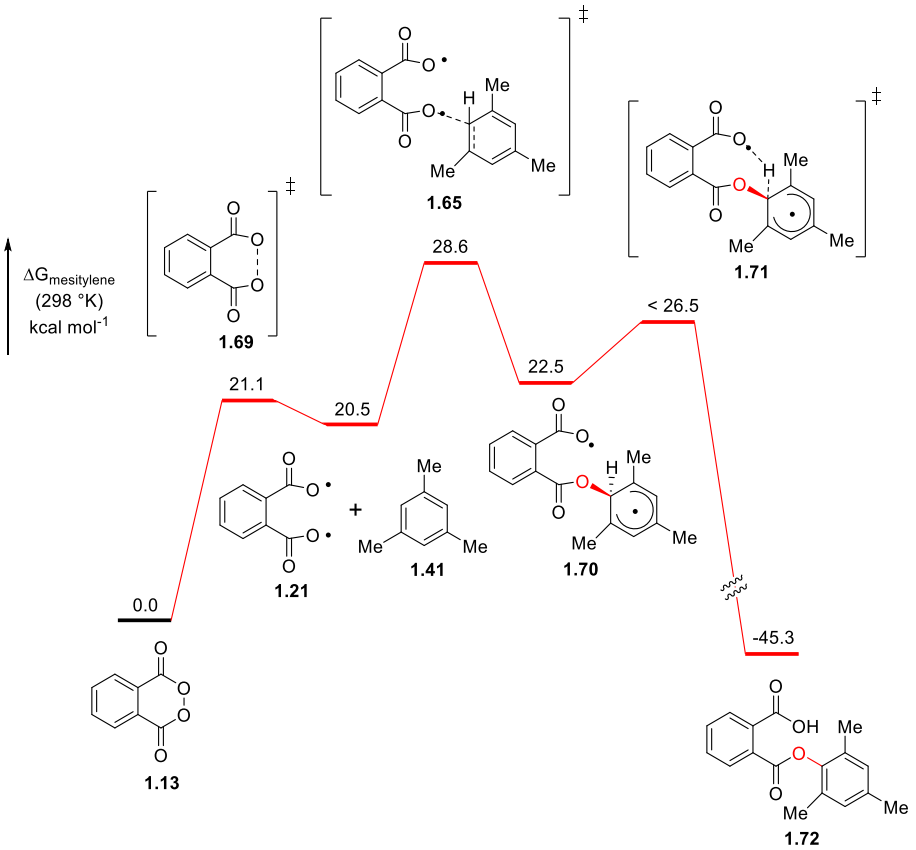

Figure 1.14. DFT-computed free energy surface and transition structures involved in the reverse rebound mechanism for the hydroxylation of mesitylene (**1.41**) at 298 °K.

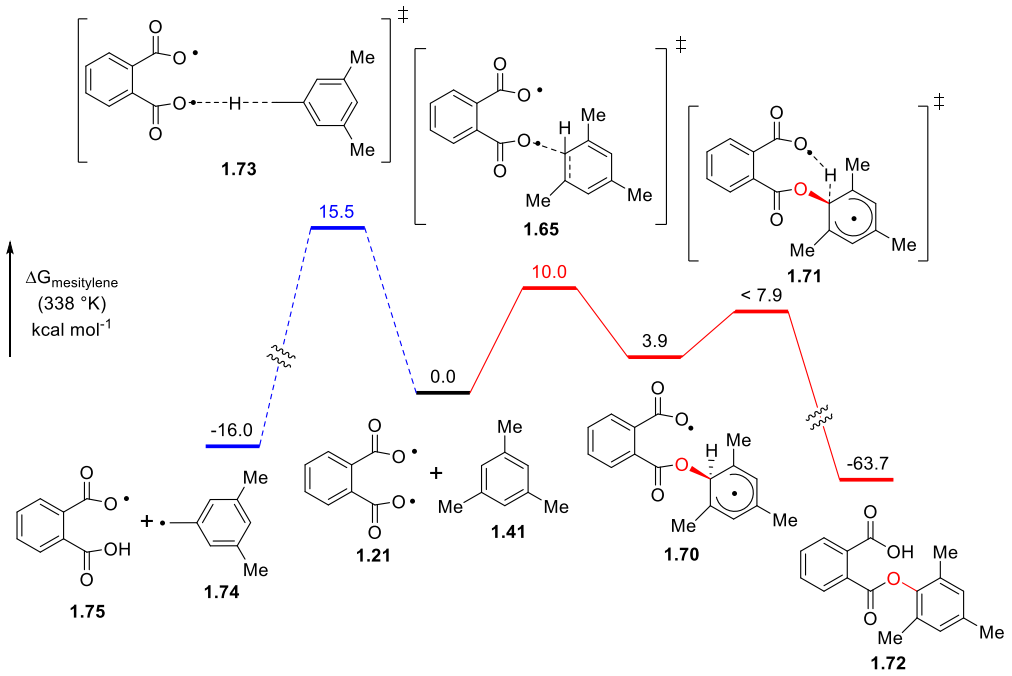

Figure 1.15. Computed free energy surfaces for aryl vs. benzylic functionalization of mesitylene at 338 °K using phthaloyl peroxide (**1.13**).

Given the similarities between benzoyl peroxide (**1.10**) and phthaloyl peroxide (**1.13**), the energy surface for benzylic vs. arene substitution was calculated by Houk and co-workers for both peroxides (Figure 1.15). In the case of phthaloyl peroxide (**1.13**), the addition of the phthaloyl radical (**1.21**) into the aromatic ring of mesitylene requires 10 kcal mol^{-1}.[74] Intramolecular hydrogen abstraction (**1.71**) is calculated to be rapid, with a barrier of less than 4 kcal mol^{-1}. Benzylic hydrogen abstraction (**1.73**) is 5.5 kcal mol^{-1} higher in energy than C-O bonding which accounts for the observed aryl selectivity for phthaloyl peroxide.

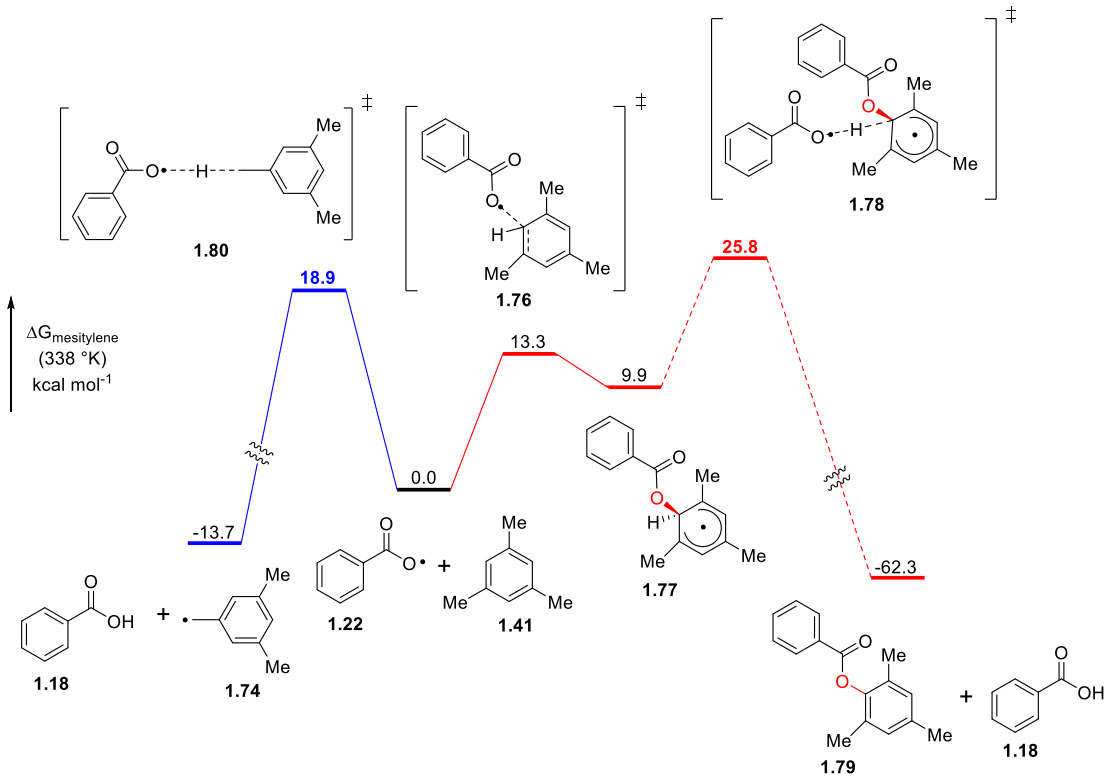

Figure 1.16. Computed free energy surfaces for aryl and benzylic functionalization using benzoyl peroxide (**1.10**).

The energetics of aryl vs. benzylic functionalization were also calculated for benzoyl peroxide to confirm that benzylic oxidation predominates using these calculation methods (**1.10**). Similar to that of phthaloyl peroxide (**1.13**), C-O bonding (**1.76**) is calculated to be lower in energy then benzylic oxidation (**1.80**). In fact, cyclohexadienyl adduct **1.77** has been observed using direct UV/Vis photolysis of benzoyl peroxide in the cavity of an EPR spectrometer at room temperature.[38] Despite the ability to add into the arene, the subsequent hydrogen abstraction is higher for benzoyl peroxide (15.9 kcal mol^{-1}) than for phthaloyl peroxide (4 kcal mol^{-1}). This is due to an entropic penalty for the bimolecular transition state (**1.78**), in contrast to the intramolecular hydrogen abstraction for phthaloyl peroxide (**1.71**). These calculations are in agreement with the experimental

observations that benzylic functionalization is favored for benzoyl peroxide in preference to aryl functionalization.

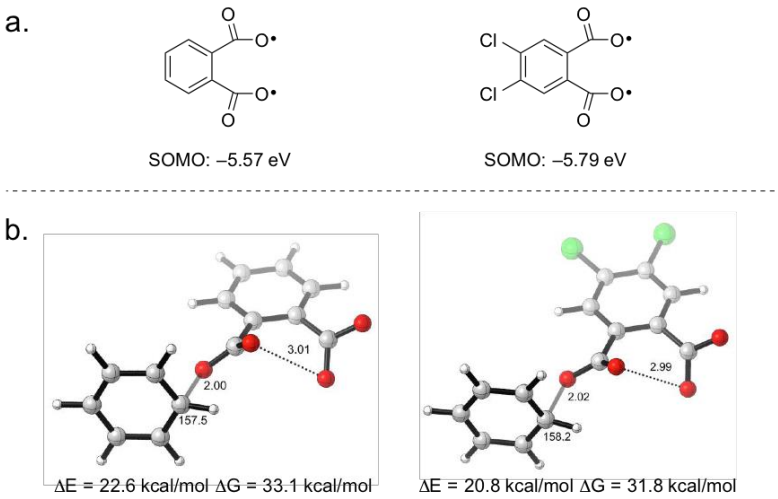

Figure 1.17. Calculations of improved peroxide.

Based on the experimentally observed enhanced reactivity of 4,5-dichlorophthaloyl peroxide (**1.33**) for olefin dihydroxylation, it was hypothesized that this increased reactivity would carry over to arene hydroxylation.[21] The same calculation methodology utilized for the parent peroxide was applied to 4,5-dichlorophthaloyl peroxide (Figure 1.17).[23] Calculations are in agreement with the experimentally determined enhanced reactivity. The SOMO for the dichloro derivative is 0.02 eV lower in energy than that of phthaloyl peroxide (Figure 1.17a). This lowers the energy gap between the SOMO-HOMO interaction in the transition state. Depictions of the C-O bonding structures with benzene are shown (Figure 1.17b) and the energy of the dichloro derivative (**1.33**) was found to be almost 2 kcal mol^{-1} lower in energy than that of phthaloyl peroxide (**1.13**).

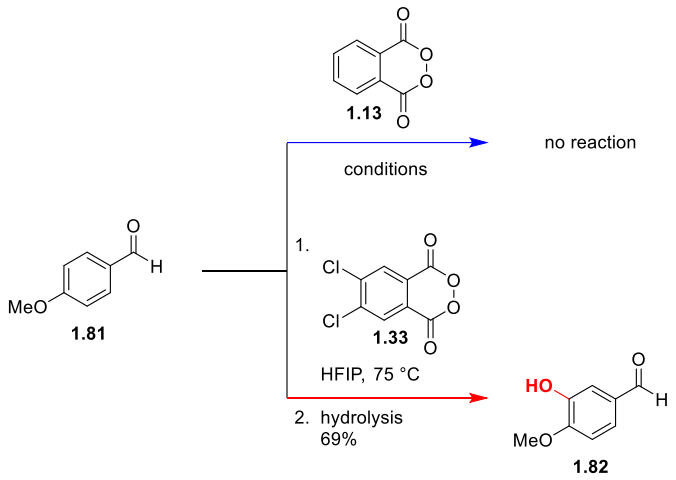

Figure 1.18. Improved reactivity of 4,5-dichlorophthaloyl peroxide (**1.33**).

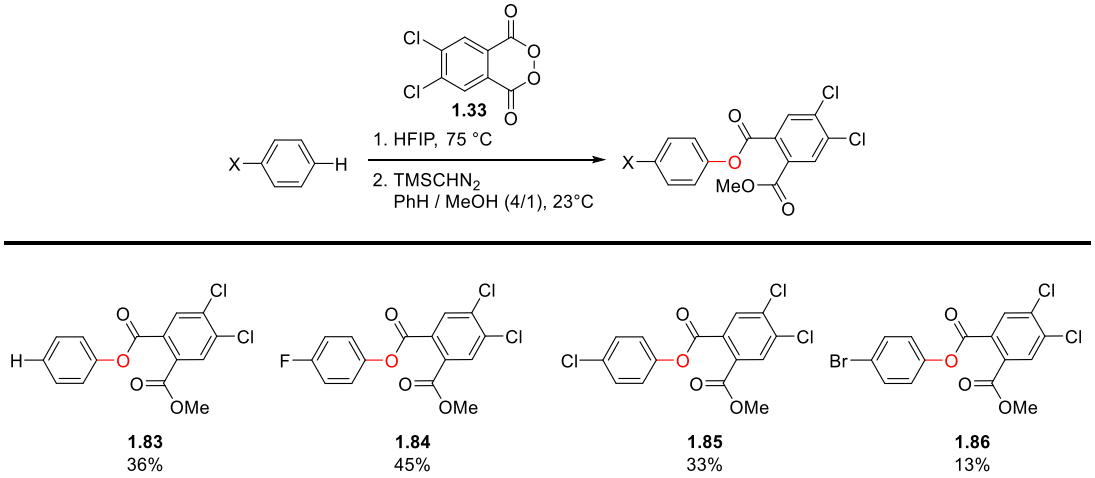

Figure 1.19. Challenging substrates prepared using 4,5-dichlorophthaloyl peroxide (**1.33**).

Previously with phthaloyl peroxide (**1.13**), electron withdrawing groups (e.g. carbonyls) require two activating groups on the ring in order to overcome the poor electronics. For example, anisaldehyde (**1.81**) does not undergo phthaloyl peroxide mediated hydroxylation (Figure 1.18). Utilizing the more reactive 4,5-dichlorophthaloyl peroxide (**1.33**), on the other hand, provides isovanillin (**1.82**) in 69% yield after hydrolysis. This suggests that only one activating group is required to overcome a carbonyl

for 4,5-dichlorophthaloyl peroxide. This enhanced reactivity observed experimentally is in agreement with the calculations which suggested that 4,5-dichlorophthaloyl peroxide would be more reactive. To showcase the improved reactivity of 4,5-dichlorophthaloyl peroxide (**1.33**), a series of halogenated arenes and benzene were subjected to 2.5 equivalents of 4,5-dichlorophthaloyl peroxide in HFIP at 75 °C (Figure 1.19). The resulting phenols were volatile, thus the crude reaction mixtures were methylated using trimethylsilyl diazomethane and then fully characterized as the phthalate methyl esters. While the yields were modest even using the more reactive peroxide, the reaction with these less reactive arenes did not result in secondary oxidation.

Unlike phthaloyl peroxide (**1.13**), arenes possessing neutral to moderately deactivating functionality were accessible using 4,5-dichlorophthaloyl peroxide (**1.33**). Primary (**1.87**) and secondary alcohols (**1.88**) were tolerated in the hydroxylation reaction, with no overoxidation observed. Similarly, a family of hydrocinnamyl derivatives possessing varying oxidation states was tested. Methyl hydrocinnamate gave the corresponding phenol (**1.91**) in 74% yield. Interestingly, protection of the carboxylate was not required, as the free carboxylic acid (**1.92**) hydroxylated in 65% yield. Hydrocinnamonitrile provided the corresponding phenol (**1.93**) in 40% yield, with recovery of 26% of starting material. Removal of a methylene spacer from methyl hydrocinnamate (**1.94**) decreased the yields (48%). The effects of placing a methoxy group *ortho*, *para* or *meta* with respect to a methyl ester was interrogated. As was observed with anisaldehyde, only one electron donating group is necessary to overcome a methyl ester attached directly to the ring, providing a 64% yield of the corresponding methyl *p*-methoxy benzoate (**1.95**). The methoxy group *ortho* to the methyl ester resulted in 53% yield of the phenol, as a 1.2:1 mixture of regioisomers (**1.96**). If the methoxy group is *meta* to the ester (**1.97**), both yields and regioselectivity decreased.

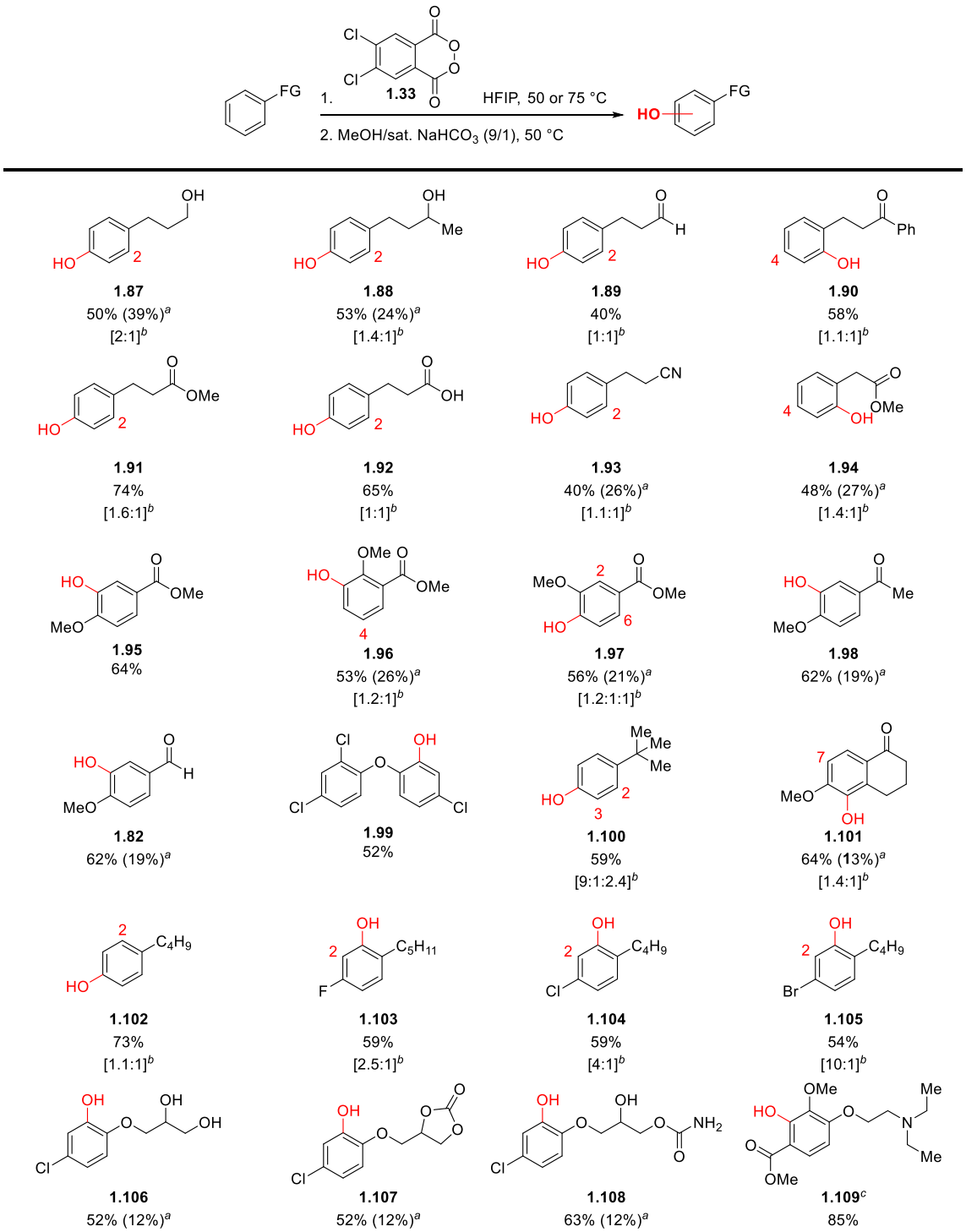

Figure 1.20. Phenols prepared using the activated peroxide 4,5-dichlorophthaloyl peroxide (**1.33**). [a] Recovered starting material. [b] Ratio of major: minor regioisomers. [c] Protonated first with *p*-toluenesulfonic acid.

Arenes processing *tert*-butyl functionality (**1.100**) increased the regioselectivity of the reaction, with respect to *n*-butyl (**1.102**). It is still noteworthy that oxidation *ortho* to this sterically demanding group is not completely abated. A series of alkyl benzenes (**1.102**–**1.105**) were hydroxylated, following the trends displayed for the halobenzenes reacted previously. Methoxy substituted 1-tetralone hydroxylated *ortho* to the methoxy functionality in 64% yield as a 1.4:1 mixture of regioisomers (**1.101**), with no Baeyer-Villiger oxidation of the ketone. Substrates possessing multiple functionality including cyclic carbonates (**1.107**) and carbamates (**1.108**) are tolerated in the reaction, giving yields of 52% and 64%, respectively. Amines are tolerated by first protonating the nitrogen with 1.0 equivalent of *p*-toluenesulfonic acid, providing high yields of this methyl vanillate derivative (**1.109**).

The FDA has mandated that in addition to testing the parent drug, metabolites present in greater than 10% must also be tested in order for final approval to be granted. The regioselectivity of the hydroxylation reaction generally follows installation of oxygen at the most electron rich carbon, analogous to cytochrome P450 oxidation. Thus using phthaloyl peroxide (**1.13**) and 4,5-dichlorophthaloyl peroxide (**1.33**), one can generate phase I oxidative metabolites from the parent drug candidate without devising a new synthetic route. The compatibility of the peroxide with a wide variety of functional groups enables late-stage chemoselective oxidation of complex small molecules.

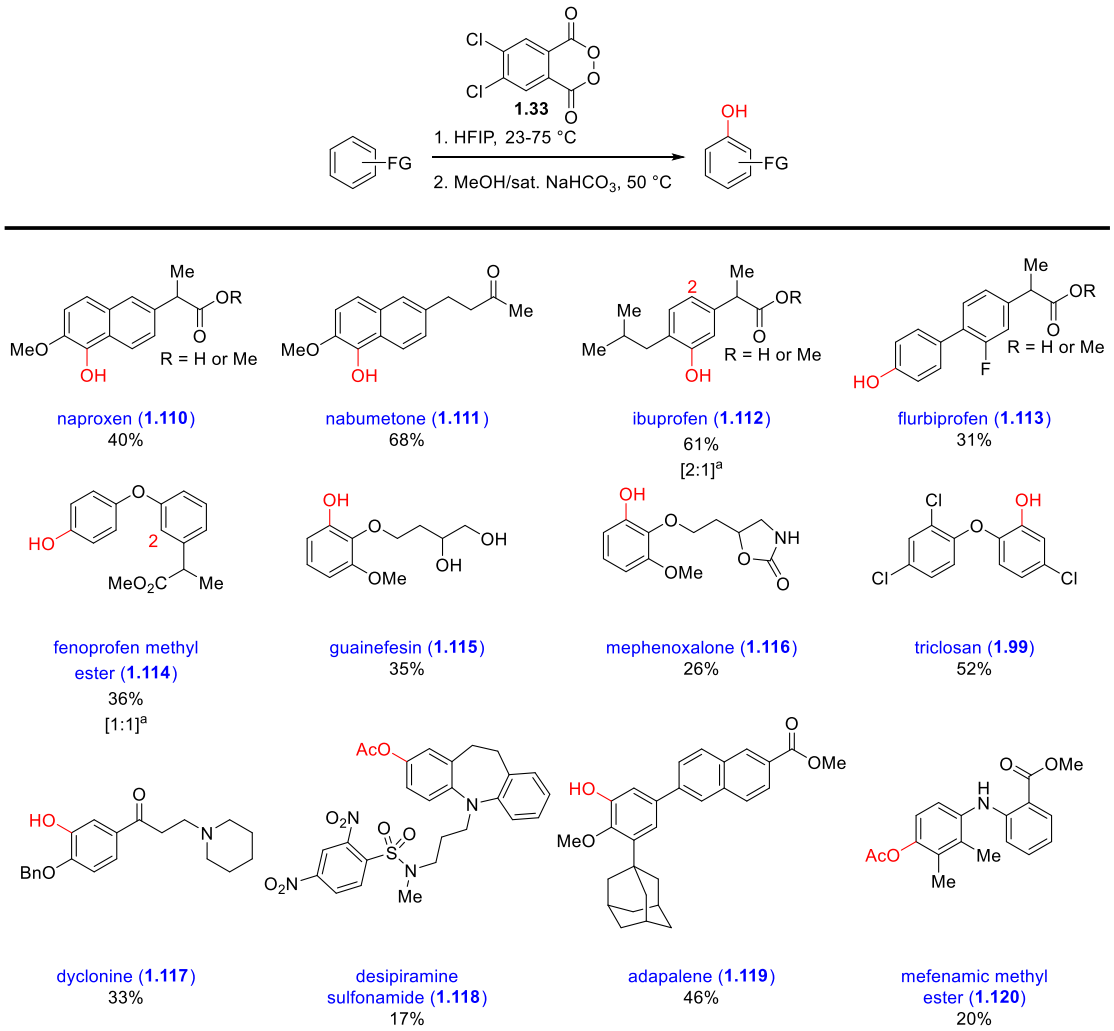

Figure 1.21. Hydroxylation of biologically relevant small molecules. [a] Ratio of major: minor regioisomers.

Given the broad functionality tolerated by the more reactive 4,5-dichlorophthaloyl peroxide (**1.33**), we subjected a variety of therapeutics, biocides, and other biologically relevant small molecules to the hydroxylation reaction (Figure 1.21). Both the free acid and methyl ester of naproxen were tolerated providing a 40% yield of **1.110**. The non-steroidal anti-inflammatory drug (NSAID) nabumetone was hydroxylated in 68% yield (**1.111**). For both naproxen and nabumetone, flash chromatography was done rapidly and under nitrogen as the resulting naphthols were prone to air-oxidation. Hydroxylation of

ibuprofen, whether as the methyl ester or carboxylate resulted in a 2:1 mixture of regioisomers, in a 61% combined yield (**1.112**). Subjecting flurbiprofen, a potent member of the NSAID family used to treat inflammation and arthritis, to the hydroxylation reaction resulted in regioselective oxidation of the more electronically rich ring, providing the phenol in 31% yield (**1.113**). This phenol is the major metabolite of the parent drug.[39] Hydroxylation of fenoprofen methyl ester resulted in a 1:1 mixture of phenols (**1.114**). The structurally related expectorant guainefesin and anxiolytic mephenoxalone gave hydroxylated products in 35% (**1.115**) and 26% (**1.116**), respectively. The low yields are a result of the highly polar products produced, rendering the aqueous workup following the hydrolysis of the phthalate ester tedious. The biocide triclosan (found in many antibacterial soaps) was synthesized by treating the corresponding trichlorinated arene with 4,5-dichlorophthaloyl peroxide, providing triclosan (**1.99**) in 52% yield. Anilines and sulfonamides (**1.118** and **1.120**) can also be hydroxylated in modest yields.

To understand the thermal stability of the peroxide, thermogravimetric analysis (TGA) was performed on solid benzoyl peroxide (**1.10**), phthaloyl peroxide (**1.13**), and 4,5-dichlorophthaloyl peroxide (**1.33**) (Figure 1.21). TGA monitors the change in mass of an analyte as a function of a gradual temperature ramp. Phthaloyl peroxide (**1.13**) undergoes a fast and energetic decomposition at 130 °C. The improved 4,5-dichlorophthaloyl peroxide (**1.33**) is more thermally stable than phthaloyl peroxide, decomposing at 135 °C. Hydrated benzoyl peroxide begins to decompose at 106 °C.

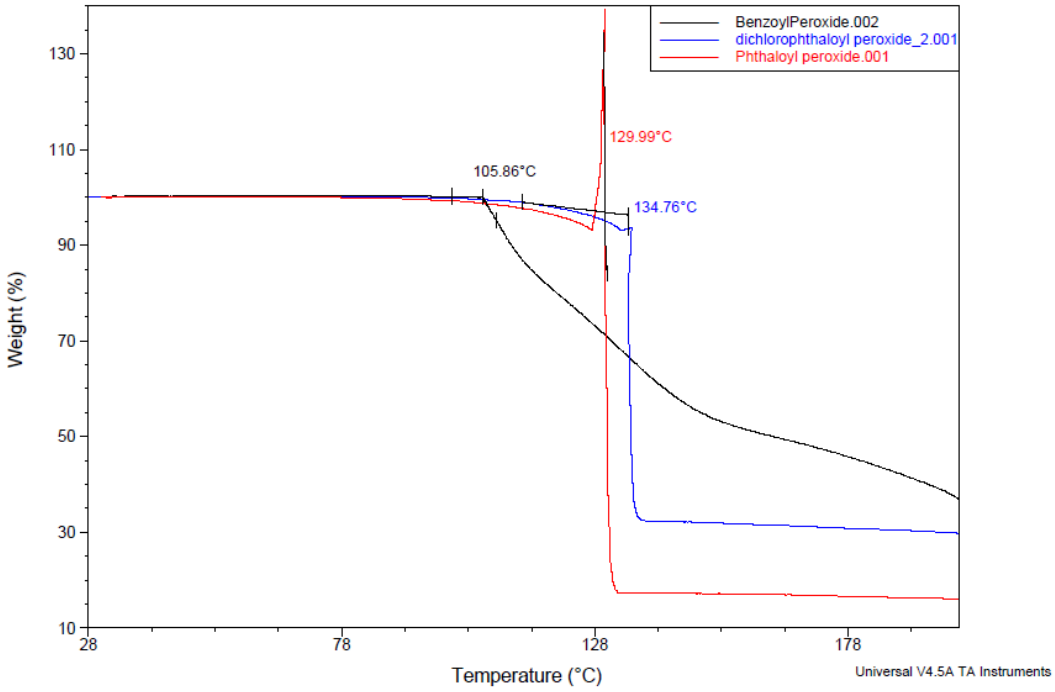

Figure 1.22. TGA of benzoyl peroxide (**1.10**), phthaloyl peroxide (**1.13**), and 4,5-dichlorophthaloyl peroxide (**1.33**).

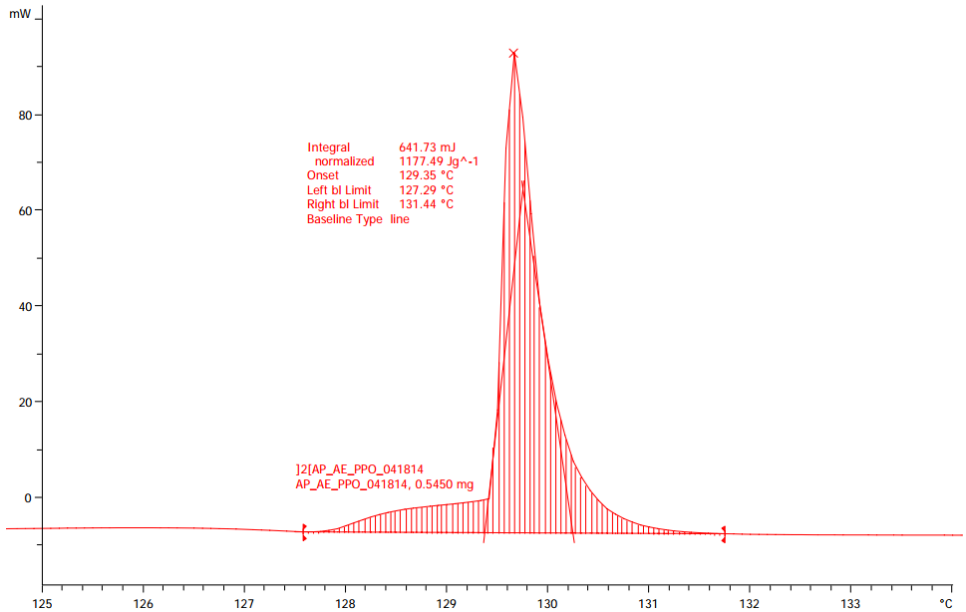

Figure 1.23. DSC thermogram of phthaloyl peroxide (**1.13**), obtained using a 5 °C min^{-1} heat ramp.

Differential scanning calorimetry (DSC) is a technique in which the difference in the heat flow between the sample and reference is monitored. The presence of an exothermic event is then used to access the stability of the analyte. A thermogram obtained in this manner indicates phthaloyl peroxide (**1.13**) has an energetic profile of 1177.49 J g^{-1} (Figure 1.23). Using DSC, anhydrous benzoyl peroxide (**1.10**) was found to have a higher decomposition enthalpy (1603.0 J g^{-1}).[40] While the energy of decomposition is lower for phthaloyl peroxide than several commercially available peroxides, the safety concerns of utilizing stoichiometric amounts of organoperoxides on scale should not be overlooked. One technique industry has pursued to circumvent the need to prepare and store large quantities of toxic or unstable reagents is to synthesize and immediately use the hazardous reagent using a flow reactor.

Reactions in flow offer several advantages over reactions performed in batch.[41-45] For example, the flow apparatus occupies a smaller footprint, and are more economical to horizontal scaling than batch reactors ("scaling out" as opposed to "scaling up").[46] Due to the higher surface area of the reactor, mixing is much more efficient, thus reactions (especially biphasic or heterogeneous solutions) are dramatically accelerated due to increased shearing forces.[42,47] Reactions run in flow can safely be run at elevated temperature[48-50] and pressure[51-53] rendering the large-scale bomb reactor unnecessary.

Exposure to toxic, unstable, and air sensitive materials are minimized in flow reactors and the accumulation of these reagents is minimal. Highly toxic substances including phosgene[54], the Vilsmeier reagent[55], diazomethane[56,57], diazoesters[58] have been prepare in flow. Additionally ozone[48], osmium tetraoxide[59], have been introduced into a flow reactor, minimizing the chances of exposure to these acutely toxic reagents.

Oxidations run in flow have also been developed. Using TEMPO and hypervalent iodine, benzylic alcohols were demonstrated to undergo conversion to the corresponding

aldehyde in flow.[60] Protocols utilizing palladium catalysis have been developed in flow, employing molecular oxygen as the stoichiometric oxidant.[61] Other examples include the use of early or late transition metals employing peroxides or oxygen as the oxidant.[61-68] More recently, Jamison reported a method to generate phenols in flow by treating an aryl Grignard with oxygen.[69]

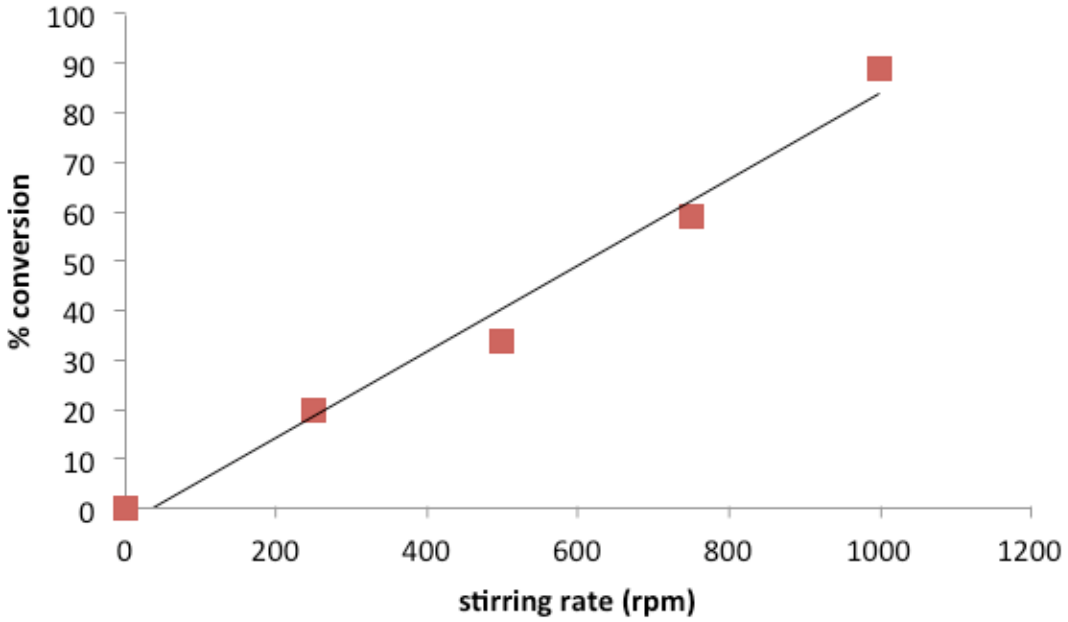

Figure 1.24. Impact of stirring on % conversion of phthaloyl peroxide (**1.13**) formation in batch. Reaction was analyzed after four hours.

Several aspects of the generation of phthaloyl peroxide (**1.13**) make it a good candidate for flow. For biphasic reactions, the rate of reaction is highly dependent on the efficiency of stirring. In the case of phthaloyl peroxide, the rate of stirring has a dramatic impact on the production of product (Figure 1.24). Related to the biphasic nature of the reaction, the scale at which the reaction was run greatly affected the product yields, as stirring is complicated in larger vessels and may require specialized equipment. On the other hand, utilizing a packed bed reactor, a tube consisting of finely ground sodium percarbonate in this case, stirring is optimized as the flow of phthaloyl chloride is forced

past the particles, maximizing contact between the surface of the solid and liquid phases (Figure 1.25).[70,71]

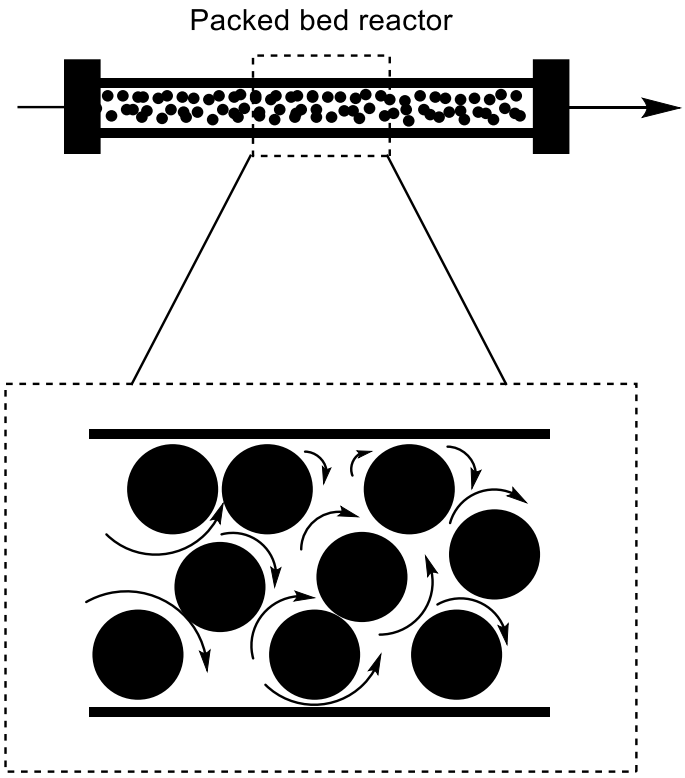

Figure 1.25. Increased stirring in packed bed reactors.

The effects of solvent on the conversion of phthaloyl peroxide (**1.13**) were investigated (Figure 1.26). The polar aprotic solvents ethyl acetate and acetone afforded moderate conversion of phthaloyl chloride (**1.30**). However, phthalic anhydride (**1.121**) was also produced in varying amounts. The need to purify the resulting peroxide from unreacted starting material and byproducts (all soluble in the solvent) was undesirable and negated the advantages of running the reaction in flow. After screening many solvents, it was found that halogenated solvents were most optimal. Trifluorotoluene, dichloroethane and methylene chloride yielded peroxide in high purity (>95% by NMR) and in comparable

isolated yields. Methylene chloride was ultimately selected due to its high volatility, simplifying its removal in the subsequent hydroxylation reaction.

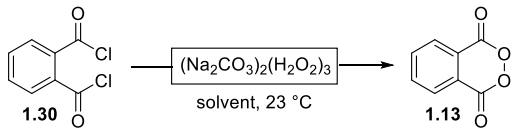

entry	solvent[a]	conversion (%)[b]
1.	ethyl acetate	68
2.	acetone	76
3.	trifluorotoluene	>95
4.	dichloroethane	>95
5.	methylene chloride	>95

Figure 1.26. Solvent optimization of peroxide (**1.13**) formation in flow. [a] Reagent grade solvent. [b] Determined *via* NMR analysis.

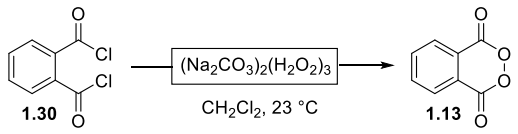

entry	flow rate (mL min^{-1})	CH_2Cl_2	BPR (psi)	conversion (%)[a]	yield (%)[b]
1.	50	anhydrous	40	>95	61
2.	167	anhydrous	40	>95	71
3.	334	anhydrous	40	>95	72
4.	167	anhydrous	none	>95	66
5.	167	reagent grade	40	>95	57
6.	167	wet	40	>95	47

Figure 1.27. Optimization of flow reaction. [a] Determined *via* NMR analysis. [b] Isolated material after removal of solvent *in vacuo*.

With an optimized solvent in hand, the effects of flow rate, amount of water present in the mobile phase, and the presence of a back pressure regulator (BPR) were investigated (Figure 1.27). The rate at which the substrate passes through the packed bed reactor has great impact on the isolated yield of the peroxide (**1.13**). In general, increasing the flow rate resulted in higher isolated yields. We found that a flow rate of 167 μL min^{-1} struck the right balance of yield and reproducibility, as high flow rates strained the syringe pump, resulting in inconsistent flow velocity through the reactor. Like the batch procedure for making phthaloyl peroxide, the amount of water present in the solvent greatly affects the yield. Using reagent grade solvent decreased the yield from 71% to 57%. Wet solvent prepared similarly to the batch solvent was even more deleterious, decreasing the yield further to 47%. Due to the continuous generation of carbon dioxide, a BPR was affixed to the reactor following passage through the packed bed reactor. While only a modest increase in isolated yield was observed, the inclusion of this device ensured constant velocity through the system.

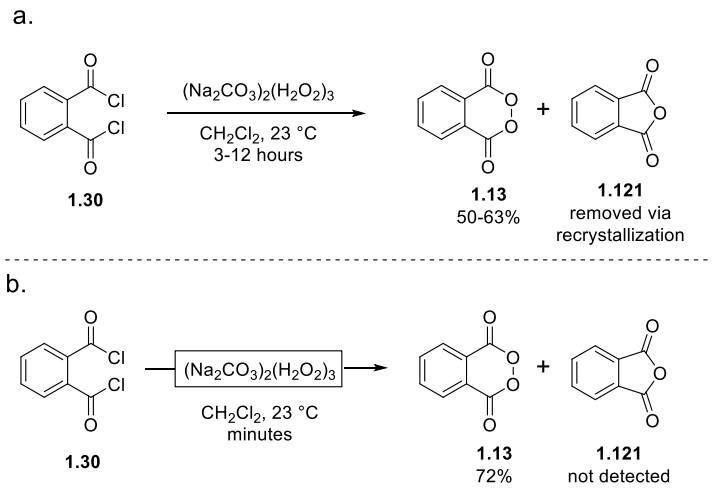

Figure 1.28. Comparison of phthaloyl peroxide (**1.13**) synthesized in (a.) batch and (b.) flow.

Remarkably, not only was the yield much higher for the flow procedure, but the peroxide (**1.13**) produced was much more pure, and did not require a final recrystallization (Figure 1.28). The flow procedure generates peroxide in minutes, as opposed to 3-12 hours (depending on the scale) in batch. Finally, this protocol yields a 0.2 M solution of phthaloyl peroxide in methylene chloride, which does not require the isolation of solid peroxide.

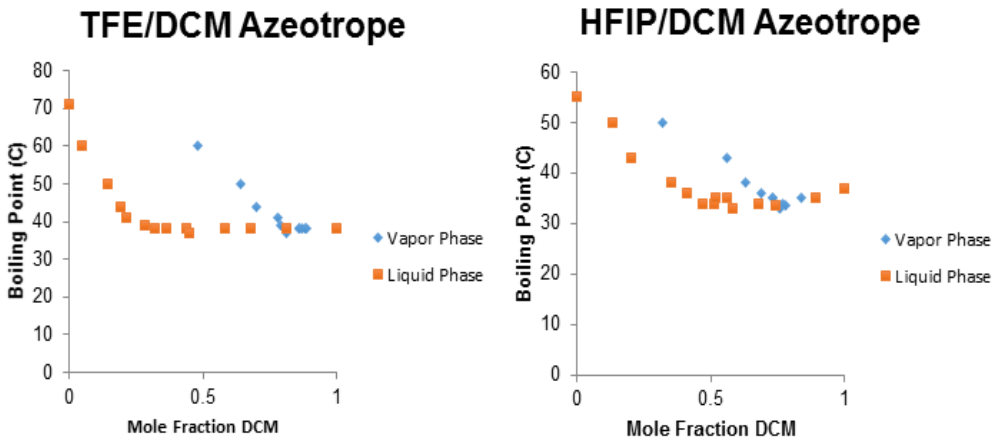

Figure 1.29. Azeotrope analysis of TFE and HFIP mixtures with methylene chloride.

However, the hydroxylation reaction employing phthaloyl peroxide (**1.13**) was optimized using fluorinated solvents.[23] Additionally, the usage of co-solvents typically decreases the yield of this reaction. For example, reaction of mesitylene in a 1:1 mixture of methylene chloride: hexafluoroisopropanol (HFIP) gave the corresponding phenol in 56% yield. The reaction ran solely in HFIP results in a 97% yield of trimethylphenol. In order to maximize yields, the solvent would need to be changed from methylene chloride to a fluorinated solvent. In-line solvent switching in flow reactors have been developed, typically utilizing a semi-permeable membrane.[72] Boiling point measurements and analysis of distillate indicated that methylene chloride and HFIP form a positive azeotrope (Figure 1.29). Consequently, removal of methylene chloride from HFIP by distillation was not

feasible. However, we found that trifluoroethanol (TFE) and methylene chloride behaved more like an ideal solution, allowing for the selective removal of methylene chloride from the TFE solution *via* distillation.

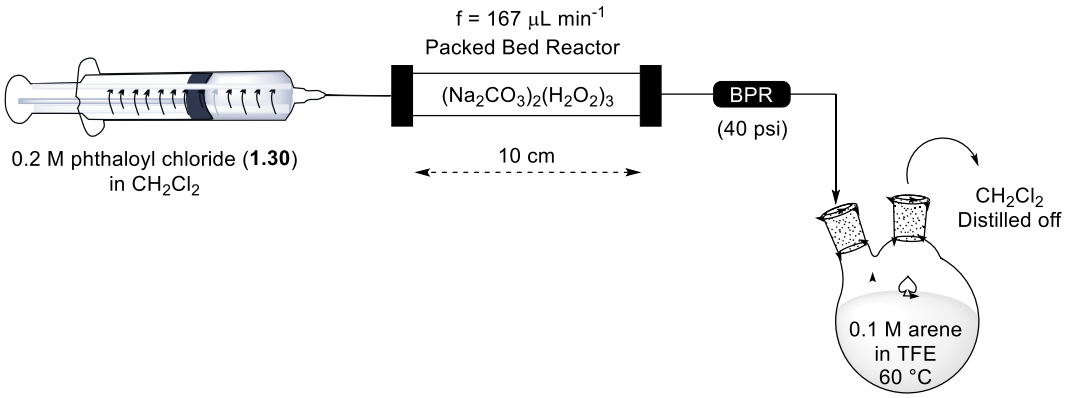

Figure 1.30. Schematic of flow apparatus.

To couple the preparation of phthaloyl peroxide (**1.13**) with the synthesis of phenols, the apparatus was assembled as depicted in Figure 1.30. A 0.2 M solution of phthaloyl chloride (**1.30**) in methylene chloride was pumped at a rate of 167 μL min^{-1} through a 10 cm packed bed reactor containing pulverized sodium percarbonate. Grinding sodium percarbonate using a mortar and pestle was found to be essential for full conversion. However, controlling the resulting particle size was necessary. For example, particles smaller than the frit porosity clogged the reactor, and uniformly sized particles increased reproducibility. Mesh sieves (140 and 325 mesh) were used to control the size of the ground sodium percarbonate by selecting for particles ranging from 46-105 μm in diameter. The feed emanating from the back pressure regulator was inserted into a two-necked flask containing the arene as a solution in TFE and equipped with a distillation apparatus. The receiving flask is submerged in an oil bath set to 60 °C, allowing for the continual removal of methylene chloride.

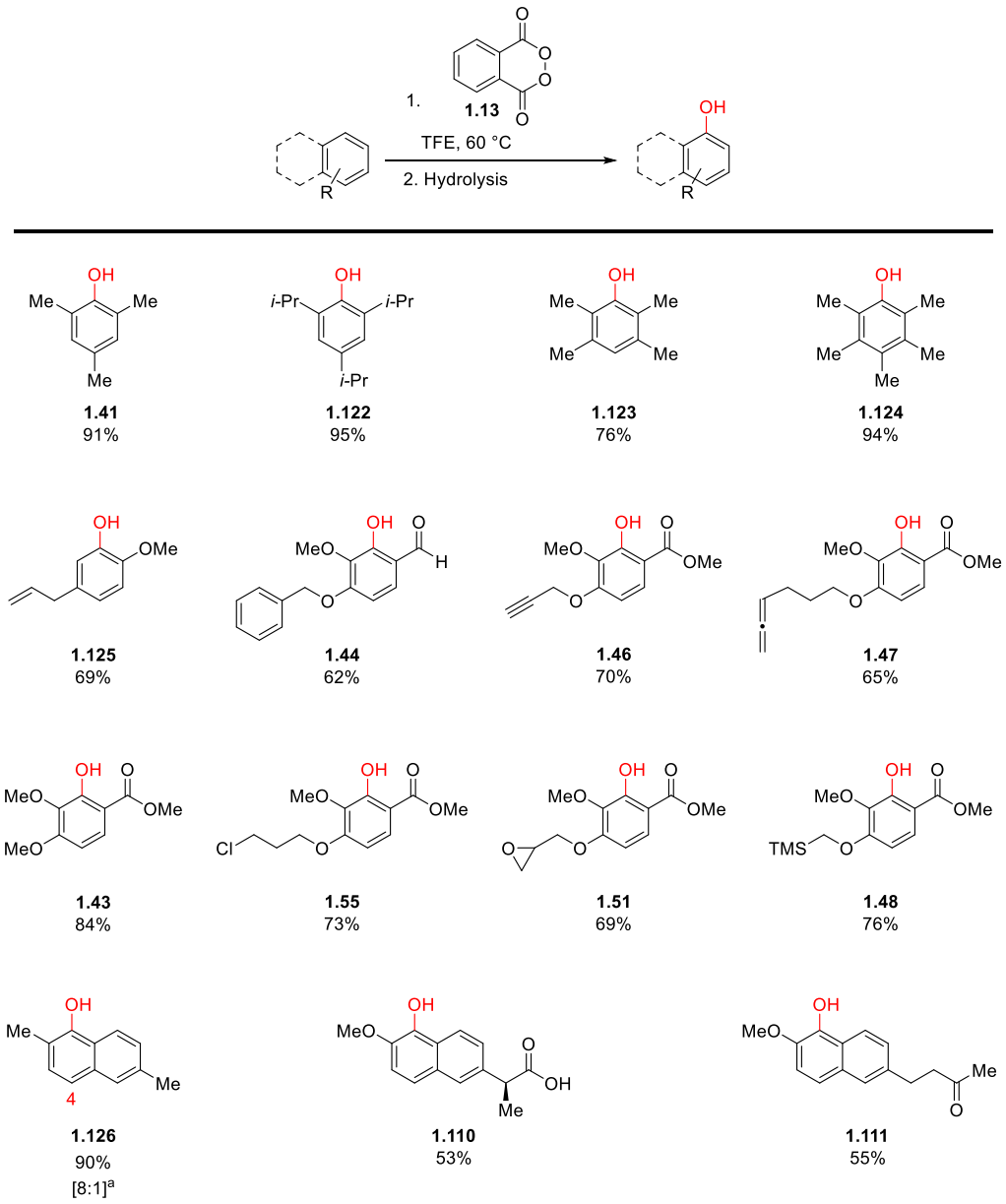

Figure 1.31. Arenes hydroxylated using phthaloyl peroxide (**1.13**) prepared in flow.
[a] Ratio of major: minor regioisomers.

Analogously to what had been previously observed in batch utilizing solid phthaloyl peroxide, a variety of arenes are oxidized in this reaction (Figure 1.31). Mesitylene is hydroxylated in 91% yield (**1.41**). Triisopropylbenzene provides phenol **1.122** in 95% yield. The sterics associated with tetramethylbenzene or pentamethylbenzene

does not impede reactivity, providing both phenols **1.123** and **1.124** in 76% and 94% yield. Allyl groups attached to the arene do not oxidize (**1.125**). When more than one arene is present, hydroxylation occurs at the more electronically rich arene (**1.44**), analogous to what is observed in batch. Alkynes and allenes do not undergo unproductive reactivity, giving good yields of phenols **1.46** and **1.47**. Naphthalene derivatives **1.110**, **1.111**, and **1.126** are obtained in good yield.

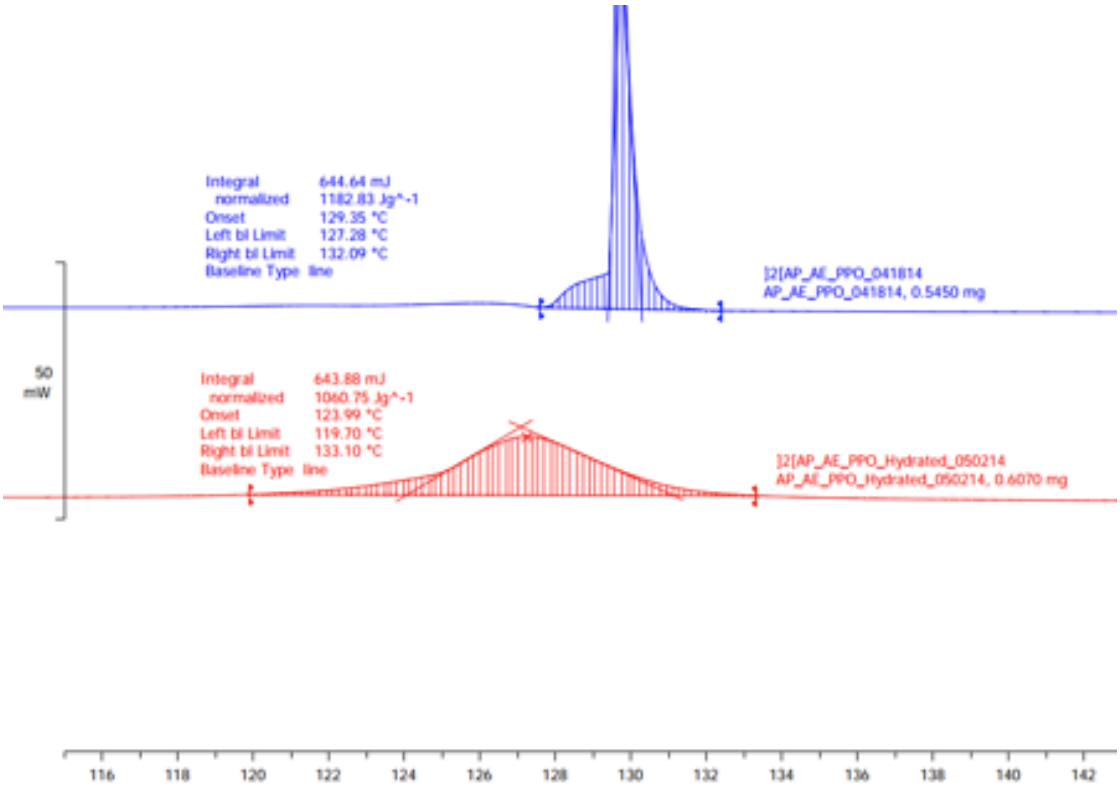

Figure 1.32. Effects of wetting phthaloyl peroxide (**1.13**) on enthalpy of decomposition.

To increase the safety of neat phthaloyl peroxide (**1.13**), the effect of wetting the solid was investigated (Figure 1.32). Despite the instability of benzoyl peroxide (**1.10**), it is commercially available and is used as a topical treatment for acne. It is kept wet in a mixture composed of at least 1% water, but typically sold as a 25% mixture. After the inclusion of only 5% water, the thermogram of phthaloyl peroxide dramatically changes. Instead of a sharp peak indicating a high energetic decomposition (detonation), the addition of water broadens the thermogram substantially. This indicates a much slower decomposition rate than that of the neat peroxide.

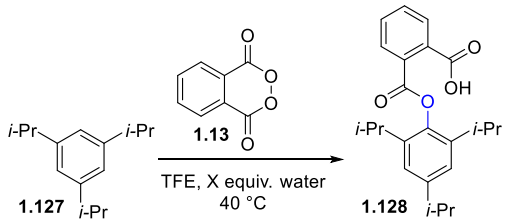

entry	equiv. water	conversion (%)[a]
1.	0	94
2.	1	90
3.	2	94
4.	8	94
5.	16	90
6.	32	73
7.	64	59
8.	128	12

Figure 1.33. Effect of water on the hydroxylation reaction. [a] Determined *via* NMR analysis.

With a method to attenuate the energetics of phthaloyl peroxide (**1.13**), the effects of water on the subsequent hydroxylation reaction were investigated (Figure 1.33). The reaction proved to be tolerant of water, up to 16 equivalents before the yield of the reaction began to be adversely affected. This demonstrates that wetting phthaloyl peroxide decreases its energetics but has little effect on its reactivity.

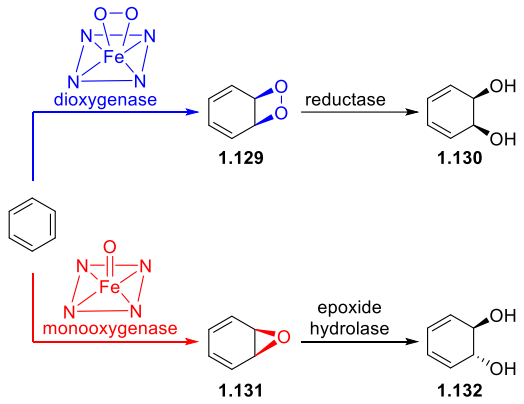

Figure 1.34. Metabolism of benzene by dioxygenase and monooxygenase.

Nature has evolved a series of enzymes capable of oxidatively processing arenes. In addition to cytochrome P450s which catalyze the insertion of one atom of dioxygen (monooxygenase), dioxygenases incorporate both atoms of dioxygen (Figure 1.34).[73-75] Both monooxygenases and dioxygenases typically harbor an iron heme cofactor as the reactive center with the catalytically active state being either an iron(V)-oxo or iron(III)-peroxo complex.[76] Upon oxidation, the resulting cyclohexadienyl adduct is further processed *via* reductive or hydrolytic steps.

While the above mentioned transformation would be immediately useful to chemical synthesis, the analogous non-biologic reaction does not exist. The lack of overoxidation in nature's oxygenase reactivity is noteworthy as the first oxidation step overcomes the barrier of aromaticity and generates a product that is itself prone to further oxidation. An analogous reaction in chemical synthesis has not been developed as the oxidant must be a strong enough oxidizer to dearomatize the arene, but not react further with the resulting cyclohexadiene. Chemical oxidations of arenes that generate dienones, which possess a reduced susceptibility towards additional oxidation, have been widely employed and extensively developed and showcase the utility of oxidative

dearomatization. However, the requirement of dienone generation is a limitation. Additionally, the resulting diene can undergoes uncontrollable Diels-Alder reactions.

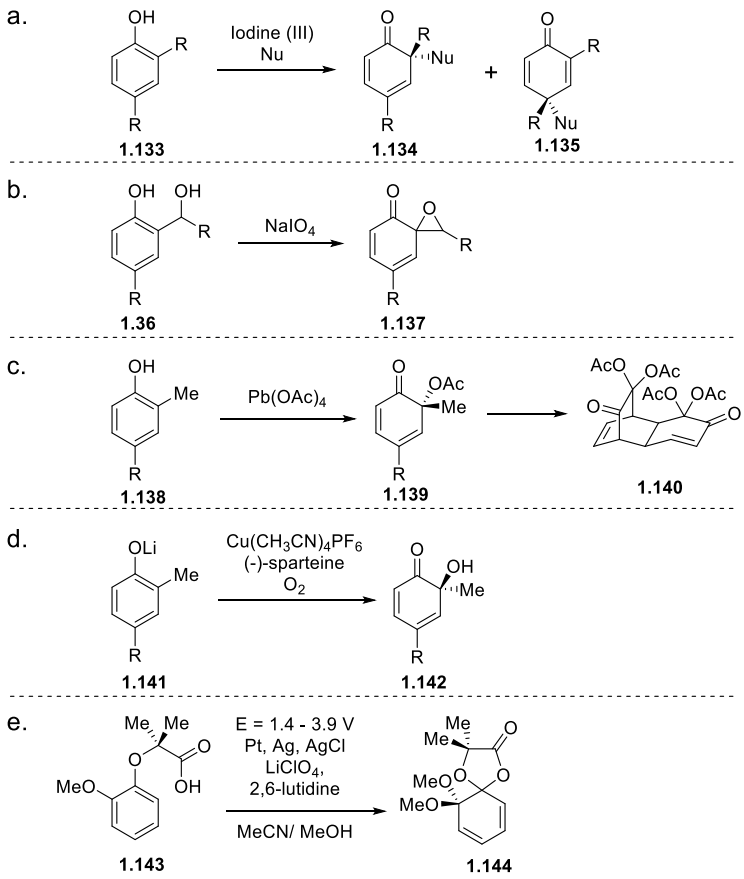

Figure 1.35. Examples of oxidative dearomatization.

Methods have been developed to access oxygenated cyclohexadiene derivatives from aromatic precursors (Figure 1.35). The most common methods employ hypervalent iodine (Figure 1.35a). Treatment of a functionalized phenol (**1.133**) with a nucleophile in the presence of an iodine(III) source, yields the dienone with addition either *ortho* (**1.134**) or *para* (**1.135**) to the phenol.[77] The Becker-Adler reaction (Figure 1.35b) is an intramolecular variant of this reaction, whereby a benzylic alcohol (**1.136**) cyclizes onto the aromatic ring, yielding the corresponding epoxide (**1.137**).[77] Acetoxylation of phenolic

compounds occurs readily using stoichiometric amounts of lead tetraacetate, affording the quinol ester (**1.139**).[78] However, dimerization occurs leading to the bridged tricycle **1.140**. A (-)-sparteine copper complex catalyzed the oxidative dearomatization of lithiated phenoxides (**1.141**), providing enantioenriched cyclohexadienones (**1.142**), which readily dimerize (Figure 1.35d).[79] Electrochemical methods also exist (Figure 1.35e).[80-83] However, these protocols often require complex electrolyte mixtures, and can be economically prohibitive due to the reliance on precious metal electrodes. These methods often are not amenable to scale. Other commonly utilized methods include use of palladium and other transition metals[78,84-87], peroxyacids[88], dimethyldioxirane[89], and biocatalysts[90-94]. However, dearomatized adducts generated by these methods are unstable and many react unproductively *via* Diels-Alder dimerization. To minimize the occurrence, bulky and/or electron withdrawing groups are added to deactivate the resulting cyclohexadienone from further reactivity.

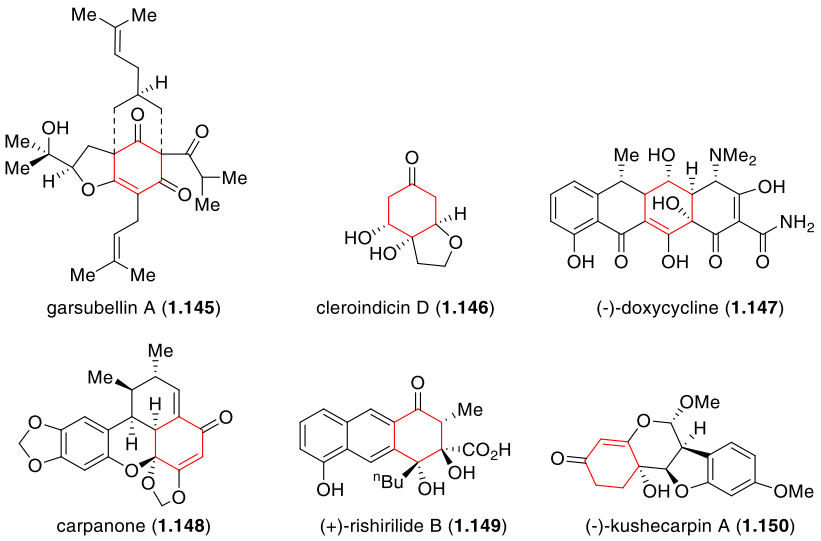

Figure 1.36. Natural products prepared using dearomatization strategies.

Oxidative dearomatization has proven to be an effective tool in chemical synthesis, rapidly converting commercial and easily-prepared arenes into highly functionalized cyclohexadienone derivatives (Figure 1.36).[95,96] This strategy increases structural complexity and aligns well with synthetic targets identified from natural sources or enables the syntheses of chemically diverse compound collections derived from a privileged core. Recently, the Njardarson group utilized hypervalent iodine to perform an oxidative dearomatization followed by Diels-Alder reaction to assemble the core of vinigrol.[97,98] Similarly, Pettus and coworkers utilized oxidative dearomatization in a key step to convert (-)-sophoracarpan A into (±)-kushecarpin A (**1.150**).[99] Dearomatization also enables access to privileged molecular scaffolds, demonstrated by Doyle[100], Tan[101], Hergenrother[102], and Porco[103].

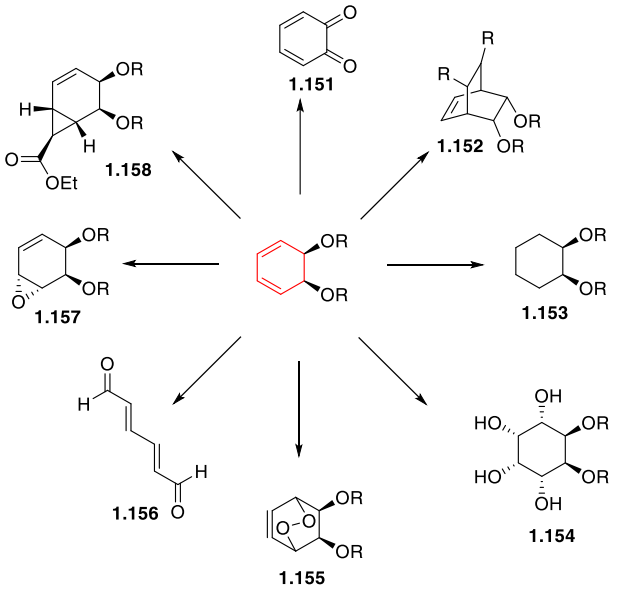

Figure 1.37. Reactivity of dearomatized adducts.

With access to cyclohexadiene derived from dearomatization, the possibility for further functionalization exists (Figure 1.37). Oxidation can occur, leading to quinones (**1.151**).[104] A Diels-Alder reaction accesses topologically complex bridged bicycles

(**1.152**).[105] Cyclohexyl derivatives (**1.153**) are produced *via* exposure of the diene to hydrogen and palladium on carbon.[106] Osmium(VIII) oxide hydroxylation of one or both olefins provides highly oxygenated cyclohexyl adducts (**1.154**).[107] Polar cycloadditions utilizing singlet oxygen gives peroxy compound **1.155**.[108] Alternatively, oxidative cleavage of the activated carbon-carbon bond yields conjugated dialdehyde **1.156**.[109] Treatment with *m*-CPBA provides the corresponding epoxide (**1.157**).[110] Additionally, rhodium-catalyzed cyclopropanation provides a bicycle[4.1]heptane (**1.158**).[111]

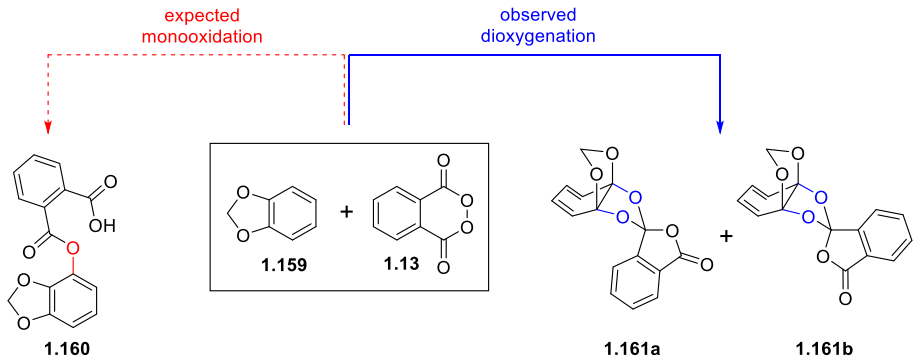

Figure 1.38. New dearomatization reactivity of phthaloyl peroxide (**1.13**).

In contrast to what others have observed previously with phthaloyl peroxide (**1.13**), subjecting 1,3-benzodioxole (**1.159**) to the standard hydroxylation protocol led to the isolation of a mixture of diastereomers of the dearomatized adduct (**1.161a** and **1.161b**). No hydroxylation (**1.160**) was observed. After reaction with phthaloyl peroxide (**1.13**), the ^{1}H-NMR signals of the starting material shift up-field, indicating a loss of aromaticity, and the hydrogens of the methylene become nonequivalent.[112] A stretch present in an IR spectrum of 1780 cm^{-1} is indicative of a lactonic orthoester.[16] Additionally a DEPT experiment confirmed that the methylene was not oxidized. Finally, X-ray structural elucidation confirmed the molecules as the bridged, dearomatized adducts (Figure 1.39, 1.40).

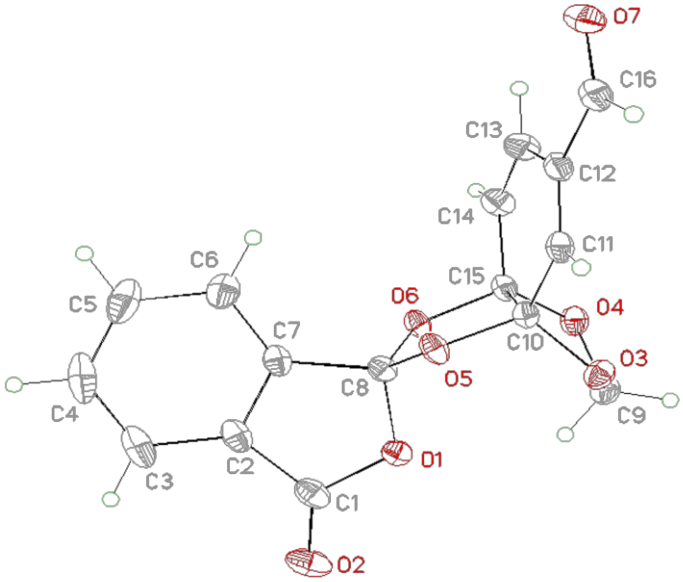

Figure 1.39. Single crystal X-ray of **1.179a**.

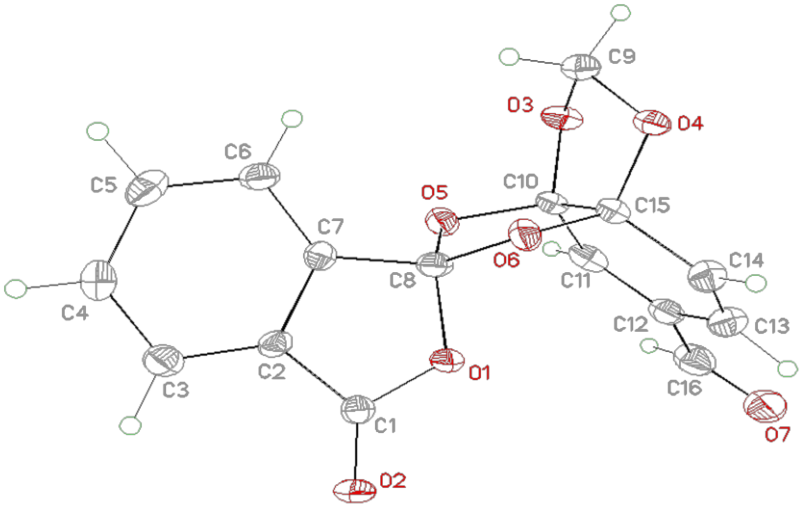

Figure 1.40. Single crystal X-ray of **1.179b**.

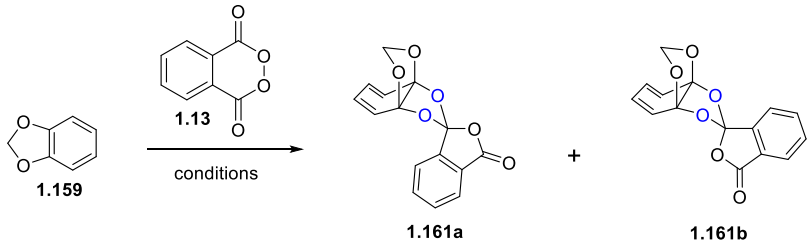

variation	equiv. PPO (**1.13**)	temperature	solvent[a]	yield[b]
-	1.5	23 °C	TFE	74%
1.	1.2	23 °C	TFE	53%
2.	3.0	23 °C	TFE	72%
3.	1.5	0 °C	TFE	37%
4.	1.5	40 °C	TFE	68%
5.	1.5	23 °C	HFIP	58%
6.	1.5	23 °C	EtOH	45%
7.	1.5	23 °C	TFT	17%
8.	1.5	23 °C	CH_2Cl_2	31%

Figure 1.41. Optimization of the dearomatization of benzodioxole using phthaloyl peroxide. [a] Reagent grade solvent. [b] Isolated yield after flash column chromatography.

The effects of varying equivalents of peroxide (**1.13**), temperature and solvent were examined in an effort to optimize the reaction (Figure 1.41). Decreasing the amount of peroxide below the standard conditions used for aryl hydroxylation led to incomplete conversion of benzodioxole (variant 1). However, increasing the amount of peroxide to three equivalents (variant 2) did not positively affect the yields. This experiment was notable, however, as no over-oxidized products were identified in these reactions despite a large excess of peroxide present. Lowering the temperature to 0 °C resulted in incomplete conversion of starting material (variant 3). Warming the reaction to 40 °C (variant 4) did not lead to higher isolated yields of the product. Analogous to that of the hydroxylation reaction, we found the commercial grade fluorinated solvents including trifluoroethanol

(TFE) and hexafluoroisopropanol (HFIP) were superior for arenes possessing electron-withdrawing substituents.[113] For electron rich substrates commercial grade trifluorotoluene (TFT) proved optimal. However, ethanol and methylene chloride also provided the dearomatized adducts with no detectable amounts of aryl hydroxylation.

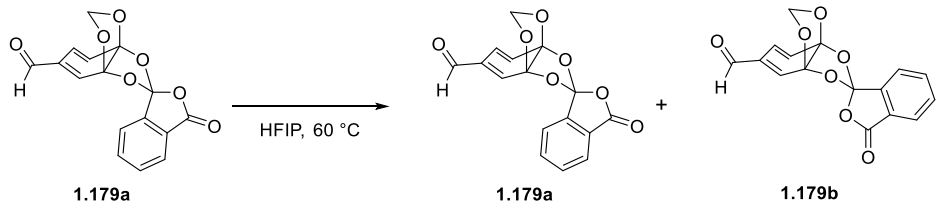

Figure 1.42. Equilibration of piperonal isomers (**1.179a** and **1.179b**).

The dearomatized adducts can be stored at 4 °C for weeks with no decrease in purity. Remarkably, the dearomatized adducts are stable to aqueous workup and silica gel chromatography. The major isomer in every case examined, is where the phthalate ester is *cis* to the methylenedioxy bridge. For most adducts, the major and minor diasteromer can be separated by chromatography. It is worth noting that heating the single isomer compound (**1.179a**) does not lead to the formation of related phenolic products (Figure 1.42). A diastereomeric mixture results due to the benzyloxy-orthoester stereocenter scrambling (**1.179a** and **1.179b**).

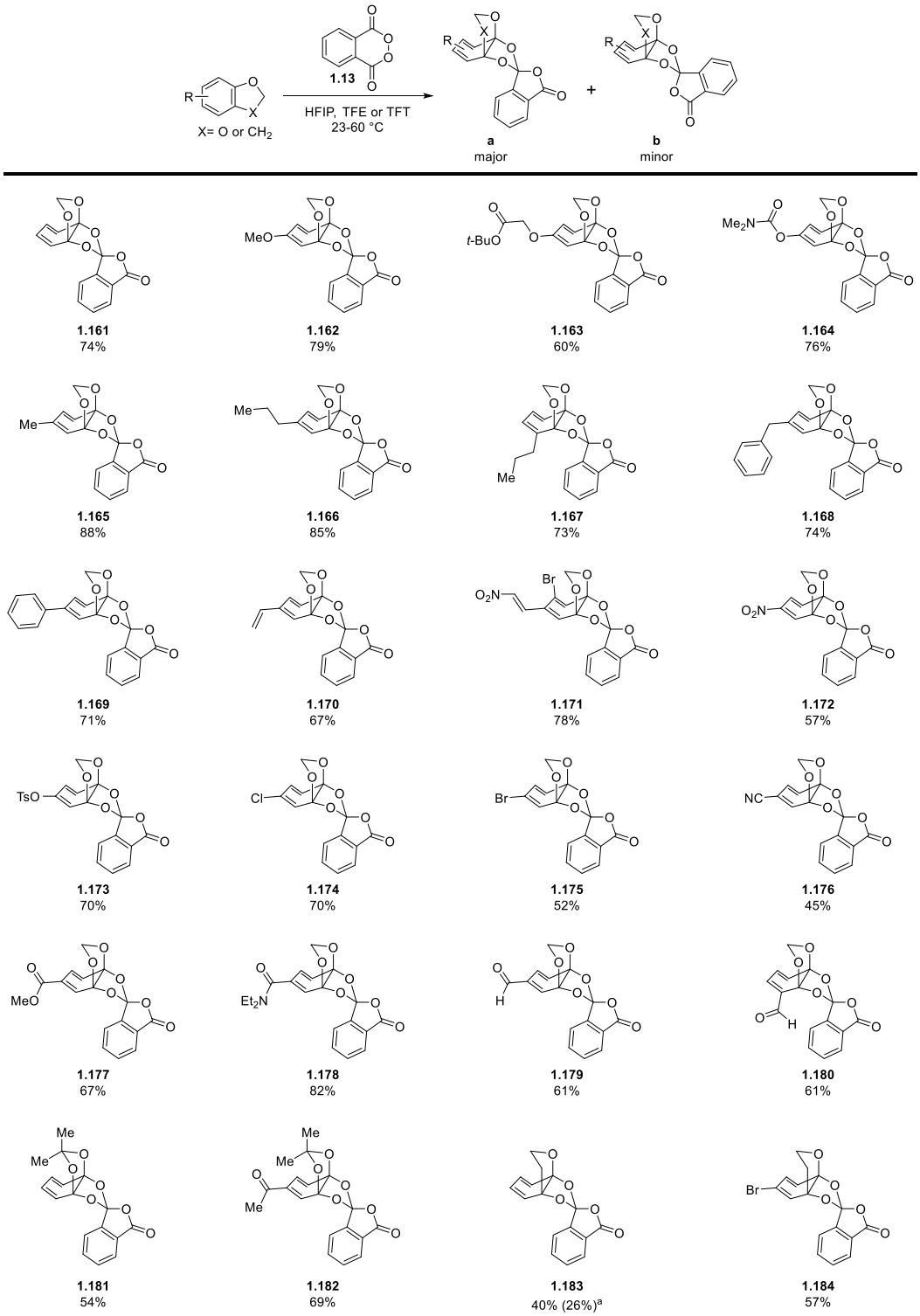

Figure 1.43. Dearomatized adducts. [a] Recovered starting material.

The reaction is chemoselective for the arene, as demonstrated by the wide variety of substituents (including many with oxidatively sensitive functionality) tolerated by the reaction (Figure 1.43). As outlined in Figure 1.41, 1,3-benzodioxole performed well under these conditions, providing a yield of 74% of the dearomatized product (**1.161**). Aryl ethers (**1.162** and **1.163**) readily dearomatize in minutes, however, these reactive substrates necessitated the use of trifluorotoluene, as the fluorinated alcohol solvents hexafluoroispropanol and trifluoroethanol led to unproductive reactions. Arenes possessing a dimethyl carbamate provide the corresponding adduct (**1.164**) in 76% yield. Aliphatic substitution on the arene is tolerated with the methyl derivative giving an 88% yield of cyclohexadiene **1.165**. Interestingly, increasing the steric environment by addition of a propyl group *meta* to the methylenedioxy ring (**1.166**) does not significantly impact the yields (85%) when compared to the smaller methyl group. A propyl group located *ortho* to the methylenedioxy ring (**1.167**) only modestly affects the yield (73%). Appended benzyl (**1.168**) or phenyl (**1.169**) groups were left unreacted, demonstrating the selectivity phthaloyl peroxide (**1.13**) has for electronically rich arenes observed previously for the hydroxylation reaction. Olefinic substitution provides the corresponding vinyl cyclohexadiene (**1.170**) in 67% yield. Neither over-oxidization nor unproductive Diels-Alder reactions were observed for this substrate, demonstrating the stability of these adducts.

For the first time, nitro substitution does not shutdown the reactivity of phthaloyl peroxide (**1.13**). The 1,3-benzodioxole core with a nitro substituent (**1.172**) provided the nitrodiene in 57% yield. If the nitro group is connected through a vinyl spacer, as with the nitro styrene (**1.171**), the yields increased. Tosylated arenes provide good yields (70%) of the corresponding dearomatized adduct **1.173**. Halogenated arenes possessing chlorine (**1.174**) or bromine (**1.175**) reacted well and can be envisioned to provide synthetic handles

for further chemical manipulation. Arenes possessing nitriles furnish the corresponding cyano-diene (**1.176**), albeit in low yield. Esters (**1.177**) and amides (**1.178**) are suitable substrates for this reaction. Other functionality susceptible to oxidation including aldehydes (**1.179**, **1.180**) remained unchanged under the reaction conditions. Interestingly, no loss in yield was observed if the aldehyde was *ortho* to the methylenedioxy ring.

Given that the steric environment associated with substituents *ortho* to the methylenedioxy ring did not drastically impact the yields of the dearomatization reaction, replacing the acetal of methylenedioxy with a dimethyl ketal was investigated. Acetonides (**1.181** and **1.182**) provided lower yields but do not completely preclude oxidative dearomatization. The importance of both oxygen atoms of the methylenedioxy was also explored. It was found that subjecting 2,3-dihydrobenzofuran to the reaction provided the dearomatized product (**1.183**) in 40% yield (with recovery of 26% of starting material) indicating that while lower yields are achieved the system still reacts to provide the oxygenated cyclohexadiene product. The bromo-dihydrobenzofuran (**1.184**) reacted providing a comparable yield to the bromomethylenedioxy derivative.

Two possible mechanisms were envisioned for the phthaloyl peroxide-mediated dearomatization reaction (Figure 1.44). Similar to what had been previously observed for the hydroxylation of arenes, a diradical mechanism is possible (Figure 1.44a). Following homolysis of the oxygen-oxygen bond of phthaloyl peroxide (**1.13**), an initial carbon-oxygen bond would be formed. This would yield a very stable cyclohexadienyl radical (**1.185**). Subsequent carbon-oxygen bond formation would provide the acetal radical (**1.186**). Recombination of the acetal radical with the phthaloyl radical would account for the observed dearomatized products (**1.161**). Alternatively, an ionic mechanism could also be plausible (Figure 1.44b).

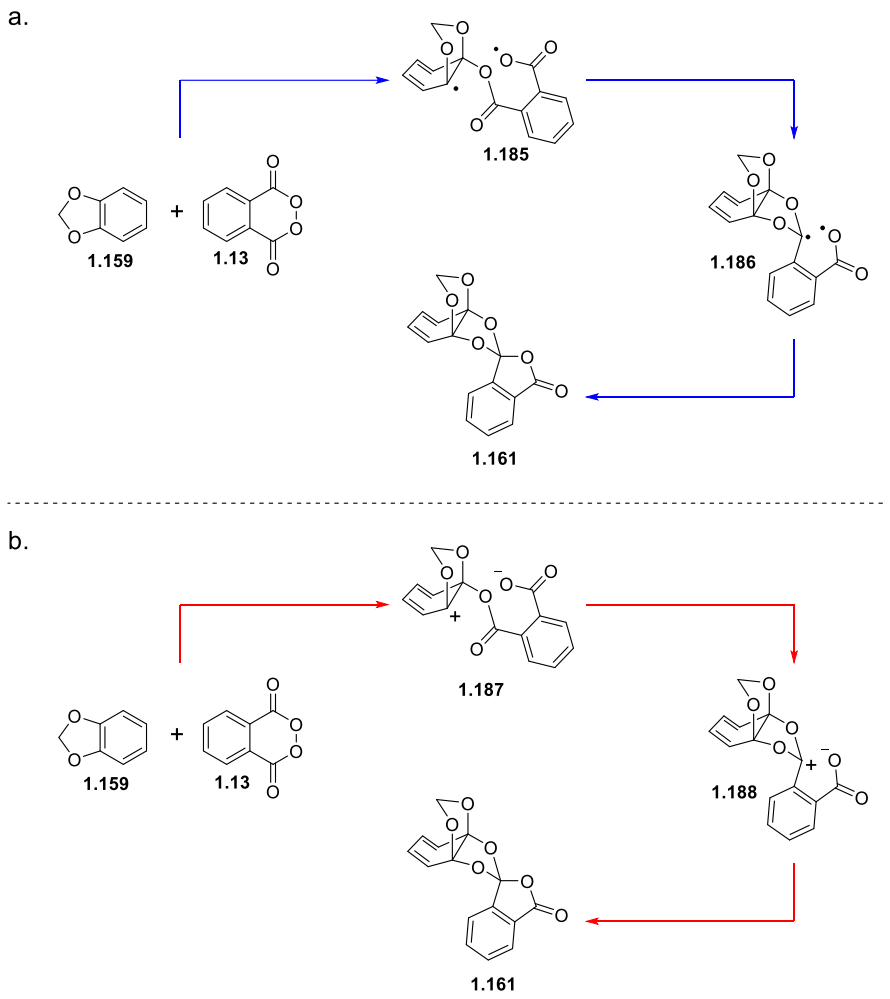

Figure 1.44. Possible mechanisms employing either (a.) radical or (b.) ionic pathway.

Benson group increment theory uses calculated heat of formation for functional groups and other groups of atoms to estimate the heat of formation for a given molecule.[114] When the estimated and experimentally determined values differ, the difference is attributed to the strain energy. Benson group additivity parameters suggest that benzodioxole substrates possess significant Baeyer (angle) strain, calculated to be 17.6 kcal mol^{-1} in the liquid state.[115] Intuitively, this is important for the formation of the first carbon-oxygen bond *ortho* to the radical-stabilizing oxygen, followed by a second carbon-oxygen

bond formation that perpetuates the relief in ring strain. Double *ipso*-addition at the ring junction alleviates this strain through re-hybridization at the carbons from sp^2 to sp^3, providing an energetic driving force for this reaction.

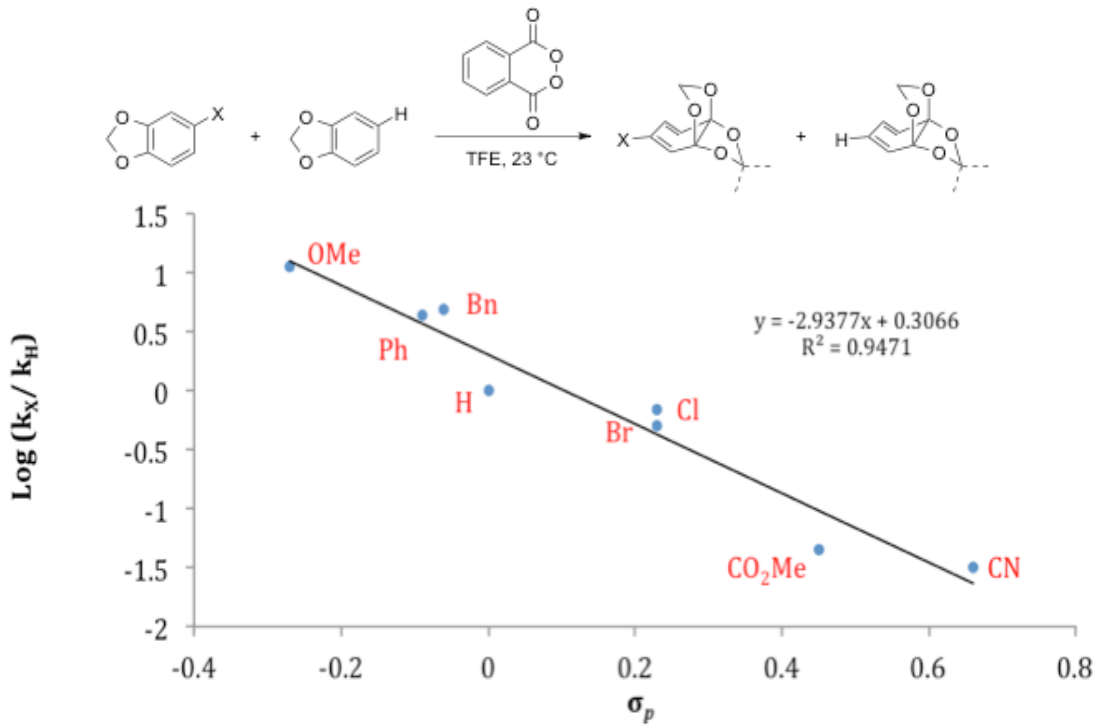

Figure 1.45. Linear free energy diagram.

The broad array of functional groups tolerated by the dearomative oxidation provided an opportunity to investigate the mechanism by Hammett plot analysis (Figure 1.45). The rates of reaction between the unfuctionalized 1,3-benzodioxole and a given substituted derivatives were obtained through direct competition reactions. A fivefold excess of each arene relative to phthaloyl peroxide (**1.13**) were reacted in TFE at 23 °C. The ratio of adducts formed was determined by crude reaction NMR analysis, providing k_X / k_H. Using σ_p or σ_p^+, a variety of Hammett plots were constructed. For the dearomatization reaction examined, σ_p values (R^2 = 0.95) provided a stronger correlation

than σ_p^+ ($R^2 = 0.91$). This is a notable departure from electrophilic aromatic substitution reactions (EAS), which tend to correlate better with σ_p^+.[116] Applying a linear regression algorithm provides a correlation (ρ) of the linear free energy and an insight into the reaction mechanism. With a ρ value of –2.94, the reaction is mildly influenced by the stabilization of polar intermediates but is not predicted to be ionic as reactions such as electrophilic aromatic substitution (EAS) possess larger negative ρ values.[117] The ρ value supports a diradical-based intermediate in the rate-determining step analogous to what was found computationally for the phthaloyl peroxide-mediated arene hydroxylation reaction.[23] Thus, a mechanistic pathway that is in agreement with this mechanism is depicted in Figure 1.44a.

4,5-DICHLOROPHTHALOYL PEROXIDE EXPERIMENTAL SECTION

Organic solutions were concentrated by rotary evaporation at ~ 20 torr. Phthaloyl peroxide was prepared as reported previously.[18] All other reagents and solvents were used directly from the supplier without further purification. Analytical thin-layer chromatography (TLC) was carried out using 0.2 mm commercial silica gel plates (silica gel 60, F254, EMD chemical) and visualized using a UV lamp. TLC plates were stained using ceric ammonium molybdate (CAM), aqueous potassium permanganate ($KMnO_4$) or iodine. Infrared spectra were recorded on a Nicolet 380 FTIR using neat thin film technique. High-resolution mass spectra (HRMS) were recorded on a Karatos MS9 and are reported as m/z (relative intensity). Accurate masses are reported for the molecular ion $[M+Na]^+$, [M+H], $[M^+]$, or [M-H]. Nuclear magnetic resonance spectra (^{1}H-NMR and ^{13}C-NMR) were recorded with a Varian Mercury 400 (400 MHz, ^{1}H at 400 MHz, ^{13}C at 100 MHz), Agilent MR 400 (400 MHz, ^{1}H at 400 MHz, ^{13}C at 100 MHz), Varian DirectDrive 400 (400 MHz, ^{1}H at 400 MHz, ^{13}C at 100 MHz), or Varian DirectDrive 600 (600 MHz, ^{1}H at 600 MHz, ^{13}C at 150 MHz). For $CDCl_3$ solutions the chemical shifts are reported as parts per million (ppm) referenced to residual protium or carbon of the solvent: δ H (7.26 ppm) and δ C (77.0 ppm). Coupling constants are reported in Hertz (Hz). Data for ^{1}H-NMR spectra are reported as follows: chemical shift (ppm, referenced to protium; s = singlet, d = doublet, t = triplet, q = quartet, p = pentet, sext = sextet, sept = septuplet, dd = doublet of doublets, td = triplet of doublets, ddd = doublet of doublet of doublets, m = multiplet, coupling constant (Hz), and integration). Melting points were measured on a MEL-TEMP device without corrections.

Safety Information

All peroxides can be dangerous when not handled correctly. The following procedures should be carried out by knowledgeable laboratory practitioners of organic synthesis. While we have not had a reaction using 4,5-dichlorophthaloyl peroxide detonate we still recommend that all reactions should be conducted with appropriate shielding as a precaution. Thermogravimetric analysis (TGA) data showed that 4,5-dichlorophthaloyl peroxide is stable below 115 ºC, however, there is a rapid loss in mass at ~135 °C indicating a potential for exothermic decomposition.

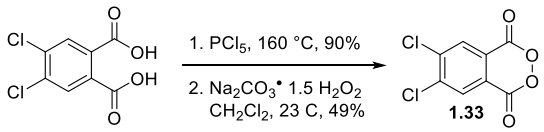

Solid 4,5-dichlorophthalic acid (50.0 g, 213 mmol, 1.0 equiv.) and solid phosphorus pentachloride (89.0 g, 427 mmol, 2.0 equiv.) were added to a flame-dried reaction vessel equipped with a stir bar. The reaction vessel was placed under a continuous flow of nitrogen and equipped with an out port leading to a saturated aqueous $NaHCO_3$ mixture. The solid mixture was then placed in an oil bath heated to 160 °C and stirred vigorously (600 rpm). **Caution: HCl Gas Evolution.** After 14 hours the reaction vessel was equipped with a fractional distillation apparatus and the dark grey-black liquid was purified by fractional distillation. The first fraction recovered (B.P. = <170 °C, 1 atm) is residual phosphorous byproducts, and was discarded. After no more distillate is collected, the distillation apparatus was placed under vacuum, and the dichloride (55.1 g, 192 mmol, 90%, >95% pure by NMR) was distilled (B.P. = 150-160 °C, 0.001 atm) as a clear colorless oil which solidified upon cooling to 23 °C.

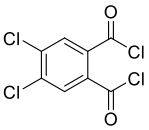

white solid, M.P. = 34 °C; **B.P.** = 155 – 160 °C (0.001 atm). **^{1}H-NMR** (400 MHz, $CDCl_3$) δ 7.98 (s, 2H).

A mixture of solid 4,5-dichlorophthaloyl chloride (25.5 g, 94 mmol, 1.0 equiv.) and sodium percabonate (16.2 g, 103 mmol, 1.1 equiv.) were diluted with non-purified methylene chloride (0.2 M, 469 mL). The white heterogeneous mixture was then placed under an atmosphere of N_2 and stirred vigorously (1000 rpm). After 24 hours the mixture was filtered over a pad of celite and carefully concentrated by rotary evaporation (water bath set to 23 °C) to reveal a pale yellow solid. This solid was dissolved in benzene (110 mL) and then pentane (220 mL) was slowly added to the stirring solution causing a slow

precipitation of a white solid. The mixture was placed in a cooling bath (0 °C) for 1 hour and then filtered cold to reveal the peroxide **1.33** as a white snow-flake solid (9.3 g, 40 mmol, 43%, 86% pure). A second precipitation of the filtrate solution after concentration provided peroxide **1.33** (2.7 g, 12 mmol, 13%, 86% pure). Concentration of the filtrate solution after the second crop provided the starting 4,5-dichlorophthaloyl dichloride (5.7 g, 21 mmol, 22%). The spectra of **1.33** matches that for 4,5-dichlorophthaloyl peroxide.

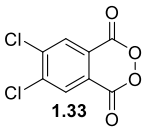

white solid; ^{1}H-NMR (400 MHz, $CDCl_3$) δ 8.34 (s, 2H); **^{13}C-NMR** (100 MHz, $CDCl_3$): δ 160.4, 142.4, 131.8, 122.6; **IR** (neat film, cm^{-1}) 1748, 906 cm^{-1}.

General Procedure A:

To flame-dried borosilicate flask equipped with a magnetic stir bar was added the corresponding arene as a solid or neat followed by the syringe addition of HFIP to provide a clear homogeneous solution with a substrate concentration of 0.1 M. In some cases, when noted, $CHCl_3$ was added to aid homogeneity. Solid 4,5-dichlorophthaloyl peroxide (**1.33**) was then added in one portion. After stirring at a rate of 500 rpm at 23 °C for 1 minute to provide full dissolution of the peroxide, the reaction vessel was capped with a polyethylene stopper, clamped, placed in an oil bath heated to 50 °C, and stirred at a rate of 500 rpm. After 24 or 48 hours the reaction was removed from the oil bath and allowed to cool to 23 °C, the stopper was removed carefully, and the HFIP was evaporated by a continuous flow of N_2 to reveal a yellow, orange, or deep red solid mixture. The crude solid mixture was then placed under an atmosphere of N_2, and a de-oxygenated mixture of MeOH / saturated aqueous $NaHCO_3$ (9: 1) was added by syringe under N_2 to provide an overall reaction

concentration of 0.1 M. The heterogeneous mixture was then placed in an oil bath heated to 50 °C and stirred at a rate of 500 rpm. After 1 hour the methanol was removed by a continuous flow of N_2, and to the mixture was added Et_2O or ethyl acetate (10 mL) and an aqueous phosphate buffer (10 mL, 0.2 M, pH = 7). The mixture was vigorously stirred (800 rpm) at 23 °C for 2 minutes to provide a biphasic solution; which was poured into a separatory funnel and partitioned. The organic layer was washed with an aqueous phosphate buffer (4 x 30 mL, 0.2 M, pH = 7) or with the combination of an aqueous saturated mixture of $NaHCO_3$ and brine (3 x 30 mL). The residual organics were back extracted with Et_2O (3 x 25 mL) or ethyl acetate (3 x 25 mL), dried over Sodium sulfate, filtered, and concentrated carefully. The crude material was then purified by silica gel chromatography using the noted solvent mixture to provide the phenolic products.

General Procedure B:

To a flame-dried borosilicate flask equipped with a magnetic stir bar was added the corresponding arene as a solid or neat followed by the syringe addition of HFIP to provide a clear homogeneous solution with a substrate concentration of 0.1 M. In some cases, when noted, $CHCl_3$ was added to aid homogeneity. Solid 4,5-dichlorophthaloyl peroxide (**1.33**) was then added in one portion. After stirring at a rate of 500 rpm at 23 °C for 1 minute to provide full dissolution of the peroxide, the reaction vessel was capped with a polyethylene stopper, clamped, placed in an oil bath heated to 75 °C, and stirred at a rate of 500 rpm. After 36 or 48 hours the reaction was removed from the oil bath and allowed to cool to 23 °C, the stopper was removed carefully, and the HFIP was evaporated by a continuous flow of N_2 to reveal a yellow, orange, or deep red solid mixture. The crude solid mixture was then placed under an atmosphere of N_2, and a de-oxygenated mixture of MeOH / saturated

aqueous $NaHCO_3$ (9: 1) was added by syringe under N_2 to provide an overall reaction concentration of 0.1 M. The heterogeneous mixture was then placed in an oil bath heated to 50 °C and stirred at a rate of 500 rpm. After 1 hour the methanol was removed by a continuous flow of N_2, and to the mixture was added Et_2O or ethyl acetate (10 mL) and an aqueous phosphate buffer (10 mL, 0.2 M, pH = 7). The mixture was vigorously stirred (800 rpm) at 23 °C for 2 minutes to provide a biphasic solution; which was poured into a separatory funnel and partitioned. The organic layer was washed with an aqueous phosphate buffer (4 x 30 mL, 0.2 M, pH = 7) or with the combination of an aqueous saturated mixture of $NaHCO_3$ and brine (3 x 30 mL). The residual organics were back extracted with Et_2O (3 x 25 mL) or ethyl acetate (3 x 25 mL), dried over sodium sulfate, filtered, and concentrated carefully. The crude material was then purified by silica gel chromatography using the noted solvent mixture to provide the phenolic products.

General Procedure C:

To flame-dried borosilicate flask equipped with a magnetic stir bar was added the corresponding arene as a solid or neat followed by the syringe addition of HFIP to provide a clear homogeneous solution with a substrate concentration of 0.1 M. In some cases, when noted, $CHCl_3$ was added to aid homogeneity. Solid 4,5-dichlorophthaloyl peroxide (**1.33**) was then added in one portion. After stirring at a rate of 500 rpm at 23 °C for 1 minute to provide full dissolution of the peroxide, the reaction vessel was capped with a polyethylene stopper, clamped, placed in an oil bath heated to 75 °C, and stirred at a rate of 500 rpm. After 36 hours the reaction was removed from the oil bath and allowed to cool to 23 °C, the stopper was removed carefully, and the HFIP was evaporated to dryness by a continuous flow of N_2 to reveal a yellow solid mixture. The crude mixture was then

dissolved in a methanol: benzene (2:7) solution providing an overall substrate concentration of 0.1 M and the now clear yellow homogeneous solution was stirred at a rate of 500 rpm. $TMSCHN_2$ (5.0 equiv., 0.2 M in Et_2O) was added in a slow dropwise fashion over 1 minute. **Caution: Rapid N_2 gas evolution**. After 30 minutes the now deep yellow – orange solution was evaporated by a continuous flow of N_2 to provide a yellow – orange gum; which was purified by silica gel chromatography using the noted solvent mixture to provide the mixed phthalate ester products.

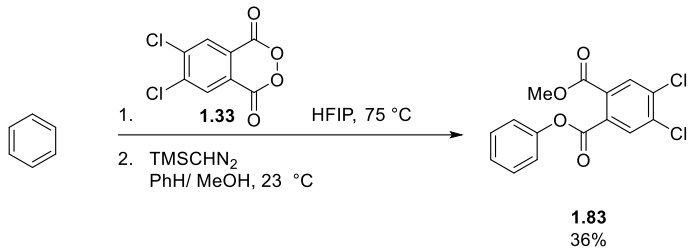

Prepared following General Procedure C using benzene (10.0 mg, 0.13 mmol, 1.0 equiv.), 4,5-dichlorophthaloyl peroxide (87.0 mg, 0.32 mmol, 2.5 equiv., (using material of 86% peroxide and 14% 4,5-dichlorophthalic anhydride)), HFIP (1.3 mL), and $TMSCHN_2$ (0.32 mL, 0.64 mmol, 5.0 equiv., 2.0 M). The crude yellow viscous oil was purified by silica gel chromatography; benzene to provide the phthalate ester **1.83** (15.1 mg, 0.05 mmol 36%) as a clear viscous oil.

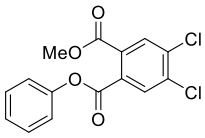

1.83

colorless oil; ^{1}H-NMR (400 MHz, $CDCl_3$) δ 7.97 (s, 1H), 7.91 (s, 1H), 7.44 (t, *J* = 7.9 Hz, 2H), 7.29 (t, *J* = 7.9, 1H), 7.25 (d, *J* = 7.2, 2H), 3.93 (s, 3H); **^{13}C-NMR** (100MHz, $CDCl_3$) δ 165.9, 164.5, 150.8, 136.4, 136.4, 131.5, 131.5, 131.4, 129.9, 128.6, 126.6, 121.5, 53.4; **IR** (neat film, cm^{-1}) 2955, 1733, 1436, 1288, 1069; **HRMS** (CI) calcd. for $C_{15}H_{10}O_4Cl_2$ $[M+H]^+$ 325.0034, obs. 325.0028.

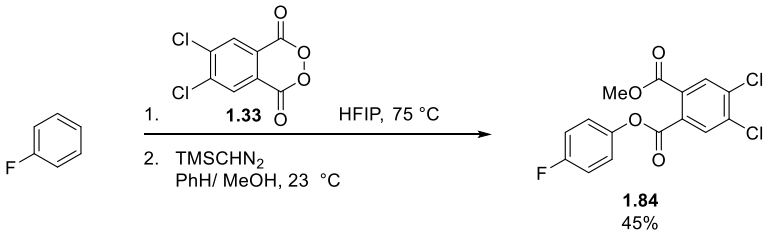

Prepared following General Procedure C using fluorobenzene (10.0 mg, 0.10 mmol, 1.0 equiv.), 4,5-dichlorophthaloyl peroxide (69.0 mg, 0.26 mmol, 2.5 equiv., (using material

of 88% peroxide and 12% 4,5-dichlorophthalic anhydride)), HFIP (1.0 mL), and $TMSCHN_2$ (0.26 ml, 0.52 mmol, 5.0 equiv., 2.0 M). The crude yellow viscous oil was purified by silica gel chromatography; benzene to provide the phthalate ester **1.84** (16.0 mg, 45%)

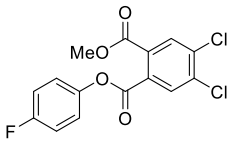

1.84

white solid, M.P. = 96 – 99 °C; $\mathbf{R_f}$ = 0.63 (silica gel, benzene);**^{1}H-NMR** (400 MHz, $CDCl_3$) δ 7.94 (s, 1H), 7.93 (s, 1H), 7.24 – 7.21 (m, 2H), 7.12 (dd, J = 8.2, 8.9, 2H), 3.93 (s, 3H); **^{13}C-NMR** (100 MHz, $CDCl_3$) δ 165.8, 164.6, 160.8 (d, J_{CF} = 245.22 Hz), 146.6, 136.5, 136.5, 131.5, 131.4, 131.3, 131.3, 123.0, 116.2, 53.4; IR (neat film, cm^{-1}) 2924, 2356, 1733, 1503, 1291, 1116; **HRMS** (ESI) calcd. for $C_{15}H_9O_4Cl_2F$ $[M+H]^+$ 342.9940, obs. 342.9934.

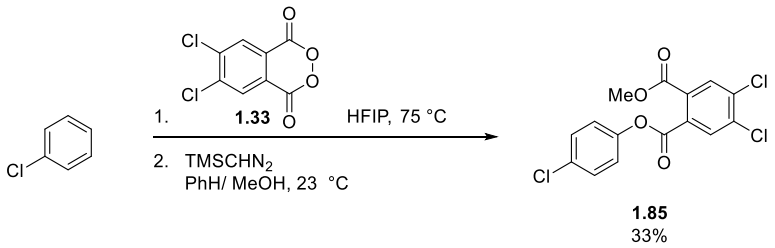

1.85
33%

Prepared following <u>General Procedure C</u> using chlorobenzene (10 mg, 0.09 mmol, 1.0 equiv.), 4,5-dichlorophthaloyl peroxide (60 mg, 0.22 mmol, 2.5 equiv., (using material of 86% and 14% 4,5-dichlorophthalic anhydride)), HFIP (0.9 mL), and $TMSCHN_2$ (0.22 mL, 0.44 mmol, 5.0 equiv., 2.0 M). The crude yellow viscous oil was purified by silica gel chromatography; benzene to provide the phthalate ester **1.85** (10.3 mg, 32%).

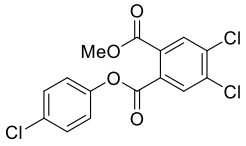

1.85

colorless oil; $\mathbf{R_f}$ = 0.69 (silica gel, benzene); **^{1}H-NMR** (400 MHz, $CDCl_3$) δ 7.93 (s, 2H), 7.40 (d, *J* = 8.9 Hz, 2H), 7.21 (d, *J* = 8.6 Hz, 2H), 3.92 (s, 3H); **^{13}C-NMR** (100 MHz, $CDCl_3$) δ 165.5, 164.2, 149.0, 136.3, 136.3, 131.8, 131.3, 131.1, 131.0, 131.0, 129.7, 122.7, 53.2; **IR** (neat film, cm^{-1}) 2955, 2924, 1733, 1503, 1487, 1288; **HRMS** (ESI) calcd. for $C_{15}H_9O_4Cl_3$ $[M+H]^+$ 358.9645, obs. 358.9636.

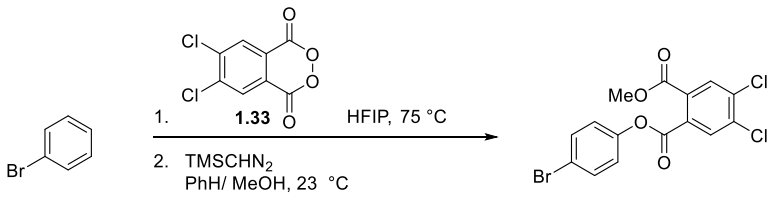

1.86
13%

Prepared following <u>General Procedure C</u> using bromobenzene (10 mg, 0.06 mmol, 1.0 equiv.), 4,5-dichlorophthaloyl peroxide (43 mg, 0.16 mmol, 2.5 equiv., (using material of 86% peroxide and 14% 4,5-dichlorophthalic anhydride)), HFIP (0.6 mL), and $TMSCHN_2$ (0.16 ml, 0.32 mmol, 5.0 equiv., 2.0 M). The crude yellow viscous oil was purified by silica gel chromatography; hexanes – 3% ethyl acetate in hexanes to provide the phthalate **1.86** (3.2 mg, 0.01 mmol, 13%).

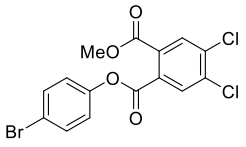

1.86

colorless oil; $\mathbf{R_f}$ = 0.40 (silica gel, 10% ethyl acetate in hexanes); **^{1}H-NMR** (400 MHz, $CDCl_3$) δ 7.93 (s, 2H), 7.55 (d, *J* = 8.9 Hz, 2H), 7.15 (d, *J* = 8.6 Hz, 2H), 3.92 (s, 3H); **^{13}CNMR** (100 MHz, $CDCl_3$) δ 165.5, 164.0, 149.6, 136.3, 132.7, 131.3, 131.1, 131.0, 131.0, 123.1, 119.5, 53.2; **IR** (neat film, cm^{-1}) 2952, 1731, 1513, 1286; **HRMS** (ESI) calcd. for $C_{15}H_9O_4Cl_2Br$ $[M+Na]^+$ 426.8931, obs. 426.8923.

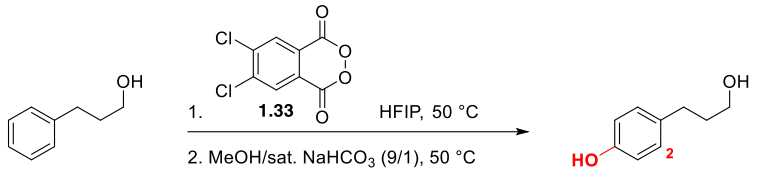

1.87

Prepared following General Procedure A using hydrocinnamyl alcohol (100 mg, 0.73 mmol, 1.0 equiv.), 4,5-dichlorophthaloyl peroxide (256 mg, 0.96 mmol, 1.3 equiv., 86%), and HFIP (7.3 mL) at 50 °C for 48 hours. The crude brown gum was purified by silica gel chromatography; 2 – 30% Et_2O in methylene chloride: hexanes (1: 1) to provide the title compounds **1.87** (56.0 mg, 0.37 mmol, 50%, 1**.87a**: **1.87b** = 2: 1) as an orange gum and the starting alcohol (39.2 mg, 0.29 mmol, 39%) as a clear colorless oil. The spectra of the title compounds match that for **1.87a** and **1.87b**.[118]

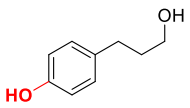

1.87a

orange gum; ^{1}H-NMR (400 MHz, $CDCl_3$) δ 7.07 (d, J = 8.6 Hz, 1H), 6.76 (d, J = 8.6 Hz, 1H), 3.67 (t, J = 6.50 Hz, 2H), 2.64 (t, J = 7.86 Hz, 2H), 1.92 – 1.82 (m, 2H).[118]

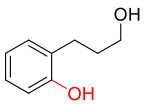

1.87b

orange gum; ^{1}H-NMR (400 MHz, $CDCl_3$) δ 7.10 (d, J = 7.52 Hz, 2H), 6.88 (d, J = 7.52 Hz, 1H), 6.85 (d, J = 7.52 Hz, 1H), 3.66 (t, J = 5.81 Hz, 2H), 2.78 (dd, J = 6.50, 7.18 Hz, 2H), 1.92 – 1.82 (m, 2H).[119]

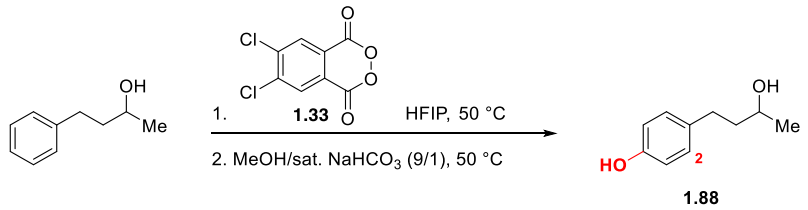

Prepared following General Procedure A using methyl hydrocinnamyl alcohol (100 mg, 0.67 mmol, 1.0 equiv.), 4,5-dichlorophthaloyl peroxide (232 mg, 0.96 mmol, 1.3 equiv., 87%), and HFIP (6.7 mL) at 50 °C for 48 hours. The crude brown gum was purified by silica gel chromatography; 2 – 30% Et_2O in methylene chloride: hexanes (1: 1) to provide the title compounds **1.88** (59.0 mg, 0.36 mmol, 53%, **1.88a: 1.88b** = 1.4: 1) as an orange gum and the starting alcohol (24.0 mg, 0.16 mmol, 24%).

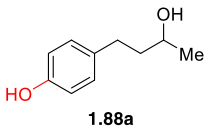

orange gum; ^{1}H-NMR (400 MHz, $CDCl_3$) δ 7.07 (d, J = 8.55 Hz, 1H), 6.75 (d, J = 8.55 Hz, 1H), 3.82 (sext, J = 6.50 Hz, 1H), 2.72 – 2.57 (m, 2H), 1.22 (d, J = 6.1 Hz, 3H).[120]

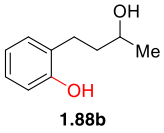

orange gum; ^{1}H-NMR (400 MHz, $CDCl_3$) δ 7.09 (m, 2H), 6.88 (m, 2H), 3.76 (sex, J = 6.84 Hz, 1H), 2.89 (m, 1H), 2.72 – 2.57 (m, 1H), 1.22 (d, J = 6.14 Hz, 3H).[121]

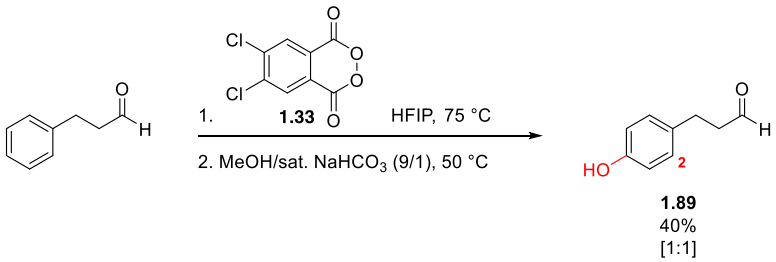

Prepared following General Procedure B using the hydrocinnamyl aldehyde (100 mg, 0.71 mmol, 1.0 equiv., 95% pure), 4,5-dichlorophthaloyl peroxide (480.0 mg, 1.8 mmol, 2.50

equiv., 86%), and HFIP (7.1 mL) at 75 °C for 36 hours. The crude brown gum was purified by silica gel chromatography; 1 – 5% Et_2O in methylene chloride: hexanes (1: 1) to provide the aldehyde **1.89a** (21.0 mg, 0.14 mmol, 20%) and the **1.89b** (21.0 mg, 0.14 mmol, 20%) as yellow gums.

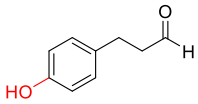

1.89a

yellow gum; ^{1}H-NMR (400 MHz, $CDCl_3$) δ 9.81 (t, *J* = 1.71 Hz, 1H), 7.06 (d, *J* = 8.55 Hz, 2H), 6.76 (d, *J* = 8.55 Hz, 2H), 4.59 (bs, 1H), 2.89 (t, *J* = 7.52 Hz, 2H), 2.74 (dd, *J* = 6.84, 7.87 Hz, 2H).[122]

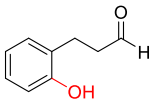

1.89b

yellow gum; ^{1}H-NMR (400 MHz, $CDCl_3$) δ 7.12 (t, *J* = 7.86, 1H), 7.07 (d, *J* = 7.18 Hz, 1H), 6.89 (t, *J* = 7.52 Hz, 1H), 6.82 (d, *J* = 7.87 Hz, 1H), 5.62 (m, 1H), 3.03 (bs, 1H,), 2.99 (m, 1H), 2.71 (dt, *J* = 5.13, 5.47 Hz, 1H), 2.06 – 1.99 (m, 2H).[123]

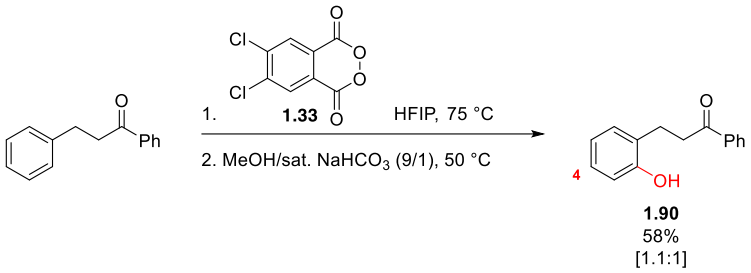

Prepared following General Procedure B using the hydrocinnamyl aryl ketone (100 mg, 0.48 mmol, 1.0 equiv.), 4,5-dichlorophthaloyl peroxide (322 mg, 1.19 mmol, 2.5 equiv., 86%), and HFIP (4.8 mL) at 75 °C for 36 hours. The crude brown gum was purified by silica gel chromatography; 1 – 10% Et_2O in methylene chloride: hexanes (1: 1) to provide **1.90a** (32.3 mg, 0.14 mmol, 30%) and **1.90b** (30.0 mg, 0.13 mmol, 28%) as orange gums.

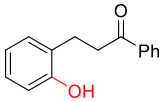

1.90a

orange gum; **^{1}H-NMR** (400 MHz, $CDCl_3$) δ 7.98 (d, *J* = 7.19 Hz, 2H), 7.88 (bs, 1H), 7.58 (t, *J* = 7.18 Hz, 1H), 7.45 (t, *J* = 7.52 Hz, 2H), 7.11 (dd, *J* = 7.18, 7.52 Hz, 2H), 6.91 (d, *J* = 7.87 Hz, 1H), 6.85 (t, *J* = 7.53 Hz, 1H), 3.46 (dd, *J* = 5.81, 6.15 Hz, 2H), 3.04 (dd, *J* = 5.81, 6.15 Hz, 2H).[124]

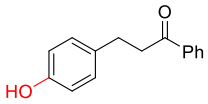

1.90b

orange gum; ^{1}H-NMR (400 MHz, $CDCl_3$) δ 7.95 (d, *J* = 6.83 Hz, 2H), 7.56 (t, *J* = 7.18 Hz, 1H), 7.45 (t, *J* = 7.52 Hz, 2H), 7.12 (d, *J* = 8.55 Hz, 2H), 6.77 (d, *J* = 8.55 Hz, 2H), 4.58 (bs, 1H), 3.26 (t, *J* = 7.68 Hz, 2H), 3.00 (dd, *J* = 7.86 Hz, 2H). [125]

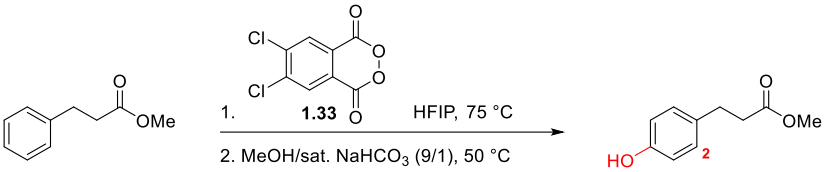

Prepared following General Procedure B using the hydrocinnamyl methyl ester (100 mg, 0.61 mmol, 1.0 equiv.), 4,5-dichlorophthaloyl peroxide (399 mg, 1.52 mmol, 2.5 equiv., 89%), and HFIP (6.1 mL) at 75 °C for 36 hours. The crude brown gum was purified by silica gel chromatography; 1 – 5% Et_2O in methylene chloride: hexanes (1: 1) to provide the esters **191** (81.3 mg, 0.55 mmol, 74%, **191a**: **191b =** 1.4: 1) as a pale yellow gum and the starting ester (5.1 mg, 0.03 mmol, 5%) as a clear colorless oil.

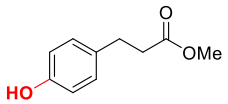

1.91a

yellow gum; ^{1}H-NMR (400 MHz, $CDCl_3$) δ 7.26 (bs, 1H), 7.06 (d, *J* = 8.55 Hz, 2H), 6.88 (d, *J* = 7.9 Hz, 2H), 3.69 (s, 3H), 2.91 (t, *J* = 6.84 Hz, 2H), 2.73 (dd, *J* = 6.15, 6.84 Hz, 2H).[126]

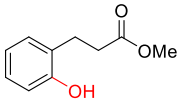

1.91b

yellow gum; ^{1}H-NMR (400 MHz, $CDCl_3$) δ 7.11 (m, 2H), 6.75 (d, J = 8.55 Hz, 2H), 3.66 (s, 3H), 2.88 (t, J = 7.9 Hz, 2H), 2.59 (t, J = 6.86 Hz, 2H).[127]

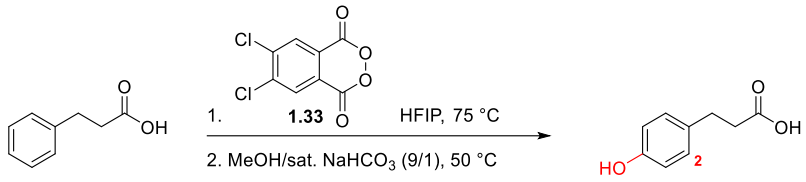

192
65%
[1:1]

Prepared following General Procedure B using hydrocinnamic acid (100 mg, 0.67 mmol, 1.0 equiv.), 4,5-dichlorophthaloyl peroxide (451.0 mg, 1.67 mmol, 2.5 equiv., 86%), $CHCl_3$ (1.7 mL), and HFIP (5.0 mL) at 75 °C for 48 hours. After removal of the HFIP and $CHCl_3$ by continuous positive flow of nitrogen, the mixed phthalate diacid was placed under an atmosphere of N_2, suspended in 1,4-dioxane (6.0 mL) added via syringe, and then a saturated aqueous mixture of $NaHCO_3$ (0.66 mL) was added via a syringe. The red-orange suspension was placed in an oil bath heated to 50 °C and stirred vigorously (700 rpm). After 1 hour the red solution was removed from the oil bath, acidified to a pH = 2 using 1 N HCl (3 mL), then diluted with ethyl acetate (20 mL), poured into a separatory funnel containing brine (20 mL), and the layers were partitioned. The organics were washed with an aqueous phosphate buffer (2 x 20 mL, 0.2 M, pH = 4) and the residual organics were extracted from the aqueous layer with a mixture of brine and ethyl acetate (4 x 30 mL). The combined organics were dried over sodium sulfate, filtered, and concentrated to reveal an orange solid. The orange solid was suspended in methylene chloride (30 mL), heated for 5 minutes, and sonicated for 1 minute. The residual orange mixture was filtered to remove the insoluble white solid 4,5-dichlorophthalic acid. The

orange filtrate solution was concentrated to reveal an orange solid which was purified by silica gel chromatography; 1% CH_3OH and 1% AcOH in methylene chloride to provide the acids **1.92** (71.8 mg, 0.43 mmol, 65%, **1.92a** : **1.92b =** 1 : 1) as an orange solid mixture and the starting acid (12.0 mg, 0.08 mmol, 12%) as a white solid.

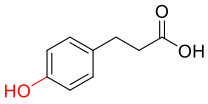

1.92a

orange solid; **^{1}H-NMR** (400 MHz, $CDCl_3$) δ 7.08 (d, *J* = 8.55 Hz, 2H), 6.76 (d, *J* = 8.21 Hz, 2H), 2.90 (t, *J* = 8.21 Hz, 2 H), 2.65 (t, *J* = 7.52 Hz, 2 H).[128]

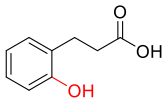

1.92b

orange solid; ^{1}H-NMR (400 MHz, $CDCl_3$) δ 7.11 (d, *J* = 8.55 Hz, 2H), 6.82 – 6.89 (m, 2H), 2.92 (t, *J* = 6.50 Hz, 2 H), 2.78 (t, *J* = 6.50 Hz, 2 H).[129]

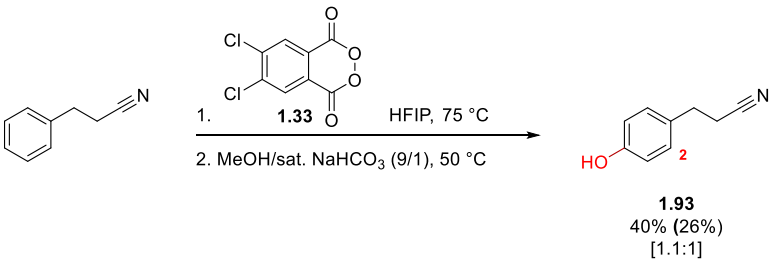

Prepared following <u>General Procedure B</u> using hydrocinnamyl nitrile (100 mg, 0.76 mmol, 1.0 equiv.), 4,5-dichlorophthaloyl peroxide (516.0 mg, 1.91 mmol, 2.5 equiv., 86%), and HFIP (7.6 mL) at 75 °C for 36 hours. The crude brown gum was purified by silica gel chromatography; 1 – 10% Et_2O in methylene chloride: hexanes (1: 1) to provide the nitriles **1.93a** (23.1 mg, 0.16 mmol, 21%) and **1.93b** (21.0 mg, 0.14 mmol, 19%) as pale yellow gums and the starting nitrile (25.8 mg, 0.20 mmol, 26%) as a clear colorless oil.

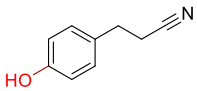

1.93a

yellow gum; **^{1}H-NMR** (400 MHz, $CDCl_3$) δ 7.11 (d, *J* = 8.55 Hz, 2H), 6.80 (d, *J* = 8.55 Hz, 2H), 4.67 (bs, 1H), 2.89 (t, *J* = 7.18 Hz, 2H), 2.58 (t, *J* = 7.52 Hz, 2H).[130]

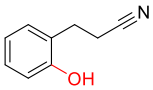

1.93b

yellow gum; **^{1}H-NMR** (400 MHz, $CDCl_3$) δ 7.17 (dd, *J* = 1.37, 7.18 Hz, 1H), 7.13 (dd, *J* = 1.71, 7.86 Hz, 1H), 6.91 (dt, *J* = 1.37, 7.18 Hz, 1H), 6.73 (d, *J* = 7.87 Hz, 1H), 4.85 (bs, 1H), 2.98 (t, *J* = 7.52 Hz, 2H), 2.67 (t, 7.52 Hz, 2H).[123]

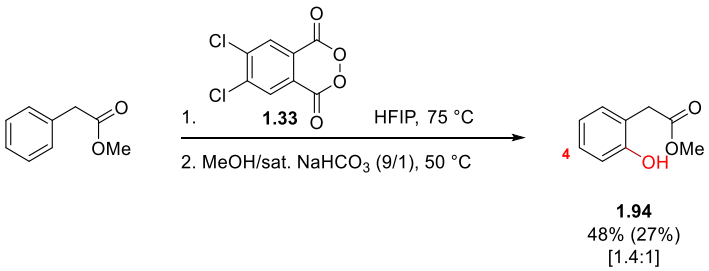

Prepared following <u>General Procedure B</u> using the methyl ester (100.0 mg, 0.67 mmol, 1.0 equiv.), 4,5-dichlorophthaloyl peroxide (436.0 mg, 1.67 mmol, 2.50 equiv., 89%), and HFIP (6.7 mL) at 75 °C for 36 hours. The crude orange gum was purified by silica gel chromatography; 1 – 10% Et_2O in methylene chloride / hexanes (1 / 1) to provide the ester **1.94** (52.4 mg, 0.32 mmol, 48%, **1.94a** : **1.94b** = 1.4 : 1) as pale yellow gums and the starting ester (27.1 mg, 0.18 mmol, 27%) as a clear colorless oil.

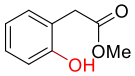

1.94a

yellow gum; **^{1}H-NMR** (400 MHz, $CDCl_3$) δ 7.33 (bs, 1H), 7.20 (m, 1H), 7.10 (dd, *J* = 1.60, 7.40 Hz, 1H), 6.94 (d, *J* = 8.20 Hz, 1H), 6.89 (dt, *J* = 1.20, 7.40 Hz, 1H), 3.75 (s, 3H), 3.68 (s, 2H).[131]

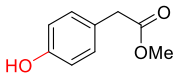

1.94b

yellow gum; ^{1}H-NMR (400 MHz, $CDCl_3$) δ 7.15 (d, J = 8.2 Hz, 2H), 6.78 (d, J = 8.60 Hz, 2H), 3.72 (s, 3 H), 3.58 (s, 2 H).[132]

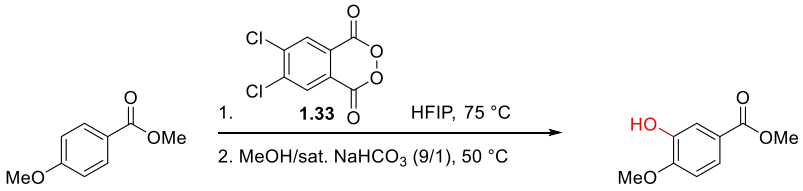

Prepared following General Procedure B using 4-methoxy methylbenzoate (100 mg, 0.60 mmol, 1.0 equiv.), 4,5-dichlorophthaloyl peroxide (408 mg, 1.50 mmol, 2.5 equiv., (using material of 86% peroxide and 14% 4,5-dichlorophthalic anhydride)), and HFIP (6.0 mL) at 75 °C for 36 hours. The crude brown foam was purified by silica gel chromatography; 1 – 20% Et_2O in methylene chloride: hexanes (1: 1) to provide the phenol **1.95** (70.0 mg, 0.39 mmol, 64%) as a yellow solid and the starting benzoate 4l (5.0 mg, 0.03 mmol, 5%) as a white solid.

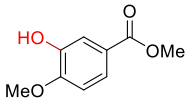

1.95

yellow solid; ^{1}H-NMR (400 MHz, $CDCl_3$): δ 7.62 (dd, 1H, J = 2.0, 8.6 Hz), 7.59 (d, 1H, J = 2.0 Hz), 6.87 (d, 1H, J = 8.6 Hz), 5.61 (s, 1H), 3.95 (s, 3H), 3.88 (s, 3H). [133]

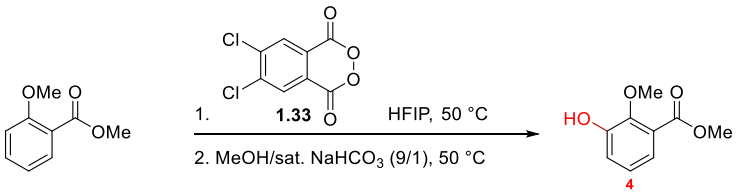

1.96
53% (26%)
[1.2:1]

Prepared following General Procedure A using methyl salicylate (100 mg, 0.60 mmol, 1.0 equiv.), 4,5-dichlorophthaloyl peroxide (212 mg, 0.78 mmol, 1.3 equiv., (using material of 86% peroxide and 14% 4,5-dichlorophthalic anhydride)), and HFIP (6.0 mL) at 50 °C for 24 hours. The crude brown foam was purified by silica gel chromatography; 1 – 20% Et_2O in methylene chloride: hexanes (1: 1) to provide the phenols **1.96a** (31.0 mg, 0.17 mmol, 28%), **1.96b** (27.2 mg, 0.15 mmol, 25%) as yellow solids and the starting salicylate (25.6 mg, 0.15 mmol, 26%) as a clear colorless oil.

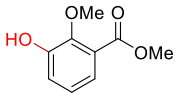

1.96a

yellow solid; ^{1}H-NMR (400 MHz, $CDCl_3$) δ 7.40 (dd, J = 1.7, 7.9 Hz, 1H), 7.15 (dd, J = 1.7, 8.2 Hz, 1H), 7.05 (t, J = 8.2 Hz, 1H), 5.91 (bs, 1H), 3.93 (s, 3H), 3.92 (s, 3H).[134]

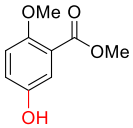

1.96b

yellow solid; ^{1}H-NMR (400 MHz, $CDCl_3$) δ 7.29 (d, J = 3.4 Hz, 1H), 6.97 (dd, J = 3.1, 8.9 Hz, 1H), 6.88 (d, J = 9.2 Hz, 1H), 4.52 (bs, 1H), 3.89 (s, 3H), 3.86 (s, 3H).[135]

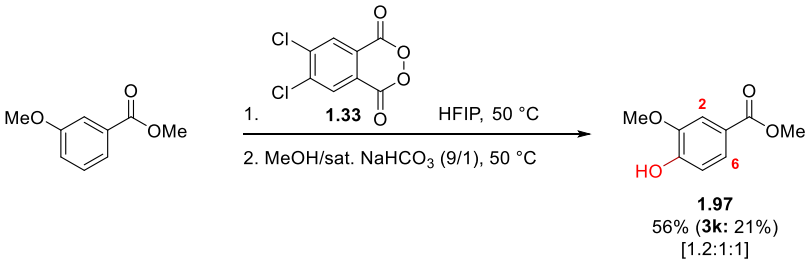

Prepared following General Procedure A using 3-methoxy methylbenzoate (100 mg, 0.60 mmol, 1.0 equiv.), 4,5-dichlorophthaloyl peroxide (212 mg, 0.78 mmol, 1.3 equiv., (using material of 86% peroxide and 14% 4,5-dichlorophthalic anhydride)), and HFIP (6.0 mL)

at 50 °C for 24 hours. The crude brown foam was purified by silica gel chromatography; 1 – 20% Et_2O in methylene chloride: hexanes (1: 1) to provide the phenols **1.97a** (22.1 mg, 0.12 mmol, 20%), **1.97b** (19.7 mg, 0.11 mmol, 18%), **1.97c** (18.8 mg, 0.10 mmol, 17%) as pale yellow solids and the starting benzoate (20.9 mg, 0.13 mmol, 21%) as a clear colorless oil.

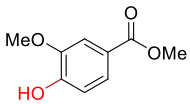

1.97a

yellow solid; ^{1}H-NMR (400 MHz, CDCl3) δ 10.37 (bs, 1H), 7.29 (d, J = 3.2 Hz, 1H), 7.08 (dd, J = 3.1, 8.9 Hz, 1H), 6.92 (d, J = 9.2 Hz, 1H), 3.95 (s, 3H), 3.78 (s, 3H).[136]

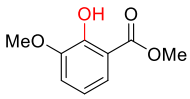

1.97b

yellow solid; ^{1}H-NMR (400 MHz, CDCl3) δ 11.00 (bs, 1H), 7.43 (dd, J = 1.5, 8.2 Hz, 1H), 7.04 (d, J = 7.9 Hz, 1H), 6.83 (t, J = 8.2 Hz, 1H), 3.95 (s, 3H), 3.91 (s, 3H).[137]

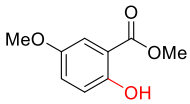

1.97c

yellow solid; ^{1}H-NMR (400 MHz, CDCl3) δ 7.64 (d, J = 8.2 Hz, 1H), 7.55 (d, J = 2.1 Hz, 1H), 6.94 (d, J = 8.2 Hz, 1H), 5.97 (bs, 1H), 3.95 (s, 3H), 3.89 (s, 3H).[137]

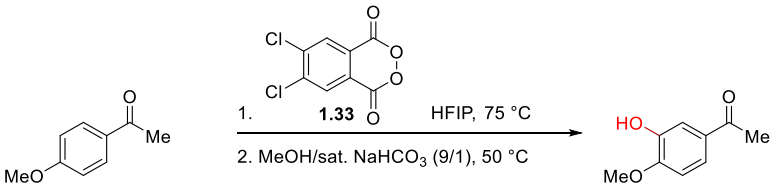

1.98
62% (19%)

Prepared following General Procedure B using 4-methoxy acetophenone (100 mg, 0.67 mmol, 1.0 equiv.), 4,5-dichlorophthaloyl peroxide (446 mg, 1.67 mmol, 2.5 equiv., (using

material of 86% peroxide and 14% 4,5-dichlorophthalic anhydride)), and HFIP (6.7 mL) at 75 °C for 36 hours. The crude brown viscous oil was purified by silica gel chromatography; 1 – 10% Et_2O in methylene chloride: hexanes (1: 1) to provide the ketone **1.98** (68.5 mg, 0.41 mmol, 62%) as a yellow solid and the starting acetophenone (18.8 mg, 0.13 mmol, 19%) as a white solid.

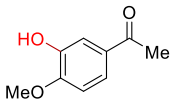

1.98

yellow solid; ^{1}H-NMR (400 MHz, $CDCl_3$) δ 7.54 – 7.52 (m, 2H), 6.89 (d, 1H, J = 8.2 Hz), 5.64 (bs, 1H), 3.97 (s, 3H), 2.55 (s, 3H).[138]

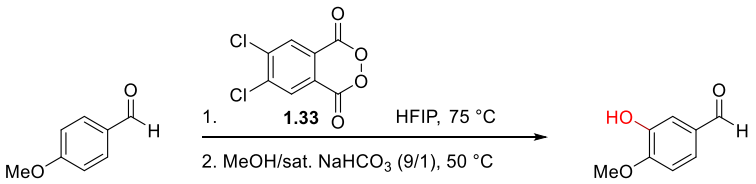

1.82
69%

Prepared following <u>General Procedure B</u> using anisaldehyde (30.0 mg, 0.22 mmol, 1.0 equiv.), 4,5-dichlorophthaloyl peroxide (239 mg, 0.88 mmol, 4.0 equiv., (using material of 86% peroxide and 14% 4,5-dichlorophthalic anhydride)), and HFIP (2.2 mL) at 75 °C for 36 hours. The crude brown viscous oil was purified by silica gel chromatography; 1 – 10% Et_2O in methylene chloride: hexanes (1: 1) to provide the aldehyde **1.82** (23.0 mg, 0.15 mmol, 69%) as a deep yellow solid.

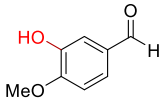

1.82

yellow solid; ^{1}H-NMR (400 MHz, $CDCl_3$) δ 9.85 (s, 1H), 7.45 – 7.43 (m, 2H), 6.98 (d, J = 8.9 Hz, 1H), 6.72 (s, 1H), 3.99 (s, 3H).[139,140]

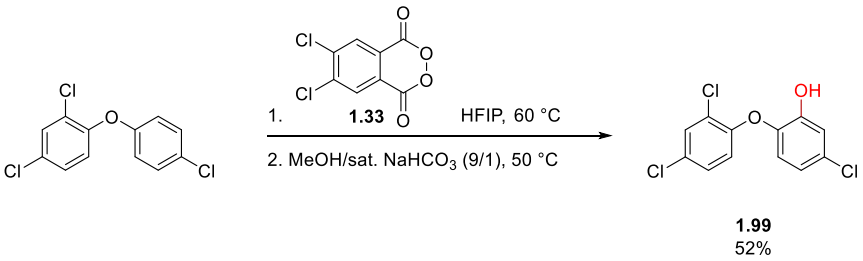

Prepared following General Procedure A using trichloride (95 mg, 0.35 mmol, 1.0 equiv.), 4,5-dichlorophthaloyl peroxide (188 mg, 0.70 mmol, 2.0 equiv., (using material of 86% peroxide and 14% 4,5-dichlorophthalic anhydride)), and HFIP (3.5 mL) at 60 °C for 24 hours. The crude brown viscous oil was purified by silica gel chromatography; 1 – 10% Et_2O in pentane to provide triclosan (**1.99**) (52.0 mg, 0.18 mmol, 52%) as a pale-yellow viscous oil and the starting trichloride (8.4 mg, 0.03 mmol, 9%). The spectra of the title compound matches that of Triclosan (**1.99**).

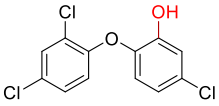

1.99

yellow oil; ^{1}H-NMR (400 MHz, $CDCl_3$) δ 7.48 (d, J = 2.2 Hz, 1H), 7.22 (dd, J = 2.4, 8.6 Hz, 1H), 7.07 (d, 1H, J = 2.4 Hz), 6.95 (d, J = 8.9 Hz, 1H), 6.81 (dd, J = 2.4, 8.9 Hz, 1H), 6.66 (d, J = 8.6 Hz, 1H), 5.63 (bs, 1H).[141]

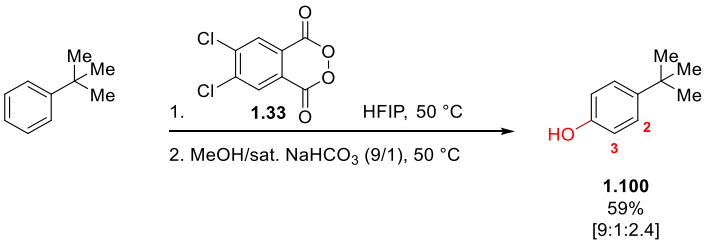

Prepared following General Procedure A using *tert*-butyl benzene (100 mg, 0.75 mmol, 1.0 equiv.), 4,5-dichlorophthaloyl peroxide (259 mg, 0.97 mmol, 1.3 equiv., (using material of 89% peroxide and 11% 4,5-dichlorophthalic anhydride)), and HFIP (7.5 mL)

at 50 °C for 24 hours. The crude brown foam was purified by silica gel chromatography; 1 – 5% Et_2O in methylene chloride: hexanes (1: 1) to provide the phenols **1.100a** and **100b** (53.4 mg, 0.36 mmol, 48%, **1.100a**: **1.100b** = 9: 1) and **1.100c** (12.6 mg, 0.08 mmol, 11%) as orange foams.

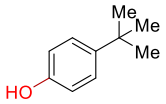

1.100a

orange foam; **^{1}H-NMR** (400 MHz, $CDCl_3$) δ 7.26 (d, J = 8.9 Hz, 2H), 6.77 (d, J = 8.9 Hz, 2H), 4.54 (bs, 1H), 1.29 (s, 9H).[139]

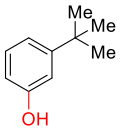

1.100b

orange foam; **^{1}H-NMR** (400 MHz, $CDCl_3$) δ 7.17 (t, J = 7.9 Hz, 1H), 6.97 (m, 1H), 6.87 (dd, J = 2.1, 2.4 Hz, 1H), 6.64 (m, 1H), 4.60 (bs, 1H), 1.30 (s, 9H).[140]

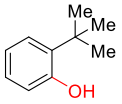

1.100c

orange foam; **^{1}H-NMR** (400 MHz, $CDCl_3$) δ 7.27 (d, J = 8.2 Hz, 1H), 7.07 (m, 1H), 6.88 (dd, J = 6.5, 8.6 Hz, 1H), 6.66 (d, J = 9.6 Hz, 1H), 4.71 (bs, 1H), 1.41 (s, 9H).[139]

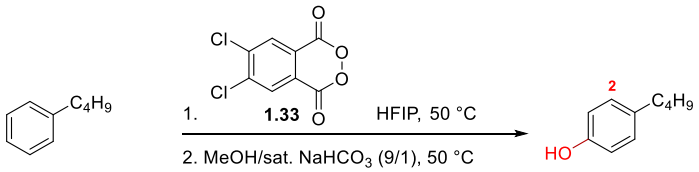

1.102
73%
[1.1:1]

Prepared following General Procedure A using butyl benzene (100 mg, 0.75 mmol, 1.0 equiv.), 4,5-dichlorophthaloyl peroxide (262 mg, 0.97 mmol, 1.3 equiv., (using material of 86% peroxide and 14% 4,5-dichlorophthalic anhydride), and HFIP (7.5 mL) at 50 °C for

24 hours. The crude orange viscous oil was purified by silica gel chromatography; 1 – 5% Et_2O in methylene chloride: hexanes (1: 1) to provide the phenols **1.102a** and **1.102b** (81.1 mg, 0.54 mmol, 73%, **1.102a**: **1.102b** = 1.2: 1) as a pale yellow viscous oil.

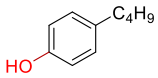

1.102a

yellow oil; ^{1}H-NMR (400 MHz, $CDCl_3$) δ 7.04 (d, *J* = 8.6 Hz, 2H), 6.74 (d, *J* = 8.3 Hz, 2H), 4.56 (bs, 1H), 2.54 (t, *J* = 7.8 Hz, 2H), 1.64 – 1.52 (m, 4H), 1.44 – 1.31 (m, 2H), 0.92 (t, *J* = 7.1 Hz, 3H).[23]

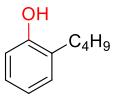

102b

yellow oil; ^{1}H-NMR (400 MHz, $CDCl_3$) δ 7.13 – 7.05 (m, 2H), 6.87 (dt, *J* = 1.1, 7.4 Hz, 1H), 6.77 – 6.74 (m, 1H), 4.64 (bs, 1H), 2.61 (t, *J* = 7.90 Hz, 2H), 1.64 – 1.52 (m, 4H), 1.44 – 1.31 (m, 2H), 0.94 (t, *J* = 7.5 Hz, 3H).[23]

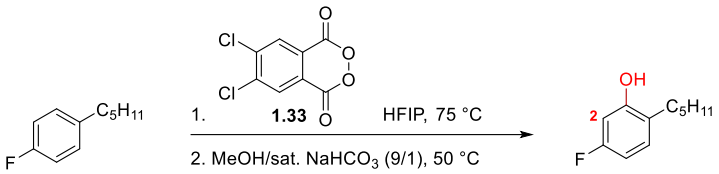

1.103
59%
[2.5:1]

Prepared following <u>General Procedure B</u> using 4-pentyl fluorobenzene (100 mg, 0.60 mmol, 1.0 equiv.), 4,5-dichlorophthaloyl peroxide (403 mg, 1.50 mmol, 2.5 equiv., (using material of 87% peroxide and 13% 4,5-dichlorophthalic anhydride), and HFIP (6.0 mL) at 75 °C for 36 hours. The crude brown viscous oil was purified by silica gel chromatography; 1 % Et_2O in methylene chloride: hexanes (1: 1) to provide the fluorophenols **1.103a** and **1.103b** (64.3 mg, 0.35 mmol, 59%, **1.103a: 1.103b** = 2.5: 1).

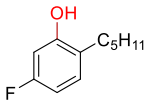

1.103a

yellow oil; R_f = 0.57 (3% Et_2O in 49% Hexanes and 48% methylene chloride);**^{1}H-NMR** (400 MHz, $CDCl_3$) δ 7.03 (dd, *J* = 6.8, 8.6 Hz, 1H), 6.57 (td, *J* = 5.8, 8.2 Hz, 1H), 6.52 (dd, *J* = 2.4, 9.9 Hz, 1H), 4.82 (bs, 1H), 2.53 (q, *J* = 8.2 Hz, 2H), 1.58 (m, 2H), 1.35 (m, 4H), 0.90 (m, 3H); **^{13}C-NMR** (100 MHz, $CDCl_3$) δ161.4 (d, J_{CF} = 243.4 Hz), 154.2 (d, J_{CF} = 10.7 Hz), 130.7 (d, J_{CF} = 9.9 Hz), 124.2 (d, J_{CF} = 3.8 Hz), 107.5, 103.0, 31.6, 29.5, 29.3, 22.5, 14.0; **IR** (neat film, cm^{-1}) 3391, 2929, 1609, 1514, 1279, 1112; **HRMS** (ESI) calcd. for $C_{11}H_{15}OF$ $[M+H]^+$ 182.1107, obs. 182.1106.

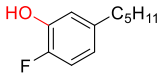

1.103b

yellow oil; ^{1}H-NMR (400 MHz, $CDCl_3$) δ 6.95 (dd, *J* = 8.2, 10.3 Hz, 1H), 6.84 (dd, *J* = 2.1, 8.6 Hz, 1H), 6.66 - 6.63 (m, 1H), 5.01 (bs, 1H), 2.53 (q, *J* = 8.2 Hz, 2H), 1.58 (m, 2H), 1.35 (m, 4H), 0.90 (m, 3H); **^{13}C-NMR** (100 MHz, $CDCl_3$) δ 149.3 (d, J_{CF} = 234.2 Hz), 143.0 (d, J_{CF} = 14.5 Hz), 140.0 (d, J_{CF} = 3.1 Hz), 120.5 (d, J_{CF} = 6.1 Hz), 117.0 (d, J_{CF} = 1.5 Hz), 115.0 (d, J_{CF} = 1.6 Hz), 35.3, 31.35, 31.0, 22.5, 14.0; **IR** (neat film, cm^{-1}) 3391, 2929, 1609, 1514, 1279, 1112; **HRMS** (ESI) calcd. for $C_{11}H_{15}OF$ $[M+H]^+$ 182.1107, obs. 182.1106.[142]

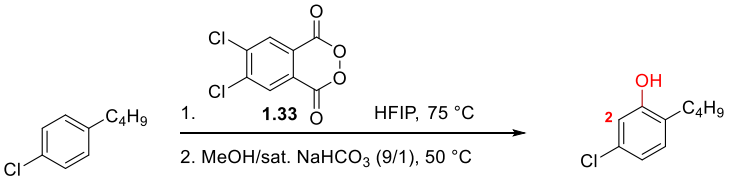

1.104
59%
[4:1]

Prepared following General Procedure B using 4-butyl chlorobenzene (100 mg, 0.59 mmol, 1.0 equiv.), 4,5-dichlorophthaloyl peroxide (406 mg, 1.48 mmol, 2.5 equiv., (using material of 85% peroxide and 15% 4,5-dichlorophthalic anhydride)), and HFIP (5.9 mL) at 75 °C for 36 hours. The crude brown viscous oil was purified by silica gel

chromatography; 1 % Et_2O in methylene chloride: hexanes (1: 1) to provide the chlorophenols **1.104a** and **1.104b** (64.4 mg, 0.35 mmol, 59%, **1.104a: 1.104b** = 4 : 1) as a yellow oil. R_f = 0.57 (3% Et_2O in 49% Hexanes and 48% methylene chloride);

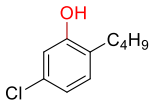

1.104a

yellow oil; ^{1}H-NMR (400 MHz, $CDCl_3$) δ 7.02 (d, *J* = 7.9 Hz, 1H), 6.5 (dd, *J* = 2.1, 8.2 Hz, 1H), 6.78 (d, *J* = 2.1 Hz, 1H), 4.69 (bs, 1H), 2.56 (t, *J* = 7.5 Hz, 2H), 1.60 – 1.53 (m, 2H), 1.37 (qt, *J* = 7.5, 7.9 Hz, 2H), 0.94 (t, *J* = 7.5 Hz, 3H); **^{13}C-NMR** (100 MHz, $CDCl_3$) δ154.2, 132.0, 131.2, 127.4, 121.1, 115.8, 32.0, 29.4, 22.7, 14.2; **IR** (neat film, cm^{-1}) 3412, 2957, 2930, 1603, 1588, 1413; **HRMS** (ESI) calcd. for $C_{10}H_{13}OCl$ $[M+H]^+$ 184.0655, obs. 184.0653.

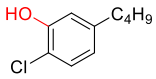

1.104b

yellow oil; ^{1}H-NMR (400 MHz, $CDCl_3$) δ 7.19 (d, *J* = 8.2 Hz, 1H), 6.86 – 6.83 (m, 1H), 6.69 (dd, *J* = 2.1, 8.2 Hz, 1H), 5.43 (bs, 1H), 2.54 (t, *J* = 7.5 Hz, 2H), 1.60 – 1.53 (m, 2H), 1.37 (qt, *J* = 7.5, 7.9 Hz, 2H), 0.92 (t, *J* = 7.1 Hz, 3H); **^{13}C-NMR** (100 MHz, $CDCl_3$) δ 151.0, 143.8, 128.5, 121.5, 116.9, 116.1, 35.1, 33.3, 22.2, 13.9; **IR** (neat film, cm^{-1}) 3412, 2957, 2930, 1603, 1588, 1413; **HRMS** (ESI) calcd. for $C_{10}H_{13}OCl$ $[M+H]^+$ 184.0655, obs. 184.0653.

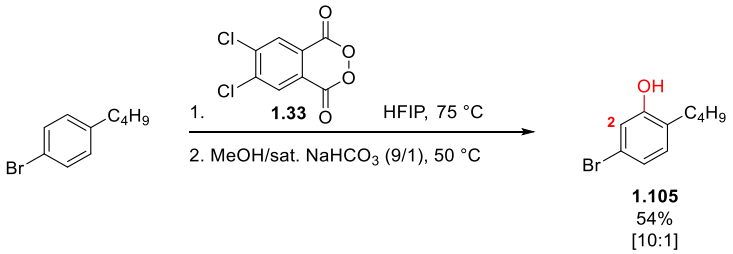

Prepared following <u>General Procedure B</u> using 4-butyl bromobenzene (100 mg, 0.47 mmol, 1.0 equiv.), 4,5-dichlorophthaloyl peroxide (321 mg, 1.17 mmol, 2.5 equiv., (using

material of 85% peroxide and 15% 4,5-dichlorophthalic anhydride), and HFIP (4.7 mL) at 75 °C for 36 hours. The crude brown viscous oil was purified by silica gel chromatography; 1 % Et_2O in methylene chloride: hexanes (1: 1) to provide the bromophenols **1.105a** and **1.105b** (58.3 mg, 0.25 mmol, 54%, **1.105a: 1.105b** = 10: 1) as a dark yellow oil. R_f = 0.57 (silica gel, 3% Et_2O in 49% Hexanes and 48% methylene chloride).

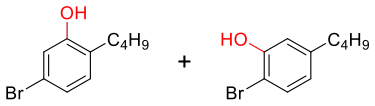

1.105a **1.105b**

yellow oil; ^{1}H-NMR (400 MHz, $CDCl_3$) δ 6.98 (d, *J* = 1.71 Hz, 1H), 6.97 (bs, 1H), 6.93 (d, *J* = 1.71 Hz, 1H), 4.72 (bs, 1H), 2.55 (t, *J* = 7.52 Hz, 2H), 1.60 – 1.53 (m, 2H), 1.42 – 1.33 (qt, *J* = 7.52, 7.52 Hz, 2H), 0.93 (t, *J* = 7.52 Hz, 3H); **^{13}C-NMR** (100 MHz, $CDCl_3$) δ 154.5, 131.6, 128.0, 124.0, 119.6, 118.6, 31.9, 29.5, 22.7, 14.2; **^{1}H NMR** (400 MHz, C_6D_6) δ 6.88 (dd, *J* = 2.0, 8.2 Hz, 1H), 6.58 (d, *J* = 8.2 Hz, 1H), 6.29 (s, 1H), 3.90 (bs, 1H), 2.36 (t, *J* = 7.9 Hz, 2H), 1.40 (dt, *J* = 7.52, 7.86 Hz, 2H), 1.17 (qt, *J* = 7.52, 7.52 Hz, 2H), 0.80 (t, *J* = 7.52 Hz, 3H); **IR** (neat film, cm^{-1}) 3390, 2957, 2928, 1408, 1123; **HRMS** (ESI) calcd. for $C_{10}H_{12}OBr$ $[M+H]^+$ 228.0150, obs. 228.0149.

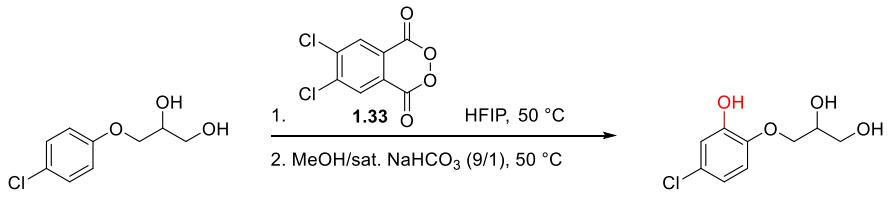

1.106
52% (12%)

Prepared following <u>General Procedure A</u> using chlorphenesin (95 mg, 0.47 mmol, 1.0 equiv.), 4,5-dichlorophthaloyl peroxide (165 mg, 0.61 mmol, 1.3 equiv., (using material of 86% and 14% 4,5-dichlorophthalic anhydride), and HFIP (4.7 mL) at 50 °C for 24 hours. After removal of the HFIP by continuous positive flow of nitrogen, the mixed phthalate

acid was placed under an atmosphere of N_2 and a de-oxygenated mixture of methanol / saturated aqueous $NaHCO_3$ (9: 1, 4.7 mL) was added via syringe under N_2. The resulting red-orange suspension was placed in an oil bath heated to 50 °C and stirred vigorously (700 rpm). After 1 hour the methanol was removed by a continuous flow of N_2 from the red solution, diluted with ethyl acetate (15 mL), an aqueous phosphate buffer (5 mL, 0.2 M, pH = 7), and brine (5 mL). The biphasic mixture was stirred vigorously (700 rpm) for 5 minutes and then poured into a separatory funnel containing brine (10 mL) and an aqueous phosphate buffer (10 mL, 0.2 M, pH = 7). After the layers were partitioned the organics were washed with a saturated aqueous mixture of $NaHCO_3$ and brine (3 x 30 mL). The residual organics were extracted from the aqueous with a mixture of brine and ethyl acetate (4 x 30 mL). The combined organics were dried over sodium sulfate, filtered, and concentrated to reveal a brown solid which was purified by silica gel chromatography; 5 - 50 % acetone in hexanes to provide the **1.106** (53.0 mg, 0.24 mmol, 52%) and chlorphenesin (11.0 mg, 0.05 mmol, 12%).

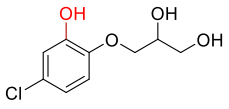

1.106

yellow oil; R_f = 0.47 (silica gel, 50% acetone in hexanes); **^{1}H-NMR** (400 MHz, $(CD_3)_2CO$) δ 8.21 (bs, 1H), 6.98 (d, *J* = 8.6 Hz, 1H), 6.85 (d, *J* = 2.4 Hz, 1H), 6.79 (dd, *J* = 2.7, 8.6 Hz, 1H), 4.39 (bs, 1H), 4.14 (d, *J* = 5.8 Hz, 1H), 4.01 (m, 2H), 3.84 (t, *J* = 5.4 Hz, 1H), 3.67 (t, *J* = 5.5 Hz, 2H); **^{13}C-NMR** (125 MHz, $(CD_3)_2CO$) δ 148.1, 145.9, 125.8, 119.0, 115.5, 114.6, 71.4, 70.4, 62.9; **IR** (neat film, cm^{-1}) 3410, 2935, 1634, 1592, 1504, 1268, 1215; **HRMS** (ESI) calcd. for $C_9H_{11}ClNaO_4$ $[M+Na]^+$ 241.0238, obs. 241.0234.

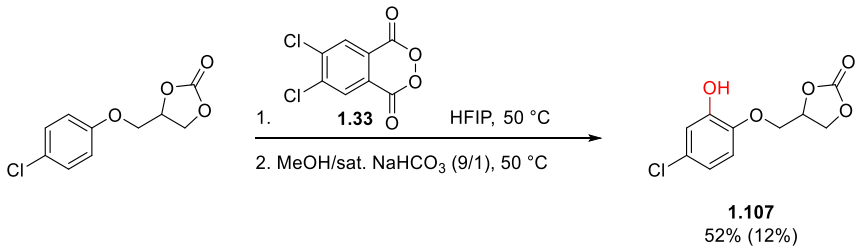

Prepared following General Procedure A using carbonate (50 mg, 0.22 mmol, 1.0 equiv.), 4,5-dichlorophthaloyl peroxide (138 mg, 0.51 mmol, 2.5 equiv., (using material of 86% peroxide and 14% 4,5-dichlorophthalic anhydride)), and HFIP (2.0 mL) at 50 °C for 24 hours. The crude brown viscous oil was purified by silica gel chromatography; 5 - 30% acetone in hexanes to provide the carbonate **1.107** (28.0 mg, 0.11 mmol, 52%) as a red – orange solid

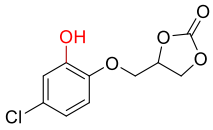

1.107

red solid, M.P. = 122 - 125°C; **R_f** = 0.46 (silica gel, 40% acetone in hexanes); **^{1}H-NMR** (400 MHz, $CDCl_3$) δ 6.98 (d, *J* = 2.4 Hz, 1H), 6.84 (dd, *J* = 2.4, 8.6 Hz, 1H), 6.78 (d, *J* = 8.6 Hz, 1H), 5.48 (bs, 1H), 5.07 (m, 1H), 4.66 (dd, *J* = 8.2, 8.9 Hz, 1H), 4.47 (dd, *J* = 5.8, 8.9 Hz, 1H), 4.30 (dd, *J* = 3.4, 10.9 Hz, 1H), 4.20 (dd, *J* = 4.4, 10.9 Hz, 1H); **^{1}H-NMR** (400 MHz, $(CD_3)_2CO$) δ 8.39 (bs, 1H), 7.01 (d, *J* = 8.7 Hz, 1H), 6.88 (d, *J* = 2.6 Hz, 1H), 6.80 (dd, *J* = 2.50, 8.5 Hz, 1H), 5.20 (m, 1H), 4.71 (t, *J* = 8.5 Hz, 1H), 4.56 (dd, *J* = 6.9, 8.5 Hz, 1H), 4.39 (dd, *J* = 3.4, 11.2 Hz, 1H), 4.33 (dd, *J* = 4.7, 11.2 Hz, 1H); **^{13}C-NMR** (150 MHz, $(CD_3)_2CO$) δ 155.5, 148.9, 146.3, 127.2, 120.0, 116.8, 115.8, 75.7, 69.5, 66.7; **IR** (neat film, cm^{-1}) 3400, 2922, 1783, 1634; **HRMS** (ESI) calcd. for $C_{10}H_9ClO_5$ $[M-H]^+$ 244.0139, obs. 244.0141.

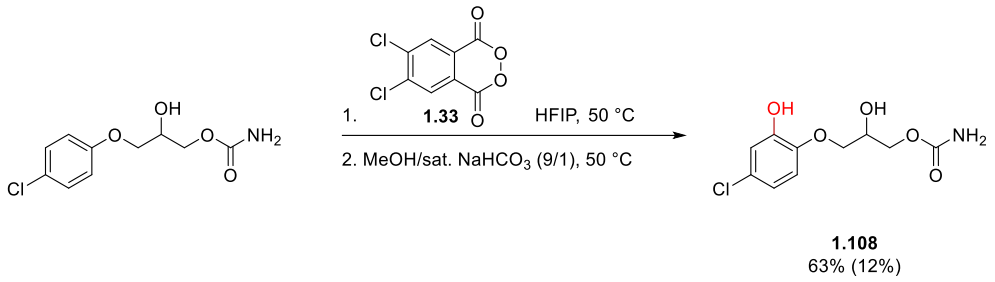

Prepared following General Procedure A using chlorphenesin carbamate (85 mg, 0.35 mmol, 1.0 equiv.), 4,5-dichlorophthaloyl peroxide (122 mg, 0.45 mmol, 1.3 equiv., (using material of 86% peroxide and 14 % 4,5-dichlorophthalic anhydride)), and HFIP (3.5 mL) at 50 °C for 24 hours. After removal of the HFIP by continuous positive flow of nitrogen, the phthalate acid was placed under an atmosphere of N_2 and a de-oxygenated mixture of methanol / saturated aqueous $NaHCO_3$ (9: 1, 3.5 mL) was added via syringe under N_2. The resulting red-orange suspension was placed in an oil bath heated to 50 °C and stirred vigorously (500 rpm). After 1 hour the methanol was removed by a continuous flow of N_2 from the red solution, diluted with ethyl acetate (15 mL), an aqueous phosphate buffer (5 mL, 0.2 M, pH = 7), and brine (5 mL). The biphasic mixture was stirred vigorously (700 rpm) for 5 minutes and then poured into a separatory funnel containing brine (10 mL) and an aqueous phosphate buffer (10 mL, 0.2 M, pH = 7). After the layers were partitioned the organics were washed with a saturated aqueous mixture of $NaHCO_3$ and brine (3 x 30 mL). The residual organics were extracted from the aqueous with a mixture of brine and ethyl acetate (4 x 30 mL). The combined organics were dried over sodium sulfate, filtered, and concentrated to reveal a brown solid which was purified by silica gel chromatography; 5 - 35% acetone in hexanes to provide the carbamate **1.108** (57.0 mg, 0.22 mmol, 63%) as an off-white solid.

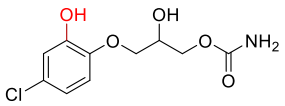

1.108

white solid, M.P. = 124 - 127°C; **R_f** = 0.45 (silica gel, 50% acetone in hexanes); **^{1}H-NMR** (400 MHz, CD_3OD) δ 6.88 (d, *J* = 8.6 Hz, 1H), 6.80 (d, *J* = 2.7 Hz, 1H), 6.74 (dd, *J* = 2.4, 8.6 Hz, 1H), 4.16 (m, 3H), 4.06 (m, 1H), 3.98 (m, 1H); **^{13}C-NMR** (100 MHz, CD_3OD) δ 158.3, 147.6, 145.6, 126.0, 118.9, 115.5, 113.8, 70.0, 68.1, 64.9; **IR** (neat film, cm^{-1}) 3369, 1706, 1501; **HRMS** (ESI) calcd. for $C_{10}H_{12}ClNNaO_5$ $[M+Na]^+$ 284.0296, obs. 284.0293.

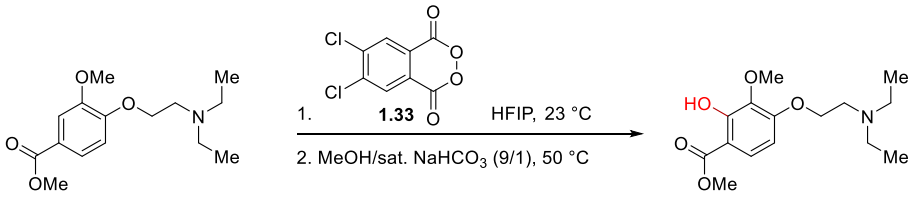

1.109
85%

To a stirred solution of amine (75.0 mg, 0.25 mmol, 1.0 equiv.) in HFIP (2.5 mL) at 23 °C was added *p*-toluenesulfonic acid (43.7 mg, 0.25 mmol, 1.0 equiv.) and then 4,5-dichlorophthaloyl peroxide (89.0 mg, 0.33 mmol, 1.3 equiv., (using material of 86% peroxide and 14% 4,5-dichlorophthalic anhydride)). After 4 hours, the solvent was removed by a continuous flow of N_2 providing the mixed phthalate acid as a red solid. The crude solid was placed under an atmosphere of N_2, suspended in a de-oxygenated mixture of methanol and saturated aqueous $NaHCO_3$ (9: 1, 2.5 mL), and placed in an oil bath heated to 50 °C. After 1 hour the reaction was then poured into an aqueous phosphate buffer (5 mL, 0.2 M, pH = 10), poured into a separatory funnel and the layers partitioned. Residual organics were extracted from the aqueous phase with ethyl acetate (3 x 5 mL). The combined organic layers were washed with an aqueous phosphate buffer (1 x 5 mL, 0.2 M, pH = 10), brine (1 x 5 mL), dried over sodium sulfate, concentrated and the crude mixture

was purified by silica gel chromatography; 1% methanol and 1% triethylamine in methylene chloride to give **1.109** (67.7 mg, 0.22 mmol, 86%).

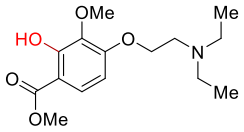

1.109

colorless oil; $\mathbf{R_f}$ = 0.40 (silica gel, 2% methanol and 2% triethylamine in methylene chloride); **^{1}H-NMR** (400 MHz, $CDCl_3$): δ 10.79 (s, 1 H), 7.55 (d, *J* = 9.0 Hz, 1H), 6.48 (d, *J* = 9.0 Hz, 1H), 4.12 (m, 2H), 3.92 (s, 3H), 3.87 (s, 3H), 2.65 (t, *J* = 7.0 Hz, 2H), 2.57 (q, *J* = 7.0 Hz, 4H), 1.99 (t, *J* = 7.4 Hz, 2H), 1.04 (t, *J* = 7.0 Hz, 6H). **^{13}C-NMR** (100 MHz, $CDCl_3$): δ 170.1, 157.3, 155.7, 136.4, 125.3, 106.5, 103.9, 66.8, 60.3, 51.8, 48.9, 46.7, 26.4, 11.2. **IR** (neat film, cm $^{-1}$): 3369, 2966, 2917, 1720, 1240. **HRMS** (ESI): $[M+H]^+$ calcd. for $C_{16}H_{26}NO_5$: 312.1806, obs. 312.1800.

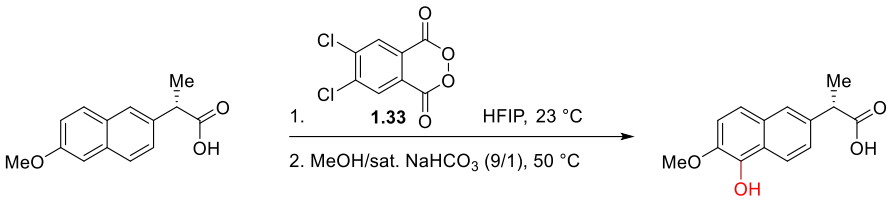

1.110
40%

Prepared following <u>General Procedure A</u> using naproxen (100 mg, 0.43 mmol, 1.0 equiv.), 4,5-dichlorophthaloyl peroxide (154 mg, 0.57 mmol, 1.3 equiv., (using material of 86% peroxide and 14% 4,5-dichlorophthalic anhydride)), and HFIP (4.3 mL) at 0 °C for 24 hours gradually warming to 23 °C. After removal of the HFIP by continuous positive flow of nitrogen, the mixed phthalate diacid was placed under an atmosphere of Argon. The crude brown solid was re-suspended in a de-oxygenated solution composed of dioxane / aqueous saturated $NaHCO_3$ (9: 1, 2.1 mL) and stirred at 50 °C. After 20 minutes the brown solution was poured into an aqueous phosphate buffer (20 mL, 0.2 M, pH = 2) and adjusted

to pH = 4. Ethyl acetate (20 mL) was added and the layers were separated. The residual organics were extracted from the aqueous layer with ethyl acetate (2 x 20 ml). The combined organics were dried over sodium sulfate, filtered, and concentrated to reveal a brown oil which was purified by silica gel chromatography; 40% Et_2O and 1% acetic acid in hexanes to provide **1.110** (43.0 mg, 0.18 mmol, 40%) as a colorless solid that decomposes in air.

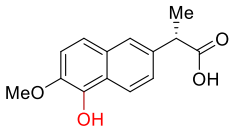

1.110

white solid, M.P. = 132 – 134 °C; $\mathbf{R_f}$ = 0.09 (silica gel, 40% Et_2O and 1% acetic acid in hexanes); **^{1}H-NMR** (400 MHz, $CDCl_3$): δ 8.11 (d, *J* = 8.9 Hz, 1H), 7.66 (d, *J* = 1.4 Hz, 1H), 7.41 (dd, *J* = 8.9, 1.7 Hz, 1H), 7.36 (d, *J* = 8.9 Hz, 1H), 7.24 (d, *J* = 8.9 Hz, 1H), 4.00 (s, 3H), 3.9 (q, J = 7.2 Hz, 1H), 1.59 (d, *J* = 7.2 Hz, 3H); ^{13}C-NMR (125 MHz, $CDCl_3$): δ 179.5, 141.3, 139.7, 135.5, 129.5, 125.9, 125.2, 123.2, 121.9, 119.5, 113.6, 57.2, 45.2, 18.1; **IR** (neat film cm $^{-1}$): 3433, 2937, 1704, 1275; **HRMS** (CI) calcd. for $C_{14}H_{14}O_4$: 246.0892, obs. 246.0894.

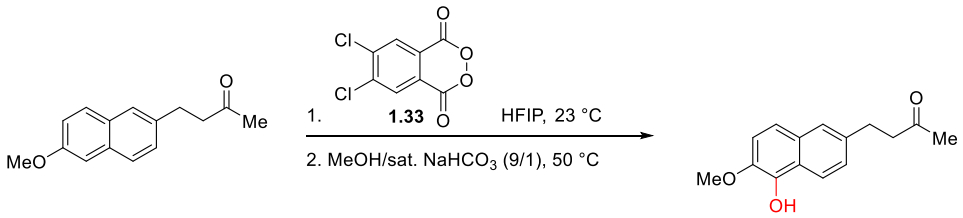

1.111
68%

Prepared following General Procedure A: A clear colorless solution of nabumetone (250.0 mg, 1.10 mmol, 1.00 equiv.) in TFE (11.0 mL) was placed in an ice water bath cooled to 0°C for 1 hour. 4,5-dichlorophthaloyl peroxide (405.0 mg, 1.42 mmol, 1.30 equiv.) was added in 8 portions over 10 minutes causing the solution to change to a dark

brown mixture. After 1 hour the TFE was removed from the black mixture by continuous positive flow of nitrogen. The brown solid mixture containing the mixed phthalate ester-acid was placed under an atmosphere of nitrogen and a deoxygenated mixture composed of methanol and aqueous saturated $NaHCO_3$ (9:1, 11.0 mL) was added. The black solution was placed in an oil bath heated to 50 °C and after 2 h the black solution was removed from the oil bath, cooled to 23 °C, diluted with an aqueous phosphate buffer (10 mL, pH = 7, 0.2 M) and ethyl acetate (10 mL), poured into a separatory funnel, partitioned, and the organic layer was washed with an aqueous phosphate buffer (3 x 30 mL, pH = 7, 0.2 M). Residual organics were extracted from the aqueous layer with ethyl acetate (3 x 20 ml), combined, dried over solid sodium sulfate, filtered, and concentrated. The crude dark brown foam was purified by silica gel chromatography; hexane – 30% ethyl acetate in hexane to afford the phenol **1.111** (183.0 mg, 0.75 mmol, 68%) as an off white amorphous foam that decomposes in air.

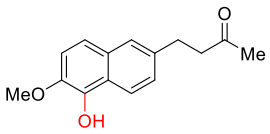

1.111

yellow solid, M.P. = 74-78 ^{0}C; **R$_f$** = 0.14 (silica gel, 3:1 hexanes: ethyl acetate); **^{1}H-NMR** (400 MHz, $CDCl_3$): δ 8.07 (d, *J* = 8.6 Hz, 1H), 7.52 (bs, 1H), 7.32 (d, *J* = 8.9 Hz, 1H), 7.28 (dd, *J* = 8.9, 2.1 Hz, 1H), 7.23 (d, *J* = 8.9 Hz, 1H), 5.99 (bs, 1H), 3.99 (s, 3H), 3.03 (t, *J* = 7.9 Hz, 2H), 2.83 (t, *J* = 7.9 Hz, 2H), 2.15 (s, 3H); **^{13}C-NMR** (100 MHz, $CDCl_3$): δ 208.1, 140.9, 139.7, 136.7, 129.7, 126.5, 125.9, 122.5, 121.5, 119.0, 113.5, 57.2, 45.1, 30.2, 29.8; **IR** (KBr, film, υ cm $^{-1}$): 3407, 2923, 1710, 1363, 1273; **HRMS** (CI) calcd. For $C_{15}H_{16}O_3$: 244.1099, obs. 244.1100.

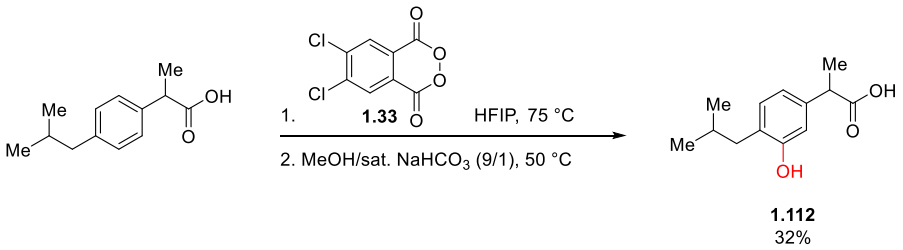

Prepared following General Procedure B using ibuprofen (50.0 mg, 0.24 mmol, 1 equiv.), HFIP (0.5 mL), and 4,5-dichlorophthaloyl peroxide (164.0 mg, 0.61 mmol, 2.50 equiv.) at 75°C for 24 hours. HFIP was removed *in vacuo* yielding a brown solid which was suspended in a deoxygenated mixture composed of methanol and aqueous saturated $NaHCO_3$ (9:1, 2.1 mL), placed in an oil bath heated to 50 °C, and after 1 h the mixture was removed from the oil bath, cooled to 23 °C, diluted with an aqueous phosphate buffer (20 mL, pH = 2, 0.2 M) and adjusted to pH = 4. Ethyl ether (20mL) was added and the layers were partitioned. Residual organics were extracted from the aqueous layer with ether (2 x 20 mL), combined, dried over solid $MgSO_4$, and concentrated. The crude brown foam was purified by silica gel chromatography; 40% Et_2O and 1% AcOH in hexane to afford the phenol **1.112** (17.2mg, 0.08 mmol, 32%).

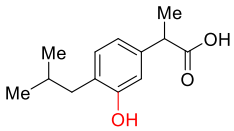

1.112

yellow oil; R_f = 0.26 (silica gel, 40% Et_2O and 1% AcOH in hexane) **^{1}H-NMR** (400 MHz, $CDCl_3$): δ 7.02 (d, *J* = 7.9 Hz, 1H), 6.80 (dd, *J* = 7.5, 1.7 Hz, 1H), 6.74 (d, *J* = 1.7 Hz,1H), 3.66 (q, *J* = 7.2 Hz, 1H), 2.44 (d, *J* = 7.5 Hz, 2H), 1.91 (dddd, *J* = 6.8 Hz, 1H),1.48 (d, *J* = 7.2 Hz, 3H), 0.92 (d, *J* = 6.8 Hz, 6H); **^{13}C-NMR** (100 MHz, $CDCl_3$): δ 179.9, 153.7, 138.7, 131.4, 126.7, 119.8, 114.3, 44.7, 39.0, 28.8, 22.5, 18.0 **IR** (neat film, cm^{-1}): 3399, 2955, 1707; **HRMS** (CI): calcd. for $C_{13}H_{18}O_3$: 222.1256, obs. 222.1255.

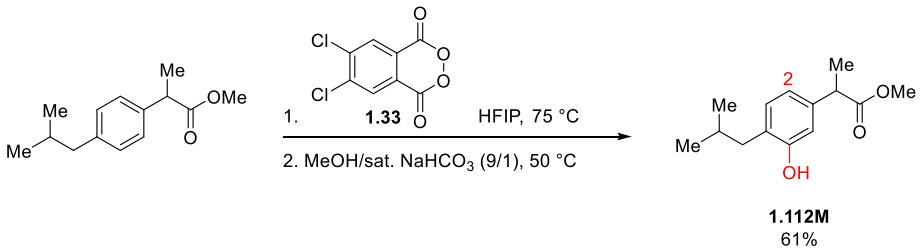

Prepared following General Procedure B using ibuprofen methyl ester (300.0 mg, 1.36 mmol, 1.0 equiv.), 4,5-dichlorophthaloyl peroxide (747.0 mg, 2.72 mmol, 2.50 equiv., 85%), and HFIP (13.6 mL) at 75 °C for 24 hours. The crude brown tar was purified by silica gel chromatography; hexane – 4% ethyl acetate in hexane to provide the starting ester (22.3 mg, 0.10 mmol, 7%) as a clear colorless oil and the phenols as a mixture which were then further purified by silica gel chromatography; 1 - 2 % Et2O in methylene chloride and hexane (1:1) to afford the phenol **1.112Ma** (130.0 mg, 0.55 mmol, 40%) and **1.112Mb** (66.0 mg, 0.28 mmol, 21%) as pale yellow oils.

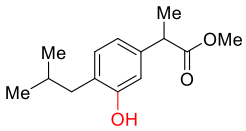

1.112Ma

yellow oil; ^{1}H-NMR (400 MHz, $CDCl_3$): δ 7.01 (d, *J* = 7.7 Hz, 1H), 6.78 (dd, *J* = 1.6, 7.7 Hz, 1H), 6.75 (d, *J* = 1.6 Hz,1H), 5.22 (bs, 1H), 3.67 (s, 1H), 3.65 (q, *J* = 7.2 Hz, 1H), 2.45 (d, *J* = 7.2 Hz, 2H), 1.92 (dddd, *J* = 6.7 Hz, 1H), 1.47 (d, *J* = 7.2 Hz, 3H), 0.92 (d, *J* = 6.7 Hz, 6H); **^{13}C-NMR** (100 MHz, $CDCl_3$): δ 175.5, 154.0, 139.4, 131.3, 126.6, 119.7, 114.0, 52.1, 45.0, 39.0, 28.8, 22.5, 18.5; **IR** (neat film, cm^{-1}): 3401, 2953, 2360, 2342, 1715.

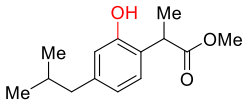

1.112Mb

yellow oil; ^{1}H-NMR (400 MHz, $CDCl_3$): δ 7.43 (bs, 1H), 6.98 (d, *J* = 7.9 Hz, 1H), 6.71 (d, *J* = 1.7 Hz, 1H), 6.67 (dd, *J* = 1.7, 7.9 Hz, 1H), 3.84 (q, *J* = 7.2 Hz, 1H) 3.73 (s, 1H), 2.39 (d, *J* = 7.2 Hz, 2H), 1.84 (dddd, *J* = 6.8 Hz, 1H), 1.54 (d, *J* = 7.2 Hz, 3H), 0.89 (d, *J* = 6.8 Hz, 6H); **^{13}C-NMR** (100 MHz, $CDCl_3$): δ 177.57, 154.30, 142.84, 128.48, 122.92, 121.66,

118.33, 52.65, 44.95, 42.03, 30.01, 22.42, 16.57 **IR** (neat film, cm^{-1}): 3401, 2953, 2360, 2342, 1734.

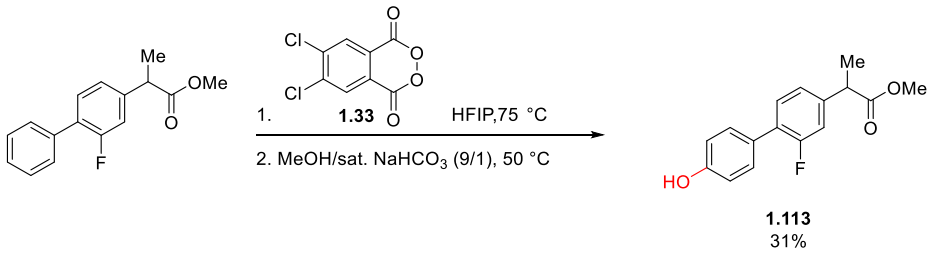

Prepared following General Procedure B using flurbiprofen methyl ester (210 mg, 0.81 mmol, 1.0 equiv.), 4,5-dichlorophthaloyl peroxide (446.0 mg, 1.6 mmol, 2.0 equiv., 85%), and HFIP (8.1 mL) at 75 °C for 24 hours. The crude dark yellow solid mixture was purified by silica gel chromatography; 1% 1,4-dioxane in benzene to afford the phenol **1.113** (69.0 mg, 0.25 mmol, 31%) as a pale yellow foam and the starting flurbiprofen (20.9 mg, 0.08 mmol, 10%).[39]

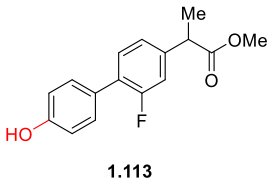

yellow foam; ^{1}H-NMR (400 MHz, $CDCl_3$): δ 7.42 (dd, *J* = 1.5, 7.1 Hz, 2H), 7.34 (t, *J* = 7.4 Hz, 1H), 7.11 (m, 2H), 6.89 (d, *J* = 8.6 Hz, 2H), 4.99 (bs, 1H), 3.75 (q, *J* = 7.0 Hz, 2H), 3.70 (s, 3H), 1.53 (d, *J* = 7.0 Hz, 3H).[39]

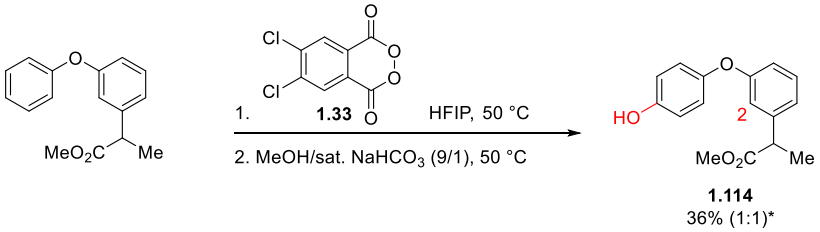

Prepared following General Procedure A using fenoprofen methyl ester (128.0 mg, 0.50 mmol, 1.0 equiv.), 4,5-dichlorophthaloyl peroxide (181.0 mg, 0.65 mmol, 1.3 equiv.), and HFIP (5.0 mL) at 50 °C for 24 hours. The crude orange foam was purified by silica gel chromatography; hexane – 12% ethyl acetate in hexane to afford the phenol **1.114a** as a white solid (24.0 mg, 0.09 mmol, 18%) and phenol **1.114b** as a pale yellow foam (24.2 mg, 0.09 mmol, 18%).

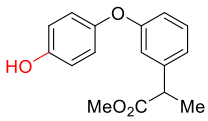

1.114a

white solid; M.P. = 102 – 105 °C; $\mathbf{R_f}$ = 0.56 (silica gel, 30% ethyl acetate in hexane) **^{1}H-NMR** (500 MHz, $CDCl_3$): δ 7.25 (m, 3H), 6.97 (d, *J* = 7.2 Hz, 1H), 6.92 (d, *J* = 8.8 Hz, 2H), 6.91 (bs, 1H), 6.81 (d, *J* = 8.8 Hz, 2H), 3.67 (q, *J* = 7.2 Hz, 1H), 1.47 (d, *J* = 7.2 Hz, 3H); **^{13}C-NMR** (125 MHz, $CDCl_3$): δ 175.1, 158.7, 152.0, 149.8, 142.2, 129.7, 121.5, 121.1, 116.8, 116. 3, 116.0, 52.2, 45.3, 18.4; **IR** (neat film, cm^{-1}): 3411, 2922, 1732, 1587, 1471, 1266, 1215; **HRMS** (CI): calcd. for $C_{16}H_{16}O_4$. 272.1049, obs. 272.1049.

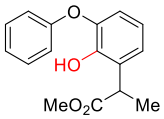

1.114b

yellow foam; ^{1}H-NMR (500 MHz, $CDCl_3$): δ 7.35 (dd, *J* = 1.2, 7.2 Hz, 2H), 7.13 (dt, *J* = 1.0, 7.2 Hz, 1H), 7.04 (m, 2H), 6.99 (dd, *J* = 2.0, 7.2 Hz, 1H), 6.83 – 6.79 (m, 2H), 5.99 (bs, 1H), 4.12 (q, *J* = 7.1 Hz, 1H), 3.71 (s, 3H), 1.53 (d, *J* = 7.1 Hz, 3H); **^{13}C-NMR** (125 MHz, $CDCl_3$): δ 175.4, 156.6, 145.0, 143.9, 129.9, 128.2, 123.7, 123.1, 120.1, 118.3, 117.1, 52.1, 39.3, 17.2.

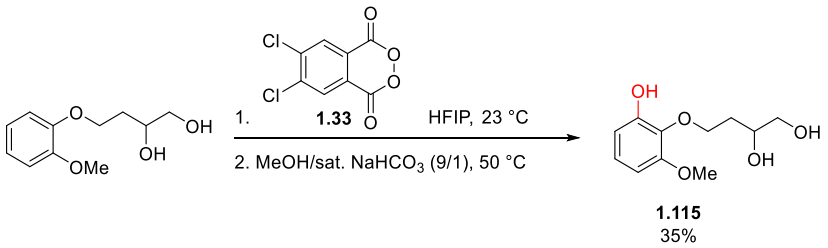

Prepared following General Procedure A using (±)-guaifenesin (75.0 mg, 0.38 mmol, 1.0 equiv.), 4,5-dichlorophthaloyl peroxide (133.0 mg, 0.49 mmol, 1.30 equiv.) in HFIP (3.8 mL) at 23 °C for 24 hours. The crude dark brown foam was purified by silica gel chromatography; 50% ethyl acetate in hexane to afford the phenol **1.115** as an opaque colorless oil (27.9 mg, 0.13 mmol, 35%).

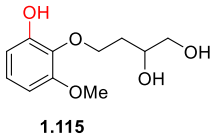

colorless oil; R_f = 0.55 (100% ethyl acetate); **^{1}H-NMR** (500 MHz, $CDCl_3$): δ 6.94 (t, *J* = 8.3 Hz, 1H), 6.59 (dd, *J* = 1.2, 8.3 Hz, 1H), 6.45 (dd, *J* = 1.2, 8.3 Hz, 1H), 4.16 (dd, *J* = 2.7, 10.3 Hz, 1H), 4.04 (m, 1H), 4.01 (t, *J* = 4.2 Hz, 1H), 3.85 (s, 3H), 3.82 (d, *J* = 3.7 Hz, 1H), 3.77 (m, 1H); **^{13}C-NMR** (125 MHz, $CDCl_3$): δ 152.9, 150.4, 135.1, 124.6, 109.2, 103.5, 74.9, 70.8, 63.7, 55.8; **IR** (neat film, cm-1): 3371, 1236, 1201; **HRMS** (ESI): calcd. for $C_{10}H_{14}O_5Na$ $[M+Na]^+$: 237.07334, obs. 237.07352.

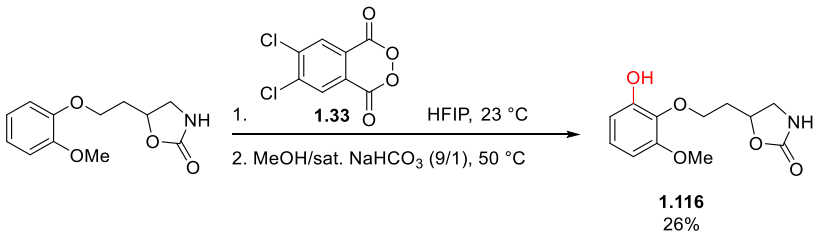

Prepared following General Procedure B using (±)-mephenoxalone (50.0 mg, 0.22 mmol, 1.0 equiv.), 4,5-dichlorophthaloyl peroxide (67.8 mg, 0.29 mmol, 1.30 equiv.), and HFIP

(2.2 mL). The crude dark brown foam was purified by silica gel chromatography; 50% ethyl acetate in hexane to afford phenol **1.116** as an opaque pale yellow oil (13.9 mg, 0.06 mmol, 26%).

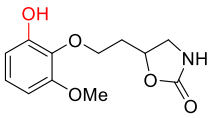

1.116

yellow oil; R_f = 0.47 (100% ethyl acetate); **^{1}H-NMR** (400 MHz, $CDCl_3$): δ 6.95 (t, *J* = 8.2 Hz, 1H), 6.61 (dd, *J* = 1.6, 8.2 Hz, 1H), 6.46 (dd, *J* = 1.2, 8.2 Hz,1H), 6.02 (s, 1H), 5.45 (s, 1H), 4.93 (m, 1H), 4.29 (dd, *J* = 3.5, 11.0 Hz, 1H), 4.14 (dd, *J* = 5.9, 11.0 Hz, 1H), 3.84 (s, 3H), 3.74 (t, *J* = 8.6 Hz, 1H), 3.58 (t, *J* = 6.6 Hz, 1H); **^{13}C-NMR** (100 MHz, $CDCl_3$): δ 158.9, 152.4, 149.7, 133.9, 124.7, 108.7, 103.8, 74.8, 73.1, 55.8, 41.9; **IR** (neat film, cm-1): 3346, 1733, 1253, 1198; **HRMS** (ESI): calcd. for $C_{11}H_{13}NO_5Na$ $[M+Na]^+$: 262.06859, obs. 262.06826.

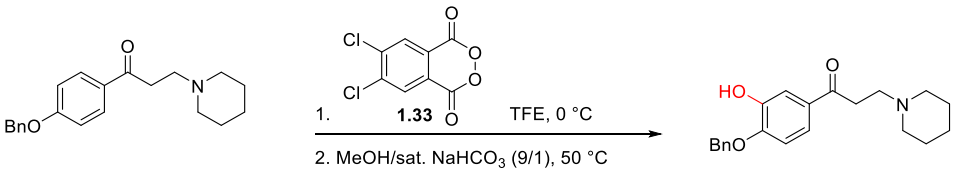

1.117
33%

Prepared following General Procedure A: To a solution of dyclonine (131.0 mg, 0.45 mmol, 1.0 equiv.) in HFIP (4.5 mL) was added *p*-toluenesulfonic acid monohydrate (86.0 mg, 0.45 mmol, 1.0 equiv.). The pale yellow solution was stirred for 2 minutes at 23 °C upon which 4,5-dichlorophthaloyl peroxide (514 mg, 1.81 mmol, 4.0 equiv., 82%) was added. The pale yellow solution was stoppered with a plastic PTFE cap and placed in an oil bath heated to 50 °C. After 12 hours the red solution was removed from the oil bath, cooled to 23 °C, and HFIP was removed by a continuous flow of nitrogen. The dark red mixture was placed under an atmosphere of nitrogen upon which a deoxygenated mixture

of methanol and a saturated aqueous mixture of $NaHCO_3$ (4.5 mL, 9:1) was added. The dark red solution was placed in an oil bath heated to 50 °C. After 2 hours the dark red solution was removed from the oil bath, cooled to 23 °C, diluted with a saturated aqueous mixture of $NaHCO_3$ (10 mL) and ethyl acetate (10 mL), poured into a separatory funnel, partitioned, and the aqueous layer was washed with a saturated aqueous mixture of $NaHCO_3$ and brine (3 x 30 mL, 1:1). Residual organics were extracted from the aqueous layer with a combination of ethyl acetate and brine (3 x 30 mL, 2:1), combined, dried over solid sodium sulfate, decanted, and concentrated. The crude black foam was purified by silica gel chromatography; 1 – 5% MeOH in methylene chloride, then 1% MeOH and 1% Et_3N in methylene chloride to afford the aminophenol **1.117** as a red solid (50.6 mg, 0.15 mmol, 33%).

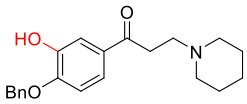

1.117

red solid, M.P. = 140 – 144 °C; $\mathbf{R_f}$ = 0.50 (5% MeOH in methylene chloride); **^{1}H-NMR** (400 MHz, $CDCl_3$): δ 7.58 (dd, *J* = 2.0, 8.2 Hz, 1H), 7.56 (d, 2.0 Hz, 1H), 6.86 (d, *J* = 8.2 Hz, 1H), 4.12 (t, *J* = 6.8 Hz, 2H), 3.64 (t, *J* = 6.8 Hz, 2H), 3.36 (t, *J* = 6.8 Hz, 2H), 3.03 (bs, 4H), 1.97 (bs, 4H), 1.83 (ddd, *J* = 7.8 Hz, 2H), 1.63 (bs, 2H), 1.51 (ddd, *J* = 7.8 Hz, 2H), 1.00 (t, *J* = 7.8 Hz, 3H); **^{13}C-NMR** 100 MHz, $CDCl_3$): δ 195.1, 151.1, 145.9, 129.1, 122.0, 114.2, 110.8, 68.8, 53.7, 52.3, 33.1, 31.0, 22.9, 22.2, 19.1, 13.8 **IR** (neat film, cm^{-1}): 3401, 2957, 2873, 1673, 1604, 1435, 1276.

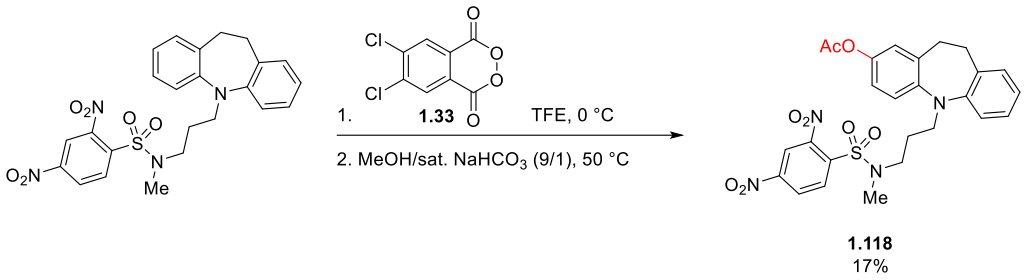

Prepared following General Procedure A: A clear yellow solution of the desipramine dinitrosulfonamide (95.0 mg, 0.19 mmol, 1.0 equiv.) in TFE and methylene chloride (4.0 mL, 1:1) was placed in an ice water bath cooled to 0 °C for 1 hour. Phthaloyl peroxide (40.0 mg, 0.25 mmol, 1.30 equiv.) was added in 5 portions over 5 minutes causing the solution to change to a dark black mixture. After 1 hour the TFE and methylene chloride were removed from the black mixture by continuous positive flow of nitrogen. The black solid tar containing the mixed phthalate esteracid was placed under an atmosphere of nitrogen and a deoxygenated mixture composed of methanol and aqueous saturated $NaHCO_3$ (9:1, 4.0 mL) was added. The black solution was placed in an oil bath heated to 50 °C. After 12 hours the black solution was removed from the oil bath, cooled to 23 °C, diluted with an aqueous phosphate buffer (10 mL, pH = 7, 0.2 M) and ethyl acetate (10 mL), poured into a separatory funnel, partitioned, and the organic layer was washed with an aqueous phosphate buffer (3 x 30 mL, pH = 7, 0.2 M). Residual organics were extracted from the aqueous layer with ethyl acetate (3 x 20 ml), combined, dried over solid sodium sulfate, filtered, and concentrated. The crude black tar was dissolved in methylene chloride (3.0 mL), pyridine (0.5 mL) and acetic anhydride (0.5 mL) were added sequentially, and the brown solution was allowed to stir at 23 °C. After 24 hours the dark brown solution was diluted with an aqueous phosphate buffer (10 mL, pH = 4, 0.2 M) and ethyl acetate (10 mL), poured into a separatory funnel, partitioned, and the organic layer was washed with an aqueous phosphate buffer (2 x 10 mL, pH = 7, 0.2 M). Residual organics were extracted from the aqueous layer with ethyl acetate (2 x 10 mL), dried over solid sodium

sulfate, decanted, and concentrated. The crude dark brown foam was purified by silica gel chromatography; hexane – 20% ethyl acetate in hexane to afford the acetate **1.118** (18.2 mg, 0.03 mmol, 17%) as a golden yellow amorphous foam.

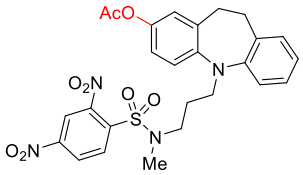

1.118

yellow foam; **R_f** = 0.66 (silica gel, 50% ethyl acetate in hexane); **^{1}H-NMR** (400 MHz, $CDCl_3$): δ 8.38 (d, *J* = 2.4 Hz, 1H), 8.34 (dd, *J* = 2.4, 8.6 Hz, 1H), 8.03 (d, *J* = 8.6 Hz, 1H), 7.11 – 7.05 (m, 3H), 6.98 (t, *J* = 7.4 Hz, 2H), 6.90 (dd, *J* = 2.3, 7.4 Hz, 1H), 6.84 (dt, *J* = 1.1, 7.4 Hz, 1H), 3.88 – 3.82 (m, 1H), 3.60 – 3.48 (m, 2H), 3.35 – 3.24 (m, 3H), 2.93 – 2.87 (m, 1H), 2.85 (s, 3H), 2.76 (dt, *J* = 4.0, 12.9 Hz, 1H), 2.33 (s, 3H), 1.74 (ddd, *J* = 7.3 Hz, 2H); **^{13}C-NMR** (125 MHz, $CDCl_3$): δ 169.0, 149.5, 148.0, 146.3, 145.1, 142.0, 139.6, 138.1, 132.4, 131.5, 130.4, 126.4, 126.0, 125.7, 125.6, 121.8, 121.4, 119.9, 119.6, 49.2, 48.5, 34.5, 33.5, 31.1, 26.1, 21.2; **IR** (neat film, cm^{-1}): 1765, 1553, 1537, 1475, 1367, 1351, 1200, 1165, 750, 736; **HRMS** (ESI): calcd. for $C_{26}H_{27}N_4O_8S$ $[M+H]^+$: 555.1550, obs. 555.1542.

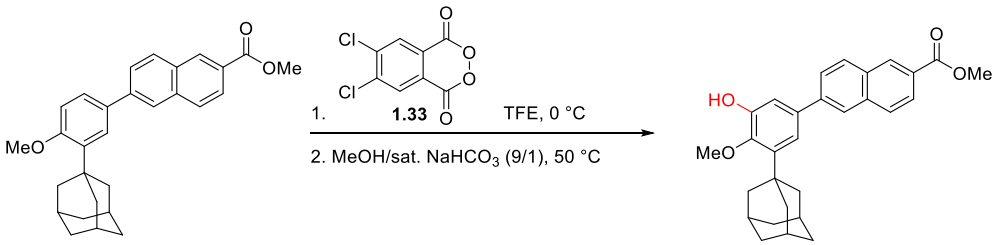

1.119
46%

Prepared using General Procedure A: A clear colorless solution of adapalene methylester (100 mg, 0.23 mmol, 1.0 equiv.) in TFE and $CHCl_3$ (9.4 mL, 1:1) was placed in an ice water bath cooled to 0 °C for 1 hour. Phthaloyl peroxide (46.0 mg, 0.28 mmol, 1.20 equiv.)

was added in 10 portions over 10 minutes changing the colorless solution to a dark brown mixture. After 2hrs the TFE and $CHCl_3$ were removed from the brown mixture by continuous positive flow of nitrogen. The black solid containing the mixed phthalate ester-acid was placed under an atmosphere of nitrogen and a deoxygenated mixture composed of methanol and aqueous saturated $NaHCO_3$ (9:1, 4.0 mL) was added. The brown solution was placed in an oil bath heated to 50 °C. After 12 hours the brown solution was removed from the oil bath, cooled to 23 °C, diluted with an aqueous phosphate buffer (10 mL, pH = 7, 0.2 M) and ethyl acetate (10 mL), poured into a separatory funnel, partitioned, and the organic layer was washed with an aqueous phosphate buffer (3 x 30 mL, pH = 7, 0.2 M). Residual organics were extracted from the aqueous layer with ethyl acetate (3 x 20 mL), combined, dried over solid sodium sulfate, filtered, and concentrated. The crude dark brown foam was purified by silica gel chromatography; hexane – 20% ethyl acetate in hexane and then purified again by silica gel chromatography; 12% 1,4-dioxane in hexane to afford the phenol **1.119** as a white solid (48.0 mg, 0.11 mmol, 46%).

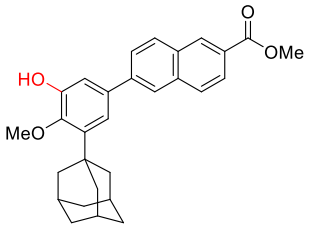

1.119

white solid, M.P. = 240 – 242 °C; **R_f** = 0.78 (silica gel, 40% 1,4-dioxane in hexane); **^{1}H-NMR** (400 MHz, $CDCl_3$): δ 8.62 (s, 1H), 8.07 (d, *J* = 8.6 Hz, 1H), 8.0 (s, 1H), 7.98 (d, *J* = 8.6 Hz, 1H), 7.91 (d, *J* = 8.6 Hz, 1H), 7.76 (d, *J* = 8.6 Hz, 1H), 7.20 (d, 2.0 Hz, 1H), 5.41 (bs, 1H), 3.99 (s, 3H), 3.90 (s, 3H), 2.15 (bs, 7H), 2.12 (bs, 2H), 1.81 (bs, 6H); **^{13}C-NMR** (100 MHz, $CDCl_3$): δ 167.3, 150.0, 147.3, 143.9, 141.0, 136.5, 135.8, 131.5, 130.8, 129.7, 128.3, 127.2, 126.4, 125.3, 118.2, 113.4, 61.4, 52.3, 41.8, 37.7, 36.9, 29.7, 29.1; **IR** (neat film, cm^{-1}): 3445, 1656.

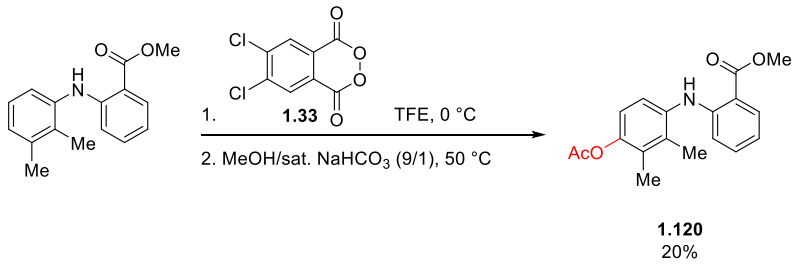

Prepared using General Procedure A: A clear colorless solution of mefenamic methyl ester (50.0 mg, 0.20 mmol, 1.0 equiv.) in TFE and methylene chloride (4.0 mL, 4:1) was placed in an ice water bath cooled to 0 °C for 30 minutes. Phthaloyl peroxide (71.0 mg, 0.43 mmol, 2.2 equiv.) was added in 5 portions over 5 minutes causing the solution to change to a dark black mixture. The mixture was allowed to warm gradually to 23 °C over 12 hours following which the TFE and methylene chloride were removed from the black mixture by continuous positive flow of nitrogen. The black solid tar was placed under an atmosphere of nitrogen and a deoxygenated mixture composed of methanol and aqueous saturated $NaHCO_3$ (9:1, 4.0 mL) was added. The black solution was placed in an oil bath heated to 50 °C. After 12 hours the black solution was removed from the oil bath, cooled to 23 °C, diluted with an aqueous phosphate buffer (10 mL, pH = 7, 0.2 M) and ethyl acetate (10 mL), poured into a separatory funnel, partitioned, and the organic layer was washed with an aqueous phosphate buffer (3 x 30 mL, pH = 7, 0.2 M). Residual organics were extracted from the aqueous layer with ethyl acetate (3 x 20 mL), combined, dried over solid sodium sulfate, decanted, and concentrated. The crude black tar was dissolved in methylene chloride (4.0 mL) upon which pyridine (155.0 mg, 0.2 mL, 1.96 mmol, 10.0 equiv.) and acetic anhydride (60.0 mg, 0.1 mL, 0.59 mmol, 3.0 equiv.) were added sequentially. After 24 h at 23 °C the dark brown solution was diluted with an aqueous phosphate buffer (10 mL, pH = 4, 0.2 M) and ethyl acetate (10 mL), poured into a separatory funnel, partitioned, and the organic layer was washed with an aqueous phosphate buffer (2 x 10 mL, pH = 7,

0.2 M). Residual organics were extracted from the aqueous layer with ethyl acetate (2 x 10 mL), dried over solid sodium sulfate, decanted, and concentrated. The crude dark brown foam was purified by silica gel chromatography; hexane – 2% ethyl acetate in hexane to afford the acetate **1.120** (12.3 mg, 0.04 mmol, 20%) as a golden yellow amorphous foam.

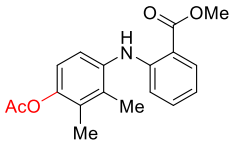

1.120

yellow foam; R_f = 0.59 (silica gel, 40% ethyl acetate in hexane); **^{1}H-NMR** (500 MHz, $CDCl_3$): δ 9.19 (bs, 1H), 7.95 (dd, *J* = 1.4, 7.1 Hz, 1H), 7.24 (m, 1H), 7.16 (d, *J* = 8.3 Hz, 1H), 6.88 (d, *J* = 8.3 Hz, 1H), 6.71 (dd, *J* = 1.1, 8.3 Hz, 1H), 6.66 (dt, *J* = 1.2, 5.9 Hz, 1H), 3.91 (s, 3H), 2.34 (s, 3H), 2.20 (s, 3H), 2.13 (s, 3H); **^{13}C-NMR** (125 MHz, $CDCl_3$): δ 169.6, 169.1, 149.4, 146.5, 136.6, 134.6, 134.2, 134.5, 130.1, 123.9, 119.8, 116.2, 113.7, 110.8, 51.7, 20.9, 14.6, 13.3; **IR** (neat film, cm^{-1}): 2918, 2360, 2340, 1760, 1703, 1252, 1195, 1090.

PREPARATION OF PHTHALOYL PEROXIDE IN FLOW EXPERIMENTAL SECTION

Construction of flow apparatus

1. Grind sodium percarbonate using a mortar and pestle. Use a 140 and 325 mesh sieve to filter particles corresponding to 46-105 μm. Ground sodium percarbonate can be stored for weeks with no loss of activity.
2. Insert a stainless steel frit inside the compression endcap bolt. Assemble the compression endcaps according to the diagram below. *Take care to not over-tighten the bolts as this will bend the ferrule, making disassembly difficult and may warp the tube*. We have found that as long as the tube is pressed tightly against the frit, the system will not leak regardless of whether the compression endcap turns under moderate force.
3. Add one pipette scoop-full of stainless steel spheres, corresponds to 0.5-0.6 grams of steel.
4. Fill the tube with ground sodium percarbonate, tapping the sides to ensure adequate packing, and leaving 3-6 mm of dead volume on the top. This corresponded to roughly 1.8-2.0 grams of sodium percarbonate.
5. Fill the remaining space with stainless steel spheres and tighten the endcap.
6. Install the inline check valve, BPR, and luer adapter.
7. After complete addition of the peroxide, the endcaps were removed carefully and the packed bed reactor was submerged in warm water to dissolve the remaining salts. After the salts had been dissolved, the tube was cleaned with water and acetone and dried in an oven (120 ^{0}C). The PFA tubing, BPR, check valve, and luer adapter were cleaned by flushing the system with methylene chloride and then air-dried.

General Flow Procedure

To a 10 mL graduated cylinder was added phthaloyl chloride (303 μL, 406 mg, 2 mmol). Anhydrous methylene chloride was added to bring the final volume to 10 mL, producing a 0.2 M solution. The flow apparatus was manually purged with anhydrous methylene chloride (1.4 mL dead volume). The solution of phthaloyl chloride was taken up into a 10 mL syringe and affixed to the luer port. A flow rate of 10 mL $hour^{-1}$ was dialed into the syringe pump. The first 3 mL (roughly twice the dead volume of the packed bed reactor) that passed through the apparatus was discarded. After 3 mL, the feed was connected through an inlet adapter to a 25mL 14/20 2-neck flask, adding the remaining 7mL of the peroxide solution (2.1 equivalents). To this flask was added 0.67 mmol of the substrate dissolved in 6.7 mL of TFE (0.1 M) and a stirbar. A distillation apparatus was affixed to the other opening. The flask was submerged in an oil bath warmed to 60 ^{0}C and followed by TLC.

Upon completion, the solvent was removed *in vacuo*, and diluted to 0.1 M with 9:1 dioxane: saturated aqueous sodium bicarbonate, sealed, and warmed to 50 ^{0}C for 12 hours to ensure complete hydrolysis of the mixed phthalate ester-acid. The contents of the flask were washed into a 60 mL seperatory funnel, and diluted with 10 mL of 0.2 M pH 7 phosphate buffer, and 20 mL of ethyl acetate. After the layers were separated, the organics were washed with additional pH 7 buffer (10 mL, twice). The combined aqueous layers were extracted with ether (10 mL, three times), and then dried over sodium sulfate. The organics were concentrated *in vacuo* and purified *via* silica gel flash chromatography.

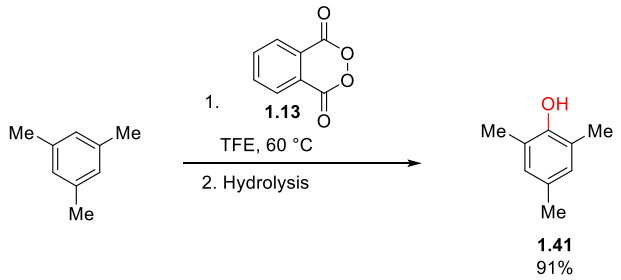

Prepared following General Flow Procedure. The reaction ran for 4 hours. After hydrolysis, the orange-brown oil was chromatographed on silica gel (10:1 hexanes: ethyl acetate) yielding **1.41** (83.2 mg, 0.611 mmol, 91%).

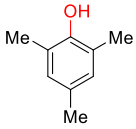

1.41

white solid, M.P. 106-107 ^{0}C; $\mathbf{R_f}$ = 0.24 (silica gel, 10:1 hexanes: ethyl acetate); **^{1}H-NMR** (400 MHz, $CDCl_3$): δ 6.79 (s, 2H), 4.43 (bs, 1H), 2.22 (s, 9H); **^{13}C-NMR** (100 MHz, $CDCl_3$): δ 149.8, 129.2, 129.0, 122.8, 20.3, 15.7; **IR** (KBr, film, υ cm $^{-1}$): 3391, 1485, 1201, 1150.[23]

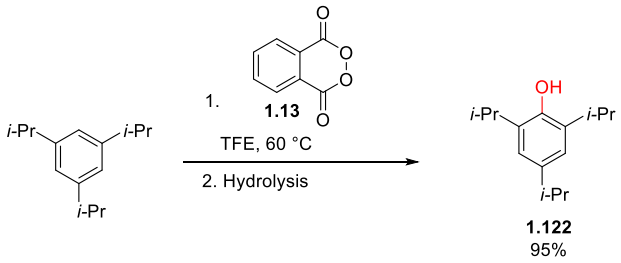

Prepared following General Flow Procedure. The reaction ran for 4 hours. After hydrolysis, the orange-brown oil was chromatographed on silica gel (15:1 hexanes: ethyl acetate) yielding **1.122** (140.5 mg, 0.638 mmol, 95%).

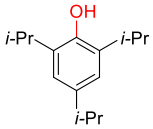

1.122

yellow oil; R_f = 0.26 (silica gel, 10:1 hexanes: ethyl acetate); **^{1}H-NMR** (400 MHz, $CDCl_3$): δ 6.91 (s, 2H), 4.62 (bs, 1H), 3.14 (sept, *J*= 7.0 Hz, 2H), 2.84 (sept, J= 7.0 Hz, 1H), 1.27 (d, *J*= 7.0 Hz, 12H), 1.24 (d, *J* = 7.0 Hz, 6H); **^{13}C-NMR** (100 MHz, $CDCl_3$): δ 147.9, 140.7, 133.3, 121.3, 33.8, 27.3, 24.3, 22.8; **IR** (KBr, film, υ cm $^{-1}$): 3571, 2960, 1470, 1200, 1154; **HRMS** (CI) calcd. for $C_{15}H_{24}O$: 220.1827, obs. 220.1828.

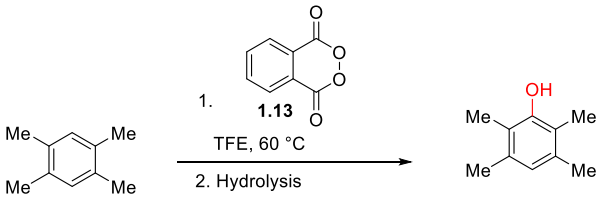

1.123
76%

Prepared following General Flow Procedure. The reaction ran for 6 hours. After hydrolysis, the orange-brown oil was chromatographed on silica gel (12:1 pentane: ether) yielding **1.123** (74.2 mg, 0.494 mmol, 74%).

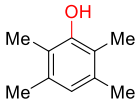

1.123

white solid, M.P. 106-107 ^{0}C**; R_f** = 0.23 (silica gel, 10:1 hexanes: ethyl acetate); **^{1}H-NMR** (400 MHz, $CDCl_3$): δ 6.60 (s, 1H), 4.59 (bs, 1H), 2.21 (s, 6H), 2.13 (s, 6H); **^{13}C-NMR** (100 MHz, $CDCl_3$): δ 151.7, 134.2, 123.5, 119.0, 19.8, 11.6; **IR** (KBr, film, υ cm $^{-1}$): 3351, 2919, 1180, 1125.[143]

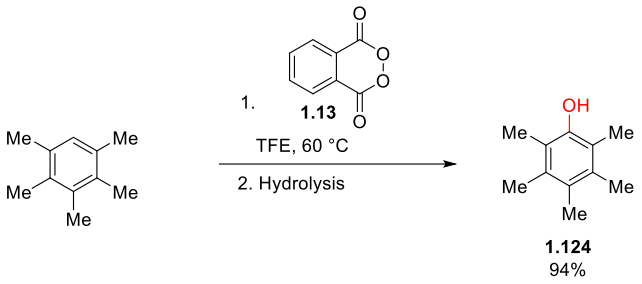

Prepared following General Flow Procedure. The reaction ran for 4 hours. After hydrolysis, the orange-brown oil was chromatographed on silica gel (10:1 hexanes: ethyl acetate) yielding **1.124** (103.2 mg, 0.628 mmol, 94%).

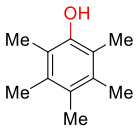

1.124

white solid, M.P. 123-124 ^{0}C; **R$_f$** = 0.20 (silica gel, 10:1 hexanes: ethyl acetate); **^{1}H-NMR** (400 MHz, $CDCl_3$): δ 4.50 (s, 1H), 2.21 (s, 6H), 2.20 (s, 6H), 2.18 (s, 3H); **^{13}C-NMR** (100 MHz, $CDCl_3$): δ 149.5, 132.9, 126.9, 118.9, 16.4, 16.3, 12.4; **IR** (KBr, film, υ cm $^{-1}$): 3343, 2916, 1384, 1125.[144]

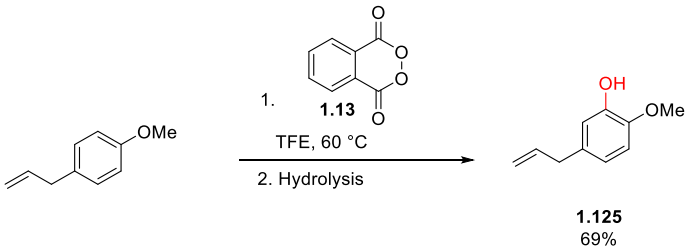

Prepared following General Flow Procedure. The reaction ran for 3 hours. After hydrolysis, the orange-brown oil was chromatographed on silica gel (10:1 hexanes: ethyl acetate) yielding **1.125** (76.3 mg, 0.465 mmol, 69%).

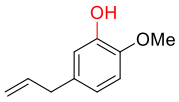

1.125

colorless oil; R_f = 0.24 (silica gel, 10:1 hexanes: ethyl acetate); **^{1}H-NMR** (400 MHz, $CDCl_3$): δ 6.79, (d, *J*= 8.1 Hz, 1H), 6.77 (d, *J*= 1.9 Hz, 1H), 6.66 (dd, *J*= 8.1, 1.9 Hz, 1H), 5.80-5.99 (m, 1H), 5.56 (s, 1H), 5.03-5.09 (m, 2H), 3.87 (s, 3H), 3.29 (d, *J*= 6.7 Hz, 2H); **^{13}C-NMR** (100 MHz, $CDCl_3$): δ 145.5, 144.9, 137.6, 133.4, 119.8, 115.5, 114.8, 110.6, 56.0, 39.6; **IR** (KBr, film, υ cm $^{-1}$): 3447, 1506, 1270, 1130; **HRMS** (ESI) calcd. for $C_{10}H_{12}O_2$ $[M+Na]^+$: 187.07300, obs. 187.07360.

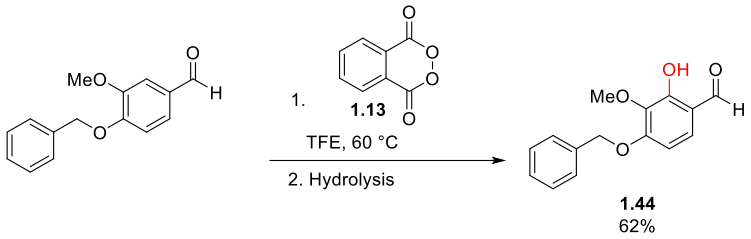

Prepared following General Flow Procedure. The reaction ran for 12 hours. An additional equivalent of peroxide (3.1 equivalents total) was added to ensure complete conversion of this substrate. After hydrolysis, the orange-brown oil was chromatographed on silica gel (10:1 to 5:1 pentane ether solvent gradient) yielding **1.44** (107.8 mg, 0.417 mmol, 62%).

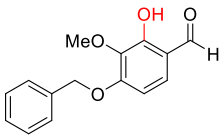

1.44

colorless oil; R_f = 0.14 (silica gel, 5:1 pentane: ether); **^{1}H-NMR** (400 MHz, $CDCl_3$): δ 11.20 (s, 1H), 9.73 (s, 1H), 7.34-7.44 (m, 5H), 7.23 (d, *J*= 8.4 Hz, 1H), 6.62 (d, *J*= 8.4 Hz, 1H), 5.24 (s, 2H), 3.93 (s, 3H); **^{13}C-NMR** (100 MHz, $CDCl_3$): δ 194.9, 158.5, 156.0, 136.6, 136.0, 130.0, 128.7, 128.3, 127.1, 116.6, 105.7, 70.8, 60.8; **IR** (KBr, film, υ cm $^{-1}$): 3255, 1652, 1520, 1452, 1388, 1264, 1102.[23]

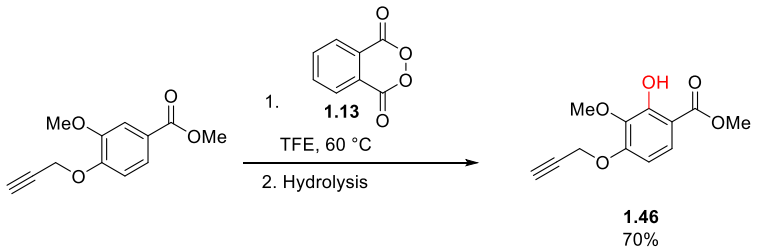

Prepared following General Flow Procedure. The reaction ran for 6 hours. After hydrolysis, the red-brown oil was chromatographed on silica gel (10:1 to 5:1 pentane: ether solvent gradient) yielding **1.46** (111.4 mg, 0.472 mmol, 70%).

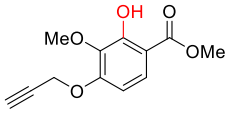

1.46

colorless oil; R_f = 0.29 (silica gel, 4:1 pentane: ether); **^{1}H-NMR** (400 MHz, $CDCl_3$): δ 10.94 (s, 1H), 7.59 (d, 9.0 Hz, 1H), 6.61 (d, *J*= 9.0 Hz, 1H), 4.81 (s, 2H), 3.93 (s, 3H), 3.90 (s, 3H), 2.53 (s, 1H); **^{13}C-NMR** (100 MHz, $CDCl_3$): δ 170.4, 156.2, 155.9, 137.3, 125.3, 107.8, 105.1, 77.9, 76.2, 60.8, 56.6, 52.2; **IR** (KBr, film, υ cm $^{-1}$): 3266, 1678, 1514, 1441, 1289, 1078.[23]

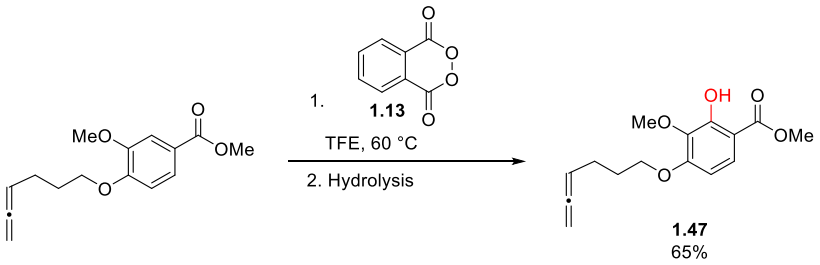

Prepared following General Flow Procedure. The reaction ran for 6 hours. After hydrolysis, the brown oil was chromatographed on silica gel (5:1 pentane: ether) yielding **1.47** (121.7 mg, 0.437 mmol, 65%).

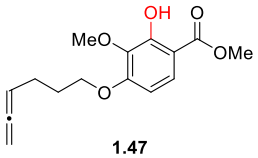

1.47

colorless oil; R_f = 0.21 (silica gel, 10:1 hexanes: ethyl acetate); **^{1}H-NMR** (400 MHz, $CDCl_3$): δ 10.88 (s, 1H), 7.56 (d, *J* = 9.2 Hz, 1H), 6.46 (d, *J* = 9.2 Hz, 1H), 5.16 (p, *J* = 6.7 Hz, 1H), 4.67-4.70 (dt, *J* = 6.7, 3.5 Hz, 2H), 4.11 (t, *J* = 6.7 Hz, 2H), 3.92 (s, 3H), 3.88 (s, 3H), 2.19-2.25 (m, 2H), 1.94-2.01 (p, *J* = 6.7 Hz, 2H); **^{13}C-NMR** (100 MHz, $CDCl_3$): δ 208.6, 170.4, 157.6, 156.1, 136.7, 125.6, 106.8, 104.2, 89.0, 75.4, 68.0, 60.7, 52.1, 28.3, 24.5; **IR** (KBr, film, υ cm $^{-1}$): 3270, 1677, 1282, 1092.[23]

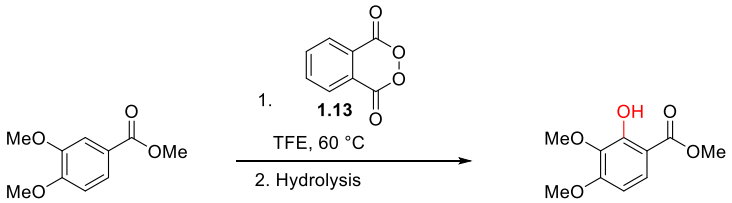

1.43
84%

Prepared following General Flow Procedure. The reaction ran for 6 hours. After hydrolysis, the red-brown oil was chromatographed on silica gel (2:1 pentane: ether) yielding the product (118.9 mg, 0.560 mmol, 84%).

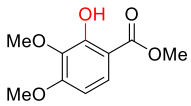

1.43

white solid, M.P. = 65-66^{0}C**; R_f** = 0.25 (silica gel, 2:1 pentane: ether); **^{1}H-NMR** (400 MHz, $CDCl_3$): δ 10.91 (s, 1H), 7.59 (d, *J*= 8.8 Hz, 1H), 6.48 (d, *J* = 8.8 Hz, 1H), 3.92 (s, 3H), 3.91 (s, 3H), 3.89 (s, 3H); **^{13}C-NMR** (100 MHz, $CDCl_3$): δ 170.4, 158.0, 155.9, 136.5, 125.7, 107.0, 103.1, 60.7, 56.0, 52.1; **IR** (KBr, film, υ cm $^{-1}$): 3172, 1678, 1439, 1285, 1090, 1033.[23]

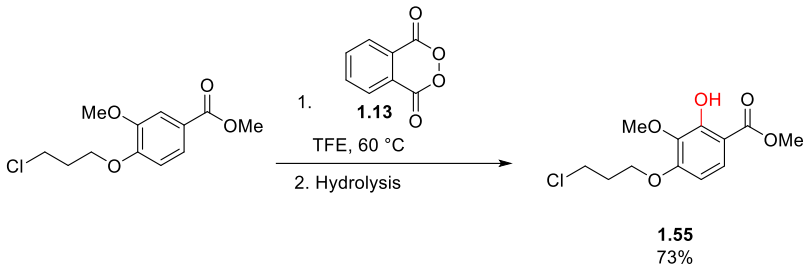

Prepared following General Flow Procedure. The reaction ran for 6 hours. After hydrolysis, the orange-brown oil was chromatographed on silica gel (10:1 hexanes: ethyl acetate) yielding **1.55** (134.8 mg, 0.491 mmol, 74%).

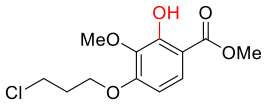

1.55

white solid, M.P. = 99-101 ^{0}C; $\mathbf{R_f}$ = 0.22 (silica gel, 5:1 pentane: ether); **^{1}H-NMR** (400 MHz, $CDCl_3$): δ 10.91 (s, 1H), 7.58 (d, *J*= 9.0 Hz, 1H), 6.49 (d, *J*= 9.0 Hz, 1H), 4.22 (t, *J*= 6.0 Hz, 2H), 3.92 (s, 3H), 3.87 (s, 3H), 3.78 (t, *J*= 6.0 Hz, 2H), 2.30 (p, *J*= 6.0 Hz, 2H); **^{13}C-NMR** (100 MHz, $CDCl_3$): δ 170.4, 157.3, 156.1, 136.8, 125.7, 107.2, 104.3, 65.2, 60.7, 52.2, 41.3, 32.0; **IR** (KBr, film, υ cm $^{-1}$): 3174, 1674, 1439, 1284, 1095.[23]

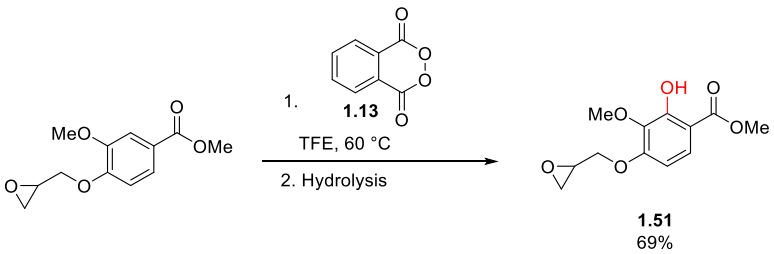

Prepared following General Flow Procedure. The reaction ran for 6 hours. After hydrolysis, the brown oil was chromatographed on silica gel (2:1 to 1:1 hexanes: ether solvent gradient) yielding **1.51** (117.3 mg, 0.461 mmol, 69%).

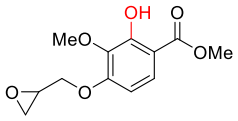

1.51

white solid, **M.P.** = 65-66 ^{0}C; **R$_f$** = 0.20 (silica gel, 1:1 hexanes: ethyl acetate); **^{1}H-NMR** (400 MHz, $CDCl_3$): δ 10.93 (s, 1H), 7.57 (d, *J*= 9.4 Hz, 1H), 6.49 (d, *J*= 9.4 Hz, 1H), 4.34 (dd, *J*= 11.3, 3.1 Hz, 1H), 4.07 (dd, *J*= 11.3, 5.9 Hz, 1H), 3.92 (s, 3H), 3.90 (s, 3H), 3.40 (m, 1H), 2.93 (t, *J*= 4.7 Hz, 1H), 2.78 (dd, *J*= 4.7, 2.7, 1H); **^{13}C-NMR** (100 MHz, $CDCl_3$): δ 170.4, 157.0, 156.2, 137.0, 125.5, 107.5, 104.7, 69.7, 60.7, 52.2, 50.0, 44.7; **IR** (KBr, film, υ cm $^{-1}$): 3194, 2930, 1673, 1439, 1283, 1092, 1032; **HRMS** (ESI) calcd. for $C_{12}H_{14}O_6$ $[M+H]^+$: 255.08630. Found: 255.08560.

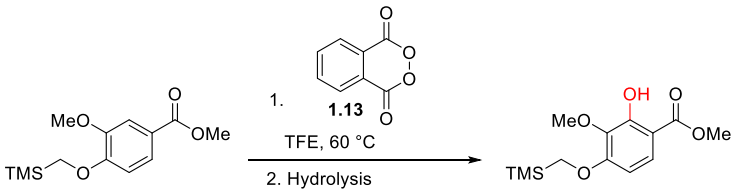

1.48
76%

Prepared following General Flow Procedure. The reaction ran for 6 hours. After hydrolysis, the orange oil was chromatographed on silica gel (10:1 to 7:1 pentane: ether solvent gradient) yielding **1.48** (145.7 mg, 0.512 mmol, 76%).

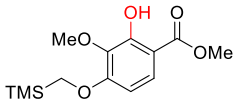

1.48

white solid, **M.P.** = 48-49 ^{0}C; **R$_f$** = 0.20 (silica gel, 7:1 pentane: ether); **^{1}H-NMR** (400 MHz, $CDCl_3$): δ 10.83 (s, 1H), 7.57 (d, *J*= 9.2 Hz, 1H), 6.58 (d, *J* = 9.2 Hz, 1H), 3.91 (s, 3H), 3.86 (s, 3H), 3.68 (s, 2H), 0.18 (s, 9H); **^{13}C-NMR** (100 MHz, $CDCl_3$): δ 170.5, 160.1, 155.8, 136.58, 125.5, 106.5, 103.6, 62.0, 60.5, 52.0, -3.0; **IR** (KBr, film, υ cm $^{-1}$): 3430, 1668, 1504, 1384, 1086, 1032; **HRMS** (ESI) calcd. for $C_{13}H_{20}O_5Si$ $[M+Na]^+$: 307.09720, obs. 307.09790.

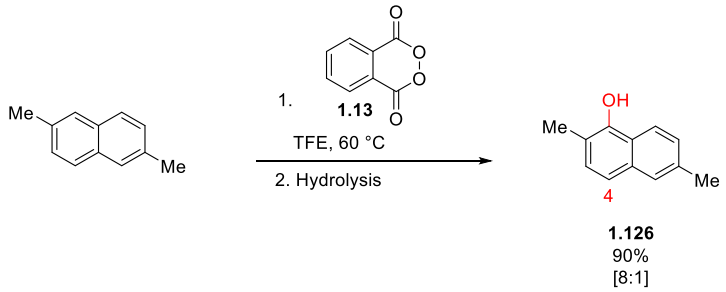

Prepared following General Flow Procedure. The reaction ran for 3 hours. After hydrolysis, the brown oil was chromatographed on silica gel (12:1 pentane: ether) yielding **1.126a** (94.4 mg, 0.548 mmol, 82%) as a solid that slowly decomposes. The regioisomer 3,7-dimethylnaphthal-1-ol (9.8 mg, 0.057 mmol, 9%) was also isolated.

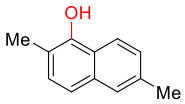

1.126a

white solid, M.P. 105-109 ^{0}C; **R$_f$** = 0.59 (silica gel, 10:1 hexanes: ethyl acetate); **^{1}H-NMR** (400 MHz, $CDCl_3$): δ 8.01 (d, *J*= 8.4 Hz, 1H), 7.54 (s, 1H), 7.30 (dd, *J*=1.6, 8.4 Hz, 1H), 7.29 (d, *J* = 8.4 Hz, 1H), 7.20 (d, *J*= 8.4 Hz, 1H), 5.13 (s, 1H), 2.50 (s, 3H), 2.40 (s, 3H); **^{13}C-NMR** (100 MHz, $CDCl_3$): δ 148.5, 134.9, 133.7, 129.0, 127.5, 126.6, 122.4, 120.7, 119.5, 115.3, 21.6, 15.6; **IR** (KBr, film, υ cm $^{-1}$): 3424, 1277, 1250.[23]

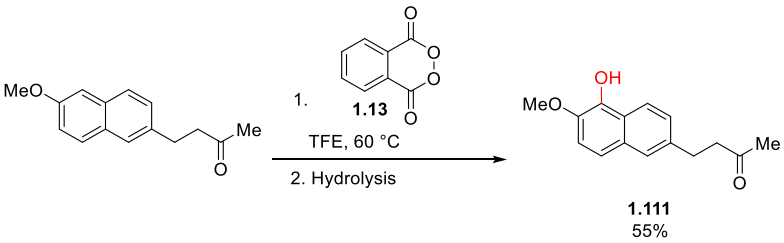

Prepared following General Flow Procedure. The reaction ran for 1 hour. After hydrolysis, the brown oil was chromatographed quickly on silica gel (3:1 hexanes: ethyl acetate)

yielding **1.111** (89.2 mg, 0.365 mmol, 55%) as a solid that decomposes in air. It was imperative to limit the time the product was exposed to silica gel.

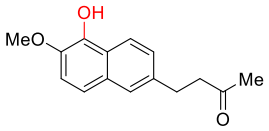

1.111

yellow solid, M.P. = 74-78 ^{0}C; **R$_f$** = 0.14 (silica gel, 3:1 hexanes: ethyl acetate); **^{1}H-NMR** (400 MHz, $CDCl_3$): δ 8.07 (d, *J* = 8.6 Hz, 1H), 7.52 (bs, 1H), 7.32 (d, *J* = 8.9 Hz, 1H), 7.28 (dd, *J* = 8.9, 2.1 Hz, 1H), 7.23 (d, *J* = 8.9 Hz, 1H), 5.99 (bs, 1H), 3.99 (s, 3H), 3.03 (t, *J* = 7.9 Hz, 2H), 2.83 (t, *J* = 7.9 Hz, 2H), 2.15 (s, 3H); **^{13}C-NMR** (100 MHz, $CDCl_3$): δ 208.1, 140.9, 139.7, 136.7, 129.7, 126.5, 125.9, 122.5, 121.5, 119.0, 113.5, 57.2, 45.1, 30.2, 29.8; **IR** (KBr, film, υ cm $^{-1}$): 3407, 2923, 1710, 1363, 1273; **HRMS** (CI) calcd. for $C_{15}H_{16}O_3$: 244.1099, obs. 244.1100.

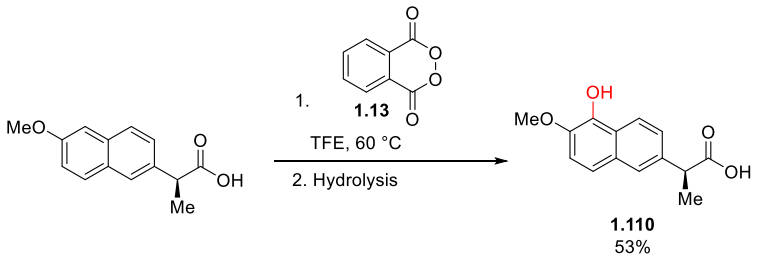

Prepared following General Flow Procedure. An additional equivalent of peroxide (3.1 equivalents total) was added to ensure complete conversion of this substrate. The reaction ran for 1 hour. Due to the carboxylic acid, the general workup procedure had to be modified. After complete hydrolysis, the reaction was poured into 0.2 M pH 2 phosphate buffer (20 mL) and adjusted to a pH of 4 using 1N NaOH solution. Ethyl acetate (20 mL) was added and the layers were separated, and the aqueous layer was extracted with additional ethyl acetate (20 mL, twice). The combined organics were dried over sodium sulfate. The brown oil was chromatographed quickly on silica gel (2:3 ether: hexanes + 1%

acetic acid) yielding **1.110** (87.6 mg, 0.356 mmol, 53%) as a solid that decomposes in air. It was imperative to limit the time the product was exposed to air on silica gel.

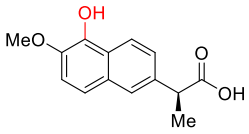

1.110

white solid, M.P. = 132-134 ^{0}C; **R$_f$** = 0.16 (silica gel, 2:3 ether: hexanes + 1% acetic acid); **^{1}H-NMR** (400 MHz, $CDCl_3$): δ 8.11 (d, *J* = 8.9 Hz, 1H), 7.66 (d, *J* = 1.4 Hz, 1H), 7.41 (dd, *J* = 8.9, 1.7 Hz, 1H), 7.36 (d, *J* = 8.9 Hz, 1H), 7.24 (d, *J* = 8.9 Hz, 1H), 5.99 (bs, 1H), 4.0 (s, 3H), 3.9 (q, J = 7.2 Hz, 1H), 1.59 (d, *J* = 7.2 Hz, 3H); **^{13}C-NMR** (125 MHz, $CDCl_3$): δ 179.5, 141.3, 139.7, 135.5, 129.5, 125.9, 125.2, 123.2, 121.9, 119.5, 113.6, 57.2, 45.2, 18.1; **IR** (KBr, film, υ cm $^{-1}$): 3433, 2937, 1704, 1275; **HRMS** (CI) calcd. for $C_{14}H_{14}O_4$: 246.0892, obs. 246.0894.

OXIDATIVE DEAROMATIZATION EXPERIMENTAL SECTION

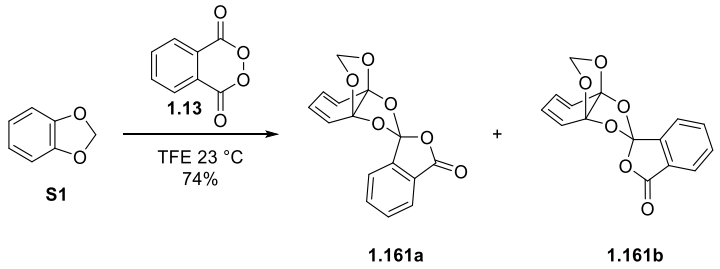

To a 25 mL round bottom flask was added neat **S1** (94 µL, 0.82 mmol, 1.0 equiv.) and trifluoroethanol (8.2 mL, 0.1 M). Solid phthaloyl peroxide (202 mg, 1.23 mmol, 1.5 equiv.) was added and the solution stirred for 30 minutes under argon at 23 ^{0}C. The solvent was removed *in vacuo* and the residue was taken up in ether (30 mL). The organic layer was washed with buffered aqueous ammonia solution (1:1 saturated aqueous sodium bicarbonate: saturated aqueous ammonium chloride, 30 mL, X 3), brine (30 mL), dried over sodium sulfate, filtered, and concentrated *in vacuo*. The resulting brown residue was purified by silica gel flash column chromatography (4:1 hexanes: ethyl acetate) yielding a mixture (**1.161a**: **1.161b**; 2.6: 1) of the two isomers (173 mg, 0.60 mmol, 74%).

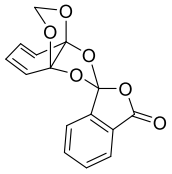

1.161a

white solid, **M.P. =** 134-136 ^{0}C; **R$_f$ =** 0.27 (silica gel, 3:1 hexanes: ethyl acetate); **^{1}H-NMR** (400 MHz, $CDCl_3$): δ 7.86 (d, *J* = 7.4 Hz, 1H), 7.69 (t, *J* = 7.4, Hz, 1H), 7.63 (t, *J* = 7.4 Hz, 1H), 7.35 (d, *J* = 7.4 Hz, 1H), 6.34 (m, 2H), 6.21 (m, 2H), 5.71 (s, 1H), 5.11 (s, 1H); **^{13}C-NMR** (100 MHz, $CDCl_3$): δ 165.3, 141.5, 134.9, 132.2, 127.6, 125.1, 124.0, 123.0, 122.9, 121.9, 107.7, 91.3; **IR** (KBr, film, υ cm $^{-1}$): 1793, 1468, 1222, 995, 967. **HRMS** (ESI) calcd. for $C_{15}H_{10}O_6$ $[M+Na]^+$: 309.03700, obs. 309.03780.

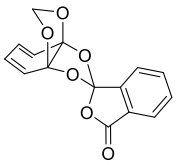

1.161b

white solid, **M.P. =** 154-155 ^{0}C; **R$_f$ =** 0.24 (silica gel, 3:1 hexanes: ethyl acetate); **^{1}H-NMR** (400 MHz, $CDCl_3$): δ 7.87 (m, *J* =1H), 7.75 (t, *J* = 7.4 Hz, 1H), 7.67- 7.69 (m, 2H), 6.30-6.32 (m, 2H), 6.23-6.26 (m, 2H), 5.34 (s, 1H), 5.20 (s, 1H); **^{13}C-NMR** (100 MHz, $CDCl_3$): δ 165.2, 140.7, 136.0, 134.8, 132.4, 128.1, 125.4, 124.2, 123.4, 122.7, 107.4, 89.8; **IR** (KBr, film, υ cm $^{-1}$): 1782, 1196, 1092, 898. **HRMS** (ESI) calcd. for $C_{15}H_{10}O_6$ $[M+Na]^+$: 309.03700, obs. 309.03730.

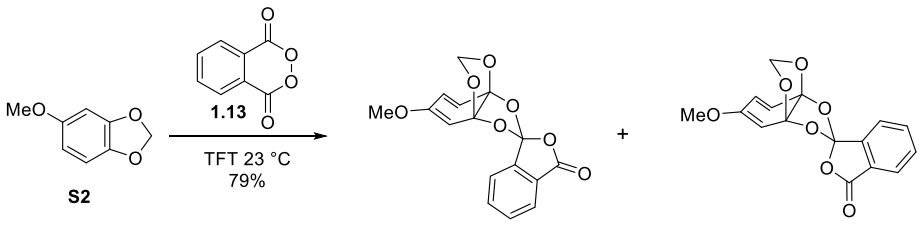

1.162a 1.162b

To a 10 mL round bottom flask was added neat **S2** (50 mg, 0.33 mmol, 1.0 equiv.) and trifluorotoluene (3.3 mL, 0.1 M). Solid phthaloyl peroxide (70 mg, 0.43 mmol, 1.2 equiv.) was added and the solution stirred for 30 minutes under argon at 23 ^{0}C. The solvent was removed *in vacuo* and the residue was taken up in ether (50 mL). The organic layer was washed with buffered aqueous ammonia solution (1:1 saturated aqueous sodium bicarbonate: saturated aqueous ammonium chloride, 30 mL, X 3), brine (30 mL), dried over sodium sulfate, filtered, and concentrated *in vacuo*. The resulting brown residue was purified by silica gel flash column chromatography (4:1 hexanes: ether) yielding a mixture (**1.162a**: **1.162b**; 3.5: 1) of the two isomers (82 mg, 0.26 mmol, 79%).

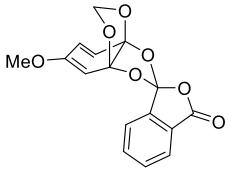

1.162a

white solid, **M.P. =** 138-140 ^{0}C; **R_f =** 0.2 (silica gel, 5:1 hexanes: ethyl acetate); **^{1}H-NMR** (400 MHz, $CDCl_3$): δ 7.87 (*J* =m, 1H), 7.70 (td, *J* = 7.4, 1.1 Hz, 1H), 7.63 (td, *J* = 7.4, 1.2 Hz, 1H), 7.38 (m, 1H), 6.33 (d, *J* = 10.2 Hz, 1H), 6.08 (dd, *J* = 10.2, 2.0 Hz, 1H), 5.73 (s, 1H), 5.34 (d, *J* = 2.0 Hz, 1H), 5.16 (s, 1H), 3.70 (s, 3H); **^{13}C-NMR** (100 MHz, $CDCl_3$): δ 165.4, 153.6, 141.6, 134.9, 132.1, 127.5, 125.04, 125.02, 124.6, 122.9, 122.1, 111.1, 107.4, 92.6, 92.0, 55.2; **IR** (KBr, film, υ cm $^{-1}$): 1794, 1410, 1094, 850. **HRMS** (ESI) calcd. for $C_{16}H_{12}O_7$ $[M+Na]^+$: 339.04750, obs. 339.04820.

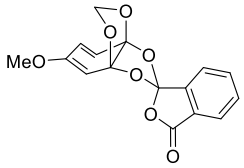

1.162b

white solid, **M.P. =** 121-123 ^{0}C; **R_f =** 0.16 (silica gel, 5:1 hexanes: ethyl acetate); **^{1}H-NMR** (400 MHz, $CDCl_3$): δ 7.86 (d, *J* = 7.2 Hz, 1H), 7.67-7.75 (m, 3H), 6.29 (d, *J* = 10.4 Hz, 1H), 6.09 (dd, *J* = 10.2, 2 Hz, 1H), 5.35 (s, 1H), 5.27 (d, *J* = 2.0 Hz, 1H), 5.24 (s, 1H), 3.70 (s, 3H); **^{13}C-NMR** (100 MHz, $CDCl_3$): δ 165.4, 154.4, 140.9, 134.8, 132.4, 128.1, 126.0, 125.3, 124.0, 122.7, 122.2, 110.8, 106.9, 91.8, 90.5, 55.2; **IR** (KBr, film, υ cm $^{-1}$): 1784, 1669, 1364, 1006, 905. **HRMS** (ESI) calcd. for $C_{16}H_{12}O_7$ $[M+Na]^+$: 339.04750, obs. 339.04830.

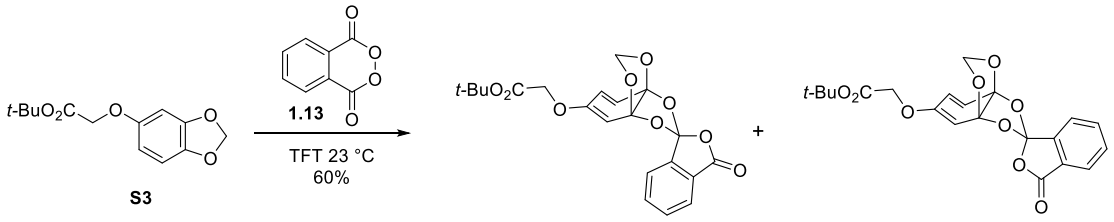

To a 4 mL vial was added neat **S3** (30 mg, 0.12 mmol, 1.0 equiv.) and trifluorotoluene (1.2 mL, 0.1 M). Solid phthaloyl peroxide (29 mg, 0.18 mmol, 1.5 equiv.) was added and the

solution stirred for 2 hours under argon at 23 ^{0}C. The solvent was removed *in vacuo* and the residue was taken up in ether (30 mL). The organic layer was washed with buffered aqueous ammonia solution (1:1 saturated aqueous sodium bicarbonate: saturated aqueous ammonium chloride, 30 mL, X 3), brine (30 mL), dried over sodium sulfate, filtered, and concentrated *in vacuo*. The resulting brown residue was purified by silica gel flash column chromatography (5:1 hexanes: ethyl acetate) yielding a mixture (**1.163a**: **1.163b**; 2.3: 1) of the two isomers (30 mg, 0.072 mmol, 60%).

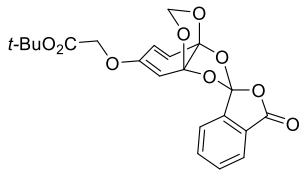

1.163a

white solid, **M.P. =** 157-159 ^{0}C; **R$_f$ =** 0.42 (silica gel, 3:1 hexanes: ethyl acetate); **^{1}H-NMR** (400 MHz, $CDCl_3$): δ 7.84 (d, *J* = 7.6 Hz, 1H), 7.7 (m, 1H), 7.63 (m, 1H), 7.39 (d, *J* = 7.6 Hz, 1H) 6.36 (d, *J* = 10.0 Hz, 1H), 6.19 (dd, *J* = 10.0, 2.0 Hz, 1H), 5.71 (s, 1H), 5.26 (d, *J* = 2.0 Hz, 1H) 5.16 (s, 1H), 4.37 (s, 2H), 1.48 (s, 9H); **^{13}C-NMR** (100 MHz, $CDCl_3$): δ 166.5, 165.3, 152.0, 141.6, 134.9, 132.1, 127.4, 125.97, 124.95, 124.5, 123.0, 122.2, 110.8, 107.28, 94.1, 92.0, 82.9, 65.3, 28.0; **IR** (KBr, film, υ cm $^{-1}$): 1792, 1751, 1521, 1394. **HRMS** (CI) calcd. for $C_{21}H_{21}O_9$: 417.1186, obs. 417.1187.

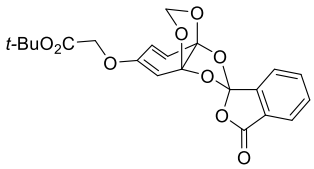

1.163b

colorless oil; **R$_f$ =** 0.35 (silica gel, 3:1 hexanes: ethyl acetate); **^{1}H-NMR** (400 MHz, $CDCl_3$): δ 7.86 (m, 1H), 7.75 (td, *J* = 7.4, 1.2 Hz, 1H), 7.65-7.69 (m, 2H), 6.32 (d, *J* = 10.2 Hz, 1H), 6.20 (dd, *J* = 10.2, 1.6 Hz, 1H), 5.38 (s, 1H), 5.23 (s, 1H), 5.21 (d, *J* = 1.6 Hz, 1H), 4.37 (d, *J* = 15.3 Hz, 1H), 4.35 (d, *J* = 15.3 Hz, 1H), 1.51 (s, 9H); **^{13}C-NMR** (100 MHz, $CDCl_3$): δ 166.5, 165.2, 152.7, 140.9, 134.8, 132.4, 128.1, 125.5, 125.3, 124.4, 122.6, 122.2, 110.5, 106.9, 93.4, 90.6, 82.8, 65.5, 28.0; **IR**

(KBr, film, υ cm $^{-1}$): 1785, 1751, 1368, 1155; **HRMS** (CI) calcd. for $C_{21}H_{21}O_9$: 417.1186, obs. 417.1186.

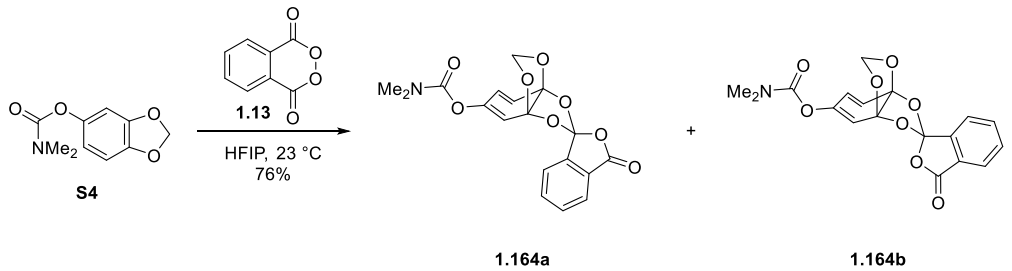

To a 4 mL vial was added **S19** (20 mg, 0.14 mmol, 1.0 equiv.) and hexafluoroisopropanol (1.4 mL, 0.1 M). Solid phthaloyl peroxide (24 mg, 0.14 mmol, 1.5 equiv.) was added and the solution stirred for 6 hours under argon at 23 ^{0}C. The solvent was removed *in vacuo* and the residue was taken up in ether (30 mL). The organic layer was washed with buffered aqueous ammonia solution (1:1 saturated aqueous sodium bicarbonate: saturated aqueous ammonium chloride, 30 mL, X 3), brine (30 mL), dried over sodium sulfate, filtered, and concentrated *in vacuo*. The resulting brown residue was purified by silica gel flash column chromatography (2: 1 to 1: 1 hexanes: ethyl acetate) yielding a mixture (**1.164a**: **1.164b**; 2.6: 1) of the two isomers (27 mg, 0.11 mmol, 76%).

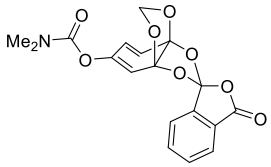

colorless oil, **R_f =** 0.35 (silica gel, 1:1 hexanes: ethyl acetate); **^{1}H-NMR** (400 MHz, $CDCl_3$): δ 7.83 (d, *J* = 7.6 Hz, 1H), 7.70 (t, *J* = 7.6 Hz, 1H), 7.62 (t, *J* = 7.6 Hz, 1H), 7.47 (d, *J* = 7.6 Hz, 1H), 6.34 (d, *J* = 10.3 Hz, 1H), 6.12 (dd, *J* = 10.3, 2.0 Hz, 1H), 6.09 (m, 1H), 5.70 (s, 1H), 5.17 (s, 1H), 3.04 (s, 3H), 3.00 (s, 3H); **^{13}C-NMR** (125 MHz, $CDCl_3$): δ 165.3, 153.5, 146.4, 141.6, 135.1, 132.1, 127.3, 124.9, 124.3, 124.3, 123.2,

122.3, 109.73, 109.70, 107.4, 92.0, 36.7, 36.5; **IR** (KBr, film, υ cm $^{-1}$): 1794, 1726, 1155, 896; **HRMS** (ESI) calcd. for $C_{18}H_{15}NO_8$ $[M+Na]^+$: 396.06900, obs. 396.06810.

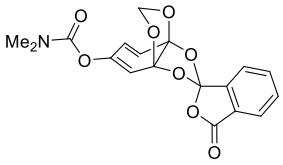

1.164b

colorless oil, **R_f =** 0.33 (silica gel, 1:1 hexanes: ethyl acetate); **^{1}H-NMR** (400 MHz, $CDCl_3$): δ 7.86 (dd, *J* = 7.6, 1 Hz, 1H), 7.75 (td, *J* = 7.6, 1.2, 1H), 7.65-7.69 (m, 2H), 6.31 (d, 10.2 Hz, 1H), 6.15 (dd, *J* = 10.2, 2 Hz, 1H), 6.12 (d, *J* = 2 Hz, 1H), 5.35 (s, 1H), 5.24 (s, 1H), 3.04 (s, 3H), 2.98 (s, 3H); **^{13}C-NMR** (100 MHz, $CDCl_3$): δ 165.3, 153.2, 146.6, 140.7, 134.8, 132.4, 128.1, 125.4, 125.3, 123.8, 122.7, 122.3, 109.4, 108.6, 107.0, 90.5, 36.6, 36.5; **IR** (KBr, film, υ cm $^{-1}$): 1785, 1727, 1154, 905; **HRMS** (ESI) calcd. for $C_{18}H_{15}NO_8$ $[M+Na]^+$: 396.06900, obs. 396.06550.

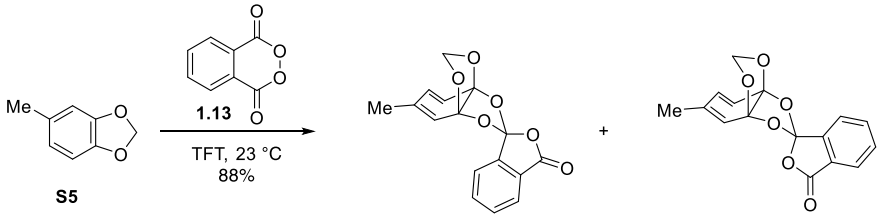

1.165a **1.165b**

To a 4 mL scintillation vial was added **S5** (30 mg, 0.22 mmol, 1.0 equiv.) and trifluorotoluene (2.2 mL, 0.1 M). Solid phthaloyl peroxide (43 mg, 0.26 mmol, 1.2 equiv.) was added and the solution stirred at 23 ^{0}C for 1 hour. The solvent was removed *in vacuo* and the residue was taken up in ethyl acetate (50 mL). The organic layer was washed with buffered aqueous ammonia solution (1:1 saturated aqueous sodium bicarbonate: saturated aqueous ammonium chloride, 30 mL, X 3), brine (30 mL), dried over sodium sulfate, filtered, and concentrated *in vacuo*. The orange residue was purified *via* silica gel

chromatography (5:1 to 3:1 hexanes: ethyl acetate) yielding a mixture (**1.165a**: **1.165b**; 8.3: 1) of the two isomers (58 mg, 0.19 mmol, 88%).

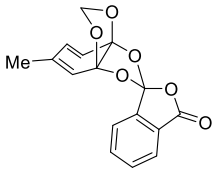

1.165a

colorless foam; R_f = 0.21 (silica gel, 5:1 hexanes: ethyl acetate); **^{1}H-NMR** (400 MHz, $CDCl_3$): δ 7.84 (m, 1H), 7.69 (td, *J* = 7.7, 1.2 Hz, 1H), 7.63 (td, *J* = 7.4, 1.2 Hz, 1H), 7.35 (m, 1H), 6.30 (d, *J* = 10.2 Hz, 1H), 6.04-6.07 (m, 2H), 5.71 (s, 1H), 5.11 (s, 1H), 1.99 (s, 3H); **^{13}C-NMR** (100 MHz, $CDCl_3$): δ 165.4, 141.6, 134.9, 132.1, 127.7, 127.6, 125.0, 123.4, 122.9, 122.0, 119.0, 108.8, 107.3, 91.6, 21.5; **IR** (KBr, film, υ cm $^{-1}$): 1794, 1283, 903, 850; **HRMS** (ESI) calcd. for $C_{16}H_{12}O_6$ $[M+Na]^+$: 323.05261, obs. 323.05291.

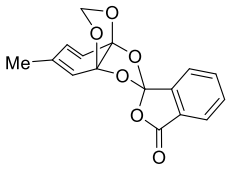

1.165b

colorless foam; R_f = 0.17 (silica gel, 5:1 hexanes: ethyl acetate); **^{1}H-NMR** (400 MHz, $CDCl_3$): δ 7.87 (m, 1H), 7.68 (m, 1H), 7.65-7.68 (m, 2H), 6.26 (d, *J* = 9.8 Hz, 1H), 6.07 (dd, *J* = 9.8, 1.1 Hz, 1H), 6.02 (m, 1H), 5.33 (s, 1H), 5.20 (s, 1H), 2.0 (s, 3H); **^{13}C-NMR** (100 MHz, $CDCl_3$): δ 165.4, 141.0, 134.8, 133.3, 132.3, 128.8, 128.1, 125.3, 122.8, 122.6, 122.2, 118.3, 108.5, 106.9, 90.1, 21.7; **IR** (KBr, film, υ cm $^{-1}$): 1784, 1284, 999, 902; **HRMS** (ESI) calcd. for $C_{16}H_{12}O_6$ $[M+Na]^+$: 323.05261, obs. 323.05305.

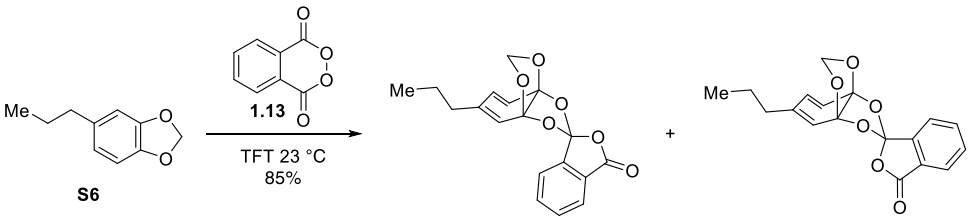

To a 4 mL scintillation vial was added **S6** (35 mg, 0.21 mmol, 1.0 equiv.) and trifluorotoluene (2.1 mL, 0.1 M). Solid phthaloyl peroxide (46 mg, 0.28 mmol, 1.5 equiv.) was added and the solution stirred at 23 ^{0}C for 30 minutes. The solvent was removed *in vacuo* and the residue was taken up in ether (30 mL). The organic layer was washed with buffered aqueous ammonia solution (1:1 saturated aqueous sodium bicarbonate: saturated aqueous ammonium chloride, 30 mL, X 3), brine (30 mL), dried over sodium sulfate, filtered, and concentrated *in vacuo*. The colorless residue was purified *via* silica gel chromatography (6:1 hexanes: ethyl acetate) yielding a mixture (**1.166a: 1.166b**; 6: 1) of the two isomers (60 mg, 0.18 mmol, 85%).

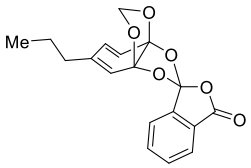

1.166a

white solid, **M.P. =** 131-132 ^{0}C; **R$_f$ =** 0.40 (silica gel, 6:1 hexanes: ethyl acetate); **^{1}H-NMR** (400 MHz, $CDCl_3$): δ 7.85 (m, 1H), 7.67 (td, *J* = 7.5, 1.2 Hz, 1H), 7.64 (td, *J* = 7.5, 1.2 Hz, 1H), 7.32 (m, 1H), 6.31 (d, *J* = 10.2 Hz, 1H), 6.10 (dd, *J* = 10.2, 1.2 Hz, 1H), 6.04 (m, 1H), 5.71 (s, 1H), 5.12 (s, 1H), 2.24-2.23 (m, 2H), 1.57 (sext, *J* = 7.4 Hz, 2H), 0.98 (t, *J* = 7.4 Hz, 3H); **^{13}C-NMR** (100 MHz, $CDCl_3$): δ 165.4, 141.6, 136.1, 134.9, 132.1, 127.5, 126.9, 125.0, 123.5, 112.8, 122.0, 118.4, 108.9, 107.5, 91.5, 37.1, 20.8, 13.5; **IR** (KBr, film, υ cm $^{-1}$): 1795, 1284, 1097, 1011, 851; **HRMS** (CI) calcd. for $C_{18}H_{16}O_6$: 328.0947, obs. 328.0945.

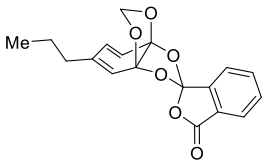

1.166b

colorless oil; **R$_f$ =** 0.27 (silica gel, 6:1 hexanes: ethyl acetate); **^{1}H-NMR** (400 MHz, $CDCl_3$): δ 7.86 (m, 1H), 7.74-7.73 (m, 1H), 7.68-7.66 (m, 2H), 6.27 (d, *J* = 10.4 Hz, 1H), 6.11 (dd, *J* = 10.4 and 1.2 Hz, 1H), 6.00 (m, 1H), 5.34 (s, 1H), 5.20 (s, 1H), 2.24-2.22 (m, 2H), 1.60-1.55 (m, 2H), 0.97 (t, *J* = 7.6 Hz, 3H); **^{13}C-NMR** (100 MHz,

$CDCl_3$): δ 165.3, 141.0, 137.3, 134.7, 132.3, 128.2, 128.1, 125.3, 122.9, 122.6, 122.2, 117.8, 108.5, 107.1, 90.1, 37.4, 20.7, 13.4; **IR** (KBr, film, υ cm^{-1}): 1784, 1411, 1284, 1057, 900, 855; **HRMS** (CI) calcd. for $C_{18}H_{16}O_6$: 328.0947, obs. 328.0948.

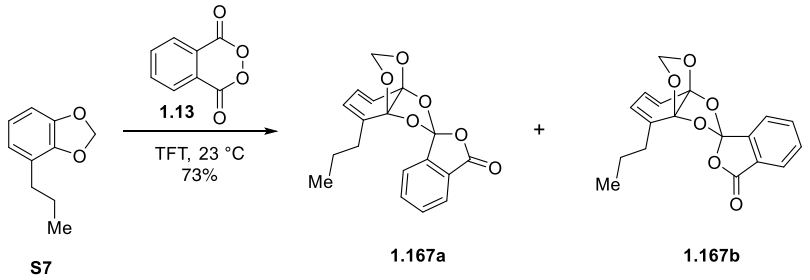

To a 4 mL scintillation vial was added **S7** (20 mg, 0.12 mmol, 1.0 equiv.) and trifluorotoluene (1.3 mL, 0.1 M). Solid phthaloyl peroxide (22 mg, 0.13 mmol, 1.1 equiv.) was added and the solution stirred at 23 ^{0}C for 2 hours. The solvent was removed *in vacuo* and the residue was taken up in ether (30 mL). The organic layer was washed with buffered aqueous ammonia solution (1:1 saturated aqueous sodium bicarbonate: saturated aqueous ammonium chloride, 30 mL, X 3), brine (30 mL), dried over sodium sulfate, filtered, and concentrated *in vacuo*. The colorless residue was purified *via* silica gel chromatography in (5:1 hexanes: ethyl acetate) yielding a mixture (**1.167a**: **1.167b**; 2.2 1) of the two isomers (29 mg, 0.089 mmol, 73%).

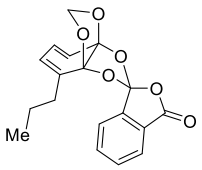

1.167a

colorless oil; R_f = 0.32 (silica gel, 5:1 hexanes: ethyl acetate); **^{1}H-NMR** (400 MHz, $CDCl_3$): δ 7.86 (m, 1H), 7.69 (td, *J* = 7.6, 1.1 Hz, 1H), 7.63 (td, *J* = 7.6, 1.1 Hz, 1H), 7.33 (m, 1H), 6.21 (dd, *J* = 9.8, 0.8 Hz, 1H), 6.16 (dd, *J* = 9.8, 5.9 Hz, 1H), 5.88 (m, 1H), 5.72 (s, 1H), 5.12 (s, 1H), 2.42 (t, *J* = 7.5 Hz, 2H), 1.61 (sext, *J* = 7.5 Hz, 2H), 0.94 (t, *J* = 7.5 Hz, 3H); **^{13}C-NMR** (100 MHz, $CDCl_3$): δ 165.4, 141.8, 138.0, 134.9, 132.1, 127.6, 125.0,

123.7, 122.8, 122.3, 121.2, 118.0, 109.8, 108.6, 91.8, 31.8, 20.8, 13.8; **IR** (KBr, film, υ cm $^{-1}$): 1791, 1360, 1283, 898, 851; **HRMS** (ESI) calcd. for $C_{18}H_{16}O_6$: 351.08390 $[M+Na]^+$, obs. 351.08480.

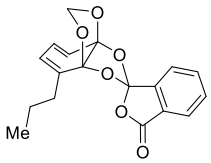

1.167b

colorless oil; R_f = 0.26 (silica gel, 5:1 hexanes: ethyl acetate); **^{1}H-NMR** (400 MHz, $CDCl_3$): δ 7.86 (m, 1H), 7.75 (m, 1H), 7.67-7.77 (m, 2H), 6.16-6.21 (m, 2H), 5.91-5.93 (m, 1H), 5.35 (s, 1H), 5.20 (s, 1H), 2.39 (m, 2H), 1.63 (sext, *J* = 7.5 Hz, 2H), 0.94 (t, *J* = 7.5 Hz, 3H); **^{13}C-NMR** (100 MHz, $CDCl_3$): δ 165.4, 140.9, 137.0, 134.8, 132.3, 128.2, 125.3, 124.9, 122.7, 122.1, 120.5, 119.2, 109.4, 108.3, 90.3, 31.9, 20.6, 13.8; **IR** (KBr, film, υ cm $^{-1}$): 1787, 1384, 899, 855; **HRMS** (ESI) calcd. for $C_{18}H_{16}O_6$ $[M+Na]^+$: 351.08390, obs. 351.08460.

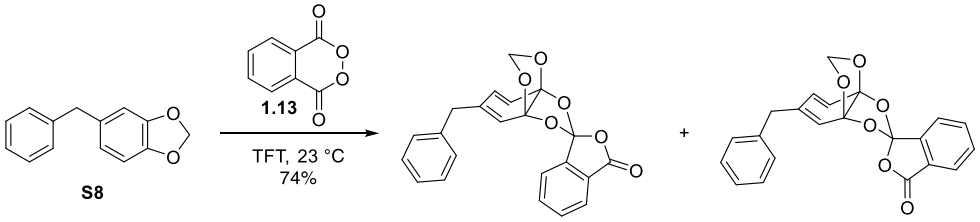

1.168a **1.168b**

To a 4 mL scintillation vial was added the **S8** (40 mg, 0.19 mmol, 1.0 equiv.) and trifluorotoluene (1.9 mL, 0.1 M). Solid phthaloyl peroxide (40 mg, 0.25 mmol, 1.3 equiv.) was added and the solution stirred at 23 ^{0}C for 18 hours. The solvent was removed *in vacuo* and the residue was taken up in ether (50 mL). The organic layer was washed with buffered aqueous ammonia solution (1:1 saturated aqueous sodium bicarbonate: saturated aqueous ammonium chloride, 30 mL, X 3), brine (30 mL), dried over sodium sulfate, filtered, and concentrated *in vacuo*. The resulting brown residue was purified by silica gel flash column

chromatography (5:1 hexanes: ethyl acetate) yielding a mixture (**1.168a**: **1.168b**; 2: 1) of the two isomers (53 mg, 0.14 mmol, 74%).

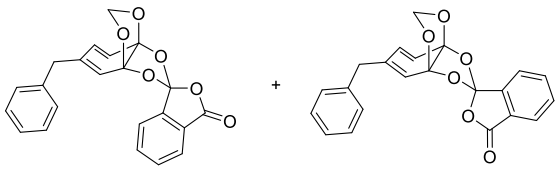

1.168a **1.168b**

pale yellow oil; **R_f =** 0.33 and 0.24 (silica gel, 5:1 hexanes: ethyl acetate); **^{1}H-NMR** (400 MHz, $CDCl_3$): δ [major isomer] 7.85 (d, *J* = 7.6, 1H), 7.67-7.70 (m, 3H), 7.34-7.21 (m, 5H), 6.28 (d, *J* =10.0 Hz, 1H), 6.11 (d, *J* =1.6 Hz, 1H), 6.04 (dd, *J* = 10.0, 1.6 Hz, 1H), 5.71 (s, 1H), 5.14 (s, 1H), 3.59 (s, 2H). [minor isomer] 7.38 (d, *J* = 7.6 Hz, 1H), 7.67-7.70 (m, 3H), 7.34-7.21 (m, 5H) 6.24 (d, *J* = 10.8 Hz, 1H), 6.11 (s, 1H), 6.03 (d, *J* =10.8 Hz, 1H), 5.35 (s, 1H), 5.22 (s, 1H), 3.61 (s, 2H); **^{13}C-NMR** (100 MHz, $CDCl_3$): δ 165.3, 165.2, 141.6, 140.8, 137.2, 137.1, 136.2, 135.2, 134.9, 134.7, 132.4, 132.1, 129.1, 129.0, 128.8, 128.7, 128.2, 127.6, 127.5, 126.9, 126.8, 126.5, 125.3, 125.1, 123.9, 123.2, 122.8, 122.7, 122.1, 122.0, 119.7, 119.5, 108.8, 108.4, 107.6, 107.1, 91.6, 90.2, 41.4, 41.4; **IR** (KBr, film, υ cm $^{-1}$): 1793, 1304, 1283, 902, 851; **HRMS** (CI) calcd. for $C_{22}H_{17}O_6$: 377.1025, obs. 377.1023.

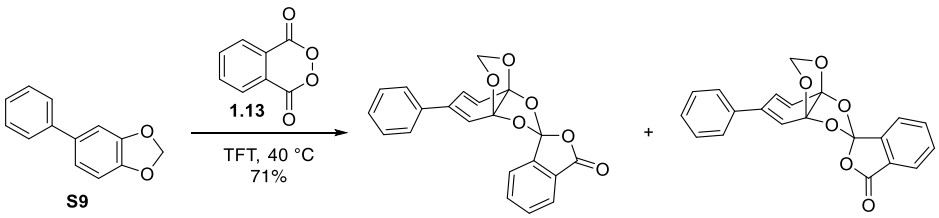

S9 **1.169a** **1.169b**

To a 4 mL scintillation vial was added **S9** (30 mg, 0.15 mmol, 1.0 equiv.) and trifluorotoluene (1.5 mL, 0.1 M). Solid phthaloyl peroxide (30 mg, 0.18 mmol, 1.2 equiv.) was added and the solution stirred at 40 ^{0}C for 6 hours. The solvent was removed *in vacuo*

and the residue was taken up in ethyl acetate (50 mL). The organic layer was washed with buffered aqueous ammonia solution (1:1 saturated aqueous sodium bicarbonate: saturated aqueous ammonium chloride, 30 mL, X 3), brine (30 mL), dried over sodium sulfate, filtered, and concentrated *in vacuo*. The orange residue was purified *via* silica gel chromatography (5:1 to 3:1 hexanes: ethyl acetate) yielding a mixture (**1.169a**: **1.169b**; 2.4: 1) of isomers (38 mg, 0.11 mmol, 71%).

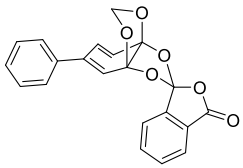

1.169a

white solid, **M.P. =** 163 ^{0}C; **R_f =** 0.46 (silica gel, 3:1 hexanes: ethyl acetate); **^{1}H-NMR** (400 MHz, $CDCl_3$): δ 7.86, (d, *J* =7.6 Hz, 1H), 7.61-7.70 (m, 2H), 7.35-7.48 (m, 6H), 6.61 (d, *J* =10.4 Hz, 1H), 6.47-6.49 (m, 2H), 5.79 (s, 1H), 5.18 (s, 1H); **^{13}C-NMR** (100 MHz, $CDCl_3$): δ 165.2, 141.3, 137.7, 135.2, 134.9, 132.1, 128.8, 128.7, 127.4, 126.3, 125.7, 124.9, 124.3, 122.9, 122.0, 119.0, 108.7, 107.4, 91.7; **IR** (KBr, film, υ cm $^{-1}$): 1795, 1368, 903, 852 ; **HRMS** (ESI) calcd. for $C_{21}H_{14}O_6$ $[M+Na]^+$: 385.06830. Found: 385.06840.

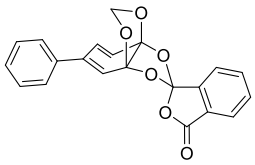

1.169b

white foam; **R_f =** 0.34 (silica gel, 3:1 hexanes: ethyl acetate); **^{1}H-NMR** (400 MHz, $CDCl_3$): δ 7.87 (d, *J* =7.6 Hz, 1H), 7.66-7.78 (m, 3H), 7.51 (m, 2H), 7.38-7.44 (m, 3H), 6.63 (dd, *J* = 10.0, 1.6 Hz, 1H), 6.44 (d, *J* =10.0 Hz, 1H), 6.41 (d, *J* = 1.6 Hz, 1H), 5.42 (s, 1H), 5.26 (s, 1H); **^{13}C-NMR** (100 MHz, $CDCl_3$): δ 165.2, 140.8, 138.0, 136.2, 134.8, 132.3, 128.7, 128.7, 128.0, 126.9, 126.4, 125.3, 123.7, 122.6, 122.2, 118.6, 108.3, 107.0, 90.3; **IR** (KBr, film, υ cm $^{-1}$): 1784, 1367, 903, 756; **HRMS** (ESI) calcd. For $C_{21}H_{14}O_6$ $[M+Na]^+$: 385.06830. Found: 385.06940.

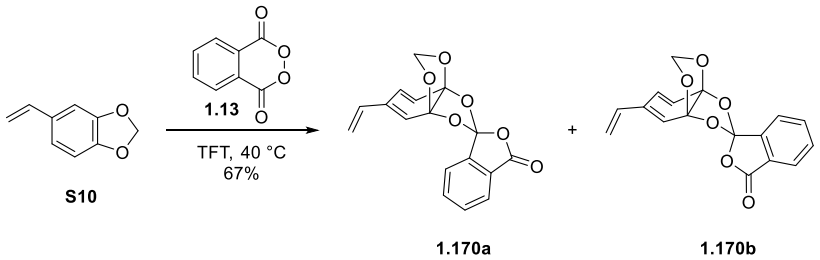

To a 4 mL vial was added **S10** (40 mg, 0.27 mmol, 1.0 equiv.) and trifluorotoluene (2.7 mL, 0.1 M). Solid phthaloyl peroxide (67 mg, 0.41 mmol, 1.5 equiv.) was added and the solution stirred for 6 hours under argon at 40 ^{0}C. The solvent was removed *in vacuo* and the residue was taken up in ethyl acetate (30 mL). The organic layer was washed with buffered aqueous ammonia solution (1:1 saturated aqueous sodium bicarbonate: saturated aqueous ammonium chloride, 30 mL, X 3), brine (30 mL), dried over sodium sulfate, filtered, and concentrated *in vacuo*. The resulting brown residue was purified by silica gel flash column chromatography (5:1 hexanes: ethyl acetate) yielding a mixture (**1.170a**: **1.170b**; 3.1: 1) of the two isomers (56 mg, 0.18 mmol, 67%).

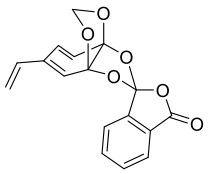

colorless oil; **R_f =** 0.24 (silica gel, 5:1 hexanes: ethyl acetate); **^{1}H-NMR** (400 MHz, $CDCl_3$): δ 7.80 (d, *J* = 7.0 Hz, 1 H), 7.67 (t, *J* = 7.0 Hz, 1H), 7.59 (t, *J* = 7.0 Hz, 1H), 7.31 (d, *J* = 7.0 Hz, 1H), 6.51 (d, *J* = 9.8 Hz, 1H), 6.42 (dd, *J* = 17.6, 10.9 Hz, 1H), 6.38 (d, *J* = 9.8 Hz, 1H), 6.16 (s, 1H), 5.71 (s, 1H), 5.62 (d, *J* = 17.6 Hz, 1H), 5.37 (d, *J* = 10.9 Hz, 1H), 5.11 (s, 1H); **^{13}C-NMR** (100 MHz, $CDCl_3$): δ 165.2, 141.4, 134.9, 134.8, 132.1, 131.9, 127.4, 125.0, 124.1, 122.9, 122.1, 121.6, 120.7, 117.6, 108.5, 107.7, 91.9; **IR** (KBr, film, υ cm $^{-1}$): 1794, 1368, 906, 852; **HRMS** (CI) calcd. For $C_{17}H_{12}O_6$: 335.05260. Found: 335.05300.

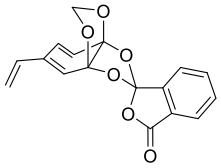

1.170b

colorless oil; **R_f =** 0.19 (silica gel, 5:1 hexanes: ethyl acetate); **^{1}H-NMR** (400 MHz, $CDCl_3$): δ 7.86 (m, 1H), 7.76 (td, *J* = 7.5, 1.1 Hz, 1H), 7.65-7.70 (m, 2H), 6.57 (dd, *J* = 10.1, 1.5 Hz, 1H), 6.44 (dd, *J* = 17.4, 11.0 Hz, 1H), 6.37 (d, *J* = 10.1 Hz, 1H), 6.15 (m, 1H), 5.63 (d, *J* = 17.4 Hz, 1H), 5.38 (m, 2H), 5.23 (s, 1H); **^{13}C-NMR** (100 MHz, $CDCl_3$): δ 165.3, 140.8, 135.0, 134.8, 132.9, 132.4, 128.1, 125.4, 123.5, 122.9, 122.7, 122.3, 120.2, 117.6, 108.3, 107.4, 90.5; **IR** (KBr, film, υ cm $^{-1}$): 1785, 1365, 1003, 905, 856; **HRMS** (CI) calcd. for $C_{17}H_{12}O_6$: 335.05260, obs. 335.05240.

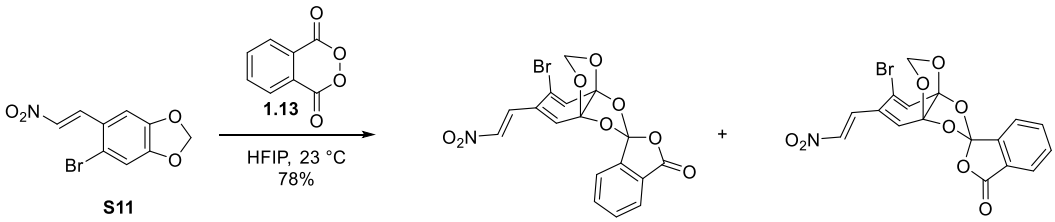

To a 4 mL scintillation vial was added **S11** (30 mg, 0.11 mmol, 1.0 equiv.) and hexafluoroisopropanol (1.1 mL, 0.1 M). Solid phthaloyl peroxide (33 mg, 0.17 mmol, 1.5 equiv.) was added and the solution stirred at 23 ^{0}C for 8 hours. The solvent was removed *in vacuo* and the residue was taken up in ethyl acetate (30 mL). The organic layer was washed with buffered aqueous ammonia solution (1:1 saturated aqueous sodium bicarbonate: saturated aqueous ammonium chloride, 30 mL, X 3), brine (30 mL), dried over sodium sulfate, filtered, and concentrated *in vacuo*. The orange residue was purified *via* silica gel chromatography (3:1 hexanes: ethyl acetate) yielding a mixture (**1.171a**: **1.171b**; 1.5: 1) of the two isomers (38 mg, 0.086 mmol, 78%).

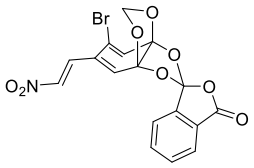

1.171a

white solid, **M.P. =** 168.170 ^{0}C; **R_f =** 0.41 (silica gel, 3:1 hexanes: ethyl acetate); **^{1}H-NMR** (400 MHz, $CDCl_3$): δ 8.02 (dd, *J* = 13.2, 1.2 Hz, 1H), 7.87 (m, 1H), 7.74 (td, *J* = 7.6, 1.2 Hz, 1H), 7.68 (td, *J* = 7.6, 1.2 Hz, 1H), 7.39 (m, 1H), 7.35 (d, *J* = 13.2 Hz, 1H), 6.89 (s, 1H), 6.62 (1H), 5.77 (s, 1H), 5.2 (s, 1H); **^{13}C-NMR** (100 MHz, $CDCl_3$): δ 164.7, 140.4, 140.2, 135.7, 135.1, 132.6, 128.4, 127.5, 127.0, 125.4, 124.4, 123.0, 122.0, 119.4, 108.1, 106.4, 92.8; **IR** (KBr, film, υ cm $^{-1}$): 1798, 1531, 1352, 1305; **HRMS** (CI) calcd. for $C_{17}H_{10}NO_8{}^{81}Br$: 436.9569, obs. 436.9568.

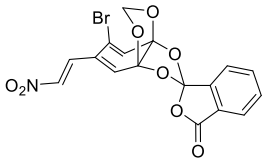

1.171b

yellow oil; **R_f =** 0.22 (silica gel, 1:1 hexanes: ethyl acetate); **^{1}H-NMR** (400 MHz, $CDCl_3$): δ 8.00 (dd, *J* = 13.2, 1.2, 1H), 7.89 (d, *J* = 7.6 Hz, 1H), 7.79 (td, *J* = 7.6, 1.2 Hz, 1H), 7.73 (td, *J* = 7.6, 1.2 Hz, 1H), 7.66 (m, 1H), 7.34 (d, *J* = 13.2 Hz, 1H), 6.84 (s, 1H), 6.57 (s, 1H), 5.38 (s, 1H), 5.27 (s, 1H); **^{13}C-NMR** (100 MHz, $CDCl_3$): δ 164.6, 140.3, 139.8, 136.0, 135.1, 132.8, 129.4, 127.9, 126.4, 125.6, 123.9, 122.7, 122.3, 120.3, 107.7, 106.0, 91.2; **IR** (KBr, film, υ cm $^{-1}$): 1788, 1530, 1366, 908, 858; **HRMS** (CI) calcd. for $C_{17}H_{10}NO_8{}^{81}Br$: 436.9569, obs. 436.9577.

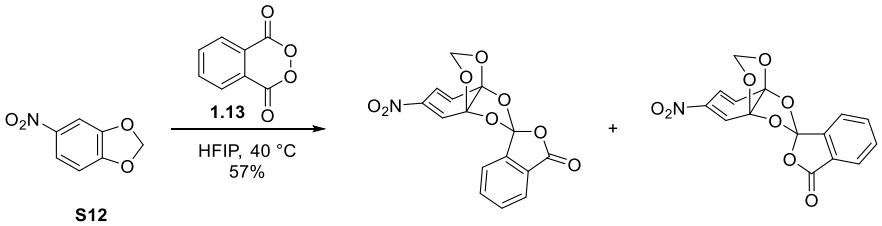

S12 1.172a 1.172b

To a 4 mL scintillation vial was added **S12** (50 mg, 0.30 mmol, 1.0 equiv.) and hexafluoroisopropanol (3.0 mL, 0.1 M). Solid phthaloyl peroxide (98 mg, 0.56 mmol, 2.0

equiv.) was added and the solution stirred at 40 ^{0}C for 24 hours. The solvent was removed *in vacuo* and the residue was taken up in ethyl acetate (50 mL). The organic layer was washed with buffered aqueous ammonia solution (1:1 saturated aqueous sodium bicarbonate: saturated aqueous ammonium chloride, 30 mL, X 3), brine (30 mL), dried over sodium sulfate, filtered, and concentrated *in vacuo*. The orange residue was purified *via* silica gel chromatography (5:1 to 3:1 hexanes: ethyl acetate) yielding a mixture (**1.172a**: **1.172b**; 1.4: 1) of the two isomers (56 mg, 0.17 mmol, 57%).

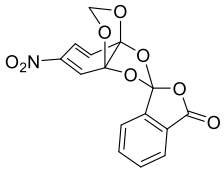

1.172a

white solid, **M.P. =** 73-75 ^{0}C; **R$_f$ =** 0.26 (silica gel, 3:1 hexanes: ethyl acetate); **^{1}H-NMR** (400 MHz, $CDCl_3$): δ 7.88 (m, 1H), 7.73 (td, *J* = 7.6, 1.2 Hz, 1H), 7.68 (td, *J* = 7.6, 1.2 Hz, 1H), 7.45 (dd, *J* = 2.0, 0.8 Hz, 1H), 7.35 (m, 1H), 6.98 (dd, *J* = 10.4, 2.0 Hz, 1H), 6.58 (dd, *J* = 10.4, 0.8 Hz, 1H), 5.81 (s, 1H), 5.20 (s, 1H); **^{13}C-NMR** (100 MHz, $CDCl_3$): δ 164.6, 145.7, 140.3, 135.2, 132.6, 127.4, 127.0, 125.3, 123.0, 122.7, 122.1, 117.2, 108.1, 107.7, 92.8; **IR** (KBr, film, υ cm $^{-1}$): 1793, 1541, 1284, 909.2; **HRMS** (CI) calcd. for $C_{15}H_{10}NO_8$: 332.0406, obs. 332.0400.

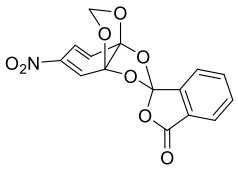

1.172b

white solid, **M.P. =** 153-154 ^{0}C; **R$_f$ =** 0.17 (silica gel, 3:1 hexanes: ethyl acetate); **^{1}H-NMR** (400 MHz, $CDCl_3$): δ 7.88 (m, 1H), 7.79 (td, *J* = 7.6, 1.2 Hz, 1H), 7.67-7.73 (m, 2H), 7.42 (dd, *J* = 2.0, 0.8 Hz, 1H) 7.01 (dd, *J* = 10.4, 2.0 Hz, 1H), 6.53 (dd, *J* = 10.4, 0.8 Hz, 1H), 5.42 (s, 1H), 5.30 (s, 1H); **^{13}C-NMR** (100 MHz, $CDCl_3$): δ 164.6, 145.7, 140.3, 135.2, 132.6, 127.4, 127.0, 125.3, 123.0, 122.7, 122.1, 117.2, 108.01, 107.87, 92.8; **IR** (KBr, film, υ cm $^{-1}$): 1795, 1634, 1405, 907; **HRMS** (CI) calcd. for $C_{15}H_{10}NO_8$: 332.0406, obs. 332.0398.

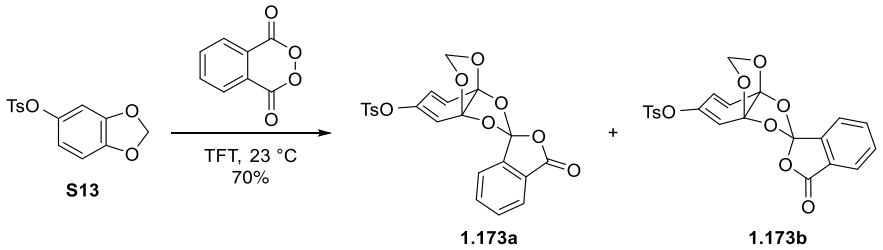

To a 4 mL scintillation vial was added **S13** (30 mg, 0.11 mmol, 1.0 equiv.) and trifluorotoluene (1.0 mL, 0.1 M). Solid phthaloyl peroxide (25 mg, 0.15 mmol, 1.5 equiv.) was added and the solution stirred at 23 ^{0}C for 14 hours. The solvent was removed *in vacuo* and the residue was taken up in ethyl acetate (30 mL). The organic layer was washed with buffered aqueous ammonia solution (1:1 saturated aqueous sodium bicarbonate: saturated aqueous ammonium chloride, 30 mL, X 3), brine (30 mL), dried over sodium sulfate, filtered, and concentrated *in vacuo*. The orange residue was purified *via* silica gel chromatography (2:1 hexanes: ethyl acetate) yielding a mixture (**1.173a**: **1.173b**; 1.3: 1) of the two isomers (33 mg, 0.072 mmol, 70%).

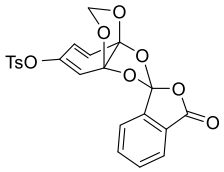

white solid, **M.P. =** 51-52 ^{0}C; **R$_f$ =** 0.40 (silica gel, 2:1 hexanes: ethyl acetate); **^{1}H-NMR** (400 MHz, $CDCl_3$): δ 7.84 (d, *J* = 7.4 Hz, 1H), 7.82 (d, *J* = 8.3 Hz, 2H), 7.73 (m, 1H), 7.66 (m, 1H), 7.36 (d, *J* = 8.3 Hz, 2H), 7.32 (d, *J* = 7.4 Hz, 1H), 6.35 (d, *J* = 10.2 Hz, 1H), 6.09 (dd, *J* = 10.2, 2.0 Hz, 1H), 5.89 (d, *J* = 2.0 Hz, 1H), 5.65 (s, 1H), 5.11 (s, 1H), 2.45 (s, 3H); **^{13}C-NMR** (100 MHz, $CDCl_3$): δ 165.0, 146.2, 145.0, 141.1, 135.0, 132.4, 132.0, 130.0, 128.4, 127.4, 125.9, 125.1, 123.2, 122.8, 122.0, 112.4, 109.0, 107.2, 92.1, 21.7; **IR** (KBr, film, υ cm $^{-1}$): 1795, 1667, 1405, 898, 850; **HRMS** (ESI) calcd. for $C_{22}H_{16}O_9S$ $[M+Na]^+$: 479.04070, obs. 479.04080.

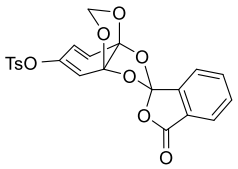

1.173b

white solid, **M.P. =** 147-148 ^{0}C; **R$_f$ =** 0.36 (silica gel, 2:1 hexanes: ethyl acetate); **^{1}H-NMR** (400 MHz, $CDCl_3$): δ 7.88-7.93 (m, 3H), 7.76 (m, 1H), 7.70 (t, *J* = 7.4 Hz, 1H), 7.64 (d, *J* = 7.4 Hz, 1H), 7.42 (d, *J* = 8.6 Hz, 2H), 6.25 (d, *J* = 11.0 Hz, 1H), 5.93-5.96 (m, 2H), 5.30 (s, 1H), 5.21 (s, 1H), 2.45 (s, 3H); **^{13}C-NMR** (100 MHz, $CDCl_3$): δ 164.8, 146.0, 145.6, 140.3, 134.9, 132.6, 131.6, 130.2, 129.9, 128.8, 128.1, 125.4, 125.3, 124.1, 122.7, 112.5, 108.6, 106.8, 90.6, 21.8; **IR** (KBr, film, υ cm $^{-1}$): 1788, 1363, 910, 856; **HRMS** (ESI) calcd. for $C_{22}H_{16}O_9S$ $[M+Na]^+$: 479.04070, obs. 479.04090.

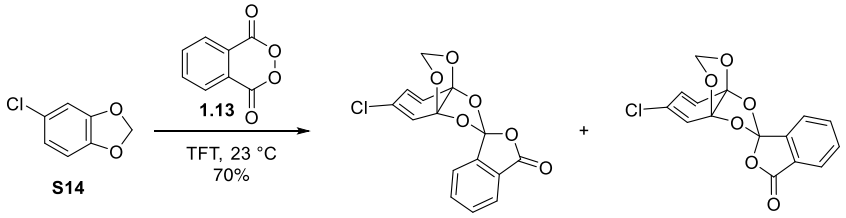

To a 4 mL vial was added **S14** (20 mg, 0.13 mmol, 1.0 equiv.) and trifluorotoluene (1.3 mL, 0.1 M). Solid phthaloyl peroxide (31 mg, 0.19 mmol, 1.5 equiv.) was added and the solution stirred for 9 hours under argon at 23 ^{0}C. The solvent was removed *in vacuo* and the residue was taken up in ether (30 mL). The organic layer was washed with buffered aqueous ammonia solution (1:1 saturated aqueous sodium bicarbonate: saturated aqueous ammonium chloride, 30 mL, X 3), brine (30 mL), dried over sodium sulfate, filtered, and concentrated *in vacuo*. The resulting brown residue was purified by silica gel flash column chromatography (5:1 hexanes: ethyl acetate) yielding a mixture (**1.174a**: **1.174b**; 1.3: 1) of the two isomers (29 mg, 0.090 mmol, 70%).

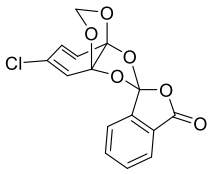

1.174a

white solid, **M.P. =** 127-128 ^{0}C; **R$_f$ =** 0.26 (silica gel, 5:1 hexanes: ethyl acetate); **^{1}H-NMR** (400 MHz, $CDCl_3$): δ 7.85 (d, *J* = 7.4 Hz, 1H), 7.72 (td, *J* = 7.4, 1.2 Hz, 1H), 7.65 (td, *J* = 7.4, 1.2 Hz, 1H), 7.39 (dd, *J* = 7.4, 1.2 Hz, 1H), 6.43 (dd, 1.6, 0.8 Hz, 1H), 6.37 (dd, *J* = 9.8, 0.8 Hz, 1H), 6.17 (dd, *J* = 9.8, 1.6 Hz, 1H), 5.73 (s, 1H), 5.15 (s, 1H); **^{13}C-NMR** (100 MHz, $CDCl_3$): δ 165.0, 141.0, 135.0, 132.4, 130.7, 127.5, 126.5, 125.2, 125.1, 123.0, 122.0, 120.1, 108.8, 106.8, 92.2; **IR** (KBr, film, υ cm $^{-1}$): 1801, 1364, 1283, 873; **HRMS** (CI) calcd. for $C_{15}H_{10}O_6{}^{35}Cl$: 321.0166, obs. 321.0167.

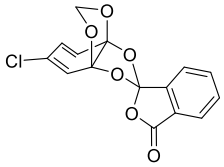

1.174b

white solid, **M.P. =** 157-158 ^{0}C; **R$_f$ =** 0.18 (silica gel, 5:1 hexanes: ethyl acetate); **^{1}H-NMR** (400 MHz, $CDCl_3$): δ 7.88 (d, *J* = 7.5 Hz, 1H), 7.77 (t, *J* = 7.5 Hz, 1H), 7.66-7.7.71 (m, 2H), 6.39 (s, 1H), 6.33 (d, *J* = 9.9 Hz, 1H), 6.20 (d, *J* = 9.9 Hz, 1H), 5.35 (s, 1H), 5.24 (s, 1H); **^{13}C-NMR** (100 MHz, $CDCl_3$): δ 165.0, 140.3, 134.9, 132.6, 131.6, 128.0, 127.7, 125.5, 124.6, 122.7, 122.2, 119.6, 108.4, 106.4, 90.6; **IR** (KBr, film, υ cm $^{-1}$): 1789, 1284, 907; **HRMS** (CI) calcd. for $C_{15}H_9O_6{}^{35}Cl$: 320.0088, obs. 320.0092.

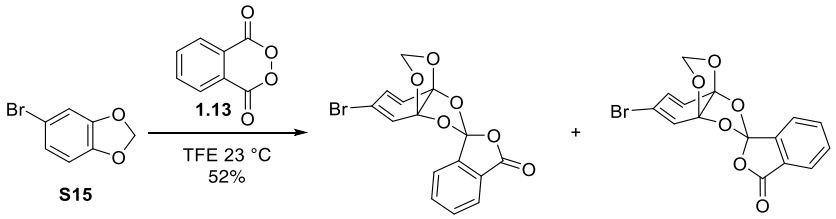

To a 4 mL scintillation vial was added **S15** (40 mg, 0.20 mmol, 1.0 equiv.) and trifluoroethanol (2.0 mL, 0.1 M). Solid phthaloyl peroxide (49 mg, 0.30 mmol, 1.5 equiv.) was added and the solution stirred at 23 ^{0}C for 18 hours. The solvent was removed *in vacuo*

and the residue was taken up in ether (30 mL). The organic layer was washed with buffered aqueous ammonia solution (1:1 saturated aqueous sodium bicarbonate: saturated aqueous ammonium chloride, 30 mL, X 3), brine (30 mL), dried over sodium sulfate, filtered, and concentrated *in vacuo*. The orange residue was purified *via* silica gel chromatography (6:1 hexanes: ethyl acetate) yielding a mixture (**1.175a**: **1.175b**; 1.2: 1) of the two isomers (38 mg, 0.10 mmol, 52%).

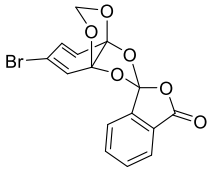

1.175a

white solid, **M.P. =** 148-150 ^{0}C; **R_f =** 0.42 (silica gel, 6:1 hexanes: ethyl acetate); **^{1}H-NMR** (400 MHz, $CDCl_3$): δ 7.86 (dd, *J* = 7.6, 1.2 Hz, 1H), 7.72 (td, *J* = 7.6, 1.2 Hz, 1H), 7.66 (td, *J* = 7.6, 1.2 Hz, 1H), 7.40 (m, 1H), 6.67 (m, 1H), 6.29 (m, 2H), 5.72 (s, 1H), 5.15 (s, 1H); **^{13}C-NMR** (100 MHz, $CDCl_3$): δ 165.0, 141.0, 135.0, 132.4, 128.3, 127.5, 125.2, 124.8, 124.1, 123.0, 122.0, 119.4, 109.0, 106.5, 92.1; **IR** (KBr, film, υ cm $^{-1}$): 1798, 1297, 1242, 1056, 853; **HRMS** (ESI) calcd. for $C_{15}H_9{}^{81}BrO_6$ $[M+Na]^+$: 388.95460, obs. 388.94520.

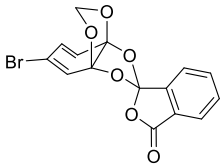

1.175b

white solid, **M.P. =** 162-164 ^{0}C; **R_f =** 0.22 (silica gel, 6:1 hexanes: ethyl acetate); **^{1}H-NMR** (400 MHz, $CDCl_3$): δ 7.88 (d, *J* = 7.6 Hz, 1H), 7.76 (td, *J* = 7.6, 1.2 Hz, 1H), 7.71-7.65 (m, 2H), 6.62 (s, 1H), 6.32 (dd, *J* = 10.0, 1.6 Hz, 1H), 6.25 (m, 1H), 5.34 (s, 1H), 5.23 (s, 1H); **^{13}C-NMR** (100 MHz, $CDCl_3$): δ 165.0, 140.3, 134.9, 132.6, 129.4, 128.1, 125.5, 124.2, 123.5, 122.7, 122.2, 120.3, 108.6, 106.1, 90.6; **IR** (KBr, film, υ cm $^{-1}$): 1788, 1365, 1283, 1096, 905, 856; **HRMS** (ESI) calcd. for $C_{15}H_9{}^{81}BrO_6$ $[M+Na]^+$: 388.94560, obs. 388.94570.

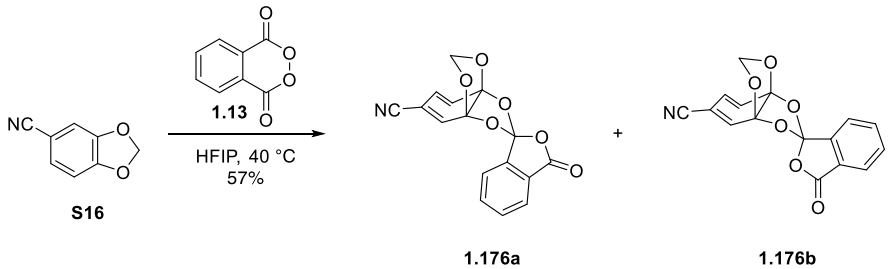

To a 4 mL scintillation vial was added **S16** (50 mg, 0.30 mmol, 1.0 equiv.) and hexafluoroisopropanol (3.0 mL, 0.1 M). Solid phthaloyl peroxide (98 mg, 0.56 mmol, 2.0 equiv.) was added and the solution stirred at 40 ^{0}C for 24 hours. The solvent was removed *in vacuo* and the residue was taken up in ethyl acetate (50 mL). The organic layer was washed with buffered aqueous ammonia solution (1:1 saturated aqueous sodium bicarbonate: saturated aqueous ammonium chloride, 30 mL, X 3), brine (30 mL), dried over sodium sulfate, filtered, and concentrated *in vacuo*. The orange residue was purified *via* silica gel chromatography (5:1 to 3:1 hexanes: ethyl acetate) yielding a mixture (**1.176a**: **1.176b**; 2.7: 1) of the two isomers (56 mg, 0.17 mmol, 57%).

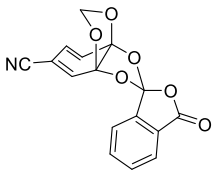

1.176a

white solid, **M.P. =** 60 ^{0}C; **R$_f$ =** 0.32 (silica gel, 4:1 hexanes: ethyl acetate); **^{1}H-NMR** (400 MHz, $CDCl_3$): δ 7.88 (m, 1H), 7.75 (td, *J* =7.2, 0.8 Hz, 1H), 7.69 (td, *J* =7.2, 0.8 Hz, 1H), 7.35 (m, 1H), 6.95 (d, *J* =1.2 Hz, 1H), 6.54 (d, *J* =10.0 Hz, 1H), 6.22 (dd, *J* =10.0, 1.2 Hz, 1H), 5.76 (s, 1H), 5.16 (s, 1H); **^{13}C-NMR** (100 MHz, $CDCl_3$): δ 164.7, 140.5, 135.2, 134.1, 132.6, 127.5, 126.6, 125.3, 122.9, 121.9, 120.4, 116.2, 110.7, 106.9, 106.1, 92.4; **IR** (KBr, film, υ cm $^{-1}$): 2360, 2340, 1794, 1284, 909, 896; **HRMS** (ESI) calcd. for $C_{16}H_9NO_6$ $[M+Na]^+$: 334.03220, obs. 334.03250.

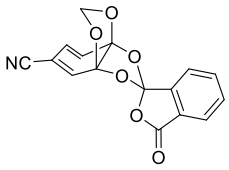

1.176b

white solid, **M.P. =** 148 ^{0}C; **R_f =** 0.17 (silica gel, 4:1 hexanes: ethyl acetate); **^{1}H-NMR** (400 MHz, $CDCl_3$): δ 7.89 m, 1H), 7.78 (t, *J* =7.6 Hz, 1H), 7.66-7.72 (m, 2H), 6.91 (s, 1H), 6.48 (d, *J* = 9.2 Hz, 1H), 6.24 (d, *J* = 9.2 Hz, 1H), 5.38 (s, 1H), 5.25 (s, 1H); **^{13}C-NMR** (100 MHz, $CDCl_3$): δ 164.6, 139.8, 135.0, 133.7, 132.8, 128.0, 126.0, 125.6, 122.7, 122.1, 121.7, 116.3, 111.6, 106.5, 105.7, 90.8; **IR** (KBr, film, υ cm $^{-1}$): 2360, 2341, 1789, 906; **HRMS** (ESI) calcd. for $C_{16}H_9NO_6$ $[M+Na]^+$: 334.03220, obs. 334.03210.

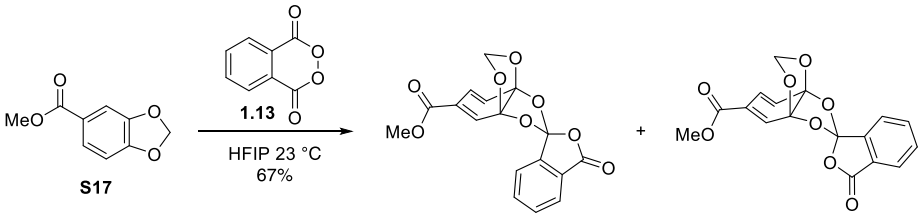

1.177a 1.177b

To a 4 mL scintillation vial was added **S17** (25 mg, 0.14 mmol, 1.0 equiv.) and hexafluoroisopropanol (1.4 mL, 0.1 M). Solid phthaloyl peroxide (34 mg, 0.21 mmol, 1.5 equiv.) was added and the solution stirred at 23 ^{0}C for 13 hours. The solvent was removed *in vacuo* and the residue was taken up in ethyl acetate (30 mL). The organic layer was washed with buffered aqueous ammonia solution (1:1 saturated aqueous sodium bicarbonate: saturated aqueous ammonium chloride, 30 mL, X 3), brine (30 mL), dried over sodium sulfate, filtered, and concentrated *in vacuo*. The orange residue was purified *via* silica gel chromatography (3:1 to 2:1 hexanes: ethyl acetate) yielding a mixture (**1.177a**: **1.177b**; 2.3: 1) of the two isomers (32 mg, 0.093 mmol, 67%).

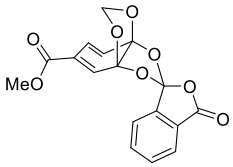

1.177a

white foam; R_f = 0.29 (silica gel, 3:1 hexanes: ethyl acetate); **^{1}H-NMR** (400 MHz, $CDCl_3$): δ 7.86 (m, 1H), 7.69 (td, *J* = 7.4, 1.6 Hz, 1H), 7.65 (td, *J* = 7.4, 1.2 Hz, 1H), 7.32 (m, 1H), 7.20 (m, 1H), 6.75 (dd, *J* = 10.2 and 1.2 Hz, 1H), 6.42 (dd, *J* = 10.2, 0.8 Hz, 1H), 5.77 (s, 1H), 5.15 (s, 1H), 3.89 (s, 3H); **^{13}C-NMR** (100 MHz, $CDCl_3$): δ 165.03, 164.99, 141.0, 135.0, 132.3, 129.0, 127.5, 126.9, 125.2, 124.6, 123.0, 122.0, 121.4, 108.1, 107.6, 92.1, 52.7; **IR** (KBr, film, υ cm $^{-1}$): 2923, 1780, 1728, 1610, 788; **HRMS** (ESI) calcd. for $C_{17}H_{12}O_8$ $[M+Na]^+$: 367.04240, obs. 367.04130.

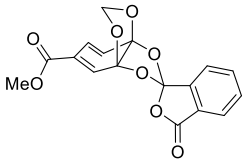

1.177b

colorless oil; **R_f =** 0.20 (silica gel, 3:1 hexanes: ethyl acetate); **^{1}H-NMR** (400 MHz, $CDCl_3$): δ 7.87 (m, 1H), 7.75 (td, *J* = 7.5, 1.0 Hz, 1H), 7.71-7.67 (m, 2H), 7.17 (m, 1H), 6.78 (dd, *J* = 10.3, 1.4 Hz, 1H), 6.38 (d, *J* = 10.3 Hz, 1H), 5.39 (s, 1H), 5.23 (s, 1H), 3.87 (s, 3H); **^{13}C-NMR** (100 MHz, $CDCl_3$): δ 164.97, 164.80, 140.3, 134.9, 132.6, 128.6, 128.0, 127.7, 125.5, 123.9, 122.69, 122.68, 122.18, 107.66, 107.2, 90.6, 52.6; **IR** (KBr, film, υ cm $^{-1}$): 2916, 1791, 1727, 1684, 1558; **HRMS** (CI) calcd. for $C_{17}H_{12}O_8$: 344.0532, obs. 344.0533.

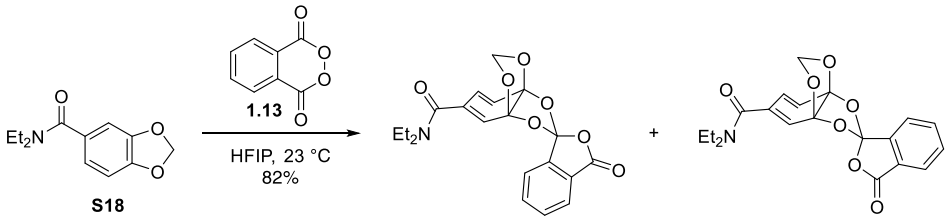

To a 4 mL scintillation vial was added **S18** (30 mg, 0.14 mmol, 1.0 equiv.) and hexafluoroisopropanol (1.4 mL, 0.1 M). Solid phthaloyl peroxide (33 mg, 0.20 mmol, 1.5

equiv.) was added and the solution stirred at 23 ^{0}C for 8 hours. The solvent was removed *in vacuo* and the residue was taken up in ethyl acetate (30 mL). The organic layer was washed with buffered aqueous ammonia solution (1:1 saturated aqueous sodium bicarbonate: saturated aqueous ammonium chloride, 30 mL, X 3), brine (30 mL), dried over sodiu m sulfate, filtered, and concentrated *in vacuo*. The orange residue was purified *via* silica gel chromatography (2:1 to 1:1 hexanes: ethyl acetate) yielding a mixture (**1.178a**: **1.178b**; 1.7: 1) of the two isomers (43 mg, 0.11 mmol, 82%).

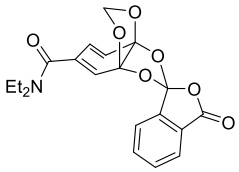

1.178a

colorless oil; **R_f =** 0.22 (silica gel, 1:1 hexanes: ethyl acetate); **^{1}H-NMR** (400 MHz, $CDCl_3$): δ 7.83 (m, 1H), 7.69 (td, *J* = 7.4, 1.1 Hz, 1H), 7.63 (td, *J* = 7.4, 1.2 Hz, 1H), 7.35 (d, *J* = 7.4 Hz, 1H), 6.43 (m, 1H), 6.31 (m, 1H), 6.22 (dd, *J* = 11.0, 1.2 Hz, 1H), 5.72 (s, 1H), 5.13 (s, 1H), 3.48 (br, 2H), 3.37 (br, 2H), 1.18-1.244 (m, 6H); **^{13}C-NMR** (100 MHz, $CDCl_3$): δ 168.0, 165.1, 141.2, 135.0, 132.3, 131.6, 127.4, 125.1, 124.8, 123.0, 123.0, 122.0, 120.4, 107.6, 107.5, 91.7, 43.2, 39.4, 14.4, 12.8; **IR** (KBr, film, υ cm $^{-1}$): 1795, 1634, 1405, 907; **HRMS** (ESI) calcd. for $C_{20}H_{19}NO_7$ $[M+Na]^+$: 408.10540, obs. 408.10590.

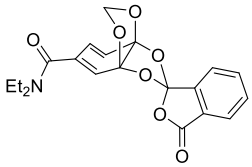

1.178b

white foam; **R_f =** 0.39 (silica gel, 1:1 hexanes: ethyl acetate); **^{1}H-NMR** (400 MHz, $CDCl_3$): δ 7.87 (m, 1H), 7.79 (td, *J* = 7.4, 0.8 Hz, 1H), 7.67-7.75 (m, 2H), 6.41 (m, 1H), 6.24 (s, 1H), 6.21 (dd, *J* = 9.8, 1.2 Hz, 1H), 3.55 (br, 2H), 3.44 (br, 2H), 1.21 (br, 6H); **^{13}C-NMR** (100 MHz, $CDCl_3$): δ 168.1, 164.8, 140.2, 134.9, 133.4, 132.5, 128.1, 125.4, 124.5, 123.6, 122.8, 122.0, 119.3, 107.4, 107.0, 90.8, 43.0, 39.2, 14.4, 12.8; **IR**

(KBr, film, υ cm $^{-1}$): 1788, 1656, 1304, 904; **HRMS** (ESI) calcd. for $C_{20}H_{19}NO_7$ $[M+Na]^+$: 408.10540, obs. 408.10540.

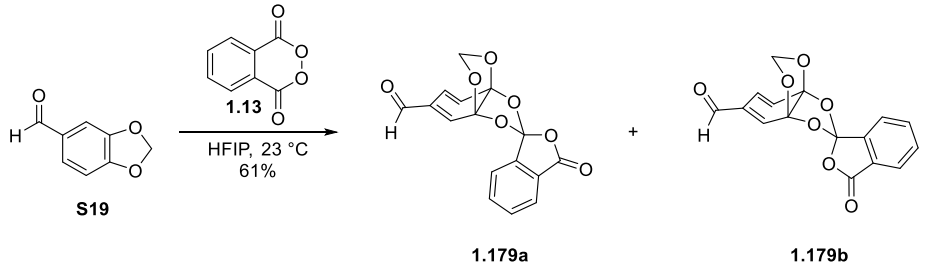

To a 10 mL flask was added piperonal (**S19**) (100 mg, 0.67 mmol, 1.0 equiv.) and hexafluoroisopropanol (6.7 mL, 0.1 M). Solid phthaloyl peroxide (164 mg, 1.0 mmol, 1.5 equiv.) was added and the solution stirred at 23 ^{0}C for 8 hours. The solvent was removed *in vacuo* and the residue was taken up in ethyl acetate (50 mL). The organic layer was washed with buffered aqueous ammonia solution (1:1 saturated aqueous sodium bicarbonate: saturated aqueous ammonium chloride, 30 mL, X 3), brine (30 mL), dried over sodium sulfate, filtered, and concentrated *in vacuo*. The resulting brown residue was purified by silica gel flash column chromatography (5:1 to 2:1 hexanes: ethyl acetate) yielding a mixture (**1.179a**: **1.179b**; 1.6: 1) of the two isomers (128 mg, 0.41 mmol, 61%).

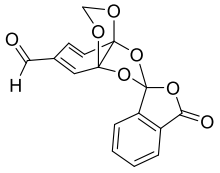

white solid, **M.P. =** 175-177 ^{0}C; **R_f =** 0.38 (silica gel, 2:1 hexanes: ethyl acetate); **^{1}H-NMR** (400 MHz, $CDCl_3$): δ 9.70 (s, 1H), 7.88 (m, 1H), 7.66-7.71 (m, 2H), 7.32 (m, 1H), 6.96 (s, 1H), 6.73 (d, *J* = 9.8 Hz, 1H), 6.50 (d, *J* = 9.8 Hz, 1H), 5.80 (s, 1H), 5.19 (s, 1H); **^{13}C-NMR** (125 MHz, $CDCl_3$): δ 190.3, 164.9, 140.9, 135.5, 135.1, 133.9, 132.5, 127.5, 125.9, 125.3, 122.9,

122.1, 118.1, 109.0, 107.4, 92.4; **IR** (KBr, film, υ cm $^{-1}$): 1790, 1689, 1134, 900, 852; **HRMS** (ESI) calcd. for $C_{16}H_{10}O_7$ $[M+Na]^+$: 337.03190, obs. 337.03240.

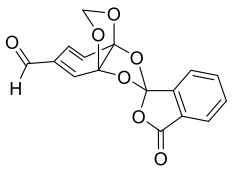

1.179b

white solid, **M.P. =** 188-191 ^{0}C; **R_f =** 0.28 (silica gel, 2:1 hexanes: ethyl acetate); **^{1}H-NMR** (400 MHz, $CDCl_3$): δ 9.67 (s, 1H), 7.87 (m, 1H), 7.78 (m, 1H), 7.68-7.72 (m, 2H), 6.94 (m, 1H), 6.77 (dd, *J* = 9.8, 1.2 Hz, 1H), 6.45 (d, *J* = 9.8 Hz, 1H), 5.43 (s, 1H), 5.27 (s, 1H); **^{13}C-NMR** (100 MHz, $CDCl_3$): δ 190.2, 164.8, 140.1, 135.1, 135.0, 134.6, 132.7, 128.0, 125.5, 125.2, 122.7, 122.2, 119.4, 108.5, 107.0, 90.9; **IR** (KBr, film, υ cm $^{-1}$): 1790, 1699, 1365, 907, 857; **HRMS** (ESI) calcd. for $C_{16}H_{10}O_7$ $[M+Na]^+$: 337.03190, obs. 337.337.03140.

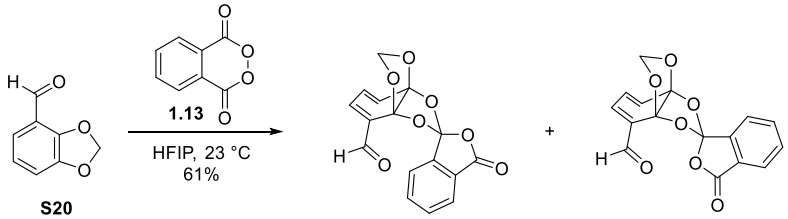

To a 4 mL scintillation vial was added **S17** (20 mg, 0.13 mmol, 1.0 equiv.) and hexafluoroisopropanol (1.3 mL, 0.1 M). Solid phthaloyl peroxide (33 mg, 0.20 mmol, 1.5 equiv.) was added and the solution stirred at 23 ^{0}C for 7 hours. The solvent was removed *in vacuo* and the residue was taken up in ethyl acetate (50 mL). The organic layer was washed with buffered aqueous ammonia solution (1:1 saturated aqueous sodium bicarbonate: saturated aqueous ammonium chloride, 30 mL, X 3), brine (30 mL), dried over sodium sulfate, filtered, and concentrated *in vacuo*. The resulting brown residue was

purified by silica gel flash column chromatography (2:1 to 1:1 hexanes: ethyl acetate) yielding a mixture (**1.180a**: **1.180b**; 1.7: 1) of the two isomers (25 mg, 0.079 mmol, 61%).

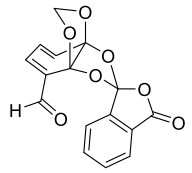

1.180a

white solid, **M.P. =** 224-225 ^{0}C; **R_f =** 0.14 (silica gel, 2:1 hexanes: ethyl acetate); **^{1}H-NMR** (400 MHz, $CDCl_3$): δ 9.74 (s, 1H), 7.85 (m , 1H), 7.67 (td, *J* = 7.4, 1.8 Hz, 1H), 7.64 (td, *J* = 7.4, 1.8 Hz, 1H), 7.28 (dd, *J* = 7.4, 1.8 Hz, 1H), 7.03 (dd, *J* = 5.9, 0.8 Hz, 1H), 6.72 (dd, *J* = 9.8, 0.8 Hz, 1H), 6.49 (dd, *J* = 9.8, 5.9 Hz, 1H), 5.84 (s, 1H), 5.19 (s, 1H) ; **^{13}C-NMR** (100 MHz, $CDCl_3$): δ 188.2, 164.8, 140.8, 135.9, 134.94, 134.89, 132.4, 130.4, 127.7, 125.2, 122.9, 122.6, 121.8, 108.4, 106.5, 92.7; **IR** (KBr, film, υ cm $^{-1}$): 1791, 1701, 1365, 1303, 906, 853; **HRMS** (ESI) calcd. for $C_{16}H_{10}O_7$ $[M+Na]^+$: 337.03190, obs. 337.03220.

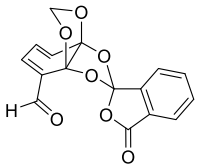

1.180b

yellow oil; **R_f =** 0.23 (silica gel, 2:1 hexanes: ethyl acetate); **^{1}H-NMR** (400 MHz, $CDCl_3$): δ 9.71 (s, 1H), 7.85 (d, *J* = 7.4 Hz, 1H), 7.75 (td, *J* = 7.4, 1.2 Hz, 1H), 7.67-7.71 (m, 2H), 7.05 (dd, *J* = 5.9, 0.8 Hz, 1H), 6.68 (dd, *J* = 9.8, 0.8 Hz, 1H), 6.51 (dd, *J* = 9.8, 5.9 Hz, 1H), 5.44 (s, 1H), 5.29 (s, 1H); **^{13}C-NMR** (100 MHz, $CDCl_3$): δ 188.7, 164.9, 139.9, 138.6, 134.9, 134.5, 132.6, 130.1, 128.0, 125.4, 123.1, 123.0, 122.5 108.0, 105.8, 91.3; **IR** (KBr, film, υ cm $^{-1}$): 1789,1697, 901, 857; **HRMS** (ESI) calcd. for $C_{16}H_{10}O_7$ $[M+Na]^+$: 337.03190, obs. 337.03220

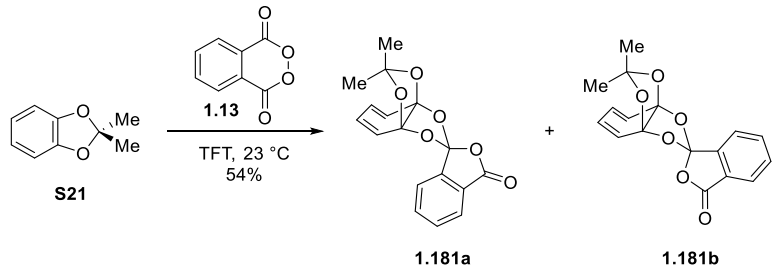

To a 4 mL scintillation vial was added **S21** (25 mg, 0.17 mmol, 1.0 equiv.) and trifluorotoluene (1.7 mL, 0.1 M). Solid phthaloyl peroxide (41 mg, 0.25 mmol, 1.5 equiv.) was added and the solution stirred at 23 ^{0}C for 8 hours. The solvent was removed *in vacuo* and the residue was purified *via* silica gel chromatography (5:1 hexanes: ethyl acetate) yielding a mixture (**1.181a**: **1.181b**; 4: 1) of the two isomers (28 mg, 0.089 mmol, 54%).

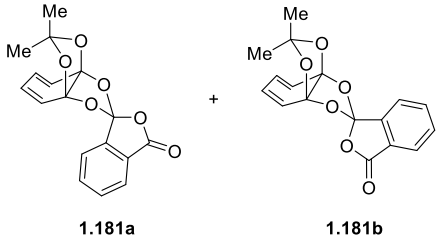

colorless oil; R_f = 0.27 (silica gel, 3:1 hexanes: ethyl acetate); **^{1}H-NMR** (400 MHz, $CDCl_3$): δ [major isomer] 7.84 (d, *J* = 8.0 Hz, 1H), 7.67 (t, *J* = 8.0 Hz, 1H), 7.61 (t, *J* = 8.0 Hz, 1H), 7.39 (d, *J* = 8.0 Hz, 1h), 6.30 (m, 2H), 6.15 (m, 2H), 1.91 (s, 3H), 1.34 (s, 3H); **^{13}C-NMR** (100 MHz, $CDCl_3$): δ 165.6, 165.4, 142.0, 140.5, 134.8, 134.7, 132.1, 132.0, 128.5, 127.4, 125.7, 125.3, 125.0, 124.7, 123.4, 122.9, 122.8, 122.1, 113.7, 112.6, 108.5, 108.4, 29.0, 28.7, 28.6, 26.9; **IR** (KBr, film, υ cm $^{-1}$): 1785, 1058, 900, 852; **HRMS** (CI) calcd. for $C_{17}H_{15}O_6$: 315.0869, obs. 315.0865.

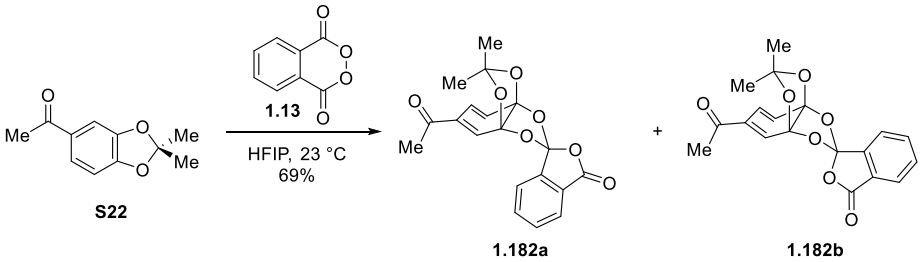

To a 4 mL scintillation vial was added **S22** (25 mg, 0.13 mmol, 1.0 equiv.) and hexafluoroisopropanol (1.3 mL, 0.1 M). Solid phthaloyl peroxide (32 mg, 0.20 mmol, 1.5 equiv.) was added and the solution stirred at 23 ^{0}C for 13 hours. Upon completion, the solvent was removed *in vacuo* and the residue was taken up in ether (30 mL). The organic layer was washed with buffered aqueous ammonia solution (1:1 saturated aqueous sodium bicarbonate: saturated aqueous ammonium chloride, 30 mL, X 3), brine (30 mL), dried over sodium sulfate, filtered, and concentrated *in vacuo*. The orange residue was purified *via* silica gel chromatography (3:1 to 2:1 hexanes: ethyl acetate) yielding a mixture (**1.182a**: **1.182b**; 1.6: 1) of the two isomers (32 mg, 0.090 mmol, 69%).

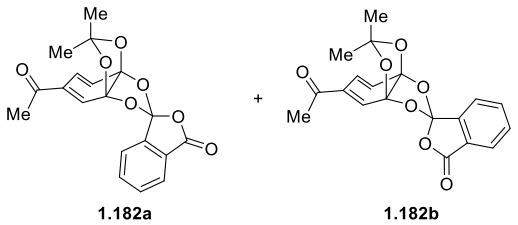

colorless foam; R_f = 0.18 (silica gel, 5:1 hexanes: ethyl acetate); **^{1}H-NMR** (400 MHz, $CDCl_3$): δ [major isomer] 7.86 (m, 1H), 7.61-7.79 (m, 2H), 7.32 (dd, *J* = 8.2, 1.1 Hz, 1H), 6.97 (d, *J* = 0.8 Hz, 1H), 6.77 (d, *J* = 10.2 Hz, 1H), 6.38 (dd, *J* = 10.2, 0.8 Hz, 1H), 2.48 (s, 3H), 1.93 (s, 3H), 1.32 (s, 3H). [minor isomer] 7.86 (m, 1H), 7.61-7.79 (m, 3H), 6.90 (d, *J* = 0.8 Hz, 1H), 6.77 (d, *J* = 9.7 Hz, 1H), 6.33 (dd, *J* = 9.7, 0.8 Hz, 1H), 2.48 (s, 3H), 1.96 (s, 3H), 1.46 (s, 3H); **^{13}C-NMR** (100 MHz, $CDCl_3$): δ 196.5, 196.3, 165.2, 165.0, 141.6, 140.1, 134.9, 134.8, 134.3, 132.8, 132.4, 132.2, 130.3, 129.6, 128.5, 127.3, 126.3, 125.5, 125.3, 125.1, 123.6, 123.4, 123.1, 122.9, 120.1, 119.3, 114.7, 113.8, 108.9, 108.8, 108.5, 108.4, 29.2, 28.68, 28.65, 26.8, 25.6; **IR** (KBr, film, υ cm $^{-1}$): 1789, 1738, 905, 853; **HRMS** (ESI) calcd. for $C_{19}H_{16}O_7$ $[M+Na]^+$: 379.07900, obs. 379.07900.

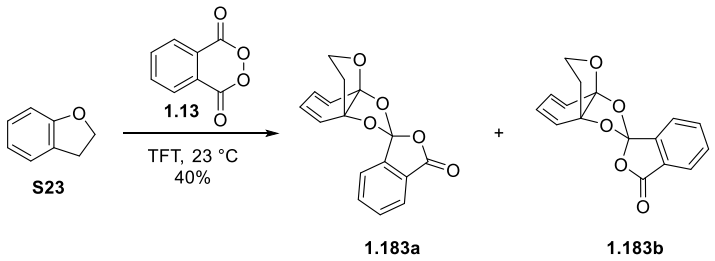

To a 4 mL scintillation vial was added **S23** (30 mg, 0.25 mmol, 1.0 equiv.) and trifluorotoluene (2.5 mL, 0.1 M). Solid phthaloyl peroxide (82 mg, 0.50 mmol, 1.5 equiv.) was added and the solution stirred at 23 ^{0}C for 13 hours. Upon completion, the solvent was removed *in vacuo* and the residue was taken up in ethyl acetate (30 mL). The organic layer was washed with buffered aqueous ammonia solution (30 mL), brine (30 mL), dried over sodium sulfate, filtered, and concentrated *in vacuo*. The orange residue was purified *via* silica gel chromatography (3:1 hexanes: ethyl acetate) yielding a mixture of the two isomers (29 mg, 0.10 mmol, 40%) and unreacted starting material (8 mg, 0.07 mmol, 27%).

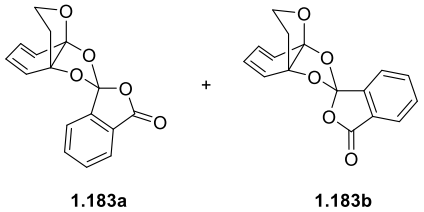

colorless oil; R_f = 0.28 (silica gel, 3:1 hexanes: ethyl acetate); **^{1}H-NMR** (400 MHz, $CDCl_3$): δ [major isomer] 7.84 (d, *J* = 7.8 Hz, 1H), 7.57-7.46 (m, 3H), 6.11-6.27 (m, 4H), 4.53 (ddd, *J* = 11.4, 8.7, 5.1 Hz, 1H), 4.0 (t, *J* = 8.7 Hz, 1H), 2.65 (dd, *J* = 13.7, 5.1 Hz, 1H), 1.98 (ddd, *J* = 13.7, 11.4, 8.7, 1H) [minor isomer] 7.57-7.74 (m, 3H), 7.34 (d, *J* = 7.8 Hz, 1H), 6.11-6.27 (m, 4H), 4.11 (ddd, *J* = 11.4, 8.6, 4.3 Hz, 1H), 3.93 (t, *J* = 8.6 Hz, 1H), 2.71 (dd, *J* = 13.7, 4.3 Hz, 1H), 2.05 (ddd, *J* = 13.7, 11.4, 8.6 Hz, 1H); **^{13}C-NMR** (100 MHz, $CDCl_3$): δ 166.1, 165.8, 142.4, 141.4, 134.7, 134.5, 132.1, 131.7, 128.3, 128.0, 127.8, 127.7, 125.2, 124.8, 124.7 123.8, 123.0, 122.8, 122.7, 122.5, 122.4, 122.2, 121.4, 111.6, 111.5, 110.6, 89.7, 88.8, 62.4, 61.9, 40.8, 39.7; **IR** (KBr, film, υ cm $^{-1}$): 1779, 891, 850; **HRMS** (ESI) calcd. for $C_{16}H_{12}O_5$ $[M+Na]^+$: 307.05770, obs. 307.05870.

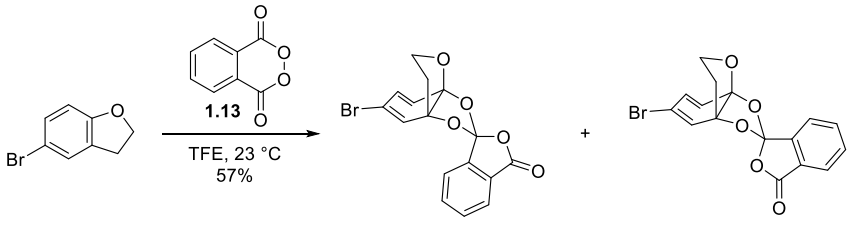

To a 4 mL scintillation vial was added the brominated derivative (50 mg, 0.25 mmol, 1.0 equiv.) and trifluoroethanol (2.5 mL, 0.1 M). Solid phthaloyl peroxide (62 mg, 0.38 mmol, 1.5 equiv.) was added and the solution stirred at 23 ^{0}C for 4 hours. The solvent was removed *in vacuo* and the residue was taken up in ethyl acetate (30 mL). The organic layer was washed with buffered aqueous ammonia solution (30 mL), brine (30 mL), dried over sodium sulfate, filtered, and concentrated *in vacuo*. The orange residue was purified *via* silica gel chromatography (3:1 hexanes: ethyl acetate) yielding a mixture of the two isomers (52 mg, 0.14 mmol, 57%).

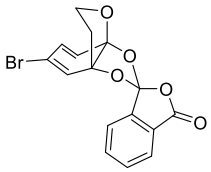

1.184a

yellow oil; R_f = 0.41 (silica gel, 3:1 hexanes: ethyl acetate); **^{1}H-NMR** (400 MHz, $CDCl_3$): δ 7.83 (d, *J* = 8.2, 0.8 Hz, 1H), 7.74 (t, *J* = 8.2 Hz, 1H), 7.64- 7.68 (m, 2H), 6.54 (s, 1H), 6.20 (d, *J* = 10.2 Hz, 1H), 6.13 (d, *J* = 10.2 Hz, 1H), 4.12 (ddd, *J* = 11.7, 8.6, 4.3 Hz, 1H), 4.04 (t, *J* = 8.6, 1H), 2.64 (dd, *J* = 13.3, 4.3 Hz, 1H), 2.05 (ddd, *J* = 13.3, 11.7, 8.6 Hz, 1H); **^{13}C-NMR** (100 MHz, $CDCl_3$): δ 165.8, 141.9, 134.9, 132.0, 127.6, 127.1, 126.2, 125.0, 122.9, 122.5, 117.5, 110.3, 91.4, 63.0, 39.6; **IR** (KBr, film, υ cm $^{-1}$): 1782, 934, 870; **HRMS** (CI) calcd. for $C_{16}H_{11}{}^{79}BrO_5$: 361.9790, obs. 361.9801.

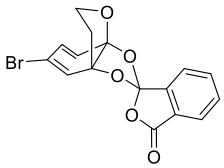

1.184b

white solid, **M.P. =** 171-176 °C; **R_f =** 0.24 (silica gel, 3:1 hexanes: ethyl acetate); **^{1}H-NMR** (400 MHz, $CDCl_3$): δ 7.86 (d, *J* = 7.4 Hz, 1H), 7.70 (t, *J* = 7.4 Hz, 1H), 7.62 (t, *J* = 7.4 Hz, 1H), 7.36 (d, *J* = 7.4 Hz, 1H), 6.56 (s, 1H), 6.20 (s, 2H), 4.54 (ddd, *J* = 11.4, 8.6, 5.5 Hz, 1H), 3.97 (t, *J* = 8.6 Hz, 1H), 2.71 (dd, *J* = 13.7, 5.5 Hz, 1H), 2.05 (ddd, *J* = 13.7, 11.4, 8.6 Hz, 1H); **^{13}C-NMR** (100 MHz, $CDCl_3$): δ 165.5, 140.9, 134.6, 132.2, 128.3, 127.9, 127.5, 125.3, 125.2, 123.1, 122.7, 117.9, 110.1, 90.4, 62.4, 40.8; **IR** (KBr, film, υ cm $^{-1}$): 1780, 1060, 895, 872; **HRMS** (CI) calcd. for $C_{16}H_{11}{}^{81}BrO_5$: 363.9769, obs. 363.9774.

Chapter 2. Synthesis and Biological Evaluation of Vinaxanthone and Xanthofulvin

The severity of injury to the spinal cord results from a debilitating combination of symptoms including loss of movement and sensation, and gain of chronic pain and spasticity.[145] Currently there is no treatment or cure to reverse and repair damage to the central nervous system (CNS). After breakage of the axonal connection, the neuron undergoes acute axonal degeneration (AAD). This period is defined by the rapid separation of the proximal end from the distal stump. With no means to receive nutrients from the now disjointed cell body, the axonal structure and membrane of the distal stump disintegrates, a process termed Wallerian degeneration.[146] This rupture in neuronal connectivity results in the chronic disability experienced by spinal cord injury (SCI) patients. Furthermore, the poor prognosis is irreversible due to the limited regrowth potential of damaged or severed neurons following AAD and Wallerian degeneration.

Working in concert, extrinsic chemorepellents present in the extracellular matrix and secreted signaling molecules impede neuronal growth. Indeed, despite the presence of endogenous stem cells in the adult CNS, no complete recovery occurs due to the surrounding inhibitory environment.[147] In the early 20th century, the histologist and Nobel laureate Santiago Ramon y Cajal observed that axotomized neurons within the CNS become swollen and were incapable of regeneration.[148] Ramon y Cajal hypothesized that the lack of regeneration was a fundamental feature of the CNS. Despite appearing quiescent, however, these cells are stalled due to an environment unconducive to axonal proliferation, resulting in chronic growth cone collapse.[149] In contrast to the CNS, upon injury to the peripheral nervous system (PNS) or embryonic nervous system, regeneration occurs into and beyond the lesion site.[150] Transplantation of optical nerves into the PNS results initially in the protuberance of surrounding PNS cells bypassing the local inhibitory

environment of the foreign CNS segment.[151] Additionally, innervation of the CNS segment occurs in the PNS environment. These experiments demonstrate the contrasting milieu of the PNS and CNS: inhibitory signals are pronounced within the CNS and are less abundant in or absent from the PNS.

Inhibitory signals are endogenous in the extracellular environment but are also upregulated in the lesion site following injury. Repulsive guidance cues are important neuronal growth inhibitors that are critical to axon pathfinding during development and are downregulated after development. Following injury, however, many of these proteins including semaphorins and myelin-associated proteins are induced, with expression patterning concentrated in the periphery of adult CNS lesions.[152-154] Additionally, scaring of the lesion site complicates regeneration, as axons cannot penetrate through the fibrotic tissue.[155] Neuroglia recruit astrocytes to the site of injury, which secrete chondroitin sulphate proteoglycans (CSPGs).[156] CSPGs are a family of extrinsic molecules that attenuate growth. Additionally, the concentration of CSPGs is highest at the center of the lesion. However, it is unclear if the scarring forms a physical barrier to prevent access of growth promoting molecules to the lesion site, or if CSPGs act directly on the growth promoting molecules to attenuate their action.[157] While CSPGs are present upon injury to the PNS, glial scaring is absent. The presence of multiple classes of inhibitory molecules and scaring of the lesion site following injury complicates regeneration of the CNS.

In addition to the presence of chemorepellents, growth factors are reduced or absent in the CNS.[158,159] A class of signaling molecules that selectively promote growth in nerve cells include nerve growth factor (NGF), brain-derived neurotrophic factor (BDNF), ciliary neurotrophic factor (CNTF), glial cell line-derived neurotrophic factor (GDNF) and neurotrophin-3 (NT-3). In addition to neurotrophic factors, signaling ligands that increase cell proliferation also promote growth, including fibroblast growth factor (FGF), insulin-

like growth factor (IGF), platelet-derived growth factor (PDGF), and vascular endothelial growth factor (VEGF). These growth factors are present in the PNS. For example, grafting a PNS segment to bridge an axotomized central neuron promotes significant protuberance of the proximal stump into the lesion, demonstrating the intrinsic permissive growth capabilities of the PNS.[160] This is in part the result of Schwann cells producing BDNF and NT-3 upon damage to the PNS.[161] Any possible therapeutic approach to regenerate severed axons must both attenuate the inhibitory environment present in the CNS and stimulate growth promoting factors.

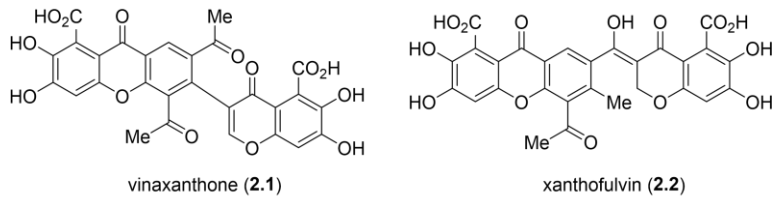

Figure 2.1. Regenerative natural products vinaxanthone (**2.1**) and xanthofulvin (**2.2**).

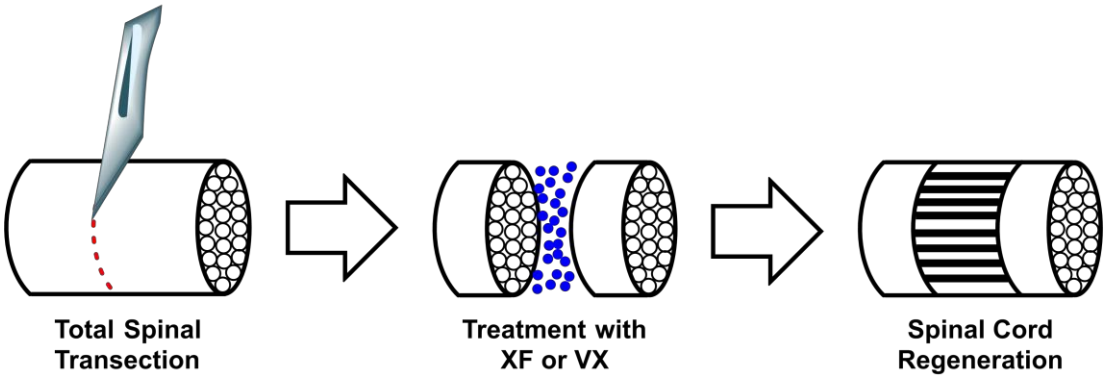

Figure 2.2. Representation of spinal cord transection and AAD followed by treatment with vinaxanthone or xanthofulvin.

Two molecules that have been shown to regenerate neurons *in vivo* are vinaxanthone (**2.1**) and xanthofulvin (**2.2**) (Figure 2.1). Following complete surgical spinal cord transection, adult rats experience immediate loss of hind limb movement. Treatment

groups were continuously administered with vinaxanthone (**2.1**) or xanthofulvin (**2.2**) in the lesion site at 0.1 mg mL^{-1} for four weeks (Figure 2.2).[162,163] Those treated with vinaxanthone (**2.1**) or xanthofulvin (**2.2**) showed a dramatic increase in hind limb movement in contrast to the control group, which exhibited virtually no recovery. Additionally, retransection of the lesion reversed the recovery experienced by the treated rats.[162] Thus the gain of function was most likely the result of reconnection of the spinal cord at the surgical site and not compensatory recovery below the lesion. Furthermore, rats treated with vinaxanthone (**2.1**) or xanthofulvin (**2.2**) exhibited enhanced regeneration and preservation of injured axons, increased remylenation, decreased apoptotic cell count, and enhancement of angiogenesis with respect to the control population. Substantial reduction in glial scaring is observed in treated animals.

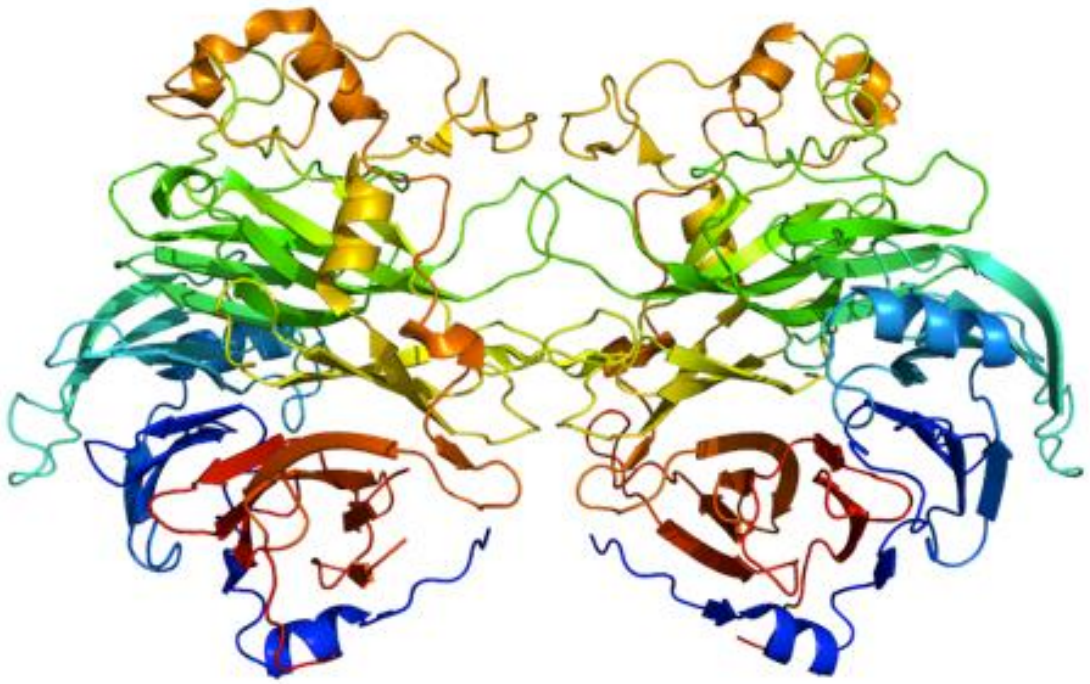

Figure 2.3. Ribbon structure of Semaphorin 3A.

Both of these small molecules were identified for their ability to inhibit semaphorin 3A (Sema3A).[153,164,165] Vinaxanthone (**2.1**) and xanthofulvin (**2.2**) reverse Sema3A-induced growth cone collapse in dorsal root ganglion (DRG) cells dose-dependently and in similar efficacy (IC_{50} vinaxanthone = 0.1 μg/ mL; IC_{50} xanthofulvin = 0.09 μg/ mL).[166] Semaphorins are one of the largest families of guidance proteins that attenuate cellular growth and migration (Figure 2.3).[167] All semaphorins possess a conserved sema domain, and have both membrane-bound and soluble forms. During embryogenesis, Sema3A expression is widespread, including in non-neuronal cells. Following development, Sema3A is found mostly in the nervous and vascular systems.[168] Sema3A is moderately expressed throughout the CNS, including in the hippocampus, entorhinal cortex, neocortex and subiculum.[169] Sema3A is also secreted following injury to neurons in the CNS, and is found in high concentrations within fibroblasts populating the lesion scar.[153,164] While Sema3A is also found in the PNS, its levels of expression are unchanged following injury.[170] Despite providing an inhibitory environment, Sema3A is vital for normal neuronal development and function, with aberrant Sema3A implicated in a variety of diseases including Alzheimer's disease.[171]

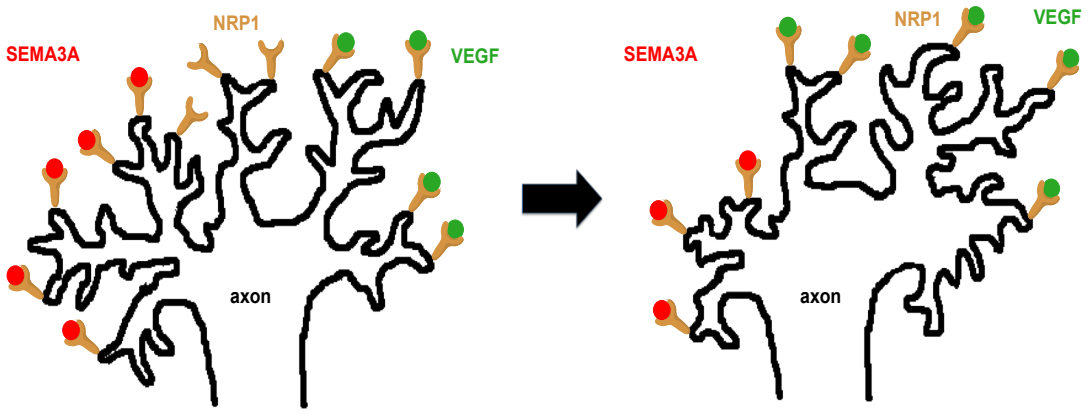

Figure 2.4. Sema3A is a chemorepellent on growing axons. It opposes the action of VEGF.

The cellular receptor for semaphorins are neuropilins and plexins. Sema3A has a high-affinity for neuropilin-1 (NRP1), but unlike other class III semaphorins, is not a ligand for neuropilin-2 or any plexins including plexin 1 (plex 1).[172,173] Activation of Sema3A mediates a NRP1/ plex 1 complex. Plex 1 is hypothesized to be responsible for the signal transduction, as it has a much larger intracellular domain than NRP1. While the precise mechanism is ambiguous, the downstream effect of Sema3A binding to NRP1 results in disruption of the microtubule and actin cytoskeleton that in turn modulates filopodia extension of the growth cone.[173,174] In addition to accommodating Sema3A, NRP1 also has a binding site for the growth promoting factor VEGF.[175] Thus, the same receptor can either promote or attenuate growth depending on the exogenous signaling molecule present (Figure 2.4).

Xanthofulvin (**2.2**) and vinaxanthone (**2.1**) act by disrupting the protein-protein interactions of Sema3A and NRP1.[168,176] A pre-mix experiment was undertaken to recapitulate the observed interaction.[177] In this experiment, Sema3A was incubated with xanthofulvin (**2.2**) for 30 minutes. DRG cells treated with this mixture exhibited significant protuberance. Treating DRG cells sequentially with Sema3A followed by xanthofulvin (**2.2**), however, resulted in little inhibition of growth cone collapse. Taken in concert, these experiments suggest that xanthofulvin (**2.2**) affects the ability of Sema3A to bind to its cellular target.[177] Additionally, xanthofulvin (**2.2**) demonstrated high levels of selectivity for Sema3A as Sema3B and Sema3F were unaffected. To rule out the modulation of other chemorepellents, xanthofulvin was assayed for affinity to Nogo-A, myelin-associated glycoprotein (MAG), and oligodendrocyte-myelin glycoproptein (OMgp). Modulation of these important signaling molecules was minimal.[178]

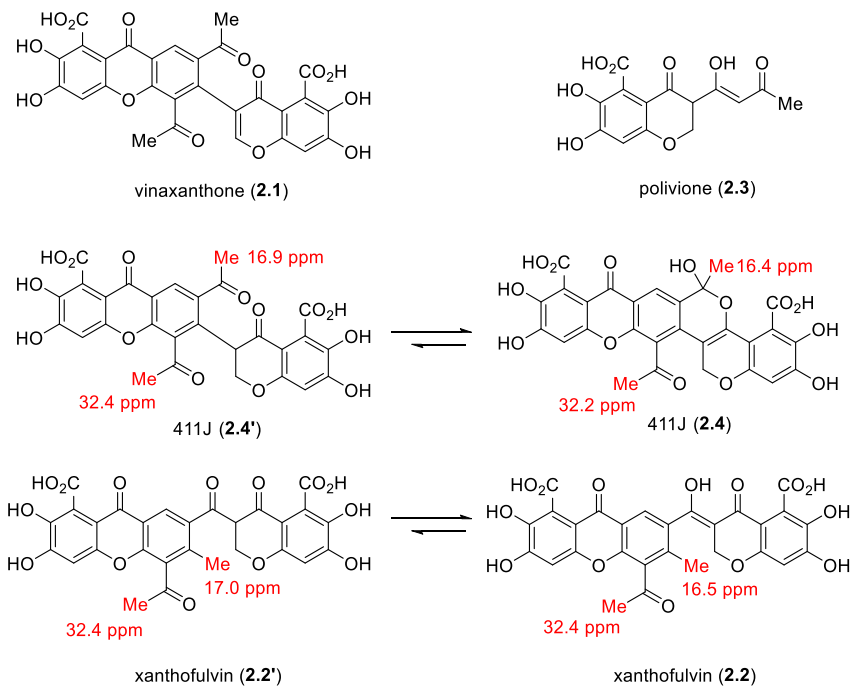

Figure 2.5. Structure of vinaxanthone (**2.1**), xanthofulvin (**2.2**).

Vinaxanthone (**2.1**) is a fungal metabolite first isolated from *Penicillium vinaceum* in 1991 (Figure 2.5).[179] This isolation produced 30 mg/ L of vinaxanthone (**2.1**). Stephen Wrigley isolated vinaxanthone in addition to polivione (**2.3**) and a molecule designated 411J (**2.4** which existed in a 4:1 mixture with hemiacetal **2.4'**).[180] More than a decade later, Sumitomo Pharmaceuticals isolated the natural product xanthofulvin (**2.2**) (also known as SM-216289) in addition to vinaxanthone (**2.1**).[166] Fermentation yielded 11 mg/ L of vinaxanthone (**2.1**) and 21 mg/ L of xanthofulvin (**2.2**). Interestingly, xanthofulvin (**2.2**) possesses identical spectral data to 411J (**2.4**). Additionally, 411J (**2.4**) and xanthofulvin (**2.2**) were co-isolated with vinaxanthone, providing evidence that both isolation groups isolated the same natural product. Rationalizing the ^{13}C-NMR data of 411J (**2.4**) and xanthofulvin (**2.2**) with the structural assignments, specifically the two methyl ketone groups of **2.4'** versus a methyl ketone and tolyl methyl group **2.2'**, led us to believe that **2.2** was intuitively the more likely structure of the natural product.[166,180]

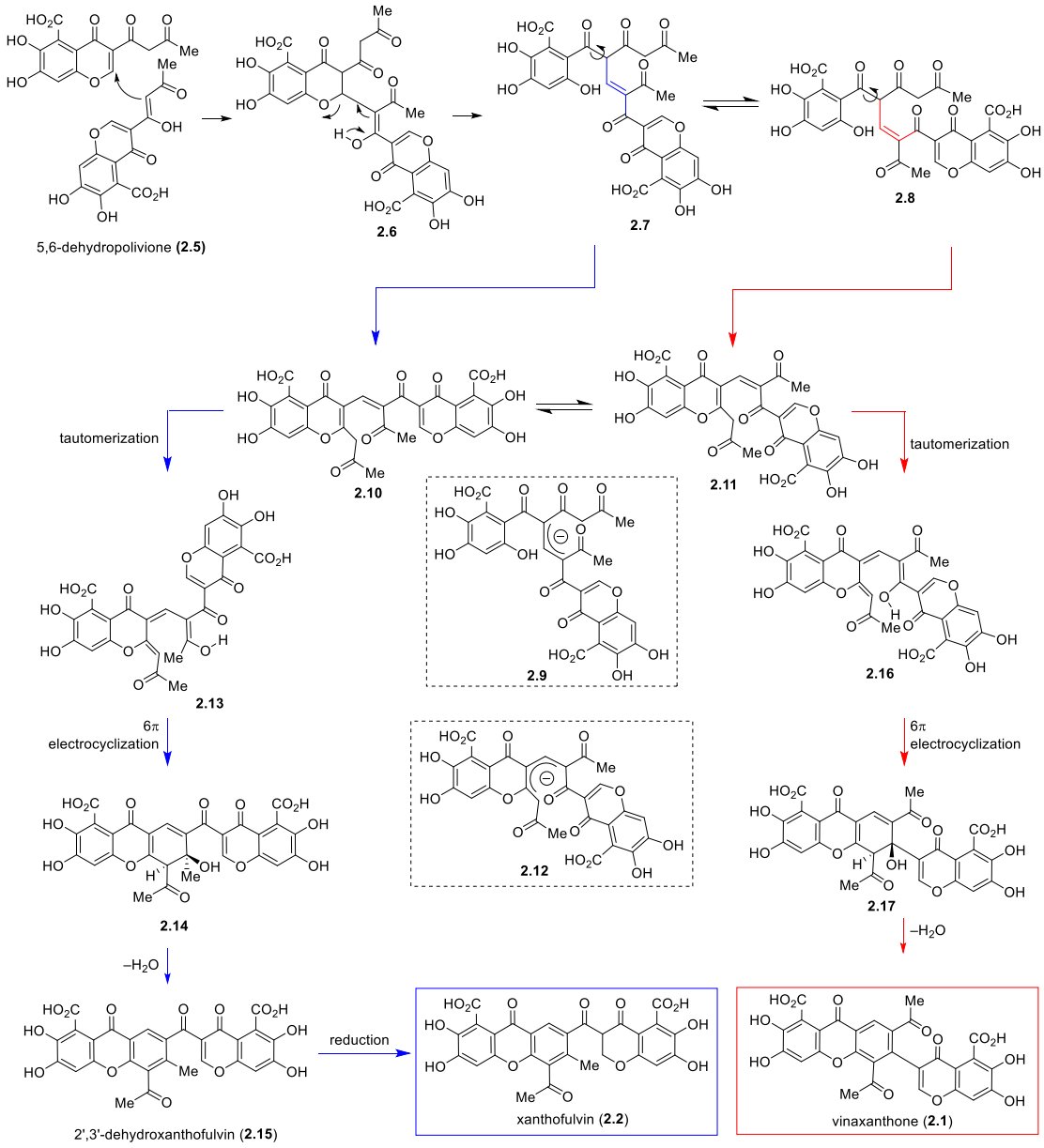

Figure 2.6. Proposal for the formation of vinaxanthone (**2.1**) or dehydro-xanthofulvin (**2.15**) from 5,6-dehydropolivione (**2.5**).

Due to their structural similarities, vinaxanthone (**2.1**) and xanthofulvin (**2.2**) were envisioned to be formed utilizing a shared biosynthetic pathway through a union of two identical triketone units of 5,6-dehydropolivione (**2.5**) (Figure 2.6). A name given due to the structural similarity with the co-isolate polivione (**2.3**). Intermolecular Michael addition

of **2.5** onto another molecule of **2.5** produces chromanone **2.6**. Elimination of the phenol gives isomeric olefins **2.7** or **2.8**. Due to the stability of anion **2.9**, the olefin geometries of **2.7** or **2.8** are envisioned to readily interconvert. Depending on the isomer, dehydrative chromenone condensation of the phenol forms **2.10** or **2.11**, in equilibrium due to the extended enolate **2.12**. Tautomerization and 6π electrocyclization of the isomeric structures **2.13** or **2.16** forms cyclohexadienes **2.14** or **2.17**. Aromatization *via* loss of water furnishes either vinaxanthone (**2.1**) or, after subsequent reduction of **2.15**, xanthofulvin (**2.2**).

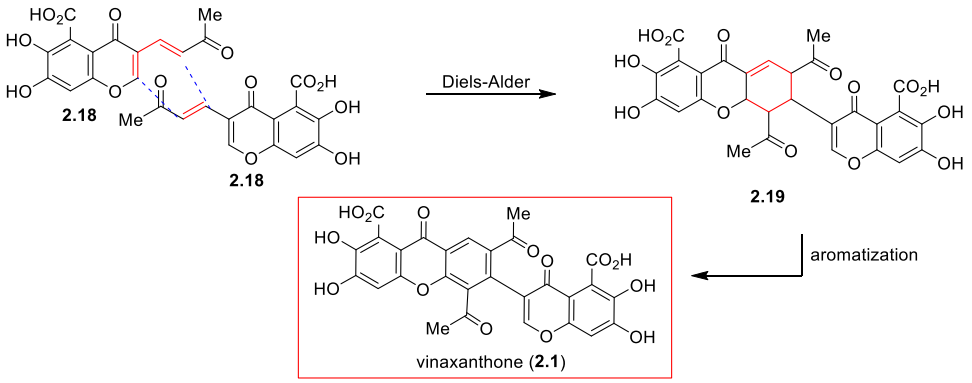

Figure 2.7. Tatsuta's biosynthetic proposal of vinaxanthone (**2.1**).

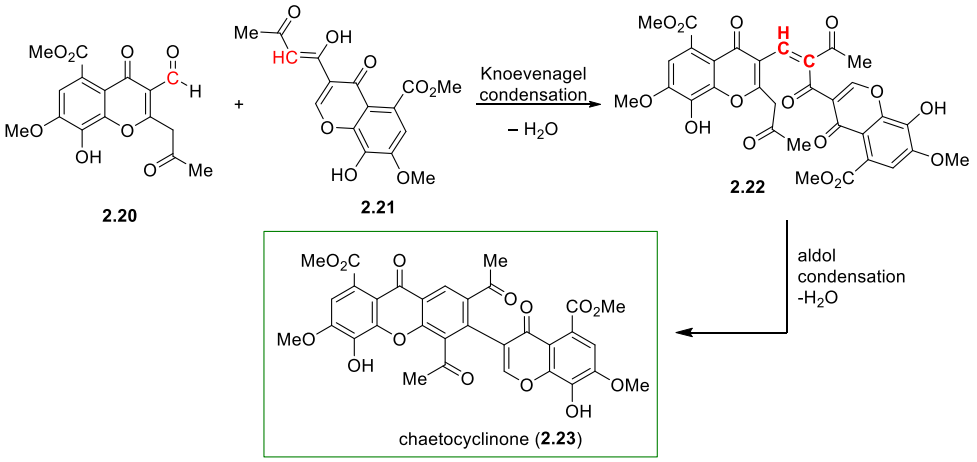

Figure 2.8. Zeeck's biosynthetic proposal for chaetocyclinone (**2.23**).

An alternative biosynthesis of vinaxanthone (**2.1**) was proposed by Tatsuta and co-workers to occur *via* an enzymatically controlled intermolecular Diels-Alder reaction between two molecules of **2.18**, followed by aromatization (Figure 2.7).[181] Axel Zeeck and co-workers proposed the biosynthesis of the structurally related natural product chaetocyclinone C (**2.23**), which inspired our proposal.[182] A Knoevenagel condensation between aldehyde **2.20** and triketone **2.21** provides adduct **2.22**. The resulting dienone undergoes an intramolecular aldol condensation and dehydration to form the natural product chaetocyclinone C (**2.23**). Chaetocyclinone C (**2.23**) in addition to vinaxanthone (**2.1**) and xanthofulvin (**2.2**) were isolated as axially achiral species. The barrier of rotation was calculated for chaetocyclinone C (**2.23**) to be 20 kcal/ mol, below the threshold for atropisomerism.[183]

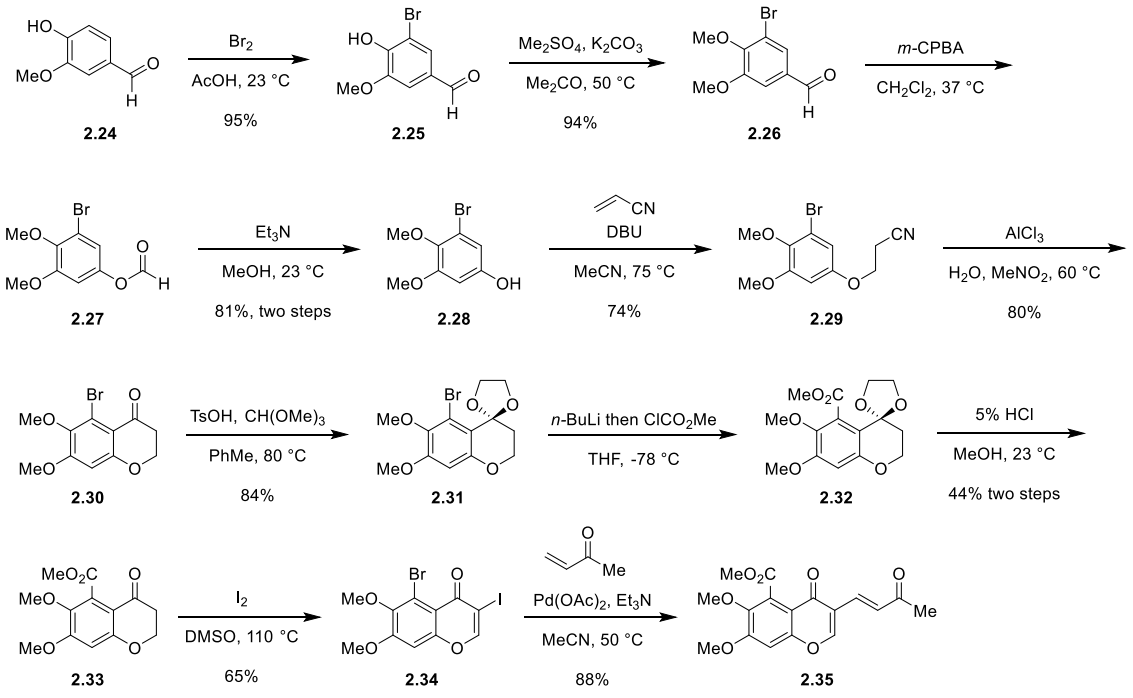

Figure 2.9. Tatsuta's synthesis of monomer enone **2.35**.

Tatsuta approached the carbocyclic core of vinaxanthone (**2.1**) *via* intermolecular Diels-Alder reaction of enone **2.35**.[181] The synthesis commenced with the bromination of vanillin (**2.24**) in acetic acid. Brominated vanillin (**2.25**) was methylated using dimethyl sulfate yielding brominated veritraldehyde (**2.26**) in 94% yield. Oxygen was installed *via* Baeyer-Villiger oxidation of the aldehyde with *meta*-chloroperoxybenzoic acid producing formate **2.27**. The resulting formate was hydrolyzed in methanol, forming phenol **2.28** in 81%. The revealed phenol added by conjugate addition into acrylonitrile in acetonitrile using 1,8-diazabicycloundec-7-ene (DBU) as base in 74% yield. The nitrile is hydrolyzed and a subsequent Friedel-Crafts acylation gives the chromanone core (**2.30**) in 84% yield. Protection of the ketone as the ketal (**2.31**), followed by lithium-halogen exchange and trapping with methyl chloroformate provides methyl ester **2.32**. Deprotection of the ketal and iodination gives 3-iodochromenone **2.34** in 65% yield. Heck cross-coupling of the iodide with methyl vinyl ketone and palladium(II) acetate catalyst in warm acetonitrile forged the enone monomer (**2.35**) in 88% yield.

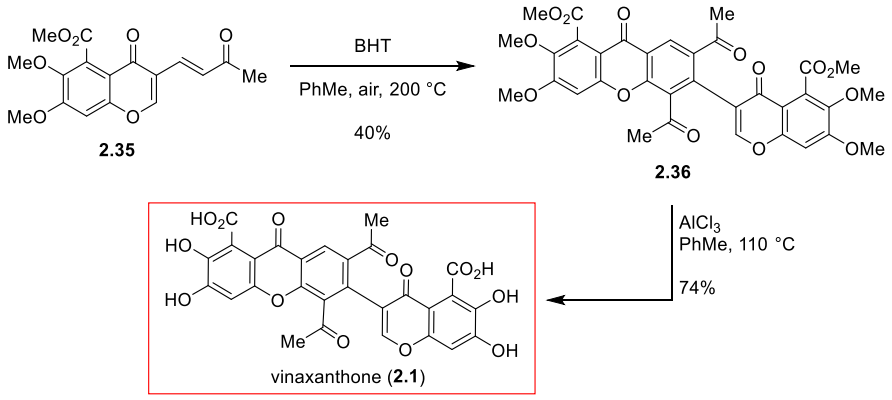

Figure 2.10. Diels-Alder reaction for the synthesis of vinaxanthone (**2.1**).

To test their biosynthetic proposal, Tatsuta heated the enone (**2.35**) in toluene at 200 °C in a sealed tube in the presence of air and butylated hydroxytoluene (BHT), forming per-methylated vinaxanthone (**2.36**) in 40% yield. BHT was added to serve as the oxidant

to re-aromatize the putative intermediary cyclohexene following intermolecular Diels-Alder reaction.[184] However, Diels-Alder cycloadditions of this type are rare in nature.[185] Global deprotection using aluminum trichloride in refluxing toluene provided vinaxanthone (**2.1**) in 74% yield.

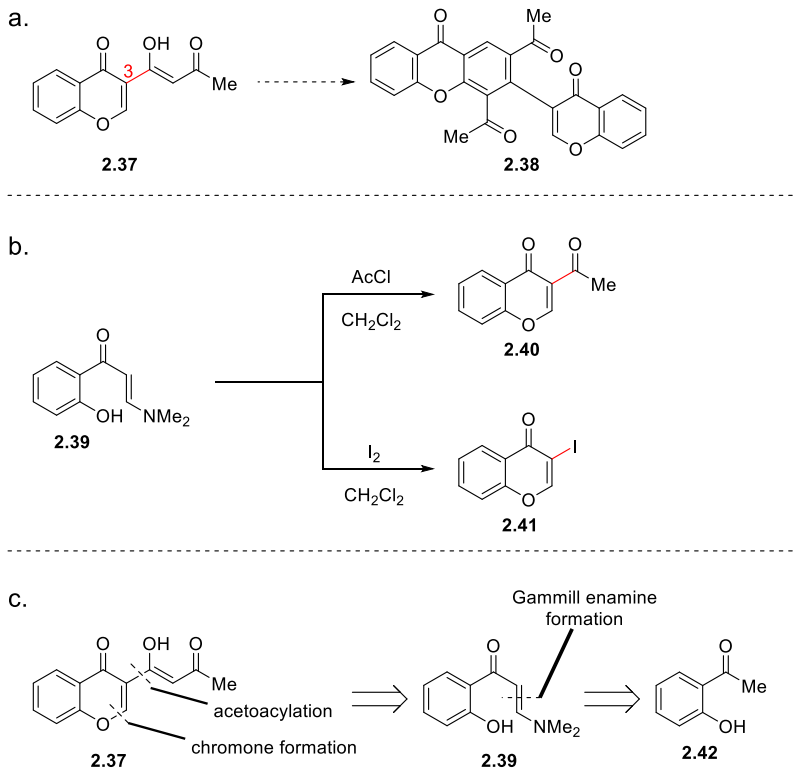

Figure 2.11. Planned route for the synthesis of deoxygenated vinaxanthone (**2.38**).

In order to test the key dimerization reaction of our proposed biomimetic strategy, the unfuncionalized triketo monomer (**2.37**) was considered (Figure 2.11). A key disconnection was the bond connecting the acetoacetyl group to the 3 position of the chromenone ring (Figure 2.11a). From there, the transformation of acetophenones into enaminone using N,N-dimethylformamide dialkyl acetals is well documented (Figure 2.11b).[186] The benefit of vinylogous amide **2.39** is twofold, it provides the lynchpin

necessary to furnish the chromenone ring through a 1-carbon-homologation and secondly, the enaminone can trap a variety of electrophiles alpha to the carbonyl in one operation.[187] For example, treatment of enaminone **2.39** with iodine in methylene chloride yields 3-iodochromenone **2.41**,[186] while acylation can be accomplished by employing acetic anhydride or acetyl chloride as the electrophile (**2.40**) (Figure 2.11b).[188] It was envisioned that an electrophilic acetoacylating agent could likewise furnish **2.37** directly from the vinylogous amide **2.39** (Figure 2.11c).

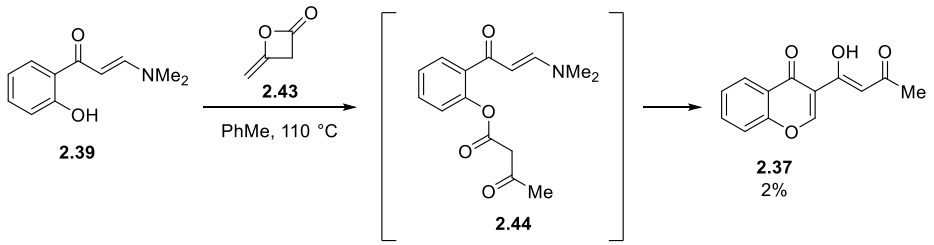

Figure 2.12. Treatment of enaminone (**2.39**) with diketene (**2.43**).

In Nature, acetoacetylation proceeds *via* stepwise chain elongation of a protein-bound malonyl moiety by an acyl unit followed by decarboxylation.[189] Synthetically, acetoacetylation can be accomplished in a variety of ways. Diketene (**2.43**) can transiently engage phenols.[190] It was hypothesized that the direct attack of phenol **2.39** into diketene (**2.43**) would yield phenyl acetoacetate **2.44** (Figure 2.12). The O-to-C transposition of the acetoacetyl unit would reveal **2.37** after loss of dimethylamine. However, engagement of enamino ketone **2.39** with diketene was inefficient. Combining diketene with the vinylogous amide in refluxing toluene only resulted in 2% isolation of the triketone (**2.37**). Neither deprotonating the phenol (**2.39**) using a variety of bases nor activating diketene *in situ* by forming the imidazolide was productive at generating acetoacetylated product **2.37**.

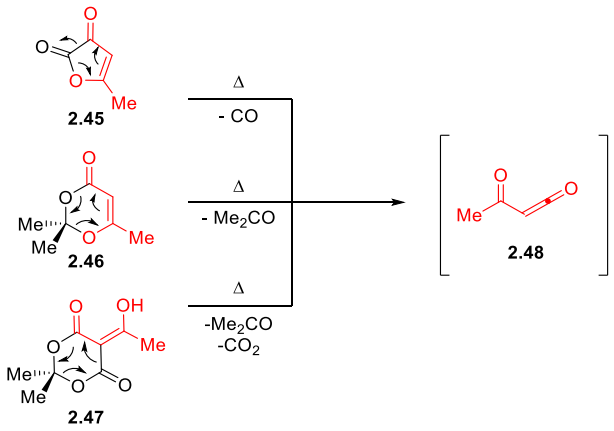

Figure 2.13. Generation of acylketene (**2.48**) *via* thermolysis of heterocycles.

The lack of reactivity exhibited by diketene (**2.43**) prompted the consideration of other acetoacetyl synthons (Figure 2.13). One such reagent is the highly reactive reagent acylketene (**2.48**).[191] Most acylketenes are generated *in situ* as only electronically stabilized or sterically hindered variants are isolable.[192] A direct route to generate acylketene (**2.48**) is through pyrolyzing β-keto esters at temperatures in excess of 200 °C.[193] Another protocol is the net-loss of hydrochloric acid from β-keto acid chlorides in the presence of an amine or alkoxide base.[194] A more appealing approach is *via* thermolysis of a variety of heterocycles. Typically acylketene can be generated at lower temperatures (often refluxing toluene), and the resulting byproducts are benign. For example, furan dione **2.45** generates acylketene through a retrocyclization, with loss of carbon monoxide.[195] The widely-used and commercially available dioxinone (**2.46**) generates acylketene through a [4+2] retro-cyclization with concomitant expulsion of an equivalent of acetone.[196,197] Another source is acyl Meldrum's acid (**2.47**), which yields acylketene via a [2+2+2] retro-cyclization, eliminating an equivalent of CO_2 in addition to acetone.[198,199]

entry	reagent	conditions	yield
1.	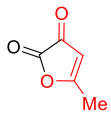 2.45	PhMe, 110 °C	3%
2.	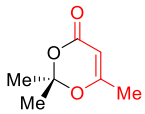 2.46	PhMe, 110 °C	11%
3.	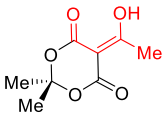 2.47	PhMe, 110 °C	16 → 43%[a]

Figure 2.14. Acetoacylation of enaminone **2.39**. [a] Isolated yields using flash chromatography with acidified silica gel.

Figure 2.14 summarizes efforts to access acylketene (**2.48**) through thermolysis. Furan dione **2.45** was prepared in two steps from acetone.[200] Exposing the enaminone (**2.39**) to furan dione **2.45** in refluxing toluene provided triketone **2.37** in 3% isolated yield. While the enaminone engaged the transient acylketene, poor yields prompted the consideration of yet another source of this reactive species. Commercially available dioxinone **2.46** provided the triketo monomer in an increased yield of 11%. Decagram quantities of acyl Meldrum's acid (**2.47**) can be generated by treating Meldrum's acid with pyridine and acyl chloride. Utilizing this precursor to acylketene (**2.48**) led to a modest increase in yield of **2.37** to 16% (entry 3). During extensive optimization of this step several observations were made and warrant further comment. Pre-warming the heating bath to well above the boiling point of toluene (145 °C) increased both yields and reproducibility. Additionally, purification of the crude material utilizing silica gel pre-acidified to a pH of 2 (using phosphoric acid) increased the yield of **2.37** using acyl Meldrum's acid to 43%.

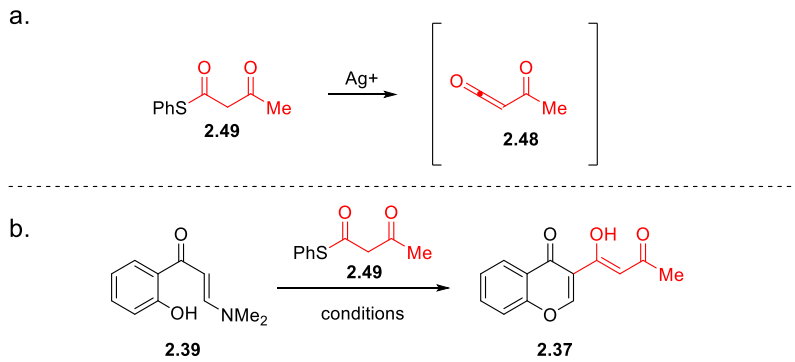

entry	thiophilic metal	thioester (**2.49**) equiv.	conditions	yield[a]
1.	1 equiv. $AgCO_2CF_3$	1 equiv.	CH_2Cl_2, 23 °C 4 days	67%
2.	1 equiv. $AgCO_2CF_3$	2 equiv.	CH_2Cl_2 23 °C 14h	51%
3.	1 equiv. Ag_2CO_3	1 equiv.	CH_2Cl_2, 23 °C 4 days	N.R.
4.	-	1 equiv.	CH_2Cl_2, 23 °C 4 days	N.R.
5.	-	1 equiv.	TFA CH_2Cl_2, 23 °C 1 day	0%

Figure 2.15. Acetoacylation of enaminone **2.39**. [a] Isolated yields using flash chromatography with acidified silica gel.

A report by Hoye discussing acylketene (**2.48**) generation under mild, ambient conditions appeared promising (Figure 2.15a).[201,202] Competition experiments suggested that activation of phenyl acetothioacetate (**2.49**) by a thiophilic metal, in this case a silver salt, followed by loss of thiophenol yielded acylketene (**2.48**) *in situ*. Adopting this procedure increased the yield of **2.37** to an acceptable 67%. Neither increasing the stoichiometry of the thioester (**2.49**) nor varying the thiophilic metal improved the yields. Additionally, the thioester alone cannot undergo triketone formation (entry 4) and trace acid did not account for product formation (entry 5). The structure of **2.37** was unambiguously confirmed by single crystal X-ray diffraction (Figure 2.16). In the liquid state, **2.37** exists entirely in the enol tautomer, with the strongly intramolecularly-bound proton appearing at δ 15.90 ppm in the ^{1}H-NMR spectrum. This crystal structure

recapitulates this observation, with hydrogen bonding occurring with the β-carbonyl (1.73 Å hydrogen bond length).

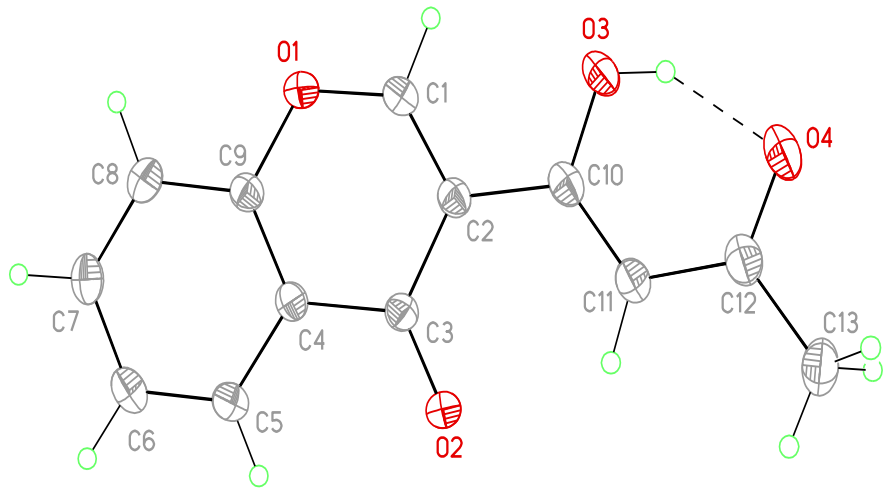

Figure 2.16. View of **2.37** showing the atom labeling scheme. Displacement ellipsoids are scaled to the 50% probability level.

The incorporation of acylketene into enaminone **2.39** led us to consider the mechanism by which this occurs (Figure 2.17). Ketene[203] and dienylketenes[204] participate in [2+2] cycloadditions. However, unlike ketene, examples of acylketene engaging in [2+2] cyclizations are rare.[205] A [4+2] inverse demand Diels-Alder could also occur. A diverse set of dienophiles can engage acylketene in this manner including imines[206] and enol ethers.[207] Hetero inverse-demand Diels-Alder provides aminal **2.50**, followed by loss of dimethylamine which furnishes pyrone **2.51**. Michael addition of the phenol into the vinylogous ester and collapse of the acetal (**2.52**) gives the desired acetoacetyl chromenone (**2.37**). To test the feasibility of this mechanistic pathway, an *o*-methoxy enamino ketone (**2.53**) was prepared, precluding the 1,2-addition pathway. Exposing this derivative to acylketene (**2.48**) yielded the methyl pyrone (**2.54**), indicating that this pathway is plausible.

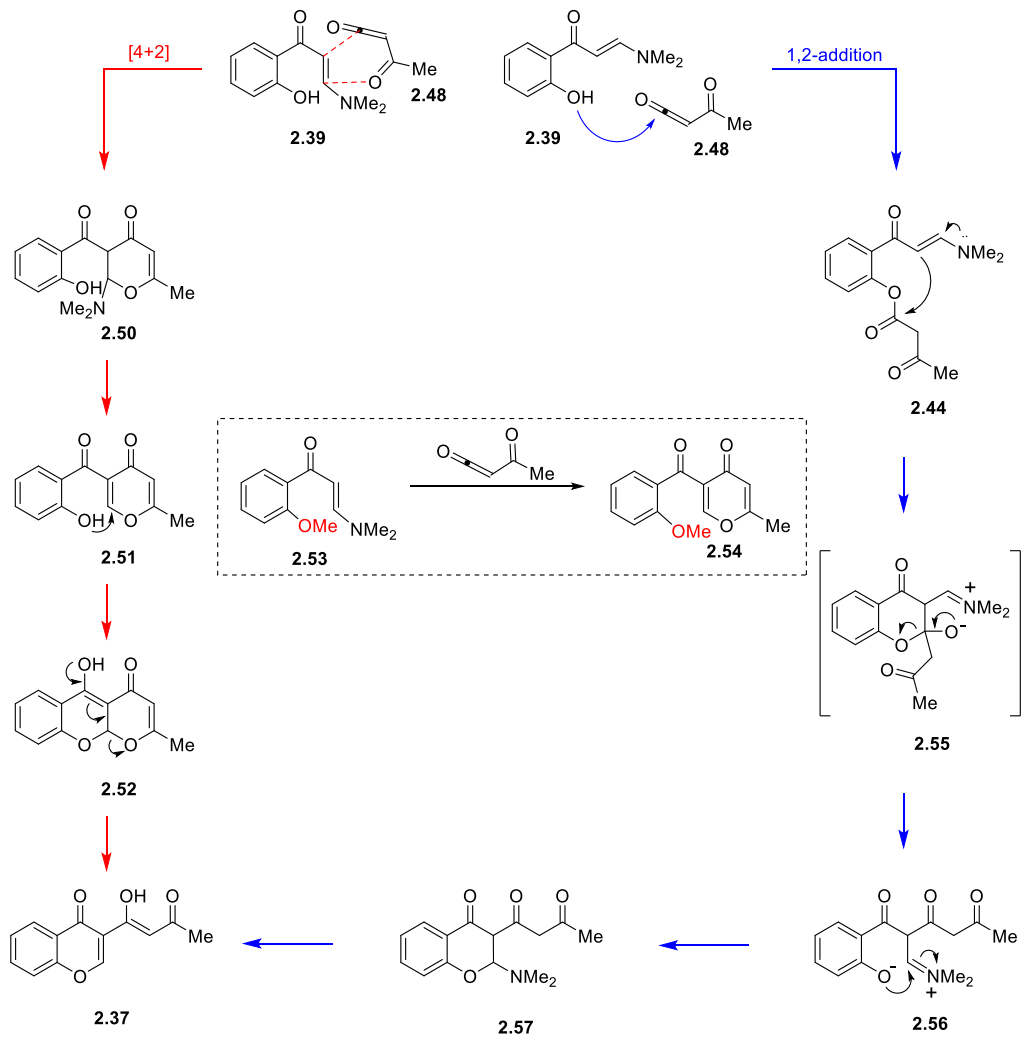

Figure 2.17. Proposed mechanism for acetoacylation of enaminone **2.39**.

However, direct engagement of the phenol cannot be ruled out. Addition of the phenol into acylketene produces the β-keto ester **2.44** after tautomerization. An O-to-C rearrangement of the dicarbonyl unit *via* addition of the enamine followed by collapse of the tetrahedral intermediate (**2.55**) with concomitant elimination of the phenoxide produces the iminium species **2.56**. Addition of the phenoxide into the iminium affords aminal **2.57**, which upon expulsion of dimethylamine, furnishes the acetoacetyl chromenone **2.37**.

Studies of the addition of protic nucleophiles into acylketene, both computationally and experimentally, have found that the 1,2-addition pathway predominates.[208]

a.

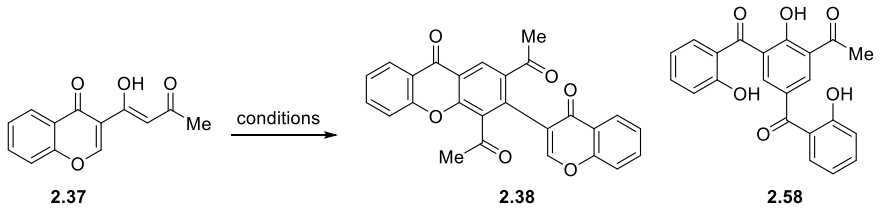

entry	conditions	yield
1.	H_2O: dioxane 1:1, 100 °C 14h	**2.38**: 72%
2.	dioxane, 90 °C 14h	N.R.
3.	HCO_2H: dioxane 1:1, 90 °C 7 days	**2.38**: 73%
4.	Et_3N MeCN, 23 °C 14h	**2.58**: 42%

b.

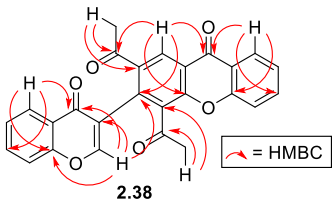

Figure 2.18. Formation of carbocyclic core of deoxygenated vinaxanthone (**2.38**).

With the tricarbonyl unit (**2.37**) in hand, the key dimerization was investigated (Figure 2.18a). It was observed that solubility required a polar aprotic solvent, and successful cyclization required the presence of water (entry 2). A 1:1 mixture of water and 1,4-dioxane was found to be ideal to generate the cyclized adduct **2.38** possessing the vinaxanthone cabocyclic scaffold. The structure of **2.38** was confirmed using 2D-NMR experiments including HMBC (Figure 2.18b). Interestingly, treatment of the triketo

monomer **2.37** with triethylamine resulted in the hydroxylated benzophenone adduct **2.58**. This product arises from a deacetoacetylation event following the initial Michael addition.

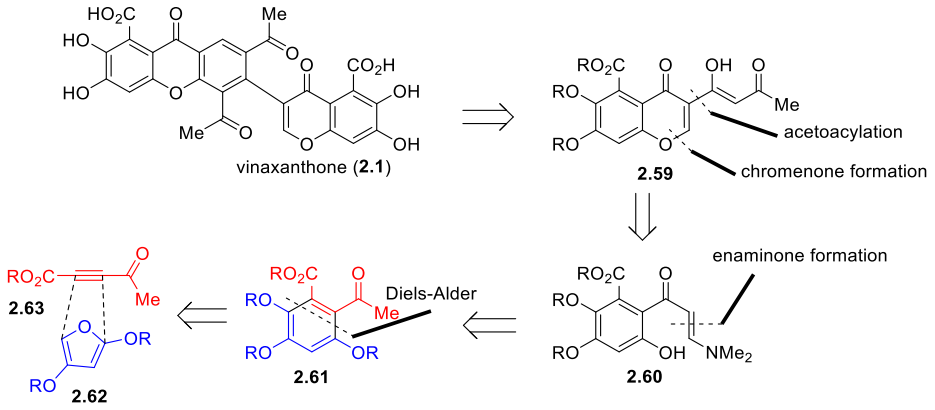

Figure 2.19. Retrosynthetic strategy for the total synthesis of vinaxanthone (**2.1**).

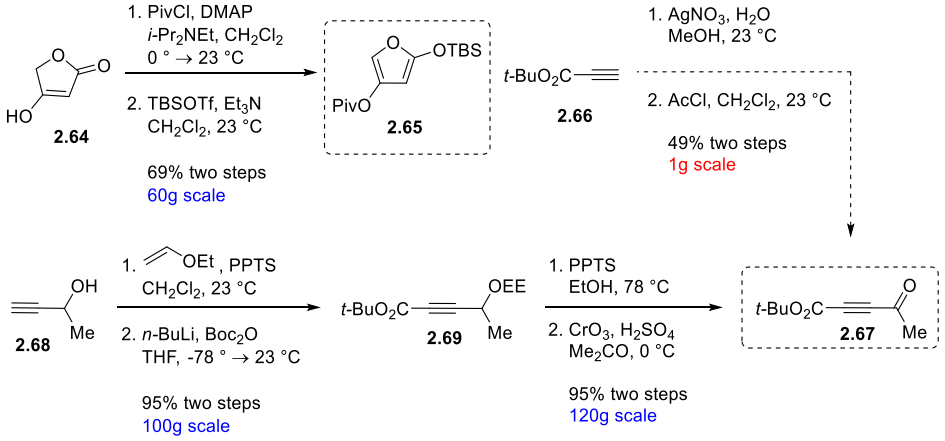

Figure 2.20. Scalable and cost-effective synthesis of diene **2.65** and dienophile **2.67**.

To approach the synthesis of vinaxanthone (**2.1**), retrosynthetic analysis followed analogously to the unfunctionalized triketone (Figure 2.19). 5,6-dehydropolivione in protected form (**2.59**) could be accessed through the acetoacylation of enaminone **2.60**. To provide rapid access to protected acetophenone **2.61**, a Diels-Alder reaction between an appropriate alkyne **2.63** and furan **2.62** was envisioned to forge the oxygenated arene. This follows from the work of T. Ross Kelly's synthesis of fredericamycin.[209]

Treatment of tetronic acid **2.64** with pivaloyl chloride yielded o-pivaloyl tetronate (Figure 2.20). Soft enolization with freshly prepared *tert*-butyldimethylsilyl triflate furnished furan **2.65** in 69% over two steps on 60g scale.[210,211] Preparation of keto ester **2.67** commenced with the protection of commercially available 3-butyn-2-ol **2.68**.[212] Alkyne deprotonation using *n*-butyl lithium followed by addition of di-*tert*-butyl dicarbonate gives the protected *tert*-butyl alkynoate **2.69** on 100g scale in 95% yield. Removal of the ethoxy ethyl protecting group with pyridinium *p*-toluenesulfonate in warm ethanol followed by oxidation of the resulting propargylic alcohol **2.69** using Jones' reagent produced keto ester **2.67** in 95% yield on 120g scale. Alternatively, the keto ester (**2.67**) could be accessed in a two-step sequence from *tert*-butyl propiolate (**2.66**).[213,214] This silver-mediated approach provided the keto ester (**2.67**) in 49% yield on 1g scale. The four-step synthesis was utilized as it was greatly amenable to scale.

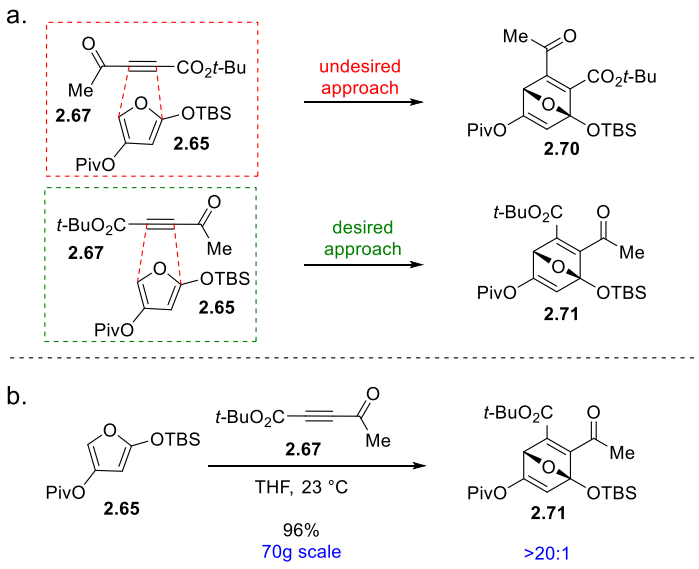

Figure 2.21. Diels-Alder reaction to form desired bicycle **2.71**.

With decagram quantities of both Diels-Alder precursors, the cycloaddition was carried out (Figure 2.21). The Diels-Alder reaction of symmetrical alkynes such as dimethyl acetylenedicarboxylate (DMAD) with furans is well documented.[215] In the case examined, however, two approaches by the dienophile (**2.67**) are possible (Figure 2.21a). While the ketone was anticipated to have the largest influence on the polarization of the dienophile, very little literature precedent exists for unsymmetrical alkyne selectivity.[209] LeCoq found that the selectivity of an aldehyde-ester alkyne was instead governed by the ester.[176] Combining the diene and dienophile at room temperature in THF forges bicycle **2.71** in 96% yield on 70g scale. Regioisomeric bicycle **2.70** was never observed. Excellent selectivity was a result of the ketone dominating the polarization of the dienophile.

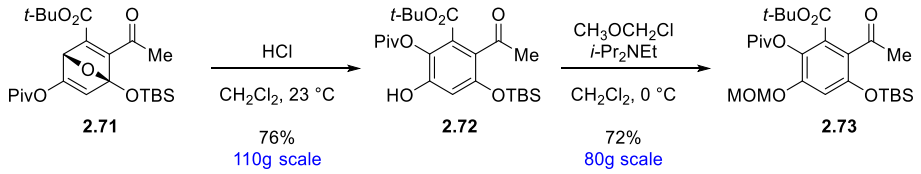

Figure 2.22. Synthesis of protected acetophenone **2.73**.

Anhydrous 4.0 M HCl in dioxane induced aromatization of the bicycle (**2.71**), forming acetophenone **2.72** in 76% yield on 110g. Using aqueous acid led to depressed yields due to protodesilylation of the furan, reverting the silyl enol ether **2.65** into pivaloyl tetronate. In the course of X-ray and ^{1}H-NMR analysis, it was determined that the pivaloyl group migrates during this reaction. It is postulated that the pivaloyl group transfers to the more nucleophilic phenol during the ring opening reaction. The remaining phenol was protected as a methoxymethyl ether using methoxymethyl chloride and Hünig's base, giving protected acetophenone (**2.73**) in 72% yield on 80g scale.

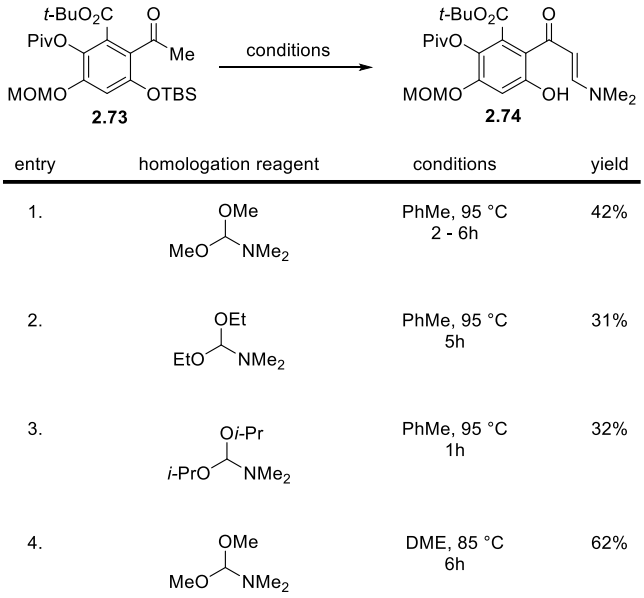

Figure 2.23. Optimization of the formation of enaminone **2.74**.

With access to large quantities of acetophenone **2.73**, the formation of enaminone **2.74** was investigated (Figure 2.23). Gammill's protocol calls for the use of commercially available N,N-dimethylformamide dimethylacetal (DMFDMA) as the homologation reagent and toluene as solvent.[186] Yields employing this procedure provided **2.74** in moderate yield (entry 1). Two additional N,N,-dimethylformamide dialkylacetal reagents were synthesized to probe whether sterics could promote more efficient ionization of the acetal. These reagents were synthesized by treating the Vilsmeier reagent with the corresponding alcohol and were purified by vacuum distillation.[216-218] Both diethyl and diisopropyl acetals proved to be less efficient than the corresponding dimethyl variant. Additionally, employing dimethoxy ethane (DME) in place of toluene was beneficial (entry 4). Yields of this step were higher and more reproducible in DME. Addition of N,N-dimethylformamide dimethylacetal furnished the hydroxyl enamino ketone **2.74** in 62% yield on 15g scale. The *in situ* generation of methoxide upon ionization of DMFDMA

conveniently desilylates the TBS phenol. Thus enaminone **2.74** was poised for acetoacylation directly.

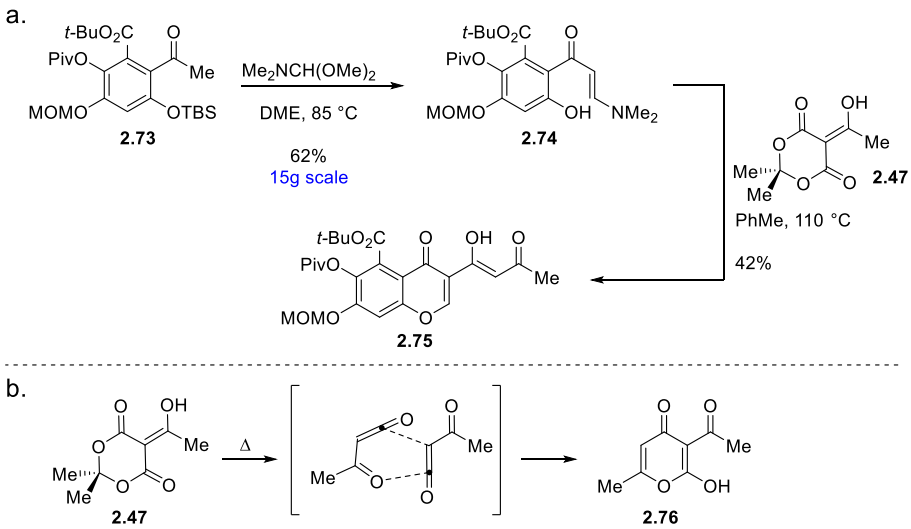

Figure 2.24. Synthesis of protected 5,6-dehydropolivione (**2.75**).

Enaminone **2.74** was subjected to the acetoacylation conditions optimized for the unfunctionalized triketone (Figure 2.24). However, utilizing Hoye's room temperature acylketene conditions yielded no desired triketo product. Employing acyl Meldrum's acid, however, furnished protected 5,6-dehydropolivione (**2.75**) in 42% yield. The differences in electronics of the model system and the oxygenated variant could rationalize the observed divergence in reactivity. In solution, the acetoacetyl group of **2.75** exists almost entirely as the enol tautomer (^{1}H-NMR: δ 15.87 ppm). The major byproduct in the acetoacylation reactions is dehydroacetic acid (**2.76**) resulting from the hetero Diels-Alder reaction between two molecules of acylketene (**2.48**) (Figure 2.24b). Three equivalents of acyl-Meldrum's acid (**2.47**) proved optimal for this reaction. Additional amounts of acyl-Meldrum's acid did not improve the isolated yield of **2.75** and the generation of dehydroacetic acid produced (**2.76**) rendered chromatographic purification tedious.

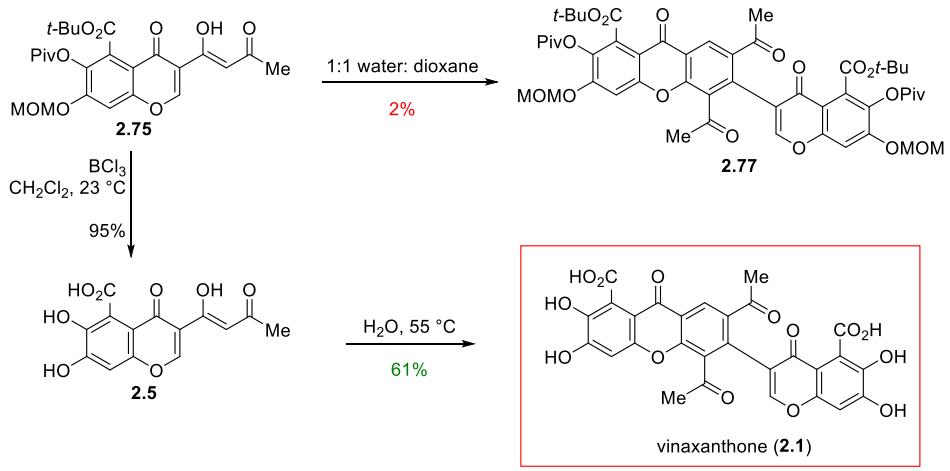

Figure 2.25. Endgame for the synthesis of vinaxanthone (**2.1**).

With protected 5,6-dehydropolivione (**2.75**) in hand, the dimerization was attempted (Figure 2.25). Under a variety of conditions, only 2% of protected vinaxanthone (**2.77**) was isolated upon warming **2.75** in 1:1 water: dioxane. An alternative strategy was pursued whereby deprotection of **2.75** occurred before the dimerization reaction. Gratifyingly, deprotection of **2.75** proceeded smoothly using boron trichloride at room temperature, providing 5,6-dehydropolivione (**2.5**) in 95% yield as a white solid. Simply stirring 5,6-dehydropolivione (**2.5**) in water at 55 °C formed vinaxanthone (**2.1**) as an off-white solid in 61% yield after trituration with methanol. The mild reactions conditions that proved optimal to forge vinaxanthone (**2.1**) from 5,6-dehydropolivione (**2.5**) supports our proposed biosynthesis. Additionally, this result could indicate that the natural product is formed in nature non-enzymatically.

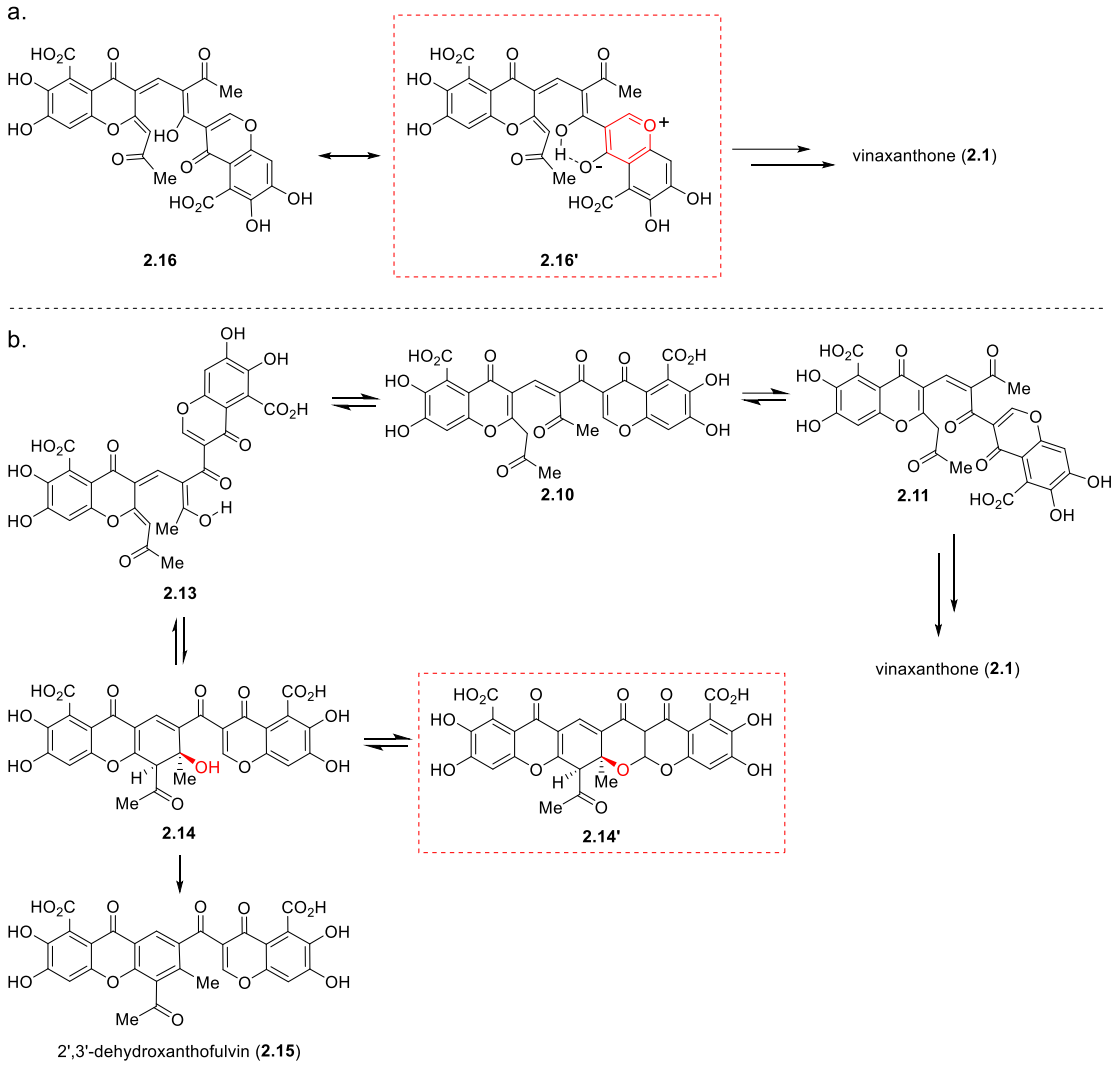

Figure 2.26. Rationale for the formation of vinaxanthone (**2.1**) over 2',3'-dehydroxanthofulvin (**2.15**).

In the dimerization of 5,6-dehydropolivione (**2.5**), only vinaxanthone (**2.1**) was isolated. To account for the formation of vinaxanthone (**2.1**) over 2',3'-dehydroxanthofulvin (**2.15**), an aromaticity-assisted hydrogen bound is invoked (Figure 2.26a).[219-222] Hydrogen bonding can significantly influence the structure, relative stability, and reactivity of heterocycles.[219] Conjugated enol **2.16** (precursor to the 6π

electrocyclization *en route* to vinaxanthone (**2.1**)) is in resonance with cyclic oxonium **2.16'**. This aromatic oxonium stabilizes the extended enol tautomer and lowers the energy of the transition state for the subsequent 6π electrocyclization reaction. An alternative explanation is that an intermediate to xanthofulvin (**2.2**) is diverted (Figure 2.26b). For example, 6π electrocyclization of **2.13** provides allylic alcohol **2.14**. The alcohol is poised to engage the proximal chromenone in a reversible 1,4-addition providing acetal **2.14'**. Formation of **2.14'** precludes the subsequent irreversible dehydration and aromatization step to form 2',3'-dehydroxanthofulvin (**2.15**).

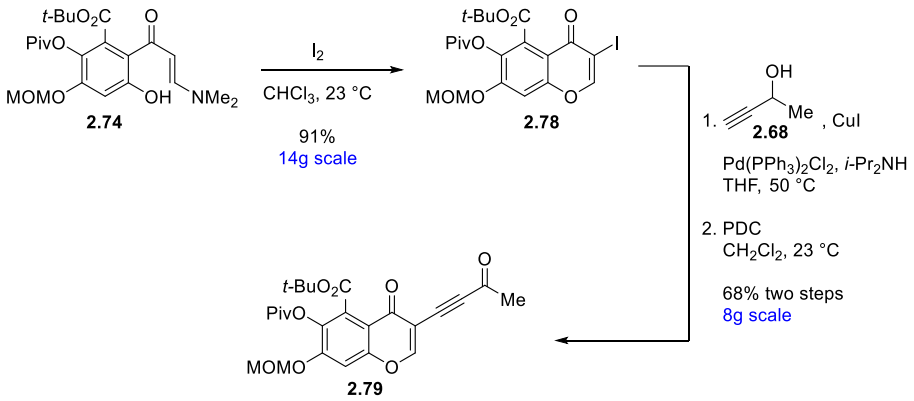

Figure 2.27. Synthesis of ynone **2.79**.

Xanthofulvin (**2.2**) was accessed *via* enaminone **2.74** (Figure 2.27). Iodination of **2.74** proceeded smoothly in chloroform, providing the corresponding 3-iodochromenone (**2.78**) as a white solid.[186,223] Sonogashira cross-coupling of the iodochromenone **2.78** with 1-butyn-2-ol (**2.68**) gives the propargylic alcohol.[224,225] Pyridinium dichromate (PDC, Cornforth reagent) oxidation of the alcohol to the ketone forms ynone **2.79** in 68% yield over two steps.[226] Alternative oxidants including manganese dioxide either provided inconsistent yields or decomposition (Swern conditions). Attempts at directly coupling 3-butyn-2-one to iodochromenone **2.78** either *via* Sonogashira or Castro-Stephens coupling

was not productive. Electronically poor alkynes, and acyl alkynes in particular are known to be poor coupling partners.[227,228]

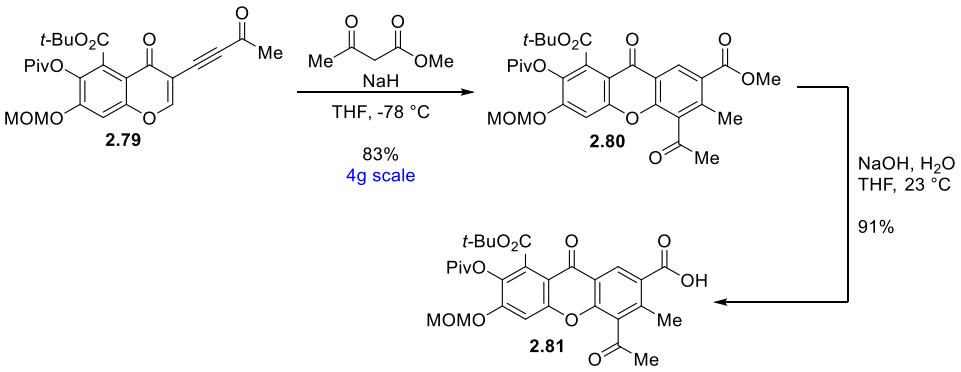

Figure 2.28. Preparation of xanthone **2.81**.

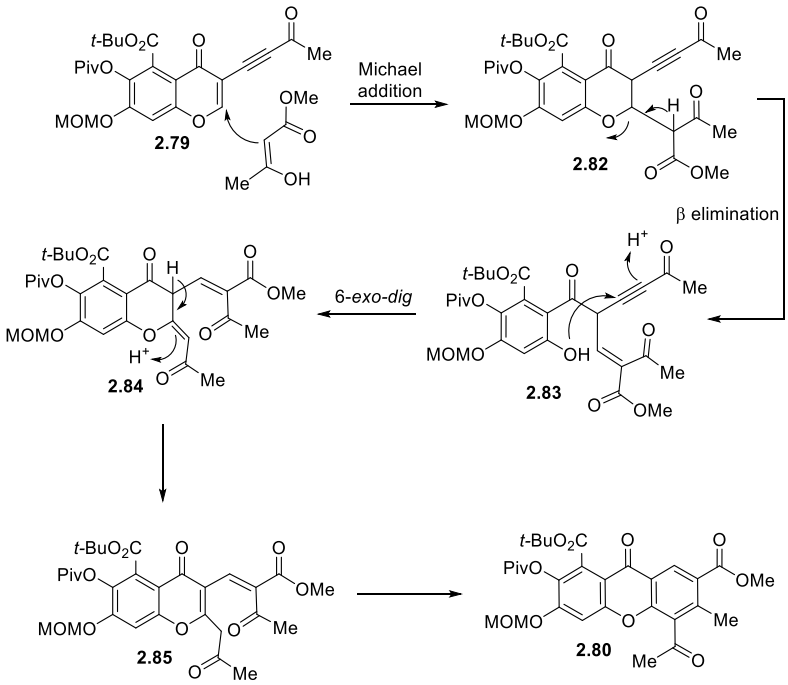

Figure 2.29. Mechanism for the formation of xanthone **2.80**.

Hu and co-workers developed a methodology for the addition and subsequent cyclizations of enolates into 3-alkynyl chromenones, yielding a variety of substituted

xanthones.[229-231] Addition of the pre-formed sodium salt of methyl acetoacetate into the ynone (**2.79**) provided xanthone **2.80** in 83% yield (Figure 2.28). In this reaction, temperature control was found to be critical to minimize deacylation. Cooling the reaction to -78 °C suppressed this byproduct and improved the yield of **2.80**. The resulting methyl ester is saponified using sodium hydroxide in 3:1 tetrahydrofuran (THF): water, yielding xanthone carboxylic acid **2.81** in 91% yield. To account for the formation of xanthone **2.80**, a mechanism is outlined in Figure 2.29. Methyl acetoacetate adds in a conjugate form, providing chromanone **2.82**. Elimination yields phenolic adduct **2.83**. A six-*exo-dig* cyclization of the phenol into the ynone forms a 2,3-disubstituted chromanone (**2.82**). The chromenone core (**2.85**) is reformed *via* isomerization of the exocyclic olefin **2.84**. Following tautomerization of the dienone, 6π electrocyclization furnishes xanthone **2.80**.

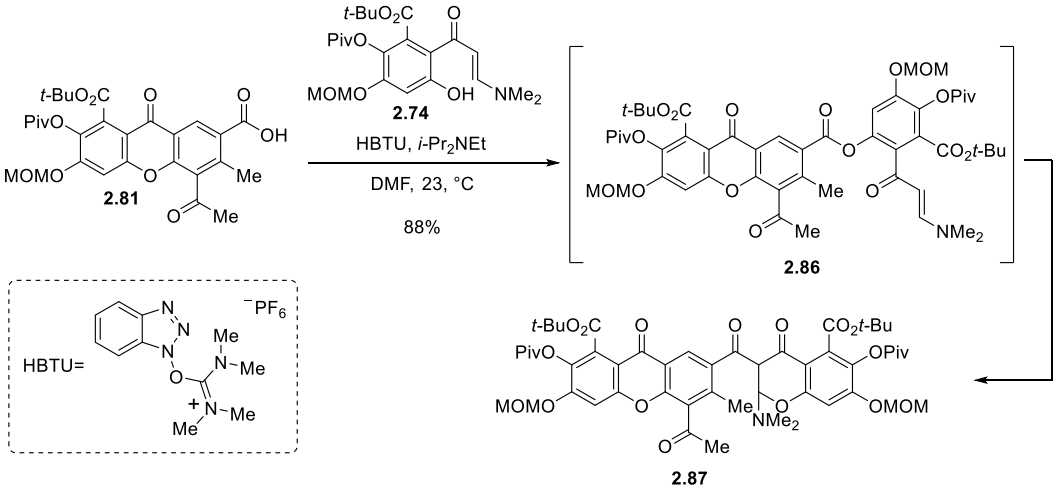

Figure 2.30. Carboxylate coupling and O-to-C migration.

To complete the construction of the carbocyclic core of xanthofulvin (**2.2**), we envisioned coupling the carboxylic acid (**2.81**) to the 3 position of the chromenone *via* ester **2.86**. After screening many coupling reagents and pre-formed electrophiles, the coupling reagent N,N,N',N'-tetramethyl-O-(1H-benzotriazol-1-yl)uranium hexafluorophosphate

(HBTU) formed the aminal (**2.87**) in 88% yield. As the byproducts are water soluble, material prepared using HBTU did not require chromatographic purification. Additionally, this procedure avoided the need to pre-form the acyl imidazolide or other activated carboxylic acid derivatives.[188] Using DCC or EDCI also promoted the rearrangement, although separation of the urea byproducts was tedious. Due to the success of using a variety of different coupling reagents, the intermediacy of benzoate **2.86** is implicated prior to the rearrangement. However, unlike previous examples utilizing enaminones to forge 3-substituted chromenones, the dimethylamino group did not eliminate under the reaction conditions.

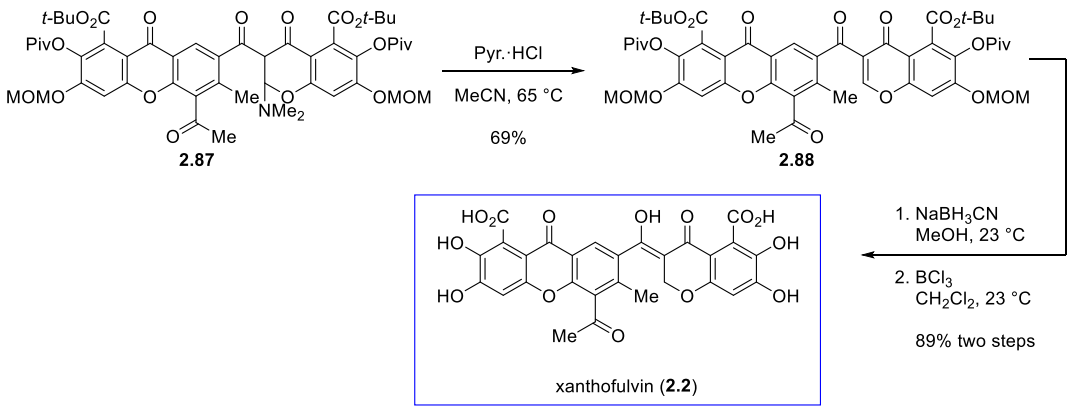

Figure 2.31. Endgame of the synthesis of xanthofulvin (**2.2**).

Elimination of dimethylamine was accomplished using anhydrous, freshly prepared pyridinium hydrochloride. Following this procedure, protected dehydroxanthofulvin (**2.88**) was formed in 69% yield. All starting material and reagents must be rigorously anhydrous, as water led to decomposition of aminal **2.87**. Conjugate reduction of the chromenone ring using sodium cyanoborohydride in methanol provided xanthofulvin in protected form. Global deprotection was achieved with boron trichloride, yielding xanthofulvin (**2.2**) after trituration with chloroform, as a yellow solid in 89% yield. Synthetic xanthofulvin (**2.2**)

matched the spectroscopic data for both isolated xanthofulvin and 411J (**2.4**), suggesting that xanthofulvin (**2.2**) is the correct structure of the natural product.[166,180]

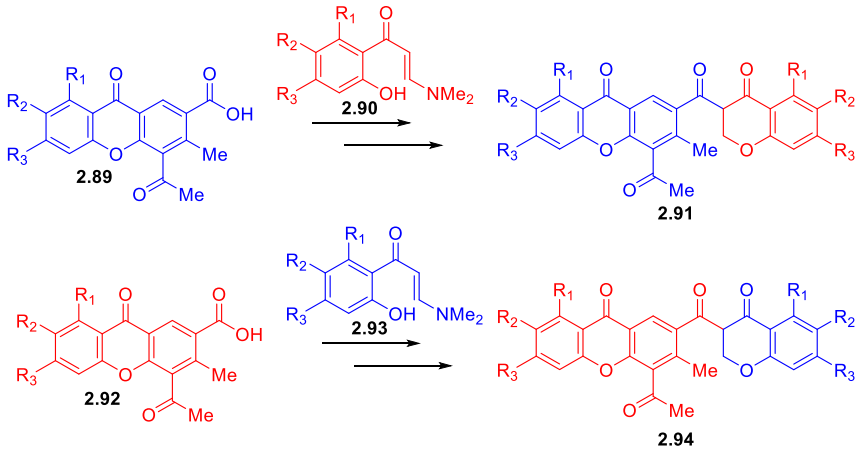

Figure 2.32. Generation of chemically edited xanthofulvin derivatives.

The advantages of the synthesis of xanthofulvin (**2.2**) is that the approach furnishes the core through a modular and controlled union of a xanthone and chromenone equivalent. Thus, in the future, new analogs of xanthofulvin can be prepared where the oxygenation pattern of the xanthone core differs from the chromenone core (Figure 2.32). Performing the O-to-C rearrangement with an enamino ketone processing oxygenation differing from that of the xanthone core, would provide a new derivative of xanthofulvin (**2.91** and **2.94**, for example). The overall goal would be to determine the effects on regeneration by manipulating the oxygenation pattern of xanthofulvin (**2.2**).

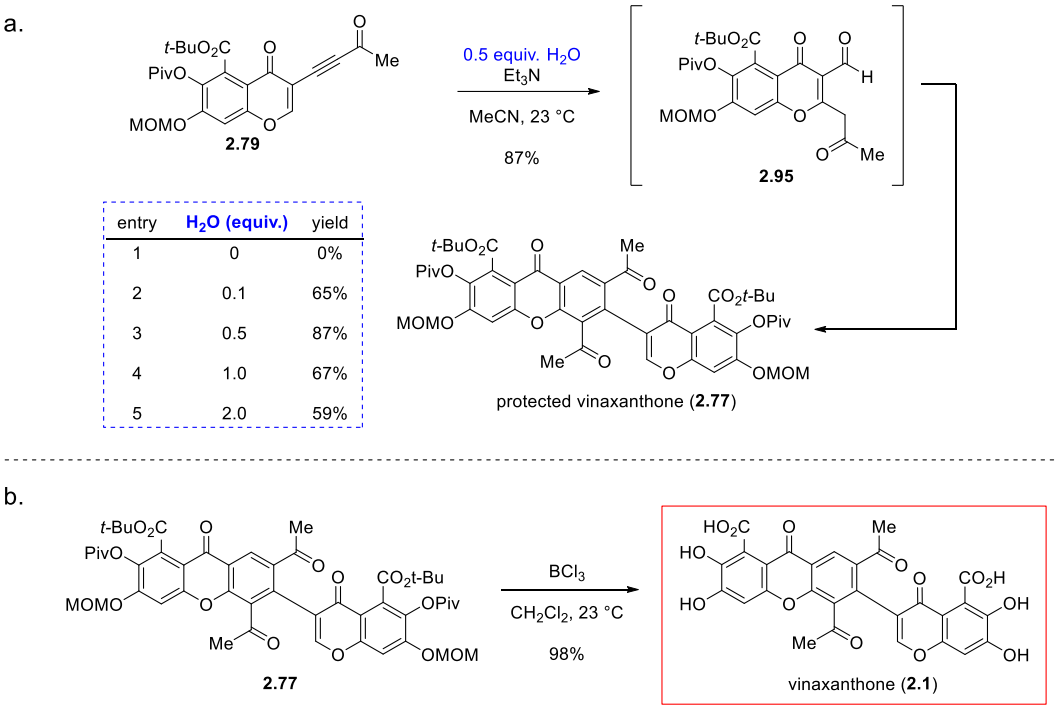

Figure 2.33. Second generation synthesis of vinaxanthone (**2.1**) from ynone **2.79**.

During the synthesis of xanthofulvin (**2.2**) it was serendipitously discovered that ynone **2.79** could be converted to protected vinaxanthone (**2.77**) with treatment of water and triethylamine at 23 °C (Figure 2.33). The amount of water was found to be critical to the reaction yield. With careful occlusion of water, unreacted starting material was re-isolated. Utilizing sub-stoichiometric amounts of water allowed for the generation of protected vinaxanthone (**2.77**) in good yield. Addition of 0.1 equivalents formed **2.77** in 65% yield. It was determined empirically that 0.5 equivalents of water was optimal, providing protected vinaxanthone in 87% yield on gram scale. Increasing the amount of water led to lower yields of **2.77**. Analogous to the first generation synthesis of vinaxanthone, deprotection utilizing boron trichloride provided vinaxanthone (**2.1**) in 98% yield.

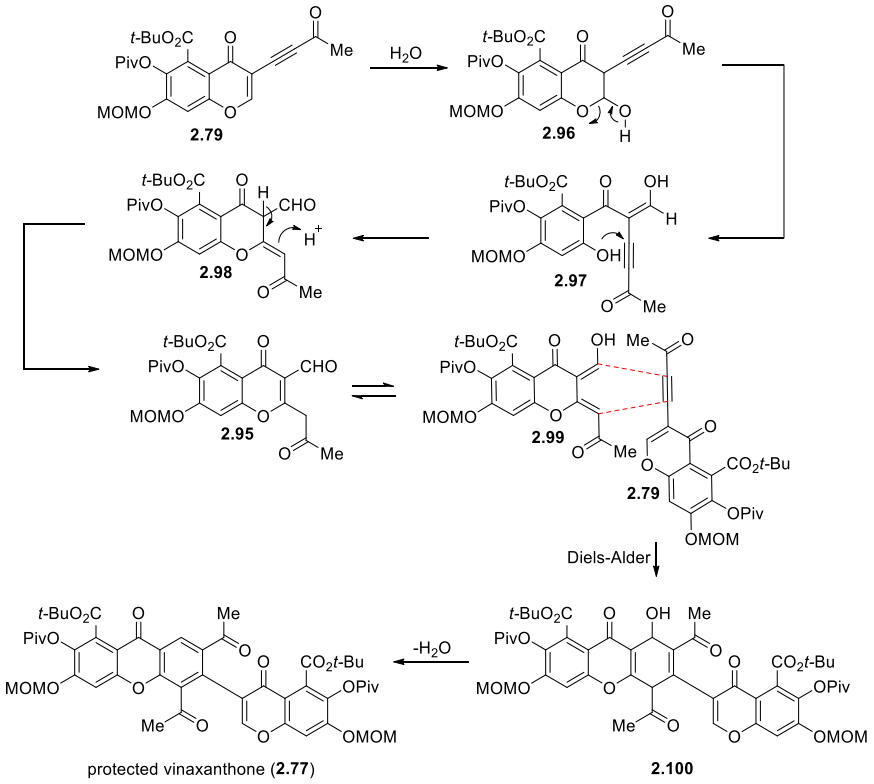

Figure 2.34. Proposed mechanisms of ynone (**2.79**) coupling to form protected vinaxanthone (**2.77**).

Based on the outcome of the optimization experiments, the mechanism for the formation of protected vinaxanthone (**2.77**) is depicted in Figure 2.34. 1,4-addition of water into the chromenone of ynone **2.79** provides hemiacetal **2.96**. Collapse of the resulting hemiacetal gives phenol **2.97**. Bond rotation and subsequent addition of the phenol into the alkynone furnishes chromanone **2.98**. Isomerization of the exocyclic olefin gives aldehyde **2.95**. Upon tautomerization of the aldehyde into its enal form (**2.99**)**,** Diels-Alder cyclization with another molecule of ynone **2.79** forms allylic alcohol **2.100**. Finally, loss of water furnishes protected vinaxanthone **2.77.** To test whether aldehyde **2.95** could be isolated discretely, ynone **2.79** was treated with 1000 equivalents of water. Hydration of the ynone (**2.79**) resulted in isolation and characterization of aldehyde **2.95,** which was

then combined with ynone **2.79**, forming **2.77** and supporting the proposed mechanism for its formation**.**

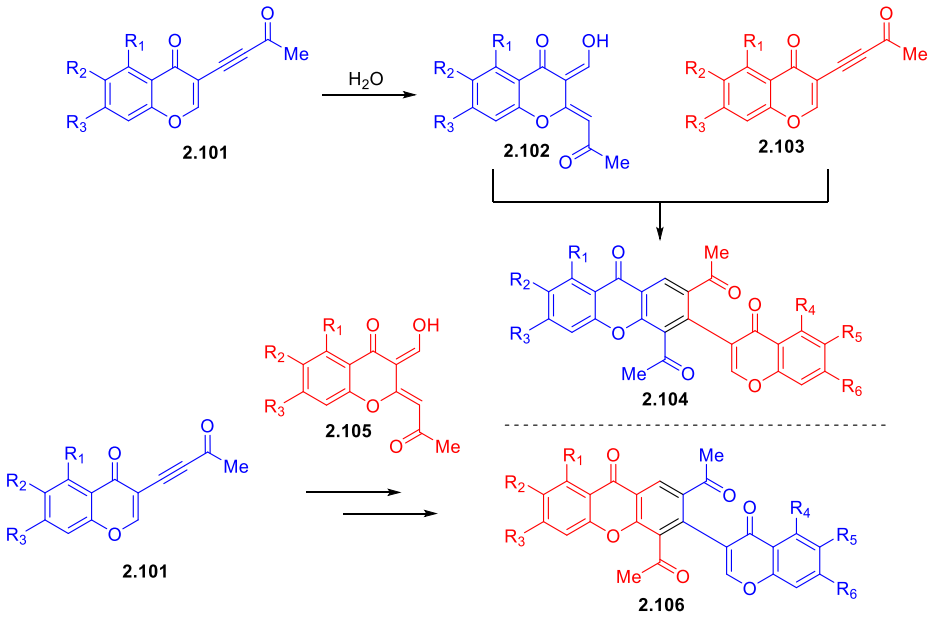

Figure 2.35. Access to chemically edited vinaxanthone analogs.

The second generation synthesis of vinaxanthone (**2.1**) provides an opportunity to generate a coupling partner *in situ* to react with another ynone (Figure 2.35). For example, hydration of ynone **2.101** provides enal **2.102**. Combining **2.102** with **2.103** provides vinaxanthone derivative **2.104**. Alternatively, ynone **2.103** could be hydrated, providing enal **2.105**. Admixture of **2.105** with ynone **2.101** gives new derivative **2.106**. With six distinct functionality to manipulate (four phenols and two carboxylates), this would provide $2^6 = 64$ possible derivatives of vinaxanthone, all accessible from the synthesis of eight ynones.

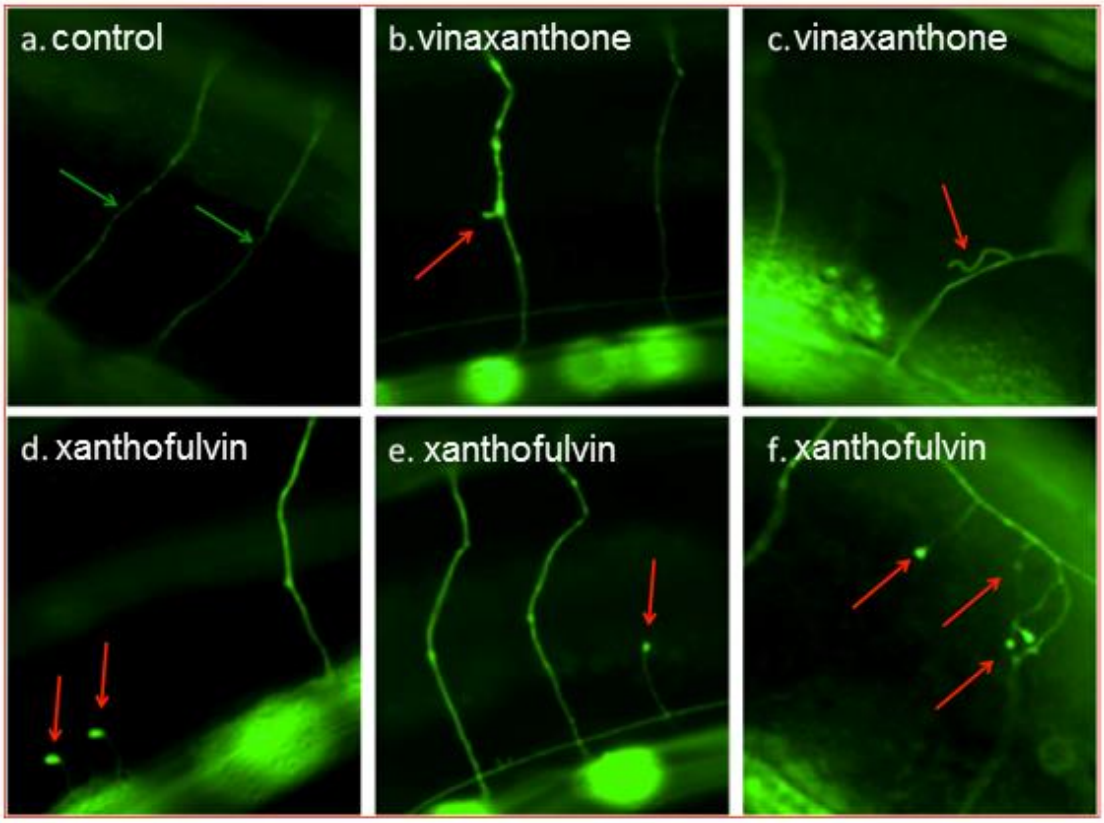

Figure 2.36. Axonal outgrowth of vinaxanthone (**2.1**) and xanthofulvin (**2.2**).

Utilizing an *in vivo* assay developed to identify small molecules that promote outgrowth of neurons, vinaxanthone (**2.1**) and xanthofulvin (**2.2**) and 25 derivatives of vinaxanthone prepared following the second generation synthesis, were screened in the nematode *Caenorhabditis elegans* (Figure 2.36).[232] Mutant, age-synchronized *C. elegans* (twenty worms observed in triplicate) possessing GFP-labeled cholinergic neurons were treated with vinaxanthone (**2.1**) or xanthofulvin (**2.2**) and then observed under fluorescence microscopy for outgrowth. Cholinergic neurons are expressed both ventrally and dorsally along the body of the worm, with commissures protruding latitudinally to connect the ventral and dorsal nerve cords. Worms are scored on whether new branching from commissures (Figure 2.36b) or sprouting from the ventral or dorsal nerve cord (Figure

2.36d) or sublateral nerve cord (Figure 2.36e) are observed. At concentrations of 2.0 μM vinaxanthone (**2.1**) and xanthofulvin (**2.2**) promoted growth in 32% and 31% of worms, respectively. The amount of outgrowth is comparable to dibutyryl cAMP, which promotes growth in 36% of worms at the same concentration and less than 18% of control worms.[233]

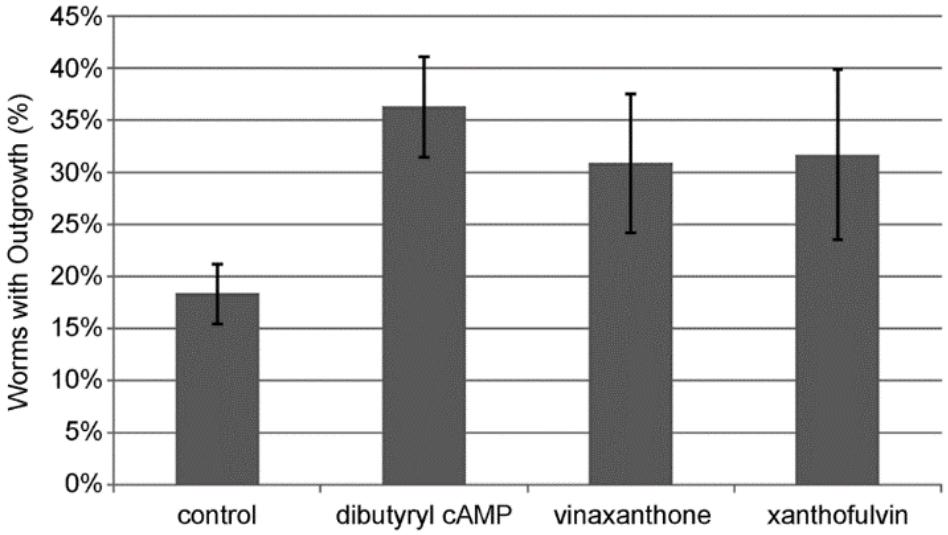

Figure 2.37. Outgrowth of vinaxanthone (**2.1**) and xanthofulvin (**2.2**) in *C. elegans*.

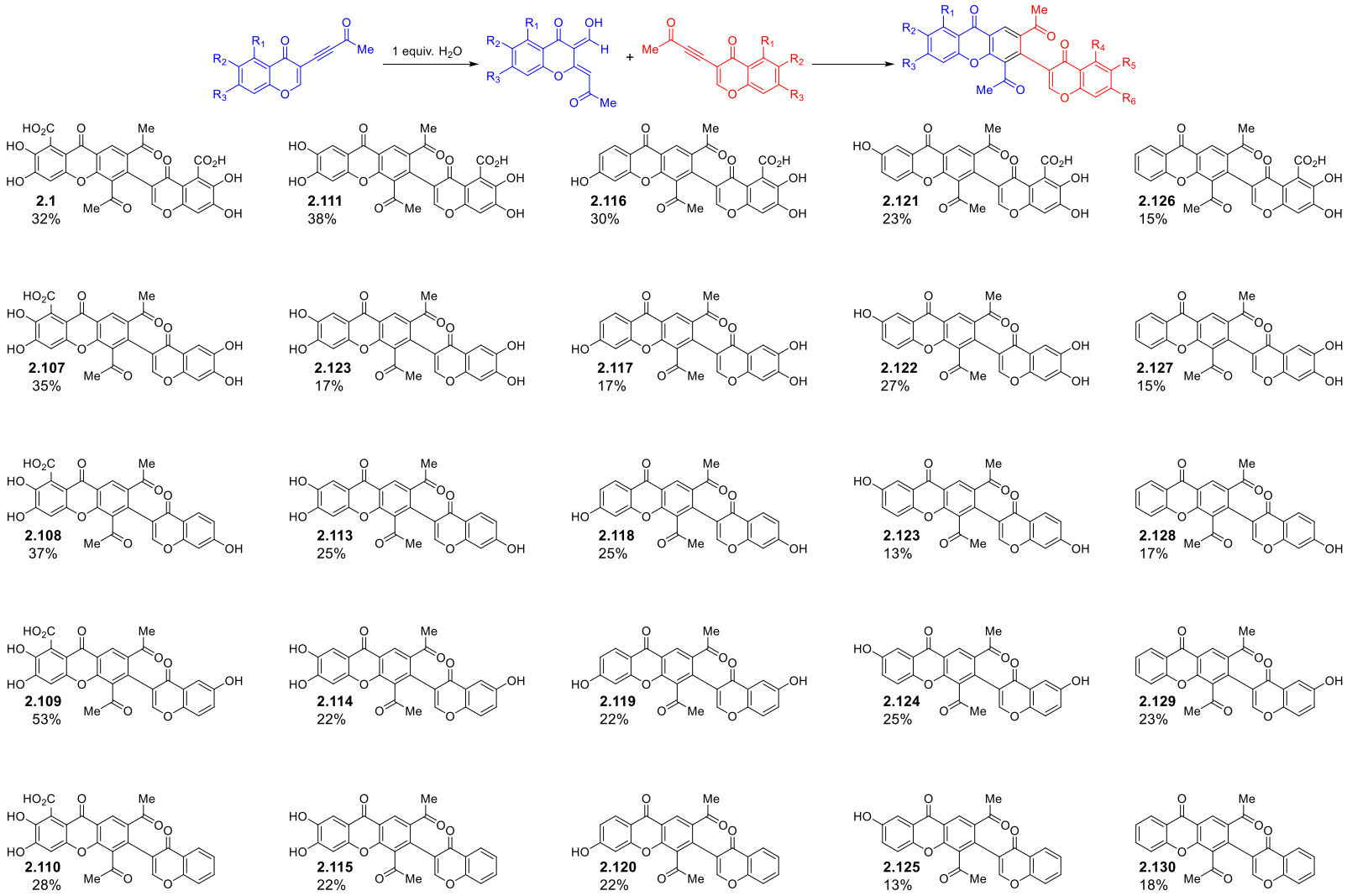

Figure 2.38. Outgrowth of chemically edited derivatives of vinaxanthone.

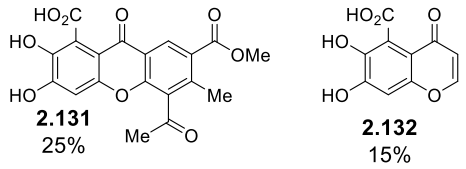

Figure 2.39. Outgrowth of xanthone methyl ester (**2.131**) and chromenone (**2.131**).

Utilizing the controlled condensation reaction developed for the second generation synthesis of vinaxanthone (**2.1**), five ynones were synthesized, resulting in 25 analogs of vinaxanthone possessing different levels of oxidation. These derivatives were subjected to the *C. elegans* outgrowth assay (Figure 2.38). Several derivatives (**2.107**, **2.108**, **2.109**, and **2.111**) matched or outperformed the outgrowth observed for vinaxanthone (**2.1**). From this data, maintaining the oxygenation pattern of the xanthone core of vinaxanthone is more critical to outgrowth than the chromenone core. Two additional truncated small molecules were also tested for outgrowth (Figure 2.39). Xanthone methyl ester **2.131** resulted in only 25% of worms with outgrowth and chromenone **2.132** displayed poor outgrowth, demonstrating the synergistic effect of both the chromone and xanthone chore of the molecule together in these natural products.

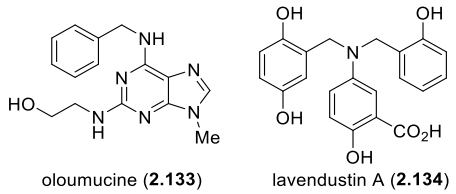

Figure 2.40. Sema3A inhibitors oloumucine (**2.133**) and lavendustin A (**2.134**).

With access to synthetic vinaxanthone (**2.1**) and xanthofulvin (**2.2**) and confirmation of the growth promoting capabilities of these molecules utilizing *C. elegans*, the biological targets were reexamined. Genetic attenuation of the NRP1/ plex 1 complex, the receptor targeted by Sema3A, does not yield axonal protuberance observed following

injury.[234] Additionally, inhibition at the post-receptor level employing olomoucine (**2.133**) or lavendustin A (**2.134**) does not promote growth (Figure 2.40).[235] The observation that vinaxanthone (**2.1**) and xanthofulvin (**2.2**) *do* promote growth and regeneration in these assays indicates they are targeting another growth promoting biological receptor in addition to Sema3A.

The poly-anionic nature of vinaxanthone (**2.1**) and xanthofulvin (**2.2**) at physiological pH could mean that the protein receptor is located on the outside of the cell, like Sema3A. An important class of transmembrane domain receptors are G-protein coupled receptors (GPCRs). GPCRs are only found in eukaryotes and are responsible for regulating the majority of important physiological processes.[236] While comprising less than one thousand of the protein-coding genes found in the human genome, these cell-surface receptors are the pharmacological target of more than half of all therapeutics.[237,238] Given the ubiquity of GPCRs as therapeutic targets, we subjected vinaxanthone (**2.1**) and xanthofulvin (**2.2**) to a panel of GPCRs.

Both vinaxanthone (**2.1**) and xanthofulvin (**2.2**) proved to be strong positive allosteric modulators of succinate receptor 1 (SUCNR1). However, neither were agonists nor antagonists of this GPCR (vinaxanthone only had 4.4% efficacy of activating SUCNR1 without succinate present). Allosteric modulators are ligands that interact with binding sites that differ topographically from the site recognized by the endogenous agonist. Positive allosteric modulators amplify the attraction of the endogenous ligand to the orthosteric site. Additionally the allosteric site tends to be more promiscuous than the orthosteric site due to decreased evolutionary pressure.[239-241]

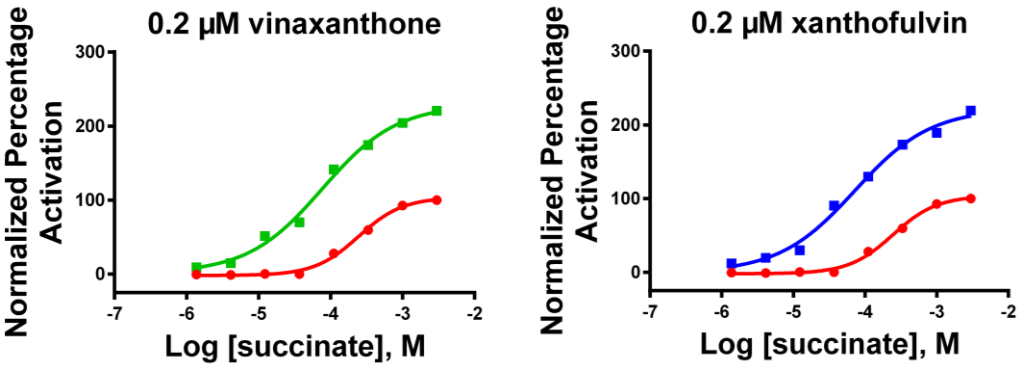

	Predicted EC_{50} Potency (μM)	Predicted Dose Ratio	Efficacy
sodium succinate	230	1	100%
sodium succinate + 0.2 μM vinaxanthone	76	0.33	230%
sodium succinate + 0.2 μM xanthofulvin	73	0.32	222%

Figure 2.41. Vinaxanthone (**2.1**) and xanthofulvin (**2.2**) are allosteric modulators of SUCNR1.

In the presence of succinate and at concentrations of 0.2 μM, vinaxanthone (**2.1**) and xanthofulvin (**2.2**) have dose ratios of 0.33 and 0.32 and efficacy of 230% and 220%, when compared to sodium succinate alone (Figure 2.41). A concentration of 0.2 μM is the same concentration that vinaxanthone (**2.1**) and xanthofulvin (**2.2**) were previously tested for Sema3A activity, demonstrating that at this concentration SUCNR1 is also activated. Vinaxanthone (**2.1**) was screened against SUCNR1 at a variety of concentrations and was found to remain active down to 1 nM (Figure 2.42).

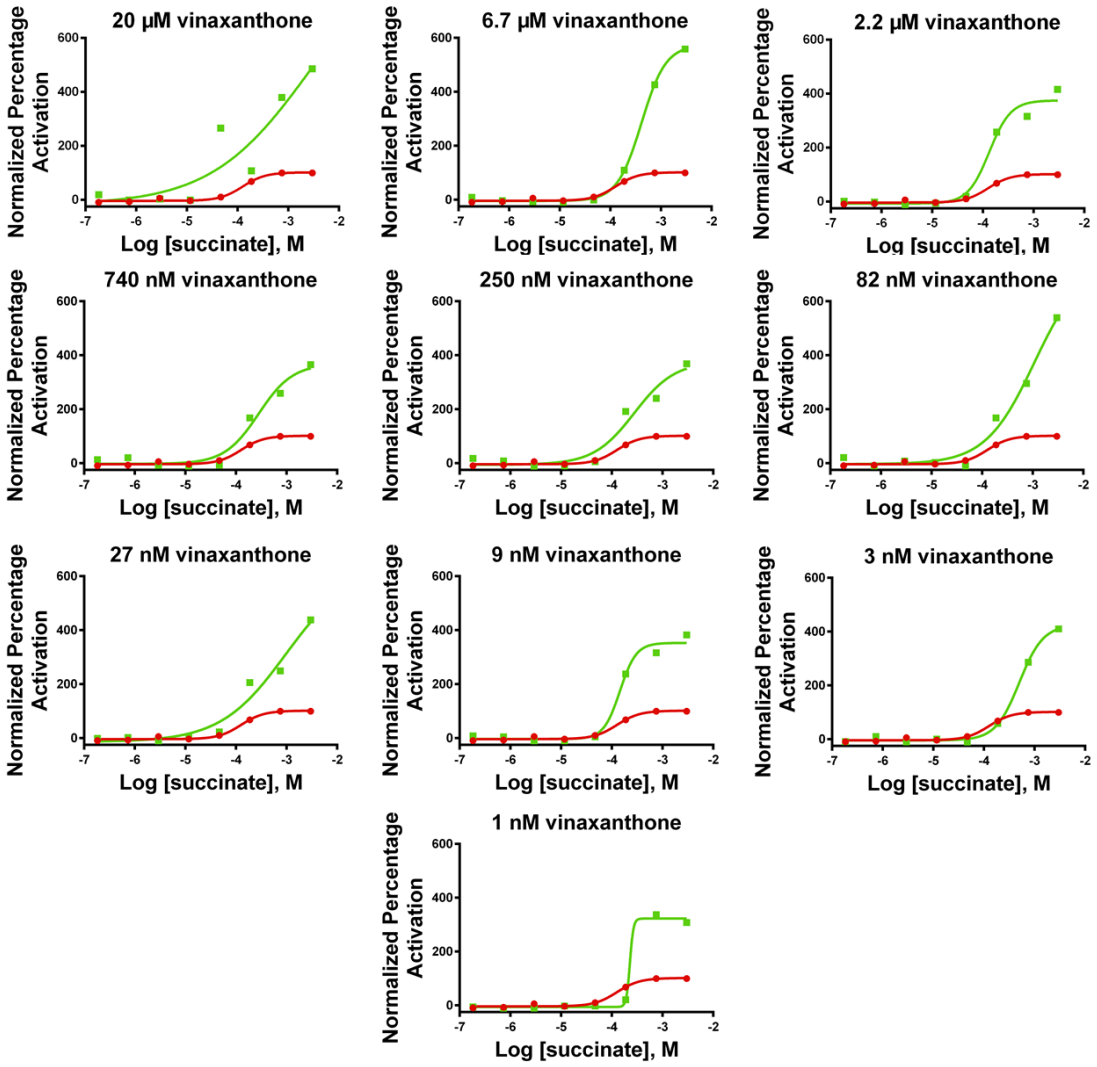

Figure 2.42. Activation of SUCNR1 at various concentrations of vinaxanthone (**2.1**).

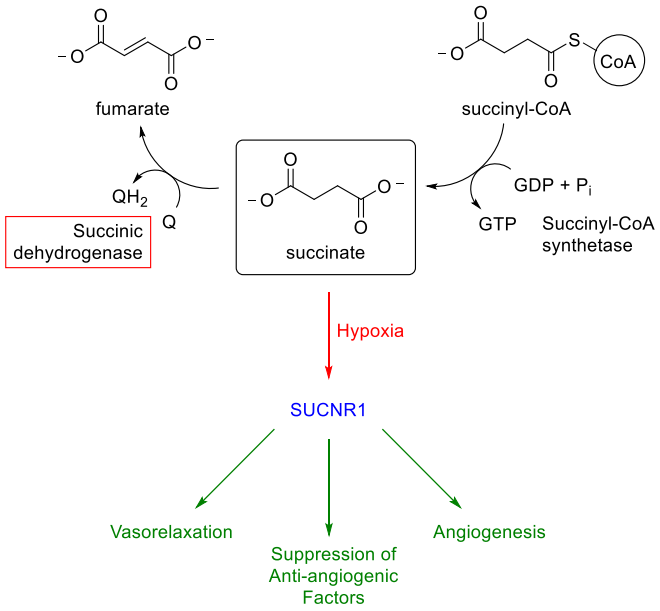

Figure 2.43. Activation of SUCNR1 leads to angiogenesis and release of cell proliferation factors.

Succinate, an intermediate in the Krebs cycle is the native ligand for SUCNR1 (identified previously as GPR91).[242] During hypoxia, nonoxidized flavin and nicotinamide nucleotide inhibit succinic dehydrogenase (Figure 2.43).[243] As a result of this inhibition, cellular concentrations of succinate increase, activating SUCNR1. In the short term, this triggers vasorelaxation which re-establishes blood flow, and thus increases oxygen and nutrient supply to the hypoxic tissue. Anti-angiogenic factors including thrombospondin-1 are also suppressed.

In addition to inhibiting anti-angiogenic factors, SUCNR1 has been shown to be a long-term regulator of pro-angiogenic factors including angiopoietin 1 and 2 and VEGF.[243] For example, genetic knockdown of SUCNR1 attenuates vasoproliferation in a mouse model. Significantly, Sema3A and VEGF share the same extracellular receptor, thus activation of VEGF opposes the action of Sema3A.[243] From this data, vinaxanthone (**2.1**) and xanthofulvin (**2.2**) inhibit Sema3A, and, through the actions of SUCNR1, stimulate the

growth promoting molecule VEGF. This dual role for vinaxanthone (**2.1**) and xanthofulvin (**2.2**) addresses the neuronal regeneration observed following injury.

MODEL SYSTEM EXPERIMENTAL SECTION

Organic solutions were concentrated by rotary evaporation at ~ 20 torr. Methylene chloride (CH_2Cl_2), diethyl ether (Et_2O), tetrahydrofuran (THF) and toluene (PhMe) were purified using a Pure-Solv MD-5 Solvent Purification System (Innovative Technology). All other reagents and solvents were used directly from the supplier without further purification. Analytical thin-layer chromatography (TLC) was carried out using 0.2 mm commercial silica gel plates (silica gel 60, F254, EMD chemical) and visualized using a UV lamp. TLC plates were stained using ceric ammonium molybdate (CAM), aqueous potassium permanganate ($KMnO_4$) or iodine. Infrared spectra were recorded on a Nicolet 380 FTIR using neat thin film technique. High-resolution mass spectra (HRMS) were recorded on a Karatos MS9 and are reported as m/z (relative intensity). Accurate masses are reported for the molecular ion $[M+Na]^+$, [M+H], $[M^+]$, or [M-H]. Nuclear magnetic resonance spectra (^{1}H-NMR and ^{13}C-NMR) were recorded with a Varian Mercury 400 (400 MHz, ^{1}H at 400 MHz, ^{13}C at 100 MHz), Agilent MR 400 (400 MHz, ^{1}H at 400 MHz, ^{13}C at 100 MHz), Varian DirectDrive 400 (400 MHz, ^{1}H at 400 MHz, ^{13}C at 100 MHz), or Varian DirectDrive 600 (600 MHz, ^{1}H at 600 MHz, ^{13}C at 150 MHz). For $CDCl_3$ solutions the chemical shifts are reported as parts per million (ppm) referenced to residual protium or carbon of the solvent: δ H (7.26 ppm) and δ C (77.0 ppm). Coupling constants are reported in Hertz (Hz). Data for ^{1}H-NMR spectra are reported as follows: chemical shift (ppm, referenced to protium; s = singlet, d = doublet, t = triplet, q = quartet, p = pentet, sext = sextet, sept = septuplet, dd = doublet of doublets, td = triplet of doublets, ddd = doublet of doublet of doublets, m = multiplet, coupling constant (Hz), and integration). Melting points were measured on a MEL-TEMP device without corrections.

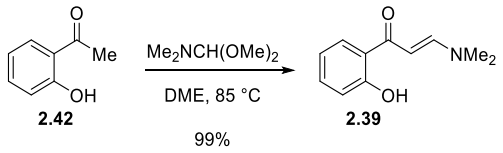

The preparation of the enamino ketone follows a modified procedure reported by Gammil. *O*-hydroxy acetophenone (**2.42**) (3.0 g, 22.0 mmol, 1.0 equiv.) and dimethylformamide dimethylacetal (8.81 mL, 66.1 mmol, 3.0 equiv.) combined in dimethoxy ethane (44.1 mL). The colorless solution heated to 95 °C and after five hours the red homogeneous solution was concentrated *in vacuo* to afford **2.39** (4.18 g, 21.9 mmol, 99% yield).

golden solid, M.P. = 128-129 °C; $\mathbf{R_f}$ = 0.24 (silica gel, 1:1 hexanes: EtOAc); **^{1}H-NMR** (400 MHz, $CDCl_3$) δ 7.89 (d, *J* = 12.0 Hz, 1H), 7.69 (dd, *J* = 7.9, 1.7 Hz, 1H), 7.35 (ddd, *J* = 8.6, 6.8, 1.7, 1H), 6.84 (dd, *J* = 8.2, 1.0 Hz, 1H), 6.81 (ddd, *J* = 7.9, 6.8, 1.0 Hz, 1H), 5.79 (d, *J* = 12.3 Hz, 1H), 3.20 (s, 3H), 2.98 (s, 3H); **^{13}C-NMR** (100 MHz, $CDCl_3$) δ 191.3, 162.8, 154.7, 133.8, 128.2, 120.2, 118.0, 117.9, 89.8, 42.3, 37.3; **IR** (film, cm $^{-1}$) 1633, 1585, 1544, 1368; **HRMS** (ESI) calcd. for $C_{11}H_{14}NO_2$ $[M+H]^+$: 192.10191, obs. 192.10219.

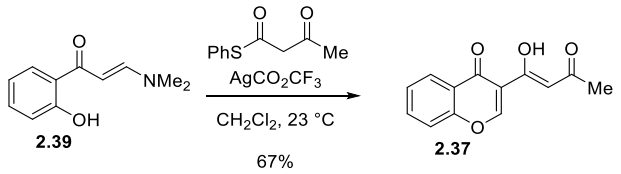

To a stirred solution of enaminone **2.39** (50.0 mg, 0.261 mmol, 1.0 equiv.) and silver trifluoroacetate (57.8 mg, 0.261 mmol, 1.0 equiv.) in dichloromethane (2.60 mL) was added phenyl thioacetoacetate (78.0 µL, 0.261 mmol, 1.0 equiv.). The flask was protected from light and the heterogeneous solution was stirred for 48 hours. The reaction was the diluted with chloroform, passed through a pad of celite, and concentrated. The resulting orange semisolid was purified using acidified silica gel* and 7:1 hexanes: EtOAc as the eluent to afford **2.37** (40.0 mg, 0.174 mmol, 67% yield).

white solid, M. P. = 142 – 144 °C; $\mathbf{R_f}$ = 0.33 (silica gel, 3:1 hexanes: EtOAc); **^{1}H-NMR** (400 MHz, $CDCl_3$) δ 15.90 (s, 1H), 8.78 (s, 1H), 8.28 (dd, *J* = 8.2, 1.7 Hz, 1H), 7.73 (ddd, *J* = 8.5, 7.2, 1.7 Hz, 1H), 7.52 (d, *J* = 8.5 Hz, 1H), 7.49 (ddd, *J* = 8.2, 7.2, 1.0 Hz, 1H), 7.12 (s, 1H), 2.24 (s, 3H); **^{13}C-NMR** (100 MHz, $CDCl_3$.) δ 224.3, 197.4, 174.7, 160.3, 155.5, 134.2, 126.3, 126.1, 124.5, 118.2, 118.1, 101.5, 26.7; **IR** (film, cm $^{-1}$) 3420, 1651, 1617, 1465; **HRMS** (ESI) calcd. for $C_{13}H_{10}NaO_4$ $[M+Na]^+$: 253.04713, obs. 253.04722.

*To a 4 L Erlenmeyer flask was added 400 g of silica gel. Added was 2.50 L of deionized water and the slurry stirred vigorously. The solution was acidified to a pH of 2 with 6.50 mL of 85% phosphoric acid. The slurry stirred for 20 minutes. The silica gel was filtered and washed with ethyl acetate, then dried in a 120 °C oven overnight.

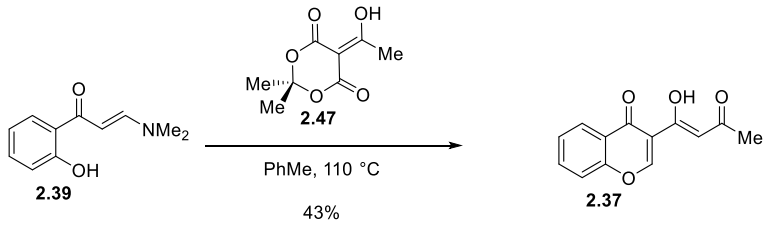

Enaminone **2.39** (3.0 g, 15.7 mmol, 1.0 equiv.) and freshly ground acyl Meldrum's acid (**37**) (8.76 g, 47.1 mmol, 3.0 equiv.) were dissolved in toluene (157 mL) and heated to reflux for 45 minutes, yielding a brown semisolid after removal of the volatiles. The crude material was purified using acidified silica gel* and 7:1 hexanes: ethyl acetate as the eluent to afford **2.37** (1.55 g, 6.73 mmol, 43%).

white solid, M. P. = 142 – 144 °C; **R**$_f$ = 0.33 (silica gel, 3:1 hexanes: EtOAc); **^{1}H-NMR** (400 MHz, $CDCl_3$) δ 15.90 (s, 1H), 8.78 (s, 1H), 8.28 (dd, *J* = 8.2, 1.7 Hz, 1H), 7.73 (ddd, *J* = 8.5, 7.2, 1.7 Hz, 1H), 7.52 (d, *J* = 8.5 Hz, 1H), 7.49 (ddd, *J* = 8.2, 7.2, 1.0 Hz, 1H), 7.12 (s, 1H), 2.24 (s, 3H); **^{13}C-NMR** (100 MHz, $CDCl_3$.) δ 224.3, 197.4, 174.7, 160.3, 155.5, 134.2, 126.3, 126.1, 124.5, 118.2, 118.1, 101.5, 26.7; **IR** (film, cm $^{-1}$) 3420, 1651, 1617, 1465; **HRMS** (ESI) calcd. for $C_{13}H_{10}NaO_4$ $[M+Na]^+$: 253.04713, obs. 253.04722.

*To a 4 L Erlenmeyer flask was added 400 g of silica gel. Added was 2.50 L of deionize d water and the slurry stirred vigorously. The solution was acidified to a pH of 2 with 6.50 mL of 85% phosphoric acid. The slurry stirred for 20 minutes. The silica gel was filtered and washed with ethyl acetate, then dried in a 120 °C oven overnight.

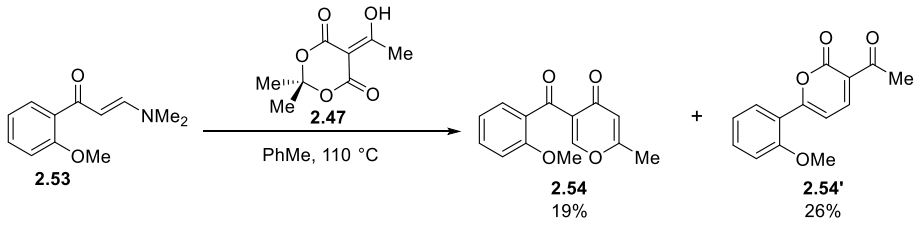

Enaminone **2.53** (120 mg, 0.59 mmol, 1.0 equiv.) and freshly ground acyl Meldrum's acid (327 mg, 1.75 mmol, 3.0 equiv.) were diluted in toluene (5.80 mL). The flask was equipped with a reflux condenser and lowered into an oil bath set to 145 °C. The reaction was heated at reflux for 45 minutes. The reaction was concentrated to yield a brown oil. The crude material was chromatographed using 7:1 hexanes: ethyl acetate as the eluent to afford **2.54** (35.0 mg, 0.14 mmol, 43 %) and **2.54'** (68.1 mg, 0.28 mmol, 48 %).

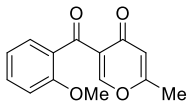

white solid; M.P. = 128 - 131 °C; **R$_f$** = 0.48 (silica gel, 100% EtOAc); **^{1}H-NMR** (400 MHz, $CDCl_3$) δ 8.10 (s, 1H), 7.63 (dd, *J* = 8.5, 1.7 Hz, 1H), 7.46 (td, *J* = 8.5, 1.7 Hz, 1H), 7.03 (td, *J* = 8.5, 1.7 Hz), 6.9 (d, *J* = 8.2 Hz, 1H), 6.17 (s, 1H), 3.72 (s. 3H), 2.30 (s, 3H); **^{13}C-NMR** (100 MHz, $CDCl_3$) δ 190.9, 175.7, 165.4, 158.8, 157.5, 134.0, 130.4, 130.3, 128.3, 120.8, 116.0, 111.3, 55.5, 19.5; **IR** (film, cm $^{-1}$) 1643, 1618.7; **HRMS** (ESI) calcd. for $C_{14}H_{12}NaO_4$ $[M+Na]^+$: 267.06278, obs. 267.06302.

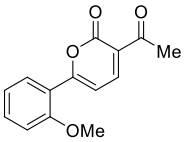

white solid; M.P. = 92 - 93 °C; **R$_f$** = 0.36 (silica gel, 1:1 hexanes: EtOAc); **^{1}H-NMR** (400 MHz, $CDCl_3$) δ 8.28 (d, *J* = 7.5 Hz, 1H), 8.02 (dd, *J* = 7.9, 1.7 Hz, 1H), 7.48 (ddd, 8.9, 6.8, 1.7 Hz, 1H), 7.32 (d, *J* = 7.5, 1H), 7.1 (dd, *J* = 7.9, 7.5 Hz, 1H), 7.02 (d, *J* = 8.2 Hz, 1H) 4.00 (s, 3H), 2.69 (s, 3H); **^{13}C-NMR** (100 MHz, $CDCl_3$) δ 195.4, 163.1, 160.5, 158.3, 148.8, 133.2, 129.7, 121.1, 120.5, 119.1, 111.6, 106.7, 55.7, 30.5; **IR** (film, cm $^{-1}$) 1730, 1672, 1600,

1530, 1256, 1244; **HRMS** (ESI) calcd. for $C_{14}H_{12}NaO_4$ $[M+Na]^+$: 267.06278, obs. 267.06313.

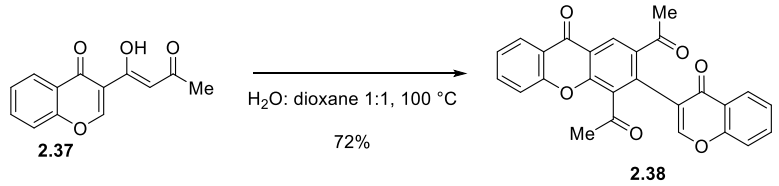

Acetoacetyl chromenone **2.37** (32.5 mg, 0.141 mmol) stirred in a 1:1 mixture of water and dioxane (1.4 mL) heated to 90 °C for 14 hours. The reaction was concentrated *in vacuo* to produce a yellow solid, which was purified by silica gel column chromatography using 99:1 dichloromethane: methanol to afford **2.38** (21.7 mg, 0.051 mmol, 72 % yield).

white solid; M.P. = 264 °C; **R_f** = 0.35 (silica gel, 1:1 hexanes: EtOAc); **^{1}H-NMR** (400 MHz, $CDCl_3$) δ 8.76 (s, 1H), 8.37 (dd, J = 7.8, 1.6 Hz, 1H), 8.22 (dd, *J* = 7.8, 1.6 Hz, 1H), 7.90 (s, 1H), 7.79 (ddd, *J* = 8.6, 7.1, 1.6 Hz, 1H), 7.73 (ddd, *J* = 8.6, 7.0, 1.6 Hz, 1H), 7.42-7.53 (m, 4H), 2.67 (s, 3H), 2.49 (s, 3H); **^{13}C-NMR** (100 MHz, $CDCl_3$) δ 201.4, 199.0, 175.7 (2 signals), 156.4, 155.7, 154.4, 153.3, 135.8, 135.7, 134.4, 134.2, 133.3, 127.6, 126.9, 126.3, 125.6, 125.2, 123.7, 121.7, 121.6, 121.0, 118.3, 118.1, 32.3, 28.9; **IR** (film, cm^{-1}) 1709, 1684, 1639, 1464; **HRMS** (ESI) calcd. for $C_{26}H_{16}NaO_6$ $[M+Na]^+$: 447.08391, obs. 447.08391.

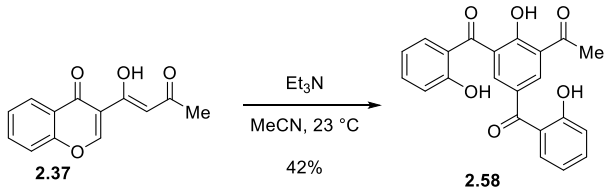

Acetoacetyl chromenone **2.37** (20.0 mg, 0.087 mmol, 1.0 equiv.) was taken up in acetonitrile (1.7 mL). Triethylamine (8.8 µL, 0.087 mmol, 1.0 equiv.) was added and the reaction stirred for 14 hours at 23 °C. The crude material was concentrated *in vacuo* to produce an orange oil, which was purified 100:10:1 hexanes: ethyl acetate: acetic acid to afford **2.58** as a yellow oil (6.90 mg, 0.0183 mmol, 42.2 %).

orange oil; R_f = 0.41 (3:1 hexanes: EtOAc); **^{1}H-NMR** (400 MHz, $CDCl_3$) δ 13.10 (s, 1H), 11.89 (s, 1H), 11.67 (s, 1H), 8.37 (d, *J* = 2.1 Hz, 1H), 7.93 (d, *J* = 2.1 Hz, 1H), 7.52-7.59 (m, 3H), 7.38 (dd, *J* = 7.9, 1.4 Hz, 1H), 7.10 (d, *J* = 7.5 Hz, 1H), 7.06 (d, *J* = 7.9 Hz, 1H), 6.93 (ddd, *J* = 8.2, 7.2, 1.0 Hz, 1H), 6.86 (ddd, *J* =8.2, 7.2, 1.0 Hz, 1H), 2.76 (s, 3H); **^{13}C-NMR** (100 MHz, C_6D_6) δ 204.4, 199.4, 198.4, 164.0, 163.8, 162.3, 137.2, 136.7, 136.3, 134.5, 133.4, 132.8, 128.6, 128.5, 120.2, 119.5, 119.2, 119.1, 119.0, 118.9, 118.7, 25.9; **IR** (film, cm $^{-1}$) 3066, 1626, , 1684, 1639, 1464; **HRMS** (ESI) calcd. for $C_{22}H_{16}NaO_6$ $[M+Na]^+$: 399.08391, obs. 399.08414.

BIOMIMETIC SYNTHESIS OF VINAXANTHONE EXPERIMENTAL SECTION

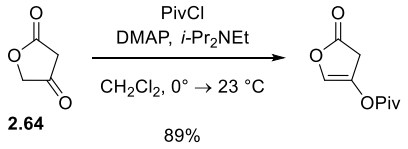

To a stirred solution of tetronic acid (**2.64**) (25.0 g, 250 mmol, 1.0 equiv.) 4-dimethylaminopyridine, (1.53 g, 12.5 mmol, 0.05 equiv.) and N,N-diisopropylethylamine (45.8 mL, 262 mmol, 1.05 equiv.) in CH_2Cl_2 (500 mL) at 0 °C was added neat pivaloyl chloride (25.9 mL, 262 mmol, 1.05 equiv.) dropwise over 40 minutes. Upon complete addition the dark-brown solution was allowed to warm to 23 °C. After 16 hours the reaction mixture was concentrated *in vacuo* to give a dark-brown oil. The residue was suspended in Et_2O (500 mL) and washed with H_2O (500 mL). The aqueous layer was extracted with Et_2O (5 x 500 mL) and the combined organic layers were dried over $MgSO_4$ and concentrated *in vacuo* to give 5-oxo-2,5-dihydrofuran-3-yl-pivalate (41.0 g, 223 mmol, 89% yield).

amber crystals, M.P. = 46-47 °C; **R_f** = 0.60 (silica gel, 1:1 hexanes: EtOAc); **^{1}H-NMR** (400 MHz, $CDCl_3$) δ 6.00 (t, *J* = 1.4 Hz, 1H), 4.91 (d, *J* = 1.4 Hz, 2H), 1.32 (s, 9H); **^{13}C-NMR** (100 MHz, $CDCl_3$) δ 173.2, 172.2, 169.1, 100.2, 68.2, 38.3, 26.4; **IR** (film, υ cm $^{-1}$) 1779, 1746, 1072.

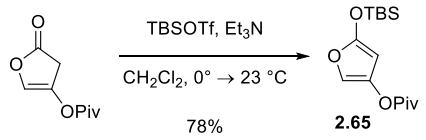

To a stirred solution of 5-oxo-2,5-dihydrofuran-3-yl-pivalate (30.0 g, 163 mmol, 1.0 equiv.) in CH_2Cl_2 (226 mL) at 0 °C was added triethylamine (29.8 mL, 212 mmol, 1.30 equiv.) in one portion. Neat *tert*-butyldimethylsilyl triflate (37.8 mL, 165 mmol, 1.01 equiv.) was then added dropwise over 10 minutes. Upon complete addition the amber solution was allowed to warm to 23 °C. After 1 hour the reaction mixture was concentrated *in vacuo* to give an amber oil. The residue was suspended in pentane (200 mL) and stirred for 1 hour. The organic layer was washed with saturated aqueous $NaHCO_3$ (100 mL), passed over solid $NaHCO_3$ (10 g), filtered and washed with brine (100 mL). The organic layer was dried over potassium carbonate and concentrated *in vacuo* to give furan **2.65** (37.9 g, 127 mmol, 78% yield).

amber oil; R_f = 0.55 (silica gel, 20: 1 hexanes: EtOAc); **^{1}H-NMR** (300 MHz, $CDCl_3$) δ 7.10 (d, J = 1.2 Hz, 1H), 5.15 (d, *J* = 1.2 Hz, 1H), 1.29 (s, 9H), 0.96 (s, 9H), 0.24 (s, 6H); **^{13}C-NMR** (100 MHz, $CDCl_3$) δ 175.3, 154.3, 139.4, 120.6, 80.1, 39.0, 27.1, 25.4, 18.0, -4.85; **IR** (film, υ cm $^{-1}$) 3202, 3141, 1753, 1627; **HRMS** (ESI) calcd. for $C_{15}H_{27}O_4Si$ $[M+H]^+$: 299.20000, obs. 299.20000.

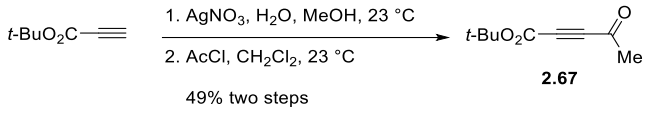

To a base-washed flask was added silver nitrate (5.39 g, 31.7 mmol, 2.0 equiv.) water (60mL) and MeOH (30 mL). Ammonium hydroxide was added dropwise (initially turning the solution into a dark brown heterogeneous solution) until the precipitate dissolved and the color dissipated. The flask was protected from light and purged with argon. To this vigorously stirring solution was added *tert*-butyl propionate (**x**) (2.18 mL, 15.85 mmol, 1.0 equiv.) as a solution in MeOH (10 mL) over 2 hours. The milky solution stirred for an additional 2 hours at 23 °C. The solution was poured into a seperatory funnel, and extracted with CCl_4 (100 mL) once and chloroform (3 x 100 mL). The combined organics were then washed with water (3 x 50 mL), dried over $CaCl_2$ and concentrated to reveal a brown/white solid. The solid was then diluted in CH_2Cl_2 (21 mL) and protected from light. Acetyl chloride (1.13 mL, 15.85 mmol, 1.0 equiv.) was added as a solution in CH_2Cl_2 (10 mL). The solution stirred at 23 °C for 20 hours. The heterogeneous solution was diluted with diethyl ether, and the solids were filtered off. The ethereal layer was washed twice with pH 7 buffer (0.2 M phosphate), brine and then dried over $MgSO_4$. The solvent was removed yielding **2.67** (1.25 g, 7.76 mmol, 49% yield).

brown oil; R_f = 0.40 (silica gel, 10:1 hexanes: EtOAc); **^{1}H-NMR** (400 MHz, $CDCl_3$) δ 2.41 (s, 3H), 1.52 (s, 9H); **^{13}C-NMR** (100 MHz, $CDCl_3$) δ 182.8, 151.0, 85.4, 79.2, 79.0, 32.3, 27.9; **IR** (film, υ cm $^{-1}$) 1716, 1689; **HRMS** (ESI) calcd. for $C_9H_{13}O_3$ $[M+H]^+$: 169.0865, obs. 169.0866.

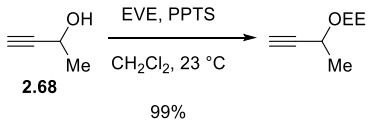

To a stirred solution of 3-butyn-2-ol (**2.68**) (100 g, 1.43 mmol, 1.0 equiv.) and ethyl vinyl ether (151 mL, 1.57 mmol, 1.1 equiv.) in CH_2Cl_2 (3 L) at 23 °C was added solid pyridinium *p*-toluenesulfonate (35.9 g, 143 mmol, 0.1 equiv.). After 1 hour the colorless solution was diluted with Et_2O (1 L) and washed with brine (2 L). The organic layer was dried over sodium sulfate and concentrated *in vacuo* to give 3-(1-ethoxyethoxy)but-1-yne as a mixture of diastereomers (201 g, 1.41 mmol, 99% yield).

colorless oil; R_f = 0.40 (silica gel, 1:1 hexanes: EtOAc); **^{1}H-NMR** (400 MHz, $CDCl_3$) δ 4.96 (q, *J* = 5.5 Hz, 1H), 4.85 (q, *J* = 5.5 Hz, 1H), 4.50 (q, *J* = 6.7 Hz, 1H), 4.35 (q, *J* = 6.7 Hz, 1H), 3.75 (m, 1H), 3.62 (m, 1H), 3.53 (m, 2H), 2.40 (s, 1H), 2.39 (s, 1H), 1.46 (d, *J* = 3.1 Hz, 3H), 1.44 (d, *J* = 3.1 Hz, 3H), 1.35 (d, *J* = 2.7 Hz, 3H), 1.34 (d, J = 2.7 Hz, 3H), 1.21 (t, J = 7.0 Hz, 6H); **^{13}C-NMR** (100 MHz, $CDCl_3$) δ 98.5, 97.5, 84.5, 83.6, 72.4, 72.0, 61.1, 60.5, 60.0, 59.9, 22.3, 21.9, 20.0, 19.9, 15.2, 14.9; **HRMS** (ESI) calcd. for $C_8H_{13}O_2$ $[M+H]^+$: 141.0916, obs. 141.0918.

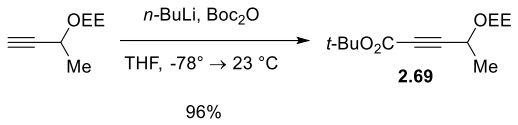

To a stirred solution of 3-(1-ethoxyethoxy)but-1-yne (110 g, 774 mmol, 1.0 equiv.) in THF (4.5 L) at −78 °C was added a solution of *n*-butyllithium in hexanes (2.0 M, 404 mL, 808 mmol, 1.05 equiv.). After 15 minutes neat liquid di-*tert*-butyl dicarbonate (186 mL, 808 mmol, 1.05 equiv.) was added over 10 minutes. Upon complete addition the amber solution was allowed to warm to 23 °C. The reaction mixture was diluted with Et_2O (1.5 L) and washed with H_2O (3 L) and brine (3 L). The organic layer was dried over $MgSO_4$ and concentrated *in vacuo* to give **2.69** as a mixture of diasteromers (180 g, 743 mmol, 96% yield).

amber oil; R_f = 0.21 (silica gel, 20:1 hexanes: EtOAc); **^{1}H-NMR** (400 MHz, $CDCl_3$) δ 4.91 (q, J = 5.1 Hz, 1H), 4.82 (q, J = 5.1 Hz, 1H), 4.56 (q, J = 6.8 Hz, 1H), 4.40 (q, J = 6.8 Hz, 1H), 3.73 (m, 1H), 3.62 (m, 1H), 3.56 (m, 1H), 3.50 (m, 1H), 1.49 (s, 18 H), 1.46 (d, J = 1.7Hz, 6H), 1.34 (d, *J* = 1.4 Hz, 6H) 1.12 (t, J = 8.5 Hz, 6H); **^{13}C-NMR** (100 MHz, C_6D_6) δ 152.6, 152.5, 99.3, 98.3, 86.1, 85.2, 82.9, 82.7, 78.3, 77.9, 61.0, 60.4, 60.3, 60.2, 27.8 (2 signals), 21.8, 21.5, 20.1, 20.0, 15.5, 15.3; **IR** (film, υ cm $^{-1}$) 1710, 1274, 1160; **HRMS** (ESI) calcd. for $C_{13}H_{22}NaO_4$ $[M+Na]^+$: 265.14103, obs. 265.14100.

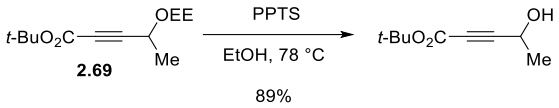

To a stirred solution of **2.69** (117g, 483 mmol, 1.0 equiv.) in ethanol (4.8 L) heated to 78 °C was added pyridinium p-toluenesulfonate (12.1g, 48.3 mmol, 0.1 equiv.). After 2 hours the amber solution was allowed to cool to 23 °C. The reaction mixture was diluted with Et_2O (2.4 L) and washed w ith brine (4 L). The organic layer was dried over $MgSO_4$ and concentrated *in vacuo* to give *tert*-butyl 4-hydroxypent-2-ynoate (73.1 g, 429 mmol, 89% yield).

amber oil; R_f = 0.30 (silica gel, 3:1 hexanes: EtOAc); **^{1}HNMR** (400 MHz, $CDCl_3$) δ 4.62 (m, 1H), 2.13 (bs, 1H), 1.51 (m, 12H); **^{13}C-NMR** (100 MHz, C_6D_6) δ 152.8, 86.8, 82.9, 77.5, 57.8, 27.8, 23.1; **IR** (film, υ cm $^{-1}$) 3400, 1709; **HRMS** (ESI) calcd. for $C_9H_{15}O_3$ $[M+H]^+$: 171.1021, obs. 171.1019.

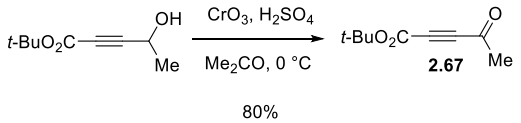

To a stirred solution of *tert*-butyl 4-(1-ethoxyethoxyl)pent-2-ynoate (73.0 g, 429 mmol, 1.0 equiv.) in Me_2CO (1.2 L) at 0 °C was added ice-cold Jones reagent (1.53 M (67.0 g CrO_3, 58.0 mL concentrated H_2SO_4 and 160 mL H_2O), 280 mL, 429 mmol, 1.0 equiv.) slowly over 15 minutes. After 30 minutes *i*-PrOH (40 mL) was added to neutralize any excess Jones reagent. The reaction mixture was diluted with CH_2Cl_2, and washed with H_2O (1 L), saturated aqueous $NaHCO_3$ (1 L) and brine (1 L). The organic layer was dried over sodium sulfate and then concentrated *in vacuo*. The crude material was passed through a plug of silica gel (1:1 pentane: ether) to give keto-ester **2.67** (57.5 g, 342 mmol, 80% yield).

amber oil; R_f = 0.40 (silica gel, 10:1 hexanes: EtOAc); **^{1}H-NMR** (400 MHz, $CDCl_3$) δ 2.41 (s, 3H), 1.52 (s, 9H); **^{13}C-NMR** (100 MHz, $CDCl_3$) δ 182.8, 151.0, 85.4, 79.2, 79.0, 32.3, 27.9; **IR** (film, υ cm $^{-1}$) 1716, 1689; **HRMS** (ESI) calcd. for $C_9H_{13}O_3$ $[M+H]^+$: 169.0865, obs. 169.0866.

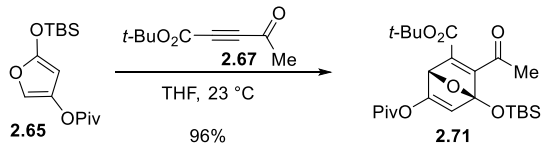

To a stirred solution of furan **2.65** (70.4 g 236 mmol, 1.0 equiv.) in THF (212 mL) at 0 °C was added keto ester **2.67** (39.7 g, 236 mmol, 1.0 equiv.) in one portion. Upon complete addition the amber solution was allowed to warm to 23 °C. After 1 hour the reaction mixture was concentrated *in vacuo* to give **2.71** as a colorless oil that was used in the next step without purification.

colorless oil; R_f = 0.35 (silica gel, 10:1 hexanes: EtOAc); **^{1}H-NMR** (400 MHz, $CDCl_3$) δ 6.38 (s, 1H), 5.24 (s, 1H), 2.43 (s, 3H), 1.47 (s, 9H), 1.25 (s, 9H), 0.90 (s, 9H), 0.20 (s, 3H), 0.18 (s, 3H); **^{13}C-NMR** (100 MHz, $CDCl_3$) δ 199.3, 174.3, 167.7, 163.7, 161.2, 146.3, 118.5, 113.9, 82.3, 78.2, 39.2, 30.7, 27.9, 26.8, 25.4, 17.7, -3.5, -3.7; **IR** (film, υ cm $^{-1}$) 1769, 1712; **HRMS** (ESI) calcd. for $C_{24}H_{38}O_7Si$ $[M+Na]^+$: 489.22790, obs. 489.22801.

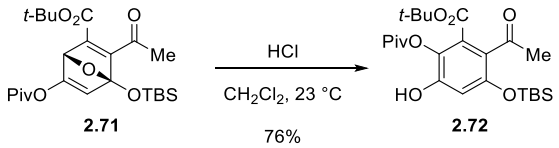

To a stirred solution of bicycle **2.71** (110 g, 236 mmol, 1.0 equiv.) in THF (471 mL) at 0 °C was added a solution of dry hydrochloric acid in dioxane (4.0 M, 47.1 mL, 47.1 mmol, 0.2 equiv.) over 5 minutes. Upon complete addition the amber solution was allowed to warm to 23 °C. After 2 hours the reaction mixture was concentrated *in vacuo*, yielding a brown oil. The crude material was purified via silica gel column chromatography (20:1 hexanes: EtOAc) to give phenol **2.72** (82.9 g, 178 mmol, 75% yield over 2-steps).

colorless oil; R_f = 0.38 (silica gel, 10:1 hexanes: EtOAc); **^{1}H-NMR** (400 MHz, $CDCl_3$) δ 10.91 (s, 1H), 6.71 (s, 1H), 2.48 (s, 3H), 1.54 (s, 9H), 1.38 (s, 9H), 0.94 (s, 9H), 0.18 (s, 9H); **^{13}C-NMR** (100 MHz, $CDCl_3$) δ 202.3, 176.3, 168.4, 148.7, 142.5, 139.7, 131.9, 119.9, 111.0, 85.7, 39.2, 32.5, 27.8, 27.2, 25.5, 18.0, -4.4; **IR** (film, υ cm $^{-1}$) 1763, 1716, 1673; **HRMS** (ESI) calcd. for $C_{24}H_{38}O_7Si$ $[M+Na]^+$: 489.22790, obs. 489.22813.

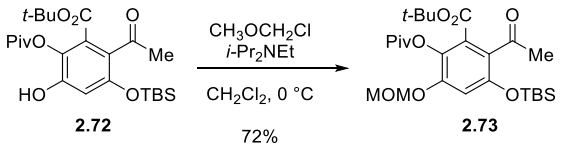

To a stirred solution of phenol **2.72** (82.9 g, 178 mmol, 1.0 equiv.) in CH_2Cl_2 (1.7 L) at 0 °C was added N,N-diisopropylethylamine (63.4 mL, 355 mmol, 2.0 equiv.). A solution of methoxymethyl chloride in toluene/ MeOAc (2.1 M, 127 mL, 267 mmol, 1.0 equiv.) was then added slowly over 20 minutes. Upon complete addition the amber solution was allowed to warm to 23 °C. After 1 hour the reaction mixture was diluted with 0.1 M HCl (500 mL) and extracted with CH_2Cl_2 (500 mL). The organic layer was dried over sodium sulfate and concentrated *in vacuo* to give an amber oil. The crude material was purified by silica gel column chromatography (10:1 hexanes: EtOAc), yielding acetophenone **2.73** (61.4 g, 120 mmol, 68% yield).

white solid; M.P. = 60-62 °C; **R_f** = 0.61 (silica gel, 3:1 hexanes: EtOAc); **^{1}H-NMR** (400 MHz, $CDCl_3$) δ 6.76 (s, 1H), 5.10 (s, 2H), 3.42 (s, 3H), 2.54 (s, 3H), 1.49 (s, 9H), 1.34 (s, 9H), 0.97 (s, 9H), 0.21 (s, 9H); **^{13}C-NMR** (100 MHz, $CDCl_3$) δ 200.9, 175.7, 163.5, 150.9, 150.4, 132.8, 128.1, 125.7, 108.6, 94.6, 82.5, 55.9, 38.9, 31.7, 27.7, 27.1, 25.6, 18.1, -4.4; **IR** (film, υ cm $^{-1}$) 1761, 1733, 1703; **HRMS** (ESI) calcd. for $C_{26}H_{42}NaO_8Si$ $[M+Na]^+$: 533.25412, obs. 533.25387.

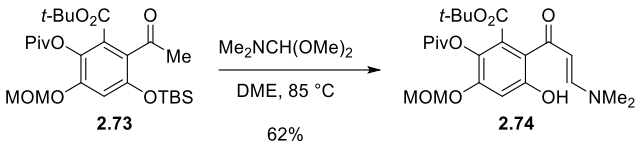

To a stirred solution of acetophenone **2.73** (15.4 g, 30.2 mmol, 1.0 equiv.) in DME at 85 °C was added N,N-dimethylformamide dimethyl acetal (16.1 mL, 121 mmol, 4.0 equiv.) in one portion. After 3 hours the amber solution was cooled to 23 °C and then concentrated *in vacuo* to give enaminone **2.74** as a dark oil. The crude material was chromatographed (1:1 hexanes: EtOAc), yielding enaminone **2.74** (8.59 g, 19.0 mmol, 63% yield).

orange solid, M.P. = 118-119 °C; **R_f** = 0.26 (silica gel, 1:1 hexanes: EtOAc); **^{1}H-NMR** (400 MHz, $CDCl_3$) δ 12.43 (bs, 1H), 7.77 (d, J = 12.2 Hz, 1H), 6.70 (s, 1H), 5.49 (d, J = 12.2 Hz, 1H), 5.13 (s, 2H), 3.41 (s, 3H), 3.15 (s, 3H), 2.84 (s, 3H), 1.47 (s, 9H), 1.34 (s, 9H); **^{13}C-NMR** (100 MHz, $CDCl_3$) δ 189.4, 175.8, 165.6, 159.3, 154.4, 151.6, 130.1, 128.5, 113.7, 104.0, 95.2, 94.0, 82.4, 56.0, 45.1, 38.7, 37.1, 27.6, 27.0; **IR** (film, υ cm $^{-1}$) 1751, 1716, 1632, 1111; **HRMS** (ESI) calcd. for $C_{23}H_{33}NNaO_8$ $[M+Na]^+$: 474.20984, obs. 474.21058.

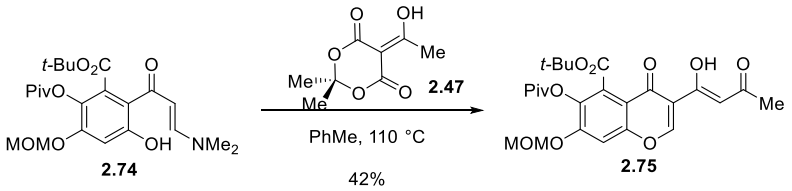

To a solution of **2.74** (1.44 g, 3.19 mmol, 1.0 equiv.) in toluene (32 mL) was added freshly ground acyl Meldrum's acid (**2.47**) (1.78 g, 9.57 mmol, 3.0 equiv.). The amber solution was heated to reflux for 45 minutes the cooled to 23 °C and concentrated *in vacuo* to give a brown solid. The crude material was purified via acidified silica gel* column chromatography (7:1 hexanes: EtOAc), yielding **2.75** (650 mg, 1.33 mmol, 42%) as a yellow solid.

yellow solid, M.P. = 181-182 °C; $\mathbf{R_f}$ = 0.24 (silica gel, 3:1 hexanes: EtOAc); **^{1}H-NMR** (400 MHz, $CDCl_3$) δ 15.87 (s, 1H), 8.66 (s, 1H), 7.23 (s, 1H), 7.05 (s, 1H), 5.24 (s, 2H), 3.45 (s, 3H), 2.22 (s, 3H), 1.65 (s, 9H), 1.38 (s, 9H); **^{13}C-NMR** (100 MHz, $CDCl_3$, The highly concentrated ^{13}C sample produced a mixture of keto and enol tautomers) δ 202.5, 197.6, 192.1, 174.3, 172.6, 163.6, 161.7, 159.4, 154.5, 154.2, 153.4, 136.7, 128.6, 120.9, 118.0, 116.3, 115.8, 103.9, 103.8, 101.7, 94.7, 83.1, 57.7, 56.7, 56.6, 39.2, 30.7, 28.2, 27.2, 26.9; **IR** (film, cm $^{-1}$) 1762, 1734, 1663, 1621; **HRMS** (ESI) calcd. for $C_{25}H_{30}NaO_{10}$ $[M+Na]^+$: 513.17312, obs. 513.17341.

*To a 4 L Erlenmeyer flask was added 400 g of silica gel. Added was 2.50 L of deionized water and the slurry stirred vigorously. The solution was acidified to a pH of 2 with 6.50 mL of 85% phosphoric acid. The slurry stirred for 20 minutes. The silica gel was filtered and washed with ethyl acetate, then dried in a 120 °C oven overnight.

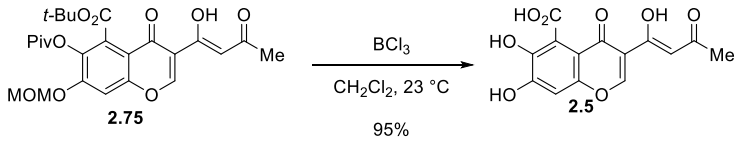

To a solution of **2.75** (50.0 mg, 0.102 mmol, 1.0 equiv.) in CH_2Cl_2 (10 mL) 0 °C was added boron trichloride solution (1.0 M in CH_2Cl_2, 1.22 mmol, 1.22 mL, 12.0 equiv.). The red heterogeneous solution warmed to 23 °C and stirred for 1 hour. The reaction was cooled to 0 °C and quenched with 2 mL of 2N HCl, and stirred at 0 °C for 5 minutes. The solution was diluted with ethyl acetate (30 mL) and the pH of the aqueous layer was adjusted to a pH of 7 using a pH 10 buffer (40 mL of 0.2 M phosphate buffer). The layers were separated and the organic layer was extracted three times with additional pH 7 buffer (30 mL of 0.2 M phosphate buffer). The combined aqueous washes were re-acidified to a pH of 2 using 2N HCl and extracted with ethyl acetate (3 x 30 mL). The organic layers were washed with brine (50 mL), dried over $MgSO_4$ and concentrated *in vacuo* to yield 5,6-dehydropolivione (**2.5**) (20.1 mg, 0.098 mmol, 96% yield) as a yellow solid.

yellow solid; M.P. = 231-232 °C; **R_f=** 0.54 (silica gel, 9:1 EtOAc: AcOH); **^{1}H-NMR** (400 MHz, $(CD_3)_2SO$) δ [enol] 16.10 (bs, 1H), 12.71 (bs, 1H), 11.55 (bs, 1H), 9.50 (bs, 1H), 8.84 (s, 1H), 6.98 (s, 1H), 6.96 (s, 1H), 2.19 (s, 3H), [keto] 12.71 (bs, 1H), 11.55 (bs, 1H), 9.50 (bs, 1H), 8.73 (s, 1H), 6.96 (s, 1H), 4.09 (s, 2H), 2.20 (s, 3H); **^{13}C-NMR** (100 MHz, $(CD_3)_2SO$) δ [enol] 196.7, 176.0, 172.3, 167.4, 160.2, 152.6, 149.8, 142.0, 120.2, 116.2, 113.2, 102.4, 100.8, 26.3, [keto] 203.0, 192.7, 173.0, 161.7, 152.6, 150.1, 120.4, 120.2, 113.6, 102.5, 57.4, 30.6; **IR** (film, cm $^{-1}$) 3280, 1617, 1473; **HRMS** (ESI) calcd. for $C_{14}H_9O_8$ $[M-H]^-$: 305.03029, obs. 305.03013.

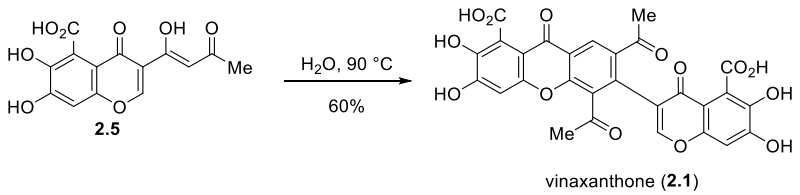

Suspended 5,6-dehydropolivione (**2.5**) (20.0 mg, 0.065 mmol) in water (0.653 mL) stirred at 90 °C for 36 hours. The reaction was diluted with 2 mL of concentrated ammonium hydroxide solution. The mixture was washed with ethyl acetate (2 x 30 mL), and acidified to a pH of 1 using concentrated HCl (10 mL) at 0 °C. The crude material was extracted with ethyl acetate (3 x 20 mL), washed with pH 2 buffer solution (20 mL) then brine (20mL) before drying over magnesium sulfate, yielding crude vinaxanthone that was purified by repeated trituration with methanol (3 x 1 mL portions) yielding pure vinaxanthone (**2.1**) as a yellow solid (11.2 mg, 0.019 mmol, 60% yield).

yellow solid; M.P. = >280 °C; **R_f**= 0.05 (sílica gel, 95:5 EtOAc: AcOH); **^{1}H-NMR** (400 MHz, $(CD_3)_2SO$) δ 12.89 (bs, 1H), 12.72 (bs, 1H), 11.69 (bs, 1H), 11.44 (bs, 1H), 9.42 (bs 2H), 9.42 (bs, 2H), 8.53 (s, 1H), 8.18 (s, 1H), 6.96 (s, 1H), 6.94 (s, 1H), 2.55 (s, 3H), 2.53 (s, 3H); **^{13}C-NMR** (125 MHz, $(CD_3)_2SO$) δ 201.1, 199.1, 172.9, 172.6, 167.4, 167.4, 154.1, 152.7, 152.5, 152.1, 150.7, 150.3, 141.7, 141.0, 136.2, 133.4, 132.6, 126.3, 120.8, 120.5, 119.8, 119.6, 112.4, 110.0, 102.4, 102.3, 32.1, 29.1; **IR** (KBr, cm $^{-1}$) 3236, 1683, 1653, 1472, 1288; **HRMS** (ESI) calcd. For $C_{28}H_{15}O_{14}$ $[M-H]^-$: 575.04673, obs. 575.04679.

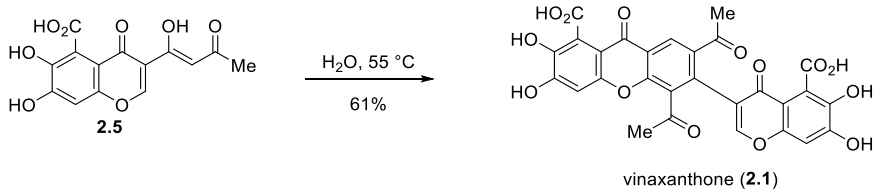

Suspended 5,6-dehydropolivione (**2.5**) (10.0 mg, 0.033 mmol, 1.0 equiv.) in water (0.327 mL) stirred at 55 °C for 4 days. The reaction was quenched with 2 mL of concentrated ammonium hydroxide. The solution was washed with ethyl acetate (2 x 20 mL), and then re-acidified to a pH of 1 using concentrated HCl at 0 °C. The crude material was extracted with ethyl acetate (3 x 20 mL), washed with pH 2 buffer (20 mL), then brine (30 mL) before drying over magnesium sulfate, yielding vinaxanthone (**2.1**) (5.7 mg, 0.0099 mmol, 61%) as a yellow solid after trituration with methanol (3 x 1mL portions).

yellow solid; M.P. = >280 °C; **R_f**= 0.05 (sílica gel, 95:5 EtOAc:AcOH); **^{1}H-NMR** (400 MHz, $(CD_3)_2SO$) δ 12.89 (bs, 1H), 12.72 (bs, 1H), 11.69 (bs, 1H), 11.44 (bs, 1H), 9.42 (bs 2H), 9.42 (bs, 2H), 8.53 (s, 1H), 8.18 (s, 1H), 6.96 (s, 1H), 6.94 (s, 1H), 2.55 (s, 3H), 2.53 (s, 3H); **^{13}C-NMR** (125 MHz, $(CD_3)_2SO$) δ 201.1, 199.1, 172.9, 172.6, 167.4, 167.4, 154.1, 152.7, 152.5, 152.1, 150.7, 150.3, 141.7, 141.0, 136.2, 133.4, 132.6, 126.3, 120.8, 120.5, 119.8, 119.6, 112.4, 110.0, 102.4, 102.3, 32.1, 29.1; **IR** (KBr, cm $^{-1}$) 3236, 1683, 1653, 1472, 1288; **HRMS** (ESI) calcd. For $C_{28}H_{15}O_{14}$ $[M-H]^-$: 575.04673, obs. 575.04679.

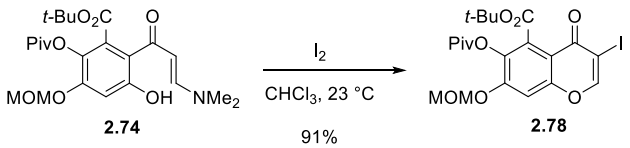

To a stirred solution of crude enaminone **2.74** (13.6 g, 30.2 mmol, 1.0 equiv.) in $CHCl_3$ (302 mL) at 23 °C was added solid iodine (15.3 g, 60.4 mmol, 2.0 equiv.) in one portion. After 40 minutes the black solution was diluted with saturated aqueous $Na_2S_2O_3$ (300 mL) and extracted with CH_2Cl_2 (300 mL). The organic layer was dried over sodium sulfate and concentrated *in vacuo* to give a tan solid. The crude material was purified via silica gel column chromatography (1:1 hexanes: EtOAc) to give iodochromone **2.78** (9.65 g, 18.1 mmol, 60% over 2-steps).

white solid, M.P. = 189-190 °C **R_f** = 0.32 (silica gel, 3:1 hexanes: EtOAc); **^{1}H-NMR** (400 MHz, $CDCl_3$): δ 8.19 (s, 1H), 7.17 (s, 1H), 5.23, (s, 2H), 3.25 (s, 3H), 1.64 (s, 9H), 1.37 (s, 9H); **^{13}C-NMR** (100 MHz, $CDCl_3$): δ 175.4, 170.9, 163.2, 156.8, 154.9, 153.3, 136.5, 128.3, 112.8, 103.5, 94.7, 86.7, 83.3, 56.6, 39.2, 28.2, 27.2; **IR** (film, υ cm $^{-1}$): 1764, 1731, 1650; **HRMS** (ESI) calcd. for $C_{21}H_{25}INaO_8$ $[M+Na]^+$: 555.04863, obs. 555.04881.

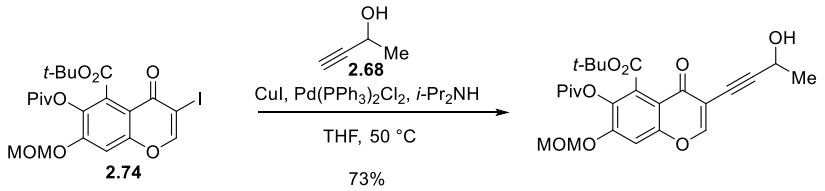

To a stirred solution of iodochromenone **2.74** (8.08 g, 15.2 mmol, 1.0 equiv.), bis(triphenylphosphine) palladium (II) dichloride (213 mg, 0.30 mmol, 0.02 equiv.) and copper iodide (289 mg, 1.54 mmol, 0.1 equiv.) in degassed THF (51 mL, 0.3 M) at 23 °C was added 3-butyn-2-ol **2.68** (4.8 mL, 60.7 mmol, 4.0 equiv.) followed by neat diisopropylamine (6.5 mL, 45.5 mmol, 3.0 equiv.). After 1 hour, the reaction mixture was diluted with aqueous 0.2 M pH = 7.0 phosphate buffer (100 mL) and extracted with CH_2Cl_2 (100 mL). The organic layer was dried over sodium sulfate and concentrated *in vacuo* to give an amber oil. The crude material was purified via silica gel column chromatography (1:1 hexanes: EtOAc) to give pure propargyl alcohol (5.23 g, 11.0 mmol, 73%).

tan solid, M.P. = 132-134 °C; **R_f** = 0.21 (silica gel, 1:1 hexanes: EtOAc); **^{1}H-NMR** (400 MHz, $CDCl_3$): δ 8.03 (s, 1H), 7.14 (s, 1H), 5.21 (s, 2H), 4.75 (m, 1H), 3.43 (s, 3H), 3.20 (bs, 1H), 1.63 (s, 9H), 1.51 (d, *J* = 6.7 Hz, 3H); **^{13}C-NMR** (100 MHz, $CDCl_3$): δ 175.5, 173.3, 163.3, 157.5, 154.6, 153.2, 136.3, 128.1, 114.5, 110.5, 103.8, 97.5, 94.6, 83.2, 73.8, 58.6, 56.6, 39.2, 28.2, 27.2, 23.8; **IR** (film, υ cm^{-1}): 3435, 1763, 1735, 1731, 1461; **HRMS** (ESI) calcd. for $C_{25}H_{30}NaO_9$ $[M+Na]^+$: 497.1782, obs. 497.1785.

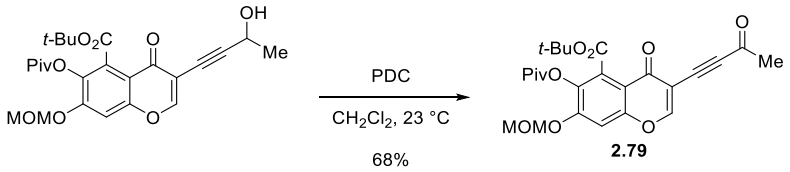

To a stirred solution of propargyl alcohol (5.23 g, 11.0 mmol, 1.0 equiv.) and activated 4.0 Å molecular sieves (2.6 g, 50% by weight) in CH_2Cl_2 (110 mL, 0.1 M) at 23 °C was added solid pyridinium dichromate (19.9 g, 55.1 mmol, 5.0 equiv.) in one portion. After 2 hours the black solution was filtered through a pad of celite and concentrated *in vacuo* to give an amber oil. The crude material was purified via silica gel column chromatography (1:1 hexanes: EtOAc) to give pure ynone **2.79** (3.54 g, 7.50 mmol, 68%) as a white solid.

white solid, M.P. = 178-179 °C; **R_f** = 0.41 (silica gel, 1:1 hexanes: EtOAc); **^{1}H-NMR** (400 MHz, $CDCl_3$): δ 8.20 (s, 1H), 7.21 (s, 1H), 5.24 (s, 2H), 3.44 (s, 3H), 2.46 (s, 3H), 1.64 (s, 9H), 1.37 (s, 9H); **^{13}C-NMR** (100 MHz, $CDCl_3$): δ 184.2, 175.4, 172.1, 163.1, 160.4, 154.6, 153.7, 136.8, 128.3, 114.6, 108.7, 104.0, 94.7, 93.5, 83.5, 81.0, 56.7, 39.2, 32.7, 28.2, 27.2; **IR** (film, υ cm^{-1}): 1762, 1734, 1672, 1620, 1459, 1264, 1246, 1155, 1091; **HRMS** (ESI) calcd. for $C_{25}H_{28}NaO_9$ $[M+Na]^+$: 495.1626, obs. 495.1632.

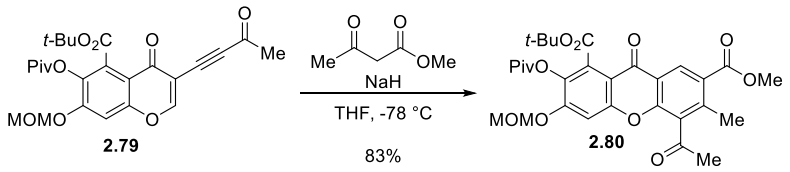

To a stirred suspension of sodium hydride (60% dispersion in mineral oil, 556 mg, 13.9 mmol, 1.0 equiv.) in THF (55.7 mL) was added methyl acetoacetate (1.50 mL, 13.9 mmol, 1.0 equiv.) dropwise over 5 min. to furnish a 0.25 M stock solution of the sodium enolate of methyl acetoacetate (stored in a Schlenk flask under argon). To a stirred solution of ynone **2.79** (500 mg, 1.06 mmol, 1.0 equiv.) in THF (88 mL) at -78 °C was added a solution of the sodium enolate of methyl acetoacetate (0.25 M THF, 8.50 mL, 2.12 mmol, 2.0 equiv.) dropwise down the side of the flask over 10 minutes. The reaction was allowed to stir at -78 °C and after 5 h, the excess sodium enolate of methyl acetoacetate was quenched with aqueous HCl (1.0 M, 1.5 mL). The resulting yellow solution was diluted with EtOAc (150 mL), washed with H_2O (3 x 50 mL), brine (50 mL), dried over sodium sulfate, and concentrated *in vacuo*. The yellow residue was chromatographed on silica gel (3:1 hexanes: EtOAc) to furnish methyl ester **2.80** (502 mg, 83 %).

tan solid, **M.P.** = 199-201 °C; **R_f** = 0.40 (silica gel, 2:1 hexanes: EtOAc); **^{1}H-NMR** (400 MHz, $CDCl_3$): δ 8.84 (s, 1H), 7.17 (s, 1H), 5.27 (s, 2H), 3.93 (s, 3H), 3.47 (s, 3H), 2.67 (s, 3H), 2.62 (s, 3H), 1.67 (s, 9H), 1.39 (s, 9H); **^{13}C-NMR** (100 MHz, CD_2Cl_2): δ 202.4, 175.9, 173.6, 166.6, 163.8, 154.8, 154.7, 153.4, 142.8, 135.8, 133.2, 129.9, 129.0, 127.6, 119.3, 112.7, 103.9, 95.1, 83.5, 56.9, 52.6, 39.5, 32.9, 28.3, 27.4, 18.2; **IR** (film, υ cm^{-1}): 1760, 1735, 1663, 1599; **HRMS** (ESI) calcd. for $C_{30}H_{34}O_{11}Na^+$ $[M+Na]^+$: 593.19933, obs. 593.19976.

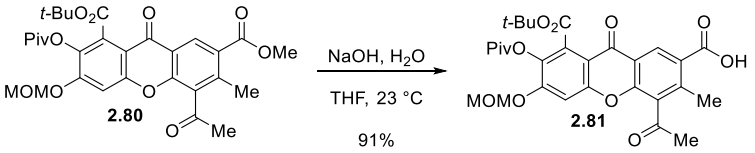

To a stirred solution of methyl ester **2.80** (920 mg, 1.61 mmol, 1.0 equiv.) in THF (65 mL, 0.025 M) at 0 °C was added 0.1 N NaOH (19.4 mL, 1.94 mmol, 1.2 equiv.) dropwise over 2 minutes. Upon complete addition the gold-orange solution was allowed to warm to 23 °C. After 36 hours, the reaction mixture was diluted with H_2O (100 mL) and washed with Et_2O (3 x 50 mL). The aqueous layer was acidified using 0.1 N HCl (20 mL), extracted with EtOAc (3 x 250 mL), dried over sodium sulfate, and concentrated *in vacuo* to give pure carboxylic acid **2.81** (816 mg, 1.43 mmol, 91%) as a white solid.

white solid, M.P. = 203-204 °C; **^{1}H-NMR** (400 MHz, $CDCl_3$): δ 8.98 (s, 1H), 7.17 (s, 1H), 5.27 (s, 2H), 3.47 (s, 3H), 2.69 (s, 3H), 2.65 (s, 3H), 1.67 (s, 9H), 1.39 (s, 9H); **^{13}C-NMR** (150 MHz, $CDCl_3$): δ 202.3, 175.6, 173.2, 168.9, 163.5, 154.5, 154.4, 153.6, 143.1, 135.8, 133.0, 131.4, 129.0, 125.7, 119.2, 112.8, 103.7, 94.8, 83.4, 56.7, 39.2, 32.8, 28.2, 27.3, 18.3; **IR** (film, υ cm^{-1}): 1760, 1688, 1666, 1619, 1596; **HRMS** (ESI) calcd. for $C_{29}H_{32}O_{11}Na^+$ $[M+Na]^+$: 579.18368, obs. 579.18373.

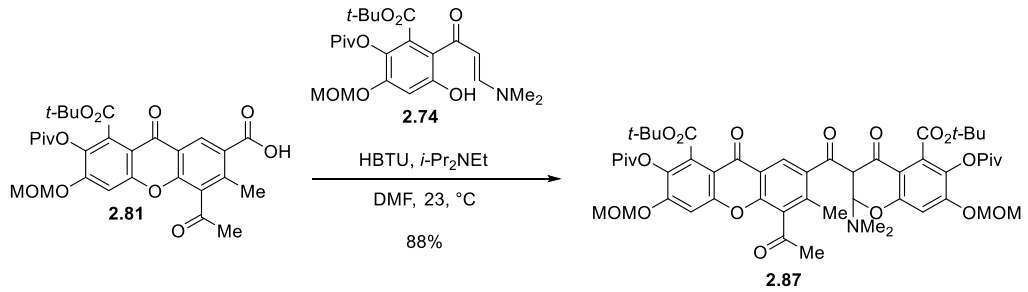

To a stirred solution of carboxylic acid **2.81** (373 mg, 0.67 mmol, 1.10 equiv.) in DMF (3.0 mL) at 23 °C was added solid HBTU (254 mg, 0.67 mmol, 1.1 equiv.) in one portion followed by N,N-diisopropylethylamine (0.27 mL, 1.52 mmol, 2.5 equiv.). The dark amber solution was stirred for 5 min. and then solid enaminone **2.74** (275 mg, 0.61 mmol, 1.10 equiv.) was added in one portion. The reaction was stirred for 6 h then diluted with 1:1 hexanes: EtOAc (100 mL) and washed with saturated aqueous LiCl solution (8 x 30 mL). The organic layer was dried over sodium sulfate and concentrated *in vacuo*. The tan residue was chromatographed on silica gel (1:2 hexanes: EtOAc with 2% Et_3N) to furnish aminal **2.87** (528 mg, 88 %).

yellow solid, M.P. = 124-126 °C; **R_f** = 0.25 (silica gel, 1:1 hexanes: EtOAc, 2% Et_3N); **^{1}H-NMR** (400 MHz, $(CD_3)_2CO$): δ 8.87 (s, 1H), 7.42 (s, 1H), 7.30 (s, 1H), 5.46 (s, 2H), 5.28 (s, 2H), 5.23 (d, *J* = 13.3 Hz, 1H), 3.47 (s, 3H), 3.44 (s, 3H), 3.07 (s, 3H), 2.86 (d, *J* = 13.3 Hz , 1H), 2.74 (s, 3H), 2.72 (s, 3H), 2.59 (s, 3H), 1.64 (s, 9H), 1.44 (s, 9H), 1.37 (s, 9H), 1.35 (s, 9H); **^{13}C-NMR** (125 MHz, $CDCl_3$): δ 202.2, 175.5, 175.3, 173.0, 163.9, 163.5, 157.5, 154.8, 154.5, 154.4, 153.4, 149.4, 144.9, 143.2, 136.4, 136.3, 135.7, 132.9, 130.9, 128.9, 128.8, 126.1, 120.1, 119.1, 112.7, 111.6, 103.6, 94.8, 94.7, 83.2, 83.1, 82.5, 56.7, 56.3, 44.9, 39.2, 39.0, 36.9, 32.8, 28.1, 27.7, 27.2, 27.1, 18.1; **IR** (film, υ cm^{-1}): 1766, 1730, 1660, 1610; **HRMS** (ESI) calcd. for $C_{52}H_{63}NO_{18}Na^+$ $[M+Na]^+$: 1012.39374, obs. 1012.39398.

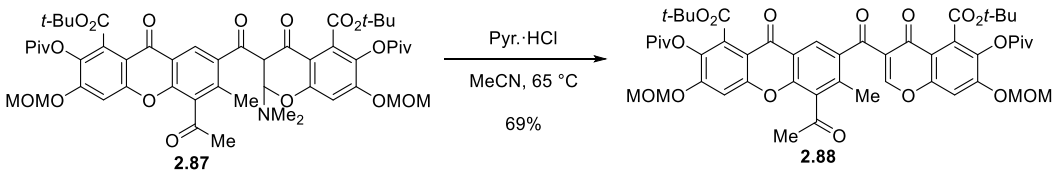

To a stirred solution of aminal **2.67** (83.6 mg, 0.084 mmol, 1.0 equiv.) in MeCN (5.6 mL) was added solid pyridinium chloride (49 mg, 0.42 mmol, 5.0 equiv.) in one portion and the resulting yellow solution was heated to 65 °C. After 18 h the reaction was concentrated and the yellow residue was chromatographed on silica gel (3:1 hexanes: EtOAc to 2:1 hexanes: EtOAc to furnish aminal **2.88** (54 mg, 69%).

yellow solid, M.P. = 185-188 °C; **R_f** = 0.21 (silica gel, 1:1 hexanes: EtOAc); **^{1}H-NMR** (400 MHz, $CDCl_3$): δ 8.43 (s, 1H), 8.25 (s, 1H), 7.27 (s, 1H), 7.17 (s, 1H), 5.26 (s, 4H), 3.48 (s, 3H), 3.47 (s, 3H), 2.68 (s, 3H), 2.45 (s, 3H), 1.61 (s, 9H), 1.42 (s, 9H), 1.38 (s, 9H), 1.35 (s, 9H); **^{13}C-NMR** (125 MHz, $CDCl_3$): δ 202.2, 192.1, 175.5, 175.3, 173.2, 172.1, 163.5, 162.9, 160.4, 154.6, 154.4, 154.3, 153.7, 152.6, 140.6, 136.8, 136.4, 135.6, 132.3, 128.9, 128.6, 127.3, 123.8, 118.7, 116.5, 112.7, 104.0, 103.6, 94.8, 94.7, 83.2, 83.1, 56.7, 56.6, 39.2, 39.1, 32.7, 28.2, 27.9, 27.3, 27.2, 17.5; **IR** (film, υ cm^{-1}): 1760, 1732, 1663, 1607, 1591; **HRMS** (ESI) calcd. for $C_{50}H_{56}O_{18}Na^+$ $[M+Na]^+$: 967.33589, obs. 967.33504.

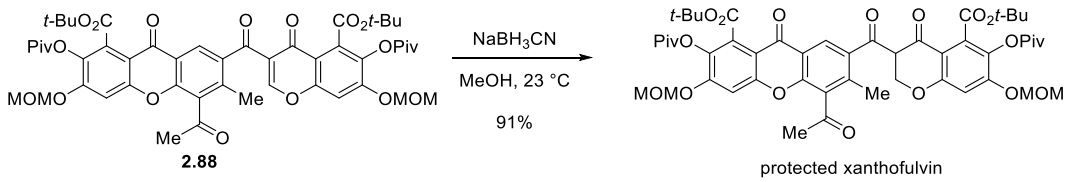

To a stirred solution of aminal **2.88** (30 mg, 0.032 mmol, 1.0 equiv.) in MeOH (0.64 mL) at 23 °C was added solid $NaBH_3CN$ (4.0 mg, 0.063 mmol, 2.0 equiv.) in one portion. After 20 minutes the chalky yellow reaction mixture was diluted with aqueous pH 7.0 phosphate buffer (0.2 M, 0.25 mL) then diluted with EtOAc (10 mL). The organic phase was separated and the aqueous layer was extracted with EtOAc (2 x 10 mL). The combined organic layers were washed with brine (10 mL), dried over sodium sulfate, and concentrated *in vacuo*. The yellow reside was chromatographed on silica gel (2:1 hexanes: EtOAc) to afford protected xanthofulvin (27 mg, 91 %).

yellow solid, M.P. = 184-186 °C; $\mathbf{R_f}$ = 0.5 (silica gel, 1:1 hexanes: EtOAc); **^{1}H-NMR** (400 MHz, $CDCl_3$): δ 15.43 (s, 1H), 8.12 (s, 1H), 7.18 (s, 1H), 6.68 (s, 1H), 5.28 (s, 2H), 5.16 (s, 2H), 4.74 (bs, 2H), 3.48 (s, 3H), 3.42 (s, 3H), 2.71 (s, 3H), 2.41 (s, 3H), 1.66 (s, 9H), 1.62 (s, 9H), 1.39 (s, 9H), 1.37 (s, 9H); **^{13}C-NMR** (150 MHz, $CDCl_3$): δ 201.9, 183.6, 175.7, 173.3, 173.1, 163.9, 163.6, 160.0, 154.9, 154.5, 152.3, 139.6, 135.7, 133.4, 132.4, 130.3, 129.3, 128.9, 126.9, 119.2, 112.7, 111.9, 103.9, 103.8, 103.5, 94.8, 94.4, 93.4. 83.3, 82.9, 66.7, 56.7, 56.5, 39.2, 39.1, 32.7, 29.7, 28.2, 28.1, 27.3, 27.2, 16.9; **IR** (film, υ cm^{-1}): 1765, 1730, 1666, 1602, 1458; **HRMS** (ESI) calcd. for $C_{50}H_{58}O_{18}Na^+$ $[M+Na]^+$: 969.35154, obs. 969.35120.

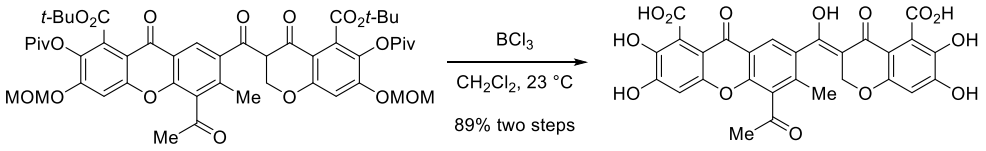

xanthofulvin (**2.2**)

To a stirred solution of protected xanthofulvin (20 mg, 0.02 mmol, 1.0 equiv.) in CH_2Cl_2 (2.1 mL) at 23 °C was added a solution of BCl_3 (1.0 M CH_2Cl_2, 0.25 mL, 0.25 mmol, 12 equiv.) and the reaction was stirred for 45 minutes. The yellow-orange solution was then treated with 12 M HCl (0.09 mL) and diluted with EtOAc (10 mL). The bright orange solution was stirred vigorously for 15 minutes and then concentrated *in vacuo*. The orange residue was diluted with MeOH (15 mL) and re-concentrated *in vacuo*. The yellow residue was triturated with $CHCl_3$ (10 mL) and then filtered. The yellow solid was then dried *in vacuo* to furnish xanthofulvin (**2.2**) (11.8 mg, 98%) as a 3.6:1 ratio of enol: keto tautomers.

yellow solid, M.P. = 252-253 °C; **R_f** = 0.14 (silica gel, 20:1 EtOAc: AcOH); **^{1}H-NMR** (500 MHz, $(CD_3)_2SO$): δ [enol] 15.61 (s, 1H), 12.75 (s, 1H), 11.62 (s, 1H), 11.23 (s, 1H), 9.33 (s, 1H), 8.69 (s, 1H), 7.95 (s, 1H), 6.93 (s, 1H), 6.39 (s, 1H), 4.66 (s, 2H), 2.70 (s, 3H), 2.31 (s, 3H). [keto] 11.15 (s, 1H), 8.88 (s, 1H), 8.51 (s, 1H), 6.92 (s, 1H), 6.42 (s, 1H), 5.01 (dd, J = 4.7 Hz, 8.1 Hz, 1H), 4.71 (dd, J = 4.2 Hz, 11.3 Hz, 1H), 4.60 (m, 1H), 2.67 (s, 3H), 2.29 (s, 3H); **^{13}C-NMR** (125 MHz, $(CD_3)_2SO$): δ [enol] 202.6, 183.7, 172.7, 172.7, 167.5, 167.5, 156.3, 154.5, 153.9, 152.2, 150.2, 140.8, 137.6, 132.4, 129.4, 128.3, 125.9, 120.7, 120.7, 118.7, 110.1, 104.4, 102.4, 102.4, 65.9, 32.4, 16.6. [keto]□202.9, 199.1, 186.3, 172.7, 167.7, 156.3, 154.7, 153.9, 150.1, 140.9, 139.2, 137.6, 134.9, 132.4, 127.7, 122.2, 120.8, 118.3, 110.1, 108.8, 102.4, 68.0, 56.3, 32.4, 17.1; **IR** (KBr, υ cm^{-1}): 3419, 2926, 1607, 1468, 1288, 1021; **HRMS** (ESI) calcd. for $C_{28}H_{17}O_{14}$ $[M-H]^-$: 577.06238, obs. 577.06186.

SECOND GENERATION SYNTHESIS OF VINAXANTHONE EXPERIMENTAL SECTION

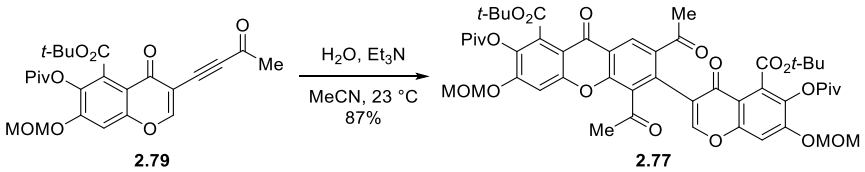

To a stirred solution of **2.79** (100 mg, 0.212 mmol, 1.0 equiv.) in MeCN (0.1 M) at 23 °C was added a 1.0 M solution of H_2O in MeCN (0.5 equiv.) and triethylamine (10 equiv.). After 16 hours, the reaction mixture was concentrated *in vacuo* to give a dark amber residue. The crude material was purified via silica gel column chromatography (5:2:1 CH_2Cl_2: EtOAc: hexanes) to give pure protected vinaxanthone **2.77** (87 mg, 0.092 mmol, 87%) as a white-tan solid.

white solid, M.P. = 224-225 °C; $\mathbf{R_f}$ = 0.68 (silica gel, 5:2:1 CH_2Cl_2: EtOAc: hexanes); **^{1}H-NMR** (400 MHz, $CDCl_3$) δ 8.62 (bs, 1H), 7.84 (bs, 1H), 7.22 (s, 1H), 7.18 (s, 1H), 5.27 (s, 2H), 5.26 (s, 2H), 3.47 (s, 3H), 3.46 (s, 3H), 2.65 (bs, 3H), 2.41 (bs, 3H), 1.68 (s, 9H), 1.58 (s, 9H), 1.39 (s, 9H), 1.37 (s, 9H); **^{13}C-NMR** (125 MHz, $CDCl_3$) δ 201.3, 198.8, 175.4 (2 signals), 173.3 (2 signals), 163.4, 163.3, 155.1, 154.6, 154.5, 154.0, 153.5, 152.6, 136.4 (2 signals), 135.9, 133.9, 132.3, 128.9, 128.2, 126.8, 121.2, 120.7, 115.0, 112.7, 103.9, 103.6, 94.7, 94.6, 83.3, 82.8, 56.7, 56.5, 39.2, 39.1, 32.5, 29.6, 28.1, 28.0, 27.2, 27.1; **IR** (film, υ cm^{-1}) 1763, 1735 1460, 1264, 1157; **HRMS** (ESI) calcd. for $C_{50}H_{56}NaO_{18}$ $[M+Na]^+$: 967.33589, obs. 967.33632.

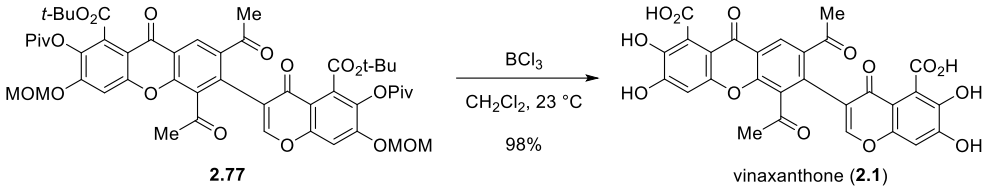

To a stirred solution of protected vinaxanthone analog **2.77** (20 mg, 0.021 mmol, 1.0 equiv.) in CH_2Cl_2 (0.1 M) at 0 °C was added 1.0 M boron trichloride (0.25 mL, 0.254 mmol, 12 equiv.). After 1 hour, the reaction mixture was diluted with EtOAc and washed with brine (5x). The organic layer was dried over sodium sulfate and concentrated *in vacuo* to give a brown/black solid. The crude material was purified by trituration with pentane: MeOH to give pure vinaxanthone (**2.1**) (12 mg, 0.021 mmol, 98%) as a yellow solid.

yellow solid; M.P. = >280 °C; **R_f**= 0.05 (sílica gel, 95:5 EtOAc:AcOH); **^{1}H-NMR** (400 MHz, $(CD_3)_2SO$) δ 12.89 (bs, 1H), 12.72 (bs, 1H), 11.69 (bs, 1H), 11.44 (bs, 1H), 9.42 (bs 2H), 9.42 (bs, 2H), 8.53 (s, 1H), 8.18 (s, 1H), 6.96 (s, 1H), 6.94 (s, 1H), 2.55 (s, 3H), 2.53 (s, 3H); **^{13}C-NMR** (125 MHz, $(CD_3)_2SO$) δ 201.1, 199.1, 172.9, 172.6, 167.4, 167.4, 154.1, 152.7, 152.5, 152.1, 150.7, 150.3, 141.7, 141.0, 136.2, 133.4, 132.6, 126.3, 120.8, 120.5, 119.8, 119.6, 112.4, 110.0, 102.4, 102.3, 32.1, 29.1; **IR** (KBr, cm $^{-1}$) 3236, 1683, 1653, 1472, 1288; **HRMS** (ESI) calcd. for $C_{28}H_{15}O_{14}$ $[M-H]^-$: 575.04673, obs. 575.04679.

Appendix A: X-ray Crystal Structures

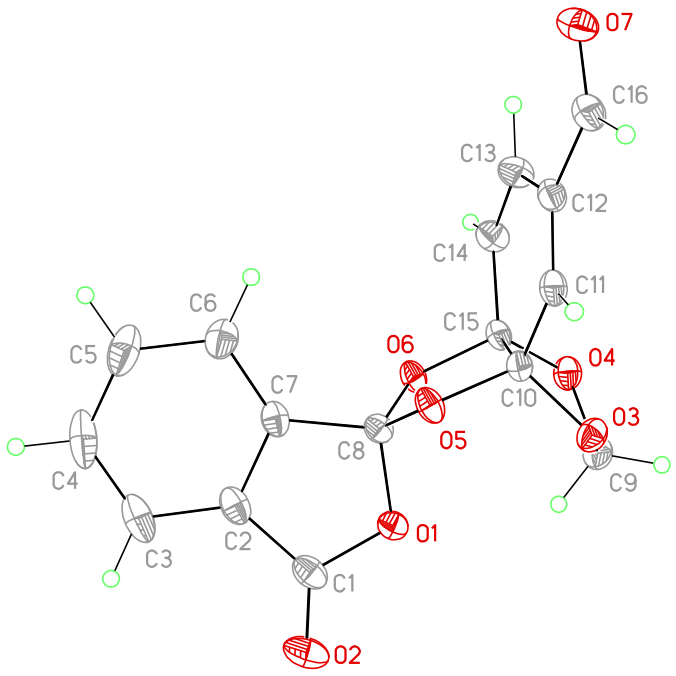

Figure A.1. View of **1.179a** showing the atom labeling scheme. Displacement ellipsoids are scaled to the 50% probability level.

Table A.1. Crystal data and structure refinement for **1.179a**.

Empirical formula	C16 H10 O7	
Formula weight	314.24	
Temperature	100(2) K	
Wavelength	0.71073 Å	
Crystal system	monoclinic	
Space group	I 2/a	
Unit cell dimensions	a = 16.170(6) Å	α= 90°.
	b = 7.239(2) Å	β= 97.61(2)°.
	c = 23.837(9) Å	γ = 90°.
Volume	2765.4(17) $Å^3$	
Z	8	

Density (calculated)	1.510 Mg/m^3
Absorption coefficient	0.121 mm^{-1}
F(000)	1296
Crystal size	0.200 x 0.180 x 0.110 mm
Theta range for data collection	2.542 to 27.488°.
Index ranges	-20<=h<=20, -9<=k<=9, -30<=l<=30
Reflections collected	24272
Independent reflections	3183 [R(int) = 0.0406]
Completeness to theta = 25.242°	100.0 %
Absorption correction	Semi-empirical from equivalents
Max. and min. transmission	1.00 and 0.822
Refinement method	Full-matrix least-squares on F^2
Data / restraints / parameters	3183 / 0 / 248
Goodness-of-fit on F^2	1.091
Final R indices [I>2sigma(I)]	R1 = 0.0362, wR2 = 0.0921
R indices (all data)	R1 = 0.0451, wR2 = 0.0976
Extinction coefficient	n/a
Largest diff. peak and hole	0.332 and -0.223 $e.Å^{-3}$

Table A.2. Atomic coordinates (x 104) and equivalent isotropic displacement parameters (Å2x 103) for 1.179a. U(eq) is defined as one third of the trace of the orthogonalized Uij tensor.

	x	y	z	U(eq)
C1	10712(1)	5585(2)	1508(1)	23(1)
C2	10885(1)	4154(2)	1948(1)	22(1)
C3	11454(1)	4143(2)	2438(1)	33(1)
C4	11509(1)	2536(3)	2756(1)	40(1)
C5	11021(1)	1001(3)	2588(1)	37(1)
C6	10447(1)	1030(2)	2098(1)	27(1)
C7	10389(1)	2646(2)	1789(1)	20(1)
C8	9847(1)	3084(2)	1247(1)	17(1)
C9	8814(1)	4031(2)	-8(1)	22(1)
C10	8524(1)	2546(2)	795(1)	17(1)
C11	7766(1)	1540(2)	928(1)	19(1)
C12	7697(1)	-281(2)	843(1)	20(1)
C13	8360(1)	-1383(2)	638(1)	24(1)
C14	9034(1)	-614(2)	474(1)	22(1)
C15	9147(1)	1426(2)	494(1)	17(1)
C16	6931(1)	-1221(2)	976(1)	22(1)
O1	10104(1)	4919(1)	1099(1)	21(1)
O2	11013(1)	7086(1)	1470(1)	34(1)
O3	8279(1)	4017(1)	425(1)	21(1)
O4	9079(1)	2170(1)	-53(1)	21(1)
O5	8998(1)	3129(1)	1311(1)	19(1)
O6	9943(1)	1863(1)	810(1)	19(1)
O7	6861(1)	-2892(1)	985(1)	27(1)

Table A.3. Bond lengths [Å] and angles [°] for 1.179a.

C1-O2	1.1994(16)	C9-H9A	0.981(14)
C1-O1	1.3766(16)	C9-H9B	0.981(14)
C1-C2	1.474(2)	C10-O3	1.4059(15)
C2-C7	1.3774(18)	C10-O5	1.4243(16)
C2-C3	1.3886(19)	C10-C11	1.4947(17)
C3-C4	1.384(3)	C10-C15	1.5427(17)
C3-H3	0.970(19)	C11-C12	1.3362(19)
C4-C5	1.391(3)	C11-H11	0.920(15)
C4-H4	0.96(2)	C12-C13	1.4698(18)
C5-C6	1.391(2)	C12-C16	1.4840(18)
C5-H5	0.954(18)	C13-C14	1.3291(19)
C6-C7	1.3795(19)	C13-H12	0.993(16)
C6-H6	0.977(16)	C14-C15	1.4880(18)
C7-C8	1.4959(18)	C14-H13	0.983(17)
C8-O6	1.3911(15)	C15-O4	1.4021(15)
C8-O5	1.4021(15)	C15-O6	1.4372(15)
C8-O1	1.4490(15)	C16-O7	1.2146(17)
C9-O4	1.4214(17)	C16-H16	1.032(15)
C9-O3	1.4322(16)		
O2-C1-O1	121.43(13)	C3-C4-H4	117.7(11)
O2-C1-C2	130.61(13)	C5-C4-H4	121.0(11)
O1-C1-C2	107.96(11)	C4-C5-C6	121.33(15)
C7-C2-C3	121.61(13)	C4-C5-H5	120.9(11)
C7-C2-C1	108.19(11)	C6-C5-H5	117.8(11)
C3-C2-C1	130.15(13)	C7-C6-C5	116.86(14)
C4-C3-C2	116.93(14)	C7-C6-H6	121.0(9)
C4-C3-H3	121.7(11)	C5-C6-H6	122.1(9)
C2-C3-H3	121.2(11)	C2-C7-C6	121.91(13)
C3-C4-C5	121.33(14)	C2-C7-C8	108.84(11)

C6-C7-C8	129.21(12)	C11-C12-C16	118.34(12)
O6-C8-O5	107.77(9)	C13-C12-C16	119.16(12)
O6-C8-O1	109.64(10)	C14-C13-C12	122.20(12)
O5-C8-O1	108.76(9)	C14-C13-H12	123.2(9)
O6-C8-C7	113.70(10)	C12-C13-H12	114.6(9)
O5-C8-C7	112.35(10)	C13-C14-C15	120.54(12)
O1-C8-C7	104.49(10)	C13-C14-H13	123.7(10)
O4-C9-O3	105.33(10)	C15-C14-H13	115.8(10)
O4-C9-H9A	109.7(8)	O4-C15-O6	110.89(10)
O3-C9-H9A	108.8(8)	O4-C15-C14	110.86(10)
O4-C9-H9B	111.0(8)	O6-C15-C14	109.49(10)
O3-C9-H9B	110.3(8)	O4-C15-C10	104.76(10)
H9A-C9-H9B	111.5(11)	O6-C15-C10	103.69(9)
O3-C10-O5	113.06(10)	C14-C15-C10	116.86(10)
O3-C10-C11	109.34(10)	O7-C16-C12	122.87(12)
O5-C10-C11	108.94(10)	O7-C16-H16	122.5(8)
O3-C10-C15	104.66(10)	C12-C16-H16	114.6(8)
O5-C10-C15	104.29(9)	C1-O1-C8	110.45(10)
C11-C10-C15	116.56(10)	C10-O3-C9	108.12(9)
C12-C11-C10	120.13(11)	C15-O4-C9	106.33(9)
C12-C11-H11	126.9(9)	C8-O5-C10	108.77(9)
C10-C11-H11	112.9(9)	C8-O6-C15	110.49(9)
C11-C12-C13	122.47(12)		

Table A.4. Anisotropic displacement parameters ($Å^2 x 10^3$) for **1.179a**. The anisotropic displacement factor exponent takes the form: $-2\pi^2[h^2 a^{*2} U^{11} + ... + 2 h k a^* b^* U^{12}]$.

	U^{11}	U^{22}	U^{33}	U^{23}	U^{13}	U^{12}
C1	18(1)	27(1)	26(1)	-7(1)	5(1)	-4(1)
C2	16(1)	32(1)	20(1)	-5(1)	3(1)	-2(1)
C3	20(1)	54(1)	24(1)	-10(1)	0(1)	-6(1)
C4	22(1)	76(1)	19(1)	2(1)	-3(1)	2(1)
C5	27(1)	58(1)	27(1)	18(1)	4(1)	4(1)
C6	21(1)	36(1)	25(1)	8(1)	4(1)	-1(1)
C7	14(1)	29(1)	17(1)	-1(1)	3(1)	-1(1)
C8	13(1)	19(1)	19(1)	-2(1)	3(1)	-1(1)
C9	20(1)	25(1)	21(1)	4(1)	3(1)	-1(1)
C10	15(1)	19(1)	16(1)	-1(1)	0(1)	1(1)
C11	13(1)	25(1)	18(1)	0(1)	1(1)	2(1)
C12	16(1)	24(1)	18(1)	1(1)	0(1)	-3(1)
C13	24(1)	21(1)	28(1)	-4(1)	5(1)	-2(1)
C14	21(1)	22(1)	25(1)	-5(1)	5(1)	0(1)
C15	14(1)	22(1)	16(1)	-1(1)	1(1)	-2(1)
C16	19(1)	27(1)	21(1)	-2(1)	3(1)	-2(1)
O1	20(1)	20(1)	22(1)	0(1)	1(1)	-3(1)
O2	32(1)	27(1)	44(1)	-6(1)	9(1)	-12(1)
O3	17(1)	22(1)	24(1)	4(1)	3(1)	3(1)
O4	21(1)	26(1)	16(1)	0(1)	2(1)	1(1)
O5	12(1)	27(1)	18(1)	-5(1)	2(1)	-1(1)
O6	13(1)	23(1)	19(1)	-5(1)	1(1)	1(1)
O7	28(1)	25(1)	29(1)	-1(1)	6(1)	-8(1)

Table A.5. Hydrogen coordinates (x 104) and isotropic displacement parameters (Å2x103) for 1.179a.

	x	y	z	U(eq)
H3	11823(12)	5180(20)	2538(8)	47(5)
H4	11909(12)	2500(30)	3091(9)	51(5)
H5	11072(11)	-110(20)	2804(8)	40(5)
H6	10116(10)	-50(20)	1968(7)	29(4)
H9A	8489(9)	4418(18)	-365(6)	15(3)
H9B	9293(9)	4850(18)	100(6)	16(3)
H11	7387(9)	2301(19)	1069(6)	18(3)
H12	8256(10)	-2740(20)	628(7)	32(4)
H13	9489(10)	-1320(20)	341(7)	35(4)
H16	6466(9)	-340(20)	1069(6)	26(4)

Table A.6. Torsion angles [°] for **1.179a**.

O2-C1-C2-C7	-178.21(14)	C13-C14-C15-C10	9.00(18)
O1-C1-C2-C7	1.11(14)	O3-C10-C15-O4	-10.35(12)
O2-C1-C2-C3	-0.8(2)	O5-C10-C15-O4	-129.32(10)
O1-C1-C2-C3	178.52(13)	C11-C10-C15-O4	110.55(11)
C7-C2-C3-C4	0.9(2)	O3-C10-C15-O6	106.00(10)
C1-C2-C3-C4	-176.20(14)	O5-C10-C15-O6	-12.98(11)
C2-C3-C4-C5	0.5(2)	C11-C10-C15-O6	-133.10(11)
C3-C4-C5-C6	-1.1(2)	O3-C10-C15-C14	-133.46(11)
C4-C5-C6-C7	0.1(2)	O5-C10-C15-C14	107.57(12)
C3-C2-C7-C6	-1.9(2)	C11-C10-C15-C14	-12.56(16)
C1-C2-C7-C6	175.76(12)	C11-C12-C16-O7	-169.94(13)
C3-C2-C7-C8	-179.98(12)	C13-C12-C16-O7	8.49(19)
C1-C2-C7-C8	-2.31(14)	O2-C1-O1-C8	179.99(12)
C5-C6-C7-C2	1.3(2)	C2-C1-O1-C8	0.59(13)
C5-C6-C7-C8	178.99(13)	O6-C8-O1-C1	-124.13(10)
C2-C7-C8-O6	122.11(11)	O5-C8-O1-C1	118.26(11)
C6-C7-C8-O6	-55.77(18)	C7-C8-O1-C1	-1.91(12)
C2-C7-C8-O5	-115.14(11)	O5-C10-O3-C9	102.61(11)
C6-C7-C8-O5	66.98(17)	C11-C10-O3-C9	-135.83(10)
C2-C7-C8-O1	2.60(13)	C15-C10-O3-C9	-10.26(12)
C6-C7-C8-O1	-175.28(12)	O4-C9-O3-C10	27.23(12)
O3-C10-C11-C12	125.65(12)	O6-C15-O4-C9	-84.17(11)
O5-C10-C11-C12	-110.34(13)	C14-C15-O4-C9	153.99(10)
C15-C10-C11-C12	7.27(17)	C10-C15-O4-C9	27.09(12)
C10-C11-C12-C13	2.08(19)	O3-C9-O4-C15	-34.07(12)
C10-C11-C12-C16	-179.55(11)	O6-C8-O5-C10	-22.56(12)
C11-C12-C13-C14	-6.4(2)	O1-C8-O5-C10	96.23(10)
C16-C12-C13-C14	175.20(13)	C7-C8-O5-C10	-148.59(10)
C12-C13-C14-C15	0.3(2)	O3-C10-O5-C8	-91.37(11)
C13-C14-C15-O4	-110.90(14)	C11-C10-O5-C8	146.85(10)
C13-C14-C15-O6	126.43(13)	C15-C10-O5-C8	21.72(12)

O5-C8-O6-C15	13.59(12)	O4-C15-O6-C8	111.84(11)
O1-C8-O6-C15	-104.64(10)	C14-C15-O6-C8	-125.51(11)
C7-C8-O6-C15	138.81(10)	C10-C15-O6-C8	-0.10(12)

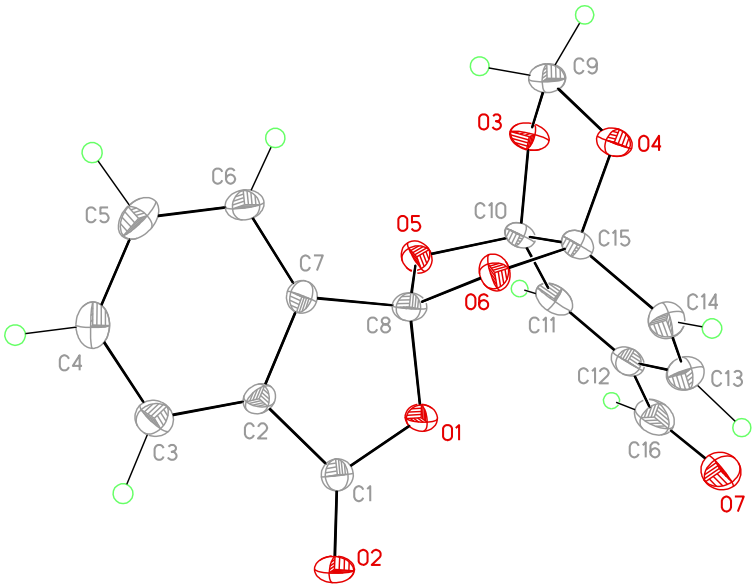

Figure A.2. View of **1.179b** showing the atom labeling scheme. Displacement ellipsoids are scaled to the 50% probability level.

Table A.7. Crystal data and structure refinement for **1.179b**.

Empirical formula	C16 H10 O7	
Formula weight	314.24	
Temperature	140(2) K	
Wavelength	0.71073 Å	
Crystal system	monoclinic	
Space group	P 21/n	
Unit cell dimensions	a = 8.5932(7) Å	α= 90°.
	b = 13.9047(9) Å	β= 108.595(4)°.
	c = 11.9833(10) Å	γ = 90°.
Volume	1357.09(18) $Å^3$	
Z	4	
Density (calculated)	1.538 Mg/m^3	
Absorption coefficient	0.123 mm^{-1}	
F(000)	648	

Crystal size	0.380 x 0.170 x 0.080 mm
Theta range for data collection	2.571 to 24.987°.
Index ranges	-10<=h<=10, -16<=k<=16, -14<=l<=14
Reflections collected	19584
Independent reflections	2385 [R(int) = 0.0838]
Completeness to theta = 25.242°	97.0 %
Absorption correction	Semi-empirical from equivalents
Max. and min. transmission	1.00 and 0.855
Refinement method	Full-matrix least-squares on F^2
Data / restraints / parameters	2385 / 0 / 249
Goodness-of-fit on F^2	1.019
Final R indices [I>2sigma(I)]	R1 = 0.0431, wR2 = 0.0845
R indices (all data)	R1 = 0.0775, wR2 = 0.0958
Extinction coefficient	$8.8(13)x10^{-6}$
Largest diff. peak and hole	0.314 and -0.201 e.$Å^{-3}$

Table A.8. Atomic coordinates (x 104) and equivalent isotropic displacement parameters (Å2x 103) for 1.179b. U(eq) is defined as one third of the trace of the orthogonalized Uij tensor.

	x	y	z	U(eq)
C1	1546(3)	6389(2)	4117(2)	19(1)
C2	-47(3)	6170(2)	3230(2)	17(1)
C3	-1265(3)	5534(2)	3293(2)	22(1)
C4	-2651(3)	5478(2)	2315(2)	24(1)
C5	-2802(3)	6024(2)	1316(2)	25(1)
C6	-1587(3)	6658(2)	1267(2)	22(1)
C7	-216(3)	6723(2)	2249(2)	17(1)
C8	1270(3)	7352(2)	2479(2)	18(1)
C9	1269(3)	9002(2)	264(2)	23(1)
C10	3018(3)	8105(2)	1670(2)	19(1)
C11	4813(3)	7951(2)	2251(2)	25(1)
C12	5618(3)	8454(2)	3224(2)	23(1)
C13	4823(3)	9172(2)	3731(2)	27(1)
C14	3243(3)	9382(2)	3292(2)	24(1)
C15	2189(3)	8860(2)	2238(2)	19(1)
C16	7401(3)	8275(2)	3775(3)	32(1)
O1	2316(2)	7066(1)	3643(1)	20(1)
O2	2184(2)	6088(1)	5092(1)	25(1)
O3	2694(2)	8413(1)	510(1)	23(1)
O4	1480(2)	9513(1)	1332(1)	22(1)
O5	2125(2)	7230(1)	1687(1)	20(1)
O6	921(2)	8328(1)	2510(1)	20(1)
O7	8251(2)	8724(1)	4622(2)	39(1)

Table A.9. Bond lengths [Å] and angles [°] for **1.179b**.

C1-O2	1.197(3)	C9-H9A	1.01(2)
C1-O1	1.373(3)	C9-H9B	1.00(2)
C1-C2	1.473(3)	C10-O3	1.395(3)
C2-C7	1.373(3)	C10-O5	1.443(3)
C2-C3	1.390(3)	C10-C11	1.491(3)
C3-C4	1.381(3)	C10-C15	1.545(3)
C3-H3	0.97(3)	C11-C12	1.346(3)
C4-C5	1.389(3)	C11-H11	0.94(2)
C4-H4	0.95(2)	C12-C13	1.449(4)
C5-C6	1.381(4)	C12-C16	1.483(3)
C5-H5	0.97(2)	C13-C14	1.323(3)
C6-C7	1.377(3)	C13-H13	1.03(2)
C6-H6	0.92(2)	C14-C15	1.487(3)
C7-C8	1.500(3)	C14-H14	1.04(3)
C8-O5	1.384(3)	C15-O4	1.397(3)
C8-O6	1.392(3)	C15-O6	1.438(3)
C8-O1	1.453(3)	C16-O7	1.217(3)
C9-O3	1.423(3)	C16-H16	1.07(3)
C9-O4	1.424(3)		
O2-C1-O1	120.9(2)	C3-C4-H4	118.6(14)
O2-C1-C2	131.5(2)	C5-C4-H4	120.2(14)
O1-C1-C2	107.63(18)	C6-C5-C4	121.5(2)
C7-C2-C3	121.8(2)	C6-C5-H5	119.9(14)
C7-C2-C1	108.8(2)	C4-C5-H5	118.6(14)
C3-C2-C1	129.4(2)	C7-C6-C5	117.2(2)
C4-C3-C2	116.7(2)	C7-C6-H6	119.9(15)
C4-C3-H3	121.8(15)	C5-C6-H6	122.9(15)
C2-C3-H3	121.5(14)	C2-C7-C6	121.5(2)
C3-C4-C5	121.3(2)	C2-C7-C8	108.55(19)

C6-C7-C8	129.9(2)	C11-C12-C16	118.1(2)
O5-C8-O6	107.72(18)	C13-C12-C16	119.1(2)
O5-C8-O1	108.91(18)	C14-C13-C12	123.1(2)
O6-C8-O1	108.30(17)	C14-C13-H13	123.2(13)
O5-C8-C7	114.14(18)	C12-C13-H13	113.6(13)
O6-C8-C7	113.28(18)	C13-C14-C15	120.1(2)
O1-C8-C7	104.26(18)	C13-C14-H14	123.0(14)
O3-C9-O4	104.26(17)	C15-C14-H14	116.9(14)
O3-C9-H9A	110.2(12)	O4-C15-O6	109.65(18)
O4-C9-H9A	108.5(13)	O4-C15-C14	109.90(18)
O3-C9-H9B	107.6(12)	O6-C15-C14	111.06(19)
O4-C9-H9B	110.0(12)	O4-C15-C10	104.31(17)
H9A-C9-H9B	115.7(17)	O6-C15-C10	103.81(16)
O3-C10-O5	109.60(17)	C14-C15-C10	117.7(2)
O3-C10-C11	110.97(19)	O7-C16-C12	123.1(3)
O5-C10-C11	110.35(18)	O7-C16-H16	125.1(15)
O3-C10-C15	104.87(17)	C12-C16-H16	111.8(15)
O5-C10-C15	104.18(17)	C1-O1-C8	110.66(17)
C11-C10-C15	116.5(2)	C10-O3-C9	105.57(17)
C12-C11-C10	120.0(2)	C15-O4-C9	105.87(17)
C12-C11-H11	127.8(14)	C8-O5-C10	107.88(16)
C10-C11-H11	112.3(14)	C8-O6-C15	108.11(17)
C11-C12-C13	122.7(2)		

Table A.10. Anisotropic displacement parameters ($Å^2 x 10^3$) for **1.179b**. The anisotropic displacement factor exponent takes the form: $-2\pi^2[h^2 a^{*2} U^{11} + ... + 2 h k a^* b^* U^{12}]$.

	U^{11}	U^{22}	U^{33}	U^{23}	U^{13}	U^{12}
C1	26(1)	13(1)	17(1)	-1(1)	4(1)	2(1)
C2	21(1)	15(1)	13(1)	-3(1)	3(1)	1(1)
C3	30(2)	19(1)	18(1)	-1(1)	10(1)	0(1)
C4	24(2)	20(1)	30(2)	-4(1)	10(1)	-5(1)
C5	19(1)	24(1)	26(2)	-7(1)	-1(1)	2(1)
C6	24(2)	21(1)	16(1)	2(1)	1(1)	3(1)
C7	21(1)	13(1)	16(1)	-2(1)	6(1)	1(1)
C8	22(1)	17(1)	14(1)	1(1)	4(1)	3(1)
C9	23(2)	23(1)	18(1)	3(1)	1(1)	2(1)
C10	22(1)	17(1)	15(1)	6(1)	4(1)	-1(1)
C11	30(2)	21(1)	26(2)	9(1)	12(1)	5(1)
C12	19(1)	23(1)	23(1)	9(1)	2(1)	-2(1)
C13	31(2)	29(1)	20(1)	0(1)	6(1)	-5(1)
C14	27(2)	24(1)	22(1)	0(1)	8(1)	-2(1)
C15	22(1)	17(1)	17(1)	4(1)	4(1)	-1(1)
C16	27(2)	32(2)	35(2)	11(1)	5(1)	1(1)
O1	20(1)	21(1)	16(1)	5(1)	0(1)	-3(1)
O2	32(1)	25(1)	14(1)	5(1)	0(1)	0(1)
O3	27(1)	25(1)	17(1)	6(1)	8(1)	5(1)
O4	30(1)	17(1)	16(1)	4(1)	3(1)	2(1)
O5	26(1)	16(1)	19(1)	1(1)	8(1)	-1(1)
O6	23(1)	14(1)	22(1)	0(1)	7(1)	-1(1)
O7	28(1)	39(1)	37(1)	9(1)	-6(1)	-7(1)

Table A.11. Hydrogen coordinates (x 10^4) and isotropic displacement parameters ($Å^2$x 10^3) for **1.179b**.

	x	y	z	U(eq)
H3	-1150(30)	5150(17)	3990(20)	33(7)
H4	-3500(30)	5048(16)	2330(20)	25(7)
H5	-3790(30)	5962(16)	650(20)	30(7)
H6	-1670(30)	7038(16)	620(20)	22(7)
H9A	260(30)	8589(15)	96(19)	16(6)
H9B	1290(30)	9460(16)	-375(19)	17(6)
H11	5240(30)	7485(16)	1860(20)	15(6)
H13	5600(30)	9488(16)	4480(20)	28(7)
H14	2670(30)	9893(18)	3660(20)	34(7)
H16	7840(30)	7740(20)	3310(20)	54(9)

Table A.12. Torsion angles [°] for **1.179b**.

O2-C1-C2-C7	179.1(2)	C13-C14-C15-C10	-1.9(3)
O1-C1-C2-C7	-0.7(2)	O3-C10-C15-O4	0.2(2)
O2-C1-C2-C3	-0.1(4)	O5-C10-C15-O4	-114.94(17)
O1-C1-C2-C3	-179.9(2)	C11-C10-C15-O4	123.3(2)
C7-C2-C3-C4	0.6(3)	O3-C10-C15-O6	115.06(17)
C1-C2-C3-C4	179.8(2)	O5-C10-C15-O6	-0.1(2)
C2-C3-C4-C5	0.7(4)	C11-C10-C15-O6	-121.86(19)
C3-C4-C5-C6	-1.2(4)	O3-C10-C15-C14	-121.8(2)
C4-C5-C6-C7	0.3(4)	O5-C10-C15-C14	123.0(2)
C3-C2-C7-C6	-1.5(4)	C11-C10-C15-C14	1.3(3)
C1-C2-C7-C6	179.1(2)	C11-C12-C16-O7	176.5(2)
C3-C2-C7-C8	177.9(2)	C13-C12-C16-O7	-2.0(4)
C1-C2-C7-C8	-1.5(2)	O2-C1-O1-C8	-177.2(2)
C5-C6-C7-C2	1.1(3)	C2-C1-O1-C8	2.6(2)
C5-C6-C7-C8	-178.2(2)	O5-C8-O1-C1	-125.63(18)
C2-C7-C8-O5	121.6(2)	O6-C8-O1-C1	117.49(19)
C6-C7-C8-O5	-59.0(3)	C7-C8-O1-C1	-3.4(2)
C2-C7-C8-O6	-114.6(2)	O5-C10-O3-C9	88.2(2)
C6-C7-C8-O6	64.8(3)	C11-C10-O3-C9	-149.7(2)
C2-C7-C8-O1	2.9(2)	C15-C10-O3-C9	-23.1(2)
C6-C7-C8-O1	-177.7(2)	O4-C9-O3-C10	38.0(2)
O3-C10-C11-C12	120.3(2)	O6-C15-O4-C9	-87.8(2)
O5-C10-C11-C12	-118.0(2)	C14-C15-O4-C9	149.8(2)
C15-C10-C11-C12	0.5(3)	C10-C15-O4-C9	22.8(2)
C10-C11-C12-C13	-1.7(4)	O3-C9-O4-C15	-38.0(2)
C10-C11-C12-C16	179.9(2)	O6-C8-O5-C10	28.8(2)
C11-C12-C13-C14	1.1(4)	O1-C8-O5-C10	-88.49(19)
C16-C12-C13-C14	179.5(2)	C7-C8-O5-C10	155.48(18)
C12-C13-C14-C15	0.8(4)	O3-C10-O5-C8	-128.79(18)
C13-C14-C15-O4	-121.0(2)	C11-C10-O5-C8	108.7(2)
C13-C14-C15-O6	117.5(2)	C15-C10-O5-C8	-17.0(2)

O5-C8-O6-C15	-28.9(2)	O4-C15-O6-C8	128.07(18)
O1-C8-O6-C15	88.7(2)	C14-C15-O6-C8	-110.3(2)
C7-C8-O6-C15	-156.16(18)	C10-C15-O6-C8	17.1(2)

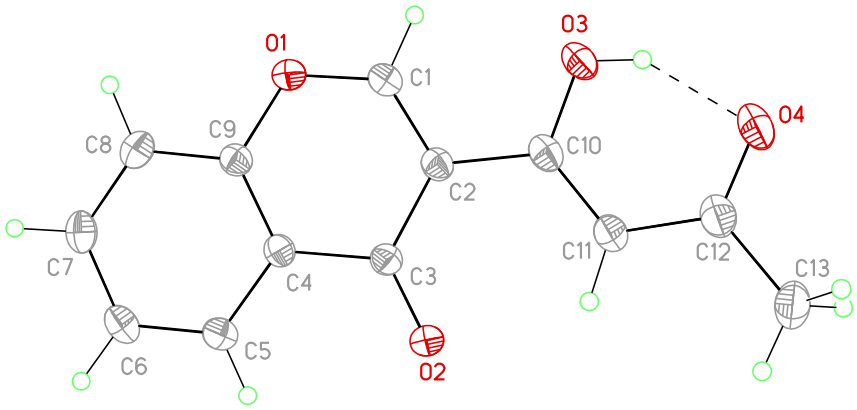

Figure A.3. View of 2.37 showing the atom labeling scheme. Displacement ellipsoids are scaled to the 50% probability level.

Table A.13. Crystal data and structure refinement for **2.37**.

Empirical formula	C13 H10 O4	
Formula weight	230.21	
Temperature	153(2) K	
Wavelength	0.71075 Å	
Crystal system	Monoclinic	
Space group	P21/c	
Unit cell dimensions	a = 12.330(2) Å	α= 90°.
	b = 6.7515(11) Å	β= 98.569(3)°.
	c = 12.628(2) Å	γ = 90°.
Volume	1039.5(3) $Å^3$	
Z	4	
Density (calculated)	1.471 Mg/m^3	
Absorption coefficient	0.110 mm^{-1}	
F(000)	480	
Crystal size	0.30 x 0.20 x 0.15 mm	
Theta range for data collection	3.26 to 27.48°.	

Index ranges	-16<=h<=16, -8<=k<=8, -16<=l<=16
Reflections collected	17516
Independent reflections	2381 [R(int) = 0.0294]
Completeness to theta = 27.48°	99.9 %
Absorption correction	Semi-empirical from equivalents
Max. and min. transmission	1.00 and 0.866
Refinement method	Full-matrix least-squares on F^2
Data / restraints / parameters	2381 / 0 / 180
Goodness-of-fit on F^2	1.099
Final R indices [I>2sigma(I)]	R1 = 0.0443, wR2 = 0.1320
R indices (all data)	R1 = 0.0521, wR2 = 0.1384
Largest diff. peak and hole	0.341 and -0.264 e.$Å^{-3}$

Table A.14. Atomic coordinates (x 10^4) and equivalent isotropic displacement parameters ($Å^2$x 10^3) for **2.37**. U(eq) is defined as one third of the trace of the orthogonalized U^{ij} tensor.

	x	y	z	U(eq)
C1	3051(1)	1605(2)	3664(1)	23(1)
C2	2563(1)	1609(2)	2630(1)	20(1)
C3	3240(1)	1435(2)	1774(1)	20(1)
C4	4433(1)	1402(2)	2157(1)	19(1)
C5	5193(1)	1382(2)	1434(1)	23(1)
C6	6302(1)	1390(2)	1801(1)	26(1)
C7	6678(1)	1407(2)	2905(1)	26(1)
C8	5951(1)	1422(2)	3631(1)	25(1)
C9	4830(1)	1426(2)	3245(1)	20(1)
C10	1354(1)	1830(2)	2442(1)	23(1)
C11	739(1)	2053(2)	1437(1)	26(1)
C12	-415(1)	2220(2)	1331(1)	28(1)
C13	-1080(1)	2515(3)	252(1)	38(1)
O1	4136(1)	1476(2)	4003(1)	25(1)
O2	2883(1)	1319(2)	814(1)	28(1)
O3	888(1)	1828(2)	3307(1)	33(1)
O4	-914(1)	2138(2)	2143(1)	38(1)

Table A.15. Bond lengths [Å] and angles [°] for **2.37**.

C1-O1	1.3450(17)	C7-H7	0.96(2)
C1-C2	1.3546(19)	C8-C9	1.3961(19)
C1-H1	0.968(19)	C8-H8	1.004(18)
C2-C3	1.4658(18)	C9-O1	1.3755(16)
C2-C10	1.4813(19)	C10-O3	1.3076(17)
C3-O2	1.2286(16)	C10-C11	1.386(2)
C3-C4	1.4789(18)	C11-C12	1.4145(19)
C4-C9	1.3878(19)	C11-H11	0.966(18)
C4-C5	1.4025(18)	C12-O4	1.2726(18)
C5-C6	1.378(2)	C12-C13	1.495(2)
C5-H5	0.946(18)	C13-H13A	0.98
C6-C7	1.402(2)	C13-H13B	0.98
C6-H6	0.970(17)	C13-H13C	0.98
C7-C8	1.374(2)	O3-H3	0.84
O1-C1-C2	125.77(12)	C5-C6-H6	120.3(10)
O1-C1-H1	110.9(11)	C7-C6-H6	119.7(10)
C2-C1-H1	123.3(11)	C8-C7-C6	120.75(13)
C1-C2-C3	119.41(12)	C8-C7-H7	122.6(12)
C1-C2-C10	116.55(12)	C6-C7-H7	116.6(12)
C3-C2-C10	124.03(12)	C7-C8-C9	118.51(13)
O2-C3-C2	125.01(12)	C7-C8-H8	122.9(11)
O2-C3-C4	120.95(12)	C9-C8-H8	118.6(11)
C2-C3-C4	114.04(11)	O1-C9-C4	121.62(12)
C9-C4-C5	118.23(12)	O1-C9-C8	116.30(12)
C9-C4-C3	120.74(12)	C4-C9-C8	122.07(13)
C5-C4-C3	121.02(12)	O3-C10-C11	121.08(12)
C6-C5-C4	120.47(13)	O3-C10-C2	115.02(12)
C6-C5-H5	120.3(11)	C11-C10-C2	123.90(12)
C4-C5-H5	119.2(11)	C10-C11-C12	120.06(13)
C5-C6-C7	119.97(13)	C10-C11-H11	124.0(11)

C12-C11-H11	116.0(11)	H13A-C13-H13B	109.5
O4-C12-C11	121.40(13)	C12-C13-H13C	109.5
O4-C12-C13	118.31(13)	H13A-C13-H13C	109.5
C11-C12-C13	120.29(13)	H13B-C13-H13C	109.5
C12-C13-H13A	109.5	C1-O1-C9	118.22(11)
C12-C13-H13B	109.5	C10-O3-H3	109.5

Table A.16. Anisotropic displacement parameters ($Å^2 x 10^3$) for **2.37**. The anisotropic displacement factor exponent takes the form: $-2\pi^2[h^2 a^{*2} U^{11} + ... + 2 h k a^* b^* U^{12}]$

	U^{11}	U^{22}	U^{33}	U^{23}	U^{13}	U^{12}
C1	22(1)	27(1)	22(1)	-1(1)	7(1)	0(1)
C2	20(1)	20(1)	22(1)	0(1)	5(1)	-1(1)
C3	20(1)	21(1)	19(1)	1(1)	4(1)	-1(1)
C4	19(1)	18(1)	21(1)	1(1)	4(1)	-1(1)
C5	24(1)	24(1)	22(1)	1(1)	6(1)	1(1)
C6	22(1)	25(1)	31(1)	4(1)	9(1)	1(1)
C7	19(1)	24(1)	35(1)	1(1)	2(1)	1(1)
C8	24(1)	25(1)	25(1)	0(1)	-2(1)	0(1)
C9	21(1)	20(1)	21(1)	0(1)	4(1)	0(1)
C10	21(1)	23(1)	27(1)	-1(1)	8(1)	-2(1)
C11	20(1)	31(1)	26(1)	-2(1)	6(1)	0(1)
C12	23(1)	30(1)	34(1)	-4(1)	5(1)	0(1)
C13	22(1)	54(1)	38(1)	-9(1)	-1(1)	4(1)
O1	22(1)	35(1)	18(1)	-1(1)	3(1)	0(1)
O2	22(1)	46(1)	18(1)	1(1)	3(1)	-1(1)
O3	22(1)	50(1)	28(1)	4(1)	11(1)	4(1)
O4	22(1)	51(1)	41(1)	2(1)	12(1)	3(1)

Table A.17. Hydrogen coordinates (x 10^4) and isotropic displacement parameters ($Å^2$x 10^3) for **2.37**.

	x	y	z	U(eq)
H13A	-1592	1407	94	58
H13B	-591	2576	-292	58
H13C	-1493	3757	247	58
H3	212	2032	3140	49
H1	2650(16)	1720(30)	4265(15)	36(5)
H5	4934(14)	1380(30)	690(15)	32(4)
H6	6826(14)	1370(20)	1300(14)	27(4)
H7	7459(17)	1450(30)	3119(16)	44(5)
H8	6191(15)	1400(30)	4427(15)	36(5)
H11	1051(15)	2130(30)	780(15)	34(5)

Table A.18. Torsion angles [°] for **2.37**.

O1-C1-C2-C3	0.9(2)
O1-C1-C2-C10	-178.05(12)
C1-C2-C3-O2	176.03(13)
C10-C2-C3-O2	-5.1(2)
C1-C2-C3-C4	-3.83(17)
C10-C2-C3-C4	175.01(12)
O2-C3-C4-C9	-176.55(12)
C2-C3-C4-C9	3.32(17)
O2-C3-C4-C5	4.67(19)
C2-C3-C4-C5	-175.46(11)
C9-C4-C5-C6	-0.07(19)
C3-C4-C5-C6	178.74(12)
C4-C5-C6-C7	0.3(2)
C5-C6-C7-C8	-0.2(2)
C6-C7-C8-C9	-0.2(2)
C5-C4-C9-O1	179.01(11)
C3-C4-C9-O1	0.20(19)
C5-C4-C9-C8	-0.34(19)
C3-C4-C9-C8	-179.15(12)
C7-C8-C9-O1	-178.89(11)
C7-C8-C9-C4	0.5(2)
C1-C2-C10-O3	-5.58(18)
C3-C2-C10-O3	175.55(12)
C1-C2-C10-C11	173.60(13)
C3-C2-C10-C11	-5.3(2)
O3-C10-C11-C12	-2.0(2)
C2-C10-C11-C12	178.88(13)
C10-C11-C12-O4	-1.2(2)
C10-C11-C12-C13	178.35(14)
C2-C1-O1-C9	2.9(2)
C4-C9-O1-C1	-3.38(18)
C8-C9-O1-C1	176.00(12)

Table A.19. Hydrogen bonds for **2.37** [Å and °].

D-H...A	d(D-H)	d(H...A)	d(D...A)	<(DHA)
O3-H3...O4	0.84	1.73	2.4840(15)	147.9

Appendix B: Catalog of Spectra

INDEX	FREQUENCY	PPM	HEIGHT
1	3190.641	7.971	38.1
2	3167.389	7.913	39.0
3	2978.300	7.441	28.7
4	2970.435	7.421	21.1
5	2905.468	7.259	41.7
6	2898.287	7.241	23.7
7	1570.901	3.925	135.2

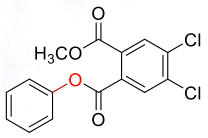

1.83

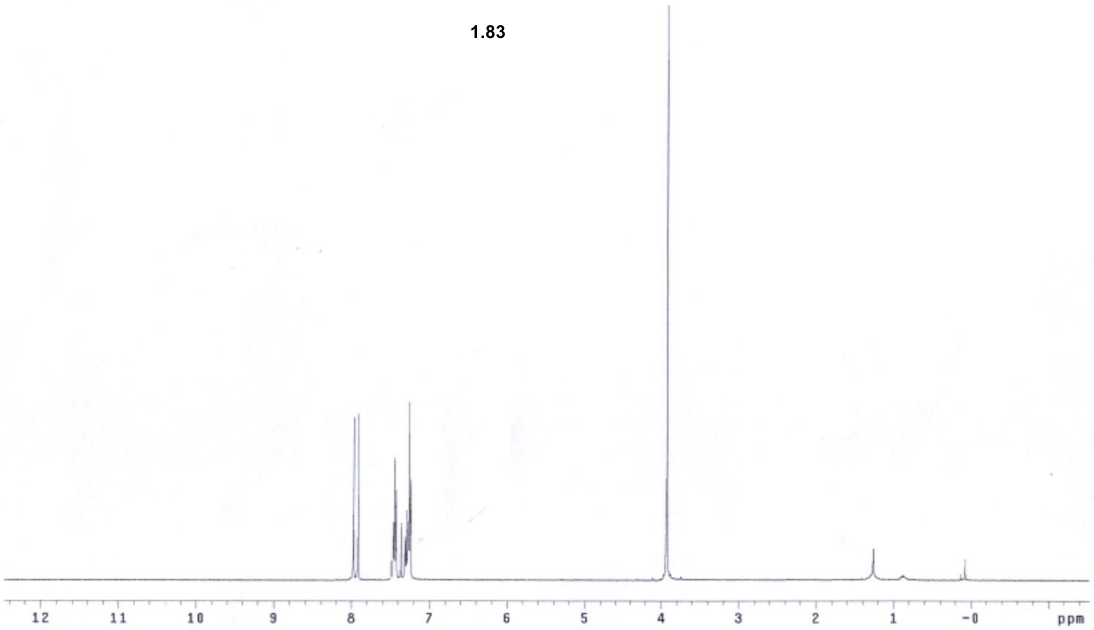

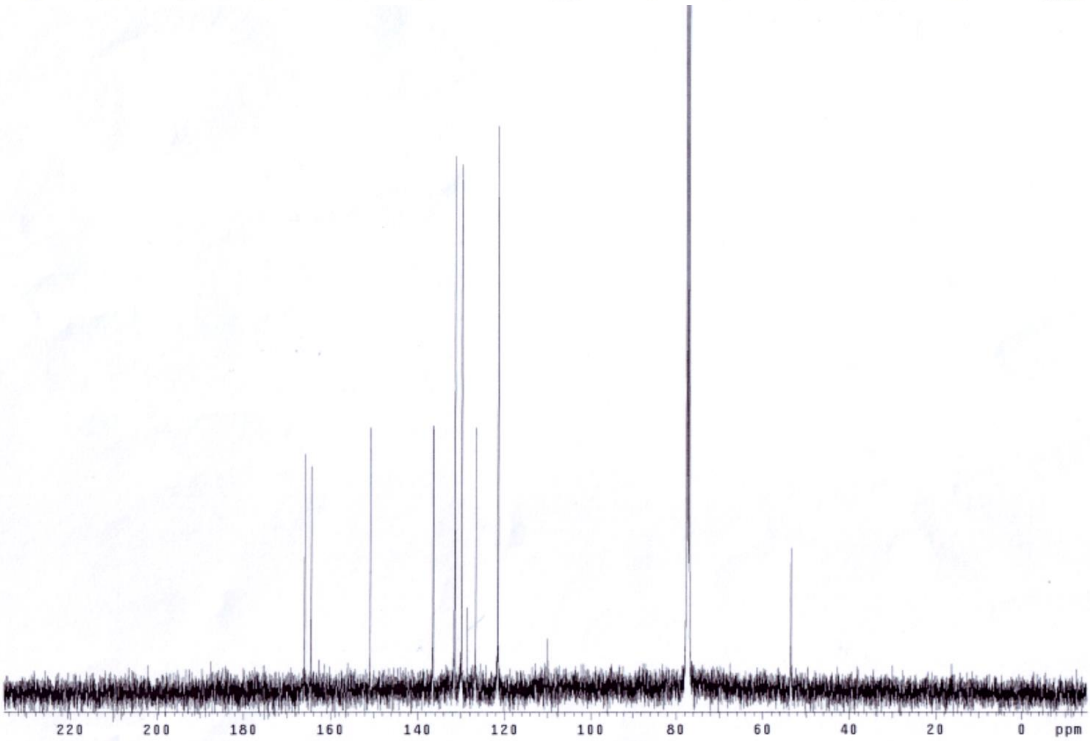

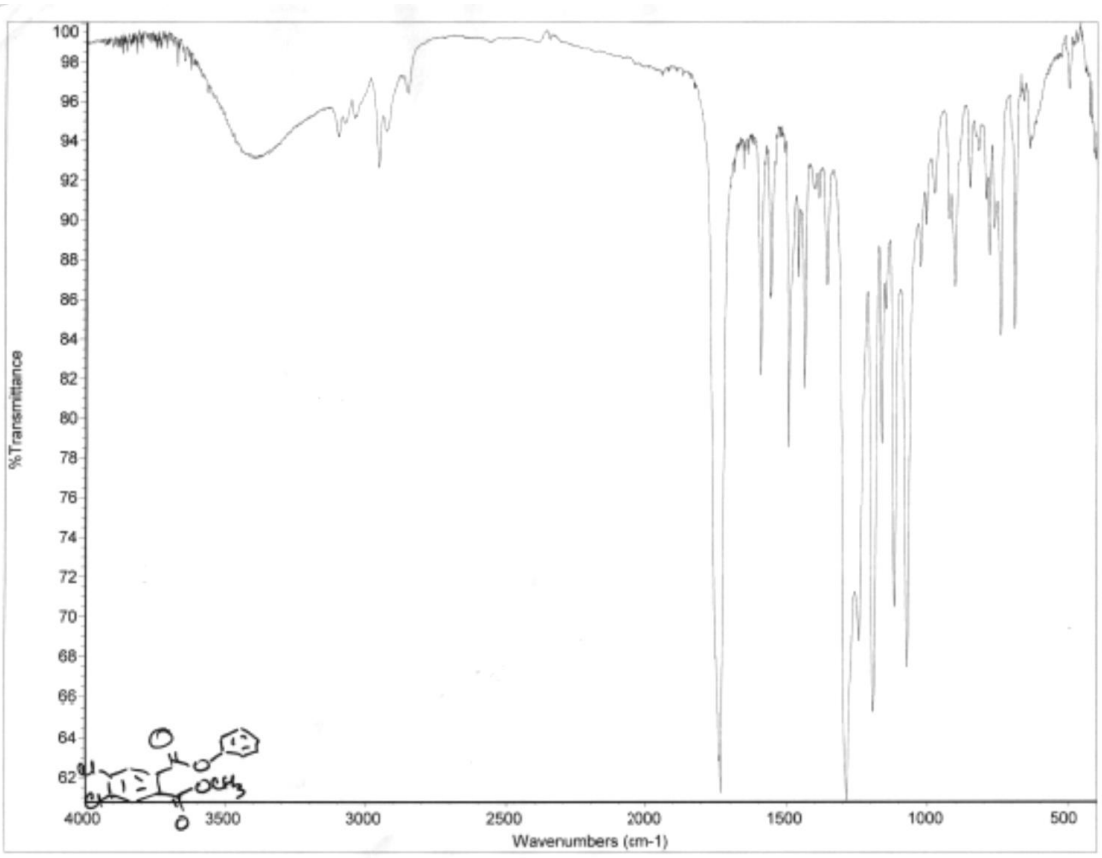
%Transmittance
100
98
96
94
92
90
88
86
84
82
80
78
76
74
72
70
68
66
64
62
4000
3500
3000
2500
2000
1500
1000
500
Wavenumbers (cm-1)

O
H3CO
Cl
O
Cl
O
F

1.84

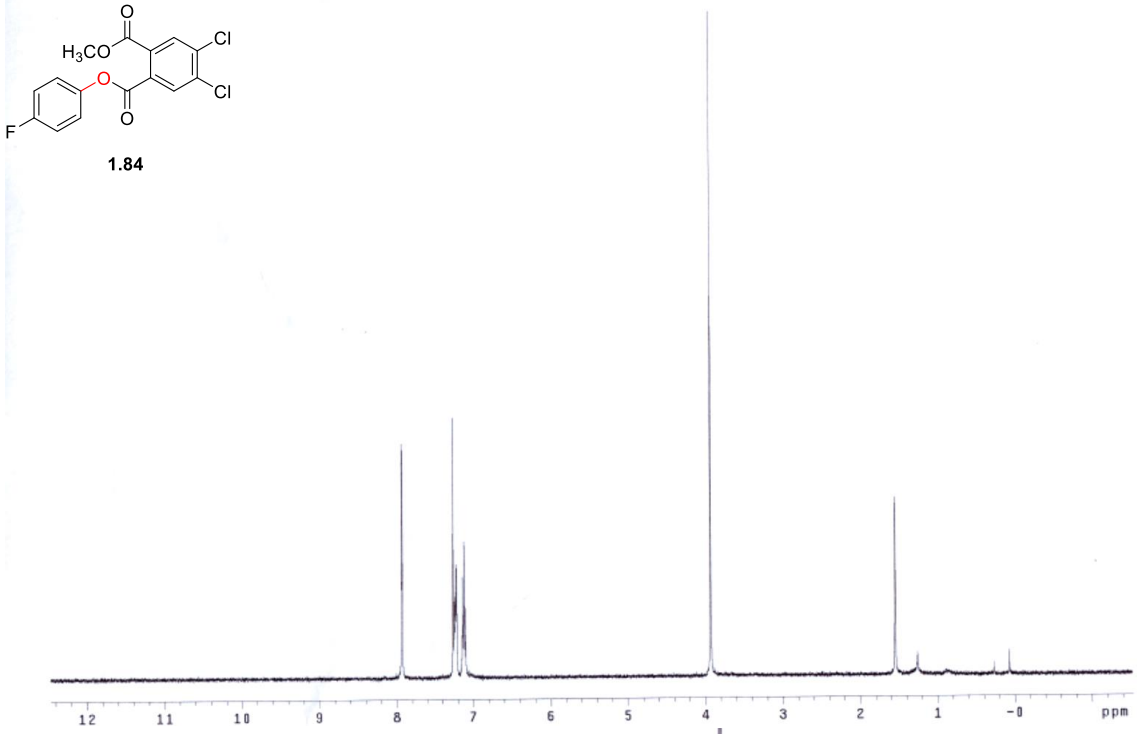
12
11
10
9
8
7
6
5
4
3
2
1
-0
ppm

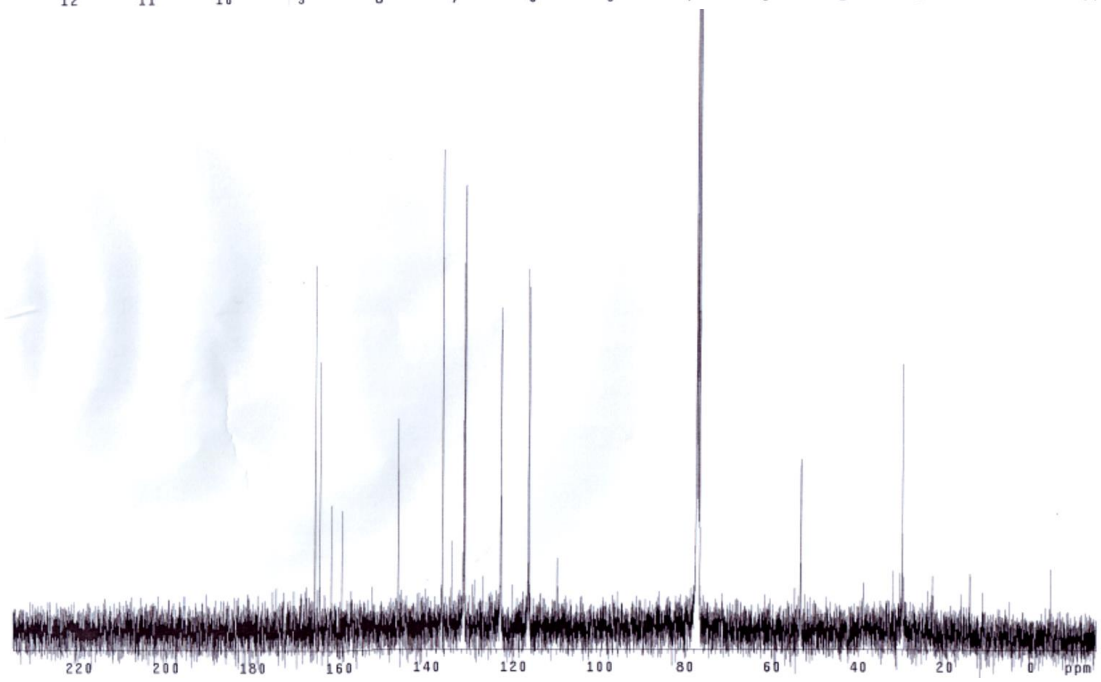
220
200
180
160
140
120
100
80
60
40
20
0
ppm

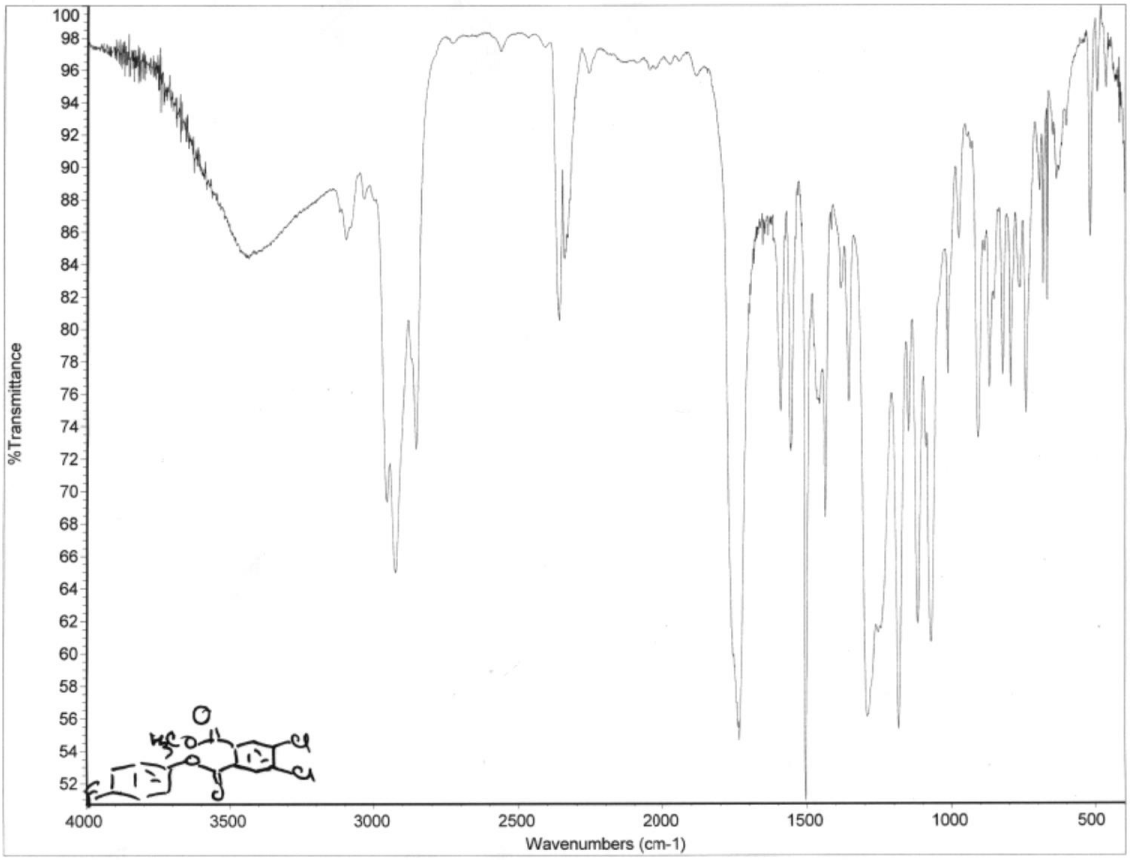
%Transmittance
100
98
96
94
92
90
88
86
84
82
80
78
76
74
72
70
68
66
64
62
60
58
56
54
52
4000
3500
3000
2500
2000
1500
1000
500
Wavenumbers (cm-1)

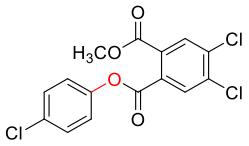
O
H3CO
Cl
O
Cl
O
Cl

1.85

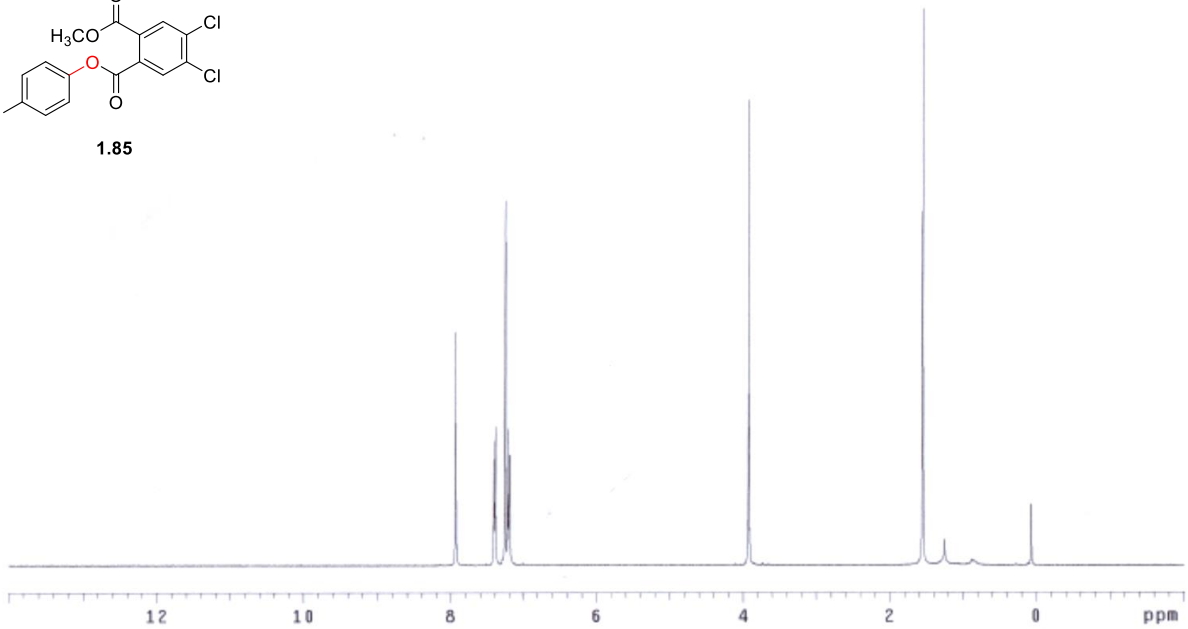
12
10
8
6
4
2
0
ppm

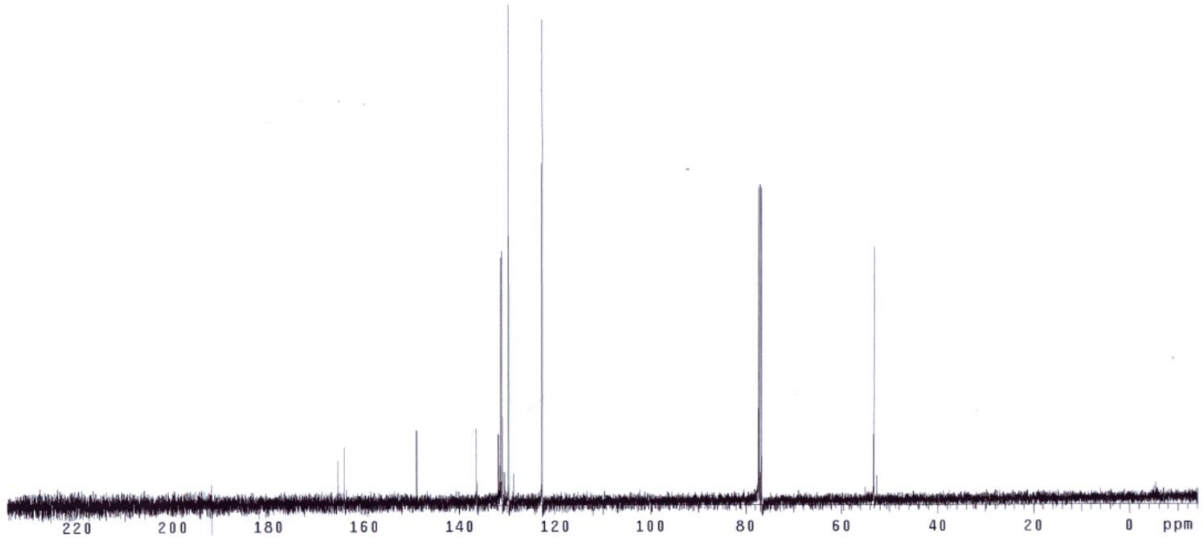
220
200
180
160
140
120
100
80
60
40
20
0
ppm

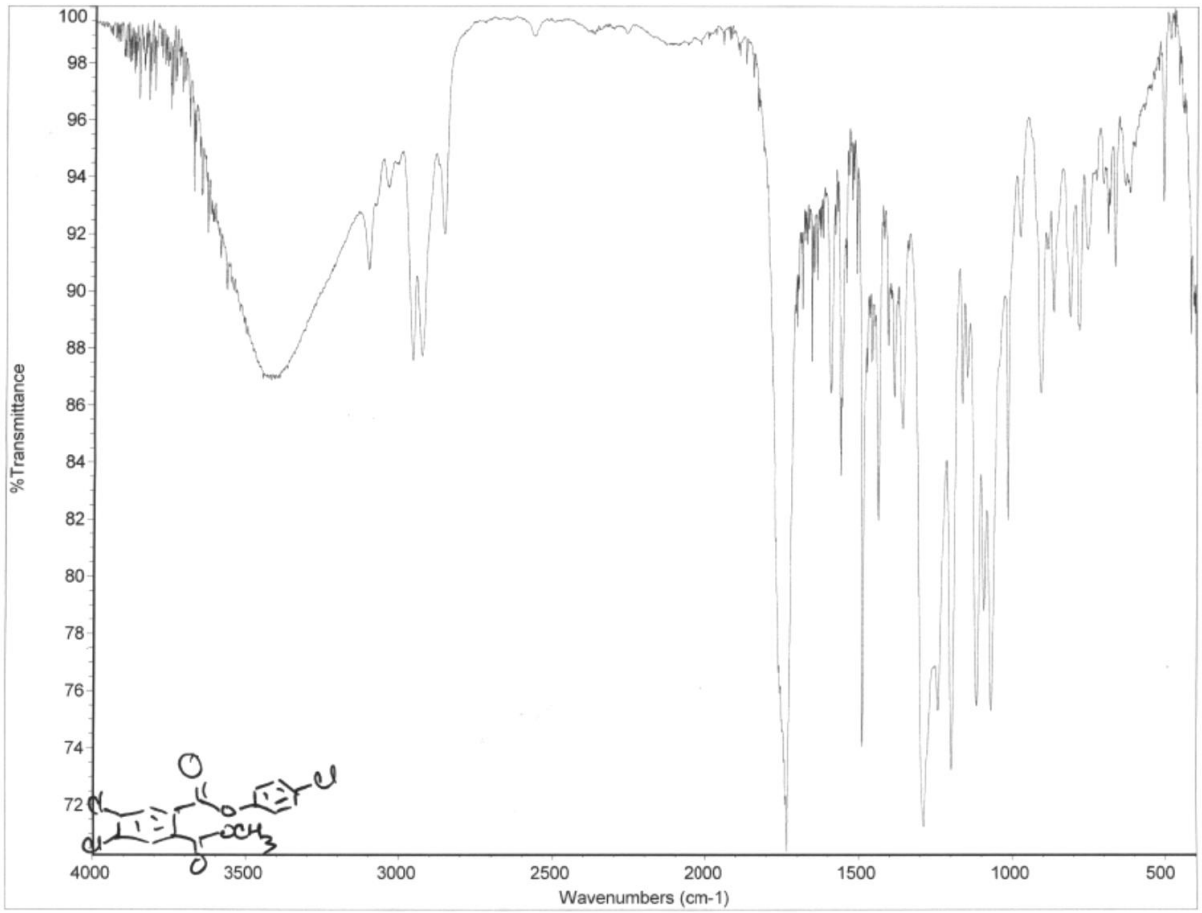
100
98
96
94
92
90
88
86
84
82
80
78
76
74
72
%Transmittance
4000
3500
3000
2500
2000
1500
1000
500
Wavenumbers (cm-1)

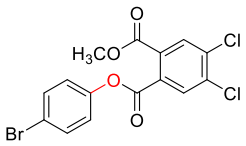
O
H3CO
Cl
O
Cl
O
Br

1.86

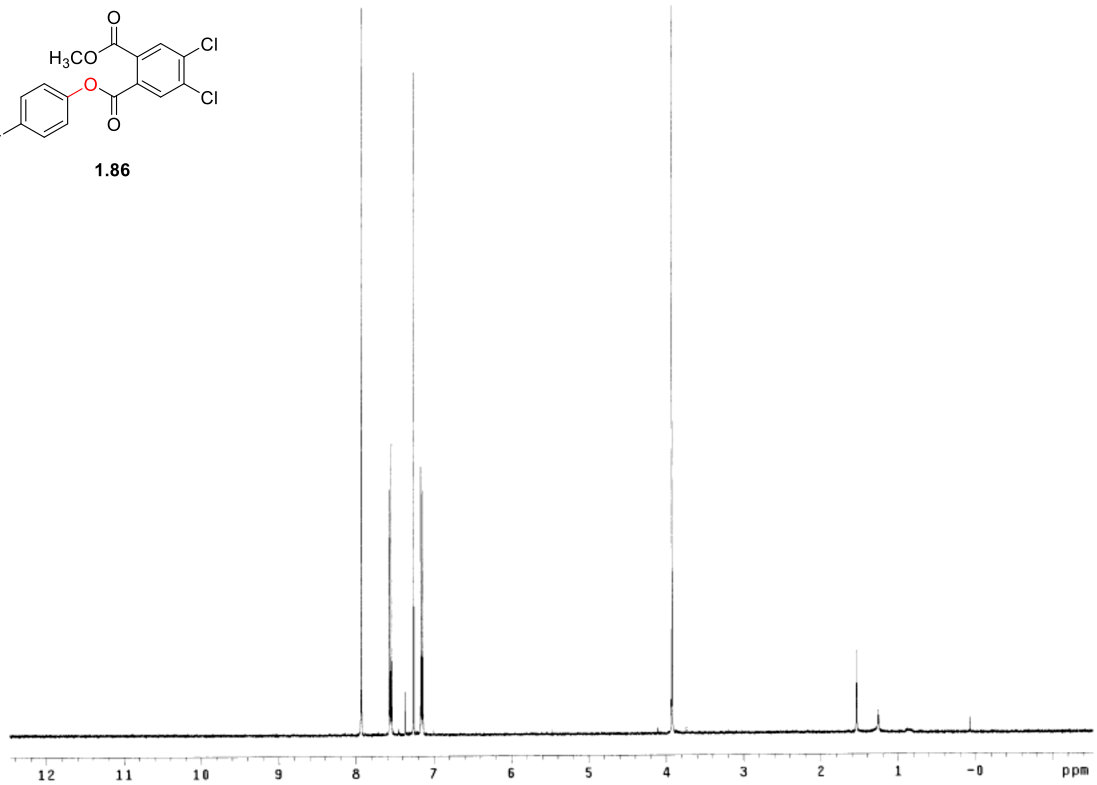
12
11
10
9
8
7
6
5
4
3
2
1
-0
ppm

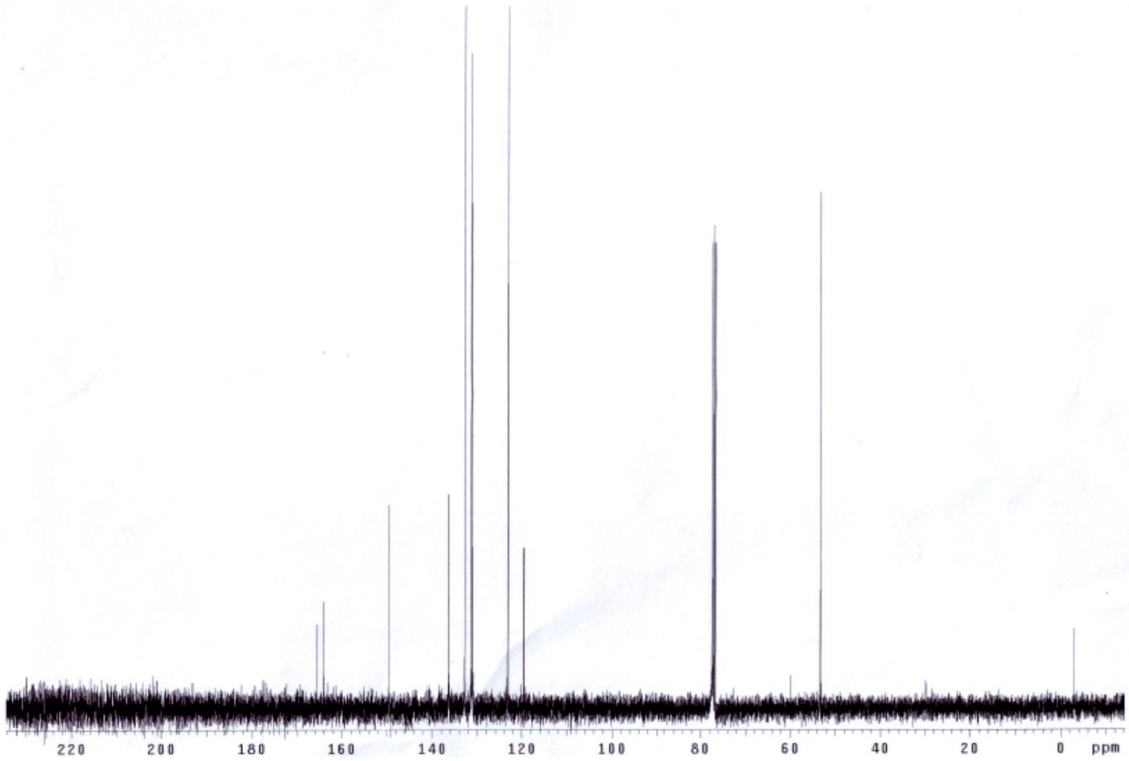
220
200
180
160
140
120
100
80
60
40
20
0
ppm

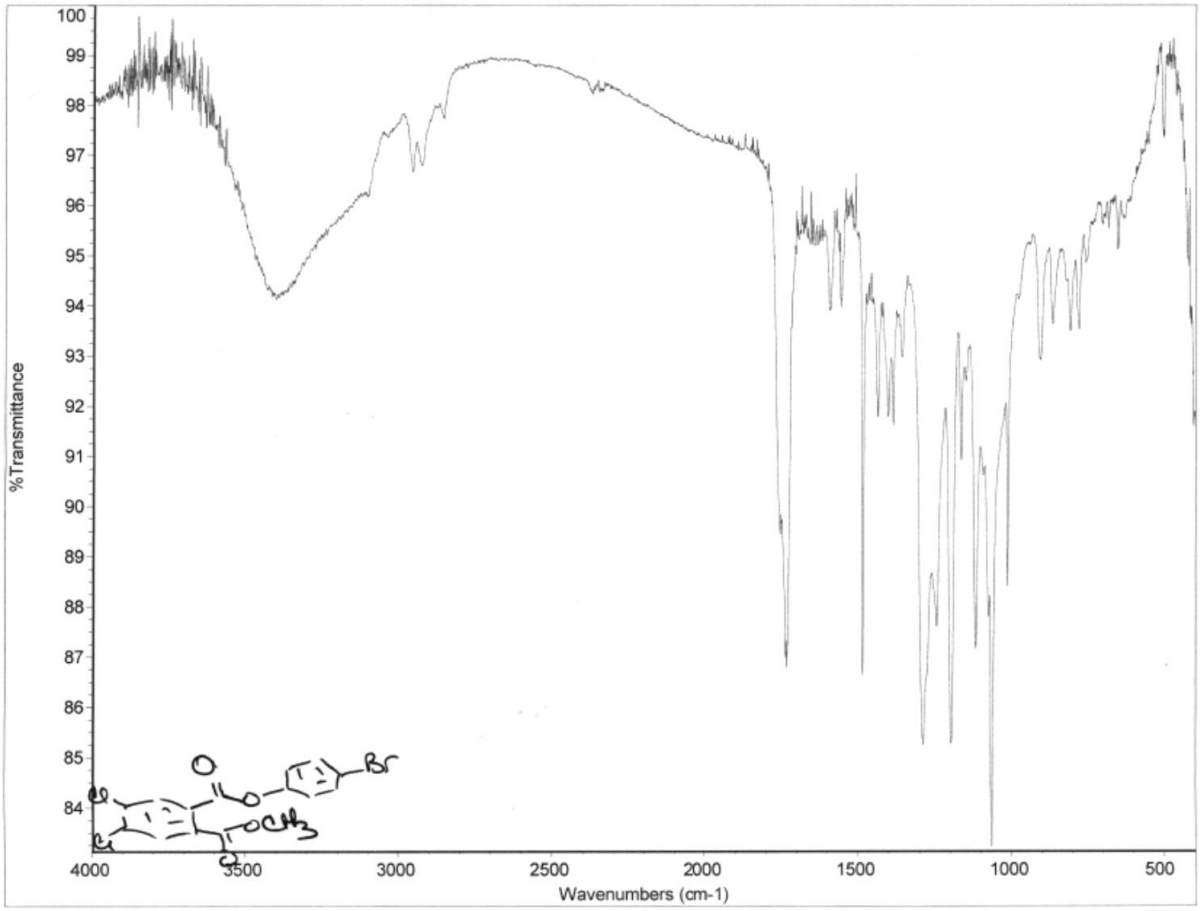
%Transmittance
100
99
98
97
96
95
94
93
92
91
90
89
88
87
86
85
84
4000
3500
3000
2500
2000
1500
1000
500
Wavenumbers (cm-1)

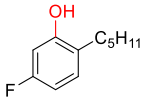
OH
C_5H_{11}
F

1.103a

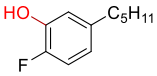
HO
C_5H_{11}
F

1.103b

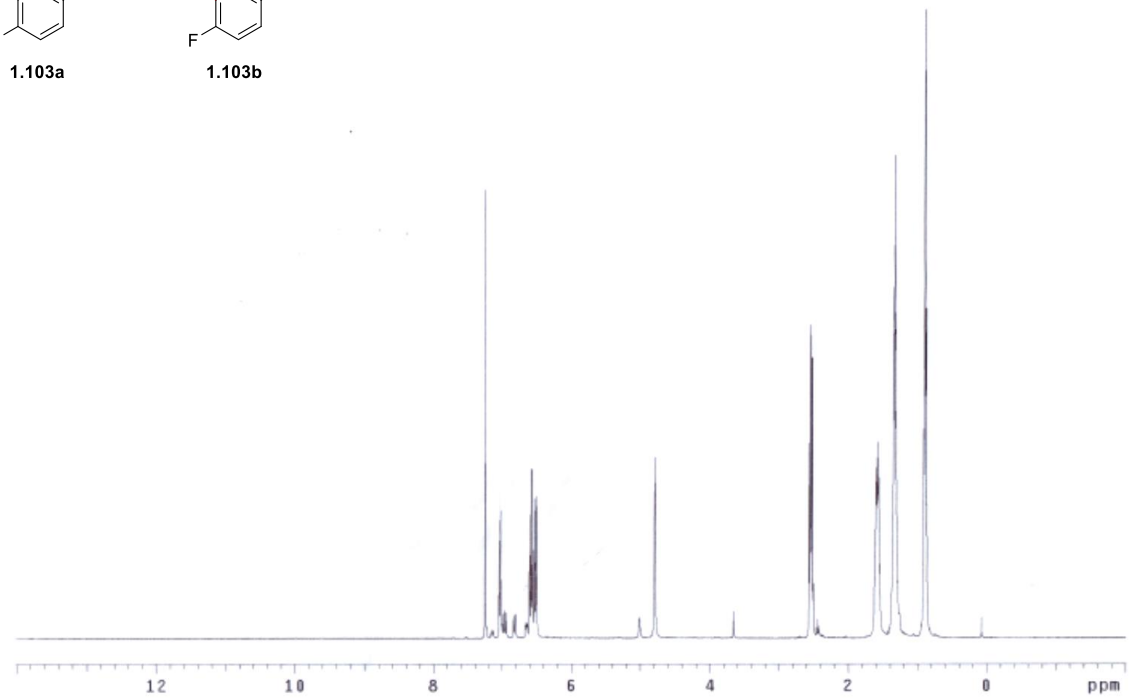
12
10
8
6
4
2
0
ppm

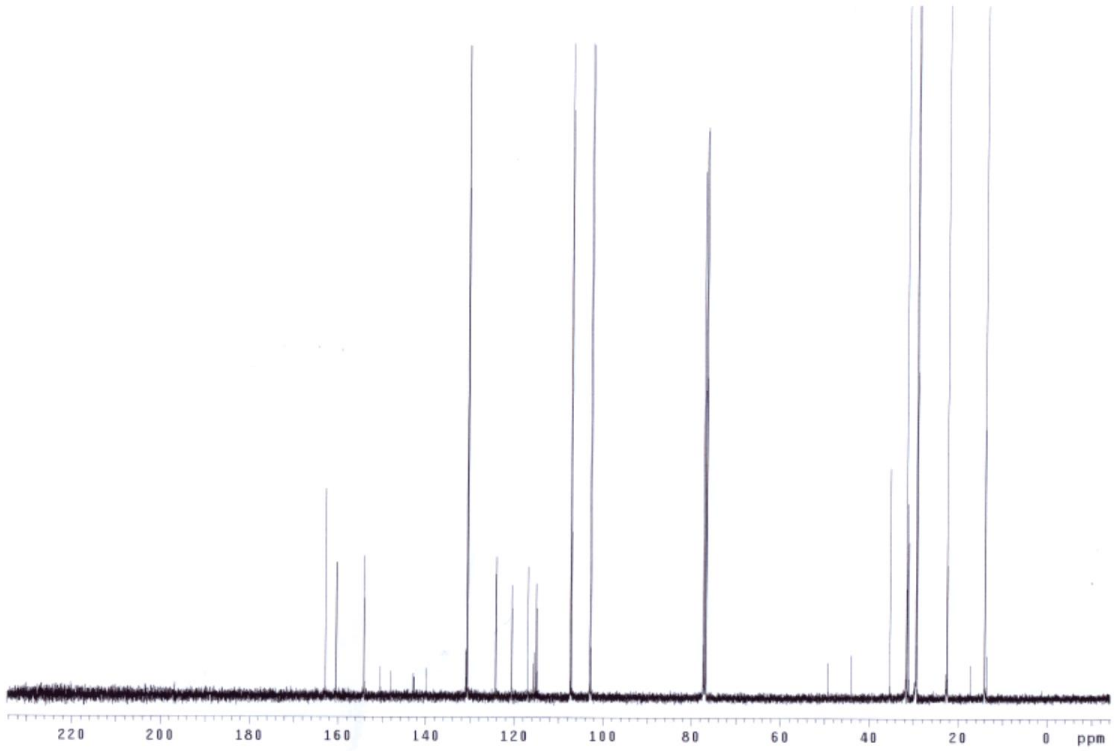
220
200
180
160
140
120
100
80
60
40
20
0
ppm

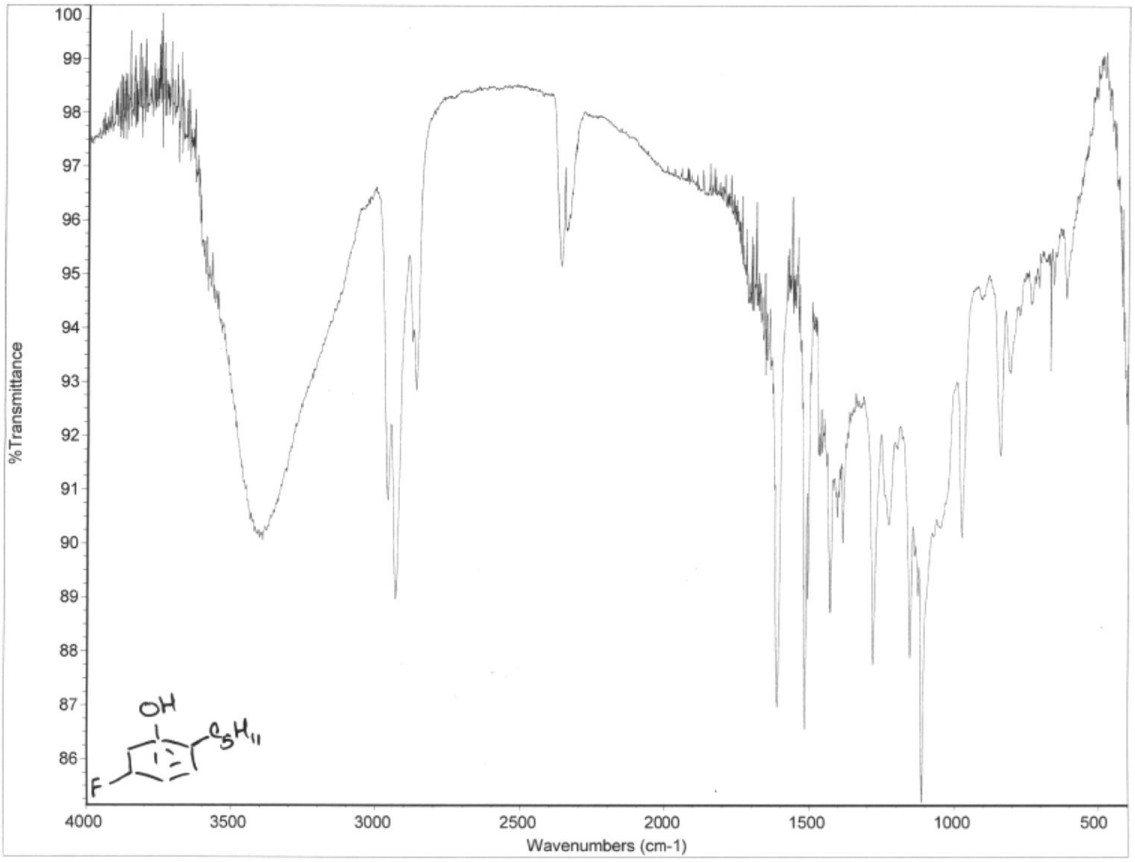
%Transmittance
100
99
98
97
96
95
94
93
92
91
90
89
88
87
86
4000
3500
3000
2500
2000
1500
1000
500
Wavenumbers (cm-1)
OH
C5H11
F

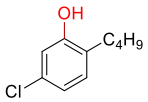
OH
C4H9
Cl

1.104a

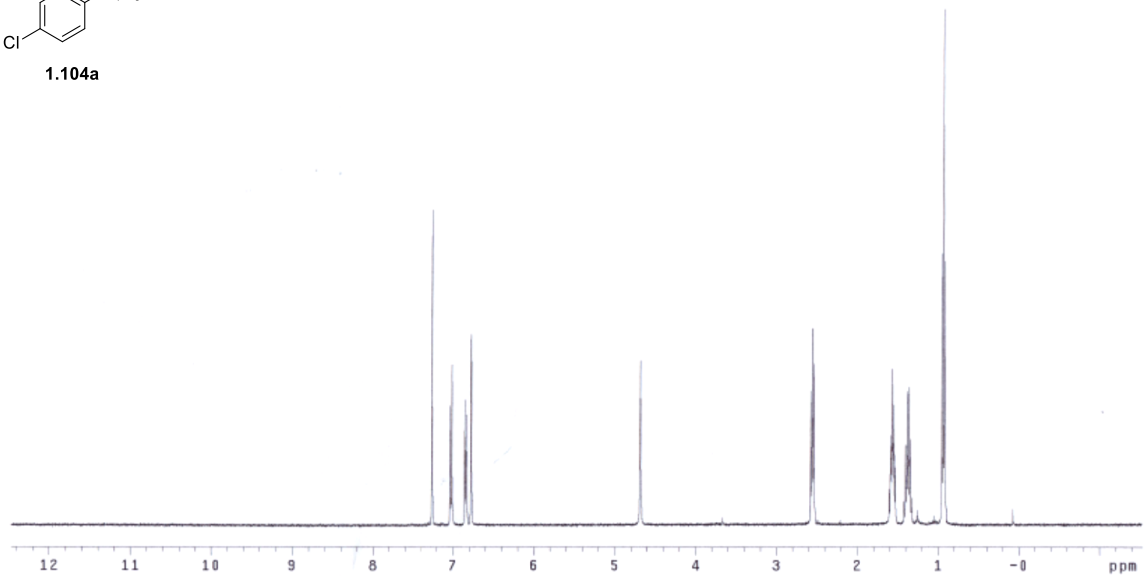
12
11
10
9
8
7
6
5
4
3
2
1
-0
ppm

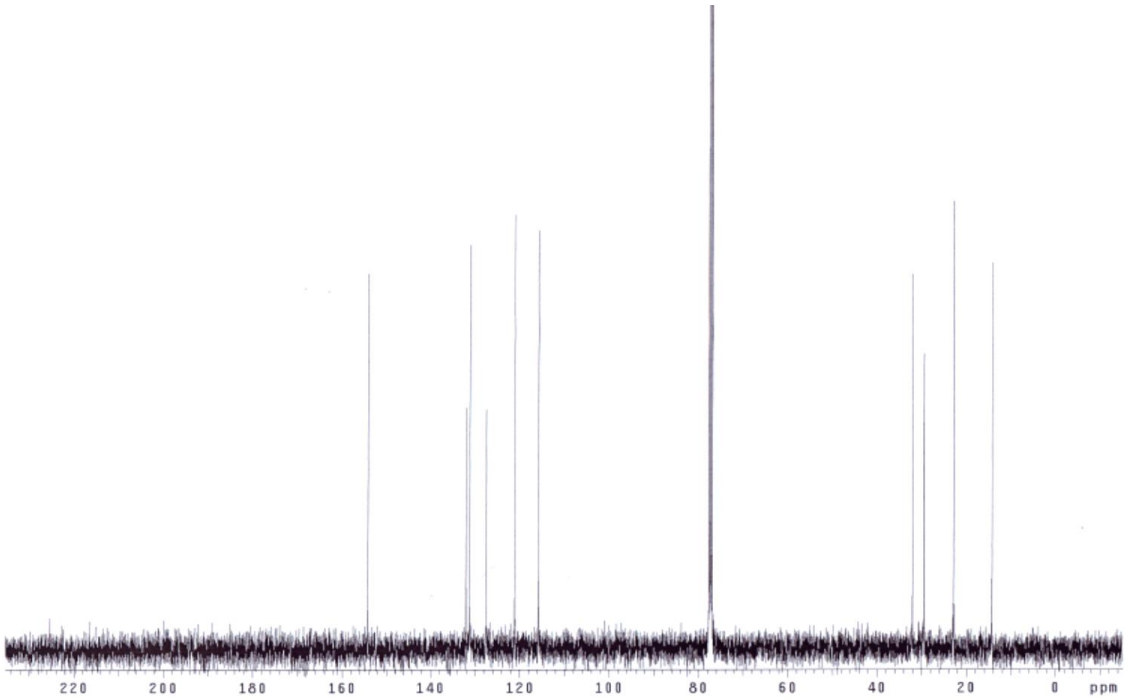
220
200
180
160
140
120
100
80
60
40
20
0
ppm

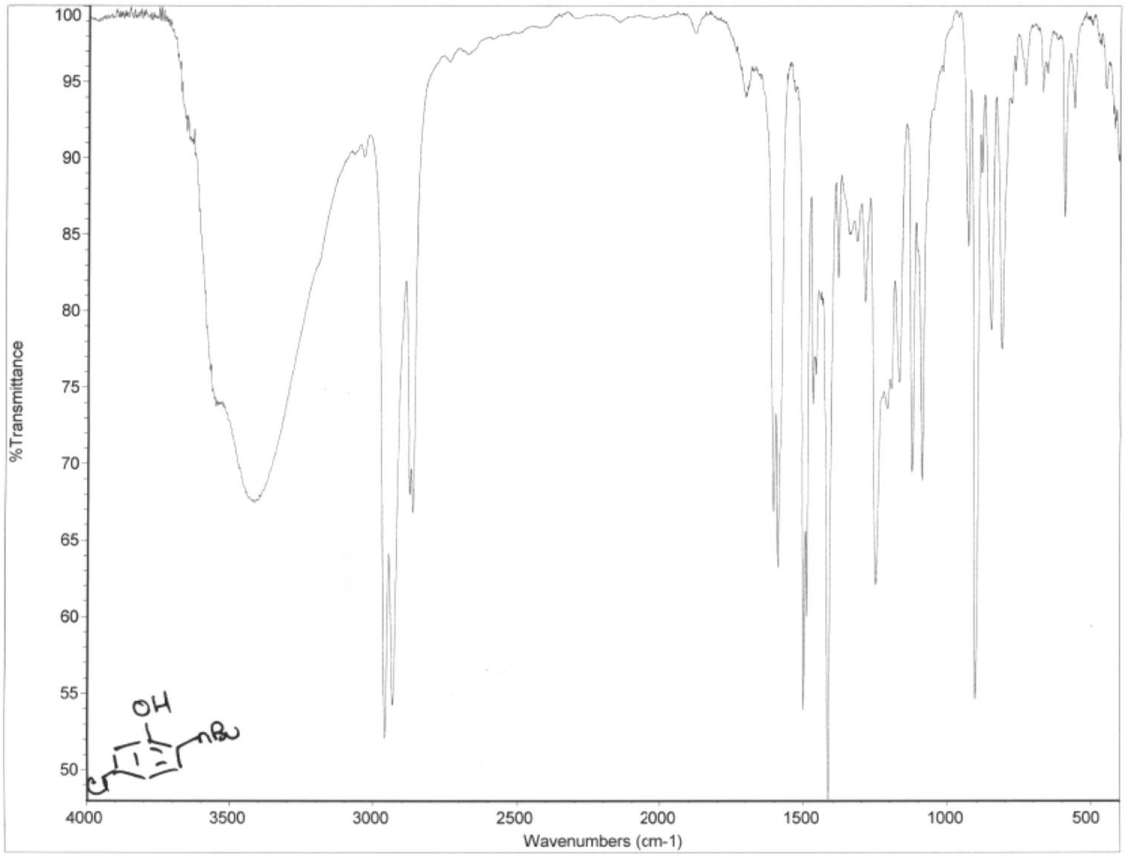
%Transmittance
100
95
90
85
80
75
70
65
60
55
50
4000
3500
3000
2500
2000
1500
1000
500
Wavenumbers (cm-1)
OH
nBu

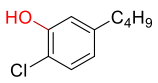
HO
C4H9
Cl

1.104b

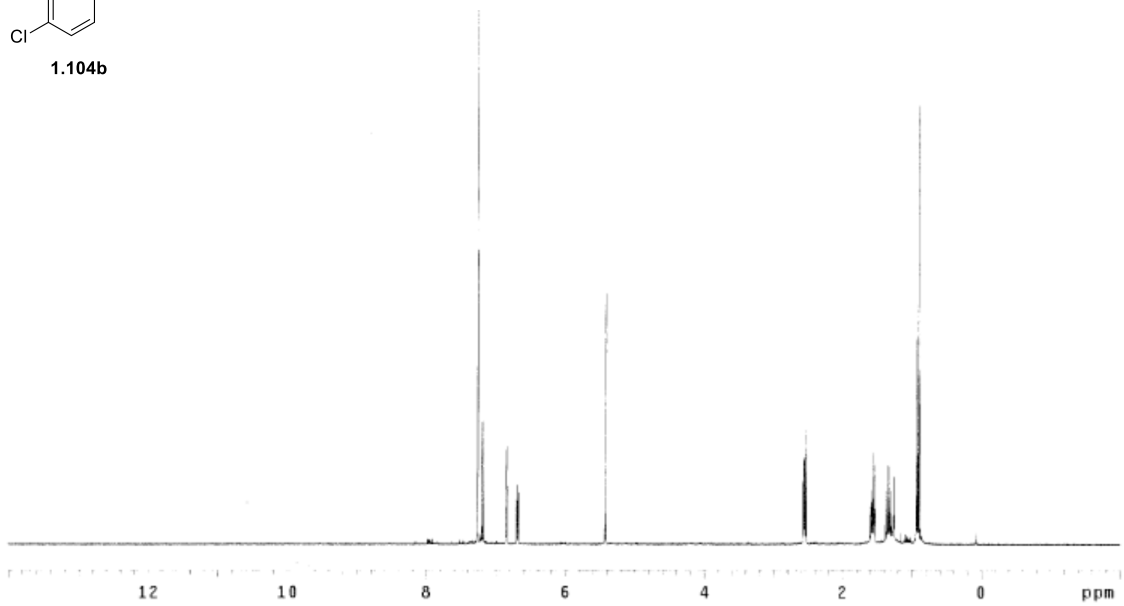
12
10
8
6
4
2
0
ppm

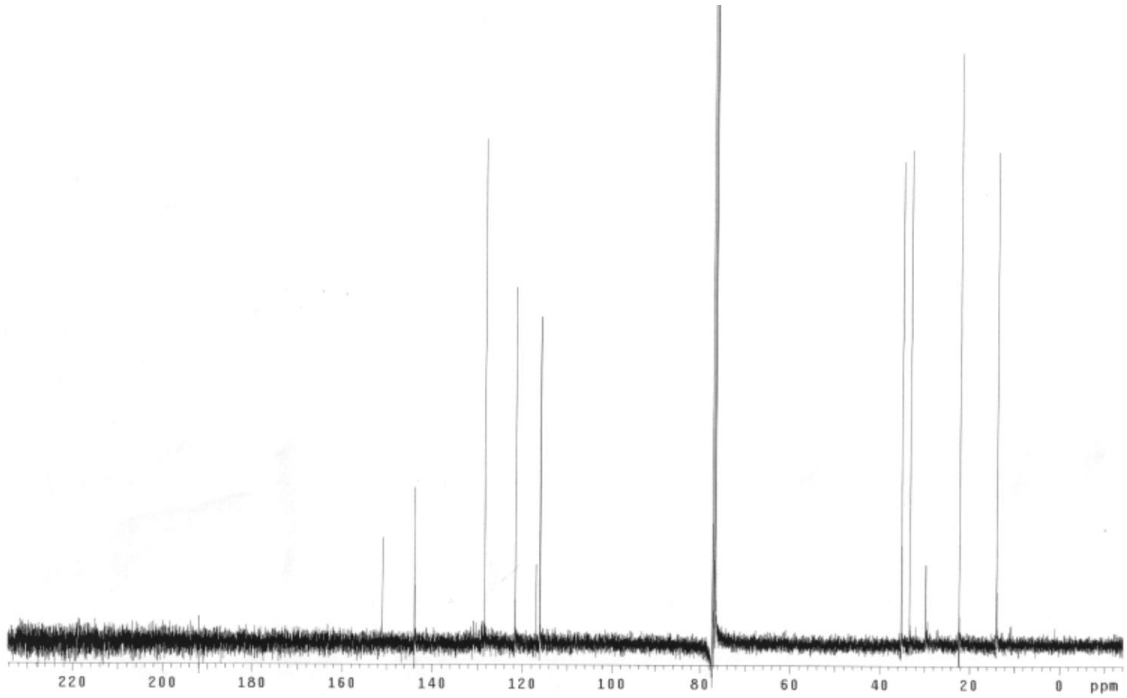
220
200
180
160
140
120
100
80
60
40
20
0
ppm

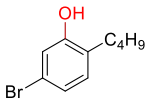
OH
C4H9
Br

1.104a

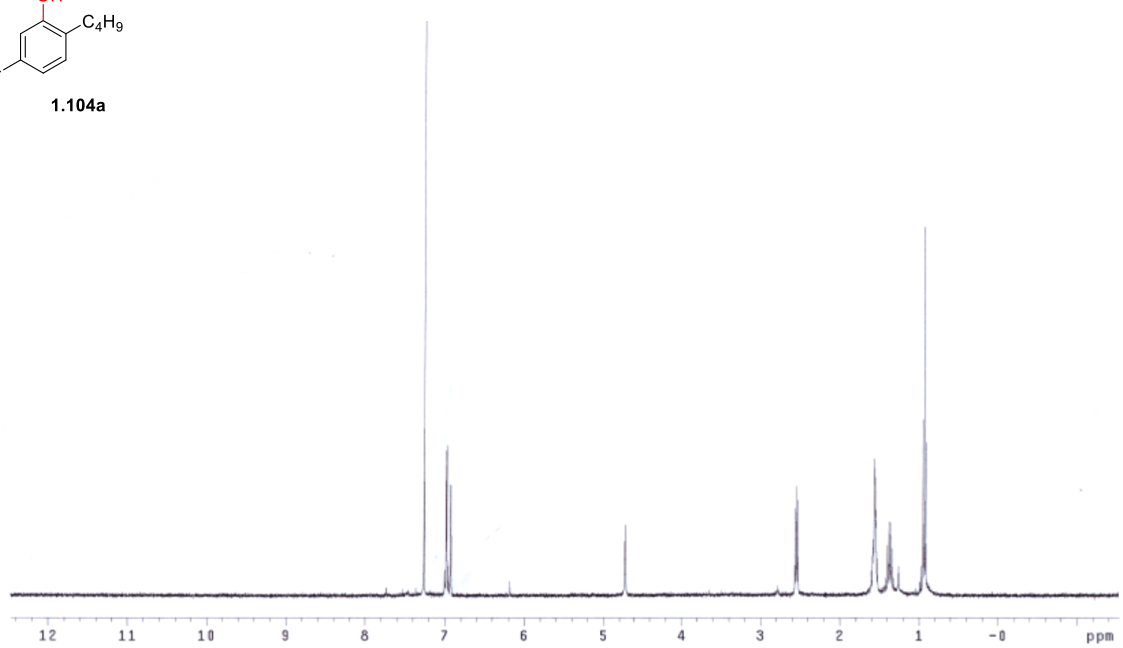
12
11
10
9
8
7
6
5
4
3
2
1
-0
ppm

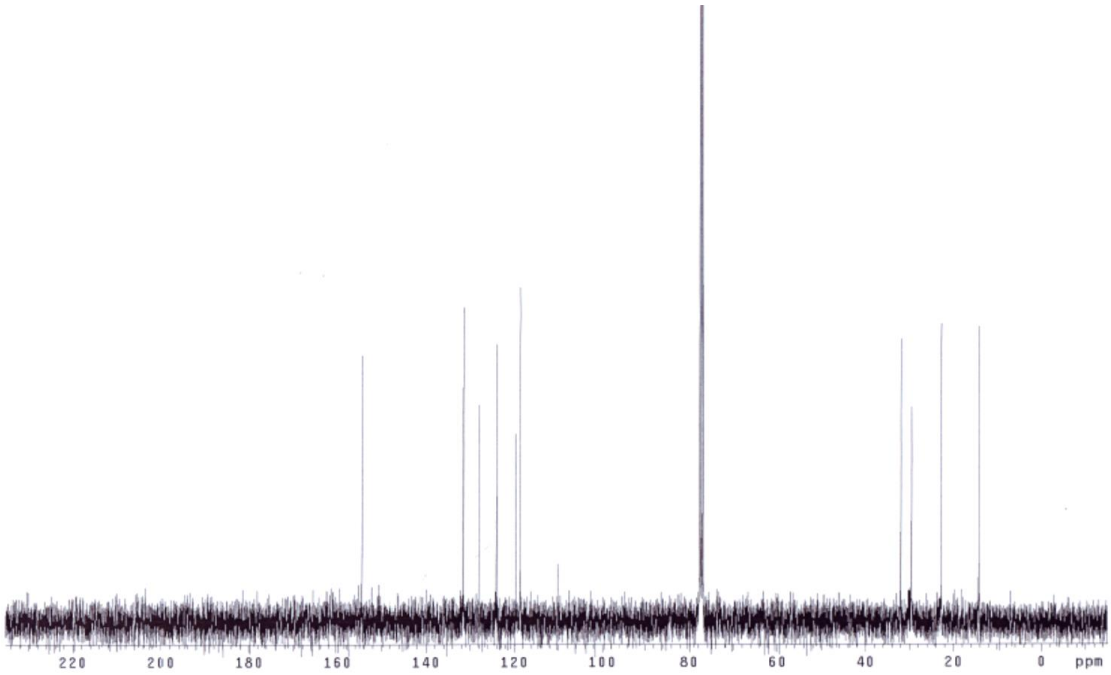
220
200
180
160
140
120
100
80
60
40
20
0
ppm

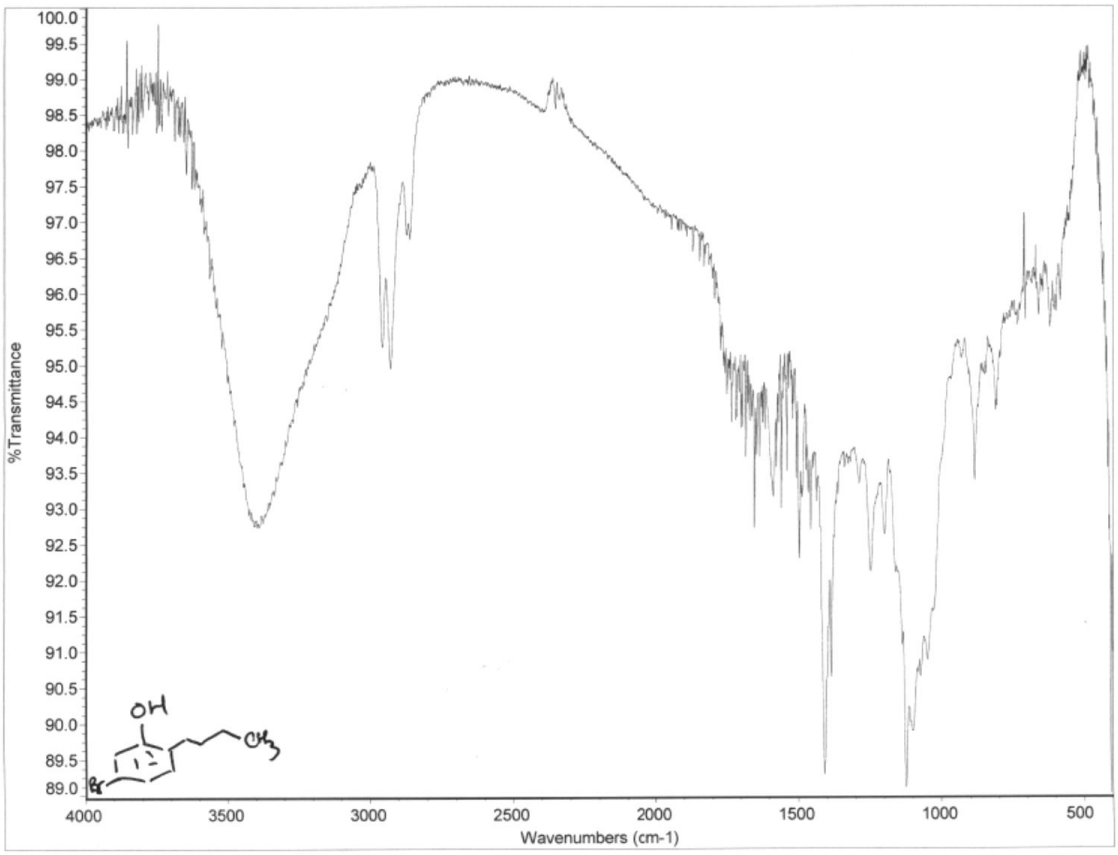
%Transmittance
100.0
99.5
99.0
98.5
98.0
97.5
97.0
96.5
96.0
95.5
95.0
94.5
94.0
93.5
93.0
92.5
92.0
91.5
91.0
90.5
90.0
89.5
89.0
4000
3500
3000
2500
2000
1500
1000
500
Wavenumbers (cm-1)
OH
CH3
Br

INDEX	FREQUENCY	PPM	HEIGHT
1	2799.145	6.983	42.7
2	2790.597	6.962	51.0
3	2742.726	6.852	49.0
4	2740.332	6.846	60.6
5	2724.262	6.806	32.9
6	2721.526	6.799	24.5
7	2715.713	6.785	26.0
8	2712.978	6.778	20.8
9	1661.190	4.150	24.6
10	1655.377	4.136	32.6
11	1605.455	4.011	38.1
12	1598.616	3.994	27.0
13	1468.339	3.668	38.7
14	1126.748	2.815	92.5
15	835.762	2.088	283.4
16	825.504	2.062	170.4
17	823.452	2.057	316.9
18	821.059	2.051	458.3
19	819.007	2.046	318.2
20	816.614	2.040	144.6

1.106

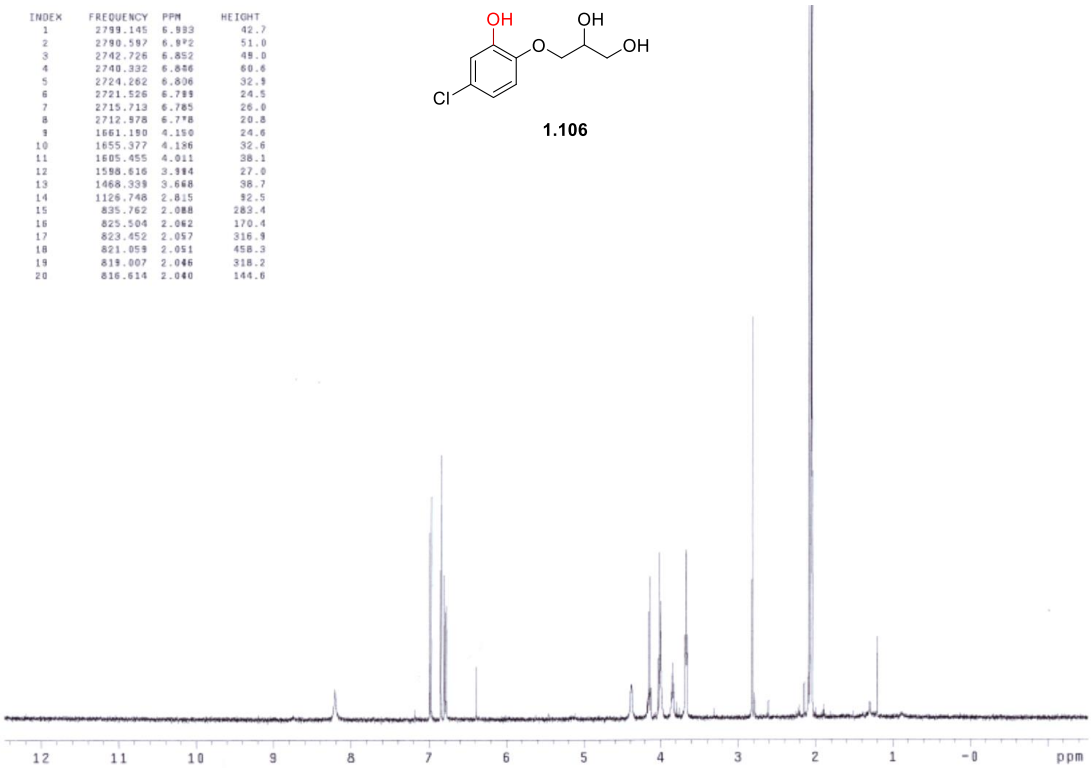

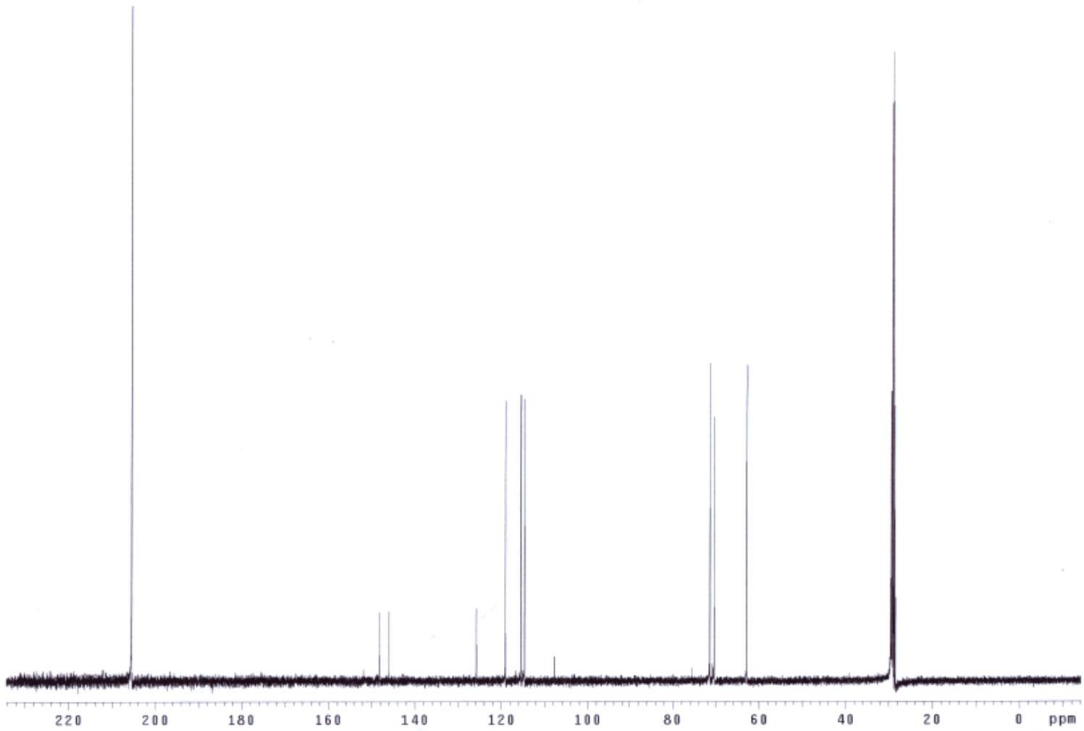

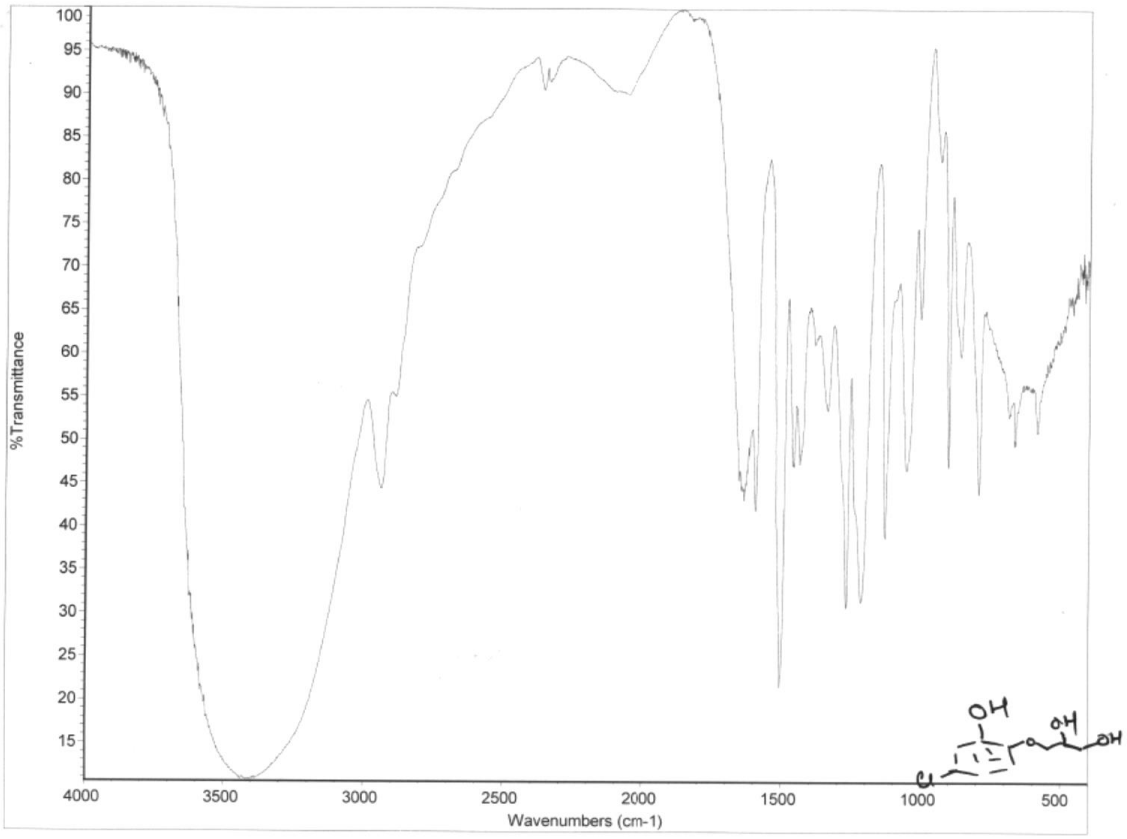
%Transmittance
100
95
90
85
80
75
70
65
60
55
50
45
40
35
30
25
20
15
4000
3500
3000
2500
2000
1500
1000
500
Wavenumbers (cm-1)
OH
OH
OH

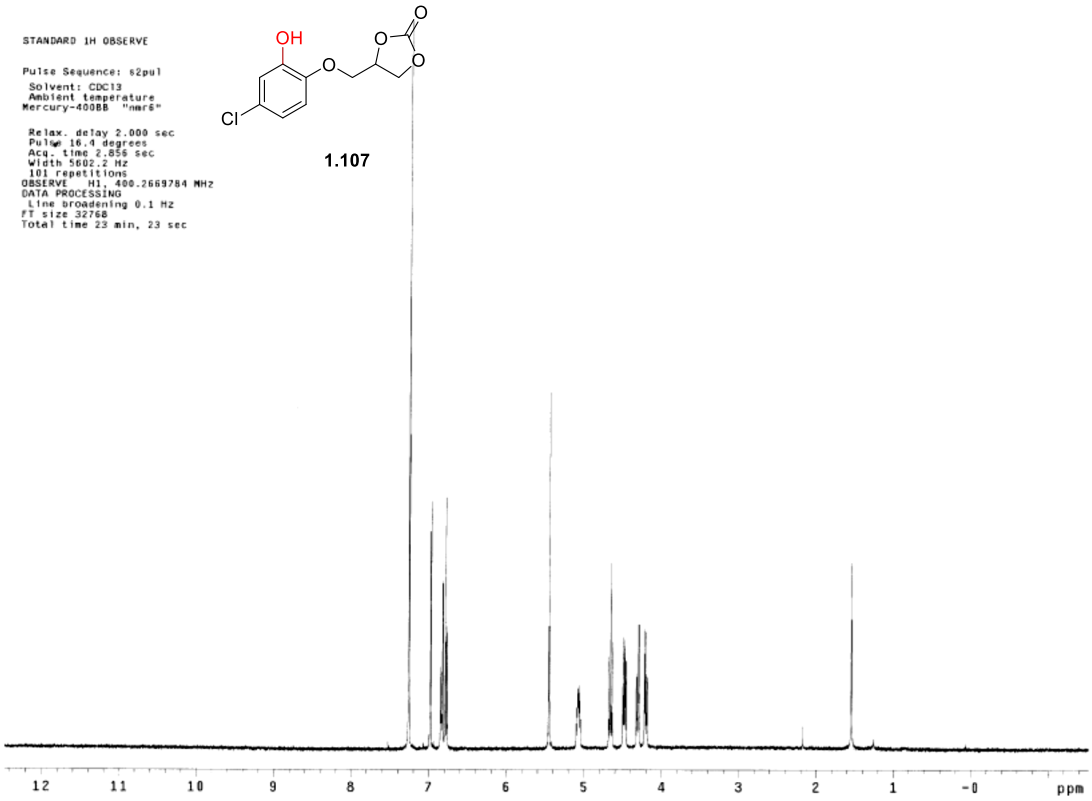
STANDARD 1H OBSERVE
Pulse Sequence: s2pul
Solvent: CDCl3
Ambient temperature
Mercury-400BB "nmr6"
Relax. delay 2.000 sec
Pulse 16.4 degrees
Acq. time 2.856 sec
Width 5602.2 Hz
101 repetitions
OBSERVE H1, 400.2669784 MHz
DATA PROCESSING
Line broadening 0.1 Hz
FT size 32768
Total time 23 min, 23 sec
OH
O
O
O
O
Cl
1.107
12
11
10
9
8
7
6
5
4
3
2
1
-0
ppm

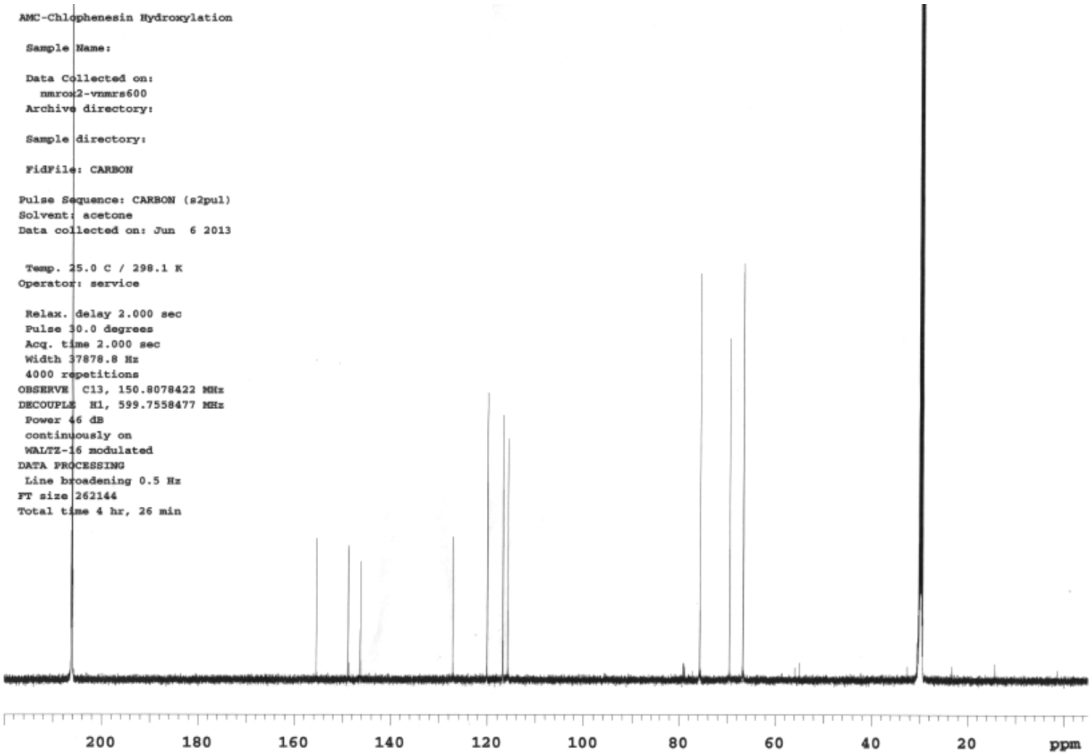
AMC-Chlophenesin Hydroxylation
Sample Name:
Data Collected on:
nmrox2-vnmrs600
Archive directory:
Sample directory:
FidFile: CARBON
Pulse Sequence: CARBON (s2pul)
Solvent: acetone
Data collected on: Jun 6 2013
Temp. 25.0 C / 298.1 K
Operator: service
Relax. delay 2.000 sec
Pulse 30.0 degrees
Acq. time 2.000 sec
Width 37878.8 Hz
4000 repetitions
OBSERVE C13, 150.8078422 MHz
DECOUPLE H1, 599.7558477 MHz
Power 46 dB
continuously on
WALTZ-16 modulated
DATA PROCESSING
Line broadening 0.5 Hz
FT size 262144
Total time 4 hr, 26 min
200
180
160
140
120
100
80
60
40
20
ppm

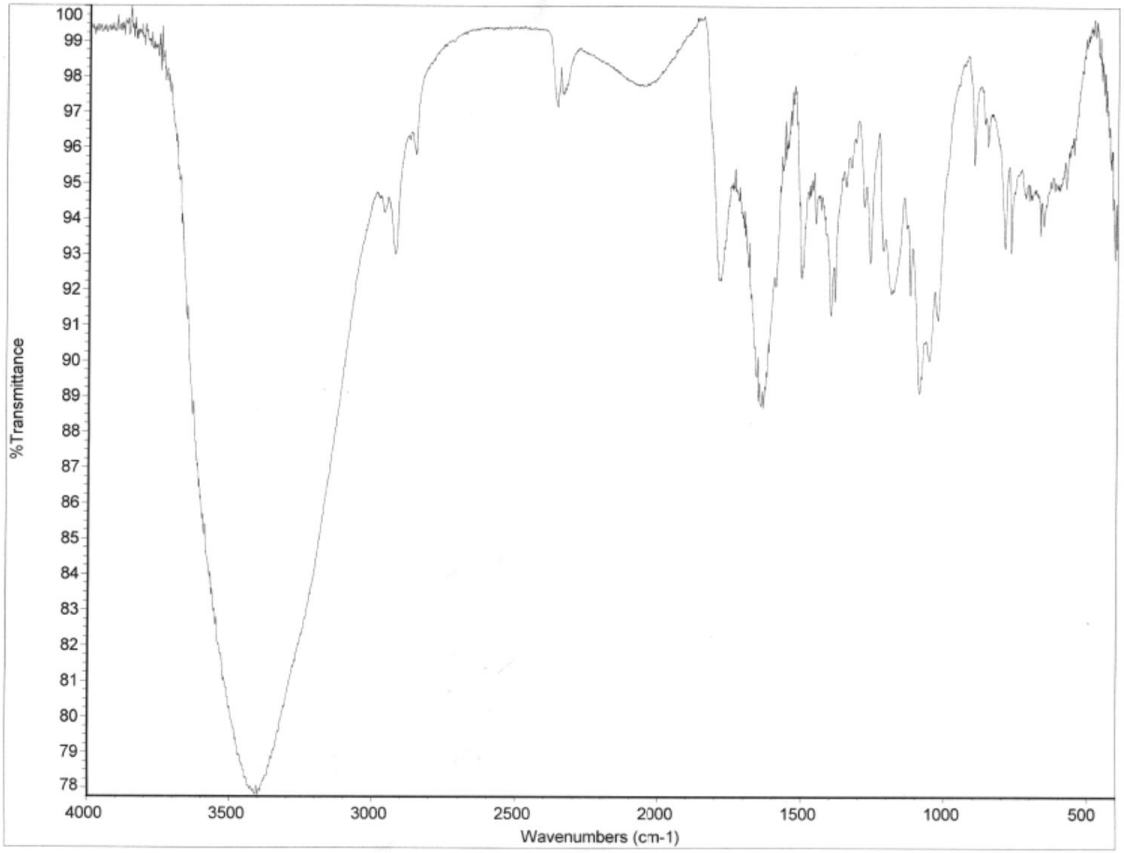
%Transmittance
100
99
98
97
96
95
94
93
92
91
90
89
88
87
86
85
84
83
82
81
80
79
78
4000
3500
3000
2500
2000
1500
1000
500
Wavenumbers (cm-1)

INDEX	FREQUENCY	PPM	HEIGHT
1	2760.506	6.897	53.0
2	2751.958	6.875	69.0
3	2723.236	6.804	65.3
4	2720.500	6.797	80.0
5	2705.797	6.760	49.8
6	2703.404	6.754	36.6
7	2697.249	6.739	35.2
8	2694.855	6.733	27.8
9	1939.524	4.846	2162.2
10	1663.925	4.157	130.6
11	1660.848	4.149	28.5
12	1633.151	4.080	20.1
13	1621.867	4.052	26.6
14	1600.326	3.998	26.4
15	1594.171	3.983	20.6
16	1325.753	3.312	668.7
17	1324.043	3.308	1274.3
18	1322.334	3.304	1733.3
19	1320.966	3.300	1157.7
20	1319.256	3.296	606.7

1.108

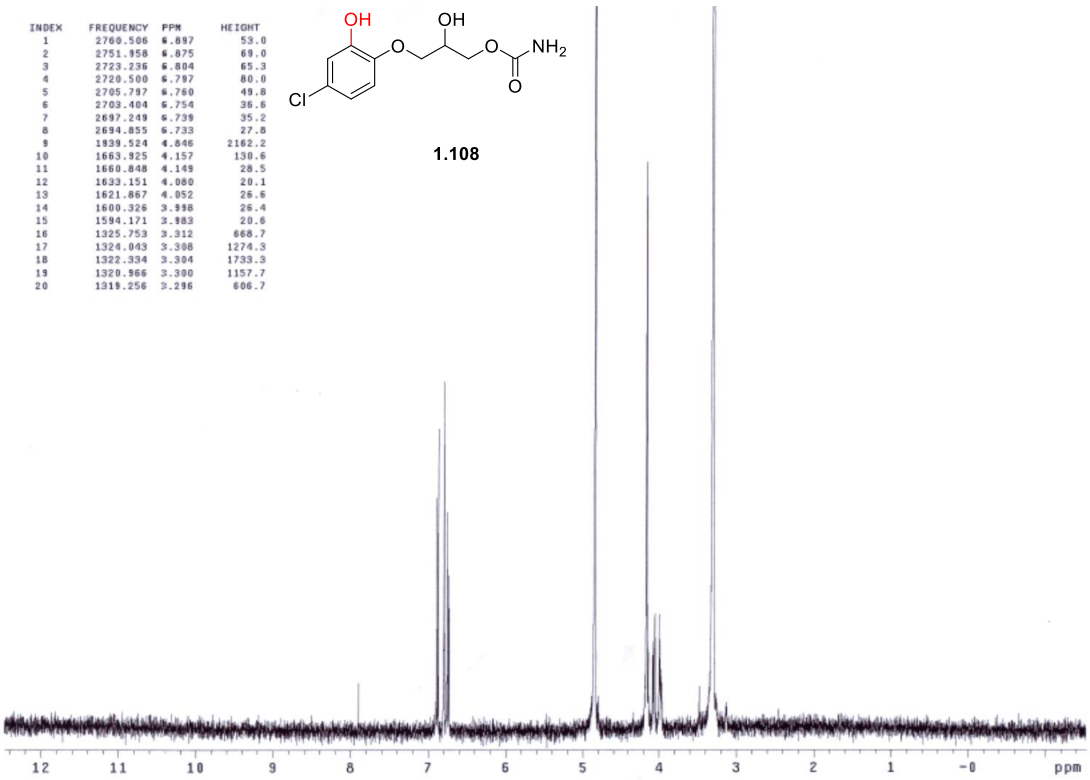

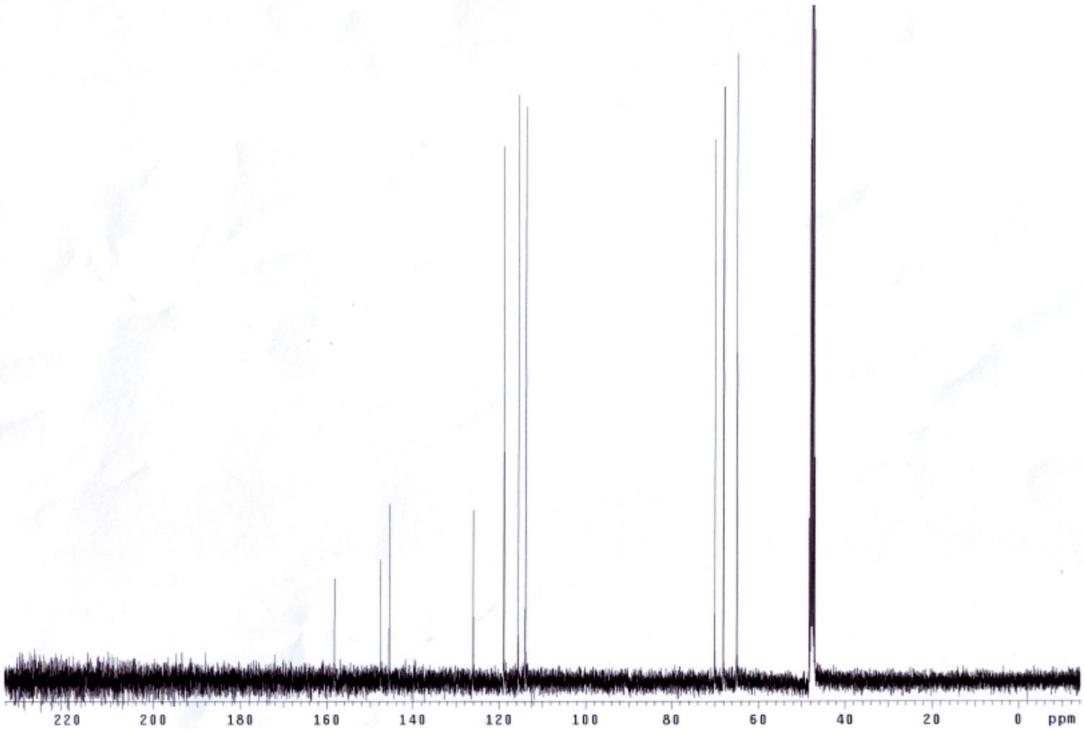

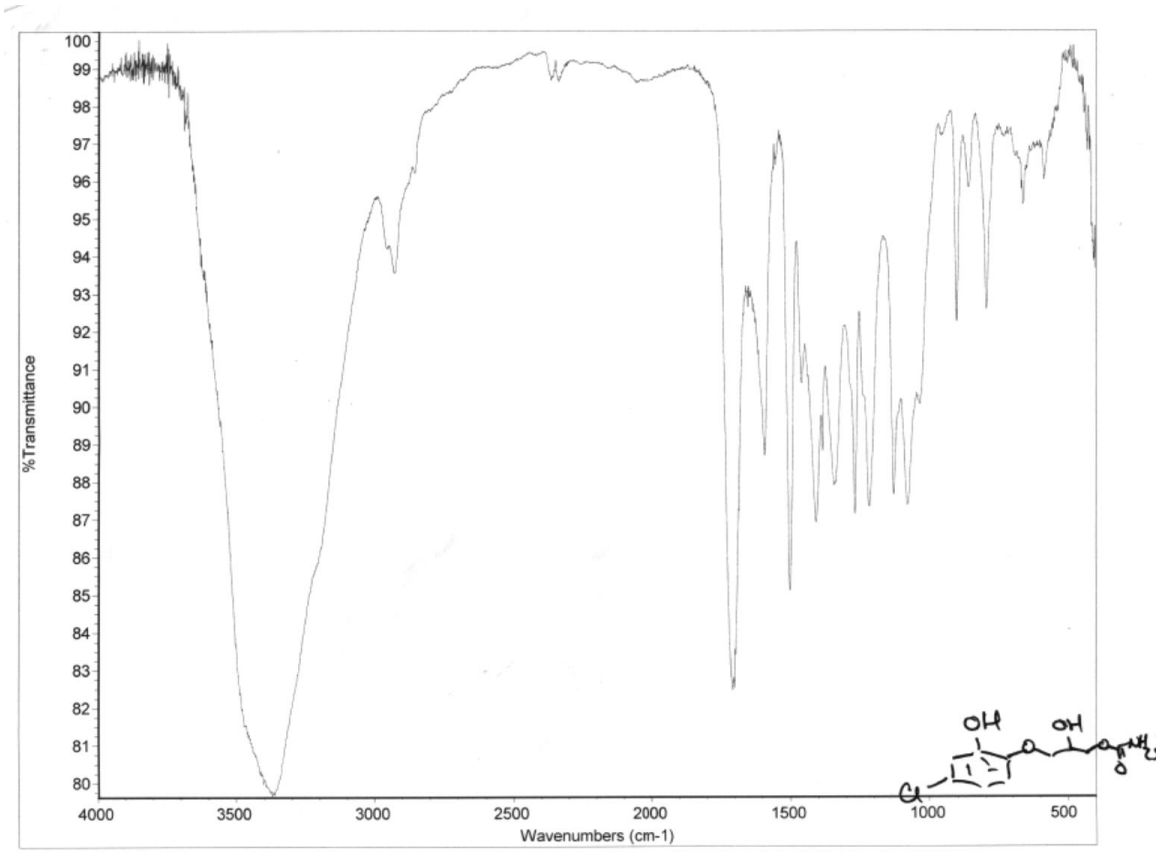
%Transmittance
100
99
98
97
96
95
94
93
92
91
90
89
88
87
86
85
84
83
82
81
80
4000
3500
3000
2500
2000
1500
1000
500
Wavenumbers (cm-1)
OH
OH
Cl

OMe
Me
HO
O
N
O
Me
OMe

1.109

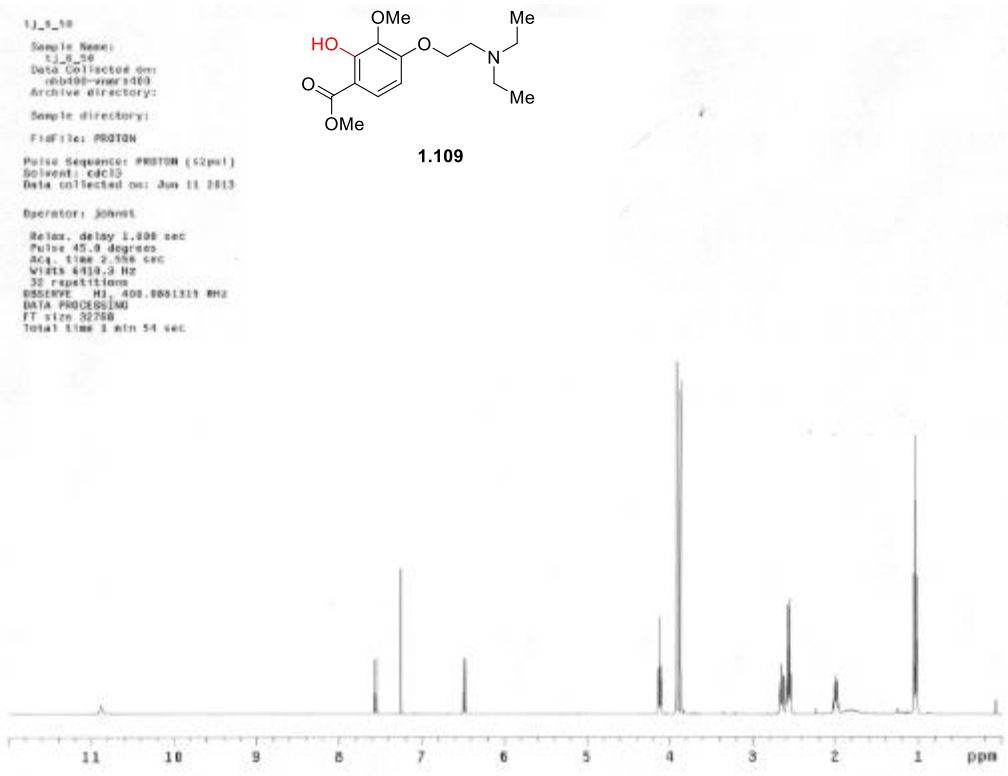
11
10
9
8
7
6
5
4
3
2
1
ppm

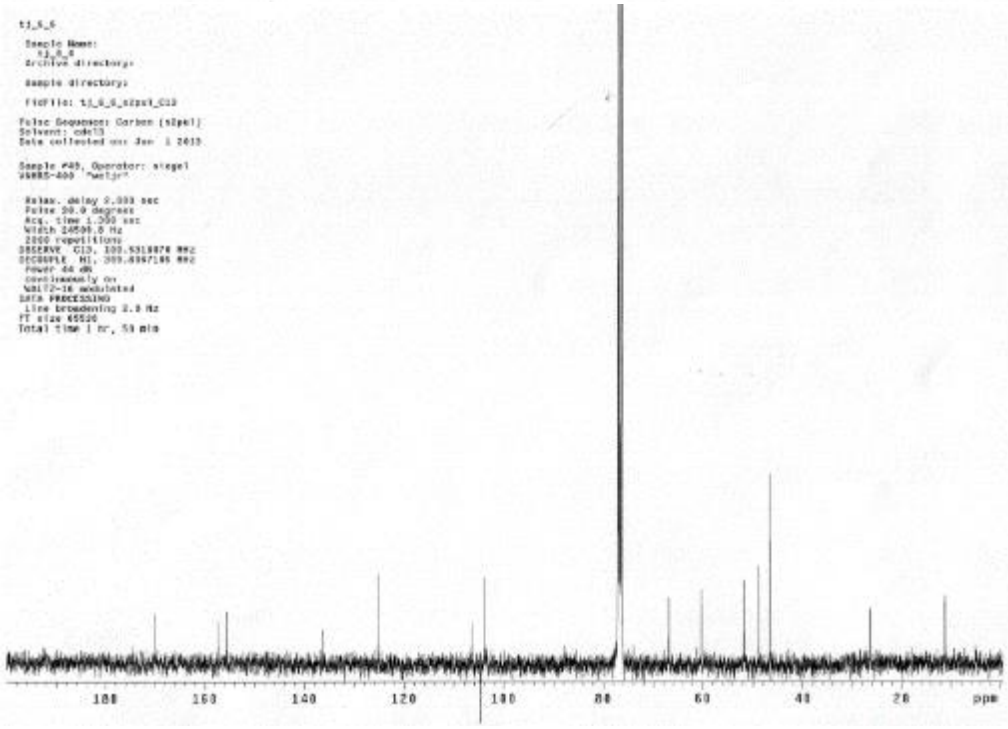
180
160
140
120
100
80
60
40
20
ppm

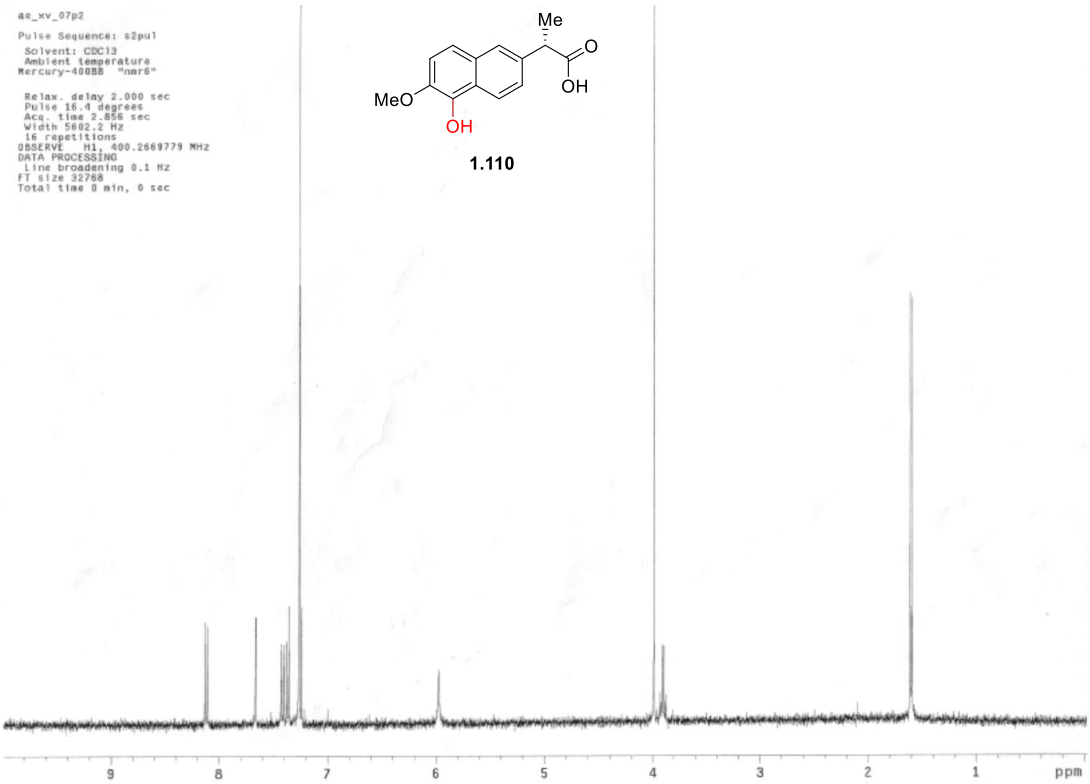
ae_xv_07p2
Pulse Sequence: s2pul
Solvent: CDCl3
Ambient temperature
Mercury-400BB "nmr6"
Relax. delay 2.000 sec
Pulse 16.4 degrees
Acq. time 2.856 sec
Width 5602.2 Hz
16 repetitions
OBSERVE H1, 400.2669779 MHz
DATA PROCESSING
Line broadening 0.1 Hz
FT size 32768
Total time 0 min, 0 sec
Me
O
OH
MeO
OH
1.110
9
8
7
6
5
4
3
2
1
ppm

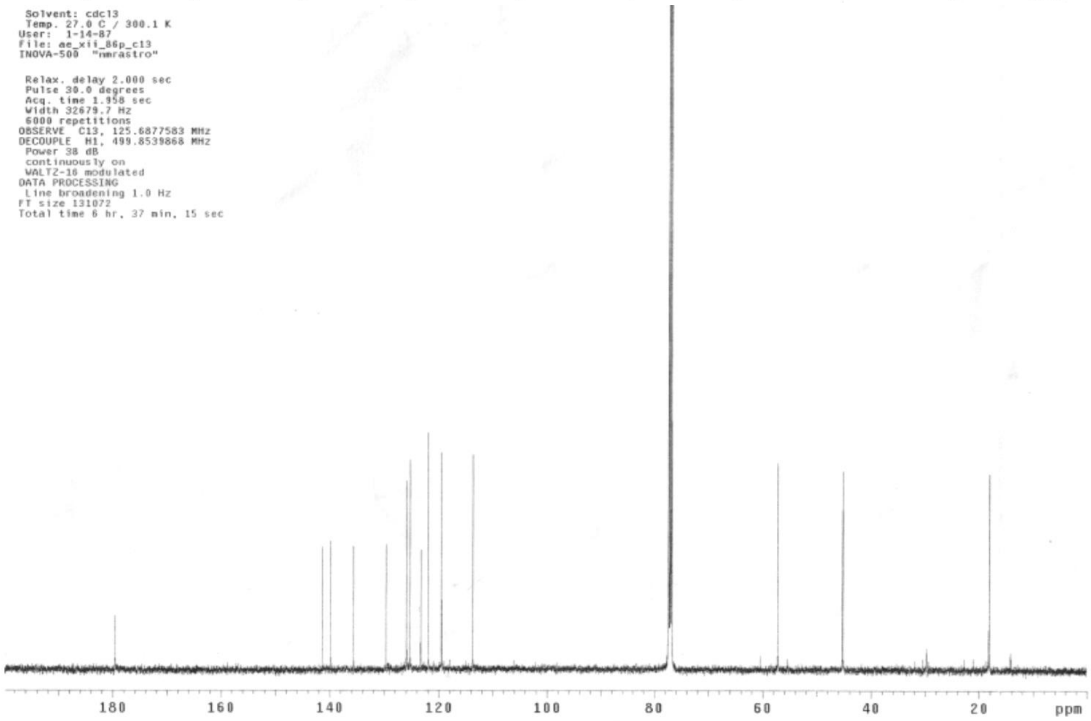
Solvent: cdcl3
Temp. 27.0 C / 300.1 K
User: 1-14-87
File: ae_xii_86p_c13
INOVA-500 "nmrastro"
Relax. delay 2.000 sec
Pulse 30.0 degrees
Acq. time 1.958 sec
Width 32679.7 Hz
6000 repetitions
OBSERVE C13, 125.6877583 MHz
DECOUPLE H1, 499.8539868 MHz
Power 38 dB
continuously on
WALTZ-16 modulated
DATA PROCESSING
Line broadening 1.0 Hz
FT size 131072
Total time 6 hr, 37 min, 15 sec
180
160
140
120
100
80
60
40
20
ppm

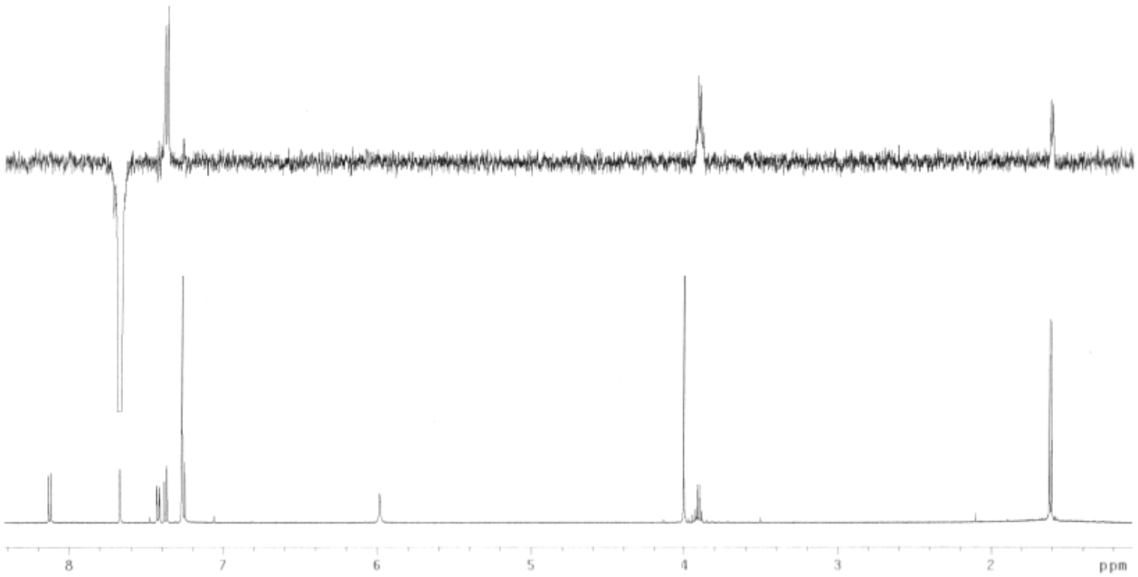
8
7
6
5
4
3
2
ppm

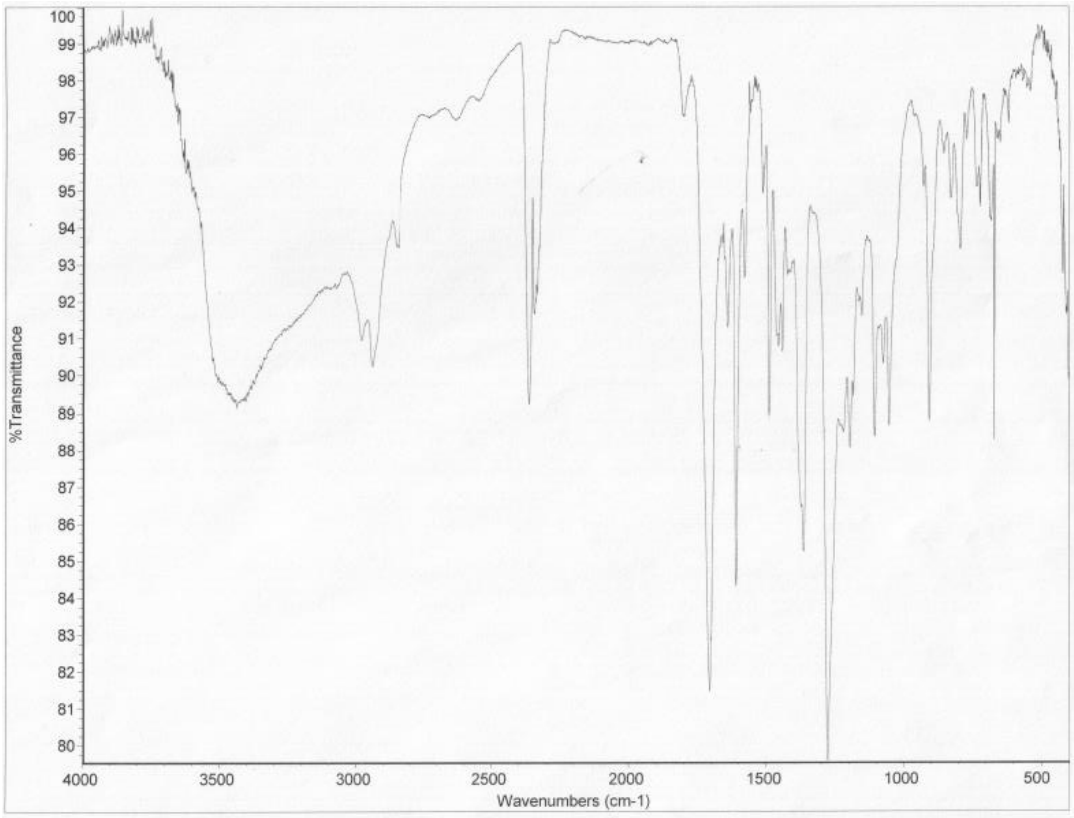
%Transmittance
100
99
98
97
96
95
94
93
92
91
90
89
88
87
86
85
84
83
82
81
80
4000
3500
3000
2500
2000
1500
1000
500
Wavenumbers (cm-1)

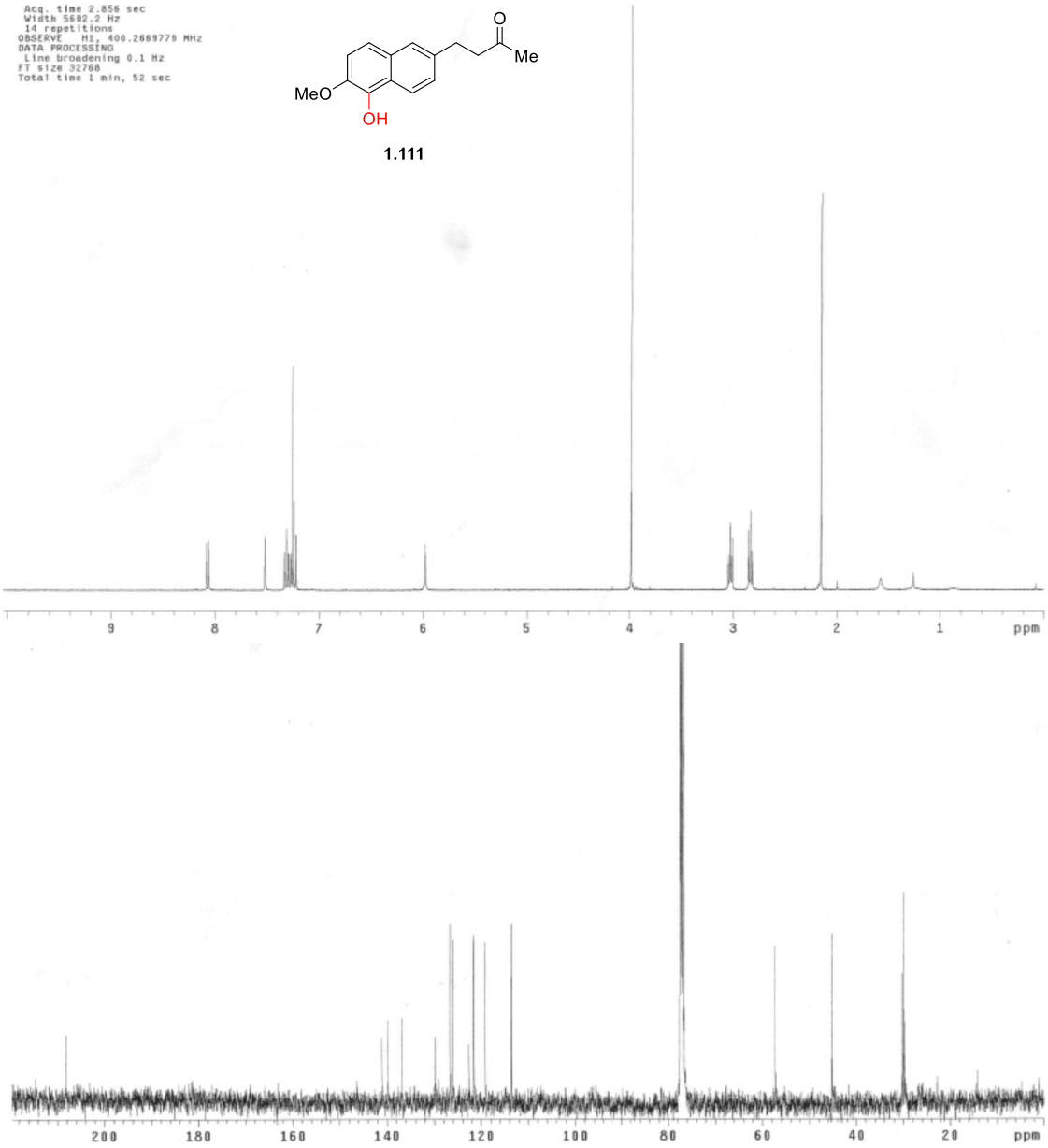
Acq. time 2.856 sec
Width 5602.2 Hz
14 repetitions
OBSERVE H1, 400.2669779 MHz
DATA PROCESSING
Line broadening 0.1 Hz
FT size 32768
Total time 1 min, 52 sec
O
Me
MeO
OH
1.111
9
8
7
6
5
4
3
2
1
ppm
200
180
160
140
120
100
80
60
40
20
ppm

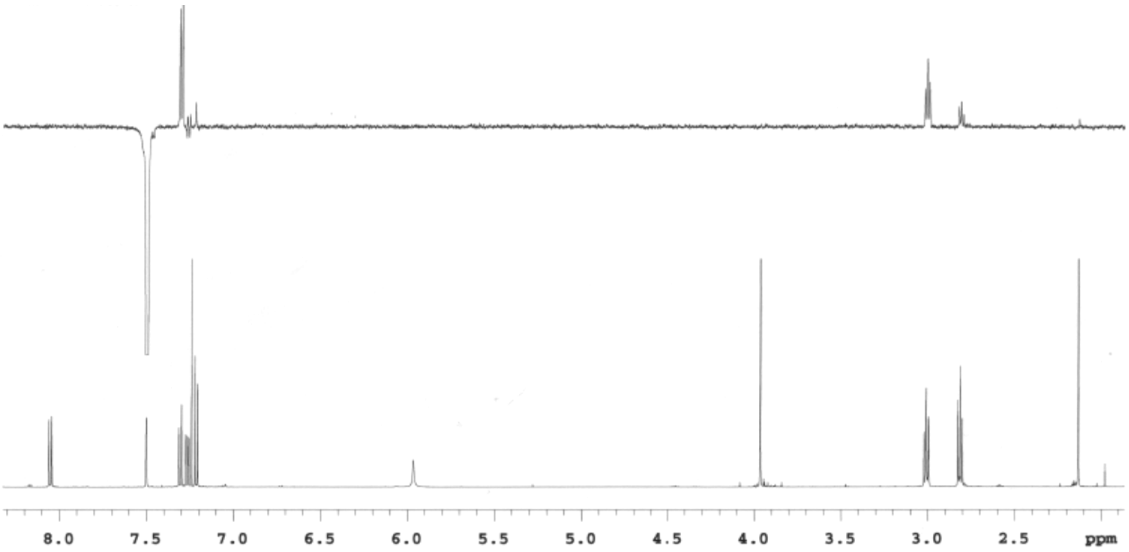

ae-hydroxy nabumetone
Selective band center: 7.50 (ppm); width: 36.2 (Hz)

Sample Name:

Data Collected on:
nmrox2-vnmrs600
Archive directory:

Sample directory:

FidFile: NOESY1D

Pulse Sequence: NOESY1D
Solvent: cdcl3
Data collected on: Jun 12 2013

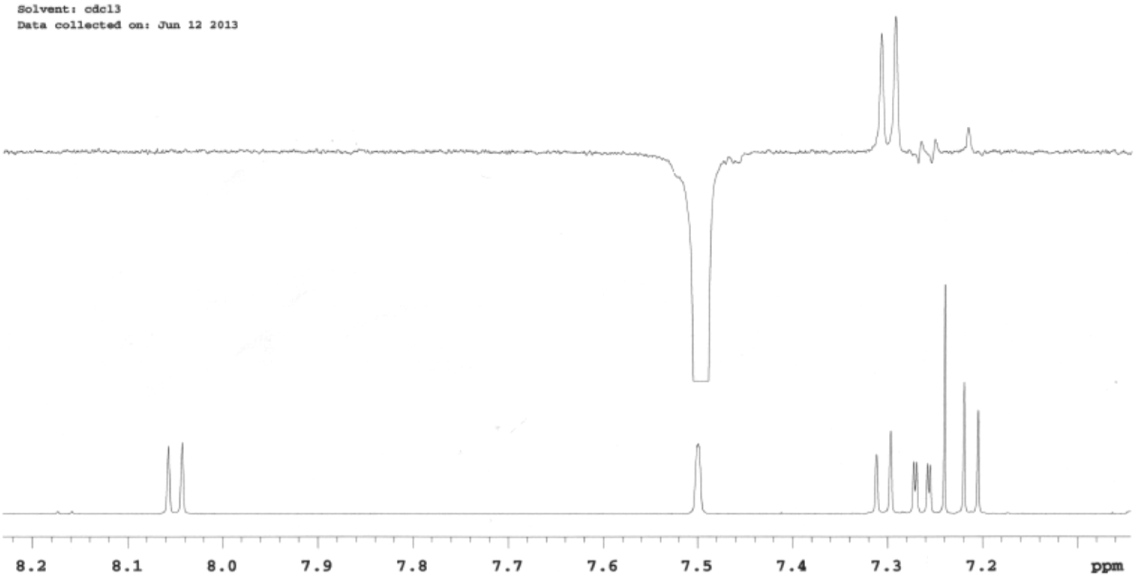

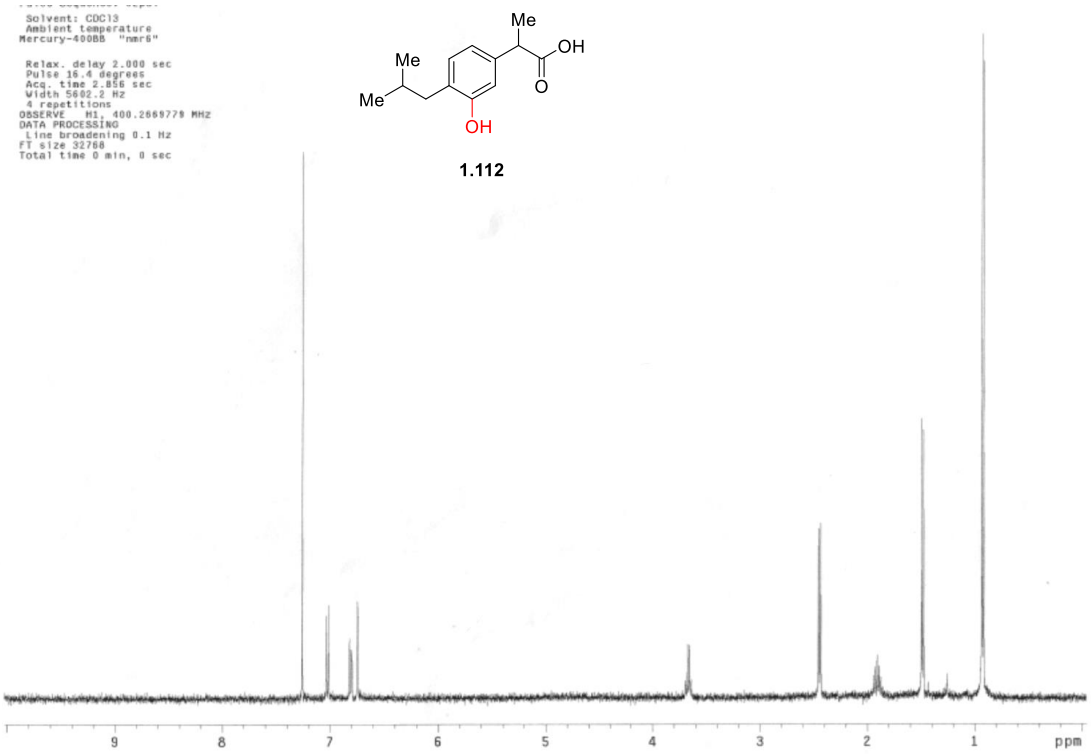
Solvent: CDCl3
Ambient temperature
Mercury-400BB "nmr6"
Relax. delay 2.000 sec
Pulse 16.4 degrees
Acq. time 2.856 sec
Width 5602.2 Hz
4 repetitions
OBSERVE H1, 400.2669779 MHz
DATA PROCESSING
Line broadening 0.1 Hz
FT size 32768
Total time 0 min, 0 sec
Me
Me
Me
OH
O
OH
1.112
9
8
7
6
5
4
3
2
1
ppm

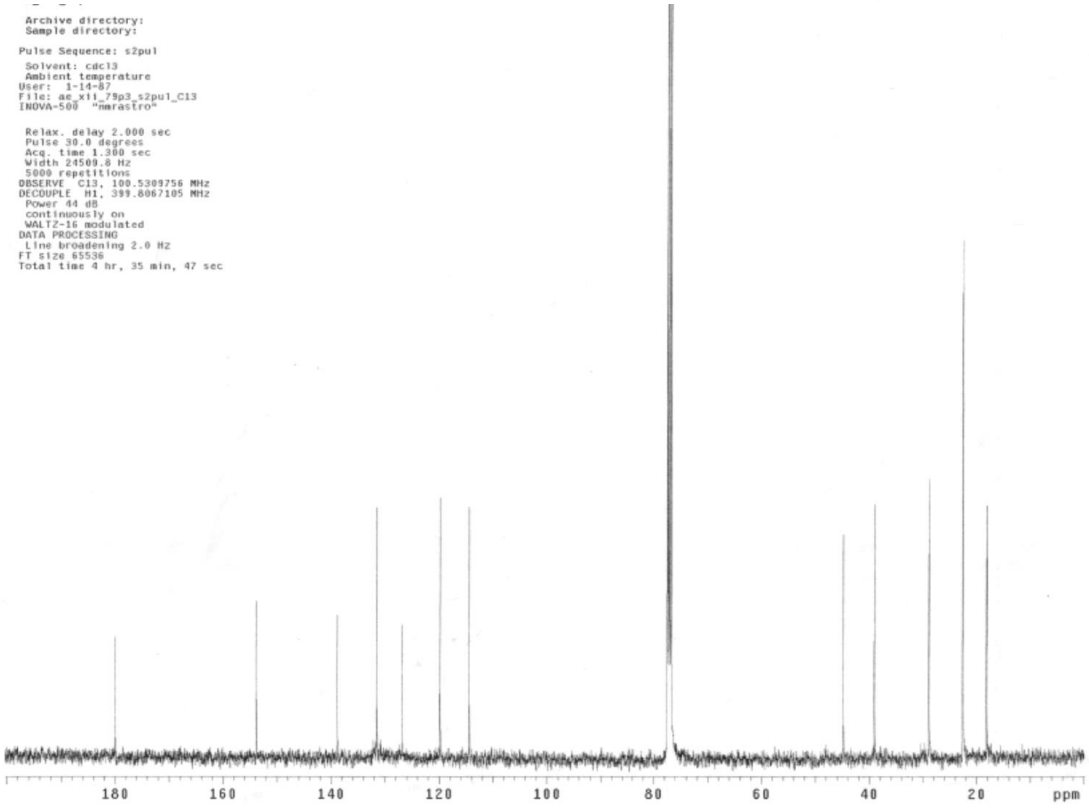
Archive directory:
Sample directory:
Pulse Sequence: s2pul
Solvent: cdcl3
Ambient temperature
User: 1-14-87
File: ae_xii_79p3_s2pul_C13
INOVA-500 "nmrastro"
Relax. delay 2.000 sec
Pulse 30.0 degrees
Acq. time 1.300 sec
Width 24509.8 Hz
5000 repetitions
OBSERVE C13, 100.5309756 MHz
DECOUPLE H1, 399.8067105 MHz
Power 44 dB
continuously on
WALTZ-16 modulated
DATA PROCESSING
Line broadening 2.0 Hz
FT size 65536
Total time 4 hr, 35 min, 47 sec
180
160
140
120
100
80
60
40
20
ppm

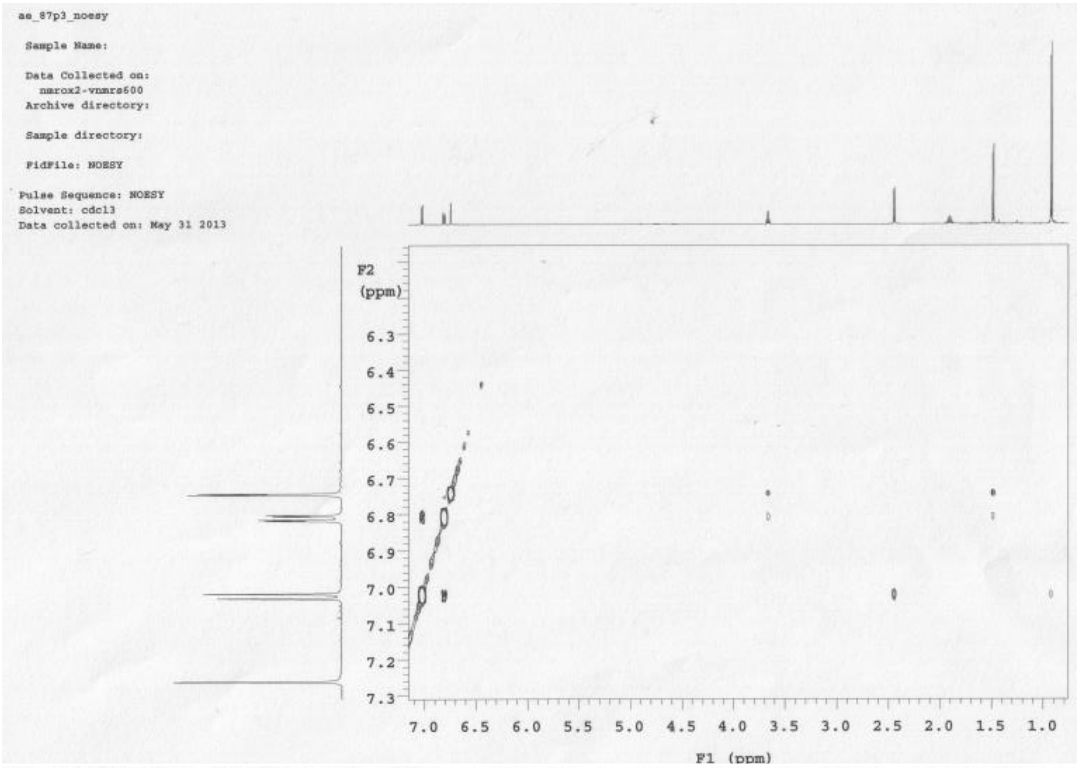
ae_87p3_noesy
Sample Name:
Data Collected on:
nmrox2-vnmrs600
Archive directory:
Sample directory:
FidFile: NOESY
Pulse Sequence: NOESY
Solvent: cdcl3
Data collected on: May 31 2013
F2
(ppm)
6.3
6.4
6.5
6.6
6.7
6.8
6.9
7.0
7.1
7.2
7.3
7.0 6.5 6.0 5.5 5.0 4.5 4.0 3.5 3.0 2.5 2.0 1.5 1.0
F1 (ppm)

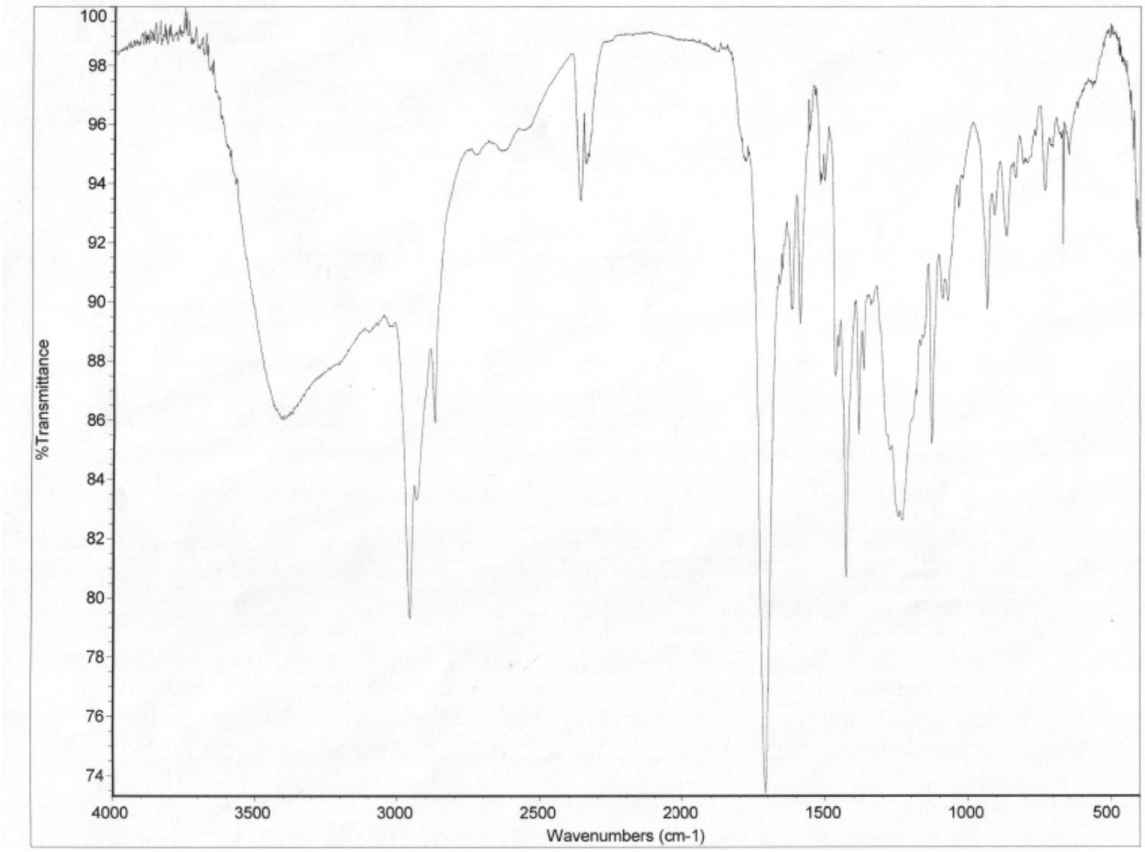
%Transmittance
100
98
96
94
92
90
88
86
84
82
80
78
76
74
4000 3500 3000 2500 2000 1500 1000 500
Wavenumbers (cm-1)

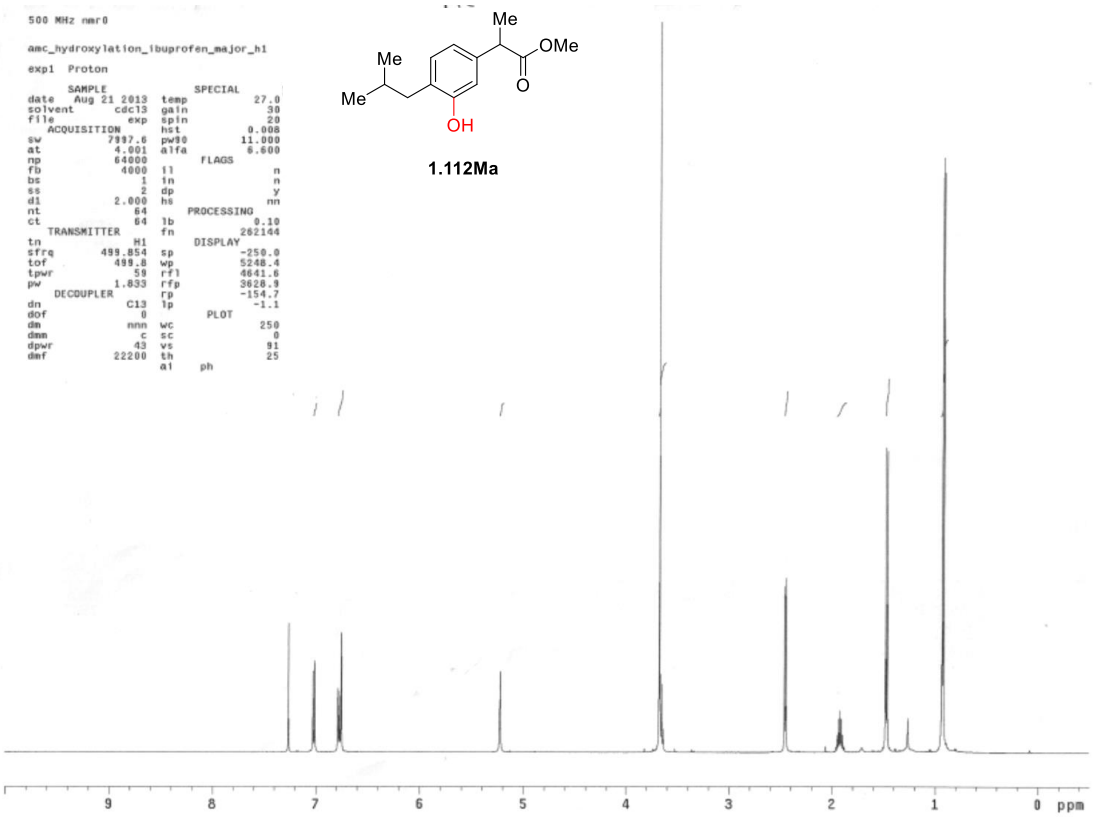
500 MHz nmr0
amc_hydroxylation_ibuprofen_major_h1
exp1 Proton
SAMPLE
date Aug 21 2013
solvent cdcl3
file exp
ACQUISITION
sw 7997.6
at 4.001
np 64000
fb 4000
bs 1
ss 2
d1 2.000
nt 64
ct 64
TRANSMITTER
tn H1
sfrq 499.854
tof 499.8
tpwr 59
pw 1.833
DECOUPLER
dn C13
dof 0
dm nnn
dmm c
dpwr 43
dmf 22200
SPECIAL
temp 27.0
gain 30
spin 20
hst 0.008
pw90 11.000
alfa 6.600
FLAGS
il n
in n
dp y
hs nn
PROCESSING
lb 0.10
fn 262144
DISPLAY
sp -250.0
wp 5248.4
rf1 4641.6
rfp 3628.9
rp -154.7
lp -1.1
PLOT
wc 250
sc 0
vs 91
th 25
al ph
Me
OMe
O
Me
Me
OH
1.112Ma
9
8
7
6
5
4
3
2
1
0 ppm

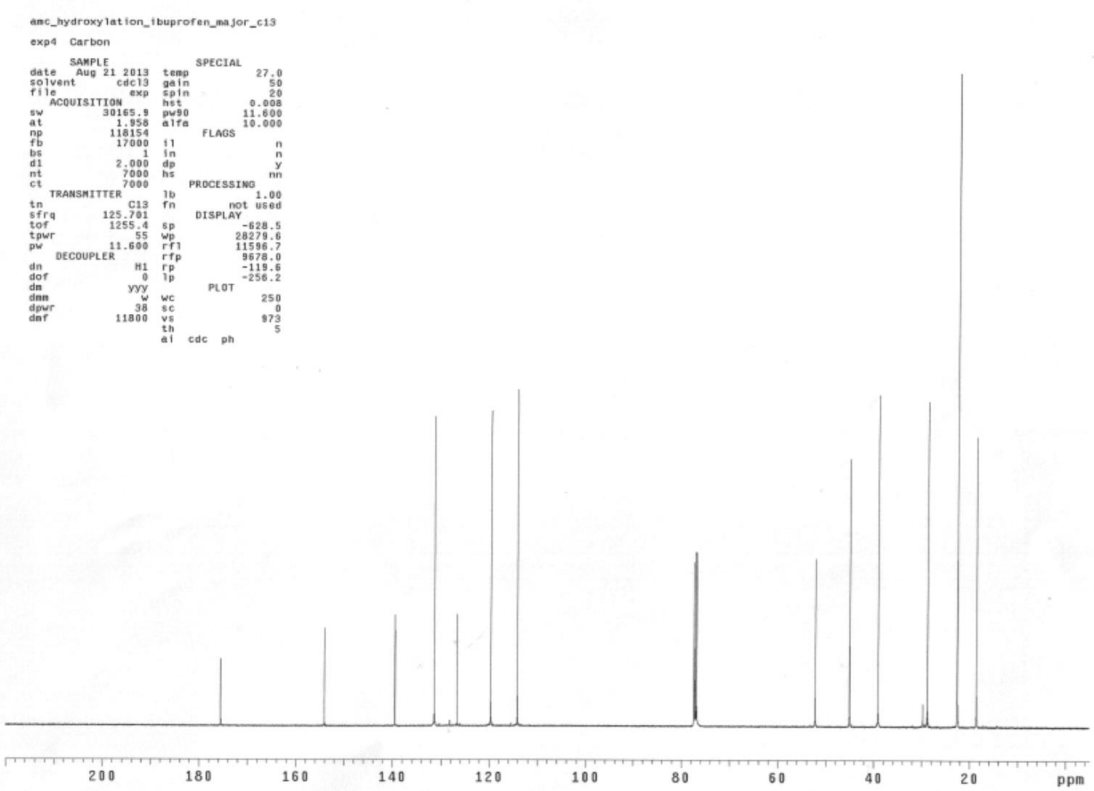
500 MHz nmr0
amc_hydroxylation_ibuprofen_major_c13
exp4 Carbon
SAMPLE
date Aug 21 2013
solvent cdcl3
file exp
ACQUISITION
sw 30165.9
at 1.958
np 118154
fb 17000
bs 1
d1 2.000
nt 7000
ct 7000
TRANSMITTER
tn C13
sfrq 125.701
tof 1255.4
tpwr 55
pw 11.600
DECOUPLER
dn H1
dof 0
dm yyy
dmm w
dpwr 38
dmf 11800
SPECIAL
temp 27.0
gain 50
spin 20
hst 0.008
pw90 11.600
alfa 10.000
FLAGS
il n
in n
dp y
hs nn
PROCESSING
lb 1.00
fn not used
DISPLAY
sp -828.5
wp 28279.6
rf1 11596.7
rfp 9678.0
rp -119.6
lp -256.2
PLOT
wc 250
sc 0
vs 973
th 5
al cdc ph
200
180
160
140
120
100
80
60
40
20
ppm

INDEX	FREQUENCY	PPM	HEIGHT
1	2905.468	7.259	72.6
2	2801.520	6.999	21.4
3	2793.656	6.979	23.3
4	2687.656	6.715	22.2
5	2685.947	6.710	26.6
6	1494.308	3.733	199.7
7	961.575	2.402	38.9
8	954.395	2.384	41.9
9	622.377	1.555	81.9
10	615.196	1.537	80.4
11	359.772	0.899	156.4
12	353.275	0.883	161.7

1.112Mb

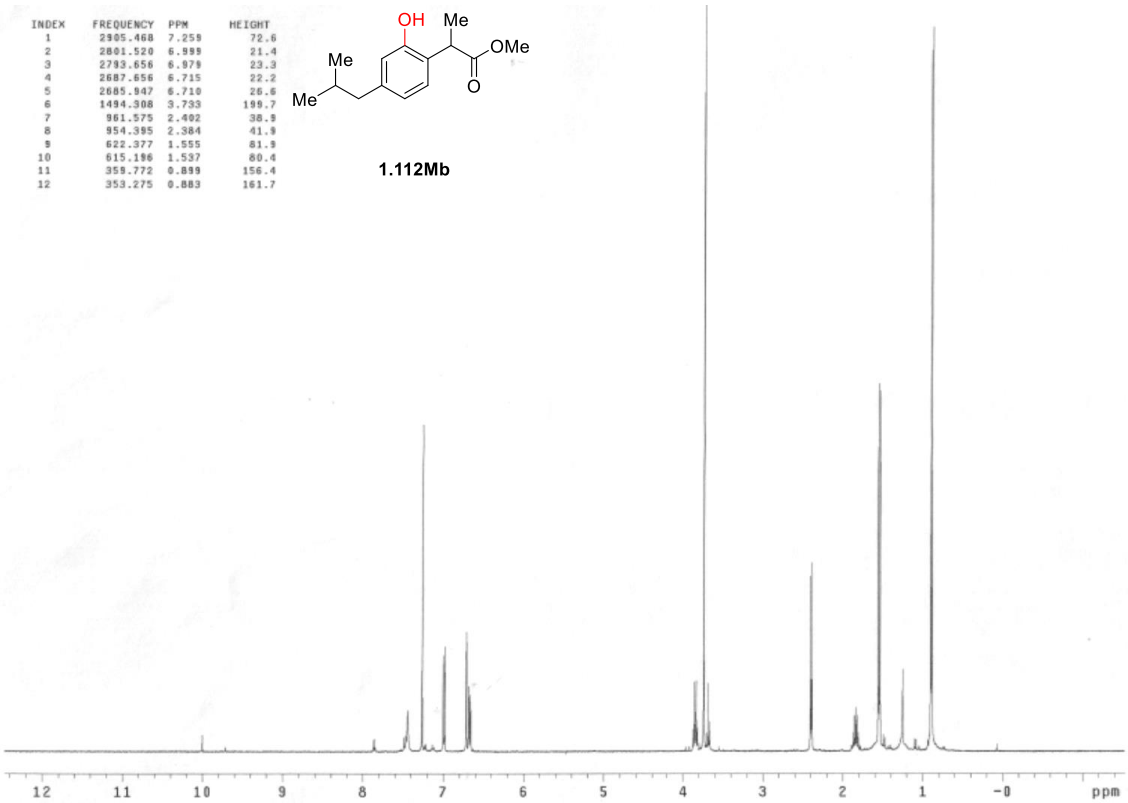

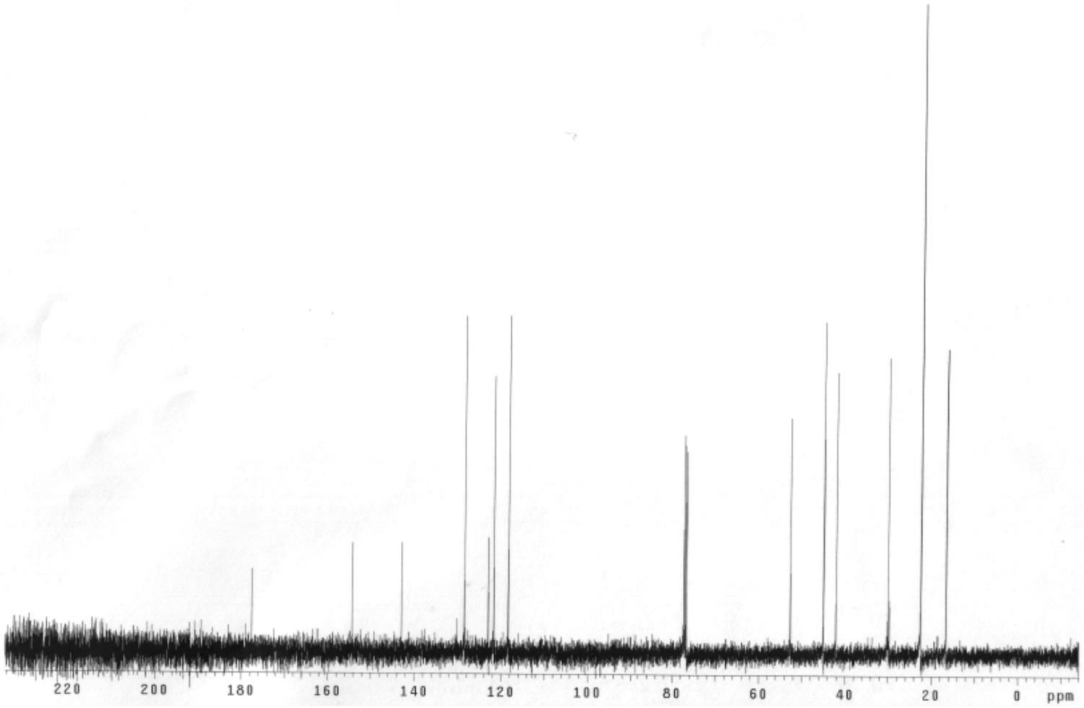

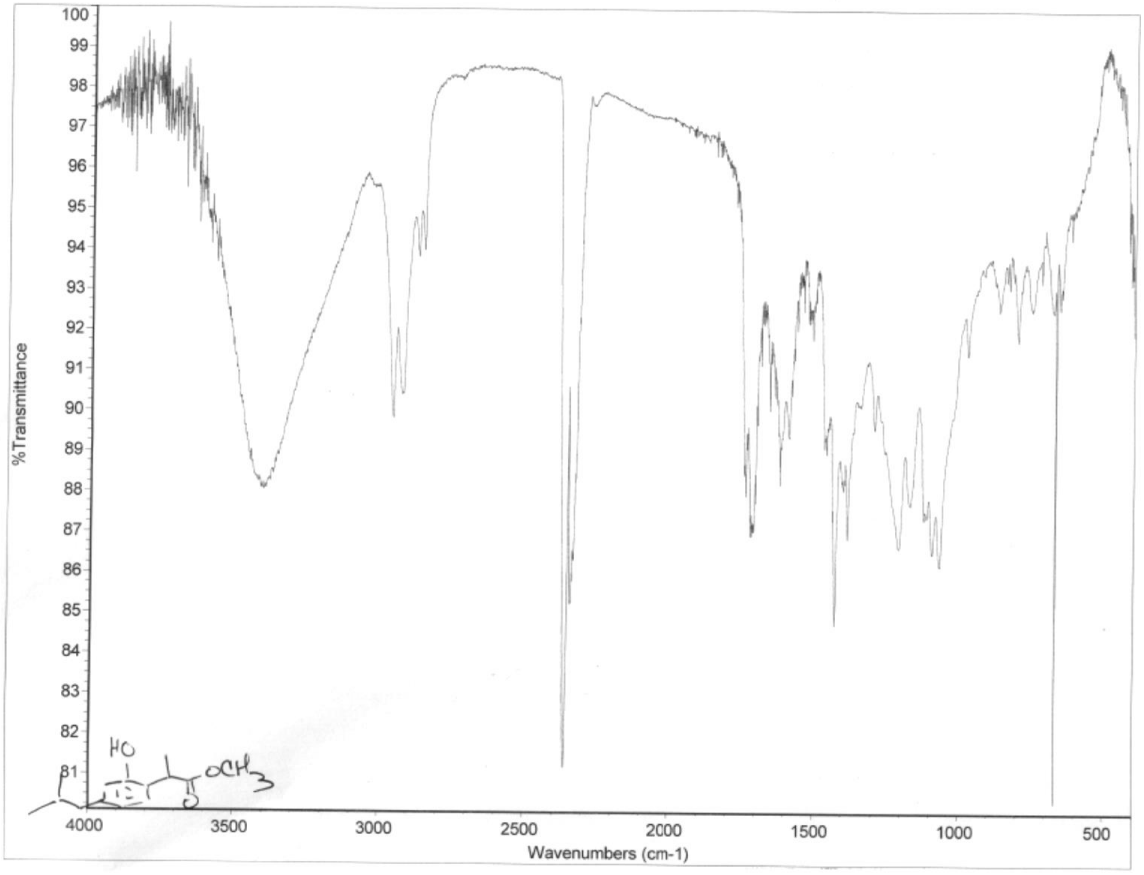
%Transmittance
100
99
98
97
96
95
94
93
92
91
90
89
88
87
86
85
84
83
82
81
4000
3500
3000
2500
2000
1500
1000
500
Wavenumbers (cm-1)
HO
OCH3

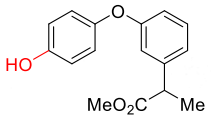

1.114a

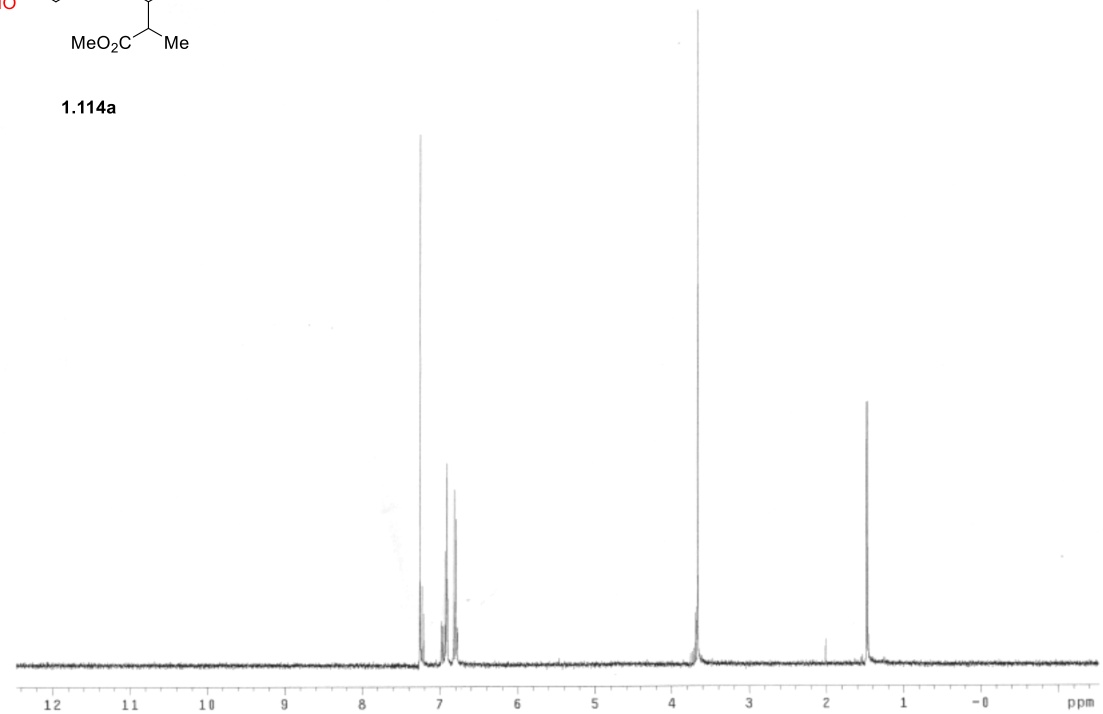

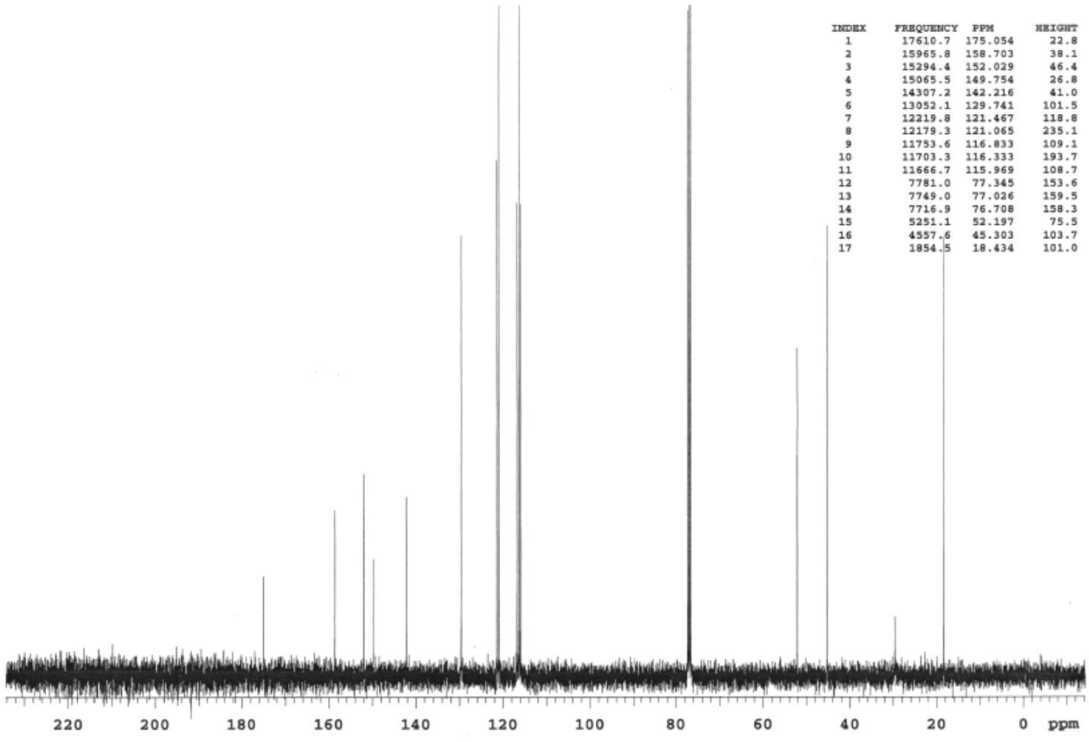

INDEX	FREQUENCY	PPM	HEIGHT
1	17610.7	175.054	22.8
2	15965.8	158.703	38.1
3	15294.4	152.029	46.4
4	15065.5	149.754	26.8
5	14307.2	142.216	41.0
6	13052.1	129.741	101.5
7	12219.8	121.467	118.8
8	12179.3	121.065	235.1
9	11753.6	116.833	109.1
10	11703.3	116.333	193.7
11	11666.7	115.969	108.7
12	7781.0	77.345	153.6
13	7749.0	77.026	159.5
14	7716.9	76.708	158.3
15	5251.1	52.197	75.5
16	4557.6	45.303	103.7
17	1854.5	18.434	101.0

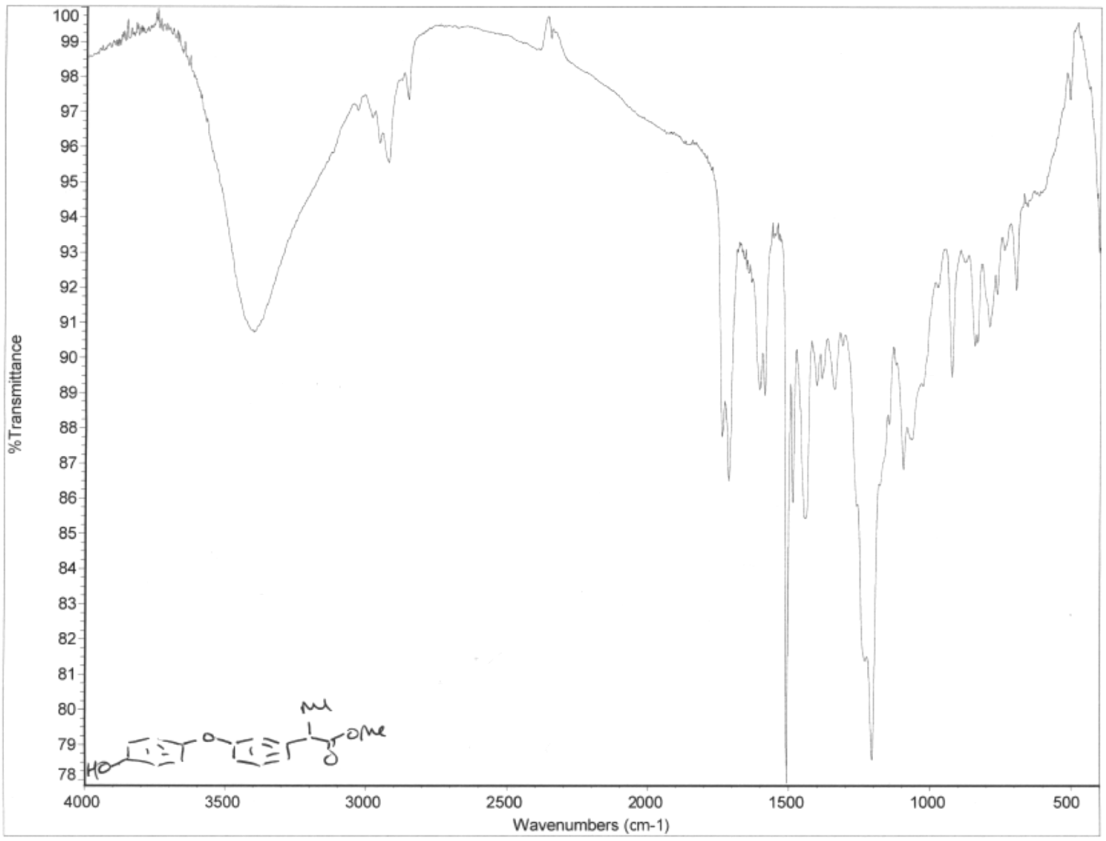
%Transmittance
100
99
98
97
96
95
94
93
92
91
90
89
88
87
86
85
84
83
82
81
80
79
78
4000
3500
3000
2500
2000
1500
1000
500
Wavenumbers (cm-1)

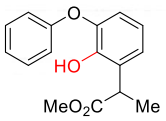
O
HO
MeO2C
Me

1.114b

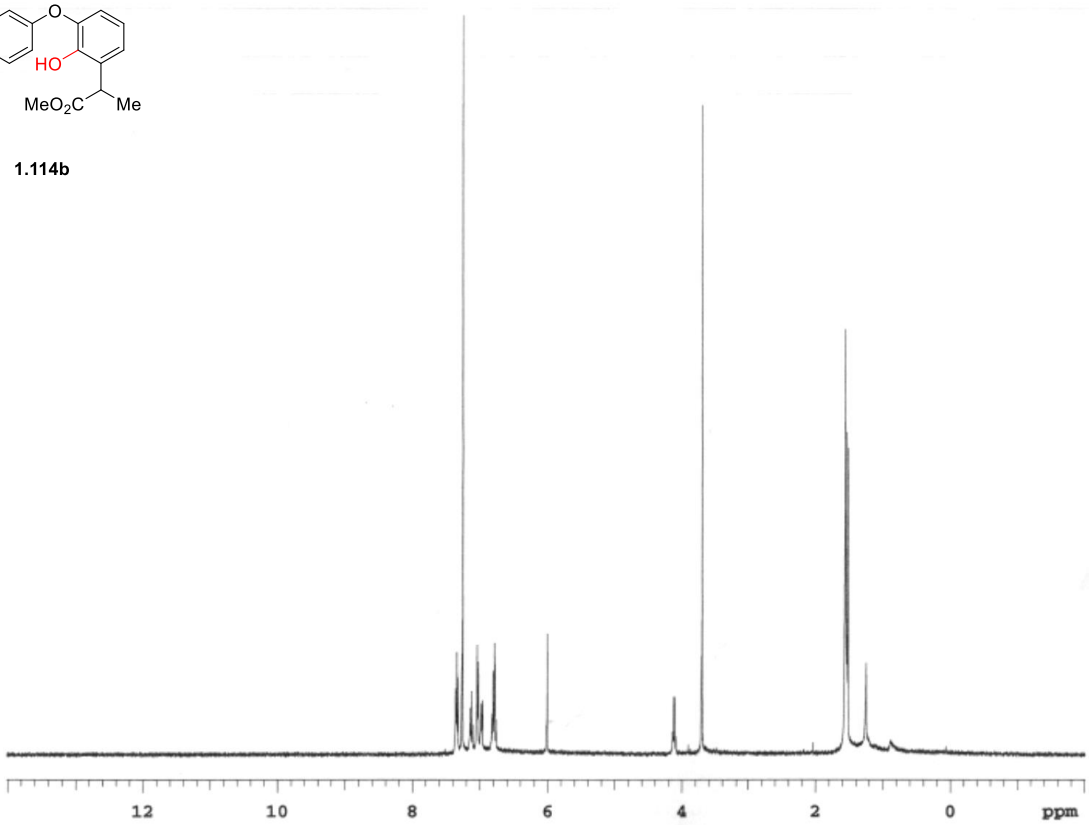
12
10
8
6
4
2
0
ppm

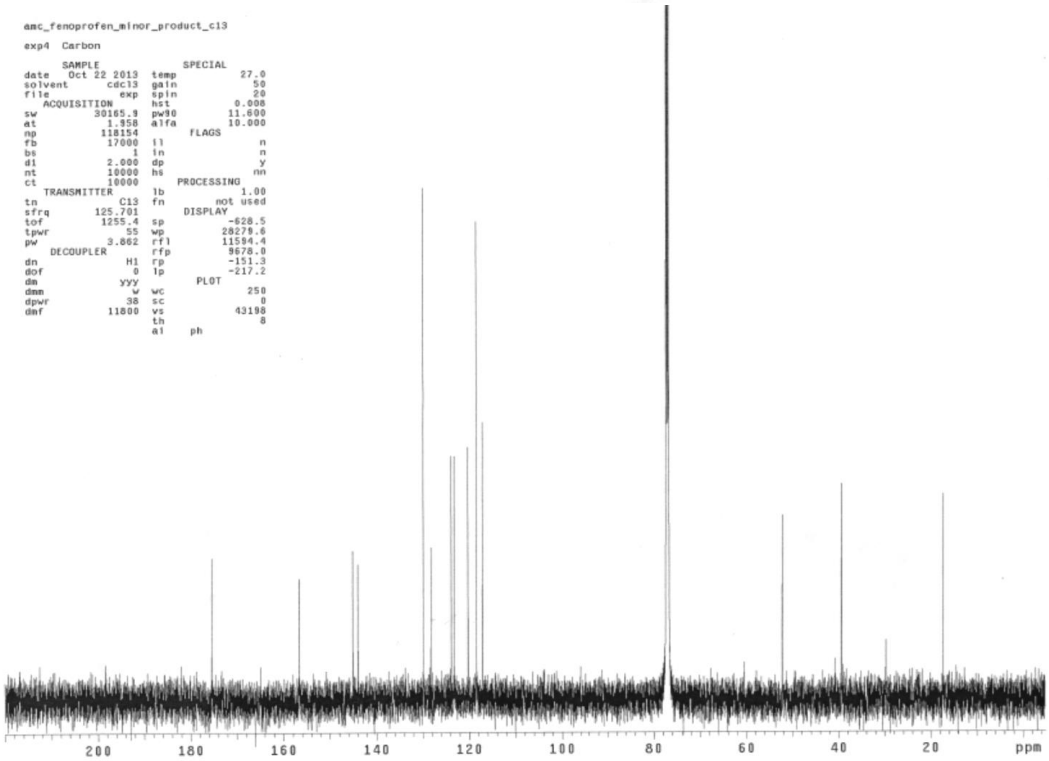
amc_fenoprofen_minor_product_c13
exp4 Carbon
SAMPLE
date Oct 22 2013
solvent cdcl3
file exp
ACQUISITION
sw 30165.9
at 1.958
np 118154
fb 17000
bs 1
d1 2.000
nt 10000
ct 10000
TRANSMITTER
tn C13
sfrq 125.701
tof 1255.4
tpwr 55
pw 3.862
DECOUPLER
dn H1
dof 0
dm yyy
dmm w
dpwr 38
dmf 11800
SPECIAL
temp 27.0
gain 50
spin 20
hst 0.008
pw90 11.600
alfa 10.000
FLAGS
ll n
in n
dp y
hs nn
PROCESSING
lb 1.00
fn not used
DISPLAY
sp -828.5
wp 28275.6
rf1 11594.4
rfp 9678.0
rp -151.3
lp -217.2
PLOT
wc 250
sc 0
vs 43198
th 8
al ph
200
180
160
140
120
100
80
60
40
20
ppm

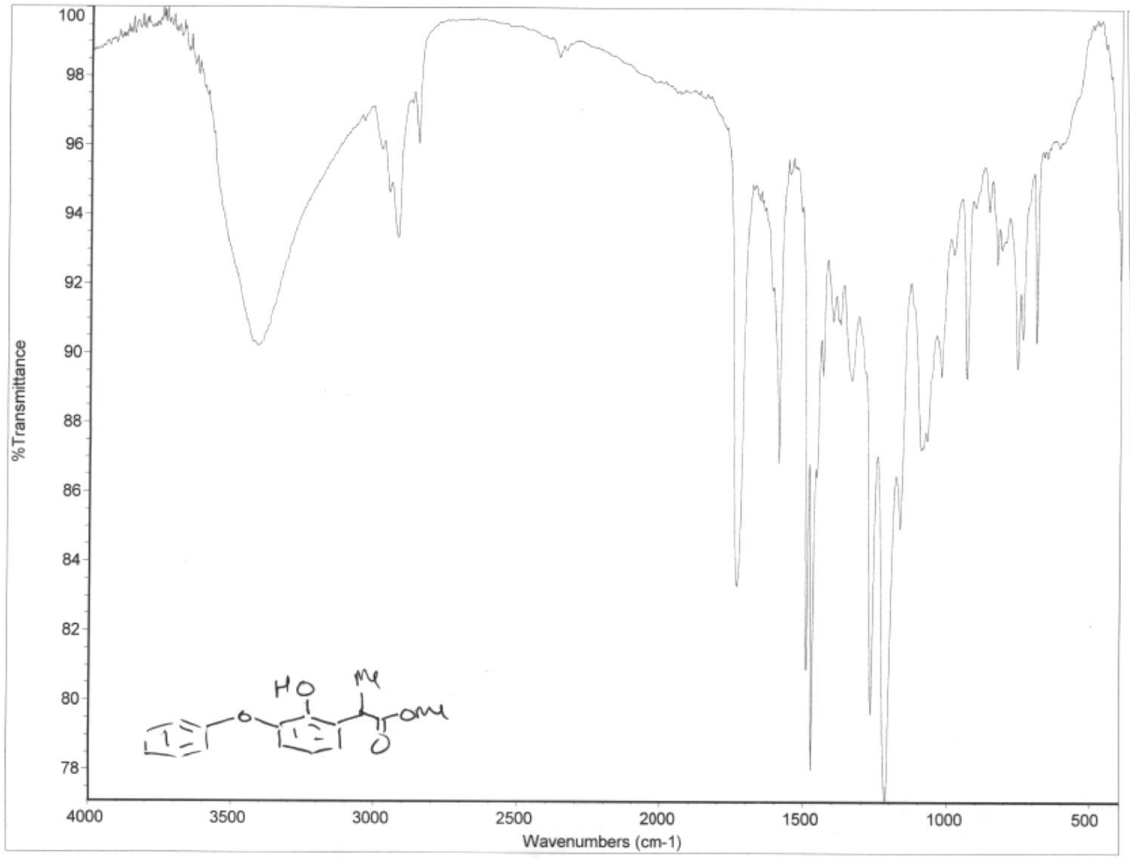
%Transmittance
100
98
96
94
92
90
88
86
84
82
80
78
4000
3500
3000
2500
2000
1500
1000
500
Wavenumbers (cm-1)
HO
Me
OMe
O

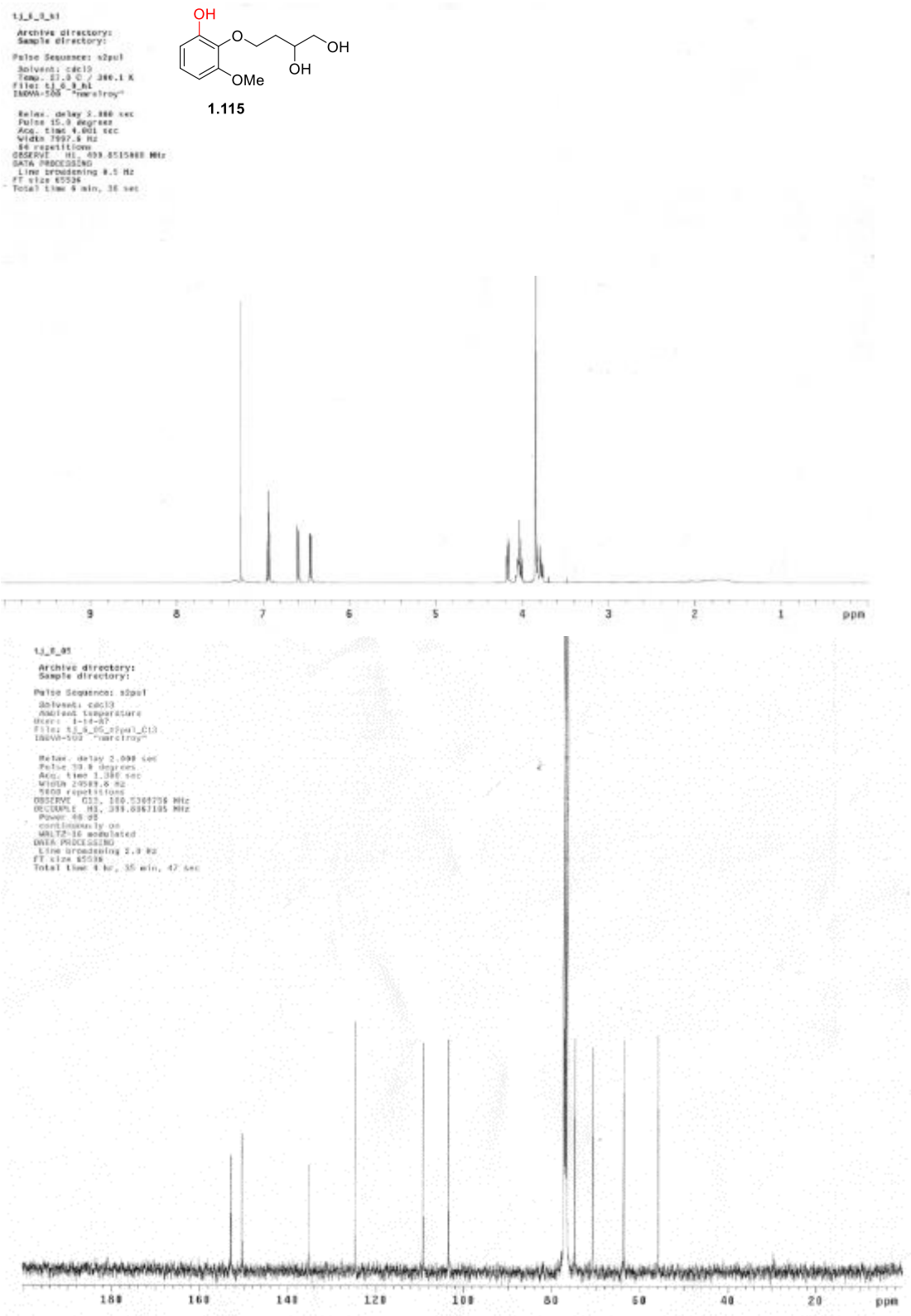
OH
O
OH
OH
OMe
1.115
9
8
7
6
5
4
3
2
1
ppm
160
140
120
100
80
60
40
20
ppm

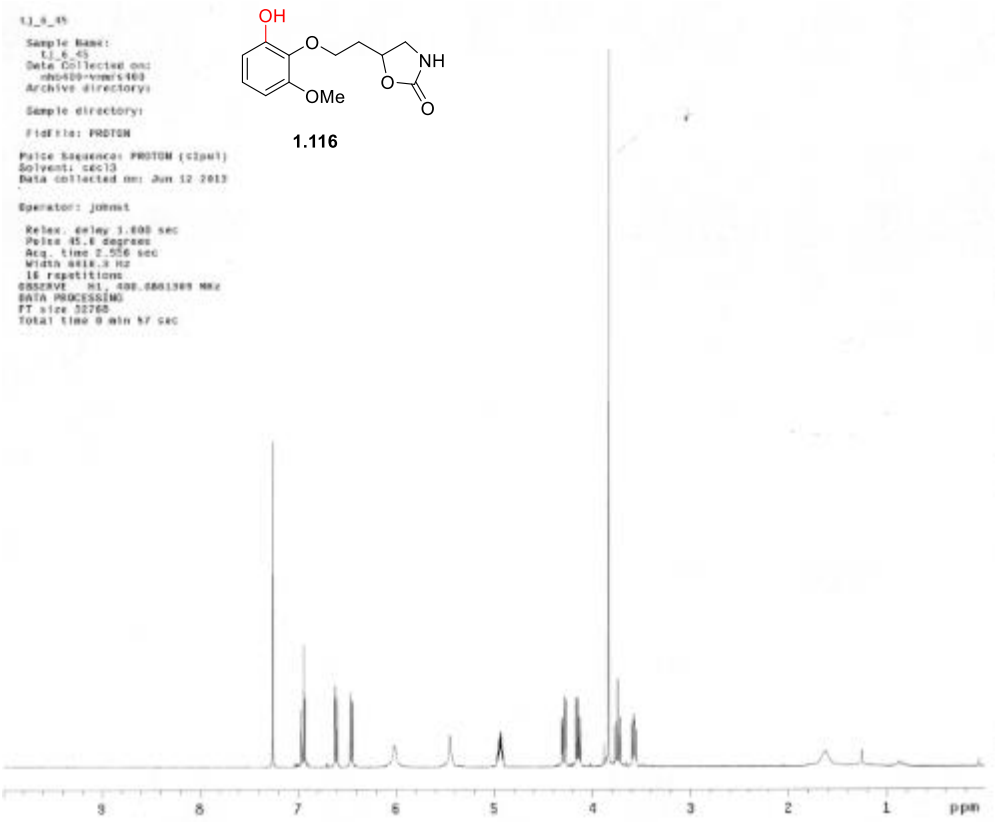
OH
O
NH
O
O
OMe
1.116
9
8
7
6
5
4
3
2
1
ppm

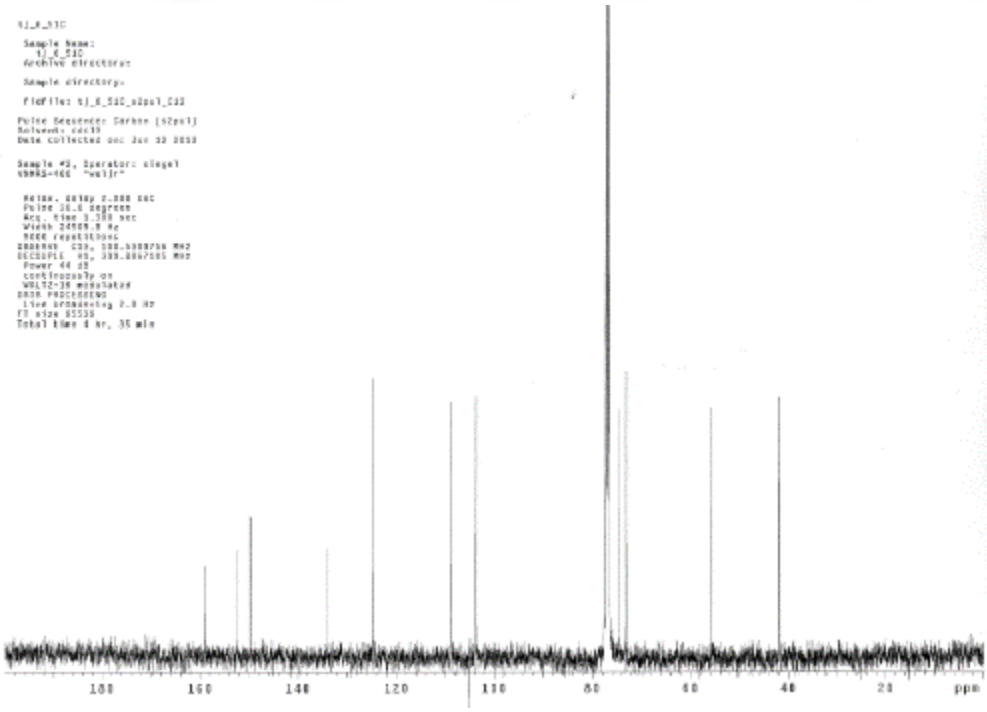
180
160
140
120
100
80
60
40
20
ppm

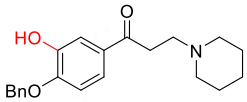
HO
O
N
BnO

1.117

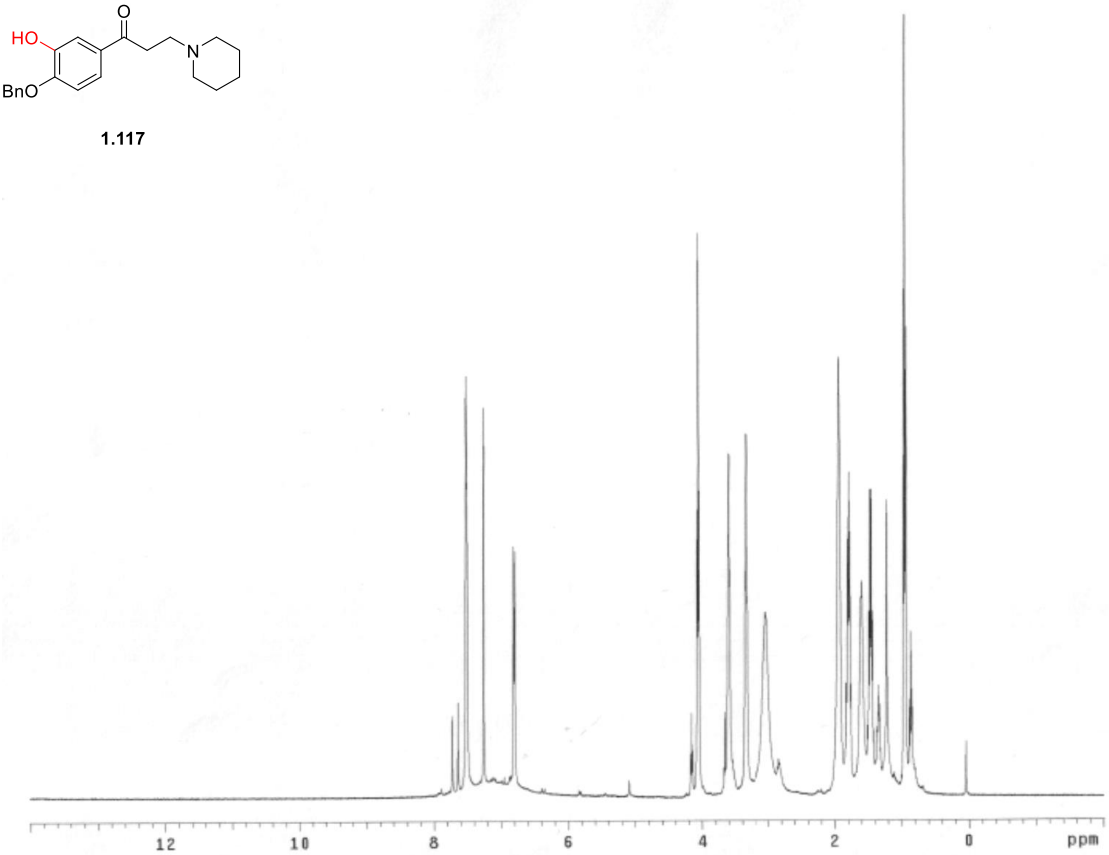
12
10
8
6
4
2
0
ppm

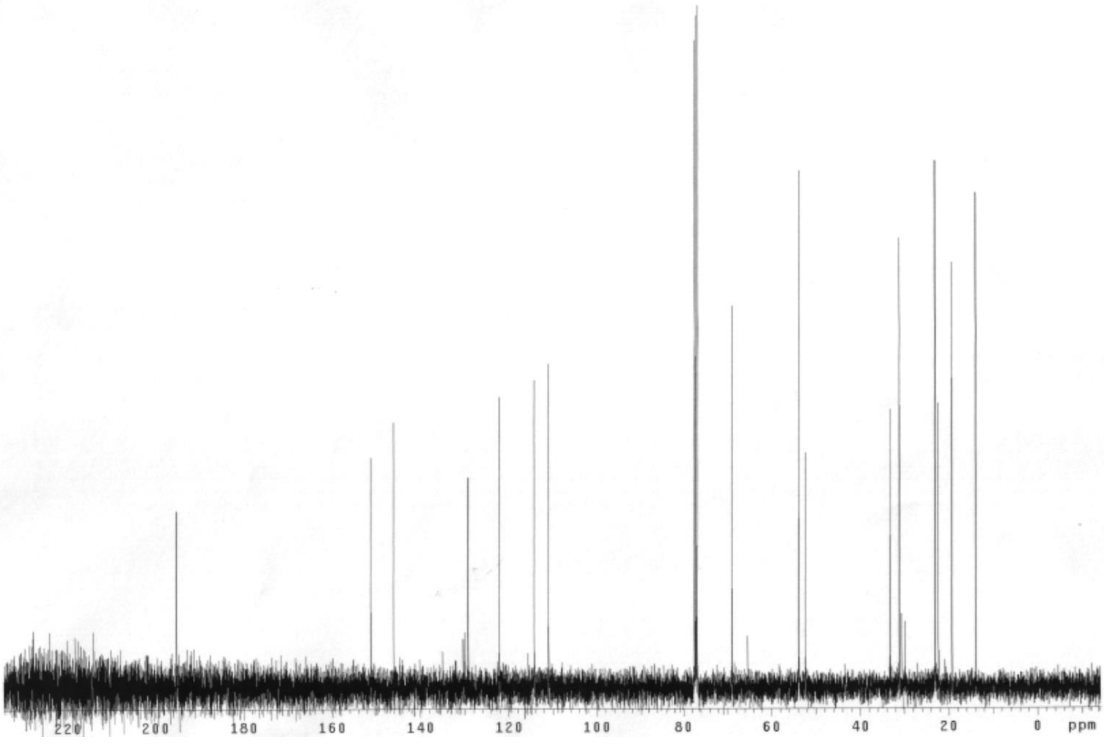
220
200
180
160
140
120
100
80
60
40
20
0
ppm

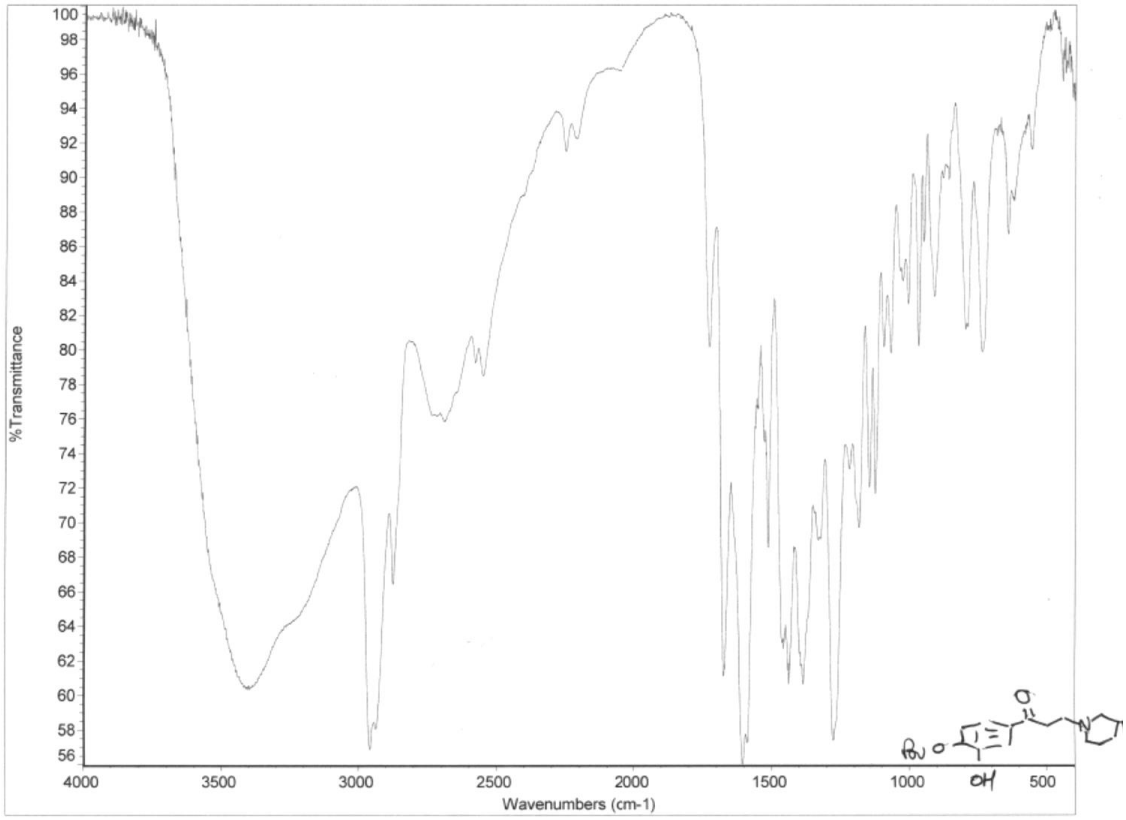
%Transmittance
100
98
96
94
92
90
88
86
84
82
80
78
76
74
72
70
68
66
64
62
60
58
56
4000
3500
3000
2500
2000
1500
1000
500
Wavenumbers (cm-1)

1.118

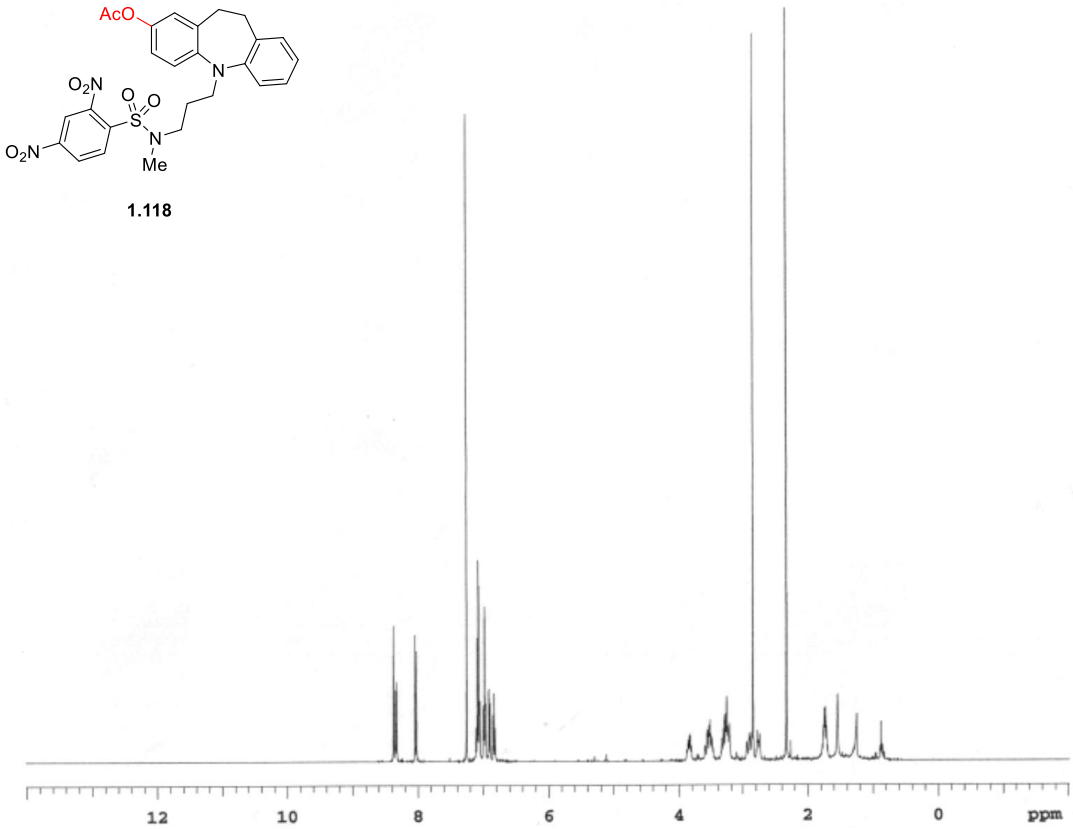


```
500 MHz nmr1

amc_desipramine_acetate_c13

exp4  Carbon

      SAMPLE                SPECIAL
date   Jan 23 2014  temp            27.0
solvent       cdcl3  gain             40
file            exp  spin             20
   ACQUISITION       hst           0.008
sw          30131.8  pw90         12.500
at            1.062  alfa         10.000
np            64000          FLAGS
fb            17000  il                n
bs                1  in                n
d1            2.000  dp                y
nt            16000  hs               nn
ct            16000          PROCESSING
   TRANSMITTER       lb             1.00
tn              C13  fn         not used
sfrq        125.584        DISPLAY
tof          1254.2  sp           -628.1
tpwr             61  wp          28253.2
pw            4.162  rf1         11579.9
    DECOUPLER        rfp          9669.0
dn               H1  rp            -95.8
dof               0  lp           -166.0
dm              yyy          PLOT
dmm               w  wc              250
dpwr             33  sc                0
dmf           12200  vs           161967
                     th                17
                     al    ph
```

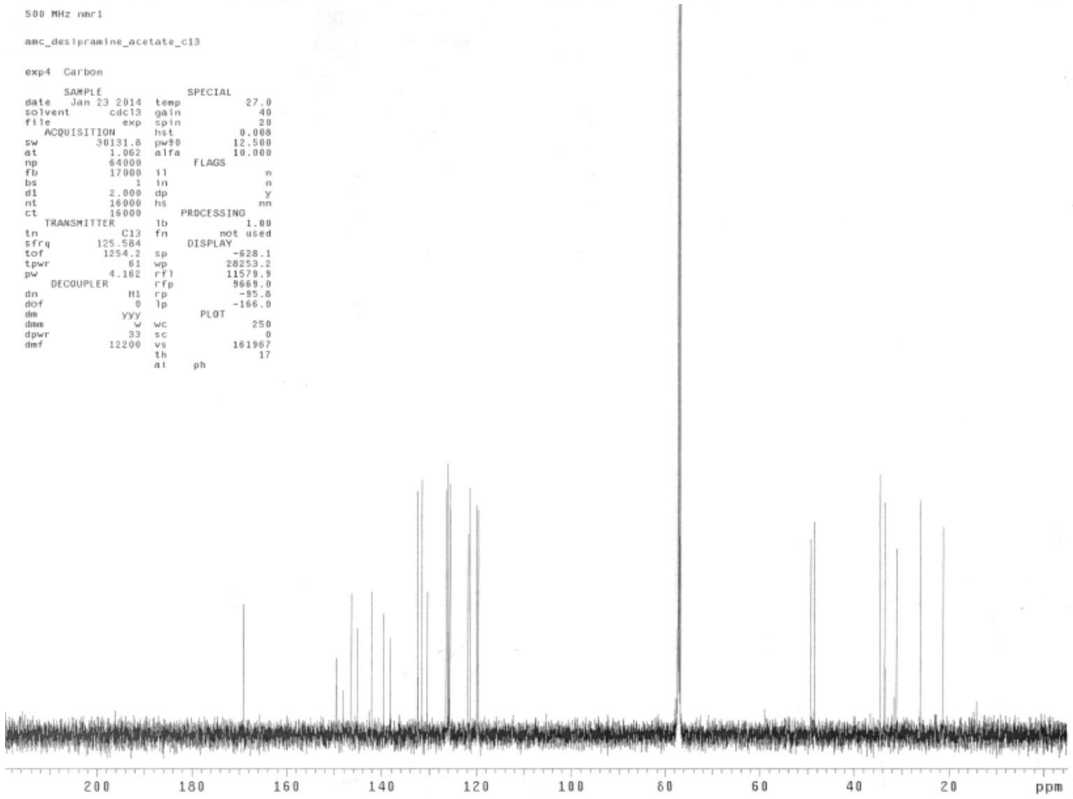

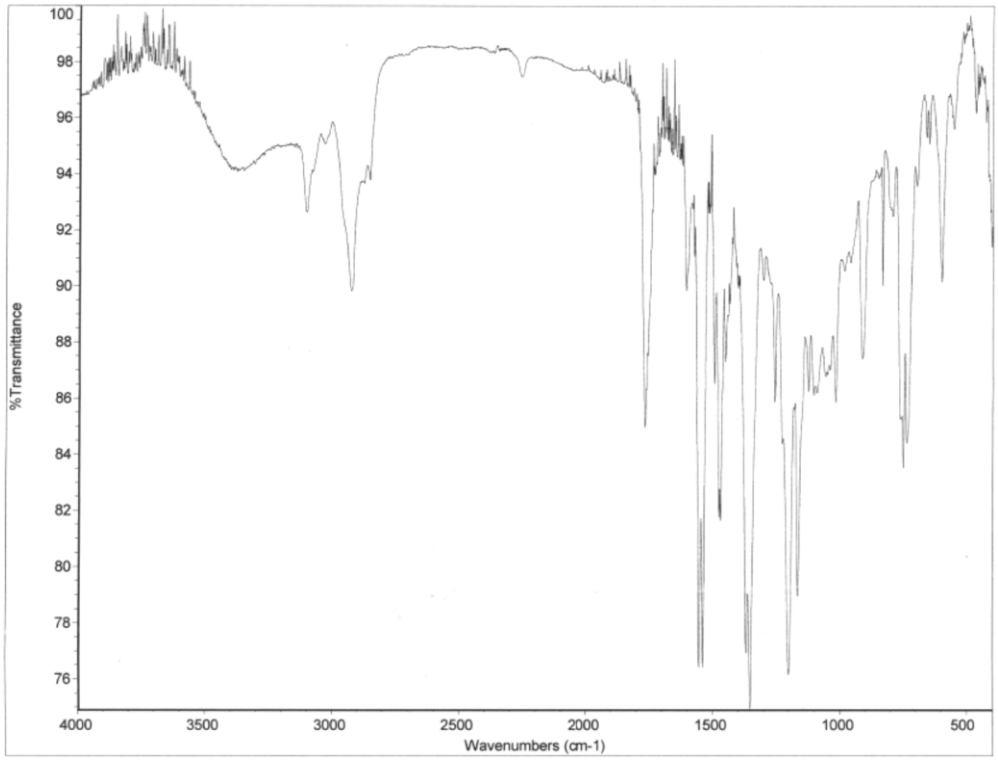
100
98
96
94
92
90
88
86
84
82
80
78
76
%Transmittance
4000
3500
3000
2500
2000
1500
1000
500
Wavenumbers (cm-1)

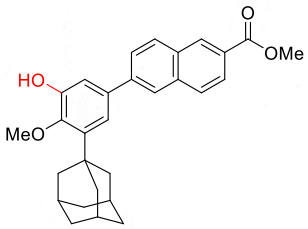
O
OMe
HO
MeO

1.119

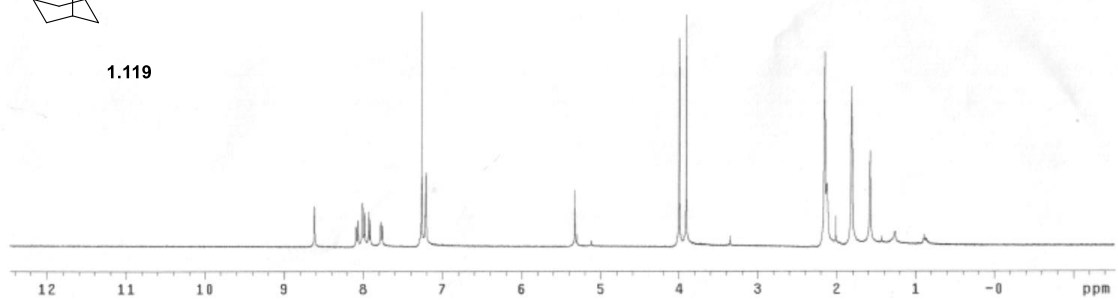
12
11
10
9
8
7
6
5
4
3
2
1
-0
ppm

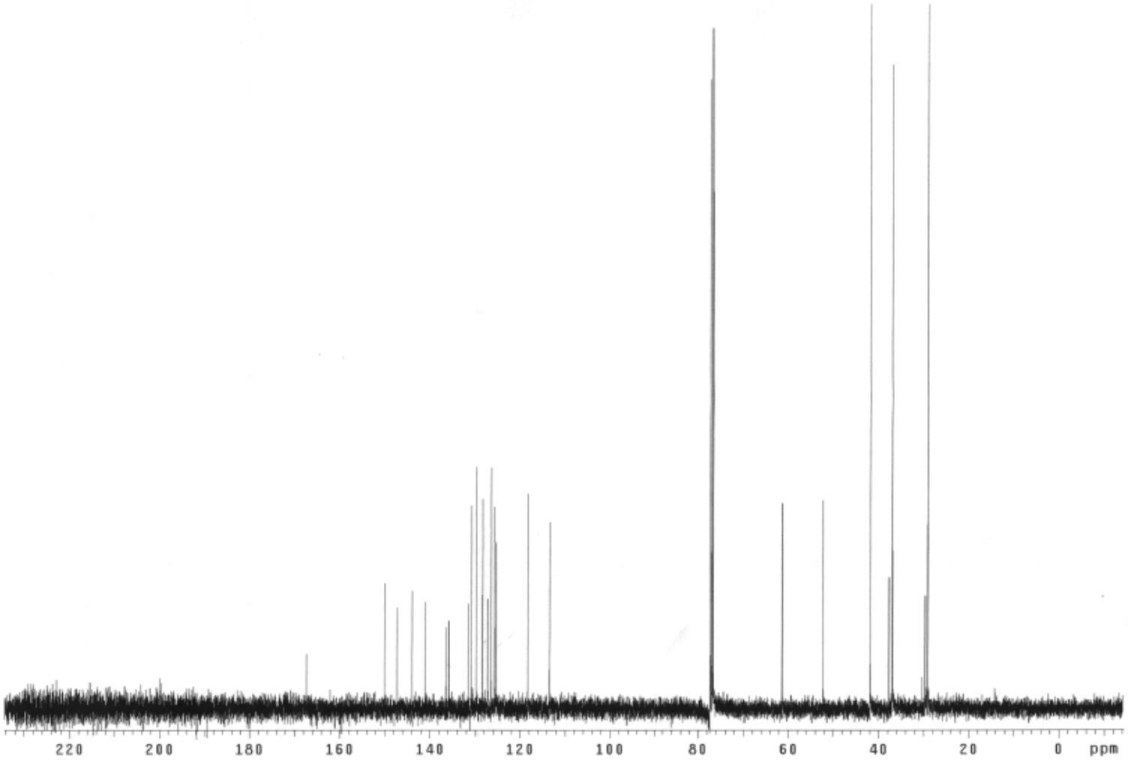
220
200
180
160
140
120
100
80
60
40
20
0
ppm

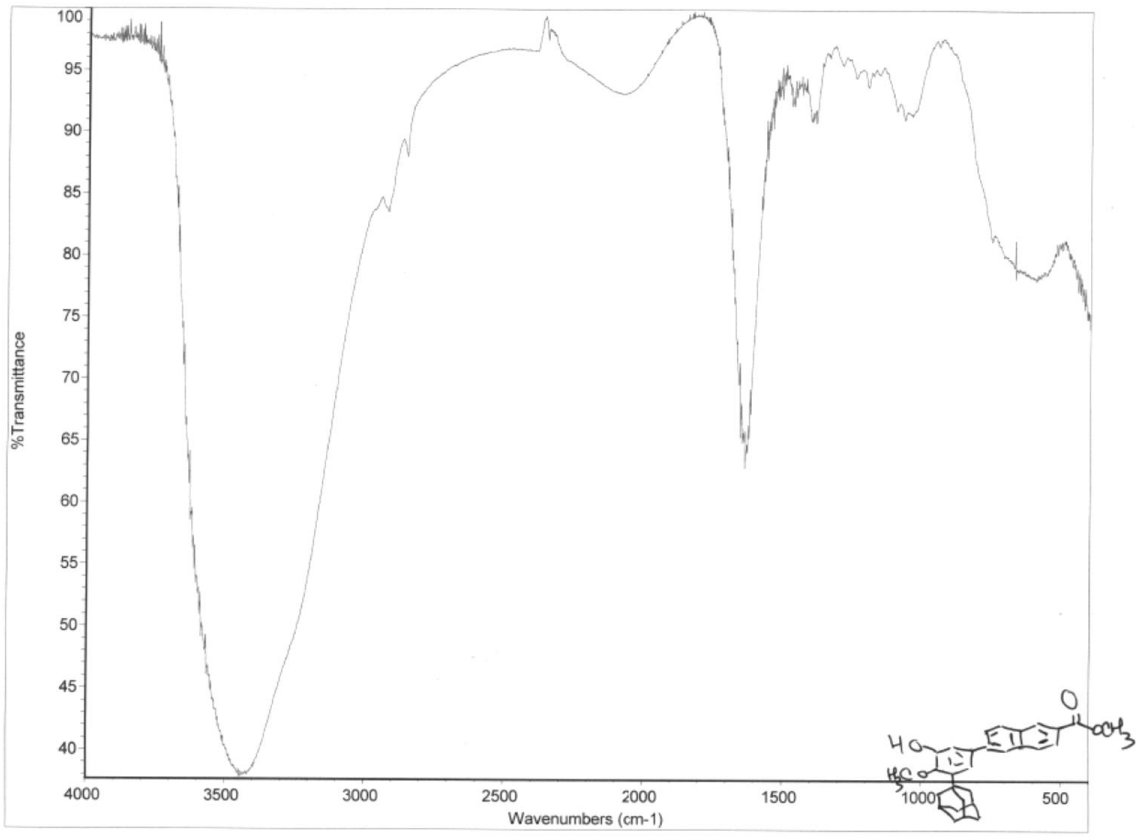
%Transmittance
100
95
90
85
80
75
70
65
60
55
50
45
40
4000
3500
3000
2500
2000
1500
1000
500
Wavenumbers (cm-1)

O
OMe
H
N
AcO
Me
Me

1.120

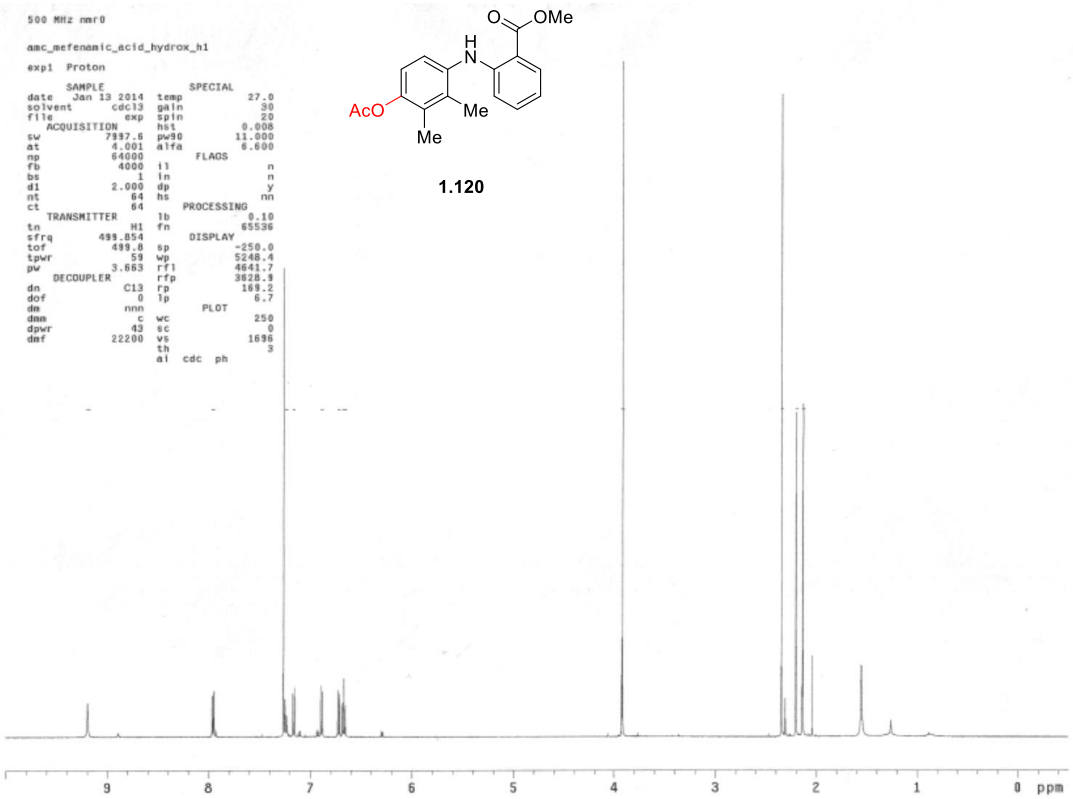
500 MHz nmr0
amc_mefenamic_acid_hydrox_h1
exp1 Proton
SAMPLE
date Jan 13 2014
solvent cdcl3
file exp
ACQUISITION
sw 7997.6
at 4.001
np 64000
fb 4000
bs 1
d1 2.000
nt 64
ct 64
TRANSMITTER
tn H1
sfrq 499.854
tof 499.8
tpwr 59
pw 3.663
DECOUPLER
dn C13
dof 0
dm nnn
dmm c
dpwr 43
dmf 22200
SPECIAL
temp 27.0
gain 30
spin 20
hst 0.008
pw90 11.000
alfa 6.600
FLAGS
il n
in n
dp y
hs nn
PROCESSING
lb 0.10
fn 65536
DISPLAY
sp -250.0
wp 5248.4
rf1 4641.7
rfp 3628.9
rp 169.2
lp 6.7
PLOT
wc 250
sc 0
vs 1696
th 3
al cdc ph
9
8
7
6
5
4
3
2
1
0 ppm

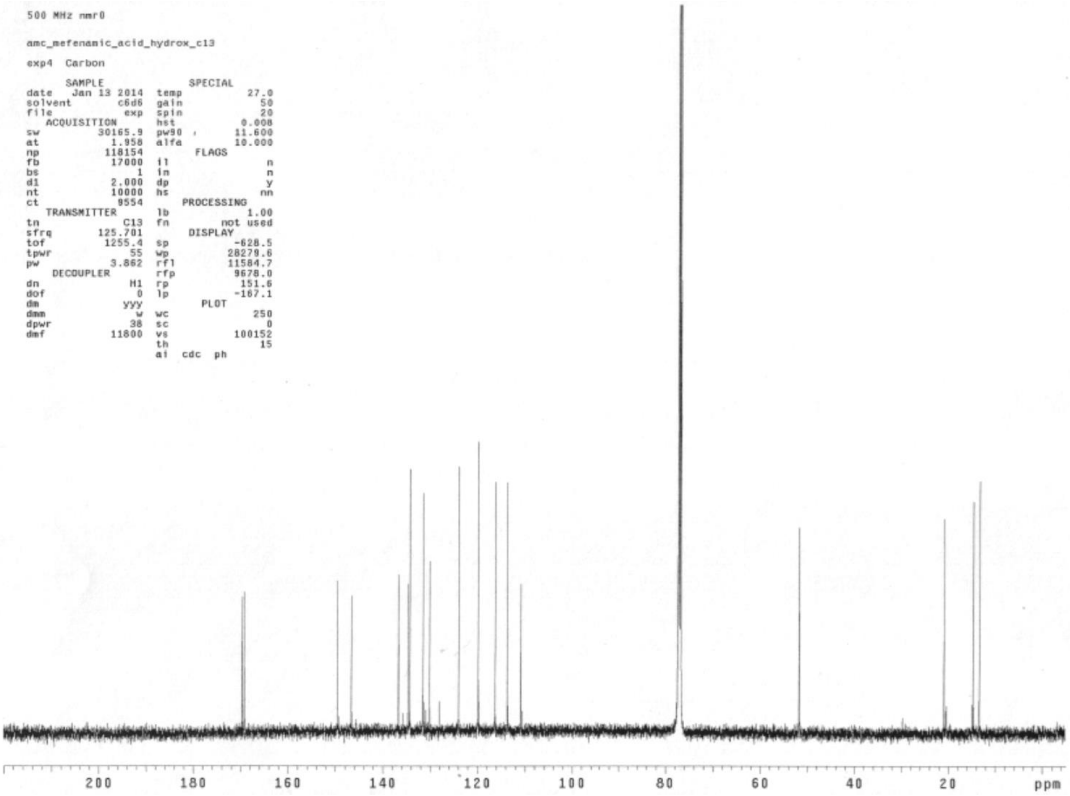
500 MHz nmr0
amc_mefenamic_acid_hydrox_c13
exp4 Carbon
SAMPLE
date Jan 13 2014
solvent c6d6
file exp
ACQUISITION
sw 30165.9
at 1.958
np 118154
fb 17000
bs 1
d1 2.000
nt 10000
ct 9554
TRANSMITTER
tn C13
sfrq 125.701
tof 1255.4
tpwr 55
pw 3.862
DECOUPLER
dn H1
dof 0
dm yyy
dmm w
dpwr 38
dmf 11800
SPECIAL
temp 27.0
gain 50
spin 20
hst 0.008
pw90 11.600
alfa 10.000
FLAGS
il n
in n
dp y
hs nn
PROCESSING
lb 1.00
fn not used
DISPLAY
sp -628.5
wp 28279.6
rf1 11584.7
rfp 9678.0
rp 151.6
lp -167.1
PLOT
wc 250
sc 0
vs 100152
th 15
al cdc ph
200
180
160
140
120
100
80
60
40
20
ppm

OH
Me
Me
Me

1.41

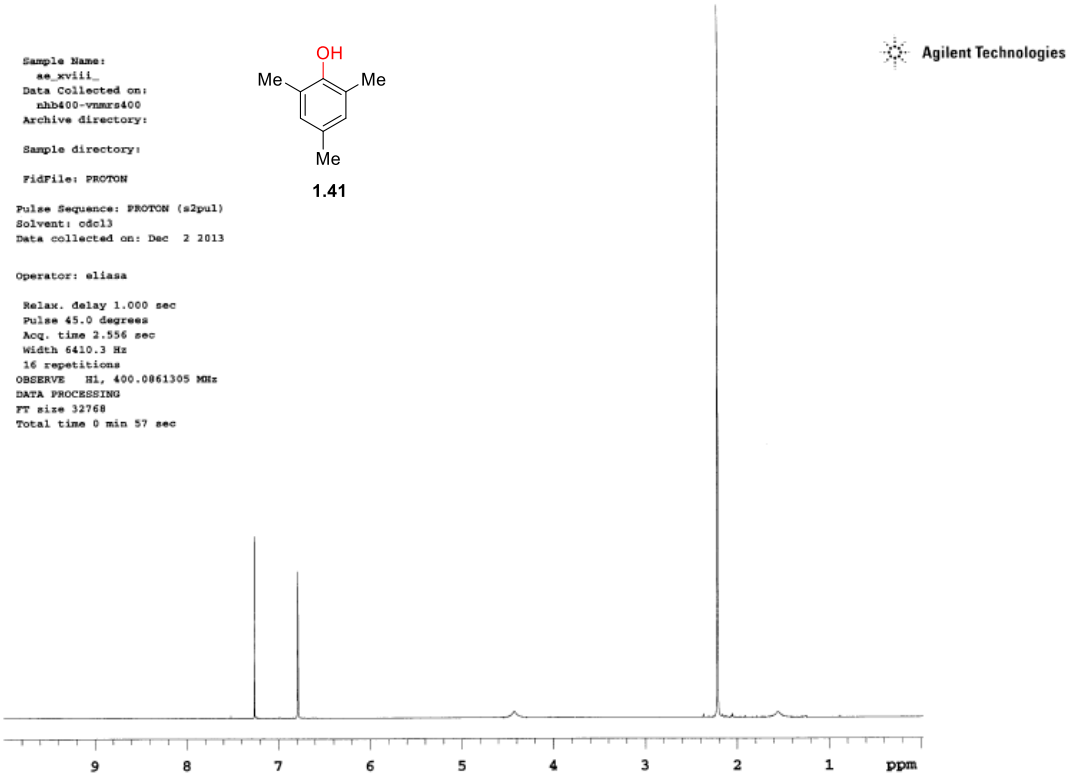
Agilent Technologies
Sample Name:
ae_xviii_
Data Collected on:
nhb400-vnmrs400
Archive directory:
Sample directory:
FidFile: PROTON
Pulse Sequence: PROTON (s2pul)
Solvent: cdcl3
Data collected on: Dec 2 2013
Operator: eliasa
Relax. delay 1.000 sec
Pulse 45.0 degrees
Acq. time 2.556 sec
Width 6410.3 Hz
16 repetitions
OBSERVE H1, 400.0861305 MHz
DATA PROCESSING
FT size 32768
Total time 0 min 57 sec
9
8
7
6
5
4
3
2
1
ppm

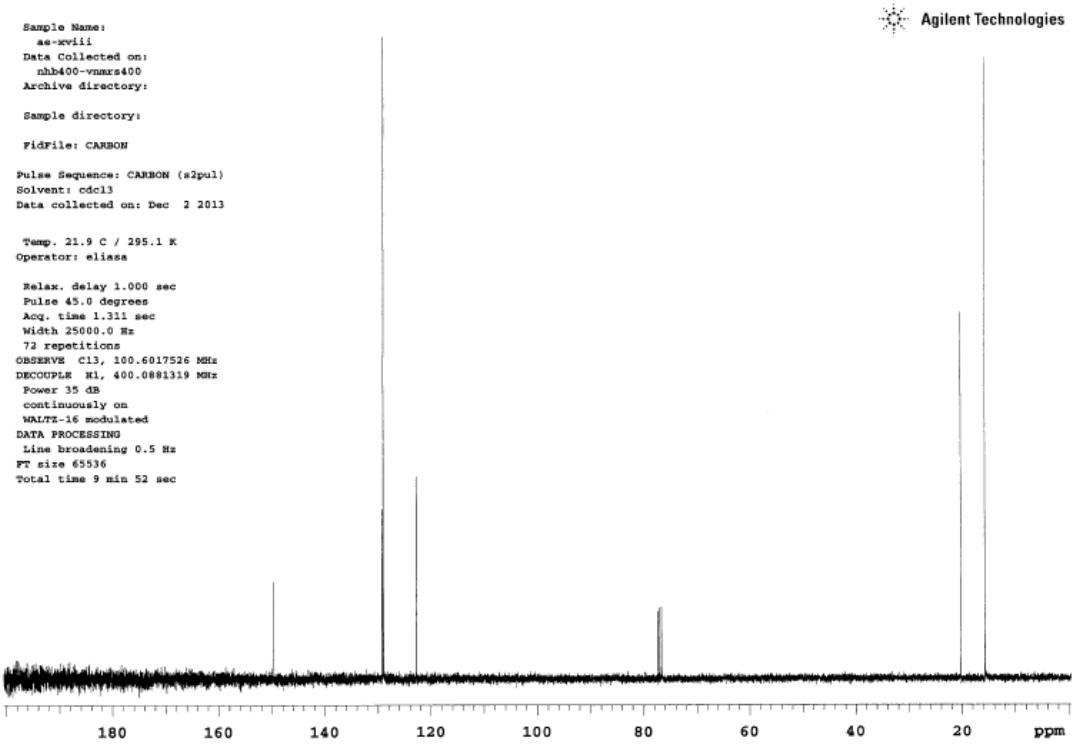
Agilent Technologies
Sample Name:
ae-xviii
Data Collected on:
nhb400-vnmrs400
Archive directory:
Sample directory:
FidFile: CARBON
Pulse Sequence: CARBON (s2pul)
Solvent: cdcl3
Data collected on: Dec 2 2013
Temp. 21.9 C / 295.1 K
Operator: eliasa
Relax. delay 1.000 sec
Pulse 45.0 degrees
Acq. time 1.311 sec
Width 25000.0 Hz
72 repetitions
OBSERVE C13, 100.6017526 MHz
DECOUPLE H1, 400.0881319 MHz
Power 35 dB
continuously on
WALTZ-16 modulated
DATA PROCESSING
Line broadening 0.5 Hz
FT size 65536
Total time 9 min 52 sec
180
160
140
120
100
80
60
40
20
ppm

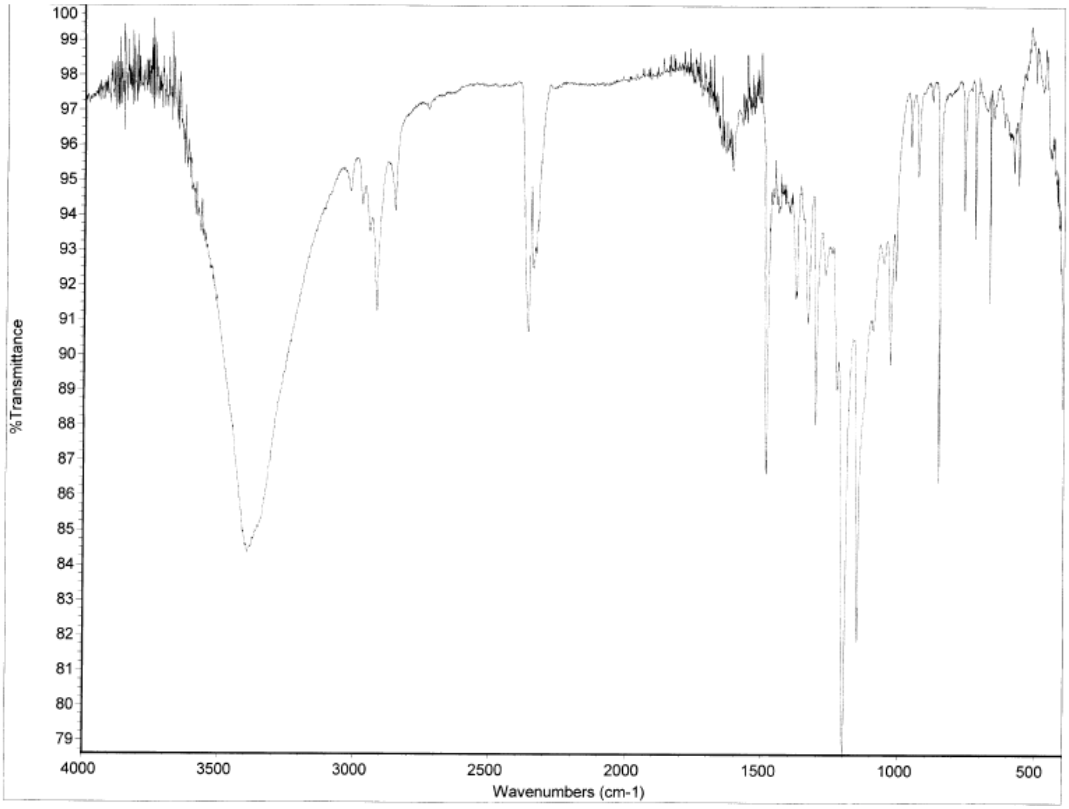
%Transmittance
100
99
98
97
96
95
94
93
92
91
90
89
88
87
86
85
84
83
82
81
80
79
4000
3500
3000
2500
2000
1500
1000
500
Wavenumbers (cm-1)

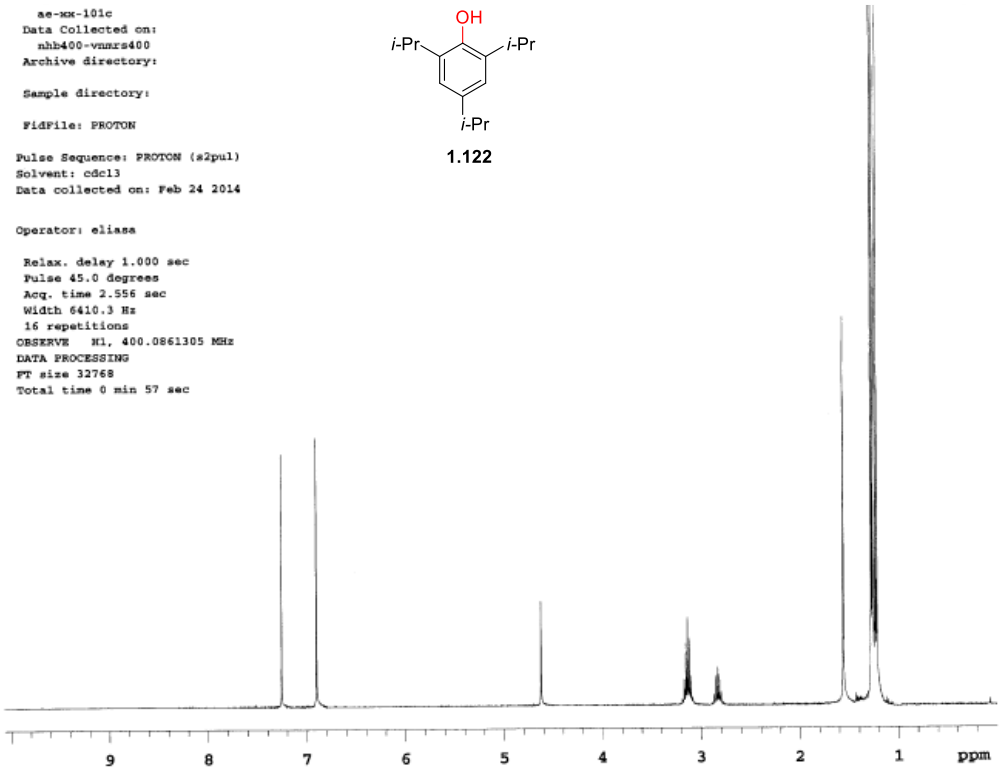
ae-xx-101c
Data Collected on:
nhb400-vnmrs400
Archive directory:
Sample directory:
FidFile: PROTON
Pulse Sequence: PROTON (s2pul)
Solvent: cdcl3
Data collected on: Feb 24 2014
Operator: eliasa
Relax. delay 1.000 sec
Pulse 45.0 degrees
Acq. time 2.556 sec
Width 6410.3 Hz
16 repetitions
OBSERVE H1, 400.0861305 MHz
DATA PROCESSING
FT size 32768
Total time 0 min 57 sec
OH
i-Pr
i-Pr
i-Pr
1.122
9
8
7
6
5
4
3
2
1
ppm

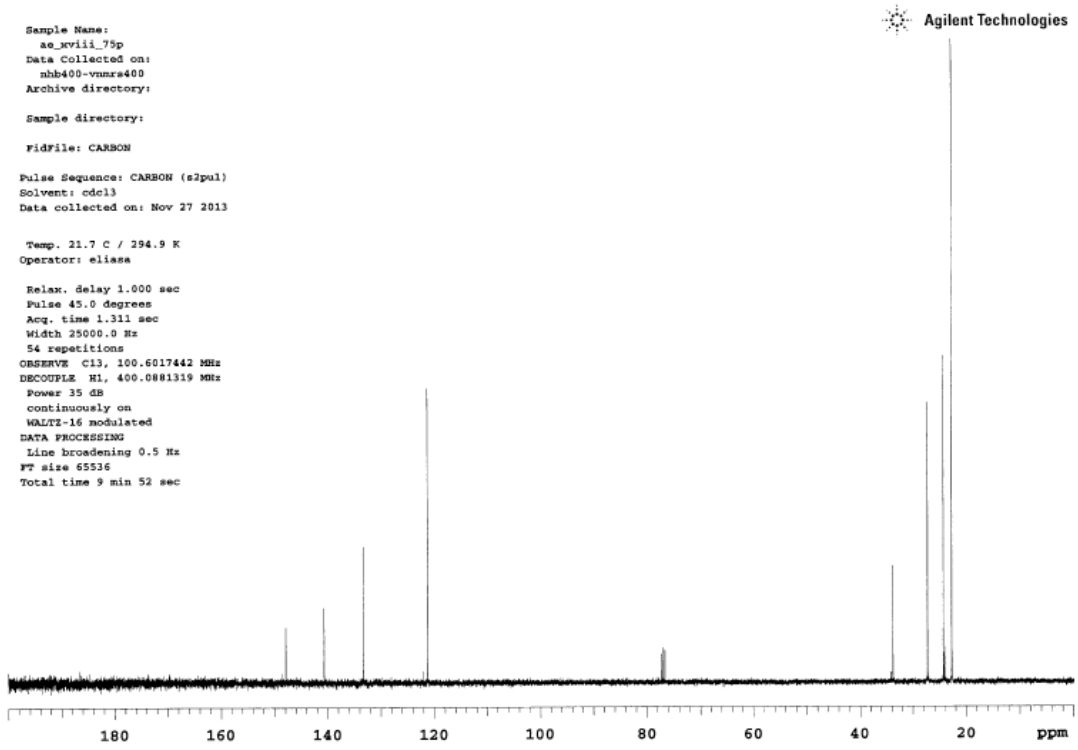
Agilent Technologies
Sample Name:
ae_xviii_75p
Data Collected on:
nhb400-vnmrs400
Archive directory:
Sample directory:
FidFile: CARBON
Pulse Sequence: CARBON (s2pul)
Solvent: cdcl3
Data collected on: Nov 27 2013
Temp. 21.7 C / 294.9 K
Operator: eliasa
Relax. delay 1.000 sec
Pulse 45.0 degrees
Acq. time 1.311 sec
Width 25000.0 Hz
54 repetitions
OBSERVE C13, 100.6017442 MHz
DECOUPLE H1, 400.0881319 MHz
Power 35 dB
continuously on
WALTZ-16 modulated
DATA PROCESSING
Line broadening 0.5 Hz
FT size 65536
Total time 9 min 52 sec
180
160
140
120
100
80
60
40
20
ppm

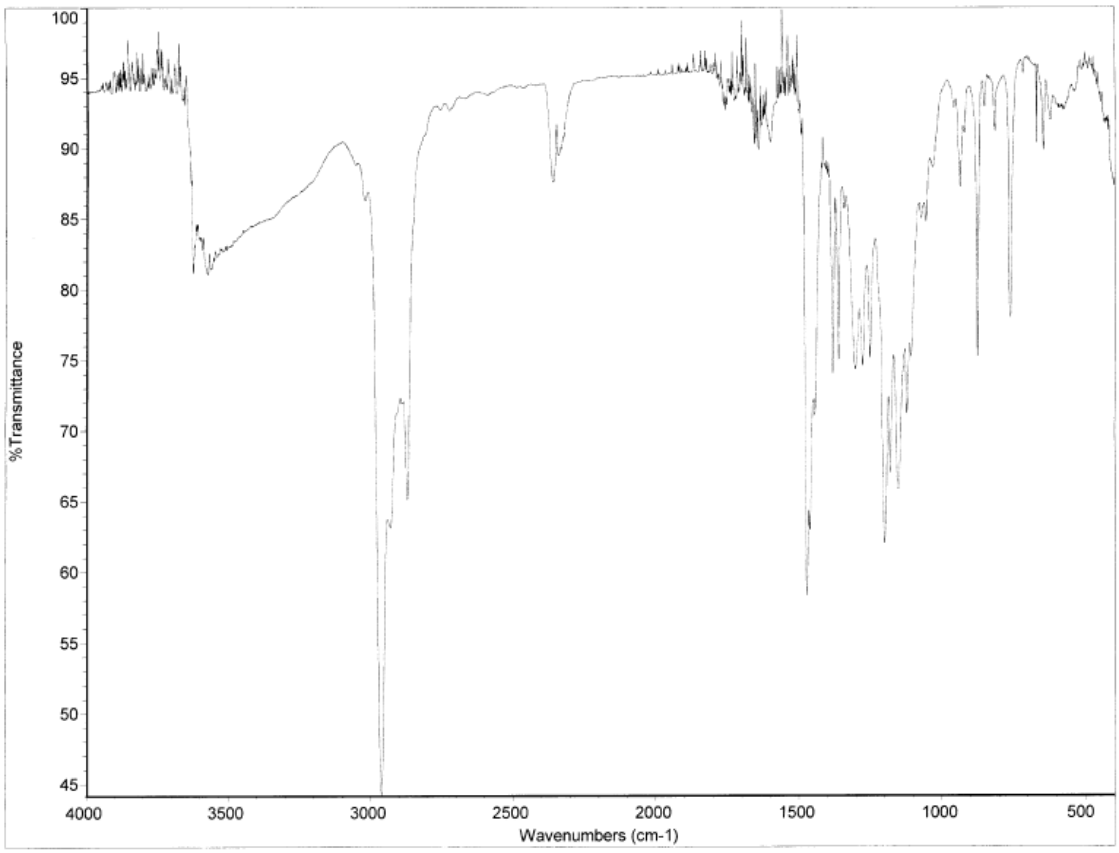
100
95
90
85
80
75
70
65
60
55
50
45
% Transmittance
4000
3500
3000
2500
2000
1500
1000
500
Wavenumbers (cm-1)

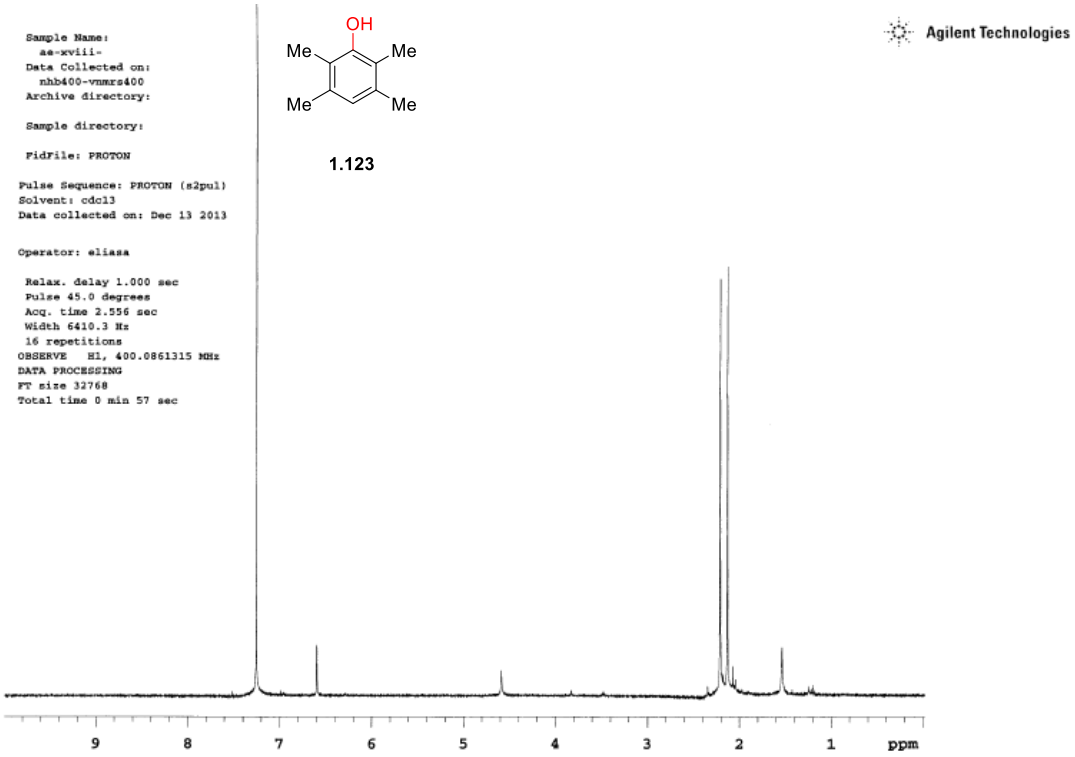
Sample Name:
ae-xviii-
Data Collected on:
nhb400-vnmrs400
Archive directory:
Sample directory:
FidFile: PROTON
Pulse Sequence: PROTON (s2pul)
Solvent: cdcl3
Data collected on: Dec 13 2013
Operator: eliasa
Relax. delay 1.000 sec
Pulse 45.0 degrees
Acq. time 2.556 sec
Width 6410.3 Hz
16 repetitions
OBSERVE H1, 400.0861315 MHz
DATA PROCESSING
FT size 32768
Total time 0 min 57 sec
OH
Me
Me
Me
Me
1.123
Agilent Technologies
9
8
7
6
5
4
3
2
1
ppm

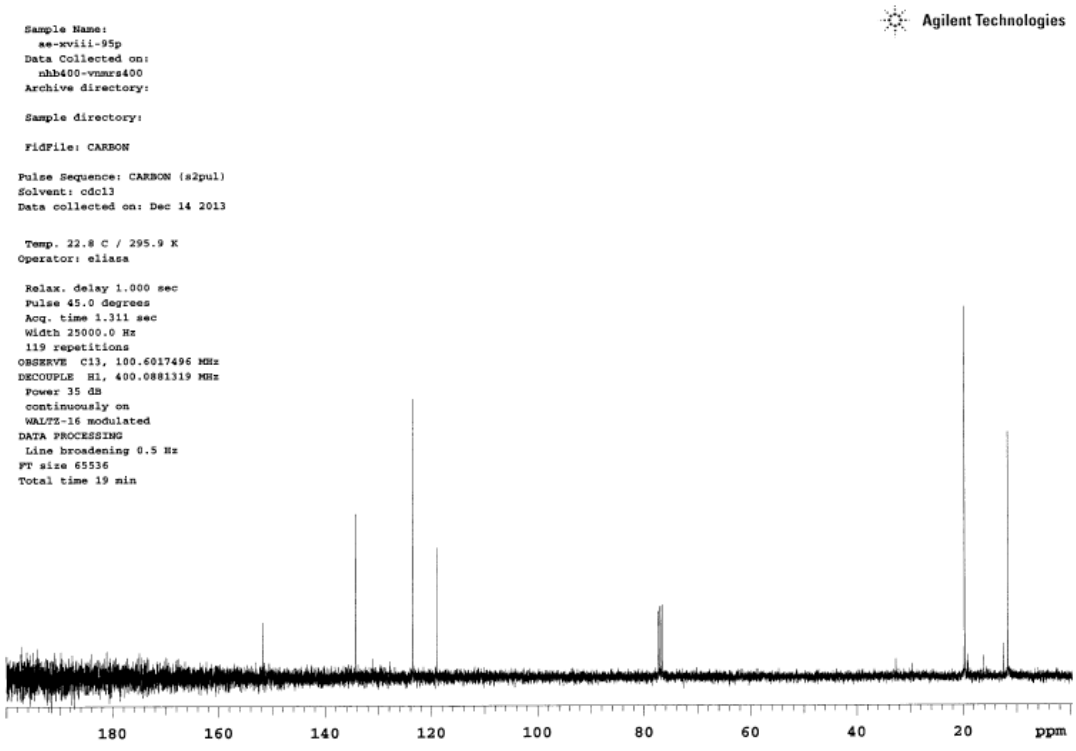
Agilent Technologies
Sample Name:
ae-xviii-95p
Data Collected on:
nhb400-vnmrs400
Archive directory:
Sample directory:
FidFile: CARBON
Pulse Sequence: CARBON (s2pul)
Solvent: cdcl3
Data collected on: Dec 14 2013
Temp. 22.8 C / 295.9 K
Operator: eliasa
Relax. delay 1.000 sec
Pulse 45.0 degrees
Acq. time 1.311 sec
Width 25000.0 Hz
119 repetitions
OBSERVE C13, 100.6017496 MHz
DECOUPLE H1, 400.0881319 MHz
Power 35 dB
continuously on
WALTZ-16 modulated
DATA PROCESSING
Line broadening 0.5 Hz
FT size 65536
Total time 19 min
180
160
140
120
100
80
60
40
20
ppm

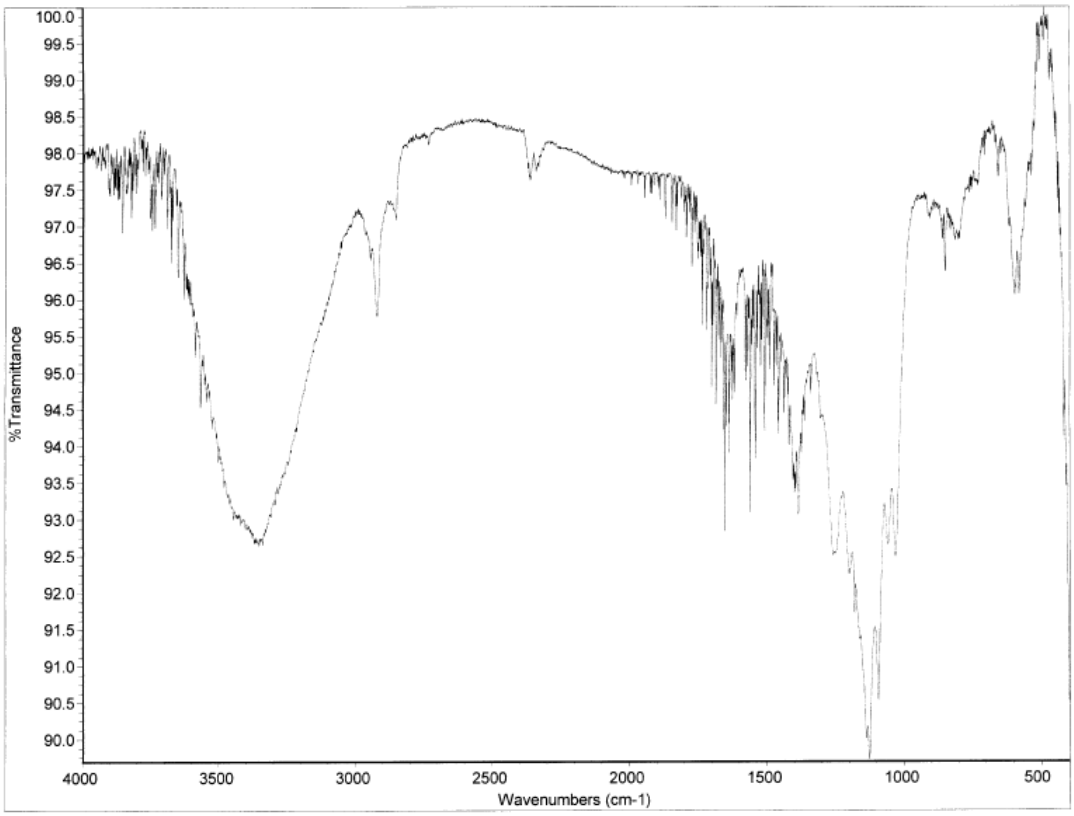
100.0
99.5
99.0
98.5
98.0
97.5
97.0
96.5
96.0
95.5
95.0
94.5
94.0
93.5
93.0
92.5
92.0
91.5
91.0
90.5
90.0
%Transmittance
4000
3500
3000
2500
2000
1500
1000
500
Wavenumbers (cm-1)

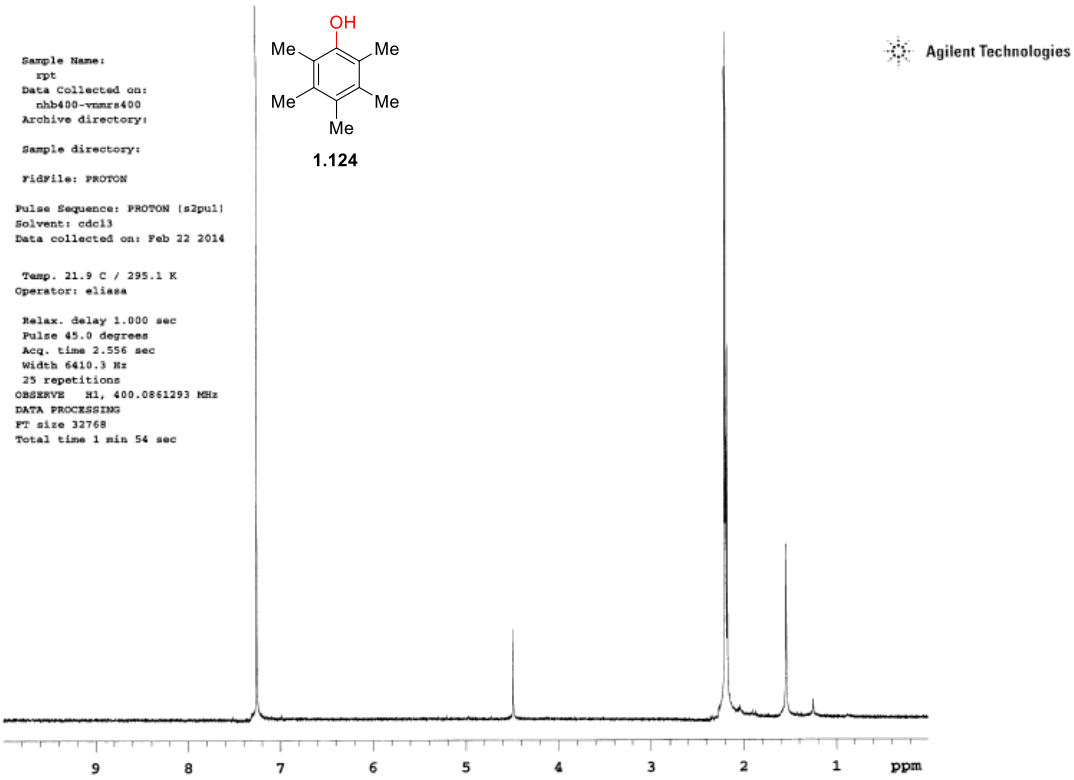
Sample Name:
rpt
Data Collected on:
nhb400-vnmrs400
Archive directory:
Sample directory:
FidFile: PROTON
Pulse Sequence: PROTON (s2pul)
Solvent: cdcl3
Data collected on: Feb 22 2014
Temp. 21.9 C / 295.1 K
Operator: elissa
Relax. delay 1.000 sec
Pulse 45.0 degrees
Acq. time 2.556 sec
Width 6410.3 Hz
25 repetitions
OBSERVE H1, 400.0861293 MHz
DATA PROCESSING
FT size 32768
Total time 1 min 54 sec
OH
Me
Me
Me
Me
Me
1.124
Agilent Technologies
9
8
7
6
5
4
3
2
1
ppm

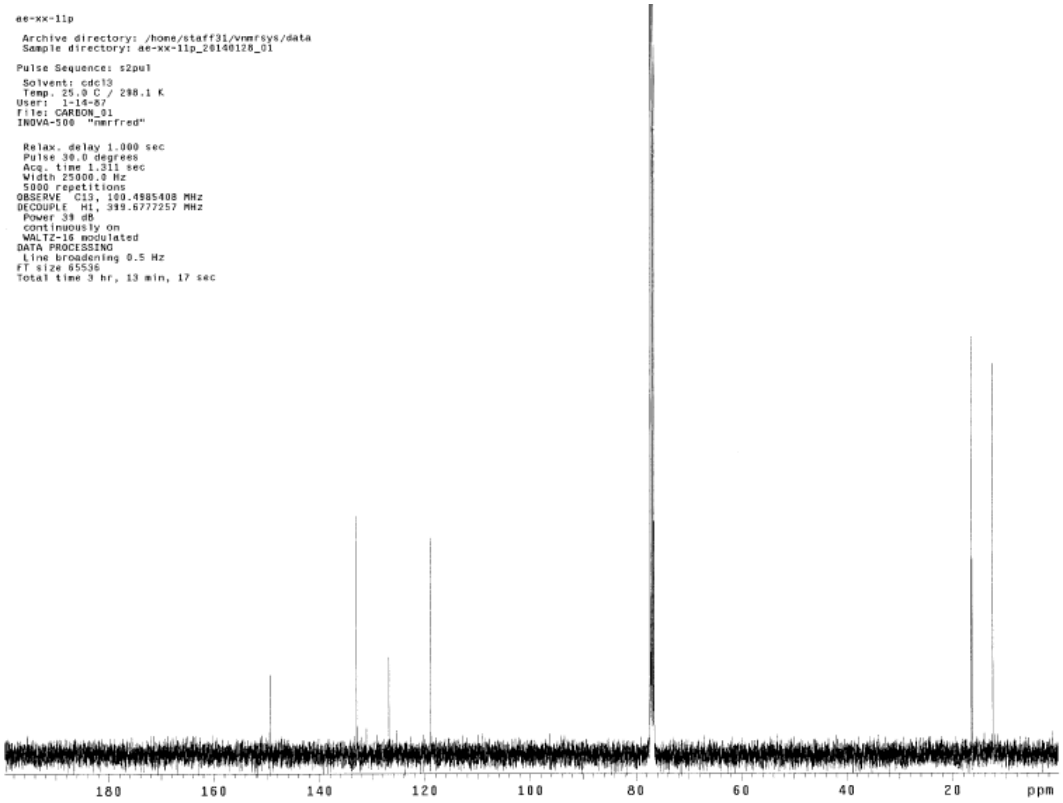
ae-xx-11p
Archive directory: /home/staff31/vnmrsys/data
Sample directory: ae-xx-11p_20140128_01
Pulse Sequence: s2pul
Solvent: cdcl3
Temp. 25.0 C / 298.1 K
User: 1-14-87
File: CARBON_01
INOVA-500 "nmrfred"
Relax. delay 1.000 sec
Pulse 30.0 degrees
Acq. time 1.311 sec
Width 25000.0 Hz
5000 repetitions
OBSERVE C13, 100.4985408 MHz
DECOUPLE H1, 399.6777257 MHz
Power 39 dB
continuously on
WALTZ-16 modulated
DATA PROCESSING
Line broadening 0.5 Hz
FT size 65536
Total time 3 hr, 13 min, 17 sec
180
160
140
120
100
80
60
40
20
ppm

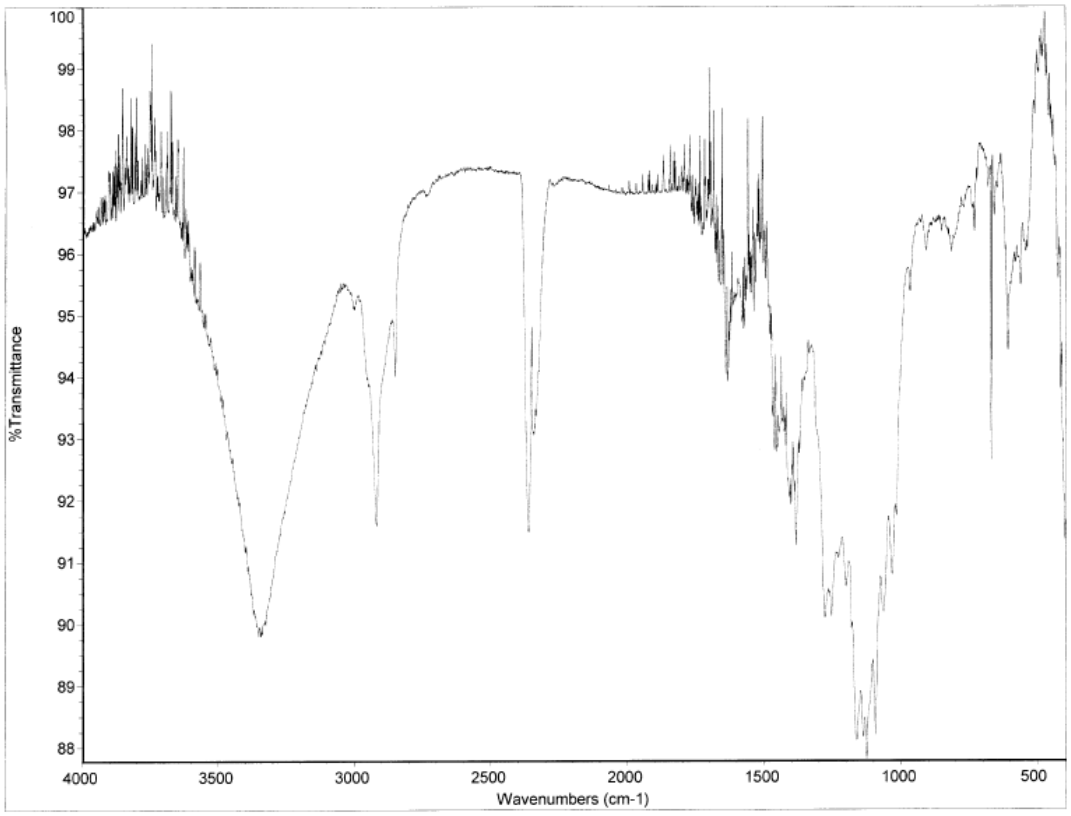
100
99
98
97
96
95
94
93
92
91
90
89
88
%Transmittance
4000
3500
3000
2500
2000
1500
1000
500
Wavenumbers (cm-1)

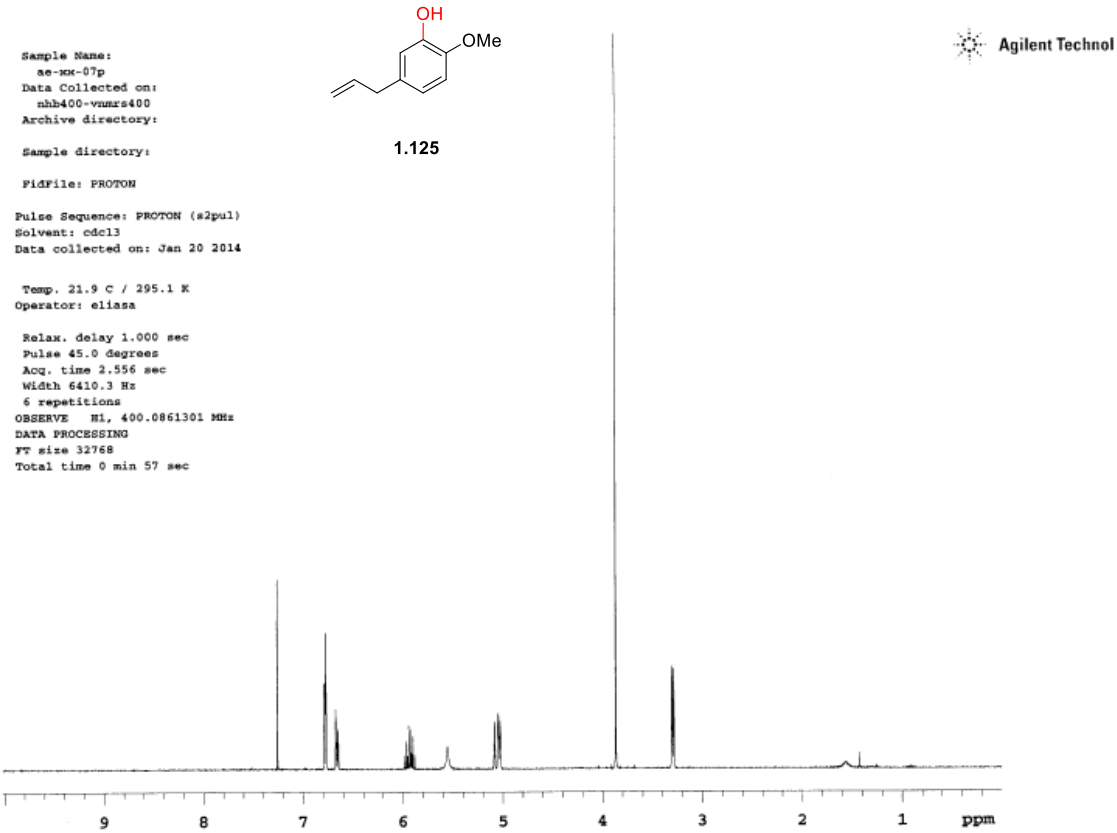
OH
OMe
1.125
Agilent Technol
Sample Name:
ae-xx-07p
Data Collected on:
nhb400-vnmrs400
Archive directory:
Sample directory:
FidFile: PROTON
Pulse Sequence: PROTON (s2pul)
Solvent: cdcl3
Data collected on: Jan 20 2014
Temp. 21.9 C / 295.1 K
Operator: eliasa
Relax. delay 1.000 sec
Pulse 45.0 degrees
Acq. time 2.556 sec
Width 6410.3 Hz
6 repetitions
OBSERVE H1, 400.0861301 MHz
DATA PROCESSING
FT size 32768
Total time 0 min 57 sec
9
8
7
6
5
4
3
2
1
ppm

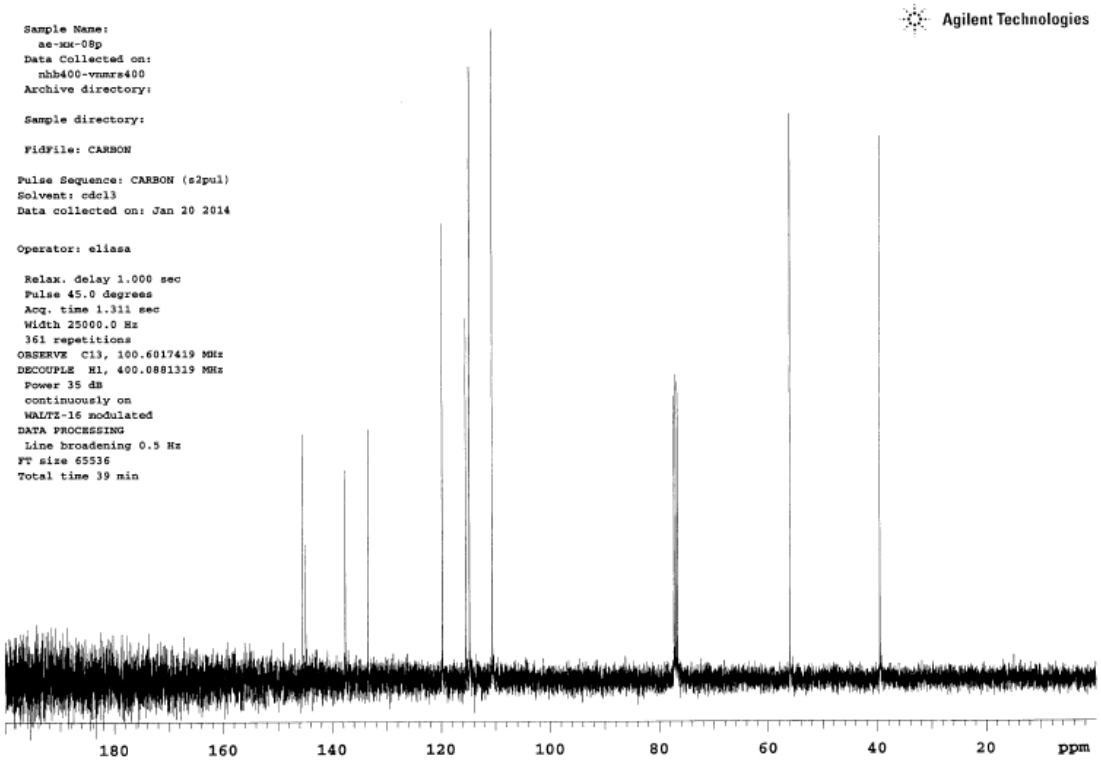
Agilent Technologies
Sample Name:
ae-xx-08p
Data Collected on:
nhb400-vnmrs400
Archive directory:
Sample directory:
FidFile: CARBON
Pulse Sequence: CARBON (s2pul)
Solvent: cdcl3
Data collected on: Jan 20 2014
Operator: eliasa
Relax. delay 1.000 sec
Pulse 45.0 degrees
Acq. time 1.311 sec
Width 25000.0 Hz
361 repetitions
OBSERVE C13, 100.6017419 MHz
DECOUPLE H1, 400.0881319 MHz
Power 35 dB
continuously on
WALTZ-16 modulated
DATA PROCESSING
Line broadening 0.5 Hz
FT size 65536
Total time 39 min
180
160
140
120
100
80
60
40
20
ppm

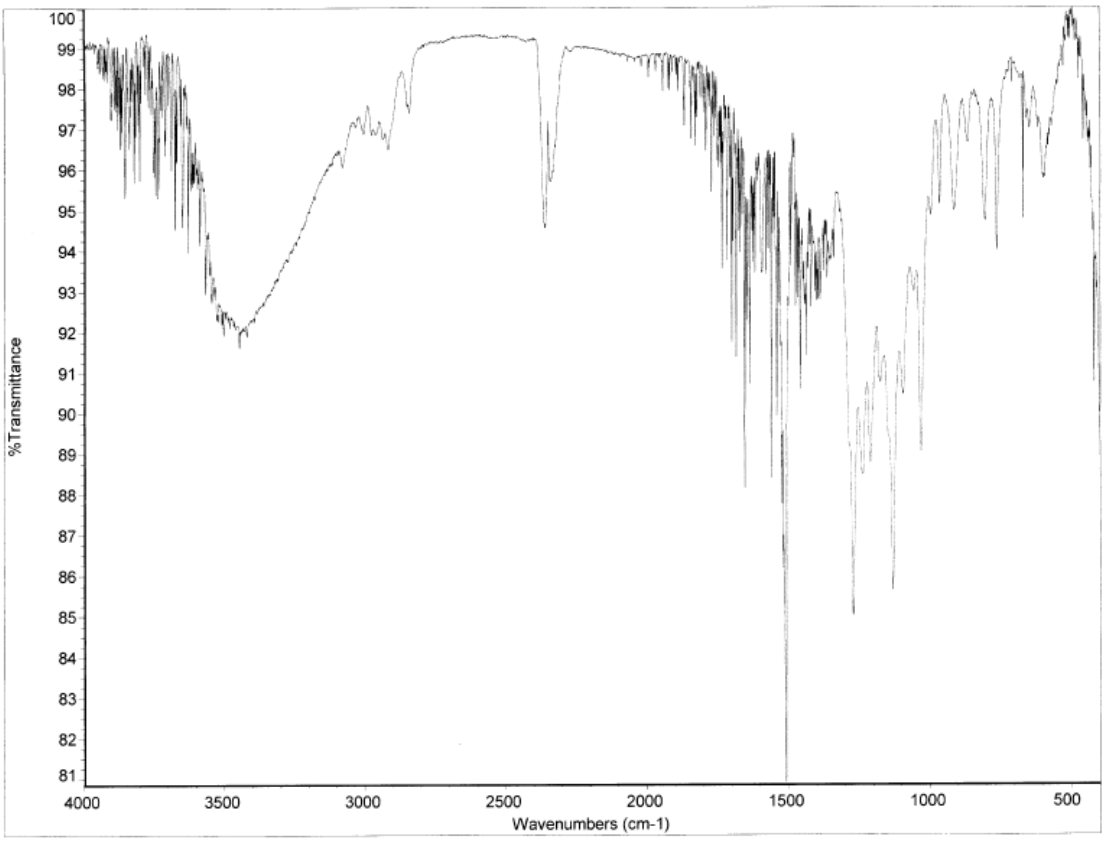
%Transmittance
100
99
98
97
96
95
94
93
92
91
90
89
88
87
86
85
84
83
82
81
4000
3500
3000
2500
2000
1500
1000
500
Wavenumbers (cm-1)

Sample Name:
ae-xx-3p2
Data Collected on:
nhb400-vnmrs400
Archive directory:

Sample directory:

FidFile: PROTON

Pulse Sequence: PROTON (s2pul)
Solvent: cdcl3
Data collected on: Jan 18 2014

Temp. 21.6 C / 294.8 K
Operator: eliasa

Relax. delay 1.000 sec
Pulse 45.0 degrees
Acq. time 2.556 sec
Width 6410.3 Hz
10 repetitions
OBSERVE H1, 400.0861305 MHz
DATA PROCESSING
FT size 32768
Total time 0 min 57 sec

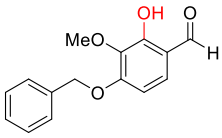

1.44

Agilent Technologies

ae_xx_03p2

Archive directory: /home/staff31/vnmrsys/data
Sample directory: ae_xx_03p2_20140117_01

Pulse Sequence: s2pul
Solvent: cdcl3
Temp. 25.0 C / 298.1 K
User: 1-14-07
File: CARBON_01
INOVA-500 "marfred"

Relax. delay 2.000 sec
Pulse 30.0 degrees
Acq. time 1.311 sec
Width 25000.0 Hz
5000 repetitions
OBSERVE C13, 100.4985415 MHz
DECOUPLE H1, 399.6777257 MHz
Power 39 dB
continuously on
WALTZ-16 modulated
DATA PROCESSING
line broadening 0.5 Hz
FT size 65536
Total time 4 hr, 36 min, 37 sec

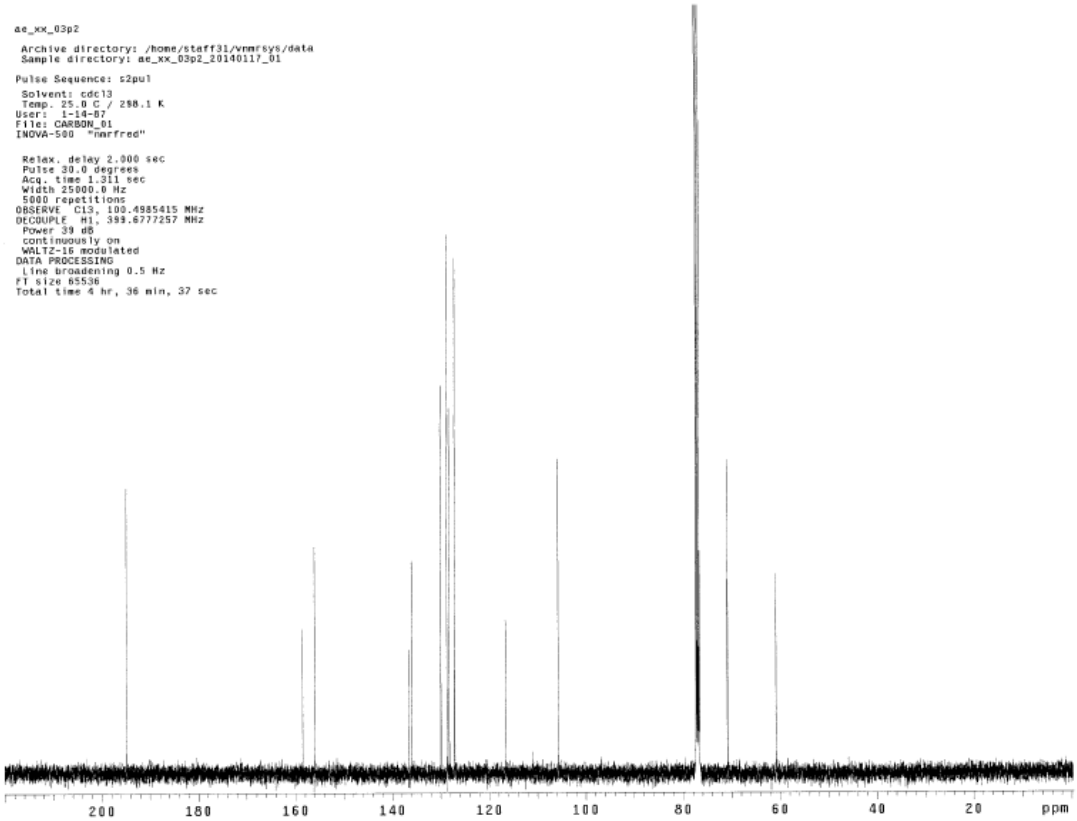

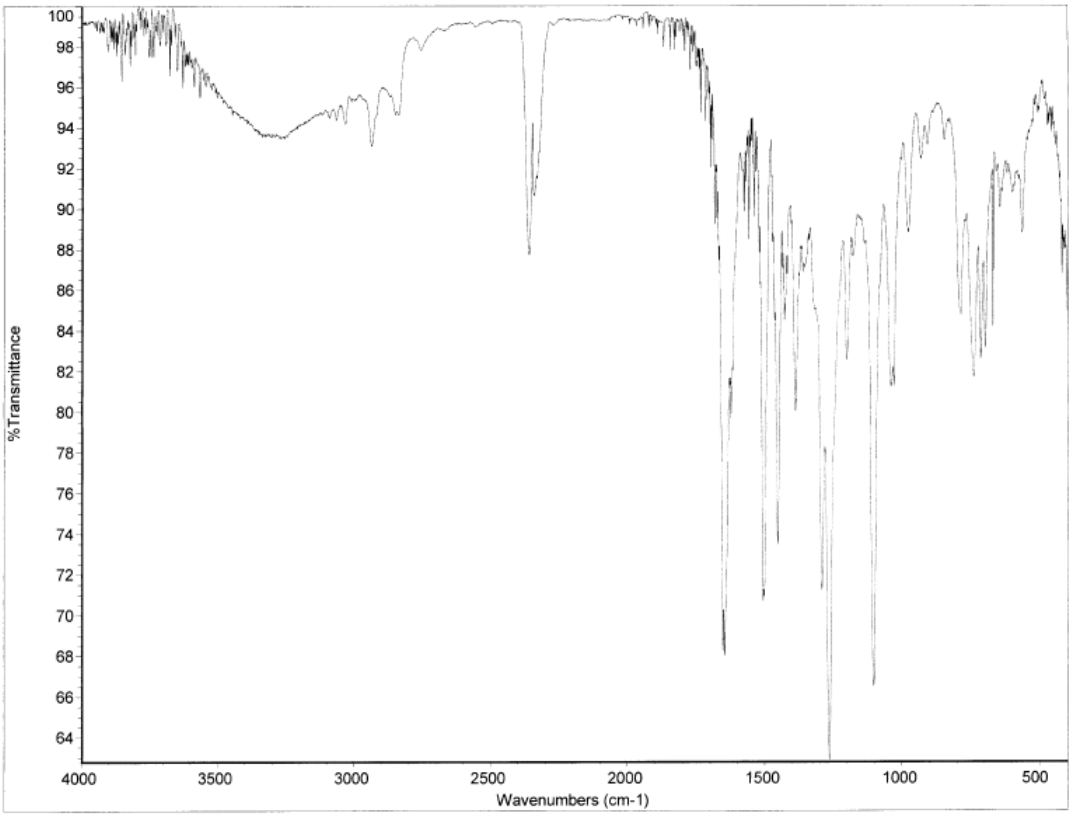
%Transmittance
100
98
96
94
92
90
88
86
84
82
80
78
76
74
72
70
68
66
64
4000
3500
3000
2500
2000
1500
1000
500
Wavenumbers (cm-1)

Sample Name:
ae-xix-11p1
Data Collected on:
nhb400-vnmrs400
Archive directory:

Sample directory:

FidFile: PROTON

Pulse Sequence: PROTON (s2pul)
Solvent: cdcl3
Data collected on: Jan 11 2014

Temp. 22.1 C / 295.2 K
Operator: eliasa

Relax. delay 1.000 sec
Pulse 45.0 degrees
Acq. time 2.556 sec
Width 6410.3 Hz
8 repetitions
OBSERVE H1, 400.0861305 MHz
DATA PROCESSING
FT size 32768
Total time 0 min 57 sec

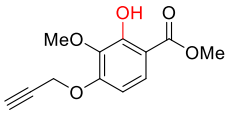

1.46

Agilent Technologies

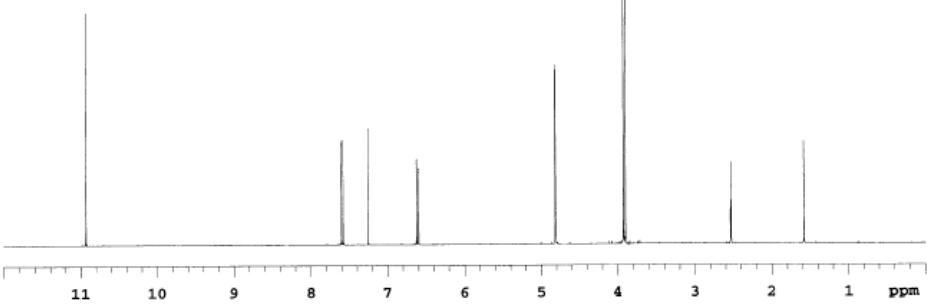

ae_xix_11

Archive directory: /home/staff31/vnmrsys/data
Sample directory: ae_xix_11_20140120_01

Pulse Sequence: s2pul

Solvent: cdcl3
Temp. 25.0 C / 298.1 K
User: 1-14-87
file: CARBON_01
INOVA-500 "nmrfred"

Relax. delay 1.000 sec
Pulse 30.0 degrees
Acq. time 1.311 sec
Width 25000.0 Hz
5000 repetitions
OBSERVE C13, 100.4985408 MHz
DECOUPLE H1, 399.6777257 MHz
Power 39 dB
continuously on
WALTZ-16 modulated
DATA PROCESSING
Line broadening 0.5 Hz
FT size 65536
Total time 3 hr, 13 min, 17 sec

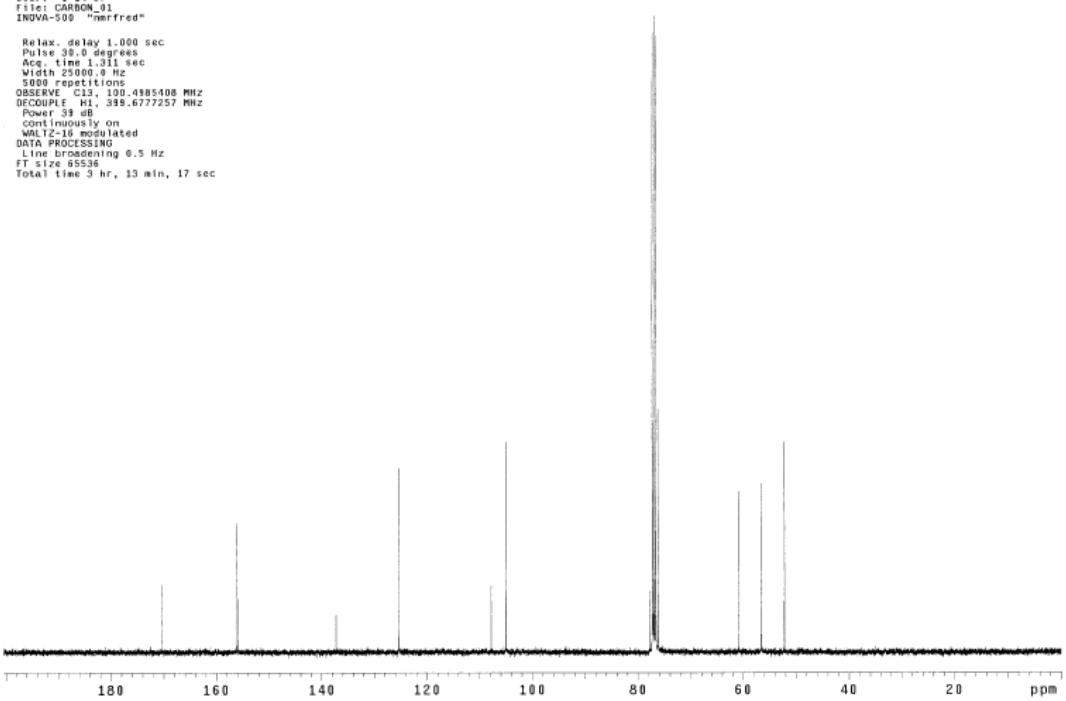

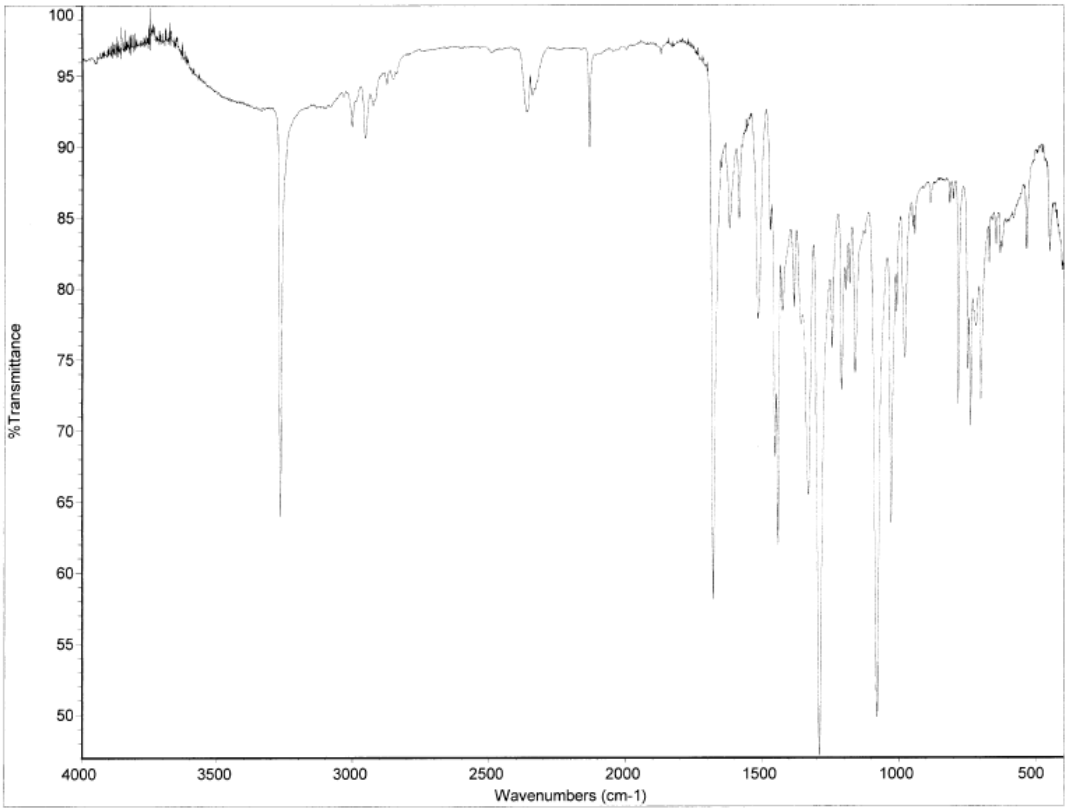
100
95
90
85
80
75
70
65
60
55
50
%Transmittance
4000
3500
3000
2500
2000
1500
1000
500
Wavenumbers (cm-1)

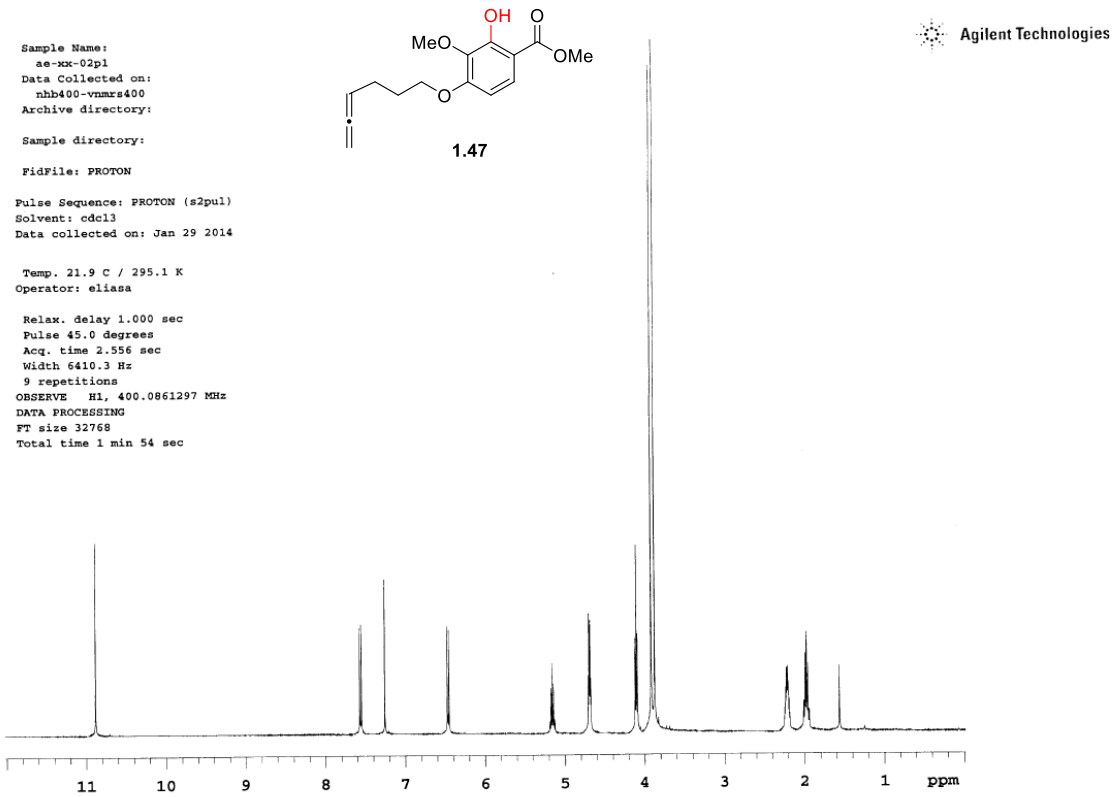
Agilent Technologies
Sample Name:
ae-xx-02p1
Data Collected on:
nhb400-vnmrs400
Archive directory:
Sample directory:
FidFile: PROTON
Pulse Sequence: PROTON (s2pul)
Solvent: cdcl3
Data collected on: Jan 29 2014
Temp. 21.9 C / 295.1 K
Operator: eliasa
Relax. delay 1.000 sec
Pulse 45.0 degrees
Acq. time 2.556 sec
Width 6410.3 Hz
9 repetitions
OBSERVE H1, 400.0861297 MHz
DATA PROCESSING
FT size 32768
Total time 1 min 54 sec
OH
O
MeO
OMe
O
1.47
11
10
9
8
7
6
5
4
3
2
1
ppm

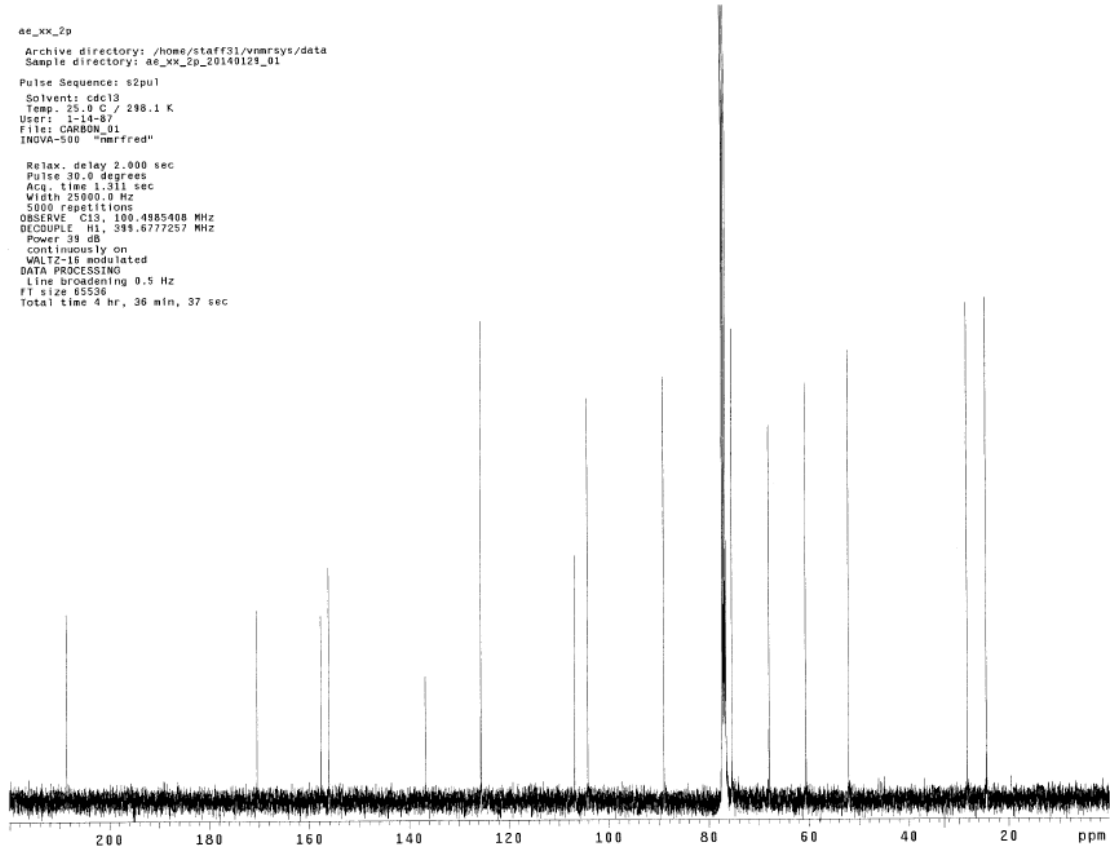
ae_xx_2p
Archive directory: /home/staff31/vnmrsys/data
Sample directory: ae_xx_2p_20140129_01
Pulse Sequence: s2pul
Solvent: cdcl3
Temp. 25.0 C / 298.1 K
User: 1-14-87
File: CARBON_01
INOVA-500 "nmrfred"
Relax. delay 2.000 sec
Pulse 30.0 degrees
Acq. time 1.311 sec
Width 25000.0 Hz
5000 repetitions
OBSERVE C13, 100.4985408 MHz
DECOUPLE H1, 399.6777257 MHz
Power 39 dB
continuously on
WALTZ-16 modulated
DATA PROCESSING
Line broadening 0.5 Hz
FT size 65536
Total time 4 hr, 36 min, 37 sec
200
180
160
140
120
100
80
60
40
20
ppm

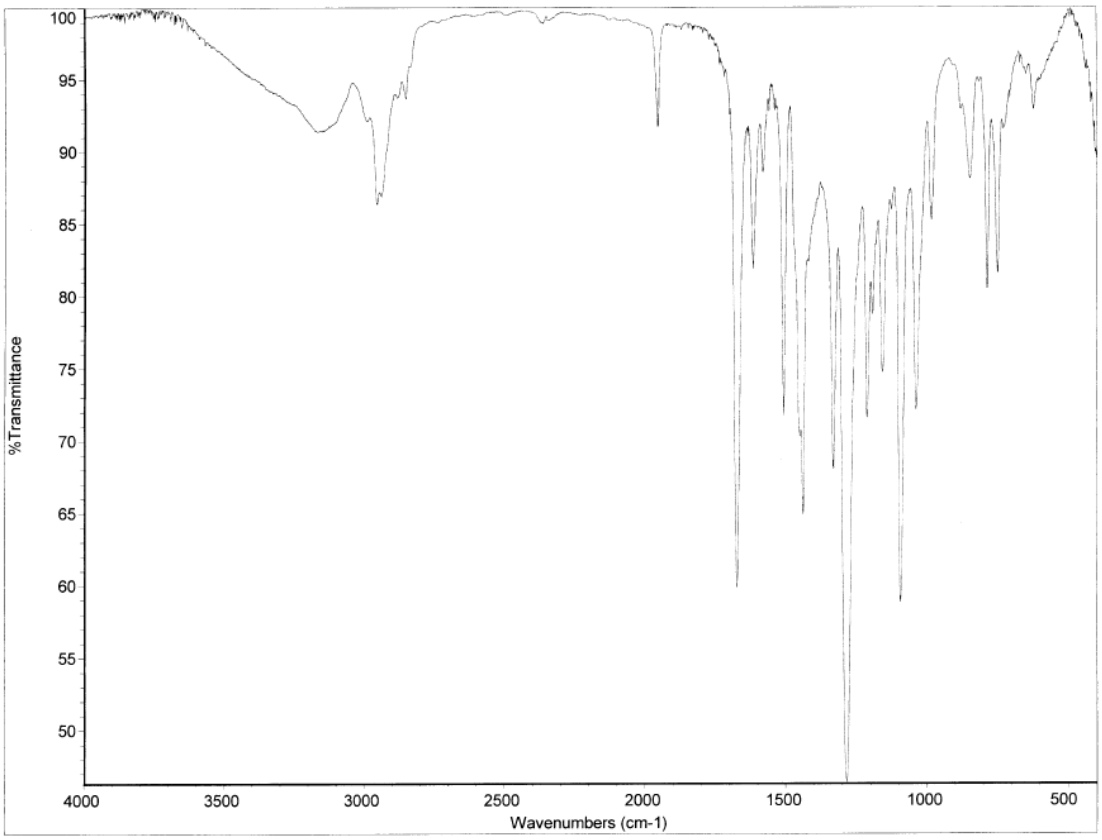
100
95
90
85
80
75
70
65
60
55
50
%Transmittance
4000
3500
3000
2500
2000
1500
1000
500
Wavenumbers (cm-1)

Agilent Technologies

Sample Name:
ae-xx-13p1
Data Collected on:
nhb400-vnmrs400
Archive directory:

Sample directory:

FidFile: PROTON

Pulse Sequence: PROTON (s2pul)
Solvent: cdcl3
Data collected on: Jan 28 2014

Temp. 22.2 C / 295.4 K
Operator: eliasa

Relax. delay 1.000 sec
Pulse 45.0 degrees
Acq. time 2.556 sec
Width 6410.3 Hz
11 repetitions
OBSERVE H1, 400.0861305 MHz
DATA PROCESSING
FT size 32768
Total time 0 min 57 sec

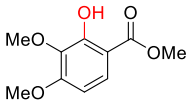

1.43

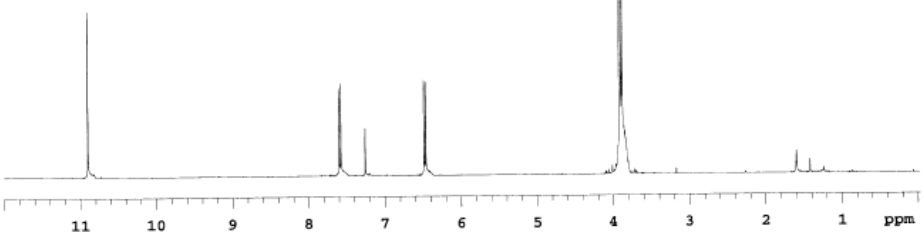

Gradient Shimming

Agilent Technologies

Sample Name:
ae-xx-13p1
Data Collected on:
nhb400-vnmrs400
Archive directory:
/home/space/data
Sample directory:
ae-xx-13p1_20140128_02
FidFile: CARBON

Pulse Sequence: CARBON (s2pul)
Solvent: cdcl3
Data collected on: Jan 28 2014

Temp. 22.3 C / 295.4 K
Operator: eliasa

Relax. delay 1.000 sec
Pulse 45.0 degrees
Acq. time 1.311 sec
Width 25000.0 Hz
311 repetitions
OBSERVE C13, 100.6017396 MHz
DECOUPLE H1, 400.0881319 MHz
Power 35 dB
continuously on
WALTZ-16 modulated
DATA PROCESSING
Line broadening 0.5 Hz
FT size 65536
Total time 19 min

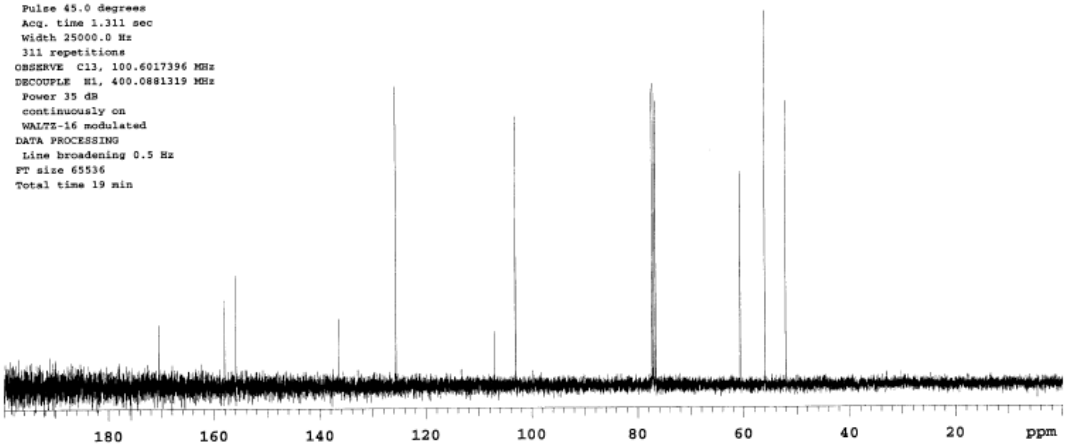

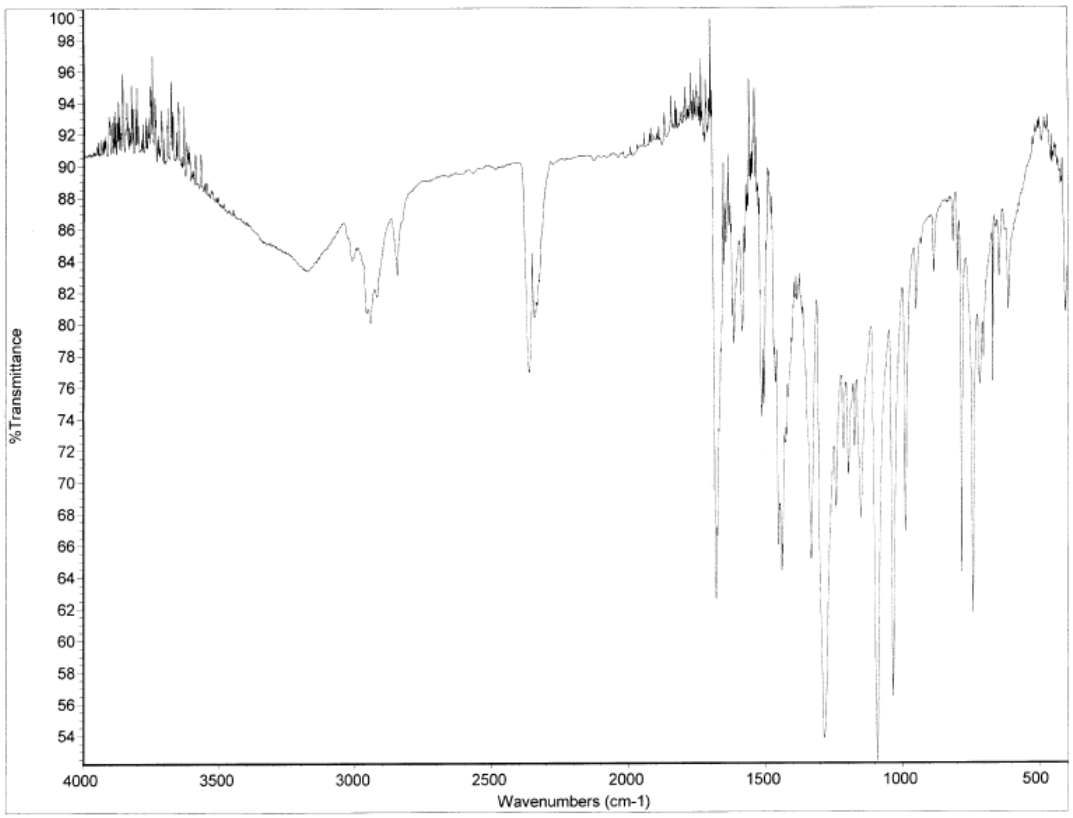
%Transmittance
100
98
96
94
92
90
88
86
84
82
80
78
76
74
72
70
68
66
64
62
60
58
56
54
4000
3500
3000
2500
2000
1500
1000
500
Wavenumbers (cm-1)

Sample Name:
ae-xix-08p1
Data Collected on:
nbb400-vnmrs400
Archive directory:

Sample directory:

FidFile: PROTON

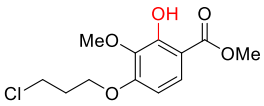

1.55

Pulse Sequence: PROTON (s2pul)
Solvent: cdcl3
Data collected on: Jan 9 2014

Operator: eliasa

Relax. delay 1.000 sec
Pulse 45.0 degrees
Acq. time 2.556 sec
Width 6410.3 Hz
16 repetitions
OBSERVE H1, 400.0861305 MHz
DATA PROCESSING
FT size 32768
Total time 0 min 57 sec

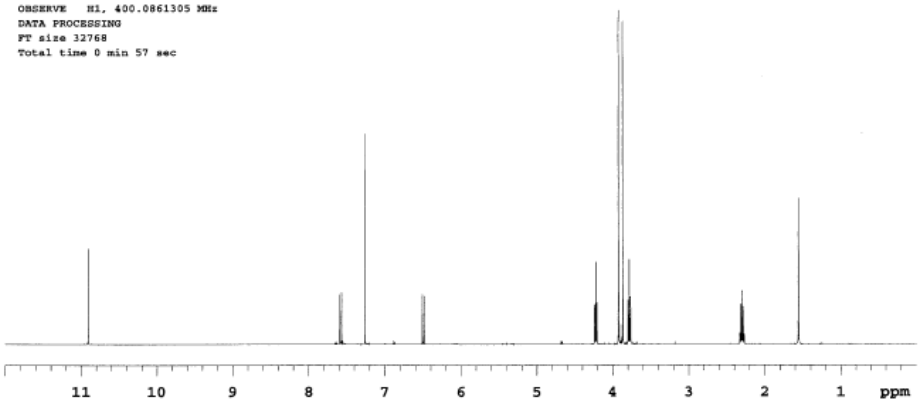

ae_xix_08p

Archive directory: /home/staff31/vnmrsys/data
Sample directory: ae_xix_08p_20140121_01

Pulse Sequence: s2pul
Solvent: cdcl3
Temp. 25.0 C / 298.1 K
User: 1-14-87
File: CARBON_01
INOVA-500 "nmrfred"

Relax. delay 2.000 sec
Pulse 30.0 degrees
Acq. time 1.311 sec
Width 25000.0 Hz
5000 repetitions
OBSERVE C13, 100.4985400 MHz
DECOUPLE H1, 399.6777257 MHz
Power 39 dB
continuously on
WALTZ-16 modulated
DATA PROCESSING
Line broadening 0.5 Hz
FT size 65536
Total time 4 hr, 36 min, 37 sec

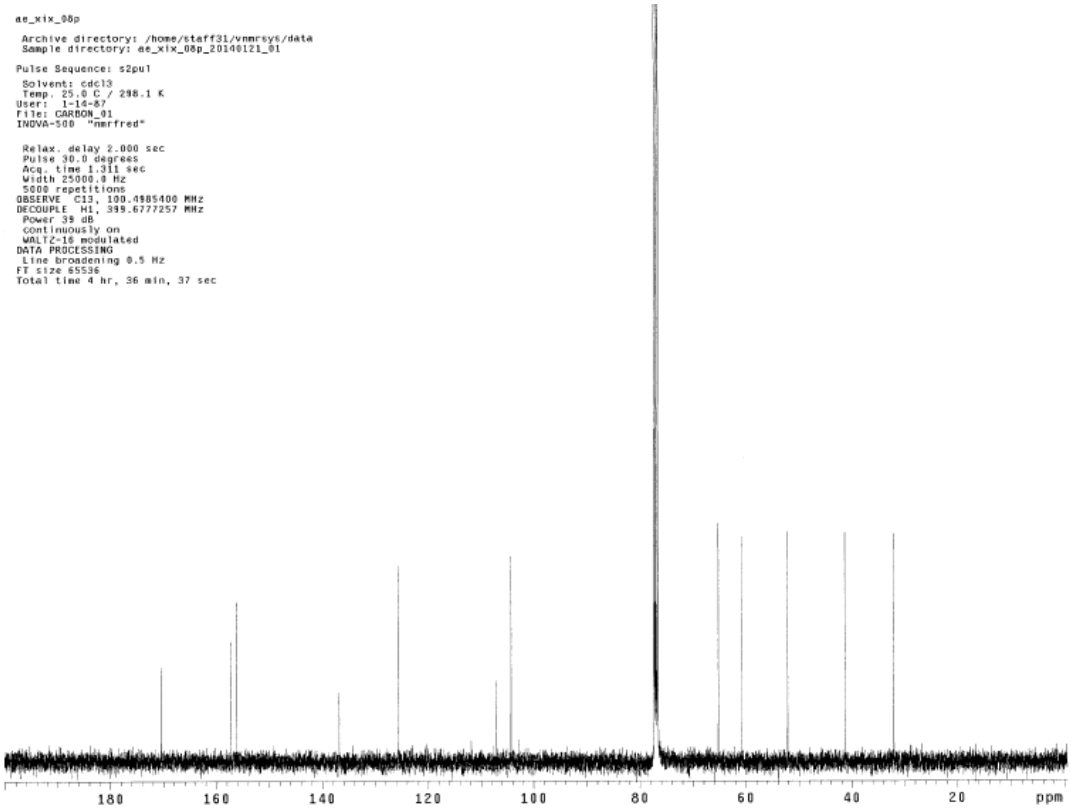

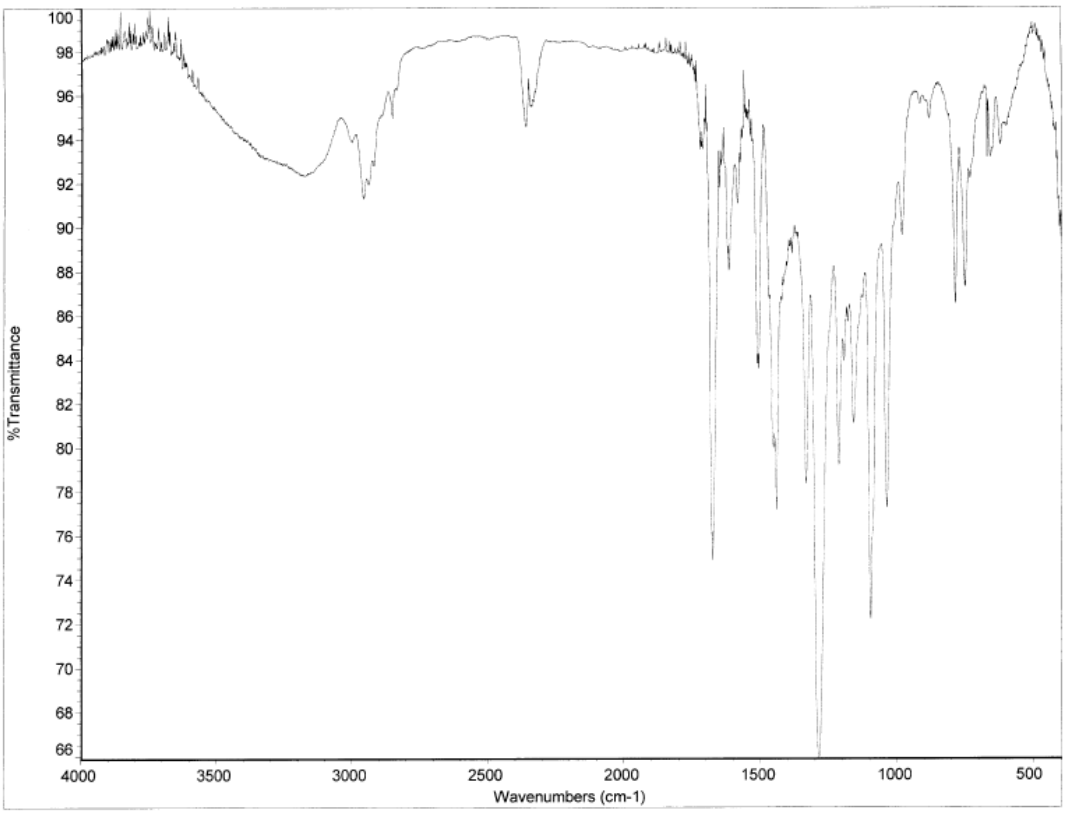
%Transmittance
100
98
96
94
92
90
88
86
84
82
80
78
76
74
72
70
68
66
4000
3500
3000
2500
2000
1500
1000
500
Wavenumbers (cm-1)

Sample Name:
ae-xix-09p1
Data Collected on:
nhb400-vnmrs400
Archive directory:

Sample directory:

FidFile: PROTON

Pulse Sequence: PROTON (s2pul)
Solvent: cdcl3
Data collected on: Jan 15 2014

Temp. 21.4 C / 294.6 K
Operator: eliasa

Relax. delay 1.000 sec
Pulse 45.0 degrees
Acq. time 2.556 sec
Width 6410.3 Hz
10 repetitions
OBSERVE H1, 400.0861301 MHz
DATA PROCESSING
FT size 32768
Total time 1 min 54 sec

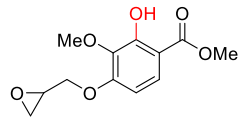

1.51

Agilent Technologies

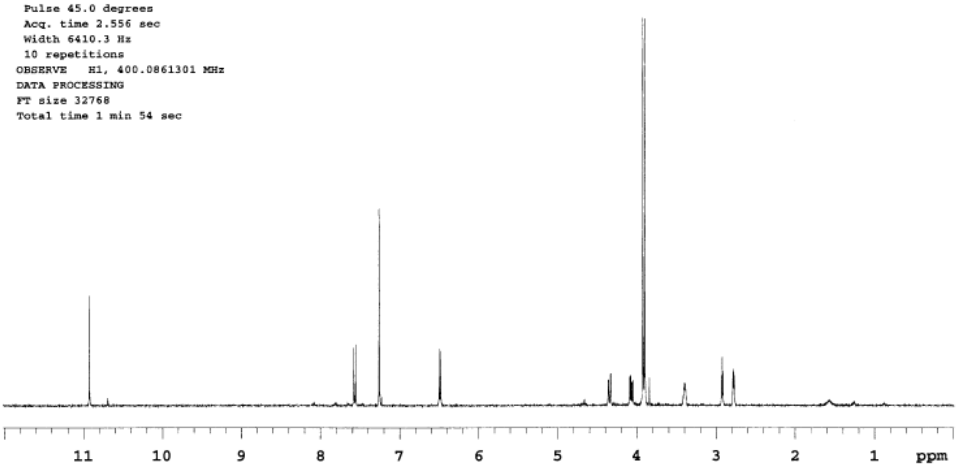

ae_xix_09p1

Archive directory: /home/staff31/vnmrsys/data
Sample directory: ae_xix_09p1_20140117_01

Pulse Sequence: s2pul
Solvent: cdcl3
Temp. 25.0 C / 298.1 K
User: 1-14-87
File: CARBON_01
INOVA-500 "nmrfred"

Relax. delay 1.000 sec
Pulse 30.0 degrees
Acq. time 1.311 sec
Width 25000.0 Hz
5000 repetitions
OBSERVE C13, 100.4985408 MHz
DECOUPLE H1, 399.6777257 MHz
Power 39 dB
continuously On
WALTZ-16 modulated
DATA PROCESSING
Line broadening 0.5 Hz
FT size 65536
Total time 3 hr, 13 min, 17 sec

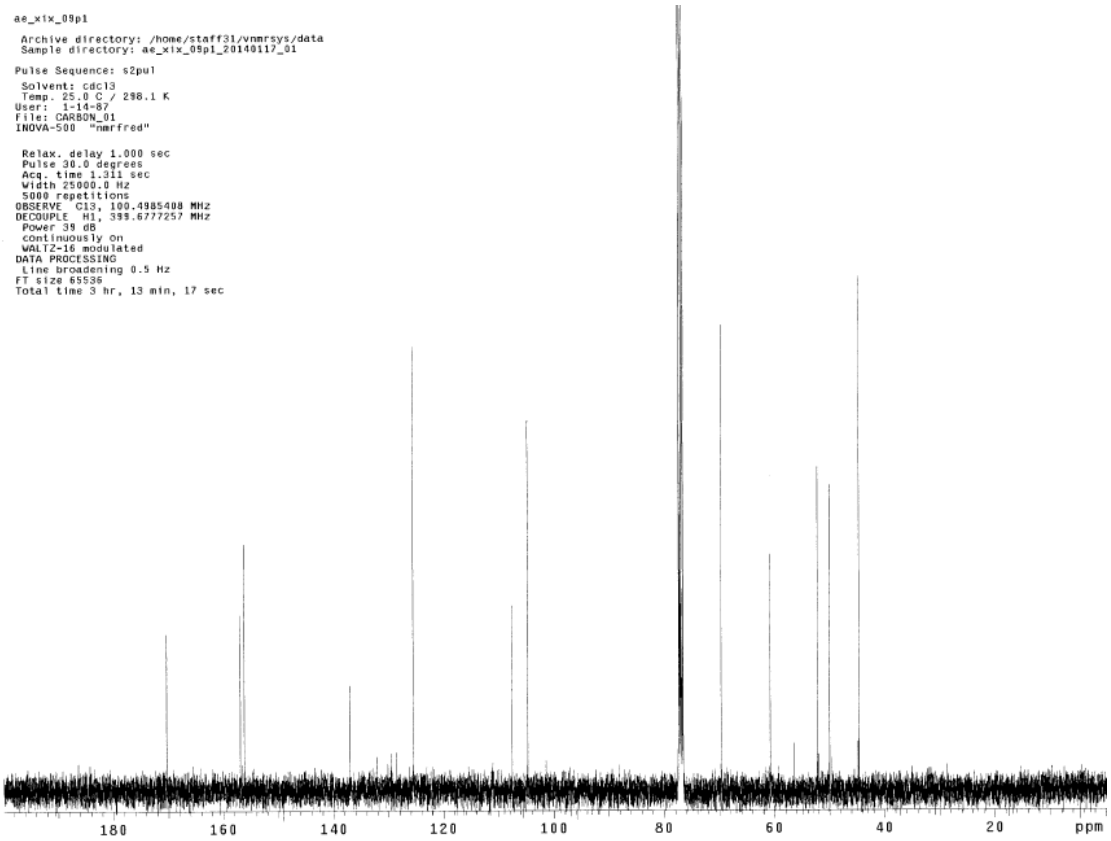

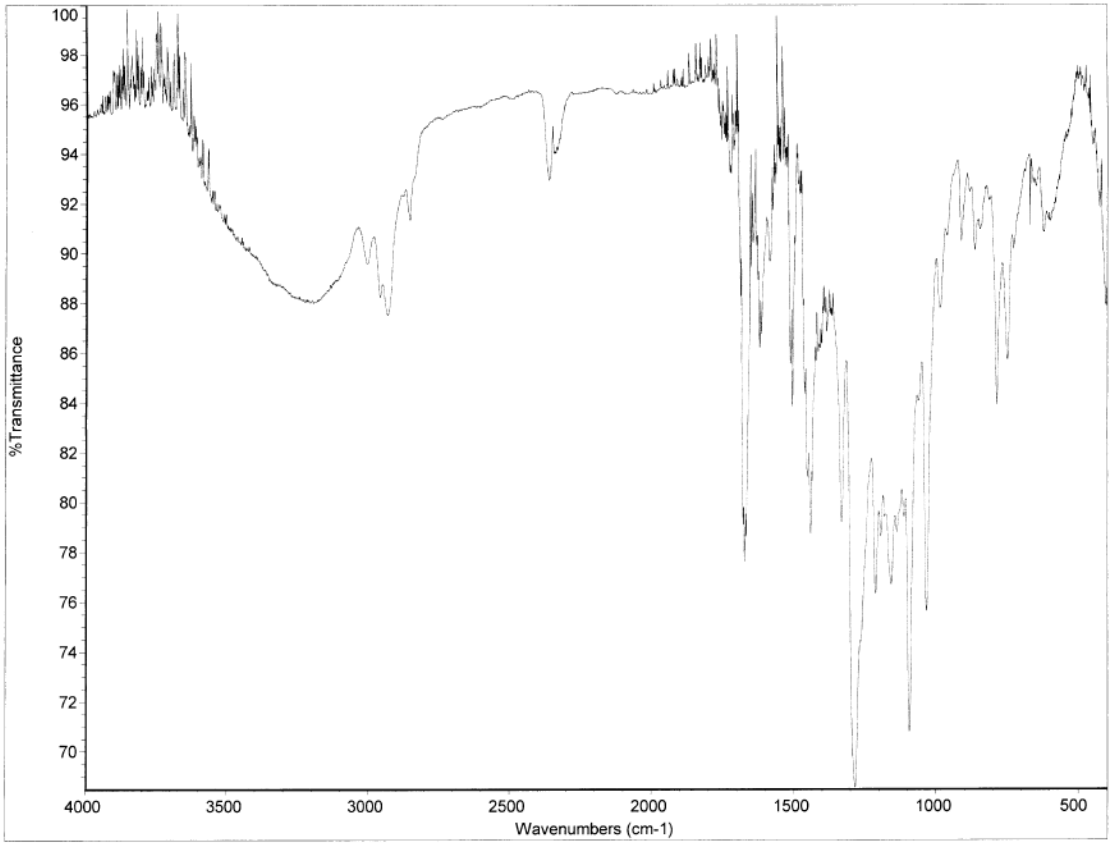
%Transmittance
100
98
96
94
92
90
88
86
84
82
80
78
76
74
72
70
4000
3500
3000
2500
2000
1500
1000
500
Wavenumbers (cm-1)

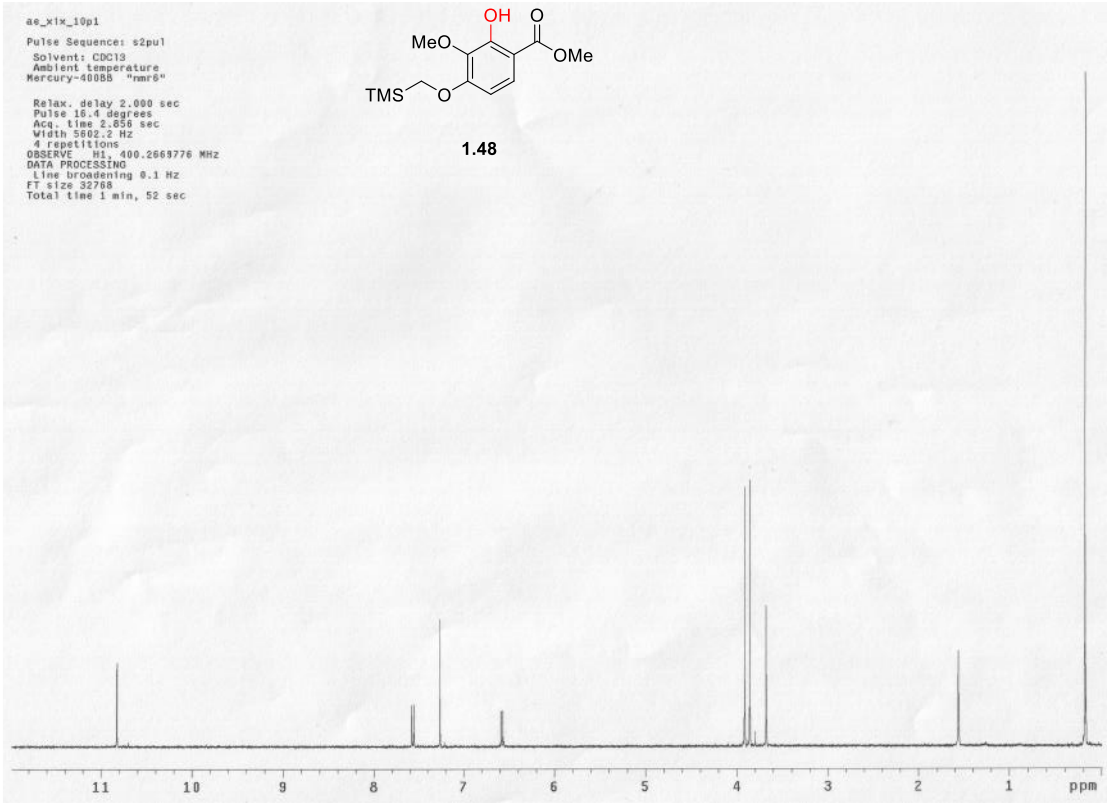
ae_xix_10p1
Pulse Sequence: s2pul
Solvent: CDCl3
Ambient temperature
Mercury-400BB "nmr6"
Relax. delay 2.000 sec
Pulse 16.4 degrees
Acq. time 2.656 sec
Width 5602.2 Hz
4 repetitions
OBSERVE H1, 400.2669776 MHz
DATA PROCESSING
Line broadening 0.1 Hz
FT size 32768
Total time 1 min, 52 sec
OH
O
MeO
OMe
TMS
O
1.48
11
10
9
8
7
6
5
4
3
2
1
ppm

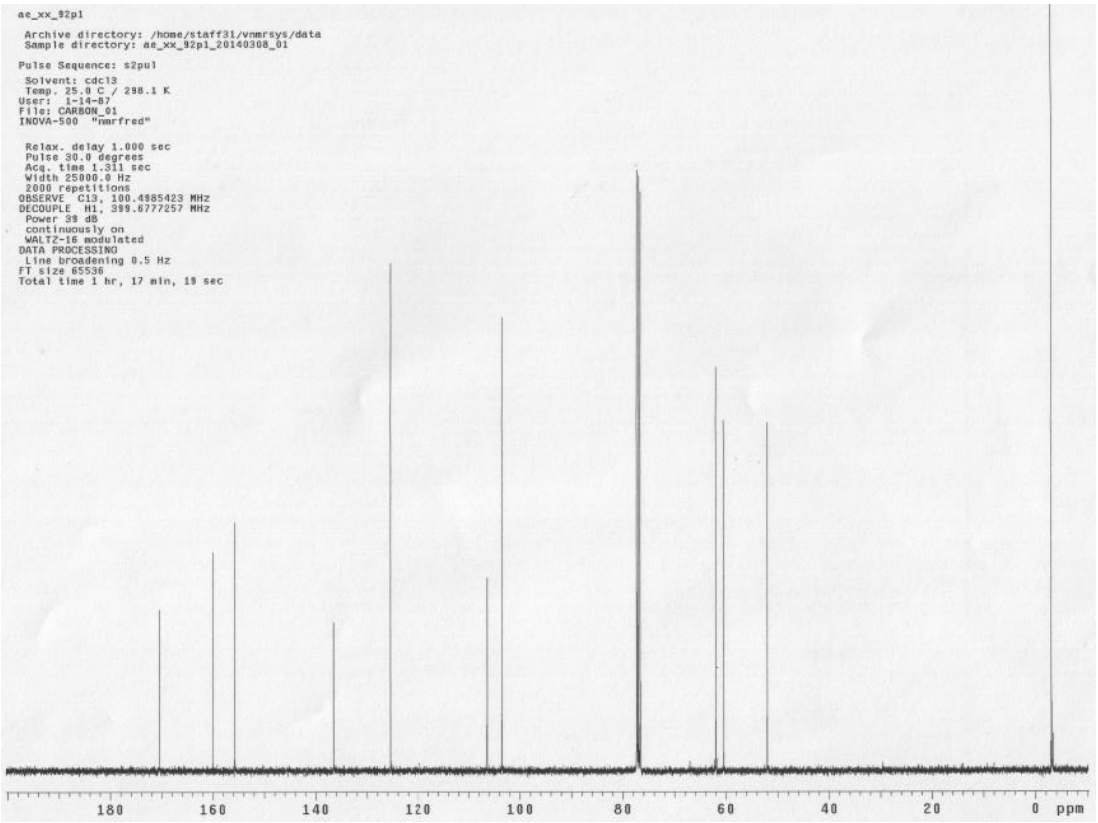
ae_xx_92p1
Archive directory: /home/staff31/vnmrsys/data
Sample directory: ae_xx_92p1_20140308_01
Pulse Sequence: s2pul
Solvent: cdcl3
Temp. 25.0 C / 298.1 K
User: 1-14-87
File: CARBON_01
INOVA-500 "nmrfred"
Relax. delay 1.000 sec
Pulse 30.0 degrees
Acq. time 1.311 sec
Width 25000.0 Hz
2000 repetitions
OBSERVE C13, 100.4985423 MHz
DECOUPLE H1, 399.6777257 MHz
Power 39 dB
continuously on
WALTZ-16 modulated
DATA PROCESSING
Line broadening 0.5 Hz
FT size 65536
Total time 1 hr, 17 min, 19 sec
180
160
140
120
100
80
60
40
20
0
ppm

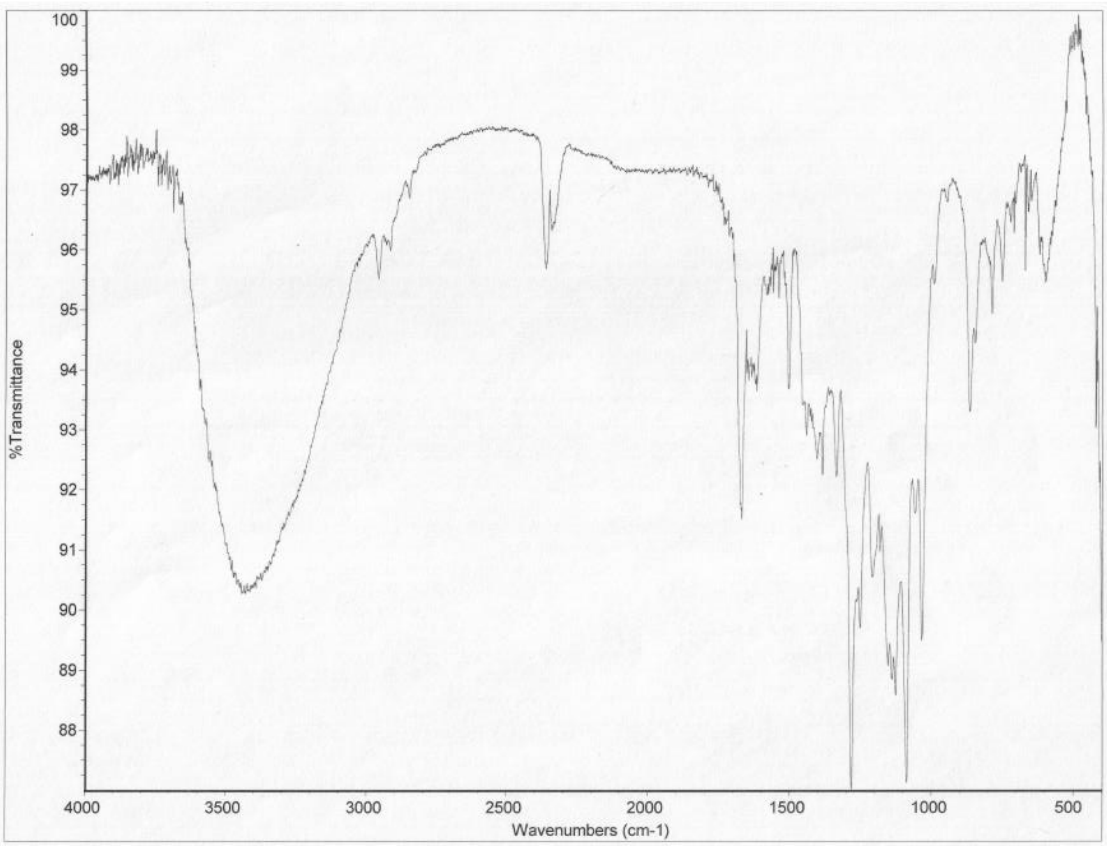
%Transmittance
100
99
98
97
96
95
94
93
92
91
90
89
88
4000
3500
3000
2500
2000
1500
1000
500
Wavenumbers (cm-1)

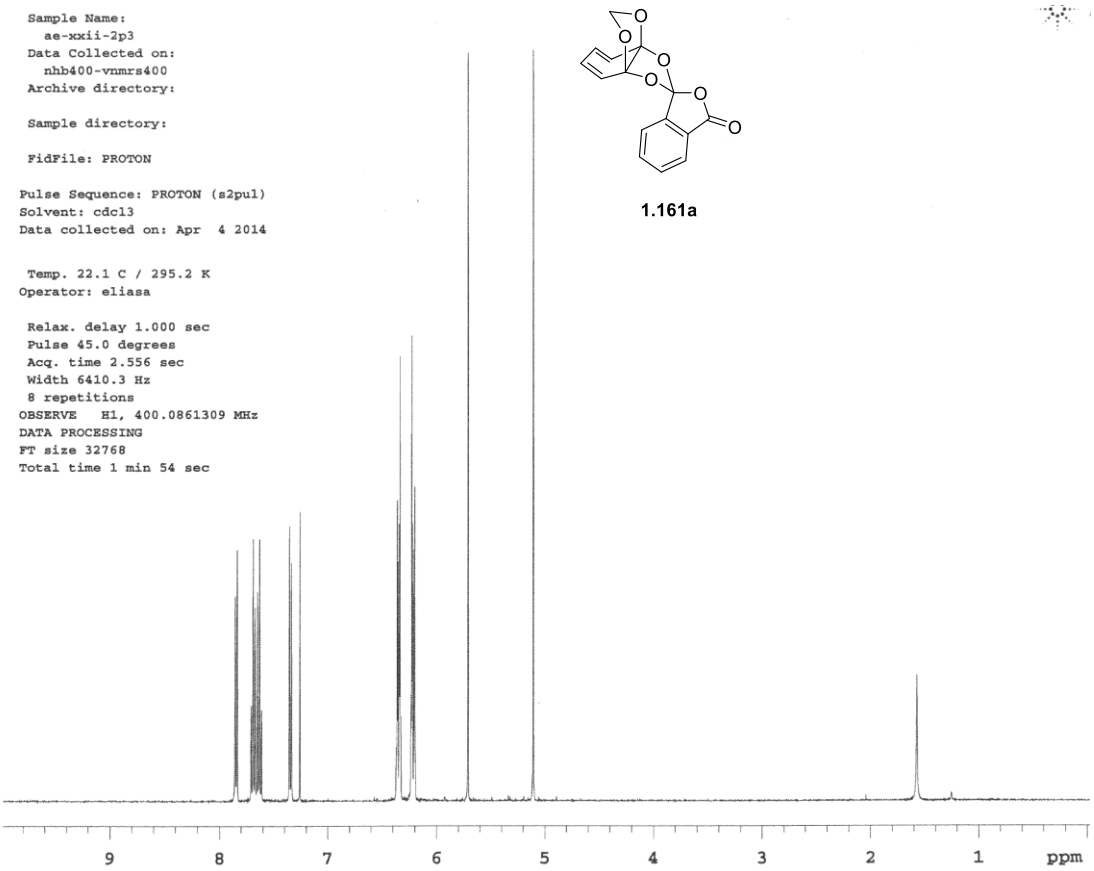
Sample Name:
ae-xxii-2p3
Data Collected on:
nhb400-vnmrs400
Archive directory:
Sample directory:
FidFile: PROTON
Pulse Sequence: PROTON (s2pul)
Solvent: cdcl3
Data collected on: Apr 4 2014
Temp. 22.1 C / 295.2 K
Operator: eliasa
Relax. delay 1.000 sec
Pulse 45.0 degrees
Acq. time 2.556 sec
Width 6410.3 Hz
8 repetitions
OBSERVE H1, 400.0861309 MHz
DATA PROCESSING
FT size 32768
Total time 1 min 54 sec
9
8
7
6
5
4
3
2
1
ppm

1.161a

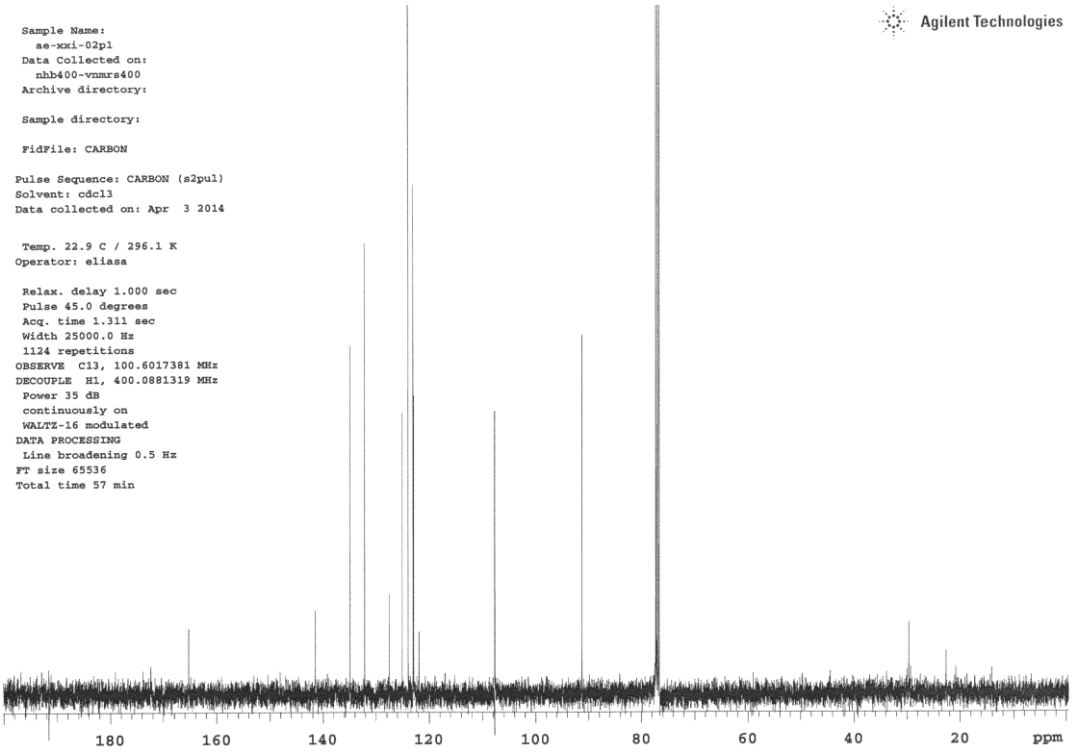
Agilent Technologies
Sample Name:
ae-xxi-02p1
Data Collected on:
nhb400-vnmrs400
Archive directory:
Sample directory:
FidFile: CARBON
Pulse Sequence: CARBON (s2pul)
Solvent: cdcl3
Data collected on: Apr 3 2014
Temp. 22.9 C / 296.1 K
Operator: eliasa
Relax. delay 1.000 sec
Pulse 45.0 degrees
Acq. time 1.311 sec
Width 25000.0 Hz
1124 repetitions
OBSERVE C13, 100.6017381 MHz
DECOUPLE H1, 400.0881319 MHz
Power 35 dB
continuously on
WALTZ-16 modulated
DATA PROCESSING
Line broadening 0.5 Hz
FT size 65536
Total time 57 min
180
160
140
120
100
80
60
40
20
ppm

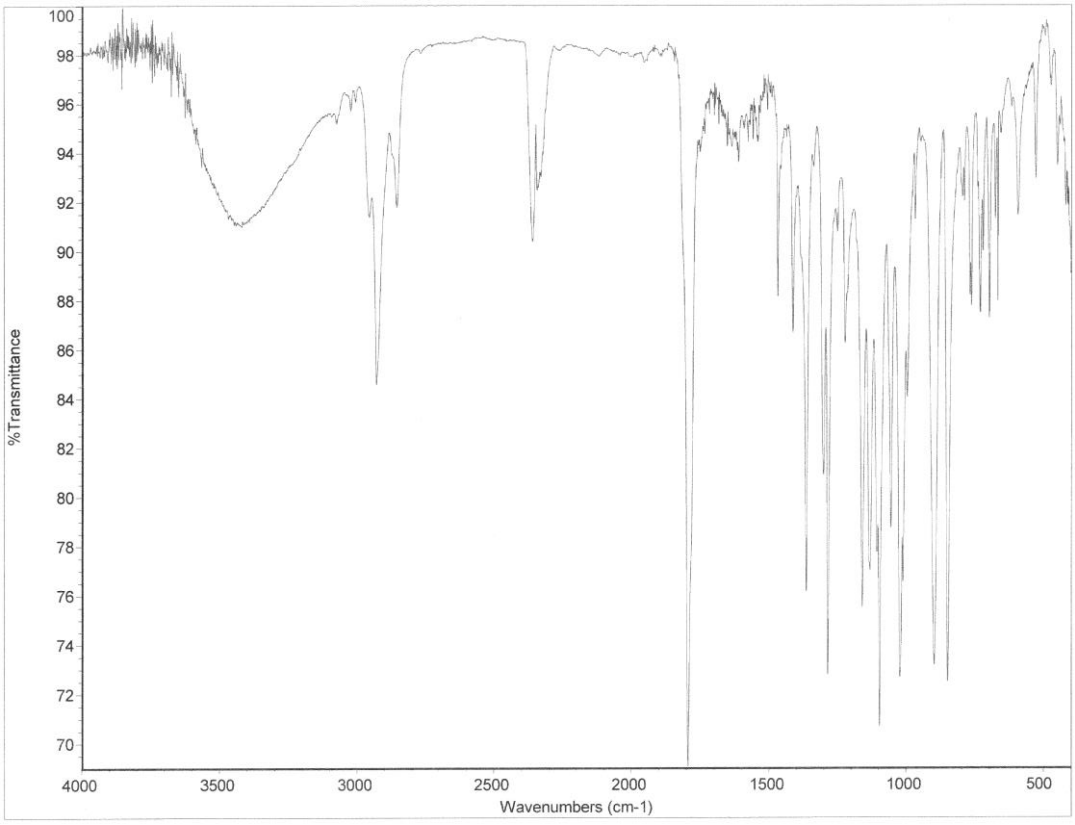
100
98
96
94
92
90
88
86
84
82
80
78
76
74
72
70
%Transmittance
4000
3500
3000
2500
2000
1500
1000
500
Wavenumbers (cm-1)

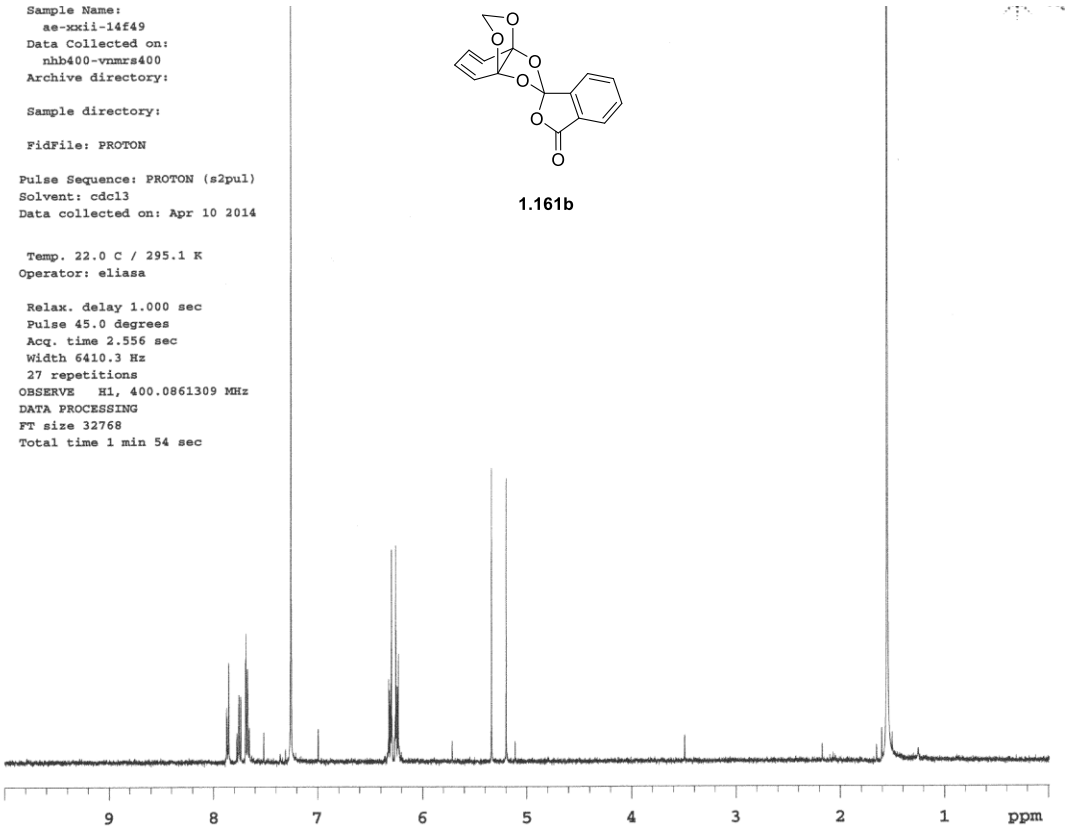
Sample Name:
ae-xxii-14f49
Data Collected on:
nhb400-vnmrs400
Archive directory:
Sample directory:
FidFile: PROTON
Pulse Sequence: PROTON (s2pul)
Solvent: cdcl3
Data collected on: Apr 10 2014
Temp. 22.0 C / 295.1 K
Operator: eliasa
Relax. delay 1.000 sec
Pulse 45.0 degrees
Acq. time 2.556 sec
Width 6410.3 Hz
27 repetitions
OBSERVE H1, 400.0861309 MHz
DATA PROCESSING
FT size 32768
Total time 1 min 54 sec
1.161b
9
8
7
6
5
4
3
2
1
ppm

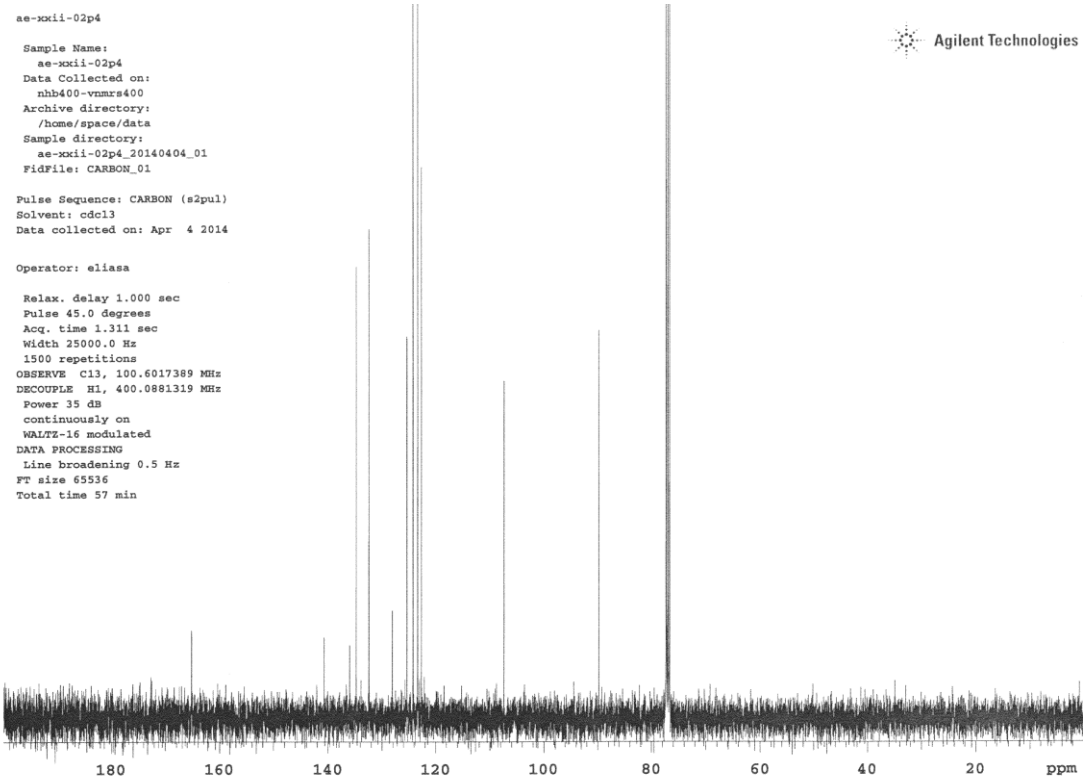
ae-xxii-02p4
Agilent Technologies
Sample Name:
ae-xxii-02p4
Data Collected on:
nhb400-vnmrs400
Archive directory:
/home/space/data
Sample directory:
ae-xxii-02p4_20140404_01
FidFile: CARBON_01
Pulse Sequence: CARBON (s2pul)
Solvent: cdcl3
Data collected on: Apr 4 2014
Operator: eliasa
Relax. delay 1.000 sec
Pulse 45.0 degrees
Acq. time 1.311 sec
Width 25000.0 Hz
1500 repetitions
OBSERVE C13, 100.6017389 MHz
DECOUPLE H1, 400.0881319 MHz
Power 35 dB
continuously on
WALTZ-16 modulated
DATA PROCESSING
Line broadening 0.5 Hz
FT size 65536
Total time 57 min
180
160
140
120
100
80
60
40
20
ppm

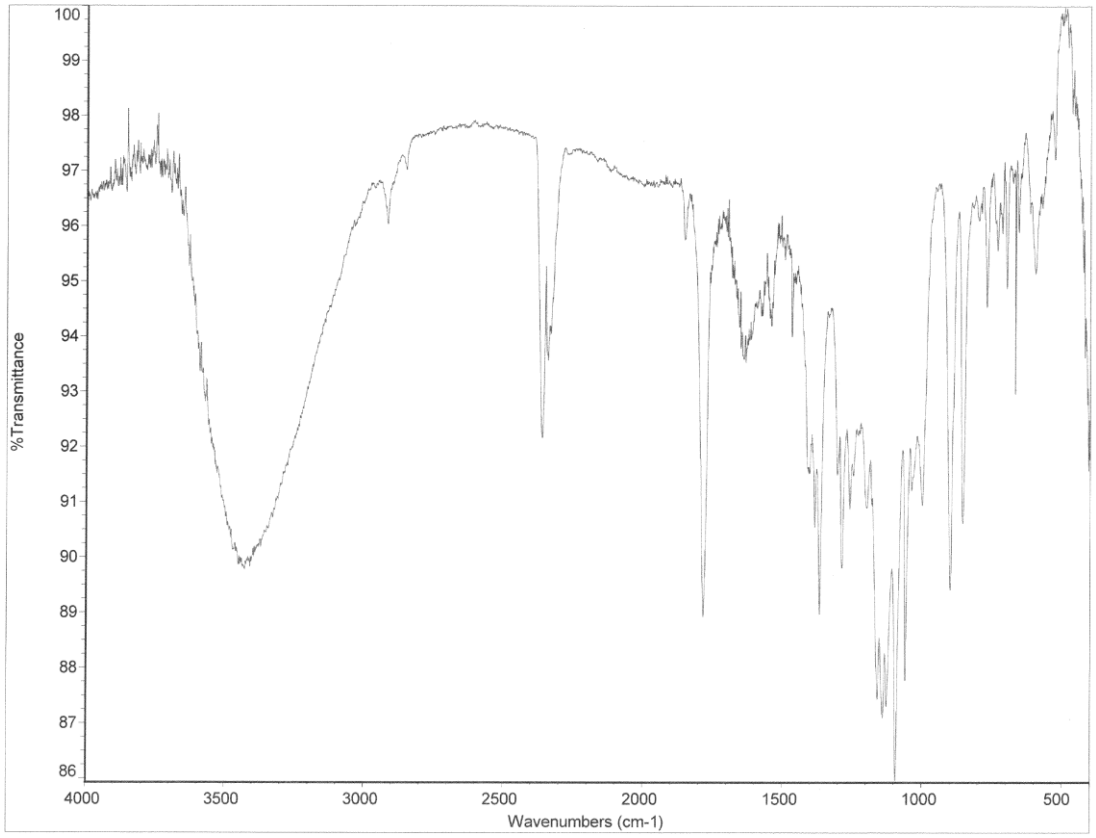
100
99
98
97
96
95
94
93
92
91
90
89
88
87
86
%Transmittance
4000
3500
3000
2500
2000
1500
1000
500
Wavenumbers (cm-1)

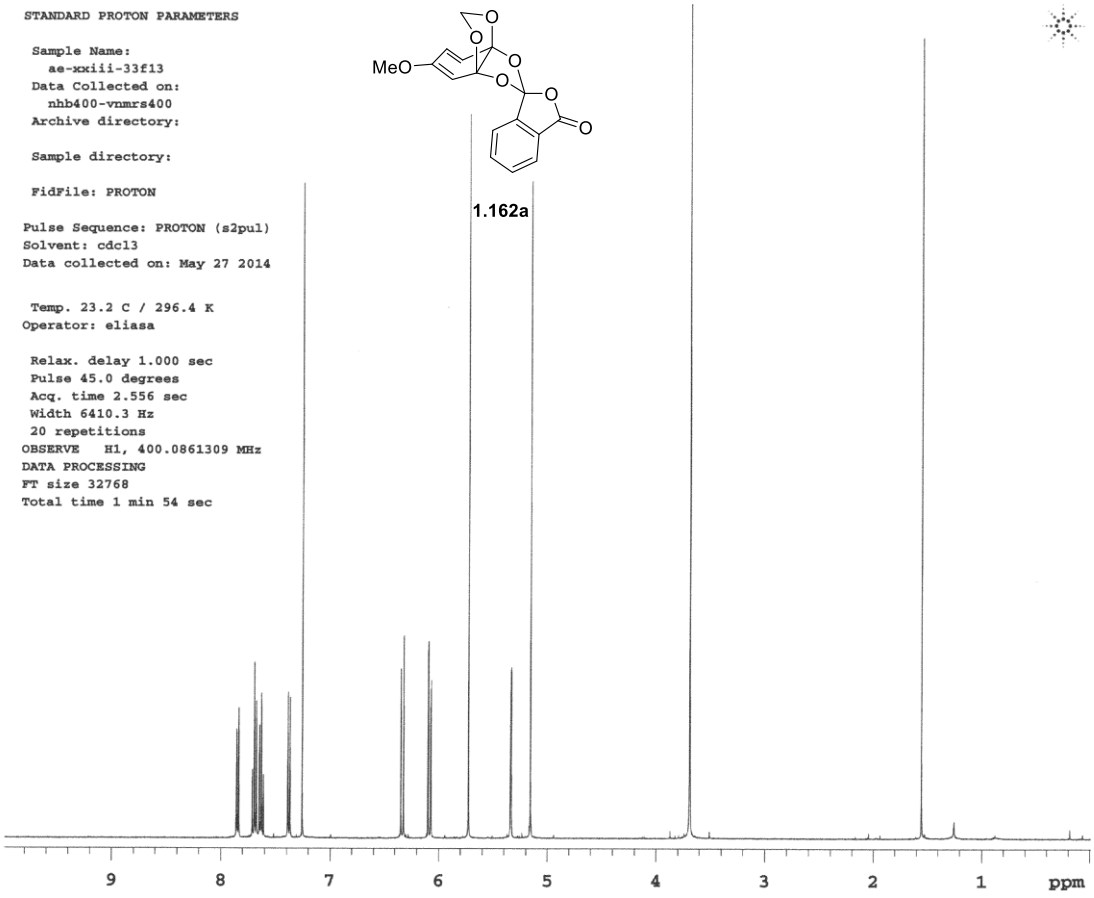
STANDARD PROTON PARAMETERS
Sample Name:
ae-xxiii-33f13
Data Collected on:
nhb400-vnmrs400
Archive directory:
Sample directory:
FidFile: PROTON
Pulse Sequence: PROTON (s2pul)
Solvent: cdcl3
Data collected on: May 27 2014
Temp. 23.2 C / 296.4 K
Operator: eliasa
Relax. delay 1.000 sec
Pulse 45.0 degrees
Acq. time 2.556 sec
Width 6410.3 Hz
20 repetitions
OBSERVE H1, 400.0861309 MHz
DATA PROCESSING
FT size 32768
Total time 1 min 54 sec
MeO
O
1.162a
9
8
7
6
5
4
3
2
1
ppm

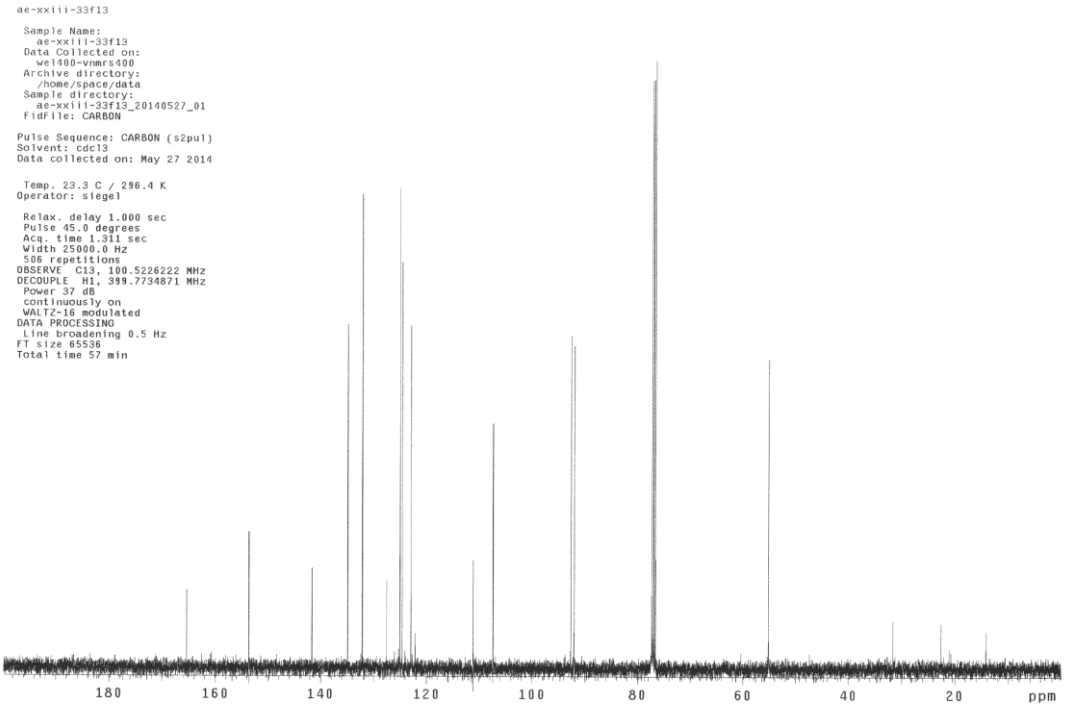
ae-xxiii-33f13
Sample Name:
ae-xxiii-33f13
Data Collected on:
wel400-vnmrs400
Archive directory:
/home/space/data
Sample directory:
ae-xxiii-33f13_20140527_01
FidFile: CARBON
Pulse Sequence: CARBON (s2pul)
Solvent: cdcl3
Data collected on: May 27 2014
Temp. 23.3 C / 296.4 K
Operator: siegel
Relax. delay 1.000 sec
Pulse 45.0 degrees
Acq. time 1.311 sec
Width 25000.0 Hz
506 repetitions
OBSERVE C13, 100.5226222 MHz
DECOUPLE H1, 399.7734871 MHz
Power 37 dB
continuously on
WALTZ-16 modulated
DATA PROCESSING
Line broadening 0.5 Hz
FT size 65536
Total time 57 min
180
160
140
120
100
80
60
40
20
ppm

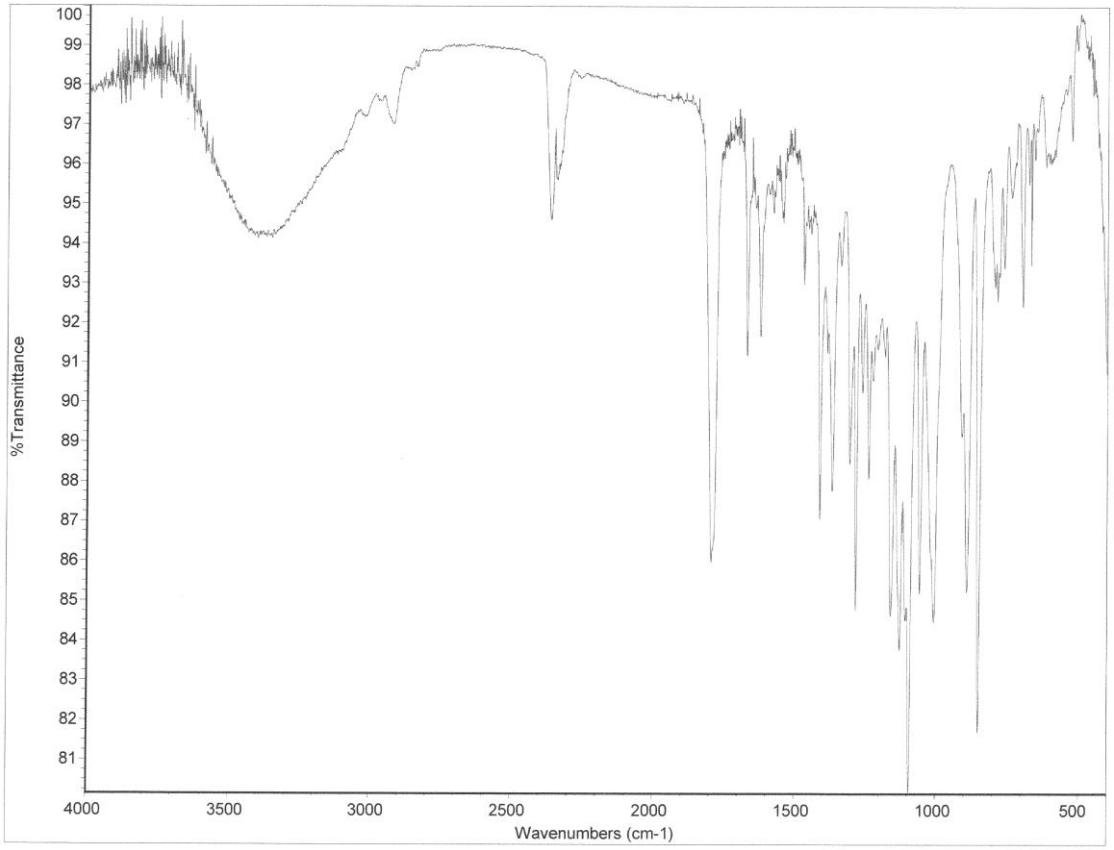
%Transmittance
100
99
98
97
96
95
94
93
92
91
90
89
88
87
86
85
84
83
82
81
4000
3500
3000
2500
2000
1500
1000
500
Wavenumbers (cm-1)

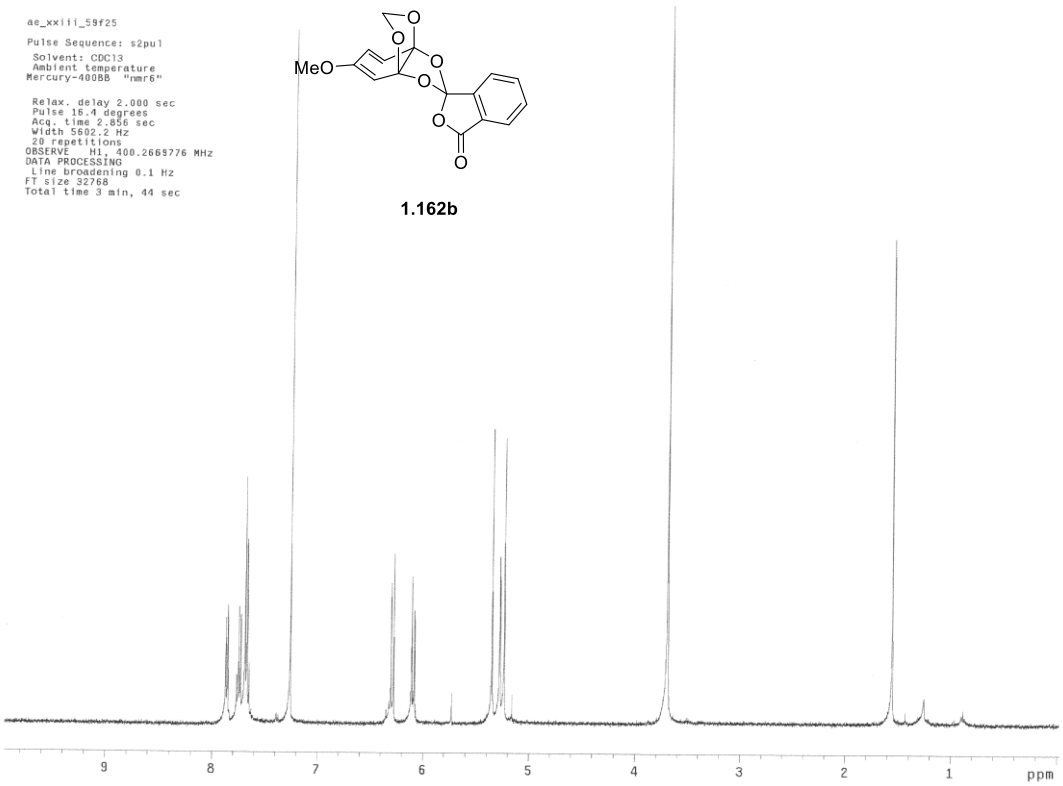
ae_xxiii_59f25
Pulse Sequence: s2pul
Solvent: CDCl3
Ambient temperature
Mercury-400BB "nmr6"
Relax. delay 2.000 sec
Pulse 16.4 degrees
Acq. time 2.856 sec
Width 5602.2 Hz
20 repetitions
OBSERVE H1, 400.2665776 MHz
DATA PROCESSING
Line broadening 0.1 Hz
FT size 32768
Total time 3 min, 44 sec
MeO
O
O
O
O
O
O
1.162b
9
8
7
6
5
4
3
2
1
ppm

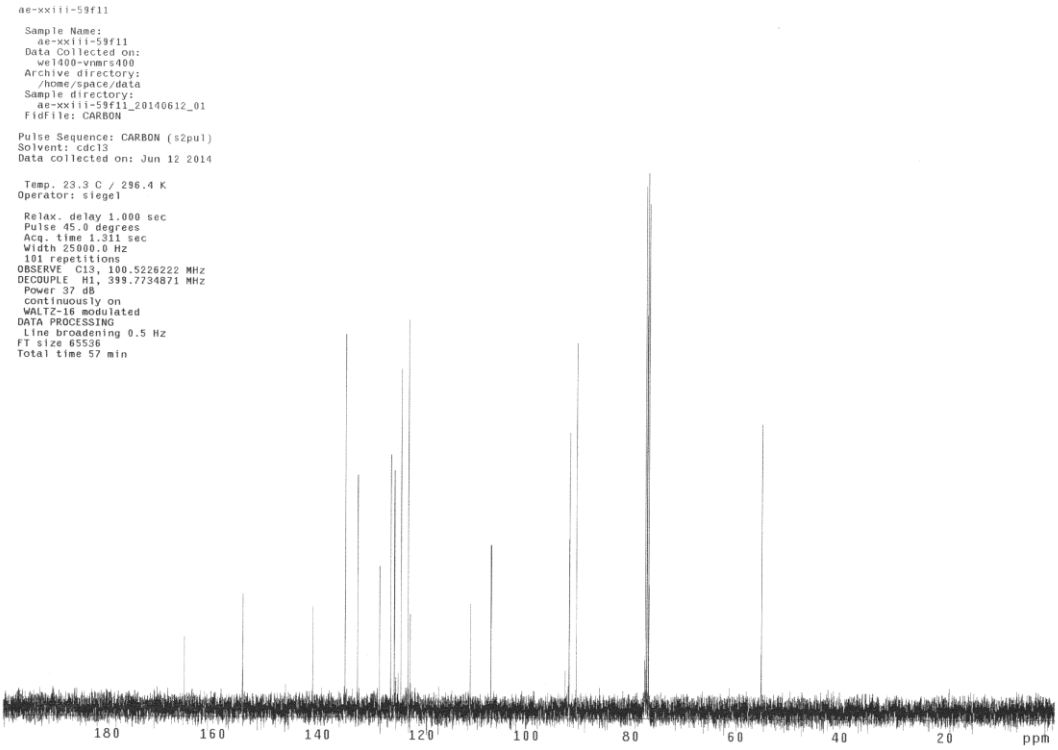
ae-xxiii-59f11
Sample Name:
ae-xxiii-59f11
Data Collected on:
wel400-vnmrs400
Archive directory:
/home/space/data
Sample directory:
ae-xxiii-59f11_20140612_01
FidFile: CARBON
Pulse Sequence: CARBON (s2pul)
Solvent: cdcl3
Data collected on: Jun 12 2014
Temp. 23.3 C / 296.4 K
Operator: siegel
Relax. delay 1.000 sec
Pulse 45.0 degrees
Acq. time 1.311 sec
Width 25000.0 Hz
101 repetitions
OBSERVE C13, 100.5226222 MHz
DECOUPLE H1, 399.7734871 MHz
Power 37 dB
continuously on
WALTZ-16 modulated
DATA PROCESSING
Line broadening 0.5 Hz
FT size 65536
Total time 57 min
180
160
140
120
100
80
60
40
20
ppm

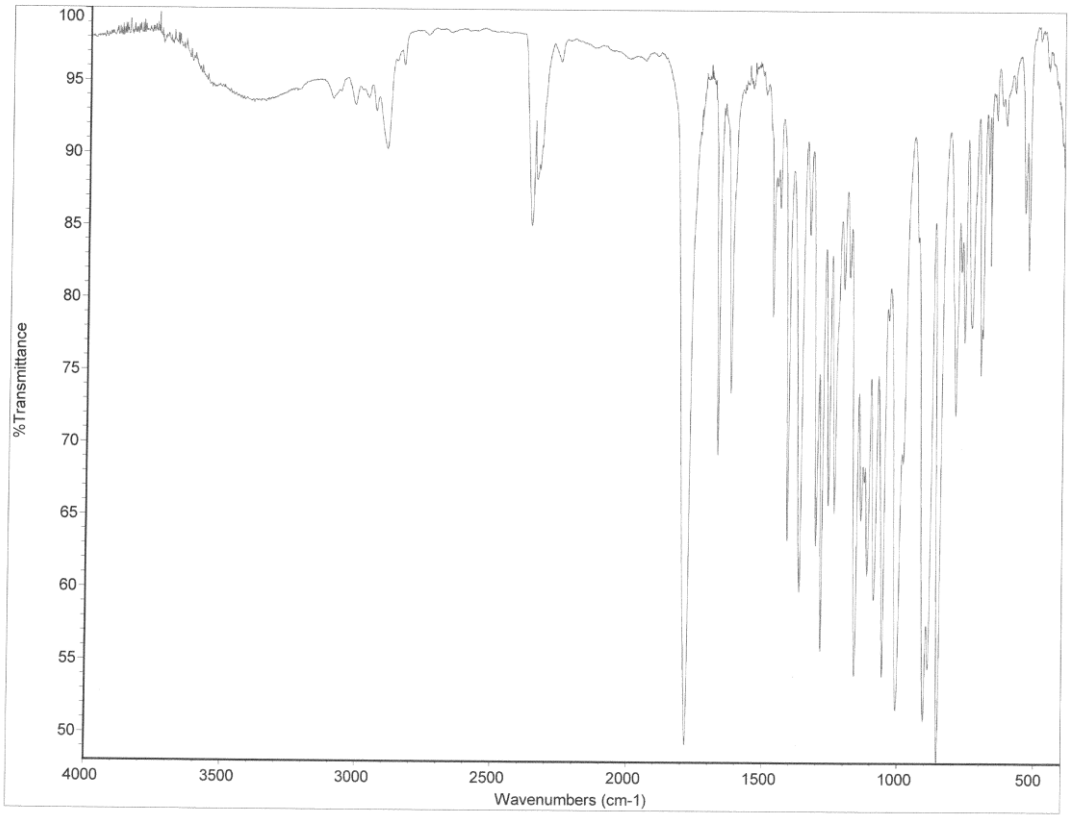
100
95
90
85
80
75
70
65
60
55
50
%Transmittance
4000
3500
3000
2500
2000
1500
1000
500
Wavenumbers (cm-1)

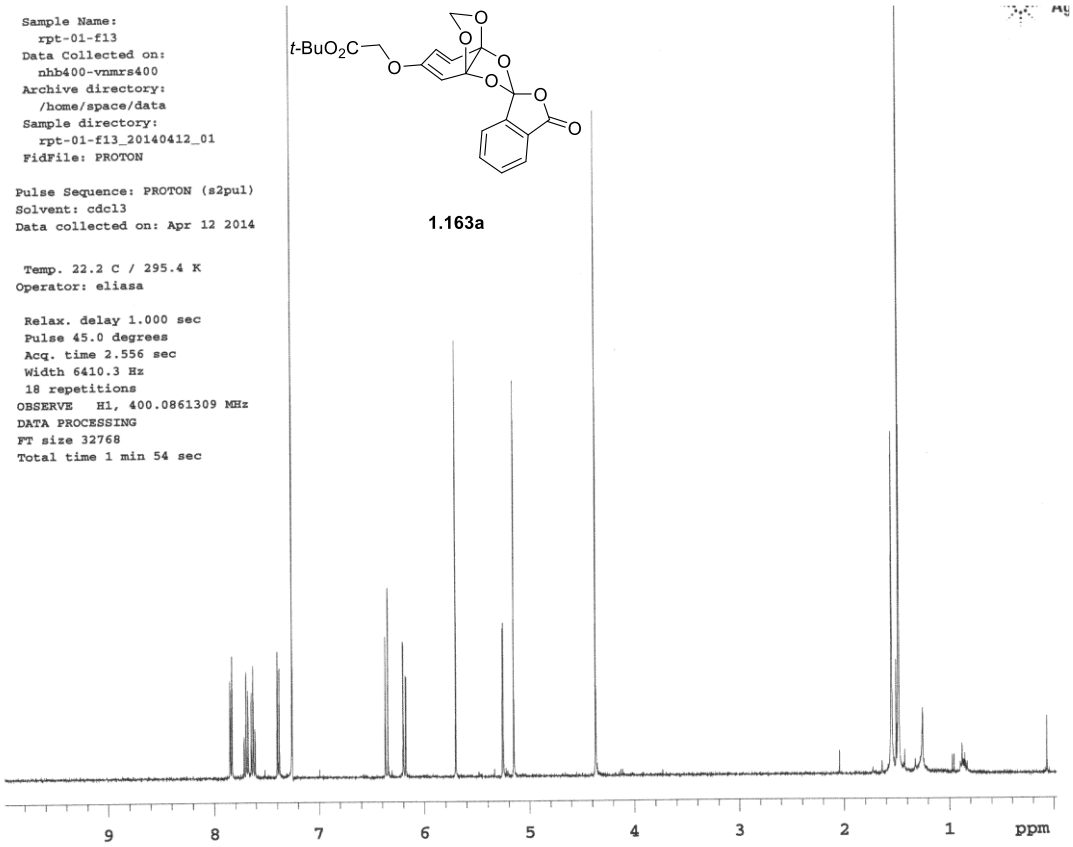
Sample Name:
rpt-01-f13
Data Collected on:
nhb400-vnmrs400
Archive directory:
/home/space/data
Sample directory:
rpt-01-f13_20140412_01
FidFile: PROTON
Pulse Sequence: PROTON (s2pul)
Solvent: cdcl3
Data collected on: Apr 12 2014
Temp. 22.2 C / 295.4 K
Operator: eliasa
Relax. delay 1.000 sec
Pulse 45.0 degrees
Acq. time 2.556 sec
Width 6410.3 Hz
18 repetitions
OBSERVE H1, 400.0861309 MHz
DATA PROCESSING
FT size 32768
Total time 1 min 54 sec
t-BuO2C
1.163a
9
8
7
6
5
4
3
2
1
ppm

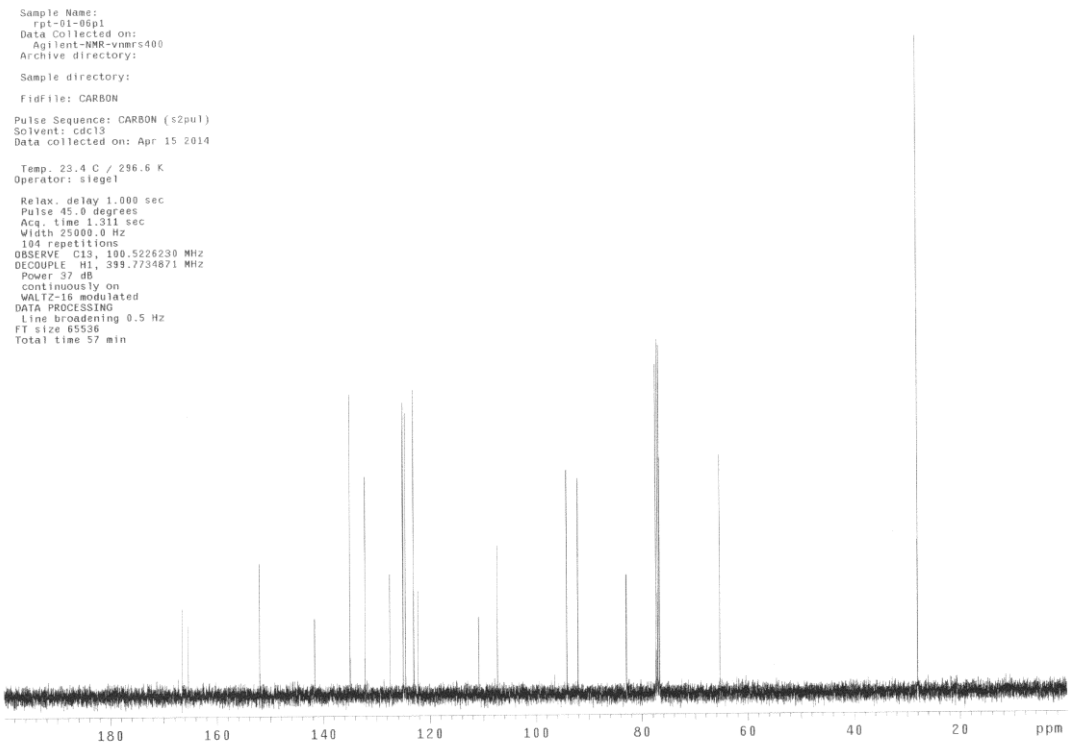
Sample Name:
rpt-01-06p1
Data Collected on:
Agilent-NMR-vnmrs400
Archive directory:
Sample directory:
FidFile: CARBON
Pulse Sequence: CARBON (s2pul)
Solvent: cdcl3
Data collected on: Apr 15 2014
Temp. 23.4 C / 296.6 K
Operator: siegel
Relax. delay 1.000 sec
Pulse 45.0 degrees
Acq. time 1.311 sec
Width 25000.0 Hz
104 repetitions
OBSERVE C13, 100.5226230 MHz
DECOUPLE H1, 399.7734871 MHz
Power 37 dB
continuously on
WALTZ-16 modulated
DATA PROCESSING
Line broadening 0.5 Hz
FT size 65536
Total time 57 min
180
160
140
120
100
80
60
40
20
ppm

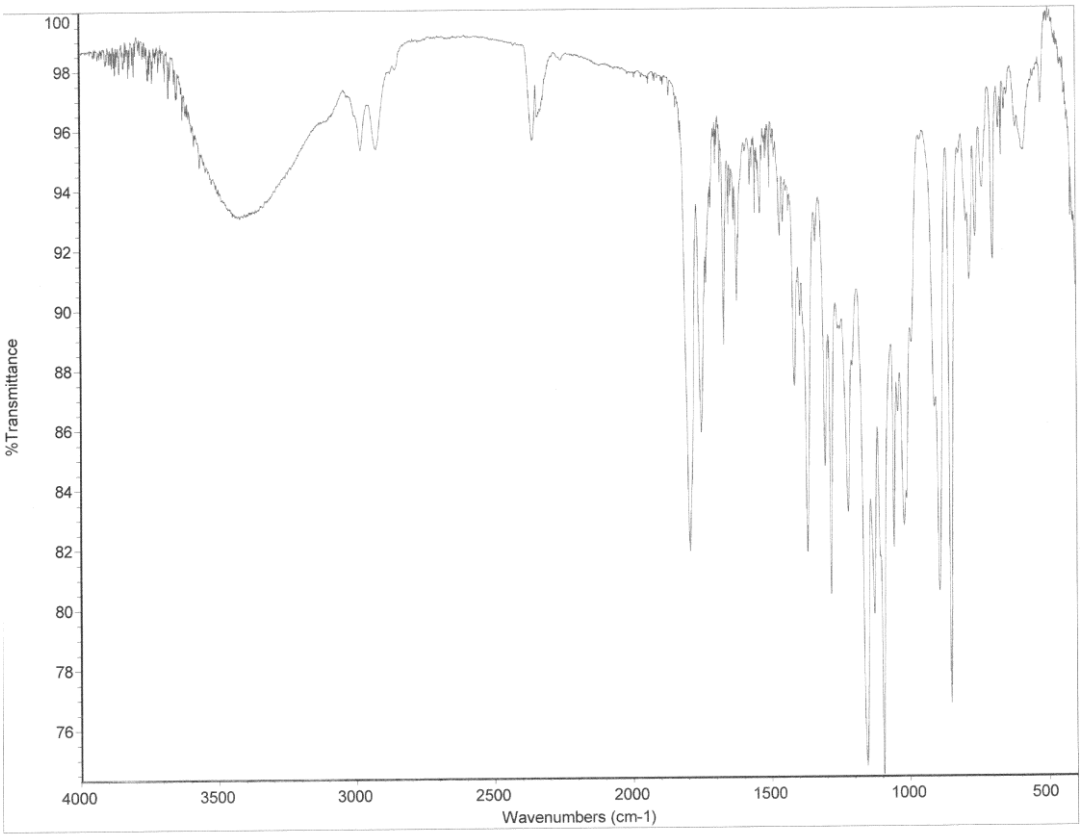
100
98
96
94
92
90
88
86
84
82
80
78
76
%Transmittance
4000
3500
3000
2500
2000
1500
1000
500
Wavenumbers (cm-1)

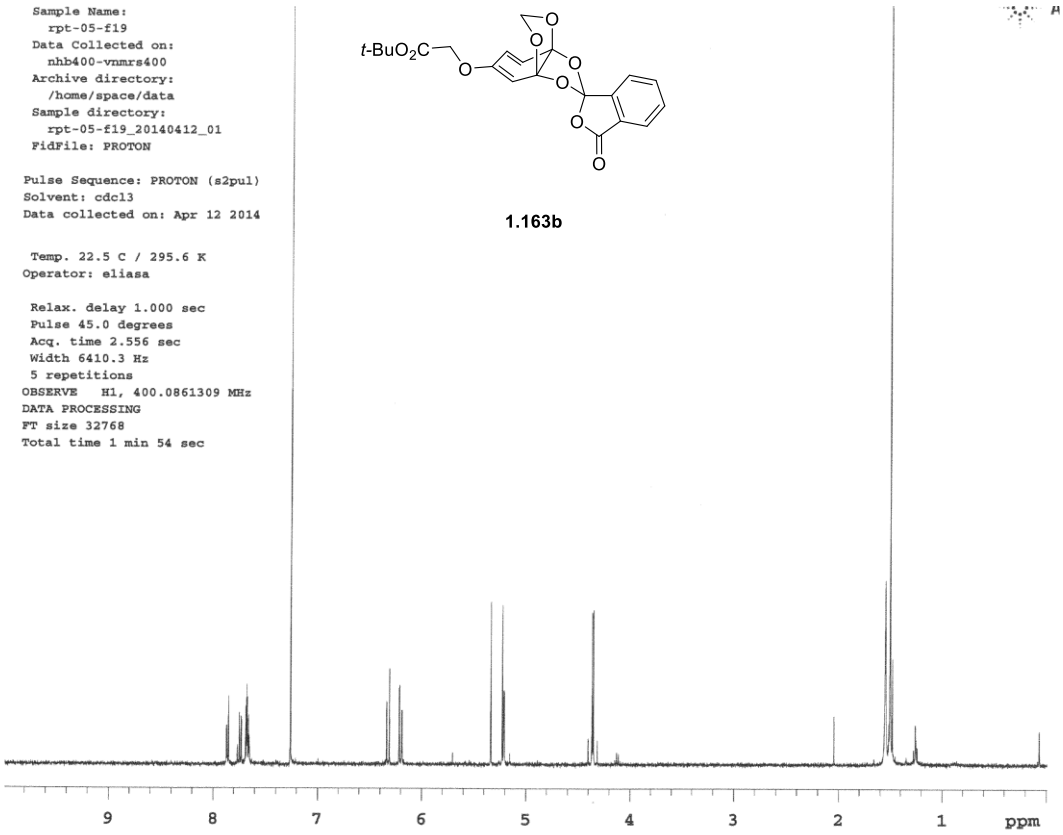
Sample Name:
rpt-05-f19
Data Collected on:
nhb400-vnmrs400
Archive directory:
/home/space/data
Sample directory:
rpt-05-f19_20140412_01
FidFile: PROTON
Pulse Sequence: PROTON (s2pul)
Solvent: cdcl3
Data collected on: Apr 12 2014
Temp. 22.5 C / 295.6 K
Operator: eliasa
Relax. delay 1.000 sec
Pulse 45.0 degrees
Acq. time 2.556 sec
Width 6410.3 Hz
5 repetitions
OBSERVE H1, 400.0861309 MHz
DATA PROCESSING
FT size 32768
Total time 1 min 54 sec
t-BuO2C
O
1.163b
9
8
7
6
5
4
3
2
1
ppm

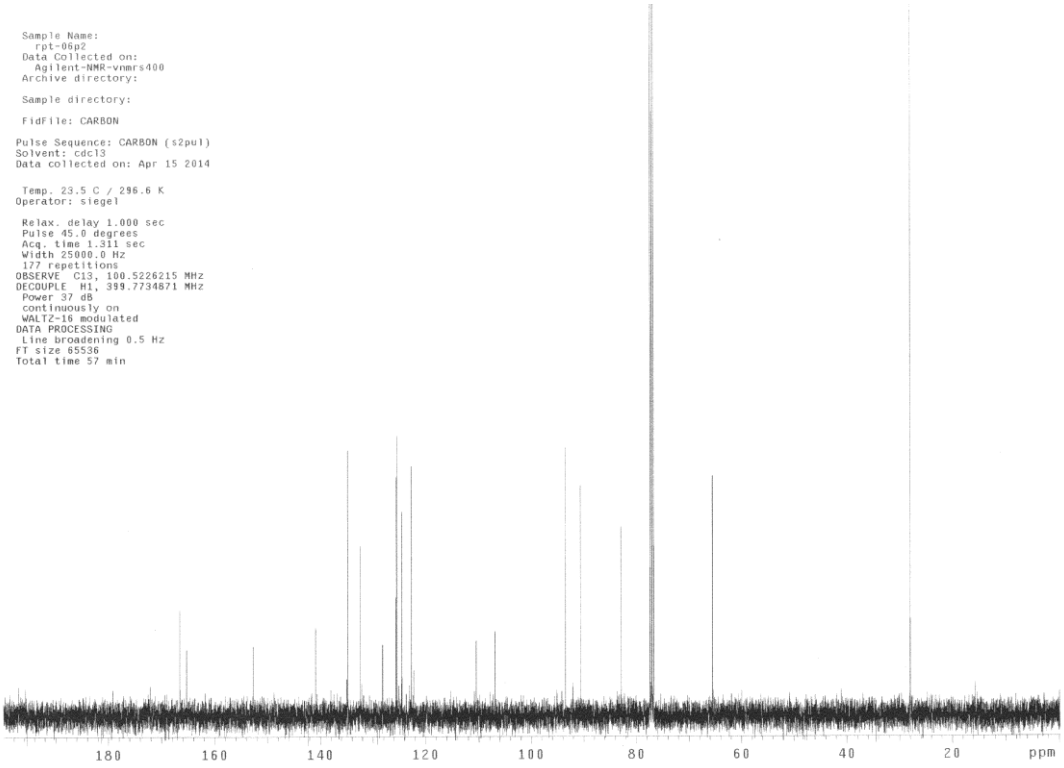
Sample Name:
rpt-06p2
Data Collected on:
Agilent-NMR-vnmrs400
Archive directory:
Sample directory:
FidFile: CARBON
Pulse Sequence: CARBON (s2pul)
Solvent: cdcl3
Data collected on: Apr 15 2014
Temp. 23.5 C / 296.6 K
Operator: siegel
Relax. delay 1.000 sec
Pulse 45.0 degrees
Acq. time 1.311 sec
Width 25000.0 Hz
177 repetitions
OBSERVE C13, 100.5226215 MHz
DECOUPLE H1, 399.7734871 MHz
Power 37 dB
continuously on
WALTZ-16 modulated
DATA PROCESSING
Line broadening 0.5 Hz
FT size 65536
Total time 57 min
180
160
140
120
100
80
60
40
20
ppm

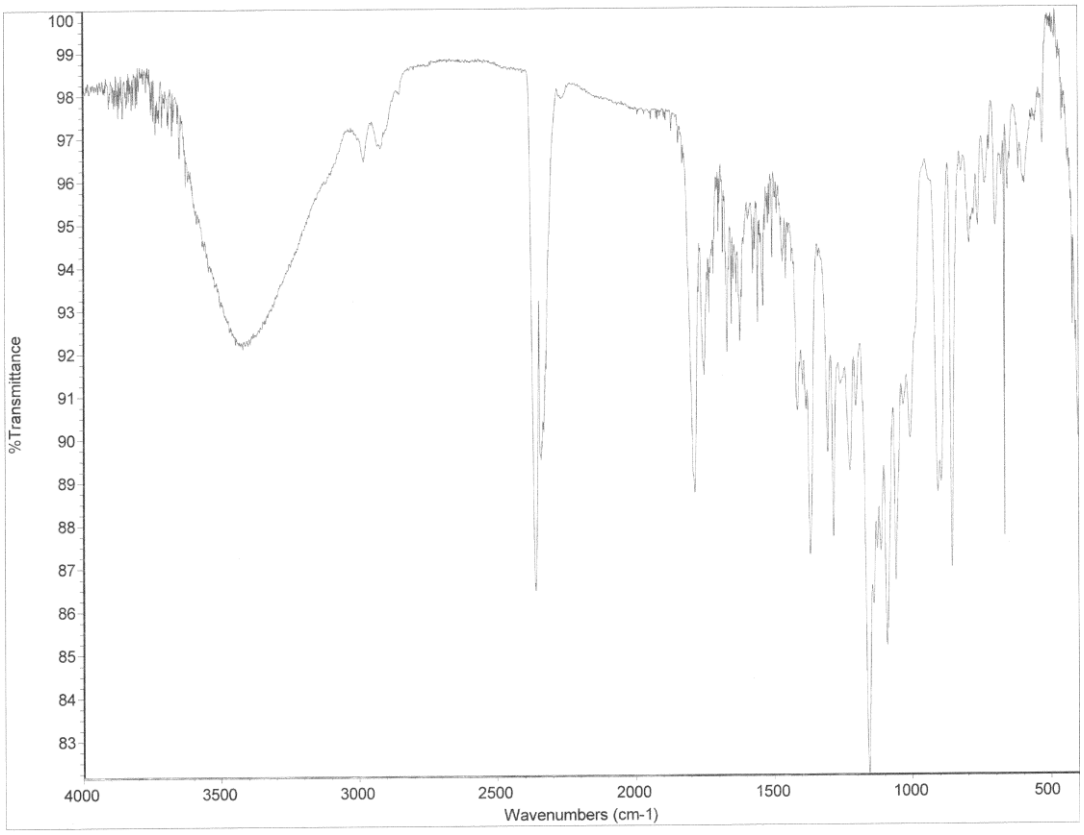
%Transmittance
100
99
98
97
96
95
94
93
92
91
90
89
88
87
86
85
84
83
4000
3500
3000
2500
2000
1500
1000
500
Wavenumbers (cm-1)

Sample Name:
ae-xxi-49p2
Data Collected on:
nhb400-vnmrs400
Archive directory:
/home/space/data
Sample directory:
ae-xxi-49p2_20140320_01
FidFile: PROTON

Pulse Sequence: PROTON (s2pul)
Solvent: cdcl3
Data collected on: Mar 20 2014

Temp. 22.3 C / 295.4 K
Operator: eliasa

Relax. delay 1.000 sec
Pulse 45.0 degrees
Acq. time 2.556 sec
Width 6410.3 Hz
9 repetitions
OBSERVE H1, 400.0858989 MHz
DATA PROCESSING
FT size 32768
Total time 0 min 57 sec

1.164a

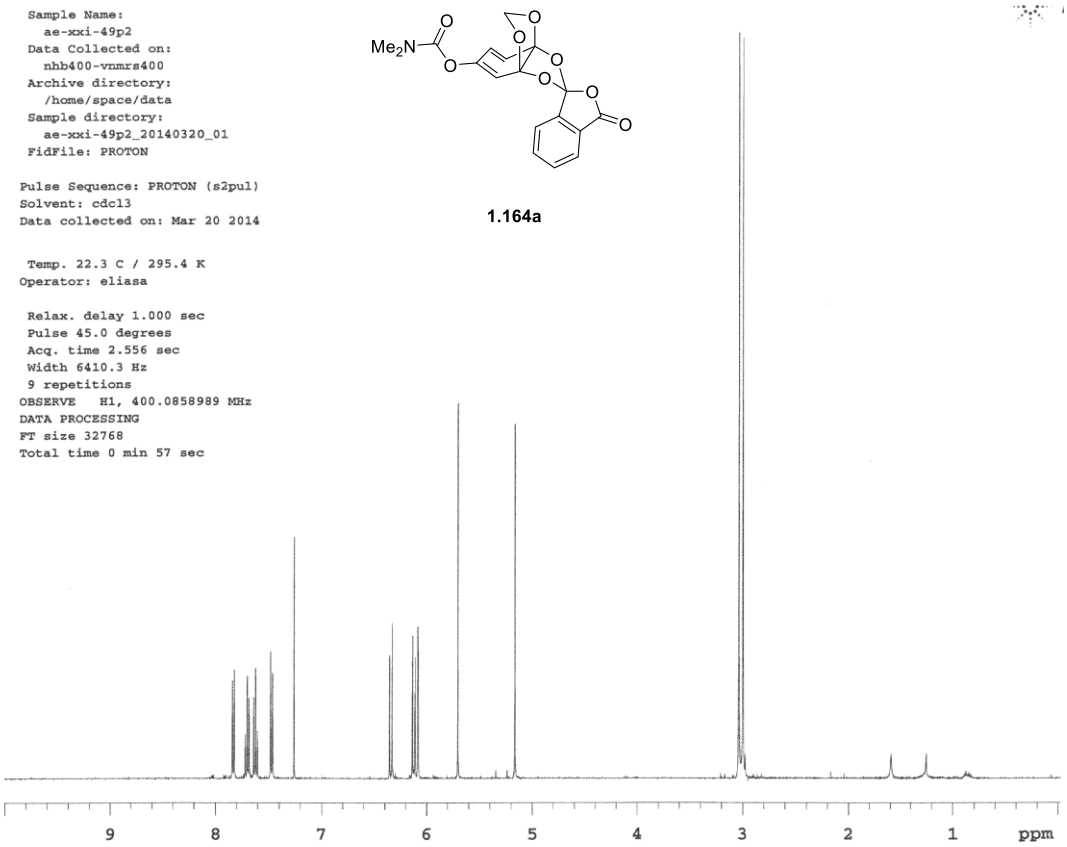

exp4 Carbon

SAMPLE		SPECIAL	
date	Mar 20 2014	temp	27.0
solvent	cdcl3	gain	40
file	exp	spin	20
ACQUISITION		hst	0.008
sw	30131.8	pw90	12.500
at	1.062	alfa	10.000
np	64000	FLAGS	
fb	17000	il	n
bs	1	in	n
d1	2.000	dp	y
nt	12000	hs	nn
ct	12000	PROCESSING	
TRANSMITTER		lb	1.00
tn	C13	fn	not used
sfrq	125.584	DISPLAY	
tof	1254.2	sp	-628.1
tpwr	61	wp	28253.2
pw	4.162	rfl	11581.7
DECOUPLER		rfp	9669.0
dn	H1	rp	269.6
dof	0	lp	-133.3
dm	yyy	PLOT	
dmm	w	wc	250
dpwr	33	sc	0
dmf	12200	vs	90740
		th	68
		al cdc ph	

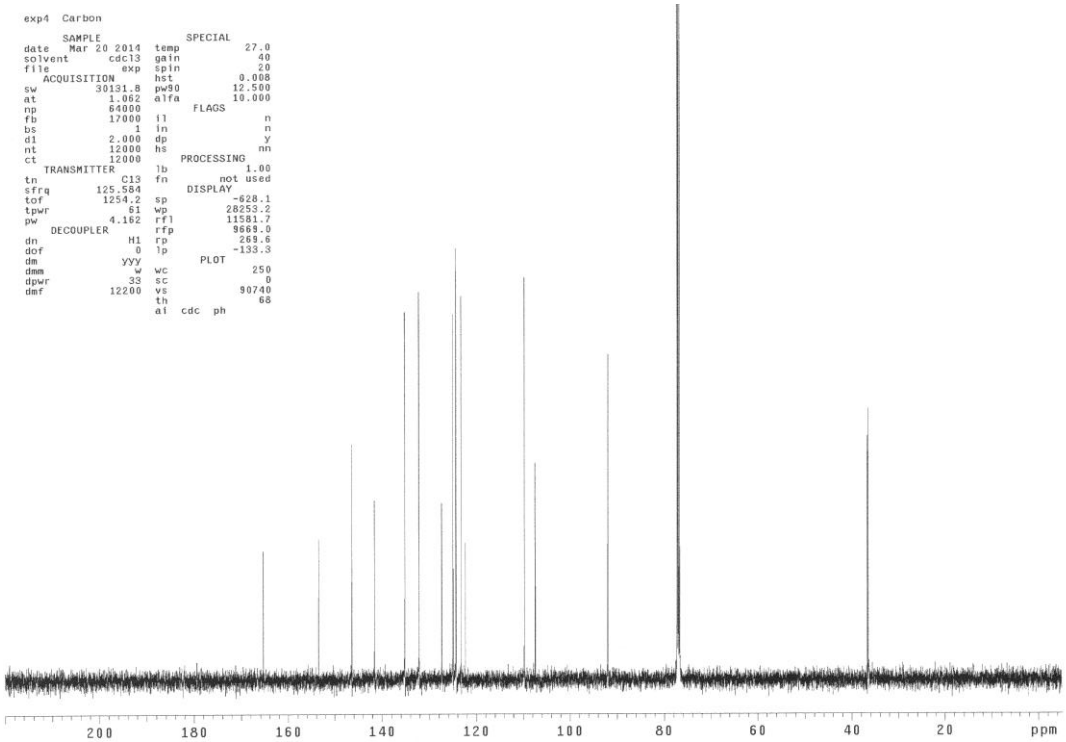

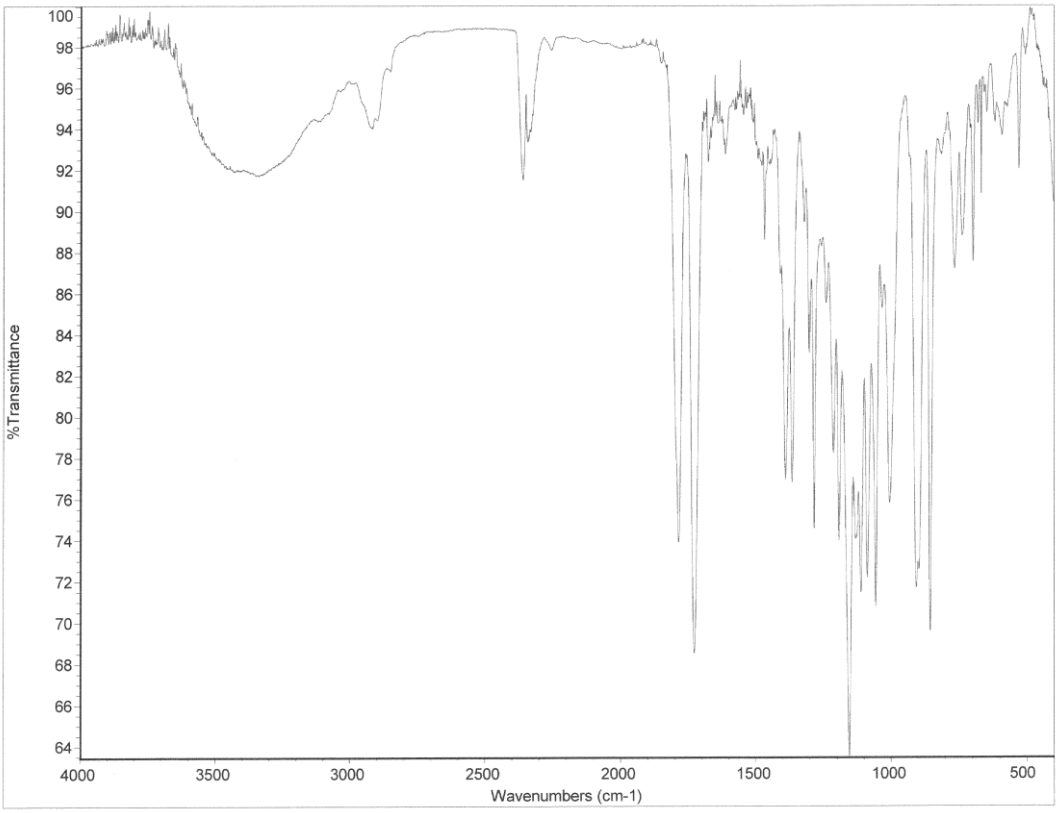
%Transmittance
100
98
96
94
92
90
88
86
84
82
80
78
76
74
72
70
68
66
64
4000
3500
3000
2500
2000
1500
1000
500
Wavenumbers (cm-1)

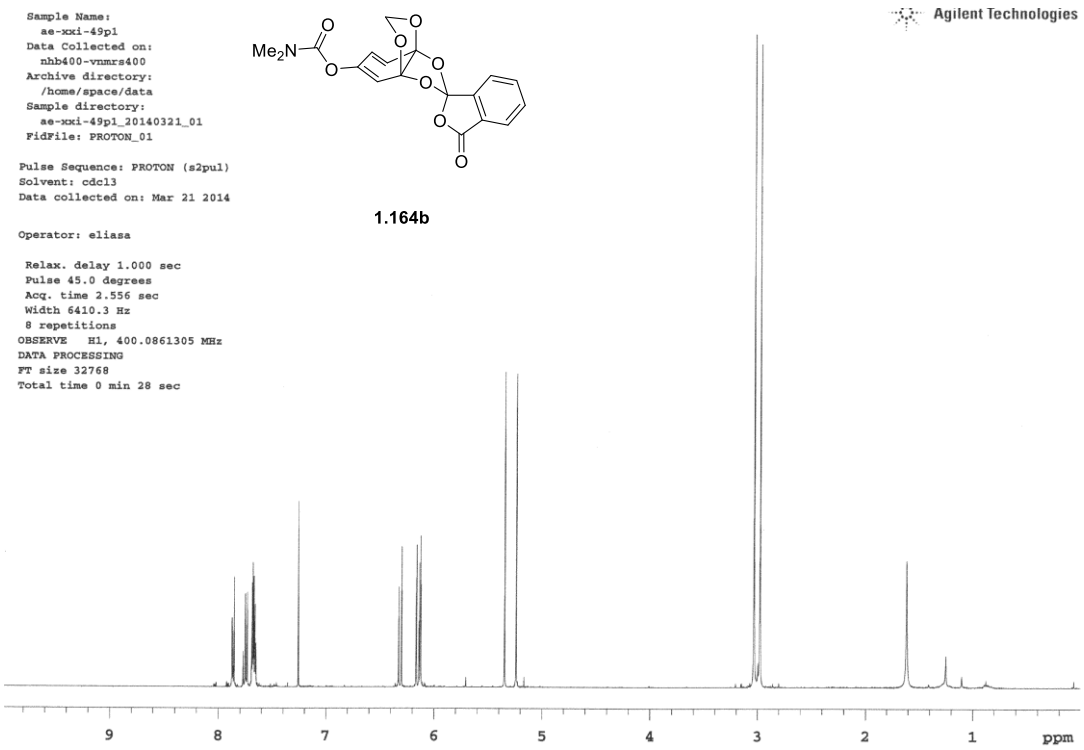
Sample Name:
ae-xxi-49p1
Data Collected on:
nhb400-vnmrs400
Archive directory:
/home/space/data
Sample directory:
ae-xxi-49p1_20140321_01
FidFile: PROTON_01
Pulse Sequence: PROTON (s2pul)
Solvent: cdcl3
Data collected on: Mar 21 2014
Operator: eliasa
Relax. delay 1.000 sec
Pulse 45.0 degrees
Acq. time 2.556 sec
Width 6410.3 Hz
8 repetitions
OBSERVE H1, 400.0861305 MHz
DATA PROCESSING
FT size 32768
Total time 0 min 28 sec
Agilent Technologies
9
8
7
6
5
4
3
2
1
ppm

1.164b

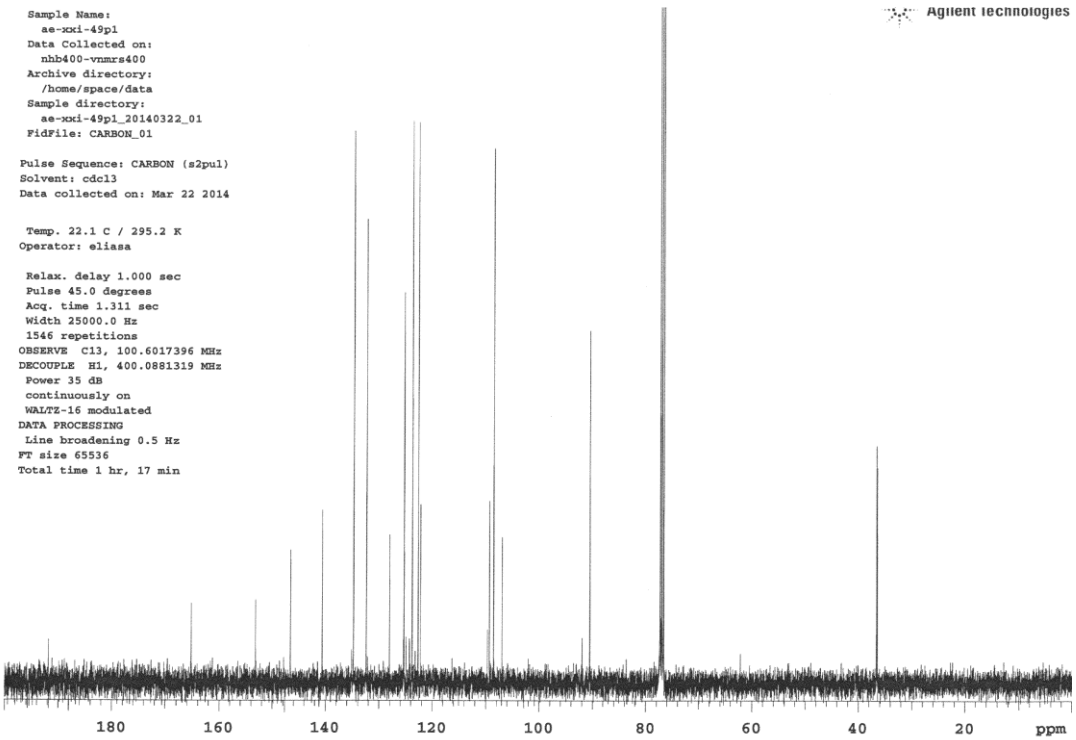
Sample Name:
ae-xxi-49p1
Data Collected on:
nhb400-vnmrs400
Archive directory:
/home/space/data
Sample directory:
ae-xxi-49p1_20140322_01
FidFile: CARBON_01
Pulse Sequence: CARBON (s2pul)
Solvent: cdcl3
Data collected on: Mar 22 2014
Temp. 22.1 C / 295.2 K
Operator: eliasa
Relax. delay 1.000 sec
Pulse 45.0 degrees
Acq. time 1.311 sec
Width 25000.0 Hz
1546 repetitions
OBSERVE C13, 100.6017396 MHz
DECOUPLE H1, 400.0881319 MHz
Power 35 dB
continuously on
WALTZ-16 modulated
DATA PROCESSING
Line broadening 0.5 Hz
FT size 65536
Total time 1 hr, 17 min
Agilent Technologies
180
160
140
120
100
80
60
40
20
ppm

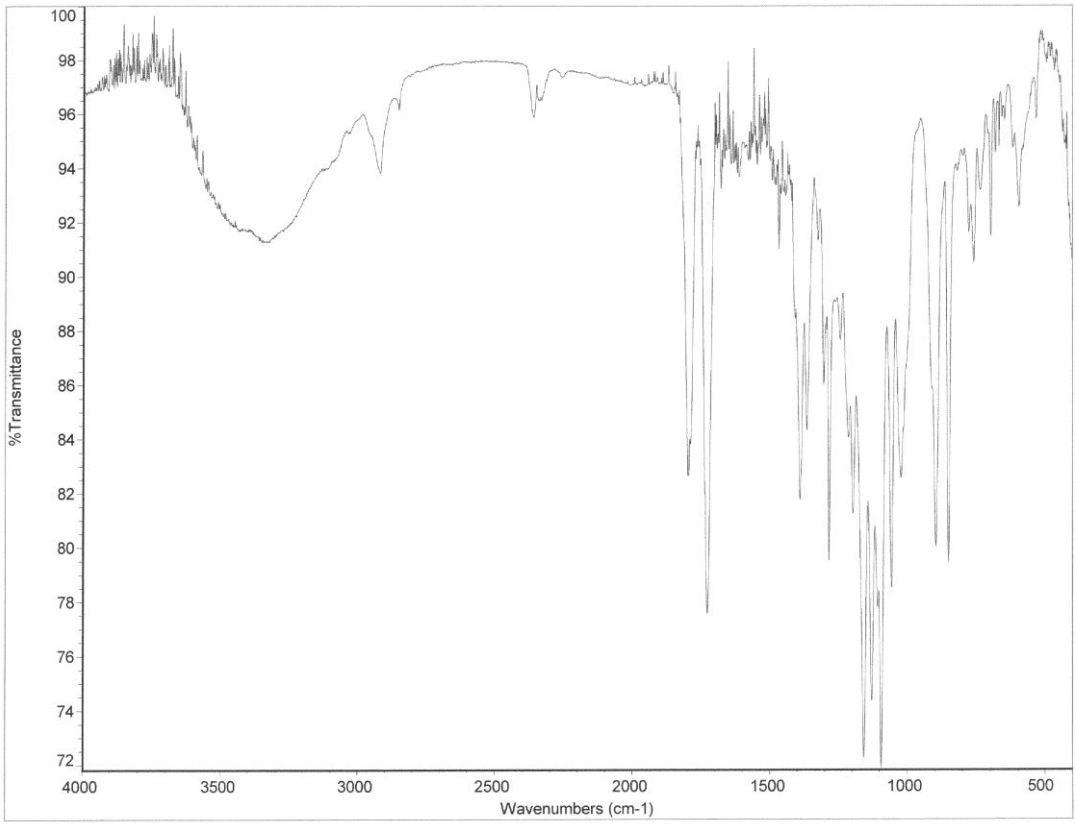
100
98
96
94
92
90
88
86
84
82
80
78
76
74
72
%Transmittance
4000
3500
3000
2500
2000
1500
1000
500
Wavenumbers (cm-1)

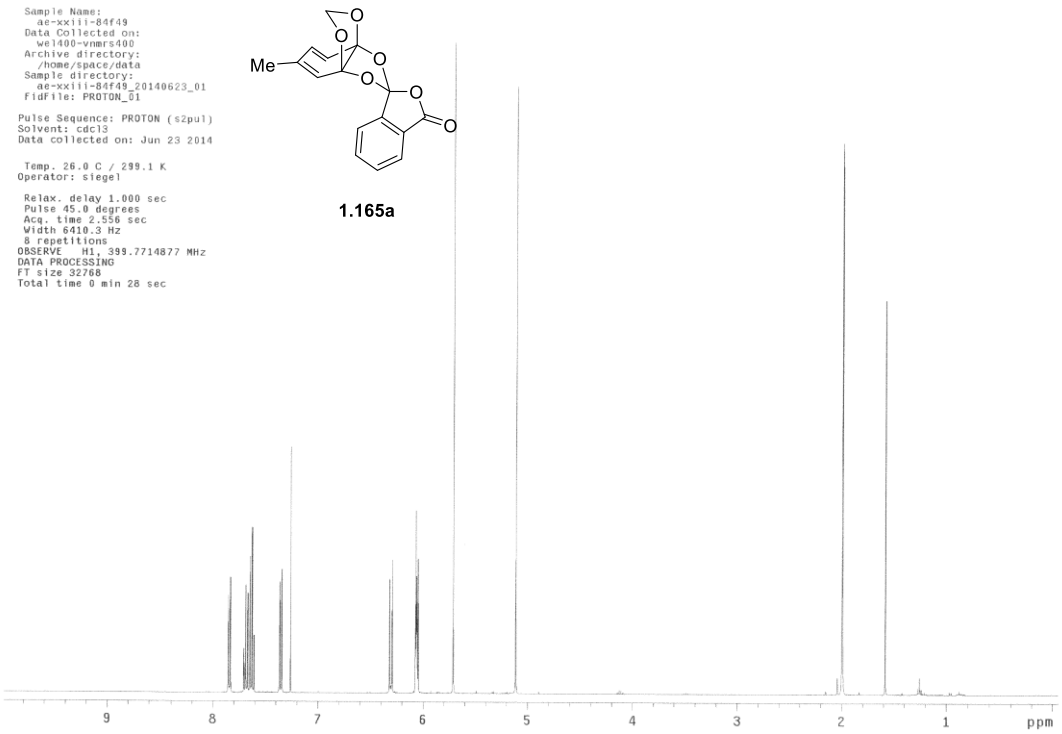
Sample Name:
ae-xxiii-84f49
Data Collected on:
wel400-vnmrs400
Archive directory:
/home/space/data
Sample directory:
ae-xxiii-84f49_20140623_01
FidFile: PROTON_01
Pulse Sequence: PROTON (s2pul)
Solvent: cdcl3
Data collected on: Jun 23 2014
Temp. 26.0 C / 299.1 K
Operator: siegel
Relax. delay 1.000 sec
Pulse 45.0 degrees
Acq. time 2.556 sec
Width 6410.3 Hz
8 repetitions
OBSERVE H1, 399.7714877 MHz
DATA PROCESSING
FT size 32768
Total time 0 min 28 sec
Me
O
1.165a
9
8
7
6
5
4
3
2
1
ppm

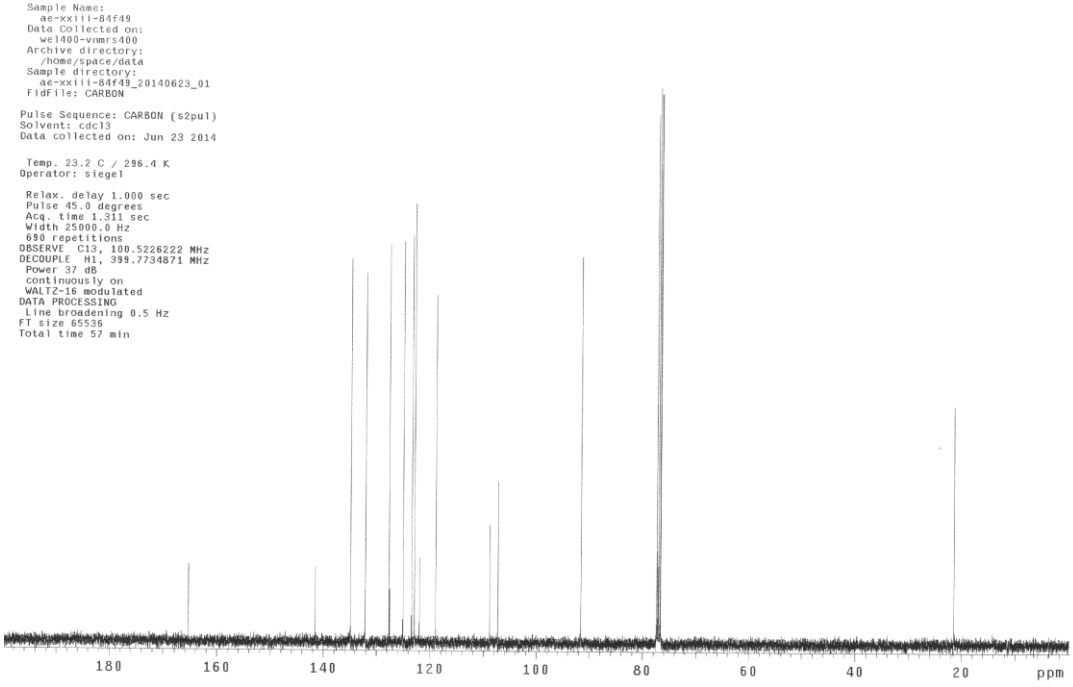
Sample Name:
ae-xxiii-84f49
Data Collected on:
wel400-vnmrs400
Archive directory:
/home/space/data
Sample directory:
ae-xxiii-84f49_20140623_01
FidFile: CARBON
Pulse Sequence: CARBON (s2pul)
Solvent: cdcl3
Data collected on: Jun 23 2014
Temp. 23.2 C / 296.4 K
Operator: siegel
Relax. delay 1.000 sec
Pulse 45.0 degrees
Acq. time 1.311 sec
Width 25000.0 Hz
690 repetitions
OBSERVE C13, 100.5226222 MHz
DECOUPLE H1, 399.7734871 MHz
Power 37 dB
continuously on
WALTZ-16 modulated
DATA PROCESSING
Line broadening 0.5 Hz
FT size 65536
Total time 57 min
180
160
140
120
100
80
60
40
20
ppm

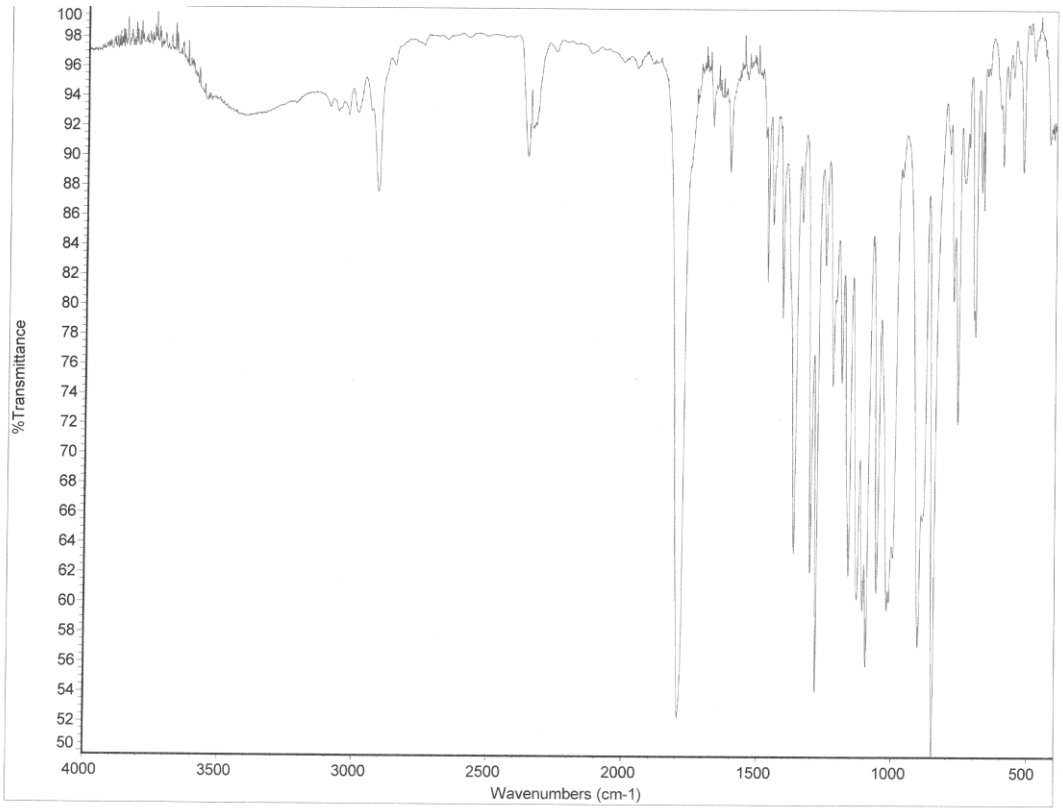
%Transmittance
100
98
96
94
92
90
88
86
84
82
80
78
76
74
72
70
68
66
64
62
60
58
56
54
52
50
4000
3500
3000
2500
2000
1500
1000
500
Wavenumbers (cm-1)

ae-xxiii-90p2
Data Collected on:
nhb400-vnmrs400
Archive directory:

Sample directory:

FidFile: PROTON

Pulse Sequence: PROTON (s2pul)
Solvent: cdcl3
Data collected on: Jun 26 2014

Temp. 23.3 C / 296.4 K
Operator: eliasa

Relax. delay 1.000 sec
Pulse 45.0 degrees
Acq. time 2.556 sec
Width 6410.3 Hz
10 repetitions
OBSERVE H1, 400.0861313 MHz
DATA PROCESSING
FT size 32768
Total time 1 min 54 sec

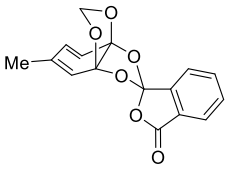

1.165b

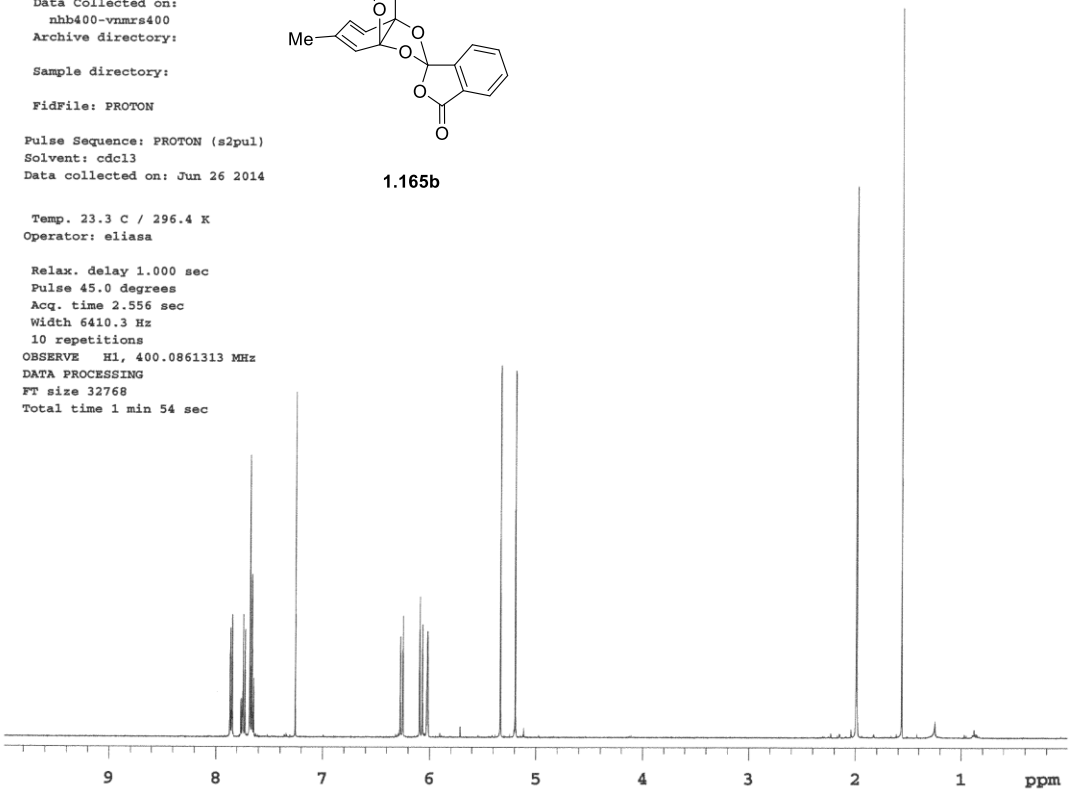

STANDARD CARBON PARAMETERS

Sample Name:
ae-xxiii-90p2
Data Collected on:
wel400-vnmrs400
Archive directory:

Sample directory:

FidFile: CARBON

Pulse Sequence: CARBON (s2pul)
Solvent: cdcl3
Data collected on: Jun 26 2014

Temp. 23.2 C / 296.4 K
Operator: siegel

Relax. delay 1.000 sec
Pulse 45.0 degrees
Acq. time 1.311 sec
Width 25000.0 Hz
590 repetitions
OBSERVE C13, 100.5226215 MHz
DECOUPLE H1, 399.7734871 MHz
Power 37 dB
continuously on
WALTZ-16 modulated
DATA PROCESSING
Line broadening 0.5 Hz
FT size 65536
Total time 57 min

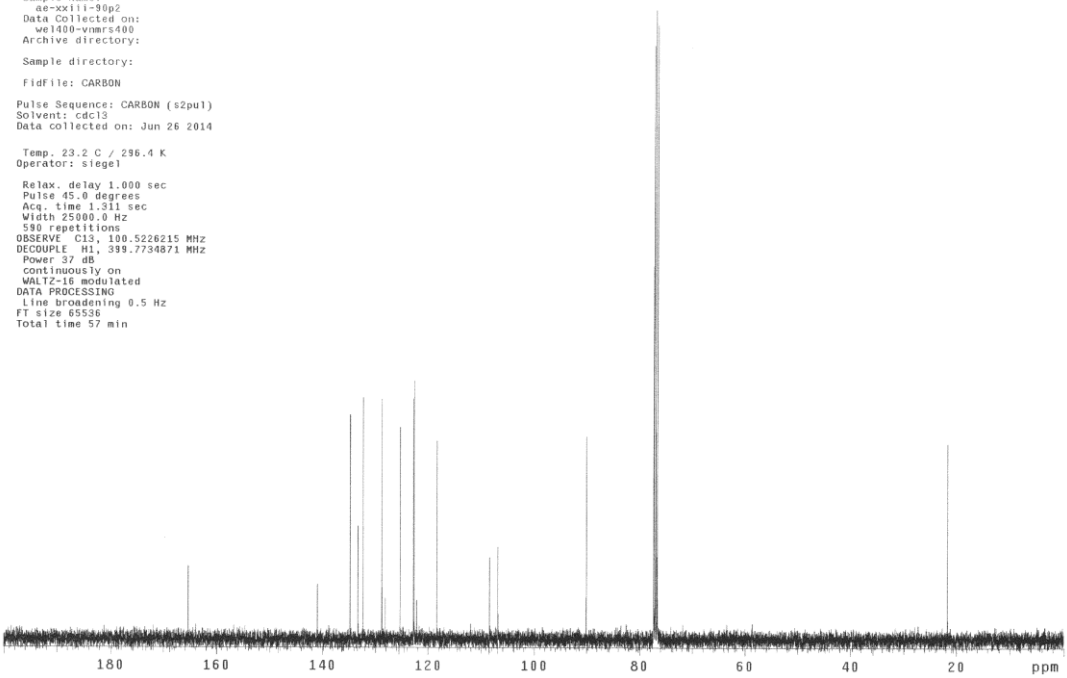

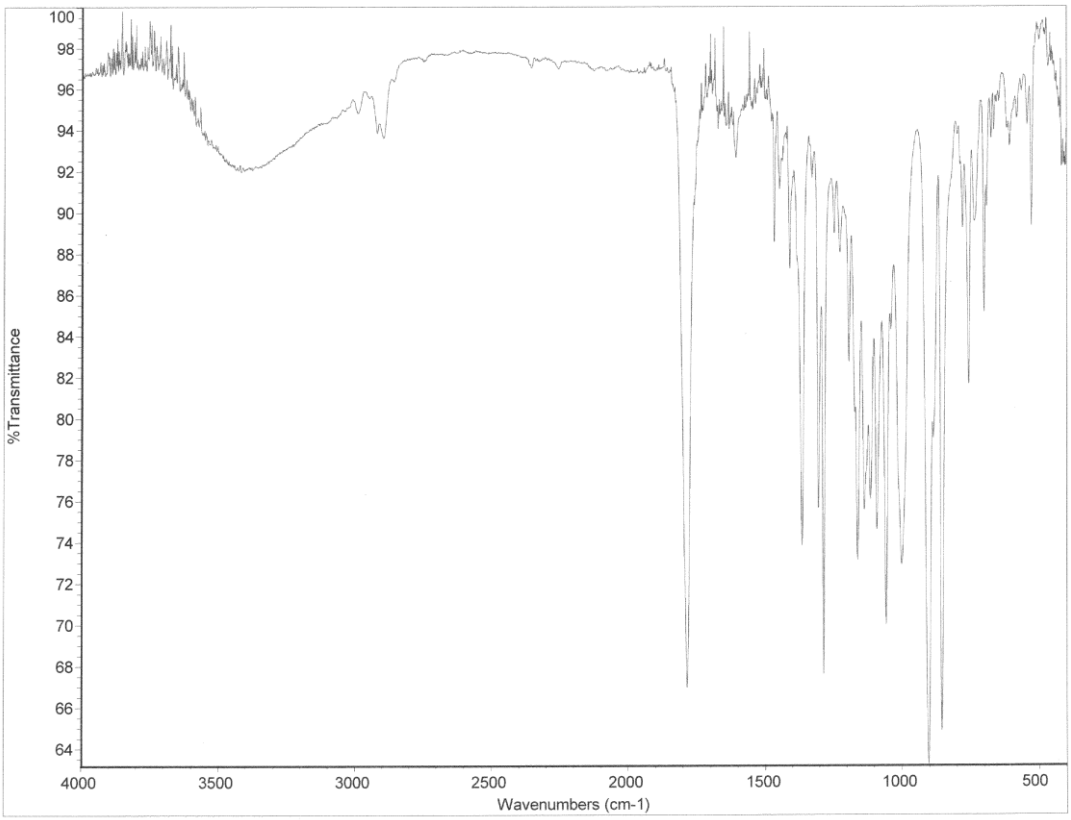
%Transmittance
100
98
96
94
92
90
88
86
84
82
80
78
76
74
72
70
68
66
64
4000
3500
3000
2500
2000
1500
1000
500
Wavenumbers (cm-1)

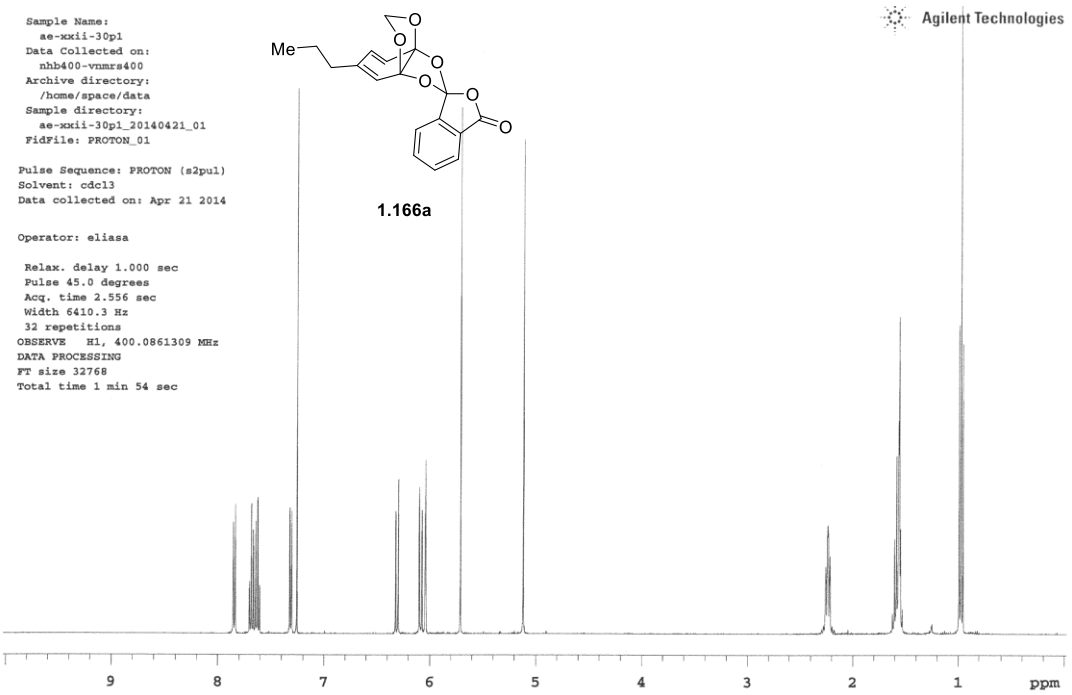
Sample Name:
ae-xxii-30p1
Data Collected on:
nhb400-vnmrs400
Archive directory:
/home/space/data
Sample directory:
ae-xxii-30p1_20140421_01
FidFile: PROTON_01
Pulse Sequence: PROTON (s2pul)
Solvent: cdcl3
Data collected on: Apr 21 2014
Operator: eliasa
Relax. delay 1.000 sec
Pulse 45.0 degrees
Acq. time 2.556 sec
Width 6410.3 Hz
32 repetitions
OBSERVE H1, 400.0861309 MHz
DATA PROCESSING
FT size 32768
Total time 1 min 54 sec
Agilent Technologies
Me
O
1.166a
9
8
7
6
5
4
3
2
1
ppm

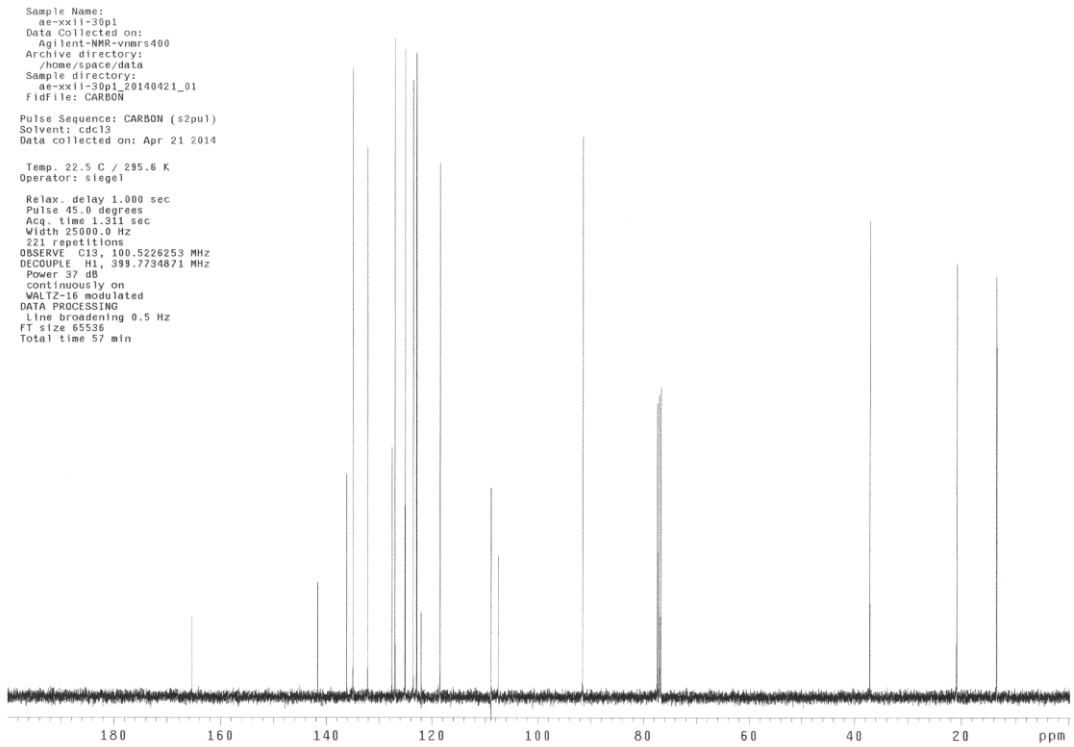
Sample Name:
ae-xxii-30p1
Data Collected on:
Agilent-NMR-vnmrs400
Archive directory:
/home/space/data
Sample directory:
ae-xxii-30p1_20140421_01
FidFile: CARBON
Pulse Sequence: CARBON (s2pul)
Solvent: cdcl3
Data collected on: Apr 21 2014
Temp. 22.5 C / 295.6 K
Operator: siegel
Relax. delay 1.000 sec
Pulse 45.0 degrees
Acq. time 1.311 sec
Width 25000.0 Hz
221 repetitions
OBSERVE C13, 100.5226253 MHz
DECOUPLE H1, 399.7734871 MHz
Power 37 dB
continuously on
WALTZ-16 modulated
DATA PROCESSING
Line broadening 0.5 Hz
FT size 65536
Total time 57 min
180
160
140
120
100
80
60
40
20
ppm

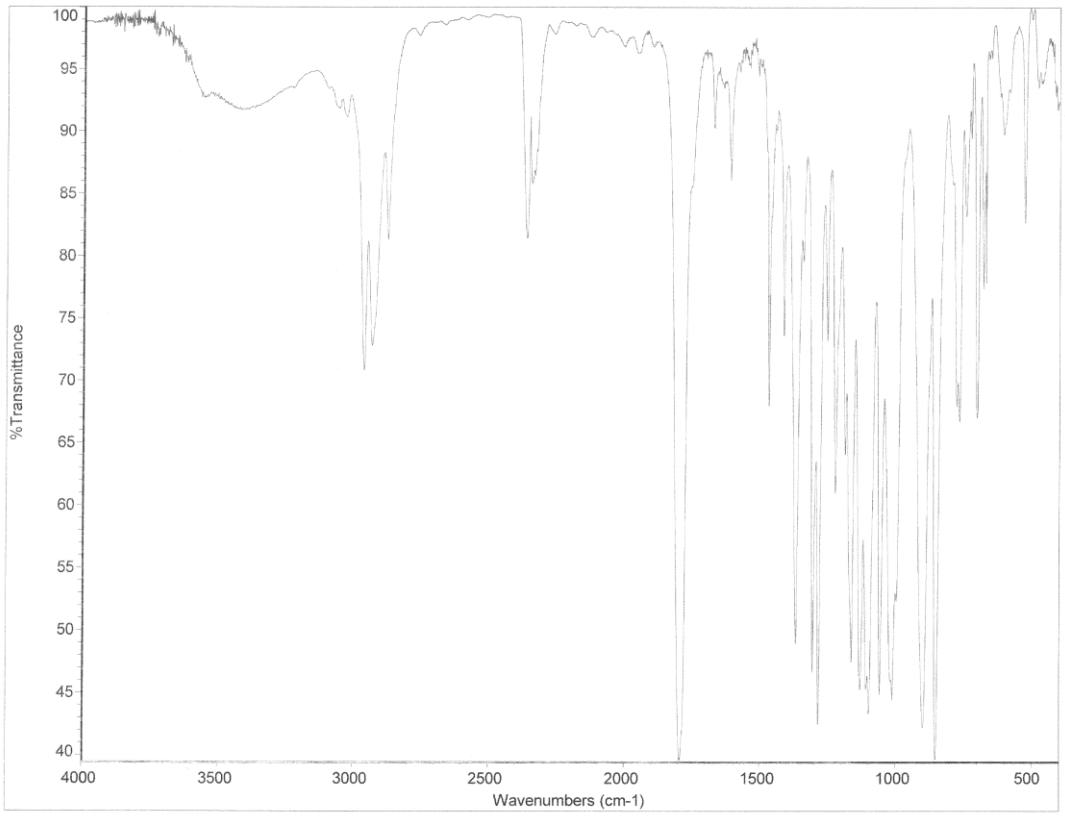
100
95
90
85
80
75
70
65
60
55
50
45
40
%Transmittance
4000
3500
3000
2500
2000
1500
1000
500
Wavenumbers (cm-1)

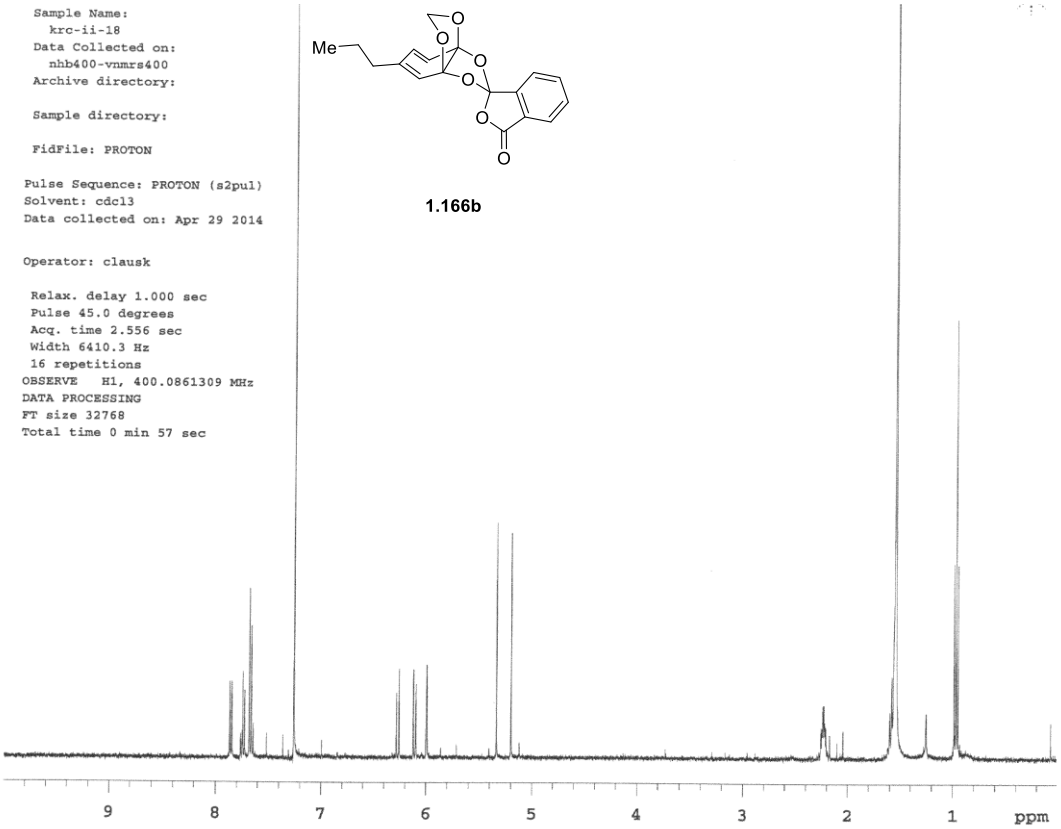
Sample Name:
krc-ii-18
Data Collected on:
nhb400-vnmrs400
Archive directory:
Sample directory:
FidFile: PROTON
Pulse Sequence: PROTON (s2pul)
Solvent: cdcl3
Data collected on: Apr 29 2014
Operator: clausk
Relax. delay 1.000 sec
Pulse 45.0 degrees
Acq. time 2.556 sec
Width 6410.3 Hz
16 repetitions
OBSERVE H1, 400.0861309 MHz
DATA PROCESSING
FT size 32768
Total time 0 min 57 sec
Me
O
O
O
O
O
O
1.166b
9
8
7
6
5
4
3
2
1
ppm

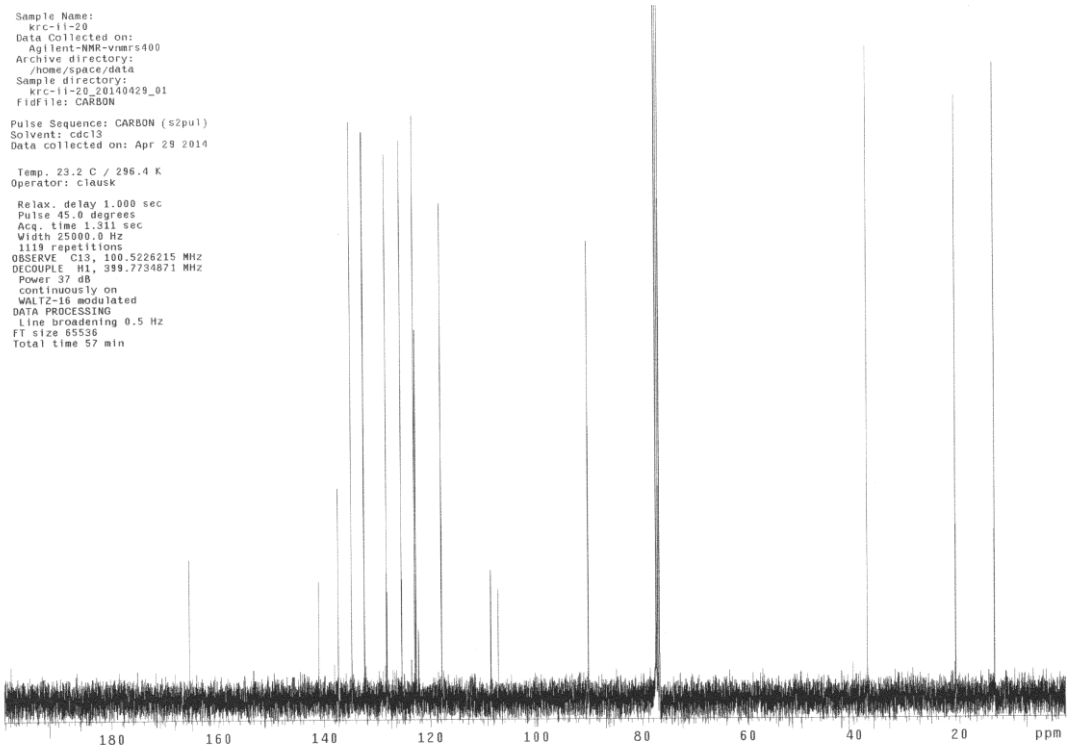
Sample Name:
krc-ii-20
Data Collected on:
Agilent-NMR-vnmrs400
Archive directory:
/home/space/data
Sample directory:
krc-ii-20_20140429_01
FidFile: CARBON
Pulse Sequence: CARBON (s2pul)
Solvent: cdcl3
Data collected on: Apr 29 2014
Temp. 23.2 C / 296.4 K
Operator: clausk
Relax. delay 1.000 sec
Pulse 45.0 degrees
Acq. time 1.311 sec
Width 25000.0 Hz
1119 repetitions
OBSERVE C13, 100.5226215 MHz
DECOUPLE H1, 399.7734871 MHz
Power 37 dB
continuously on
WALTZ-16 modulated
DATA PROCESSING
Line broadening 0.5 Hz
FT size 65536
Total time 57 min
180
160
140
120
100
80
60
40
20
ppm

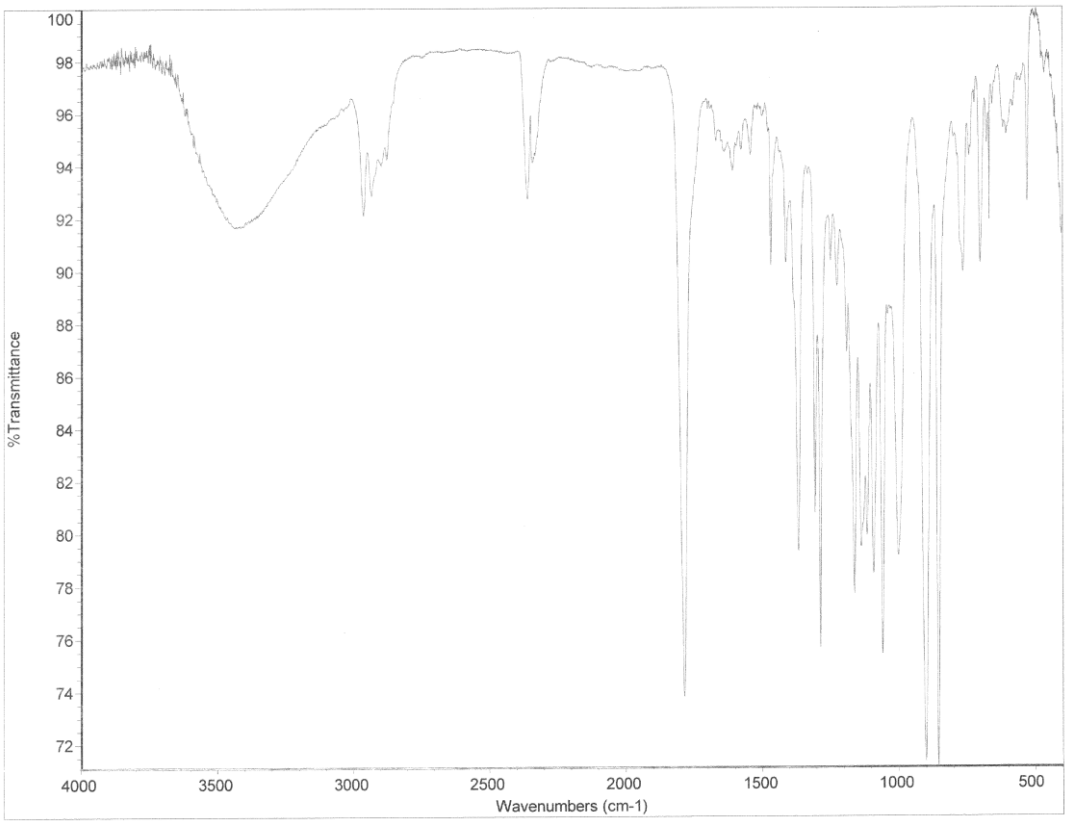
100
98
96
94
92
90
88
86
84
82
80
78
76
74
72
%Transmittance
4000
3500
3000
2500
2000
1500
1000
500
Wavenumbers (cm-1)

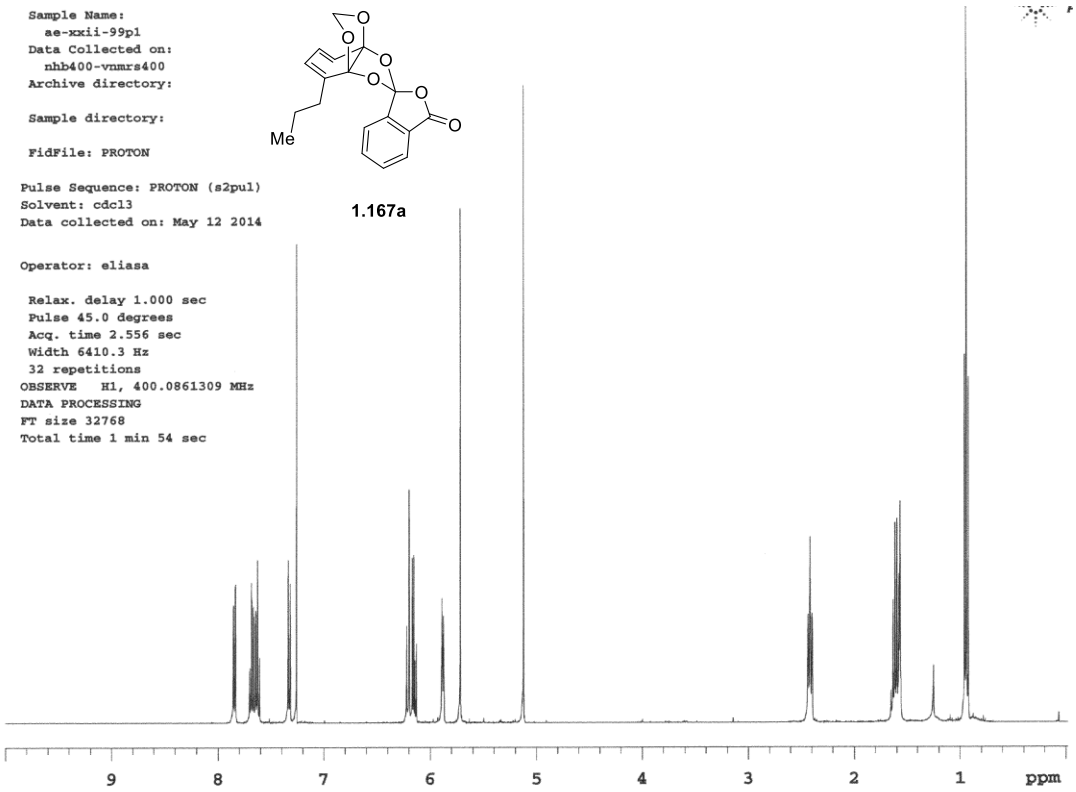
Sample Name:
ae-xxii-99p1
Data Collected on:
nhb400-vnmrs400
Archive directory:
Sample directory:
FidFile: PROTON
Pulse Sequence: PROTON (s2pul)
Solvent: cdcl3
Data collected on: May 12 2014
Operator: eliasa
Relax. delay 1.000 sec
Pulse 45.0 degrees
Acq. time 2.556 sec
Width 6410.3 Hz
32 repetitions
OBSERVE H1, 400.0861309 MHz
DATA PROCESSING
FT size 32768
Total time 1 min 54 sec
Me
O
1.167a
9
8
7
6
5
4
3
2
1
ppm

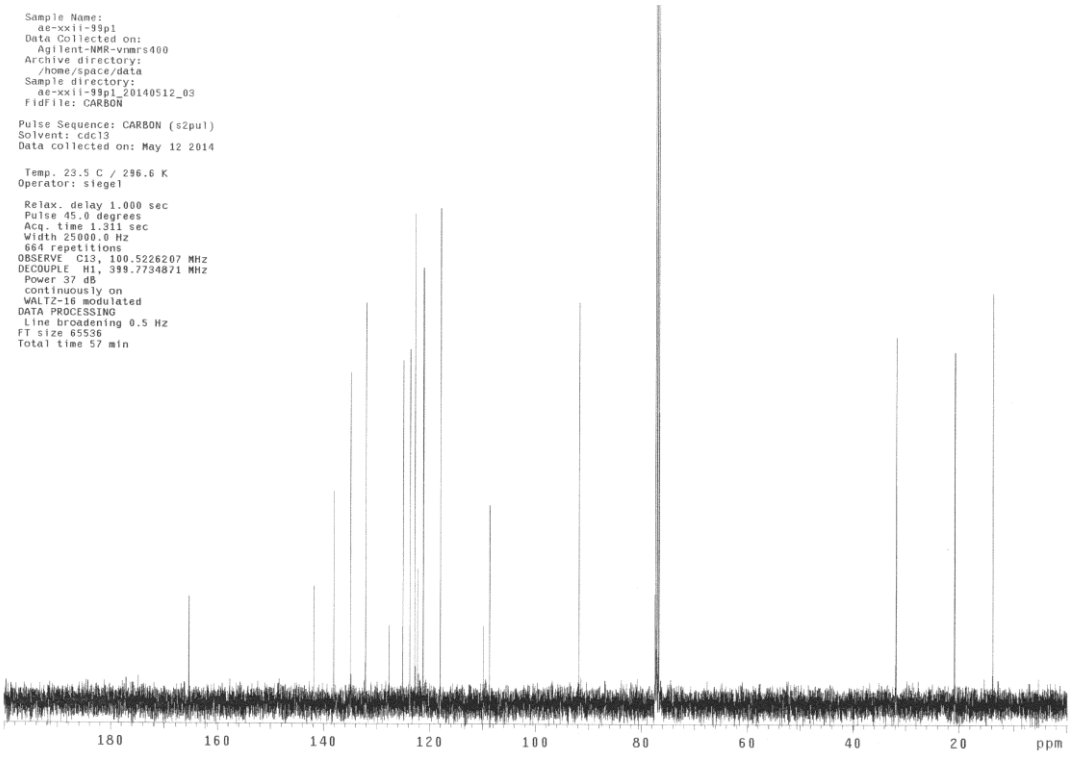
Sample Name:
ae-xxii-99p1
Data Collected on:
Agilent-NMR-vnmrs400
Archive directory:
/home/space/data
Sample directory:
ae-xxii-99p1_20140512_03
FidFile: CARBON
Pulse Sequence: CARBON (s2pul)
Solvent: cdcl3
Data collected on: May 12 2014
Temp. 23.5 C / 296.6 K
Operator: siegel
Relax. delay 1.000 sec
Pulse 45.0 degrees
Acq. time 1.311 sec
Width 25000.0 Hz
664 repetitions
OBSERVE C13, 100.5226207 MHz
DECOUPLE H1, 399.7734871 MHz
Power 37 dB
continuously on
WALTZ-16 modulated
DATA PROCESSING
Line broadening 0.5 Hz
FT size 65536
Total time 57 min
180
160
140
120
100
80
60
40
20
ppm

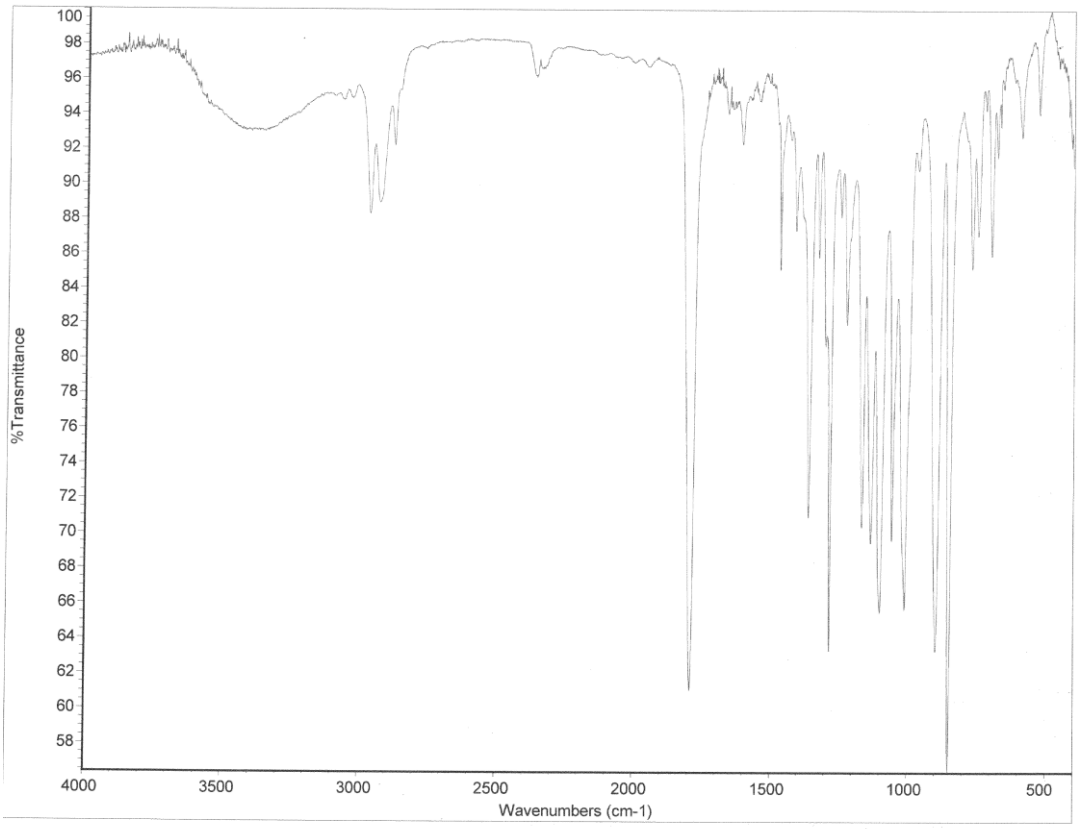
%Transmittance
100
98
96
94
92
90
88
86
84
82
80
78
76
74
72
70
68
66
64
62
60
58
4000
3500
3000
2500
2000
1500
1000
500
Wavenumbers (cm-1)

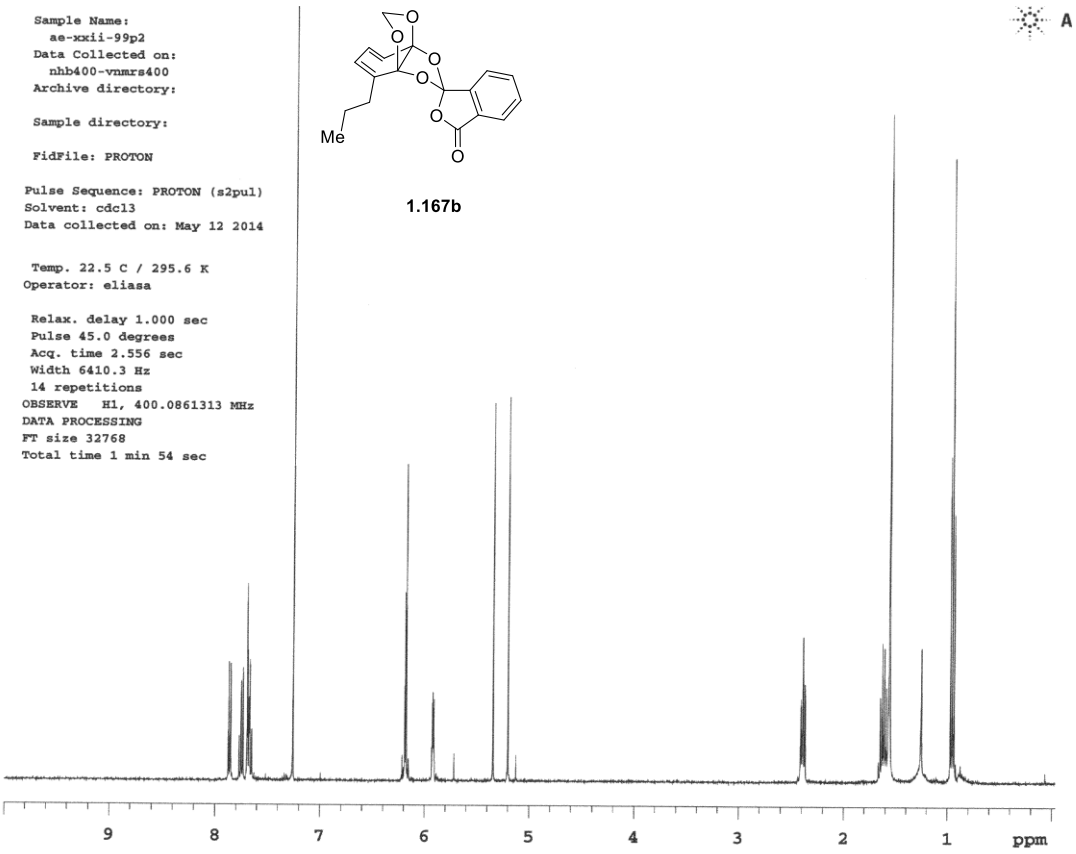
Sample Name:
ae-xxii-99p2
Data Collected on:
nhb400-vnmrs400
Archive directory:
Sample directory:
FidFile: PROTON
Pulse Sequence: PROTON (s2pul)
Solvent: cdcl3
Data collected on: May 12 2014
Temp. 22.5 C / 295.6 K
Operator: eliasa
Relax. delay 1.000 sec
Pulse 45.0 degrees
Acq. time 2.556 sec
Width 6410.3 Hz
14 repetitions
OBSERVE H1, 400.0861313 MHz
DATA PROCESSING
FT size 32768
Total time 1 min 54 sec
Me
O
1.167b
A
9
8
7
6
5
4
3
2
1
ppm

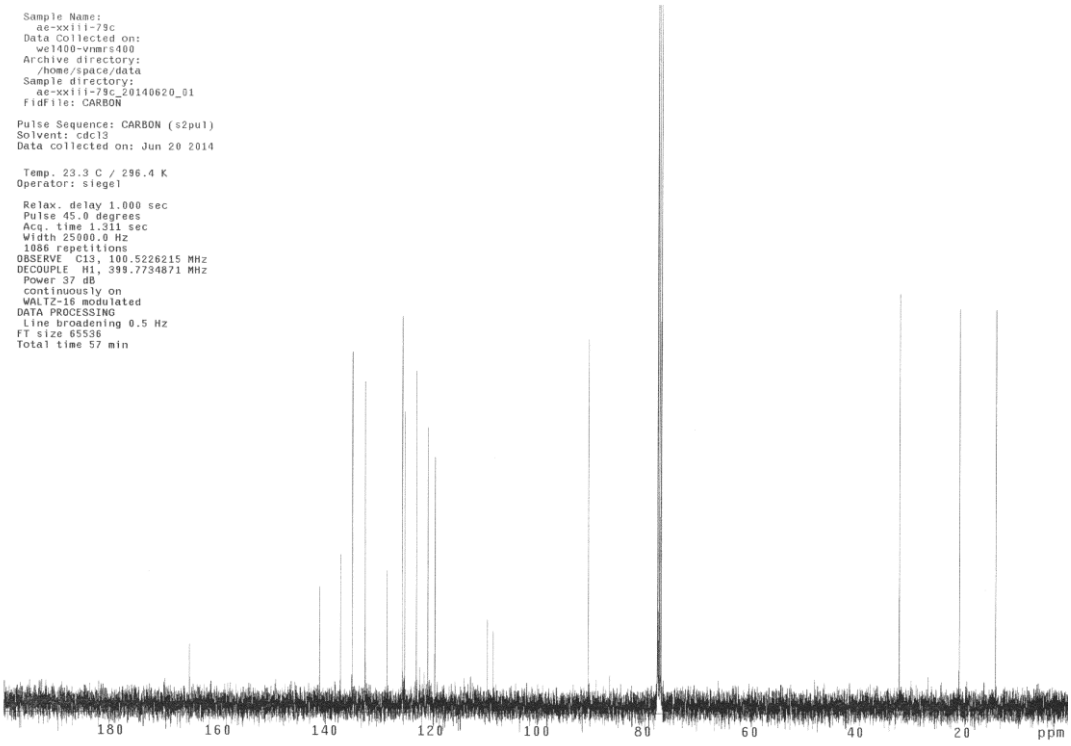
Sample Name:
ae-xxiii-79c
Data Collected on:
wel400-vnmrs400
Archive directory:
/home/space/data
Sample directory:
ae-xxiii-79c_20140620_01
FidFile: CARBON
Pulse Sequence: CARBON (s2pul)
Solvent: cdcl3
Data collected on: Jun 20 2014
Temp. 23.3 C / 296.4 K
Operator: siegel
Relax. delay 1.000 sec
Pulse 45.0 degrees
Acq. time 1.311 sec
Width 25000.0 Hz
1086 repetitions
OBSERVE C13, 100.5226215 MHz
DECOUPLE H1, 399.7734871 MHz
Power 37 dB
continuously on
WALTZ-16 modulated
DATA PROCESSING
Line broadening 0.5 Hz
FT size 65536
Total time 57 min
180
160
140
120
100
80
60
40
20
ppm

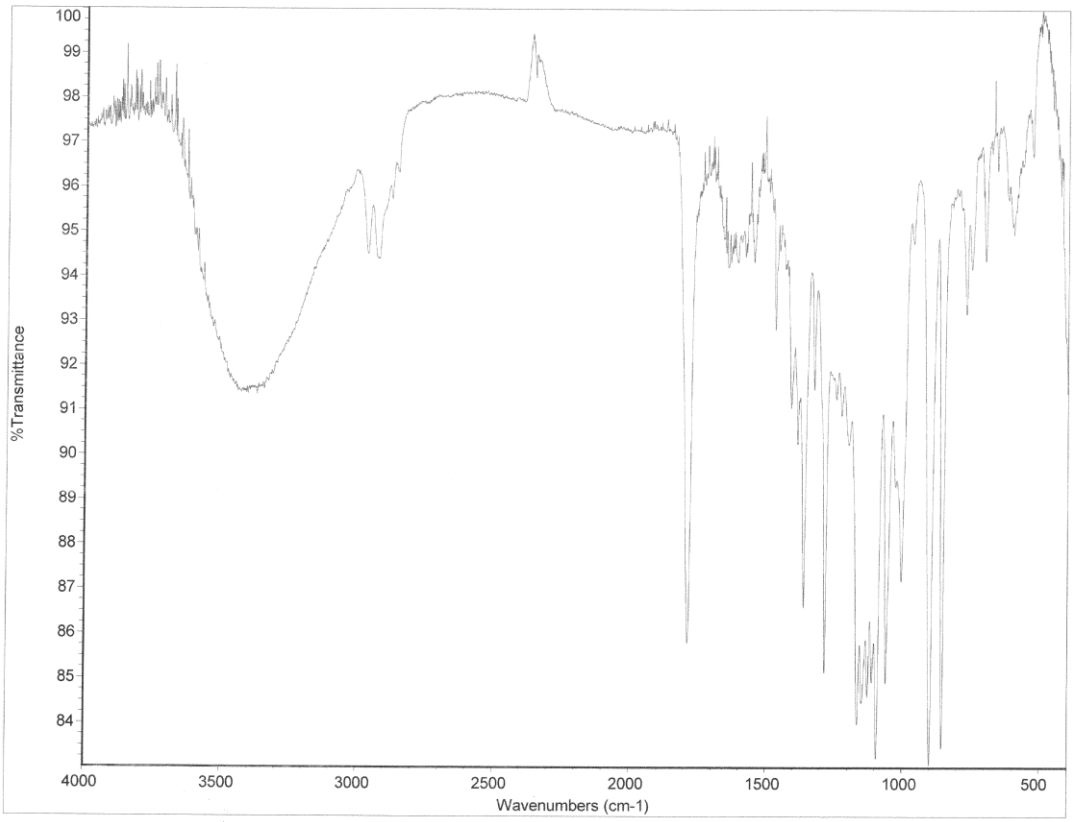
%Transmittence
100
99
98
97
96
95
94
93
92
91
90
89
88
87
86
85
84
4000
3500
3000
2500
2000
1500
1000
500
Wavenumbers (cm-1)

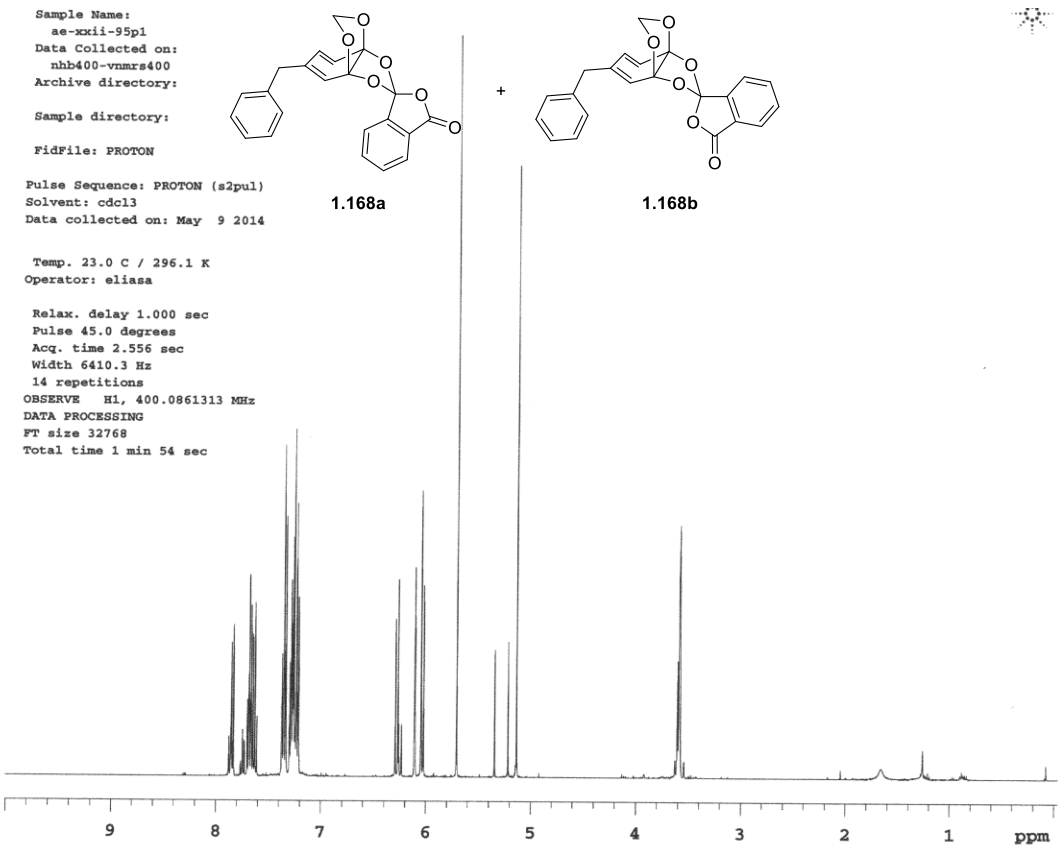
Sample Name:
ae-xxii-95p1
Data Collected on:
nhb400-vnmrs400
Archive directory:
Sample directory:
FidFile: PROTON
Pulse Sequence: PROTON (s2pul)
Solvent: cdcl3
Data collected on: May 9 2014
Temp. 23.0 C / 296.1 K
Operator: eliasa
Relax. delay 1.000 sec
Pulse 45.0 degrees
Acq. time 2.556 sec
Width 6410.3 Hz
14 repetitions
OBSERVE H1, 400.0861313 MHz
DATA PROCESSING
FT size 32768
Total time 1 min 54 sec
1.168a
+
1.168b
9
8
7
6
5
4
3
2
1
ppm

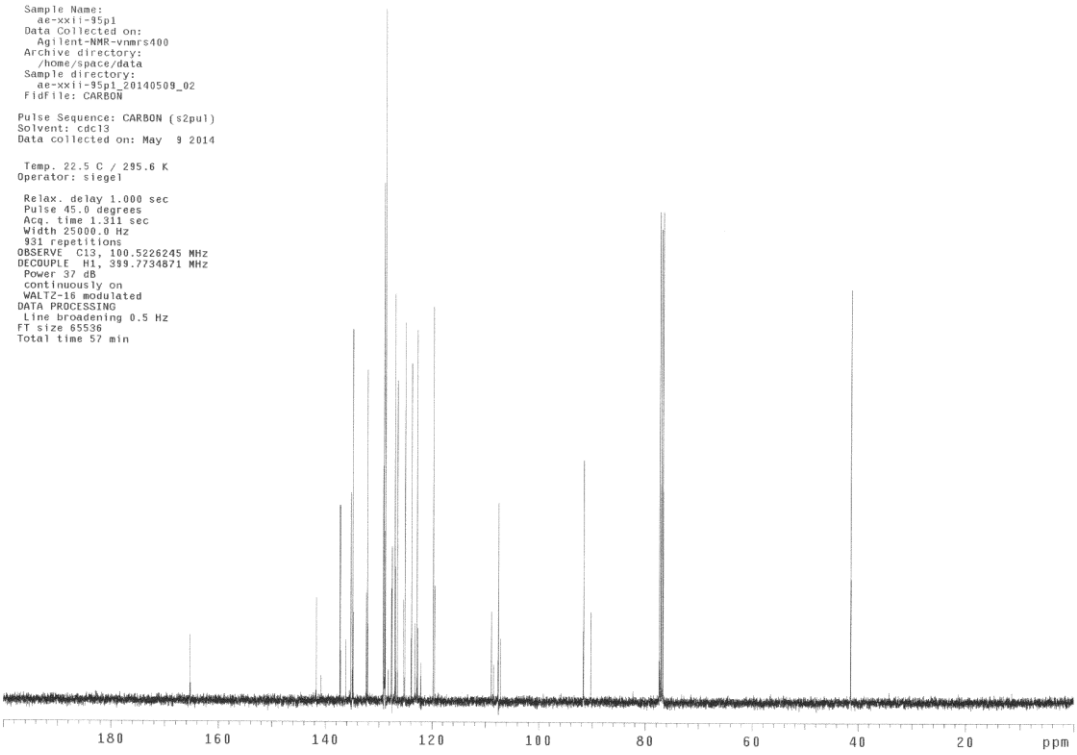
Sample Name:
ae-xxii-95p1
Data Collected on:
Agilent-NMR-vnmrs400
Archive directory:
/home/space/data
Sample directory:
ae-xxii-95p1_20140509_02
Fidfile: CARBON
Pulse Sequence: CARBON (s2pul)
Solvent: cdcl3
Data collected on: May 9 2014
Temp. 22.5 C / 295.6 K
Operator: siegel
Relax. delay 1.000 sec
Pulse 45.0 degrees
Acq. time 1.311 sec
Width 25000.0 Hz
931 repetitions
OBSERVE C13, 100.5226245 MHz
DECOUPLE H1, 399.7734871 MHz
Power 37 dB
continuously on
WALTZ-16 modulated
DATA PROCESSING
Line broadening 0.5 Hz
FT size 65536
Total time 57 min
180
160
140
120
100
80
60
40
20
ppm

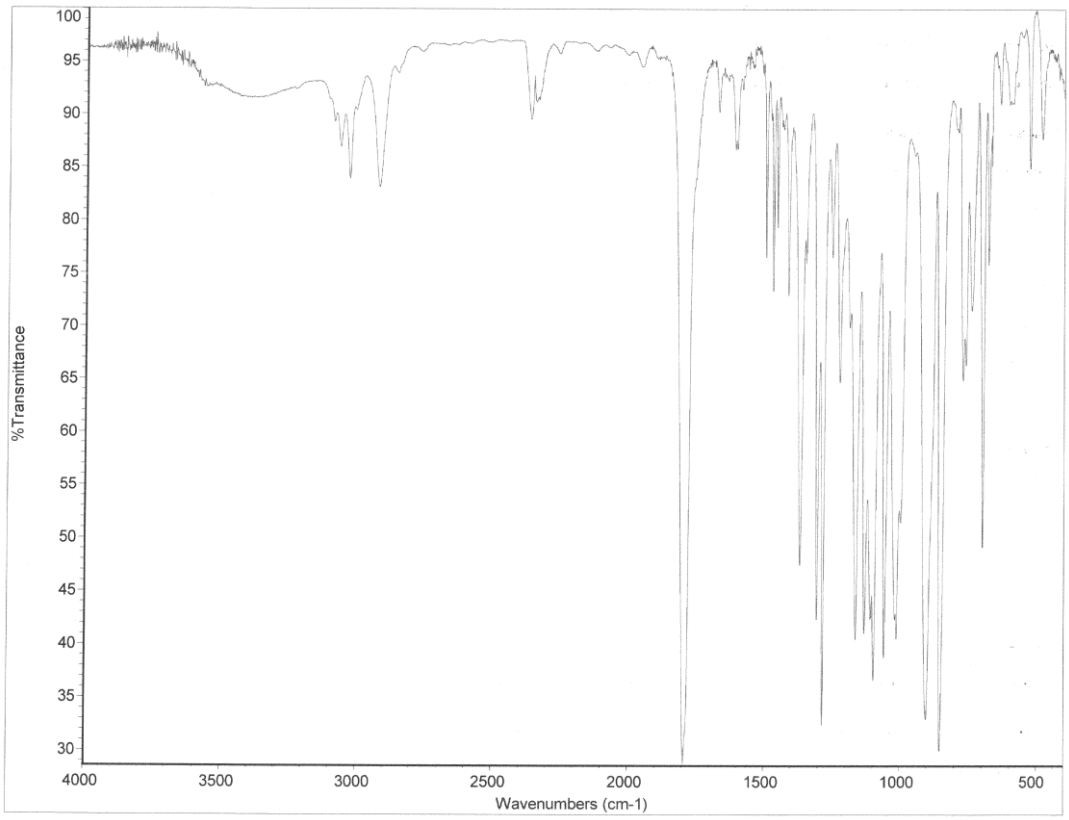
%Transmittance
100
95
90
85
80
75
70
65
60
55
50
45
40
35
30
4000
3500
3000
2500
2000
1500
1000
500
Wavenumbers (cm-1)

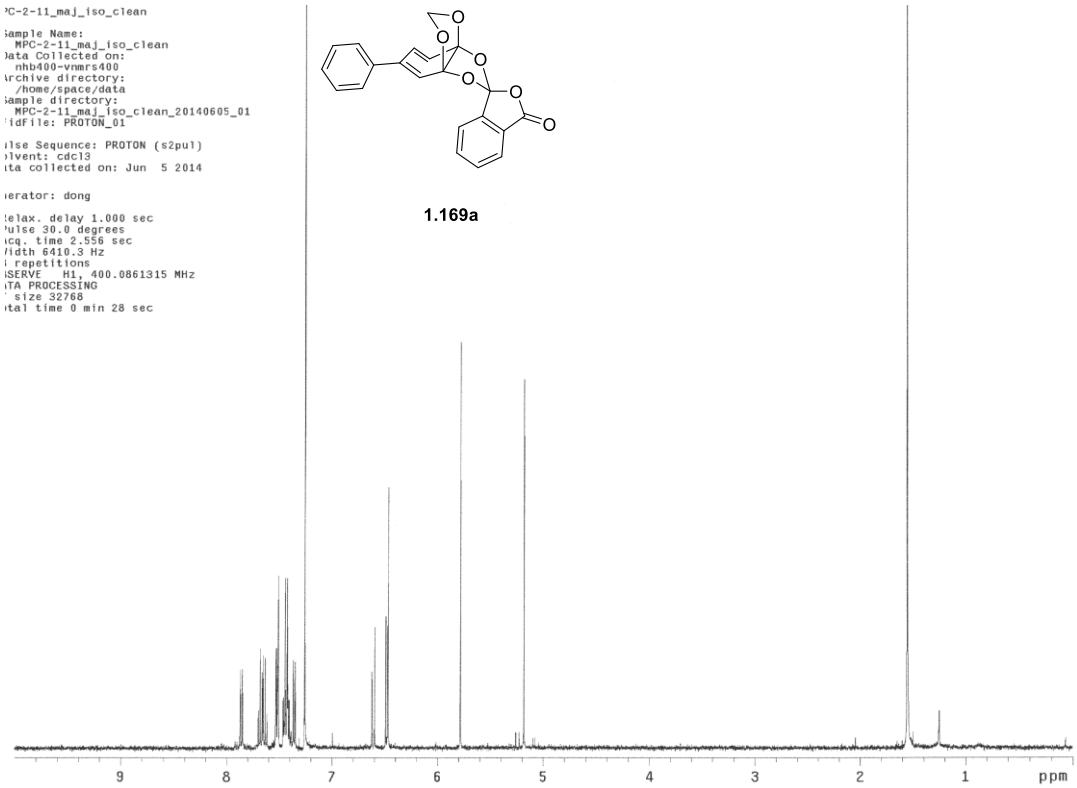
PC-2-11_maj_iso_clean
Sample Name:
MPC-2-11_maj_iso_clean
Data Collected on:
nhb400-vnmrs400
Archive directory:
/home/space/data
Sample directory:
MPC-2-11_maj_iso_clean_20140605_01
FidFile: PROTON_01
Pulse Sequence: PROTON (s2pul)
Solvent: cdcl3
Data collected on: Jun 5 2014
Operator: dong
Relax. delay 1.000 sec
Pulse 30.0 degrees
Acq. time 2.556 sec
Width 6410.3 Hz
1 repetitions
OBSERVE H1, 400.0861315 MHz
DATA PROCESSING
FT size 32768
Total time 0 min 28 sec
1.169a
9
8
7
6
5
4
3
2
1
ppm

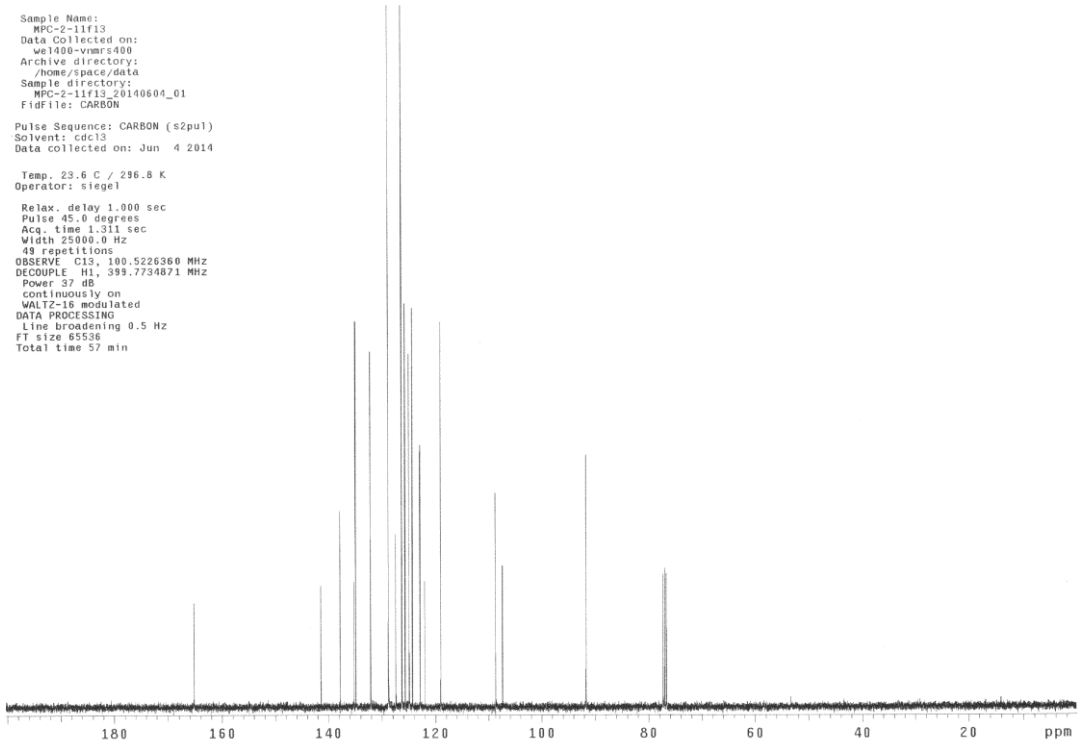
Sample Name:
MPC-2-11f13
Data Collected on:
we1400-vnmrs400
Archive directory:
/home/space/data
Sample directory:
MPC-2-11f13_20140604_01
FidFile: CARBON
Pulse Sequence: CARBON (s2pul)
Solvent: cdcl3
Data collected on: Jun 4 2014
Temp. 23.6 C / 296.8 K
Operator: siegel
Relax. delay 1.000 sec
Pulse 45.0 degrees
Acq. time 1.311 sec
Width 25000.0 Hz
49 repetitions
OBSERVE C13, 100.5226360 MHz
DECOUPLE H1, 399.7734871 MHz
Power 37 dB
continuously on
WALTZ-16 modulated
DATA PROCESSING
Line broadening 0.5 Hz
FT size 65536
Total time 57 min
180
160
140
120
100
80
60
40
20
ppm

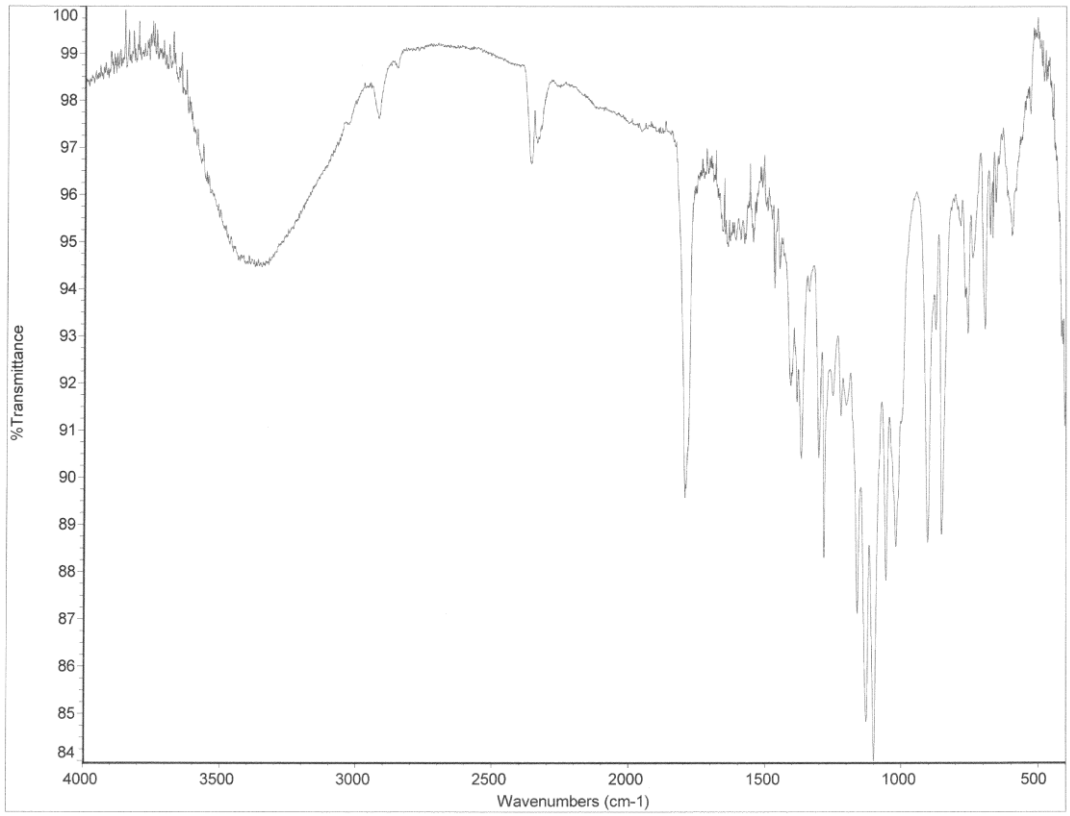
%Transmittance
100
99
98
97
96
95
94
93
92
91
90
89
88
87
86
85
84
4000
3500
3000
2500
2000
1500
1000
500
Wavenumbers (cm-1)

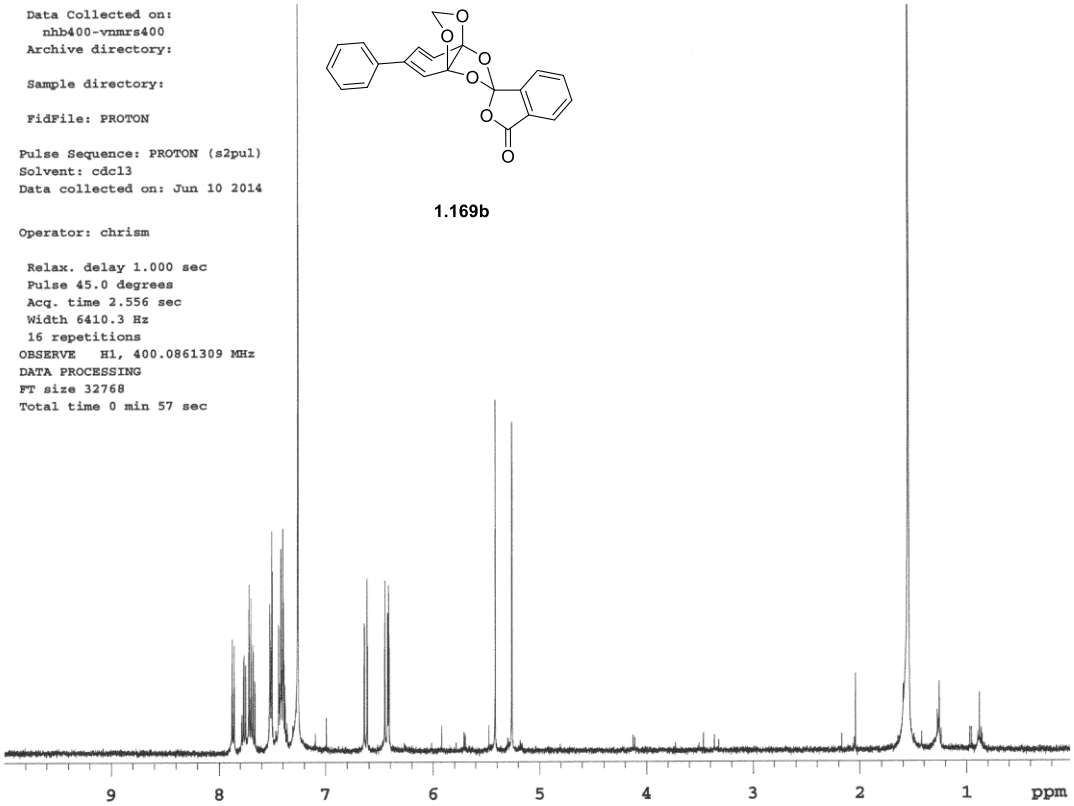
Data Collected on:
nhb400-vnmrs400
Archive directory:
Sample directory:
FidFile: PROTON
Pulse Sequence: PROTON (s2pul)
Solvent: cdcl3
Data collected on: Jun 10 2014
Operator: chrism
Relax. delay 1.000 sec
Pulse 45.0 degrees
Acq. time 2.556 sec
Width 6410.3 Hz
16 repetitions
OBSERVE H1, 400.0861309 MHz
DATA PROCESSING
FT size 32768
Total time 0 min 57 sec
1.169b
9
8
7
6
5
4
3
2
1
ppm

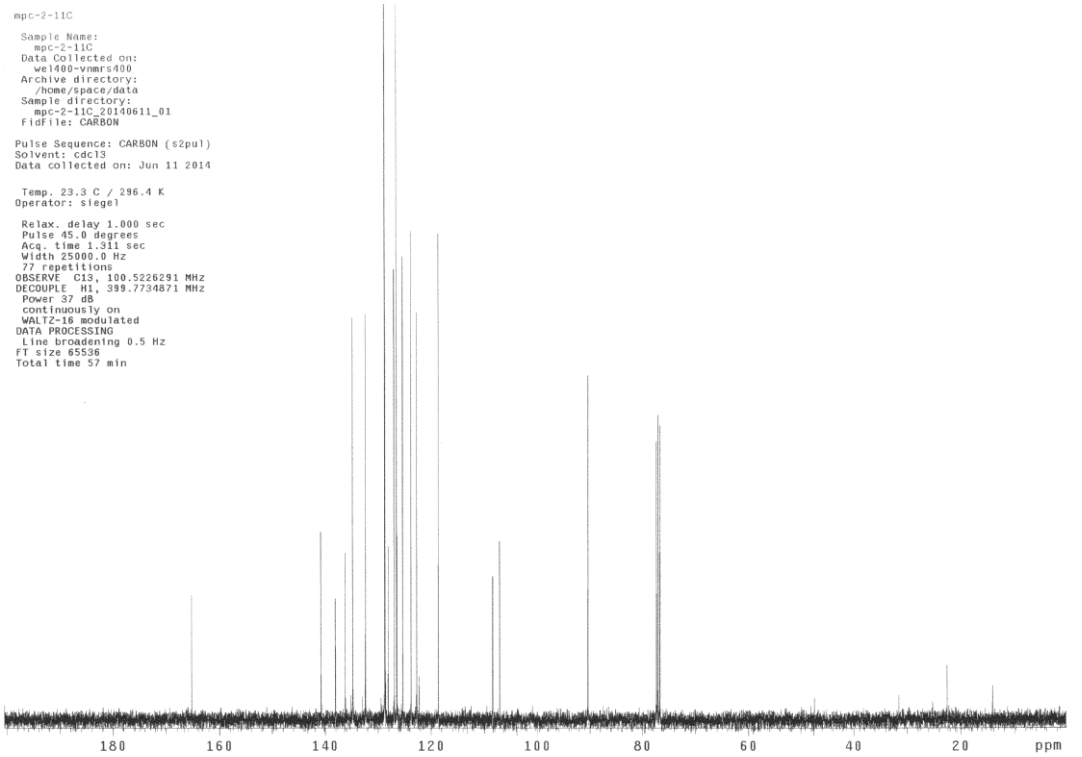
mpc-2-11C
Sample Name:
mpc-2-11C
Data Collected on:
wel400-vnmrs400
Archive directory:
/home/space/data
Sample directory:
mpc-2-11C_20140611_01
FidFile: CARBON
Pulse Sequence: CARBON (s2pul)
Solvent: cdcl3
Data collected on: Jun 11 2014
Temp. 23.3 C / 296.4 K
Operator: siegel
Relax. delay 1.000 sec
Pulse 45.0 degrees
Acq. time 1.311 sec
Width 25000.0 Hz
77 repetitions
OBSERVE C13, 100.5226291 MHz
DECOUPLE H1, 399.7734871 MHz
Power 37 dB
continuously on
WALTZ-16 modulated
DATA PROCESSING
Line broadening 0.5 Hz
FT size 65536
Total time 57 min
180
160
140
120
100
80
60
40
20
ppm

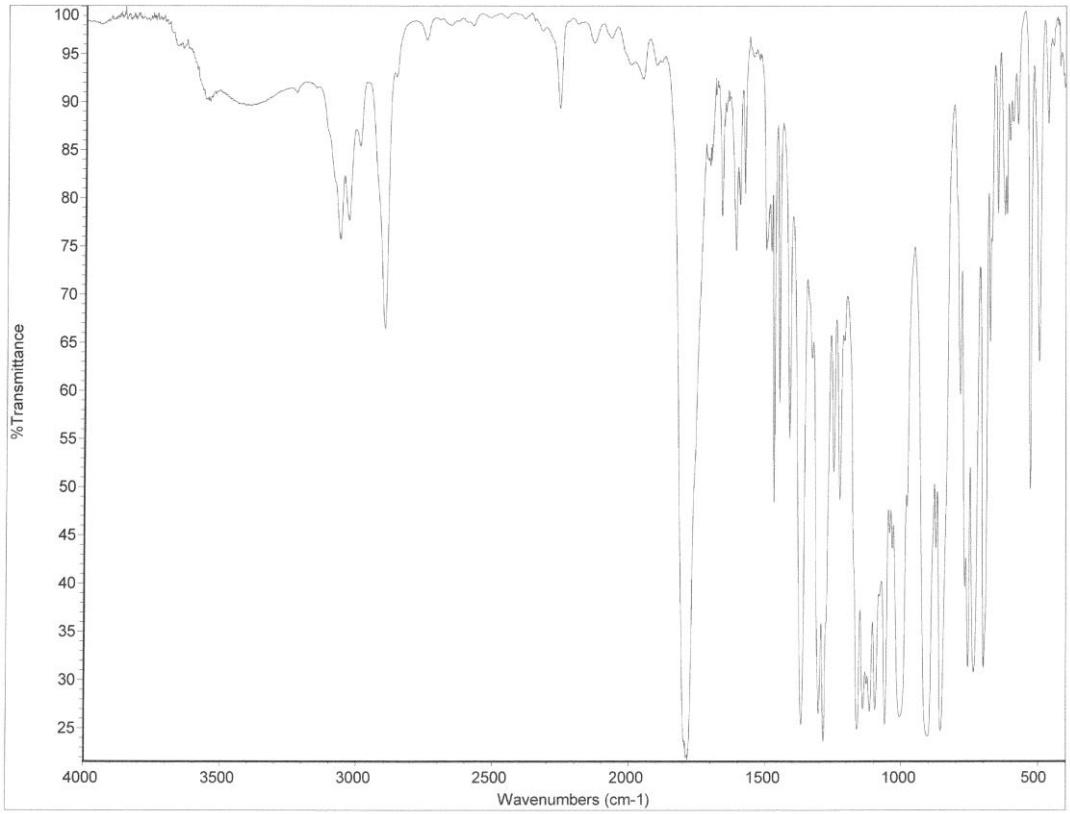
%Transmittance
100
95
90
85
80
75
70
65
60
55
50
45
40
35
30
25
4000
3500
3000
2500
2000
1500
1000
500
Wavenumbers (cm-1)

Sample Name:
RB-29
Data Collected on:
nhbrobo-vnmrs400
Archive directory:
/home/staff31/vnmrsys/data
Sample directory:
RB-29_20140627_01
FidFile: PROTON_01

Pulse Sequence: PROTON (s2pul)
Solvent: cdcl3
Data collected on: Jun 27 2014

Temp. 25.0 C / 298.1 K
Sample #7, Operator: siegel

Relax. delay 1.000 sec
Pulse 30.0 degrees
Acq. time 2.556 sec
Width 6410.3 Hz
16 repetitions
OBSERVE H1, 399.6757273 MHz
DATA PROCESSING
FT size 32768
Total time 0 min 57 sec

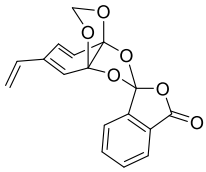

1.170a

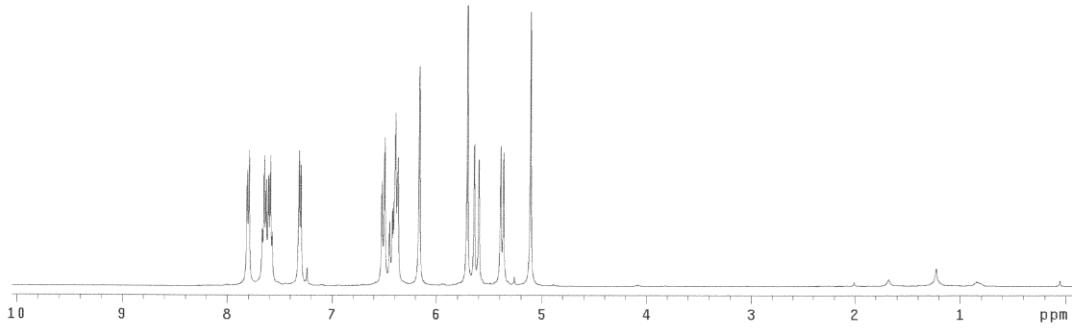

Sample Name:
RB-29
Data Collected on:
nhbrobo-vnmrs400
Archive directory:
/home/staff31/vnmrsys/data
Sample directory:
RB-29_20140627_01
FidFile: CARBON_01

Pulse Sequence: CARBON (s2pul)
Solvent: cdcl3
Data collected on: Jun 27 2014

Temp. 25.0 C / 298.1 K
Sample #7, Operator: siegel

Relax. delay 1.000 sec
Pulse 30.0 degrees
Acq. time 1.311 sec
Width 25000.0 Hz
512 repetitions
OBSERVE C13, 100.4985476 MHz
DECOUPLE H1, 399.6777257 MHz
Power 39 dB
continuously on
WALTZ-16 modulated
DATA PROCESSING
Line broadening 0.5 Hz
FT size 65536
Total time 13 min

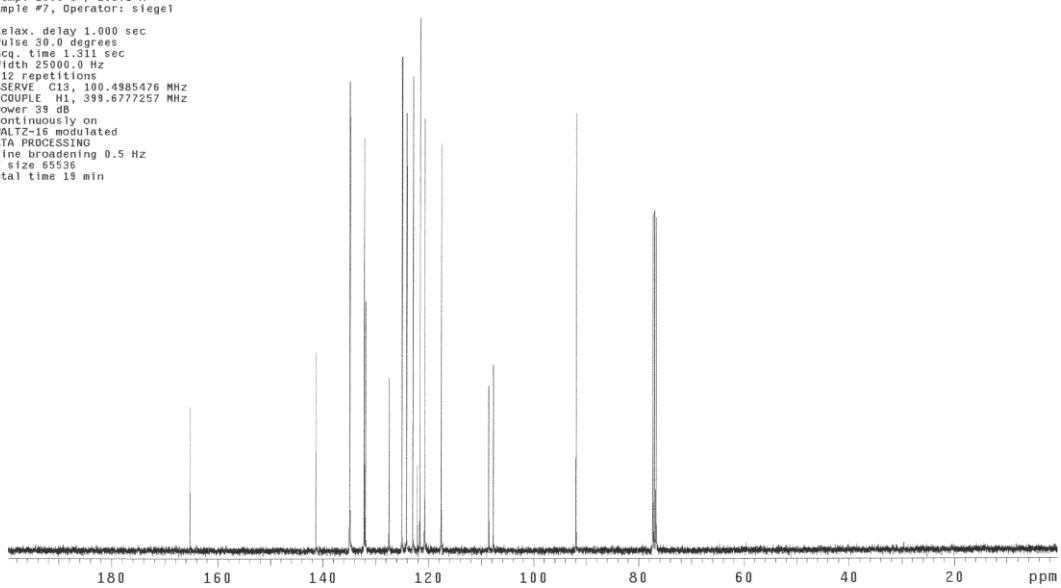

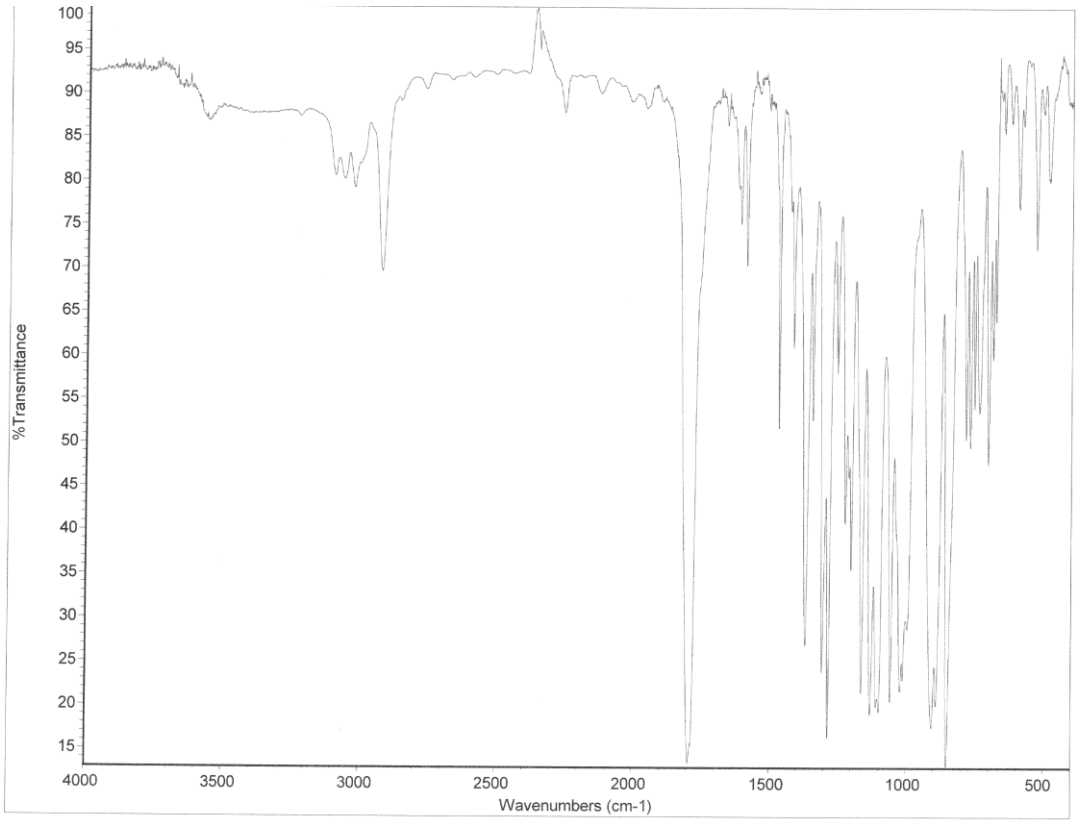
%Transmittance
100
95
90
85
80
75
70
65
60
55
50
45
40
35
30
25
20
15
4000
3500
3000
2500
2000
1500
1000
500
Wavenumbers (cm-1)

Sample Name:
ae-xxiii-97f24
Data Collected on:
nhb400-vnmrs400
Archive directory:

Sample directory:

FidFile: PROTON

Pulse Sequence: PROTON (s2pul)
Solvent: cdcl3
Data collected on: Jul 3 2014

Temp. 22.9 C / 296.1 K
Operator: siegel

Relax. delay 1.000 sec
Pulse 45.0 degrees
Acq. time 2.556 sec
Width 6410.3 Hz
16 repetitions
OBSERVE H1, 400.0861309 MHz
DATA PROCESSING
FT size 32768
Total time 1 min 54 sec

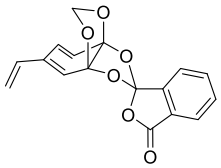

1.170b

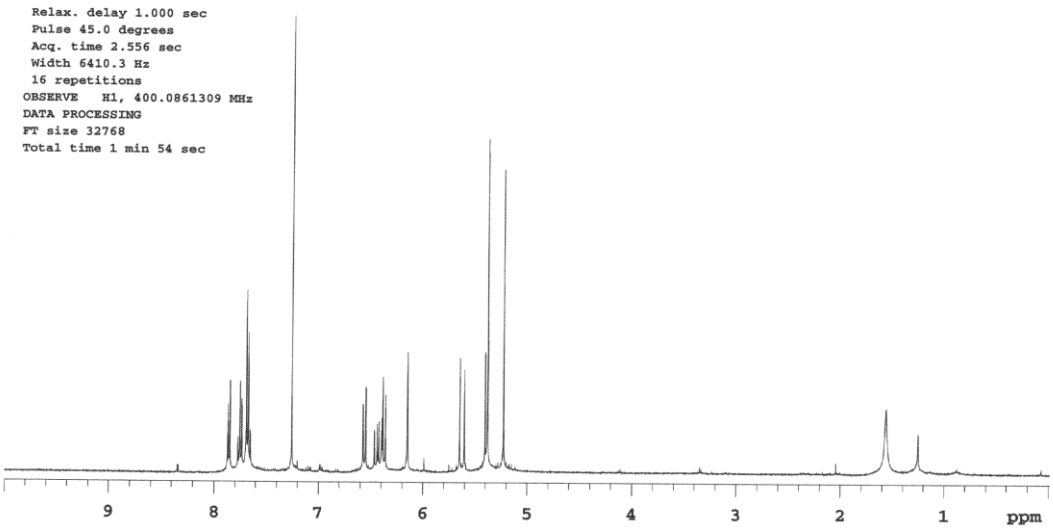

Sample Name:
ae-xxiii-97f29
Data Collected on:
wel400-vnmrs400
Archive directory:
/home/space/data
Sample directory:
ae-xxiii-97f29_20140704_01
FidFile: CARBON

Pulse Sequence: CARBON (s2pul)
Solvent: cdcl3
Data collected on: Jul 4 2014

Temp. 23.2 C / 296.4 K
Operator: siegel

Relax. delay 2.000 sec
Pulse 30.0 degrees
Acq. time 1.311 sec
Width 25000.0 Hz
1301 repetitions
OBSERVE C13, 100.5226207 MHz
DECOUPLE H1, 399.7734871 MHz
Power 37 dB
continuously on
WALTZ-16 modulated
DATA PROCESSING
Line broadening 0.5 Hz
FT size 65536
Total time 1 hr, 22 min

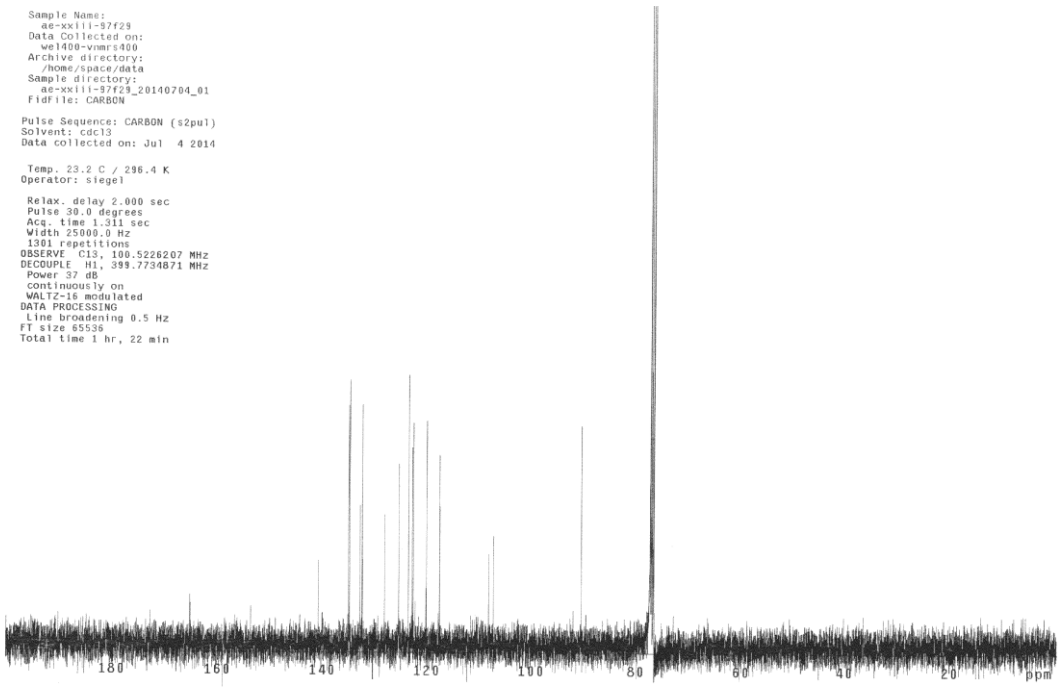

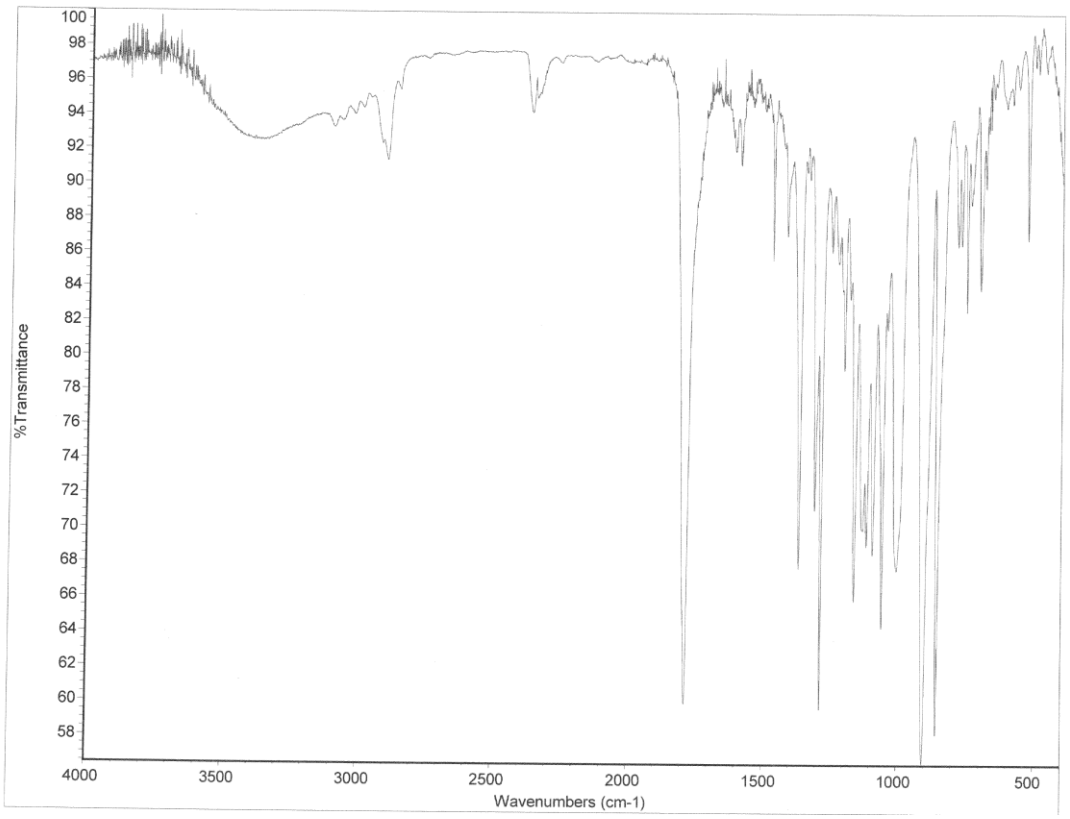
%Transmittance
100
98
96
94
92
90
88
86
84
82
80
78
76
74
72
70
68
66
64
62
60
58
4000
3500
3000
2500
2000
1500
1000
500
Wavenumbers (cm-1)

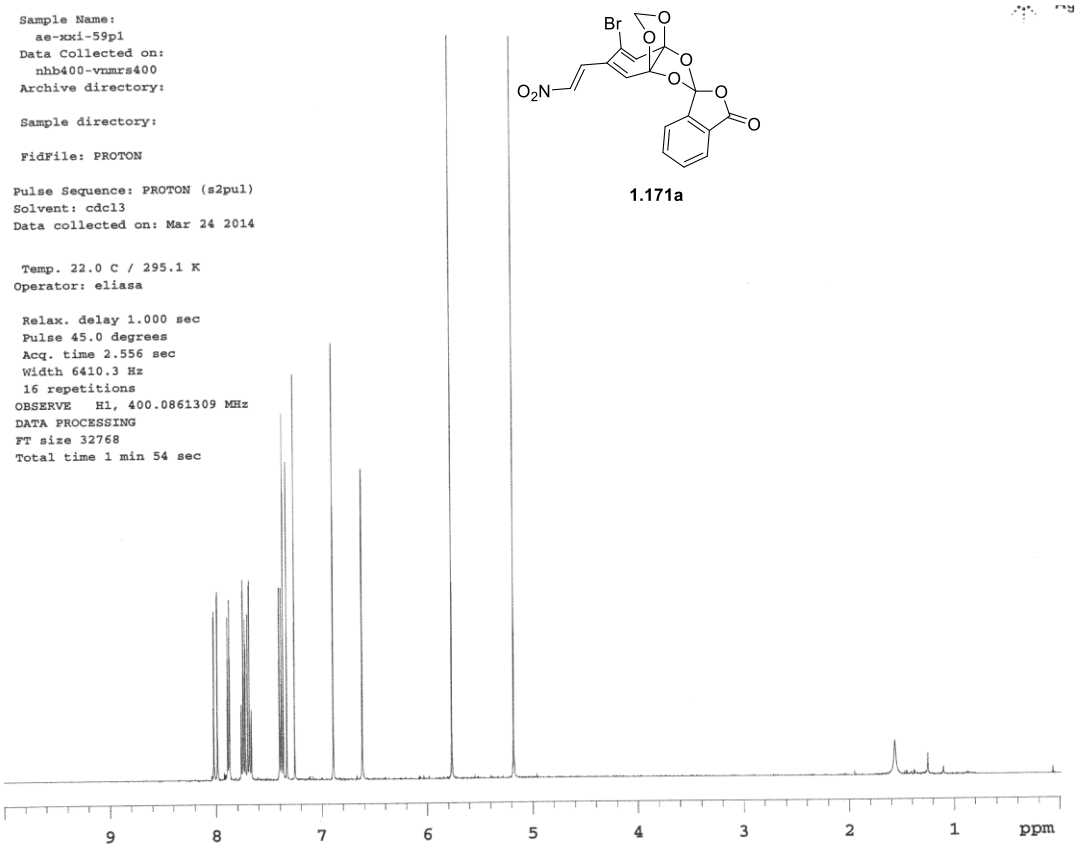
Sample Name:
ae-xxi-59p1
Data Collected on:
nhb400-vnmrs400
Archive directory:
Sample directory:
FidFile: PROTON
Pulse Sequence: PROTON (s2pul)
Solvent: cdcl3
Data collected on: Mar 24 2014
Temp. 22.0 C / 295.1 K
Operator: eliasa
Relax. delay 1.000 sec
Pulse 45.0 degrees
Acq. time 2.556 sec
Width 6410.3 Hz
16 repetitions
OBSERVE H1, 400.0861309 MHz
DATA PROCESSING
FT size 32768
Total time 1 min 54 sec
Br
O
O
O
O
O
O
O
O_2N
1.171a
9
8
7
6
5
4
3
2
1
ppm

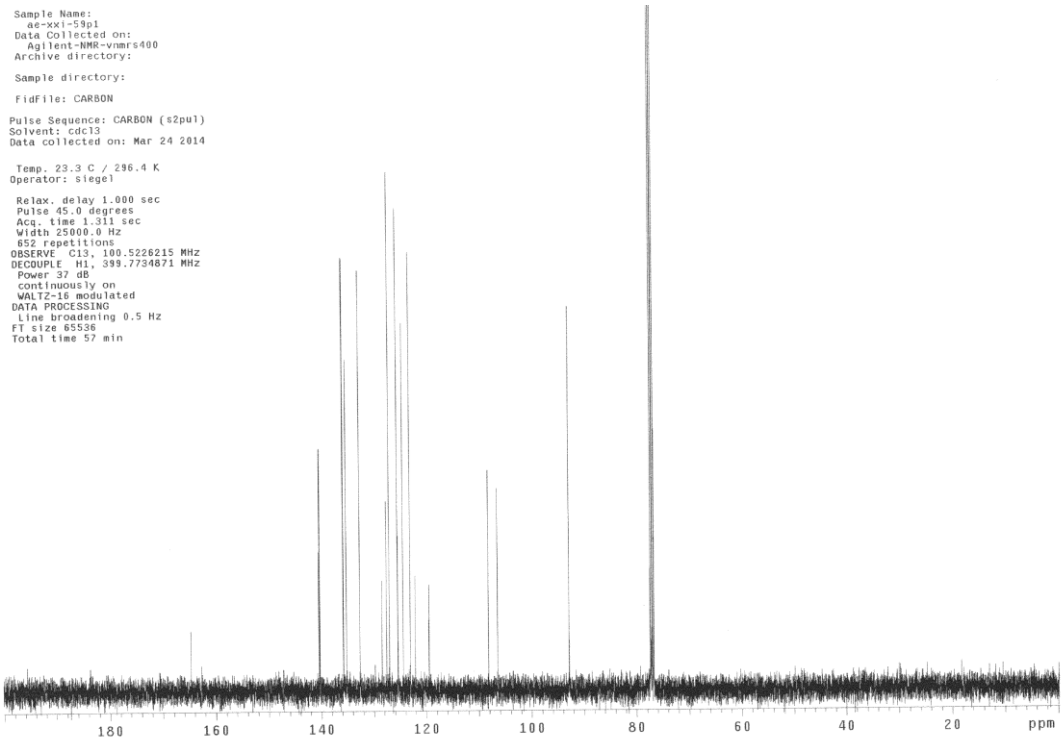
Sample Name:
ae-xxi-59p1
Data Collected on:
Agilent-NMR-vnmrs400
Archive directory:
Sample directory:
FidFile: CARBON
Pulse Sequence: CARBON (s2pul)
Solvent: cdcl3
Data collected on: Mar 24 2014
Temp. 23.3 C / 296.4 K
Operator: siegel
Relax. delay 1.000 sec
Pulse 45.0 degrees
Acq. time 1.311 sec
Width 25000.0 Hz
652 repetitions
OBSERVE C13, 100.5226215 MHz
DECOUPLE H1, 399.7734871 MHz
Power 37 dB
continuously on
WALTZ-16 modulated
DATA PROCESSING
Line broadening 0.5 Hz
FT size 65536
Total time 57 min
180
160
140
120
100
80
60
40
20
ppm

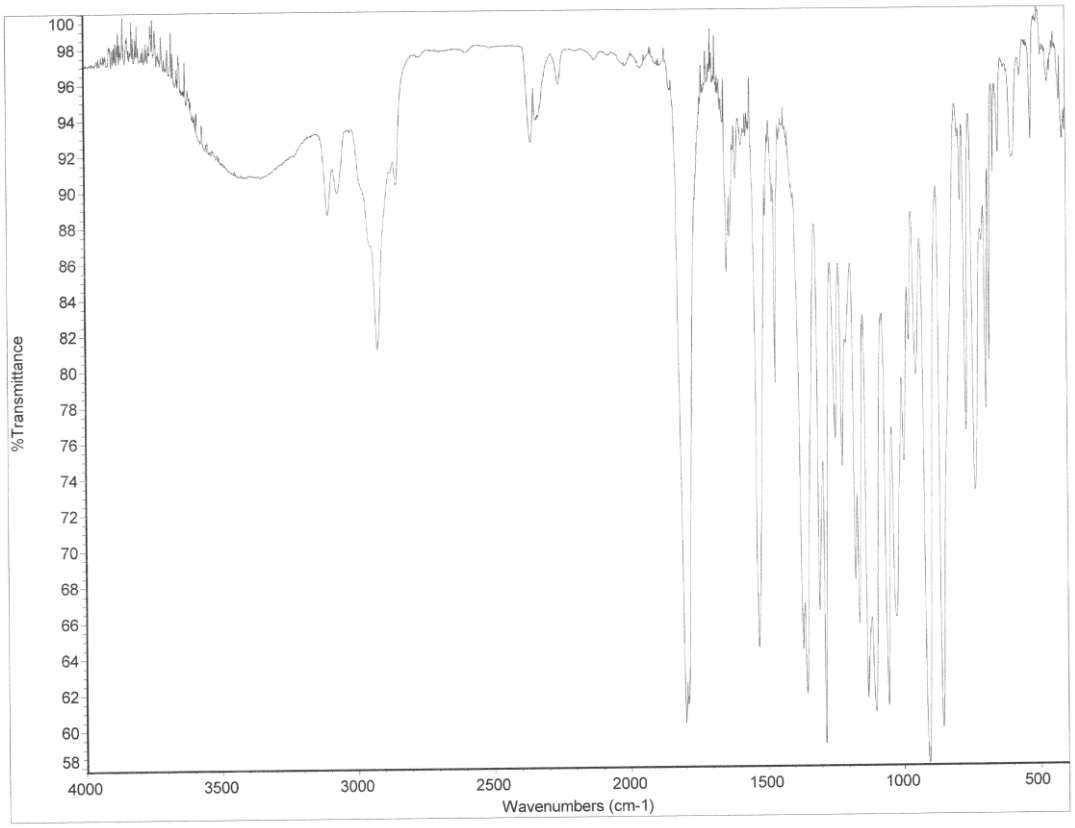
%Transmittance
100
98
96
94
92
90
88
86
84
82
80
78
76
74
72
70
68
66
64
62
60
58
4000
3500
3000
2500
2000
1500
1000
500
Wavenumbers (cm-1)

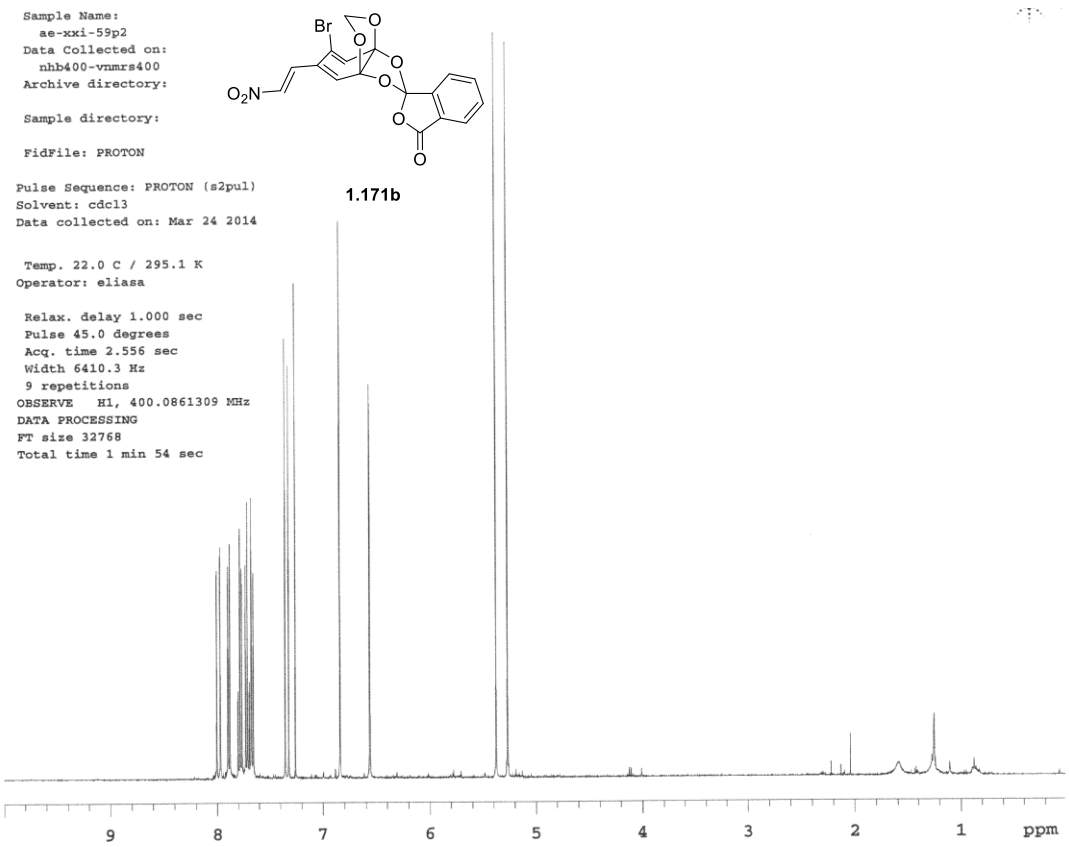
Sample Name:
ae-xxi-59p2
Data Collected on:
nhb400-vnmrs400
Archive directory:
Sample directory:
FidFile: PROTON
Pulse Sequence: PROTON (s2pul)
Solvent: cdcl3
Data collected on: Mar 24 2014
Temp. 22.0 C / 295.1 K
Operator: eliasa
Relax. delay 1.000 sec
Pulse 45.0 degrees
Acq. time 2.556 sec
Width 6410.3 Hz
9 repetitions
OBSERVE H1, 400.0861309 MHz
DATA PROCESSING
FT size 32768
Total time 1 min 54 sec
Br
O
O
O
O
O
O
O_2N
1.171b
9
8
7
6
5
4
3
2
1
ppm

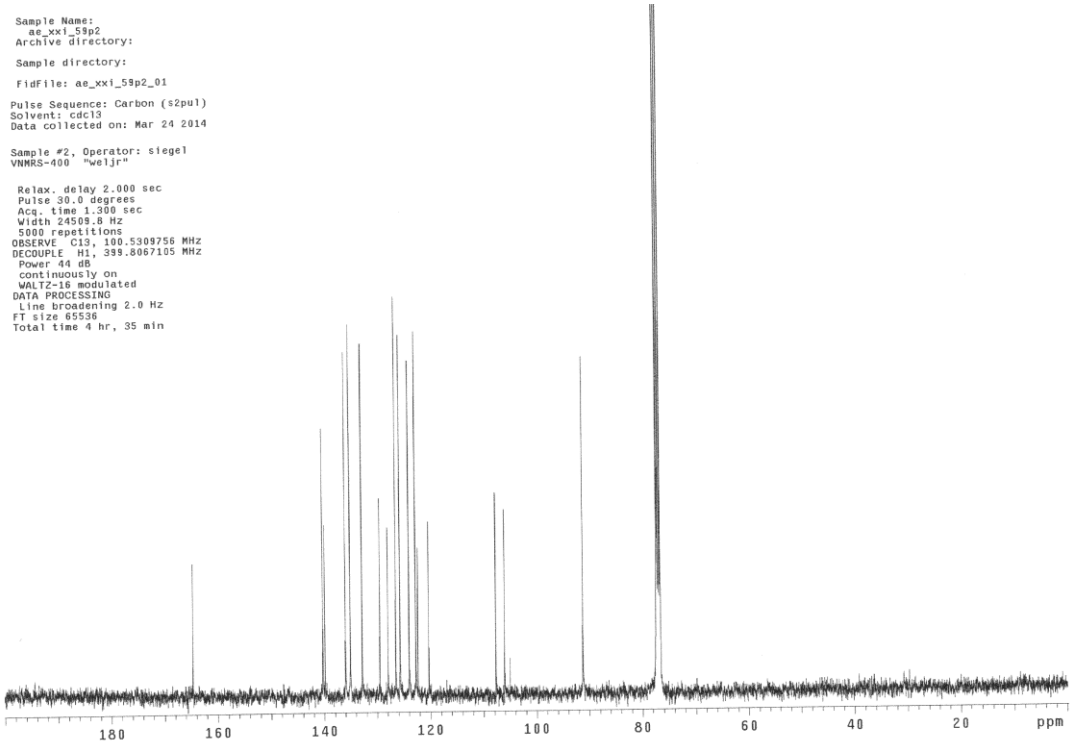
Sample Name:
ae_xxi_59p2
Archive directory:
Sample directory:
FidFile: ae_xxi_59p2_01
Pulse Sequence: Carbon (s2pul)
Solvent: cdcl3
Data collected on: Mar 24 2014
Sample #2, Operator: siegel
VNMRS-400 "weljr"
Relax. delay 2.000 sec
Pulse 30.0 degrees
Acq. time 1.300 sec
Width 24509.8 Hz
5000 repetitions
OBSERVE C13, 100.5309756 MHz
DECOUPLE H1, 399.8067105 MHz
Power 44 dB
continuously on
WALTZ-16 modulated
DATA PROCESSING
Line broadening 2.0 Hz
FT size 65536
Total time 4 hr, 35 min
180
160
140
120
100
80
60
40
20
ppm

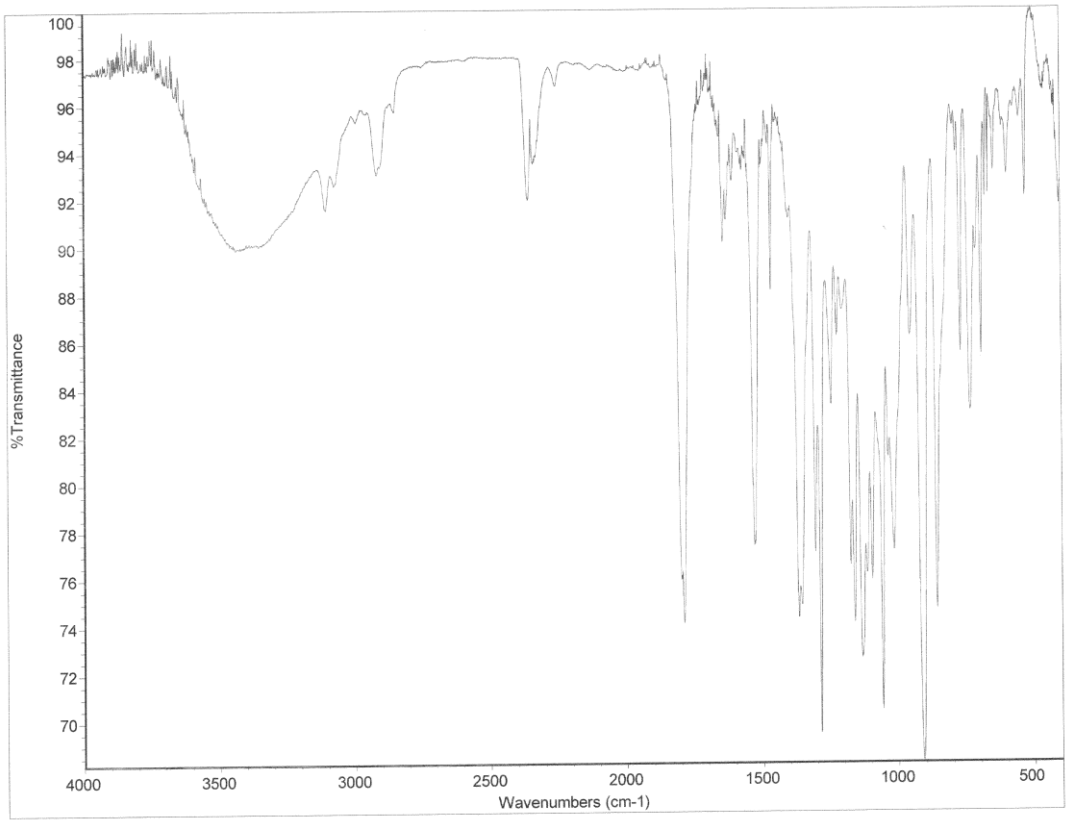
%Transmittance
100
98
96
94
92
90
88
86
84
82
80
78
76
74
72
70
4000
3500
3000
2500
2000
1500
1000
500
Wavenumbers (cm-1)

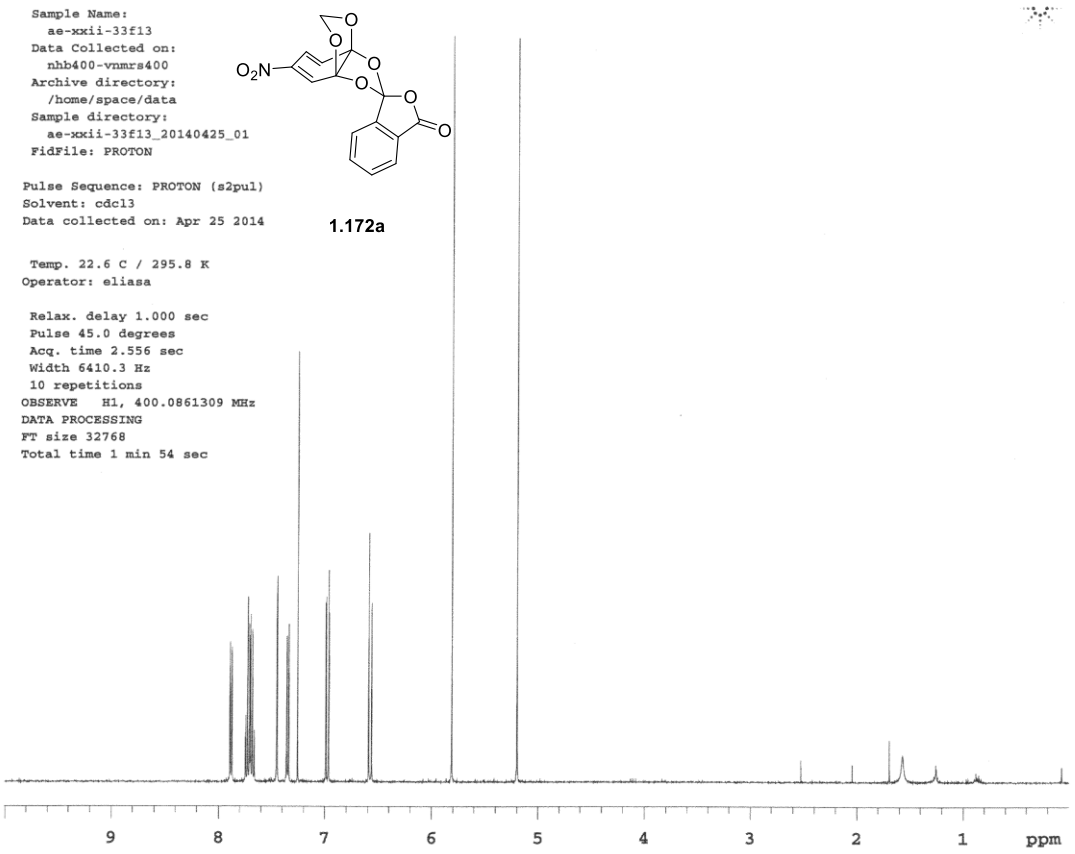
Sample Name:
ae-xxii-33f13
Data Collected on:
nhb400-vnmrs400
Archive directory:
/home/space/data
Sample directory:
ae-xxii-33f13_20140425_01
FidFile: PROTON
Pulse Sequence: PROTON (s2pul)
Solvent: cdcl3
Data collected on: Apr 25 2014
Temp. 22.6 C / 295.8 K
Operator: eliasa
Relax. delay 1.000 sec
Pulse 45.0 degrees
Acq. time 2.556 sec
Width 6410.3 Hz
10 repetitions
OBSERVE H1, 400.0861309 MHz
DATA PROCESSING
FT size 32768
Total time 1 min 54 sec
O2N
1.172a
9
8
7
6
5
4
3
2
1
ppm

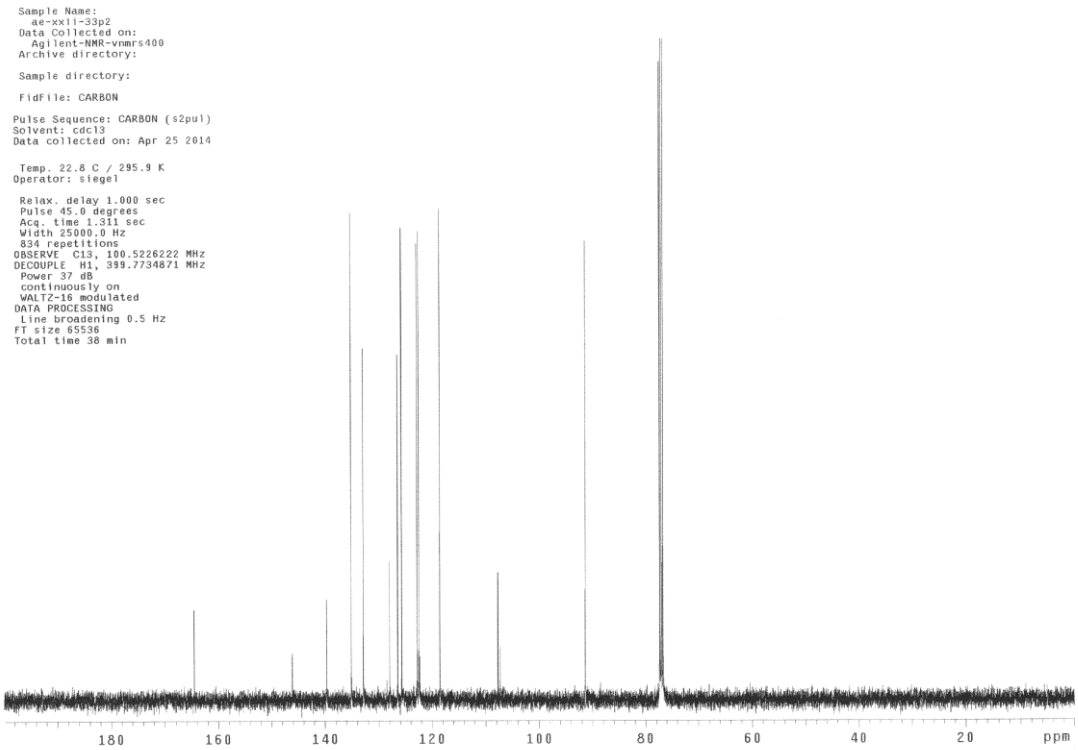
Sample Name:
ae-xxii-33p2
Data Collected on:
Agilent-NMR-vnmrs400
Archive directory:
Sample directory:
FidFile: CARBON
Pulse Sequence: CARBON (s2pul)
Solvent: cdcl3
Data collected on: Apr 25 2014
Temp. 22.8 C / 295.9 K
Operator: siegel
Relax. delay 1.000 sec
Pulse 45.0 degrees
Acq. time 1.311 sec
Width 25000.0 Hz
834 repetitions
OBSERVE C13, 100.5226222 MHz
DECOUPLE H1, 399.7734871 MHz
Power 37 dB
continuously on
WALTZ-16 modulated
DATA PROCESSING
Line broadening 0.5 Hz
FT size 65536
Total time 38 min
180
160
140
120
100
80
60
40
20
ppm

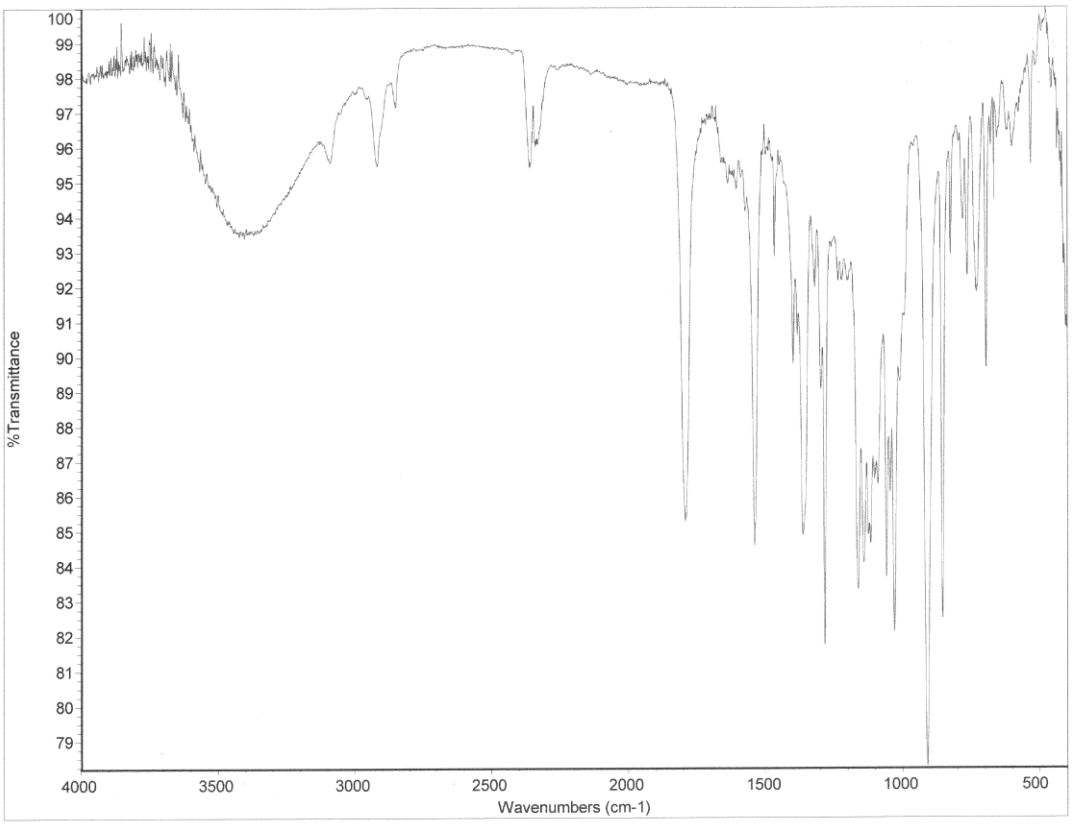
%Transmittance
100
99
98
97
96
95
94
93
92
91
90
89
88
87
86
85
84
83
82
81
80
79
4000
3500
3000
2500
2000
1500
1000
500
Wavenumbers (cm-1)

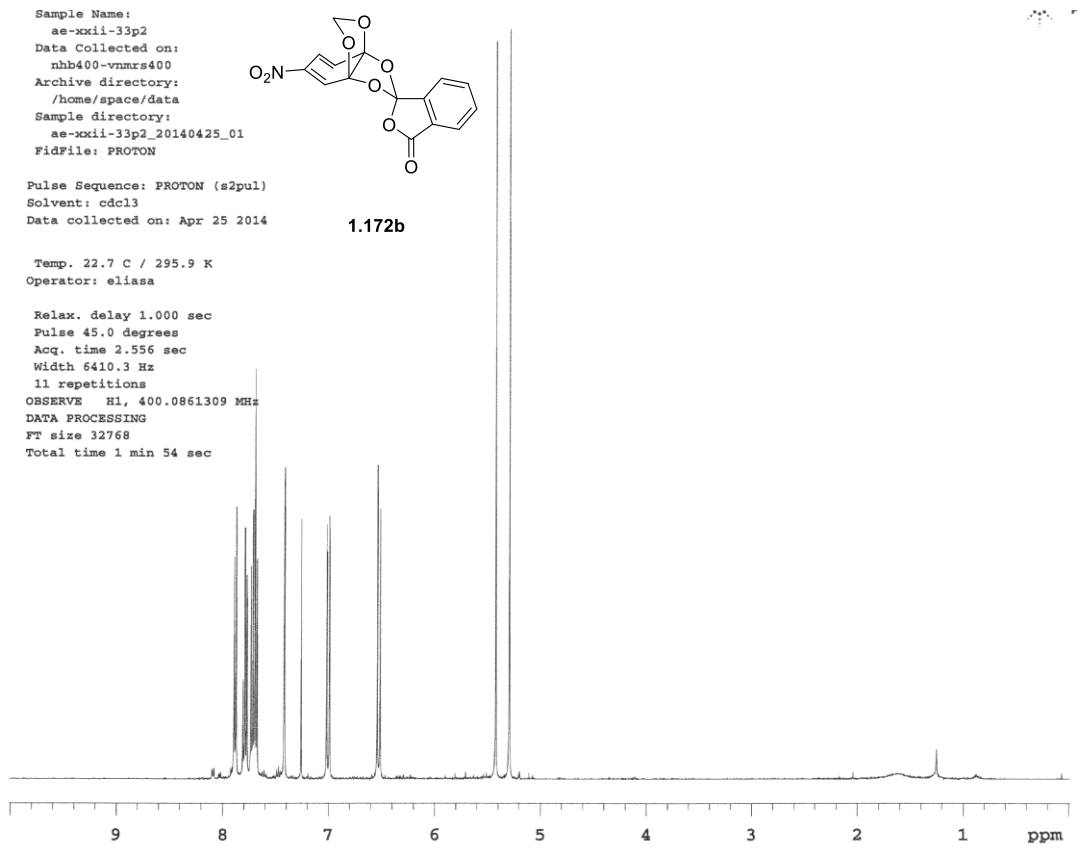
Sample Name:
ae-xxii-33p2
Data Collected on:
nhb400-vnmrs400
Archive directory:
/home/space/data
Sample directory:
ae-xxii-33p2_20140425_01
FidFile: PROTON
Pulse Sequence: PROTON (s2pul)
Solvent: cdcl3
Data collected on: Apr 25 2014
Temp. 22.7 C / 295.9 K
Operator: eliasa
Relax. delay 1.000 sec
Pulse 45.0 degrees
Acq. time 2.556 sec
Width 6410.3 Hz
11 repetitions
OBSERVE H1, 400.0861309 MHz
DATA PROCESSING
FT size 32768
Total time 1 min 54 sec
1.172b
9
8
7
6
5
4
3
2
1
ppm

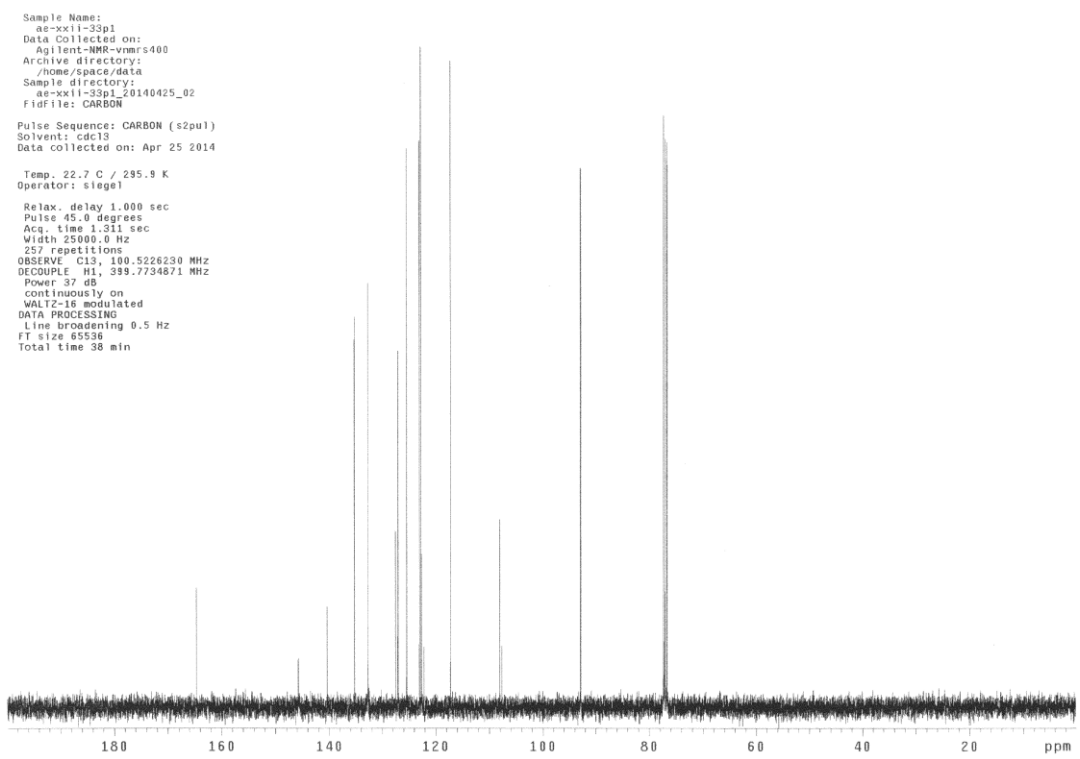
Sample Name:
ae-xxii-33p1
Data Collected on:
Agilent-NMR-vnmrs400
Archive directory:
/home/space/data
Sample directory:
ae-xxii-33p1_20140425_02
FidFile: CARBON
Pulse Sequence: CARBON (s2pul)
Solvent: cdcl3
Data collected on: Apr 25 2014
Temp. 22.7 C / 295.9 K
Operator: siegel
Relax. delay 1.000 sec
Pulse 45.0 degrees
Acq. time 1.311 sec
Width 25000.0 Hz
257 repetitions
OBSERVE C13, 100.5226230 MHz
DECOUPLE H1, 399.7734871 MHz
Power 37 dB
continuously on
WALTZ-16 modulated
DATA PROCESSING
Line broadening 0.5 Hz
FT size 65536
Total time 38 min
180
160
140
120
100
80
60
40
20
ppm

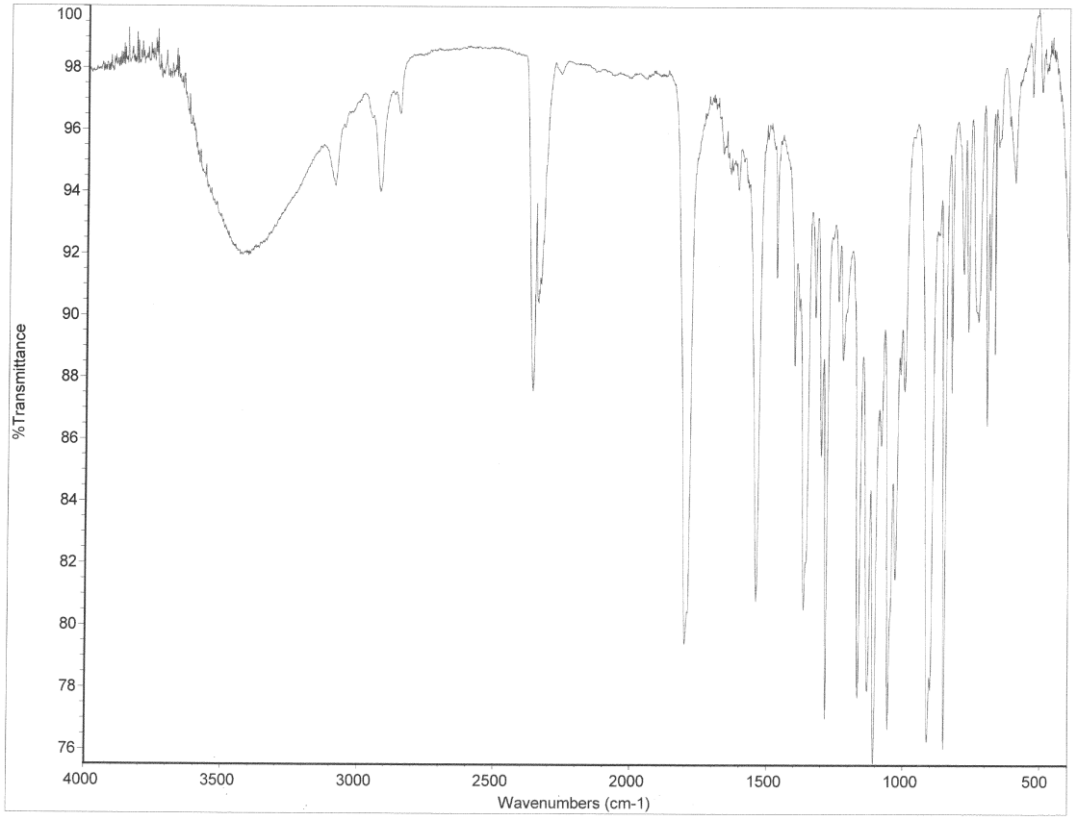
100
98
96
94
92
90
88
86
84
82
80
78
76
%Transmittance
4000
3500
3000
2500
2000
1500
1000
500
Wavenumbers (cm-1)

Sample Name:
ae-xxiv-01f29
Data Collected on:
nhb400-vnmrs400
Archive directory:
/home/space/data
Sample directory:
ae-xxiv-01f29_20140709_01
FidFile: PROTON

Pulse Sequence: PROTON (s2pul)
Solvent: cdcl3
Data collected on: Jul 9 2014

Temp. 22.2 C / 295.4 K
Operator: eliasa

Relax. delay 1.000 sec
Pulse 30.0 degrees
Acq. time 2.556 sec
Width 6410.3 Hz
15 repetitions
OBSERVE H1, 400.0861309 MHz
DATA PROCESSING
FT size 32768
Total time 0 min 57 sec

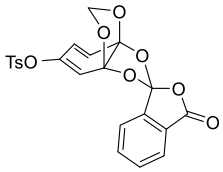

1.173a

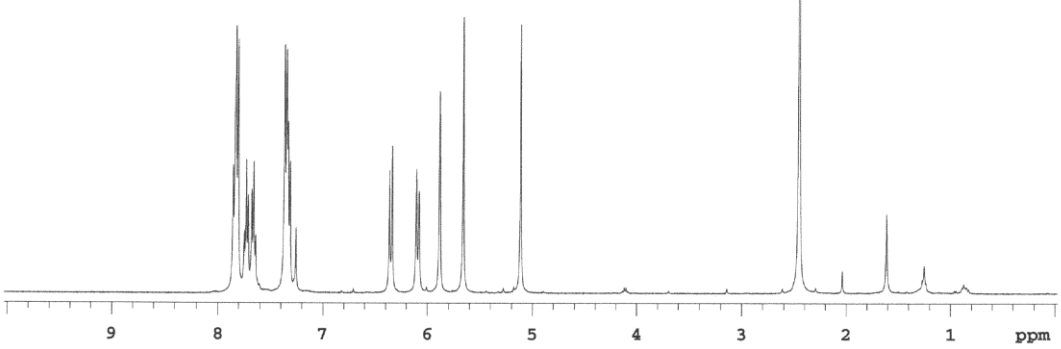

STANDARD CARBON PARAMETERS

Sample Name:
ae-xxiv-f29
Data Collected on:
we1400-vnmrs400
Archive directory:
/home/space/data
Sample directory:
ae-xxiv-f29_20140708_01
FidFile: CARBON

Pulse Sequence: CARBON (s2pul)
Solvent: cdcl3
Data collected on: Jul 8 2014

Temp. 23.4 C / 296.6 K
Operator: siegel

Relax. delay 1.000 sec
Pulse 45.0 degrees
Acq. time 1.311 sec
Width 25000.0 Hz
80 repetitions
OBSERVE C13, 100.5226253 MHz
DECOUPLE H1, 399.7734871 MHz
Power 37 dB
continuously on
WALTZ-16 modulated
DATA PROCESSING
Line broadening 0.5 Hz
FT size 65536
Total time 4 min 56 sec

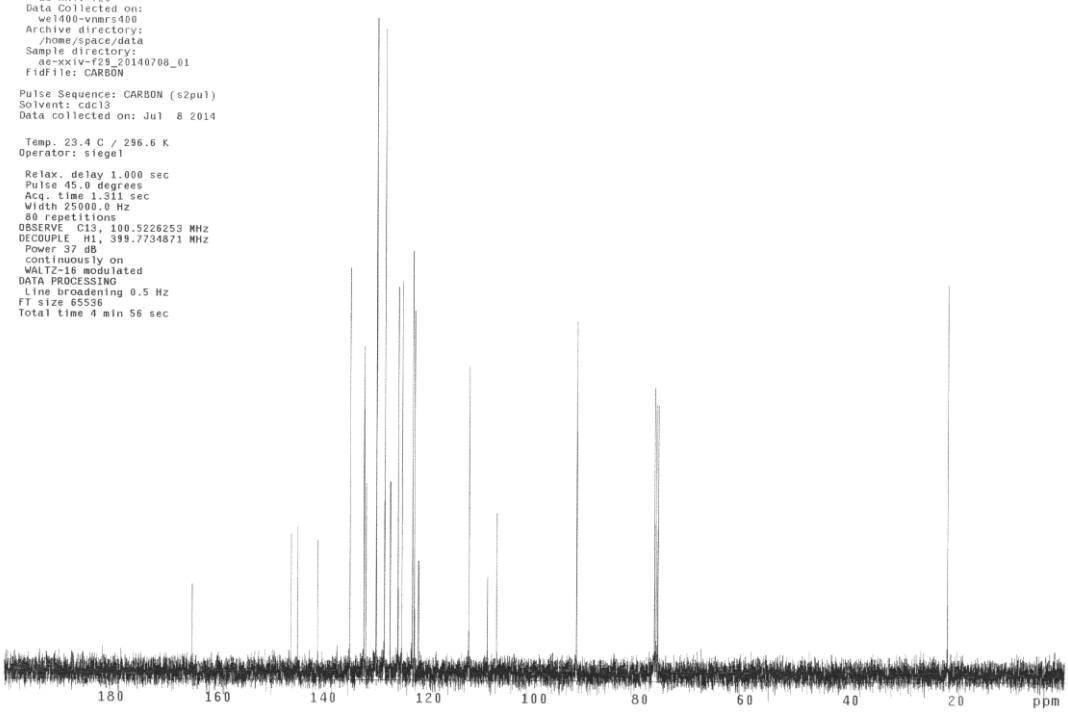

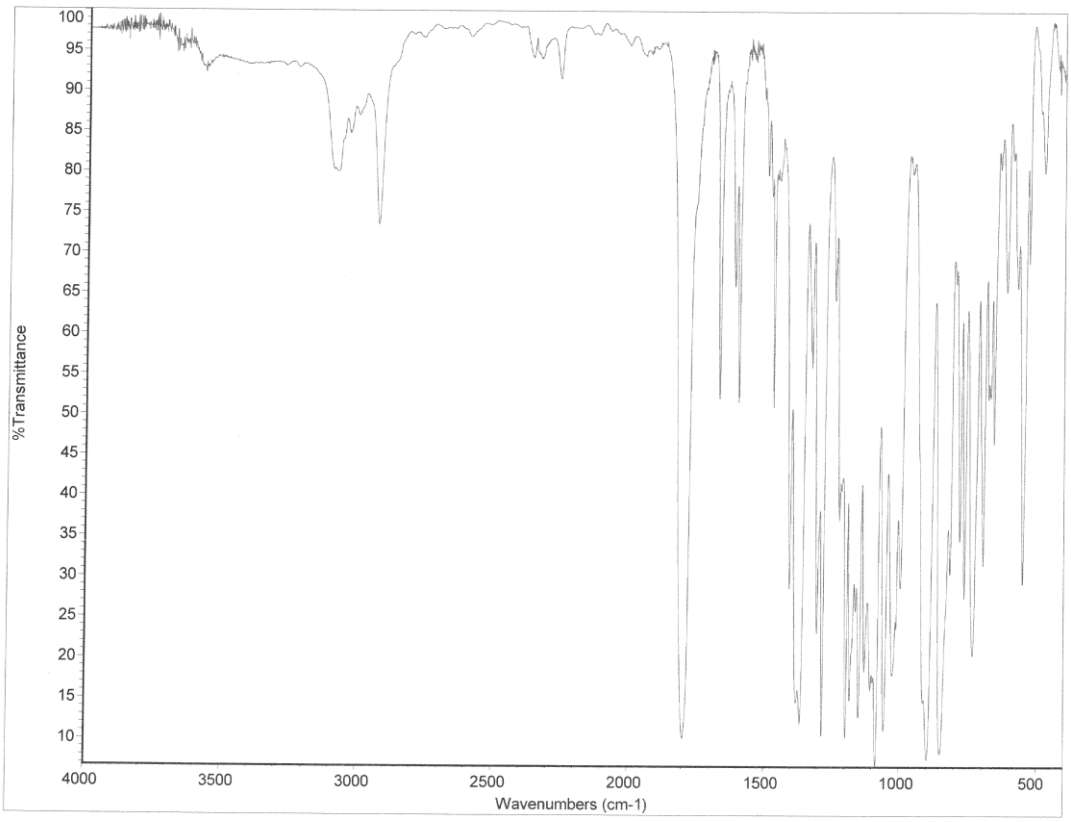
%Transmittance
100
95
90
85
80
75
70
65
60
55
50
45
40
35
30
25
20
15
10
4000
3500
3000
2500
2000
1500
1000
500
Wavenumbers (cm-1)

TsO
O
O
O
O
O
O
O

1.173b

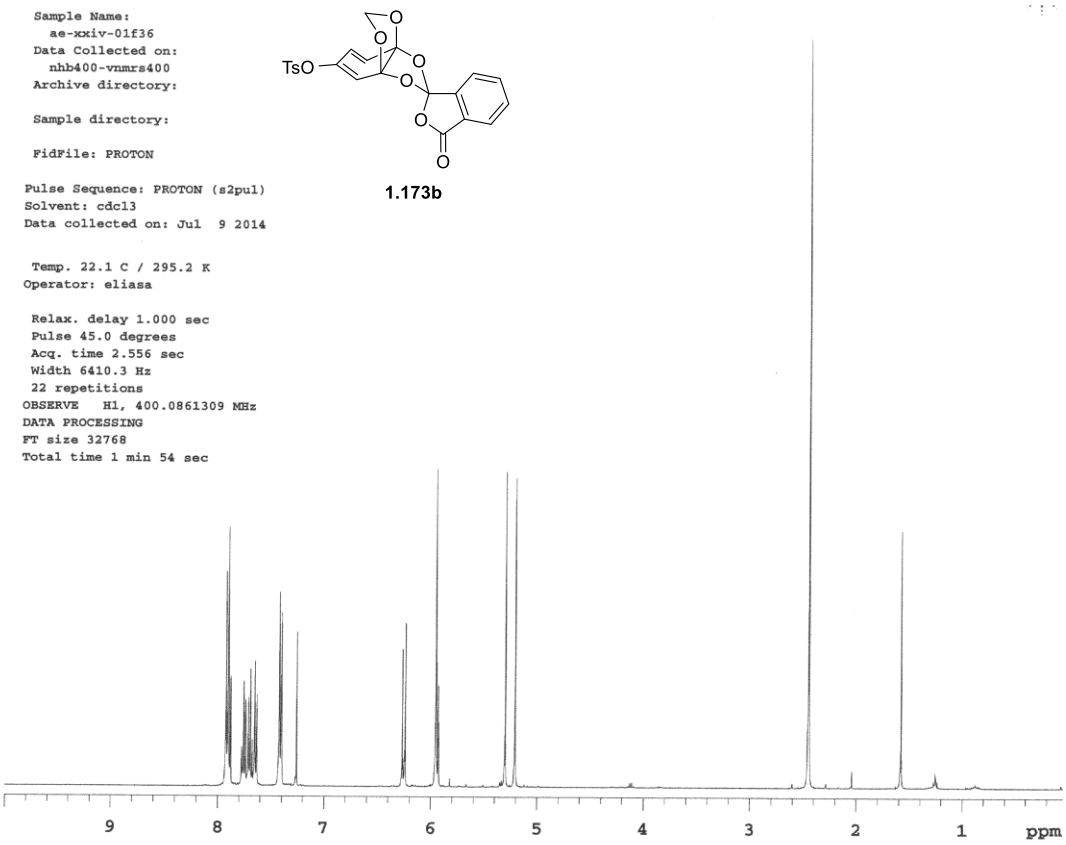
Sample Name:
ae-xxiv-01f36
Data Collected on:
nhb400-vnmrs400
Archive directory:
Sample directory:
FidFile: PROTON
Pulse Sequence: PROTON (s2pul)
Solvent: cdcl3
Data collected on: Jul 9 2014
Temp. 22.1 C / 295.2 K
Operator: eliasa
Relax. delay 1.000 sec
Pulse 45.0 degrees
Acq. time 2.556 sec
Width 6410.3 Hz
22 repetitions
OBSERVE H1, 400.0861309 MHz
DATA PROCESSING
FT size 32768
Total time 1 min 54 sec
9
8
7
6
5
4
3
2
1
ppm

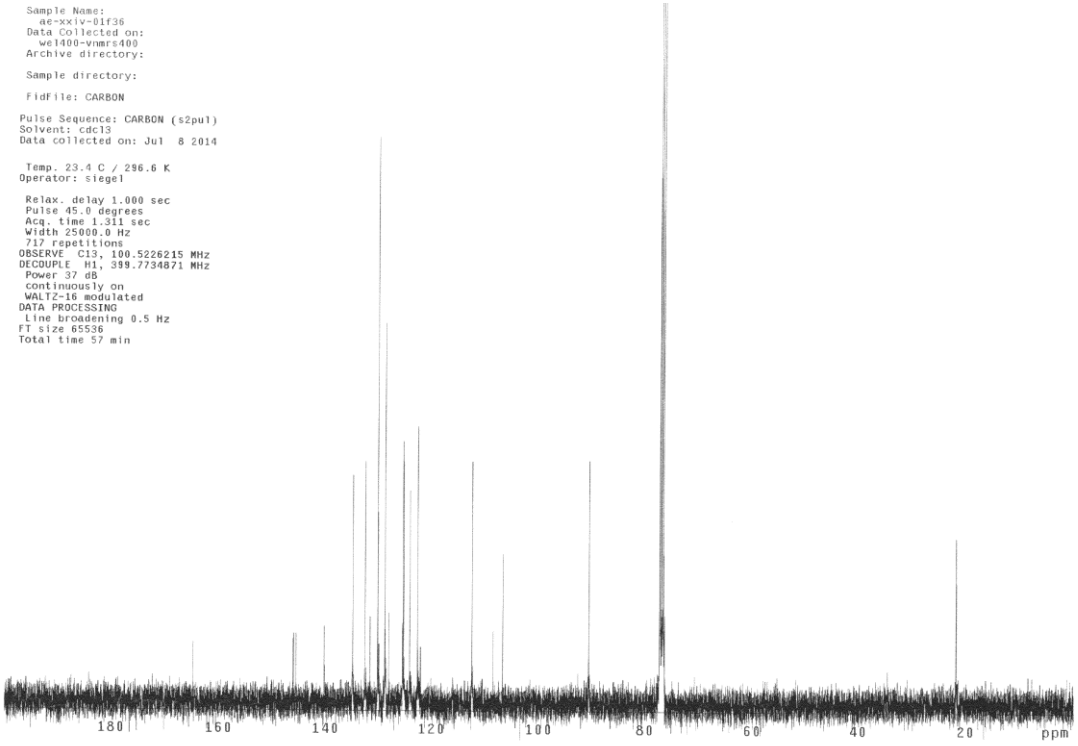
Sample Name:
ae-xxiv-01f36
Data Collected on:
wel400-vnmrs400
Archive directory:
Sample directory:
FidFile: CARBON
Pulse Sequence: CARBON (s2pul)
Solvent: cdcl3
Data collected on: Jul 8 2014
Temp. 23.4 C / 296.6 K
Operator: siegel
Relax. delay 1.000 sec
Pulse 45.0 degrees
Acq. time 1.311 sec
Width 25000.0 Hz
717 repetitions
OBSERVE C13, 100.5226215 MHz
DECOUPLE H1, 399.7734871 MHz
Power 37 dB
continuously on
WALTZ-16 modulated
DATA PROCESSING
Line broadening 0.5 Hz
FT size 65536
Total time 57 min
180
160
140
120
100
80
60
40
20
ppm

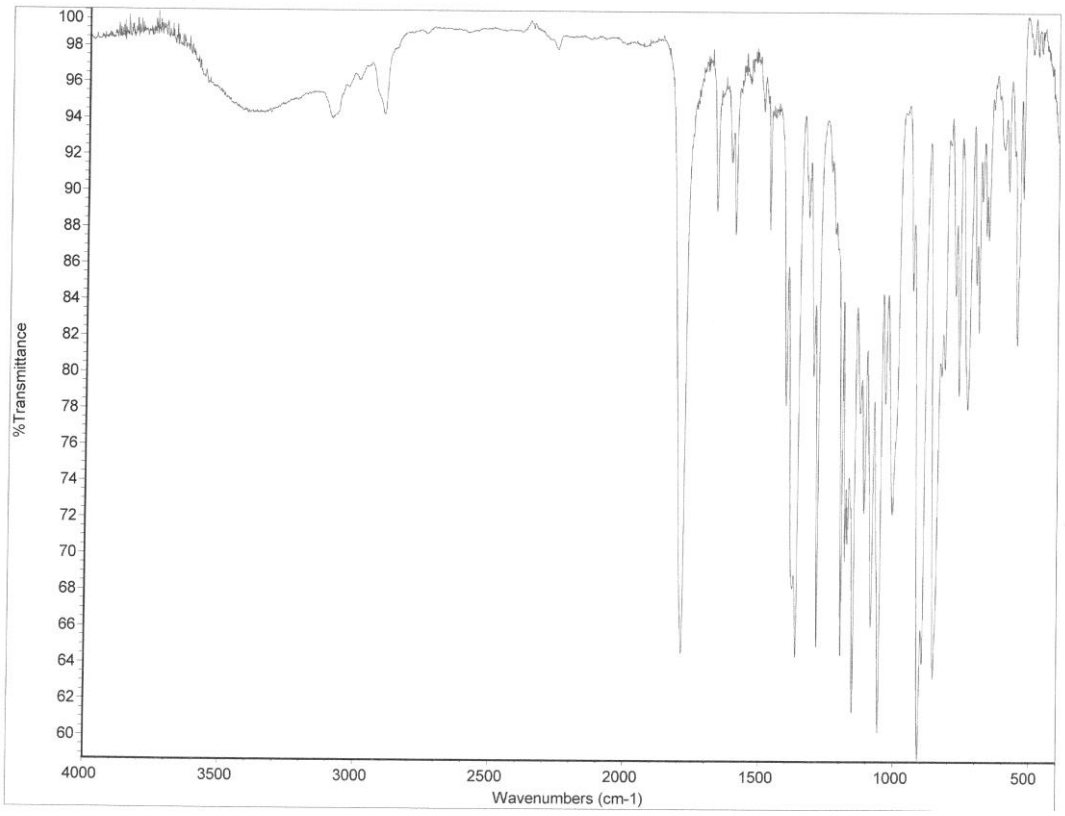
%Transmittance
100
98
96
94
92
90
88
86
84
82
80
78
76
74
72
70
68
66
64
62
60
4000
3500
3000
2500
2000
1500
1000
500
Wavenumbers (cm-1)

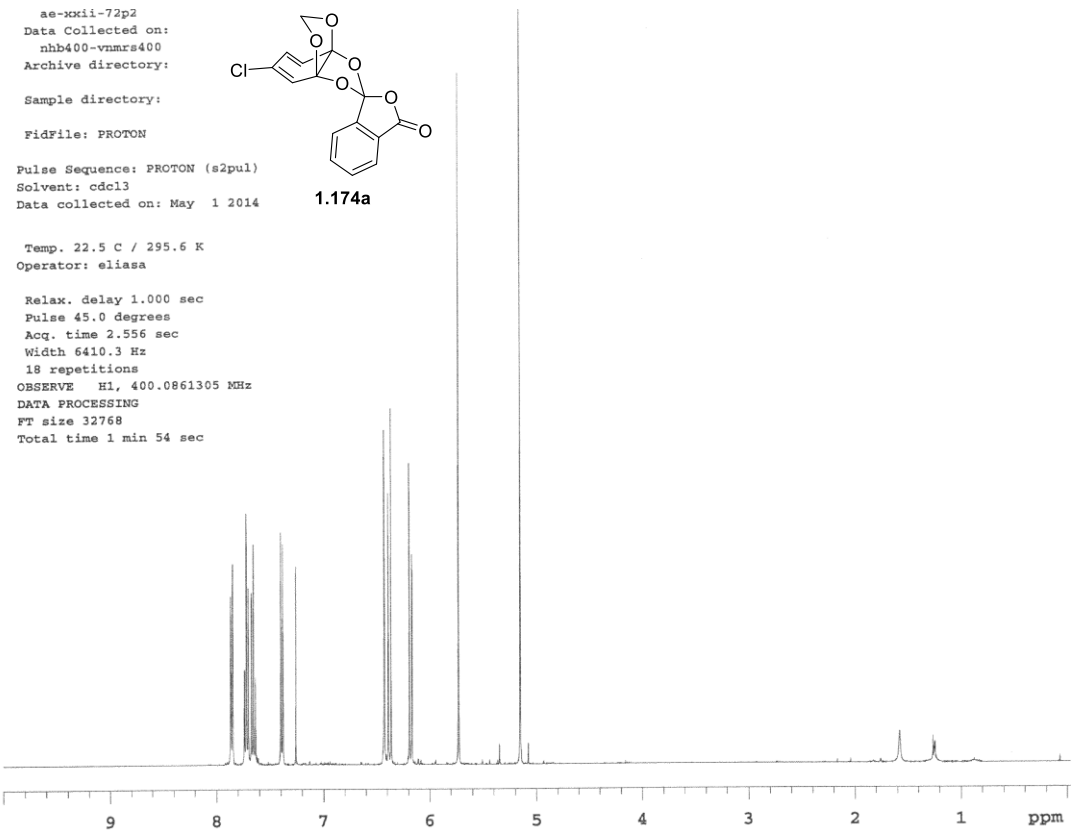
ae-xxii-72p2
Data Collected on:
nhb400-vnmrs400
Archive directory:
Sample directory:
FidFile: PROTON
Pulse Sequence: PROTON (s2pul)
Solvent: cdcl3
Data collected on: May 1 2014
Temp. 22.5 C / 295.6 K
Operator: eliasa
Relax. delay 1.000 sec
Pulse 45.0 degrees
Acq. time 2.556 sec
Width 6410.3 Hz
18 repetitions
OBSERVE H1, 400.0861305 MHz
DATA PROCESSING
FT size 32768
Total time 1 min 54 sec
Cl
O
1.174a
9
8
7
6
5
4
3
2
1
ppm

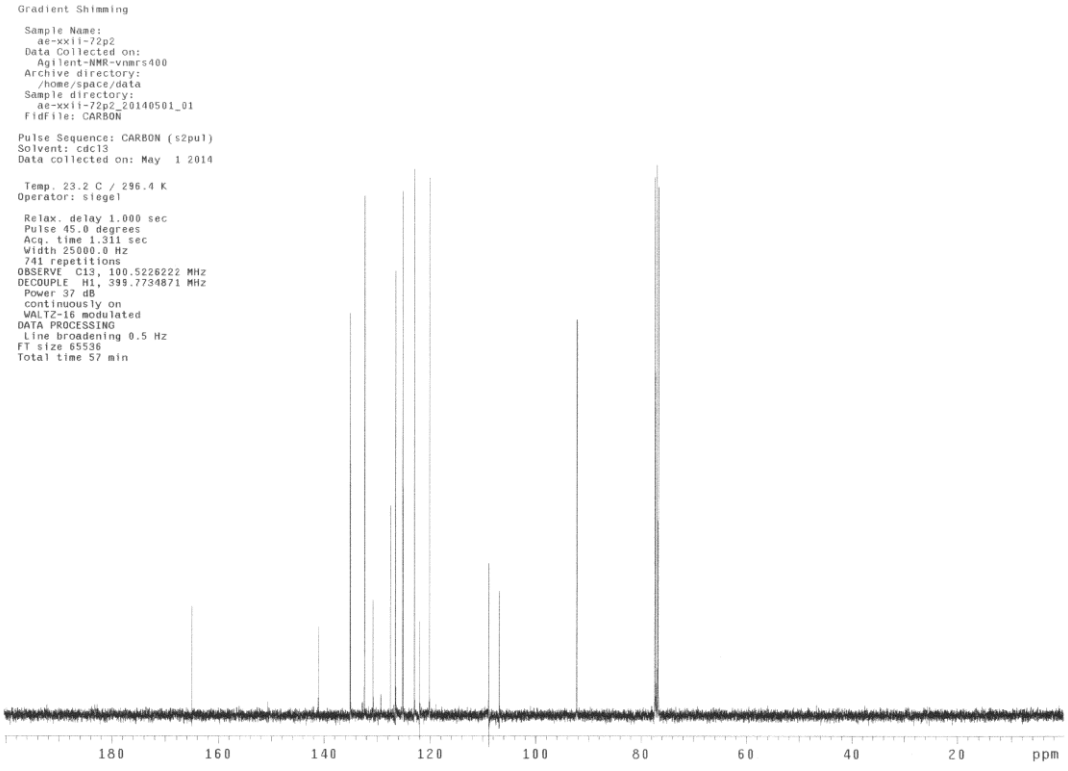
Gradient Shimming
Sample Name:
ae-xxii-72p2
Data Collected on:
Agilent-NMR-vnmrs400
Archive directory:
/home/space/data
Sample directory:
ae-xxii-72p2_20140501_01
FidFile: CARBON
Pulse Sequence: CARBON (s2pul)
Solvent: cdcl3
Data collected on: May 1 2014
Temp. 23.2 C / 296.4 K
Operator: siegel
Relax. delay 1.000 sec
Pulse 45.0 degrees
Acq. time 1.311 sec
Width 25000.0 Hz
741 repetitions
OBSERVE C13, 100.5226222 MHz
DECOUPLE H1, 399.7734871 MHz
Power 37 dB
continuously on
WALTZ-16 modulated
DATA PROCESSING
Line broadening 0.5 Hz
FT size 65536
Total time 57 min
180
160
140
120
100
80
60
40
20
ppm

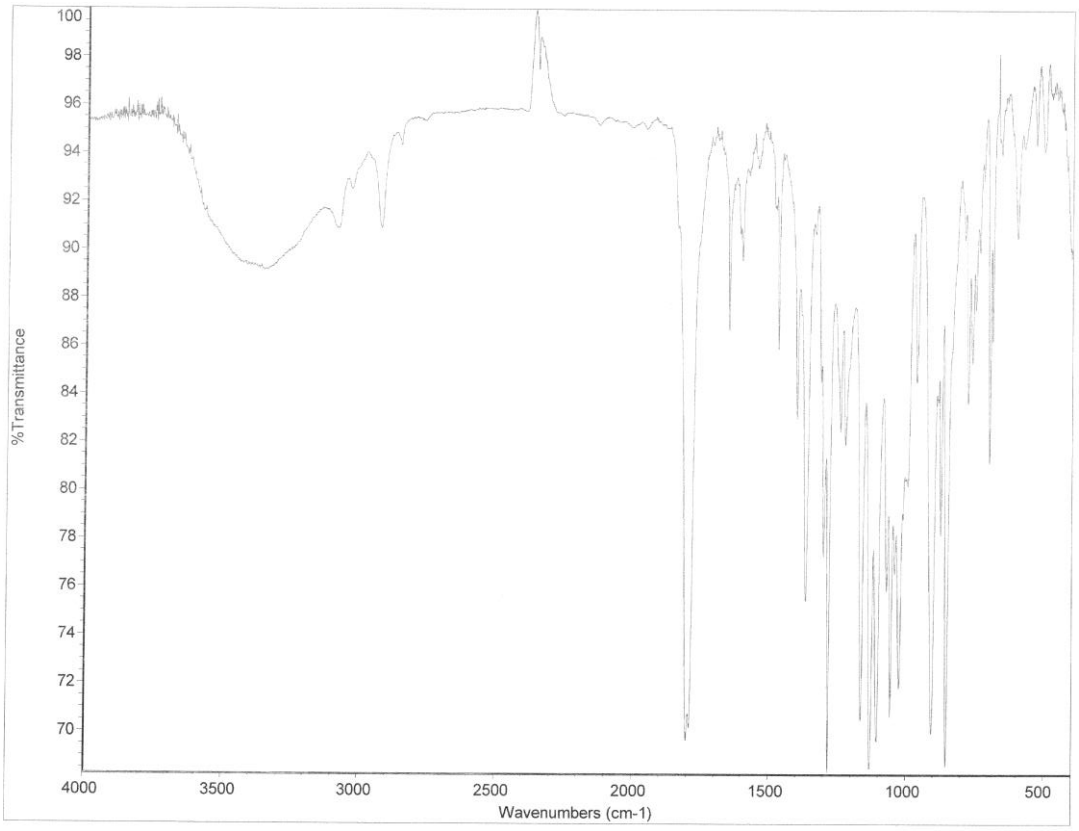
%Transmittance
100
98
96
94
92
90
88
86
84
82
80
78
76
74
72
70
4000
3500
3000
2500
2000
1500
1000
500
Wavenumbers (cm-1)

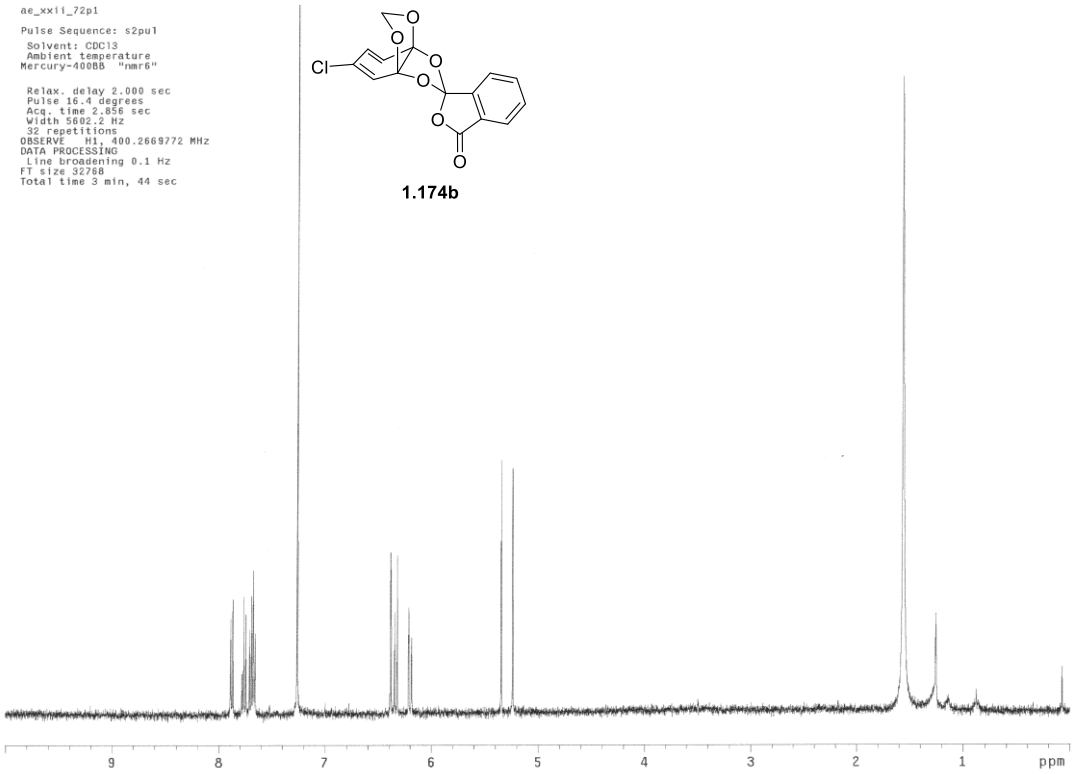
ae_xxii_72p1
Pulse Sequence: s2pul
Solvent: CDCl3
Ambient temperature
Mercury-400BB "nmr6"
Relax. delay 2.000 sec
Pulse 16.4 degrees
Acq. time 2.856 sec
Width 5602.2 Hz
32 repetitions
OBSERVE H1, 400.2669772 MHz
DATA PROCESSING
Line broadening 0.1 Hz
FT size 32768
Total time 3 min, 44 sec
Cl
O
1.174b
9
8
7
6
5
4
3
2
1
ppm

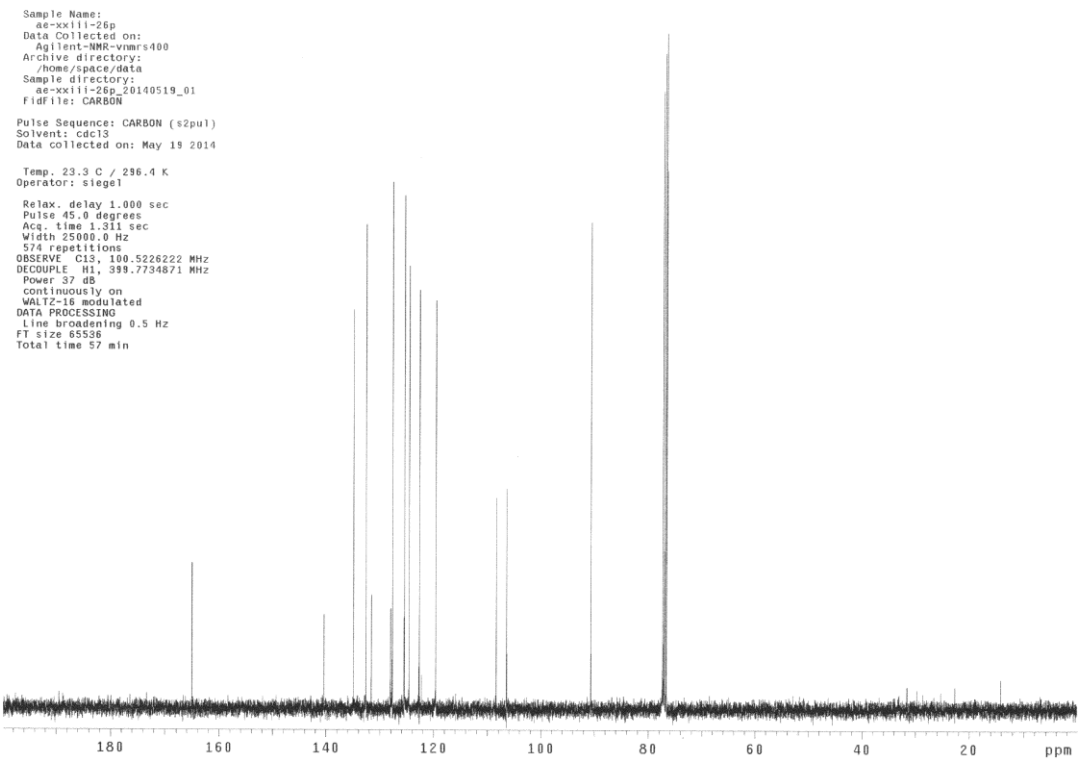
Sample Name:
ae-xxiii-26p
Data Collected on:
Agilent-NMR-vnmrs400
Archive directory:
/home/space/data
Sample directory:
ae-xxiii-26p_20140519_01
FidFile: CARBON
Pulse Sequence: CARBON (s2pul)
Solvent: cdcl3
Data collected on: May 19 2014
Temp. 23.3 C / 296.4 K
Operator: siegel
Relax. delay 1.000 sec
Pulse 45.0 degrees
Acq. time 1.311 sec
Width 25000.0 Hz
574 repetitions
OBSERVE C13, 100.5226222 MHz
DECOUPLE H1, 399.7734871 MHz
Power 37 dB
continuously on
WALTZ-16 modulated
DATA PROCESSING
Line broadening 0.5 Hz
FT size 65536
Total time 57 min
180
160
140
120
100
80
60
40
20
ppm

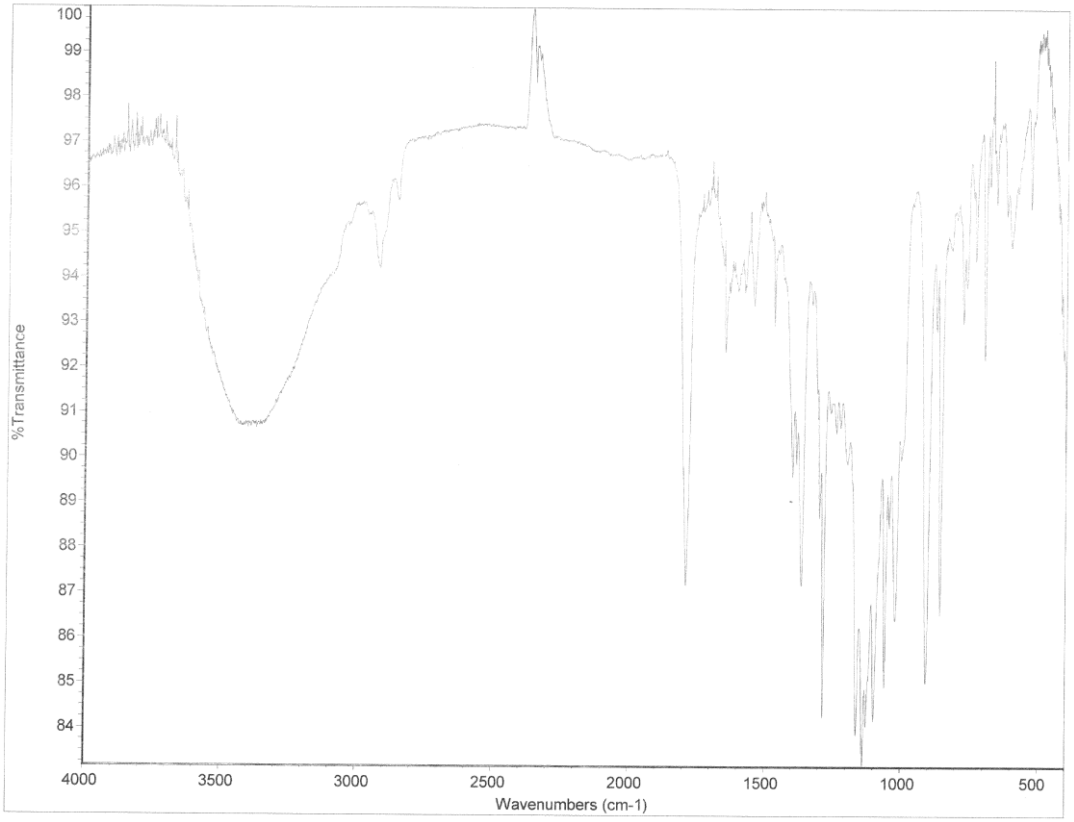
100
99
98
97
96
95
94
93
92
91
90
89
88
87
86
85
84
% Transmittance
4000
3500
3000
2500
2000
1500
1000
500
Wavenumbers (cm-1)

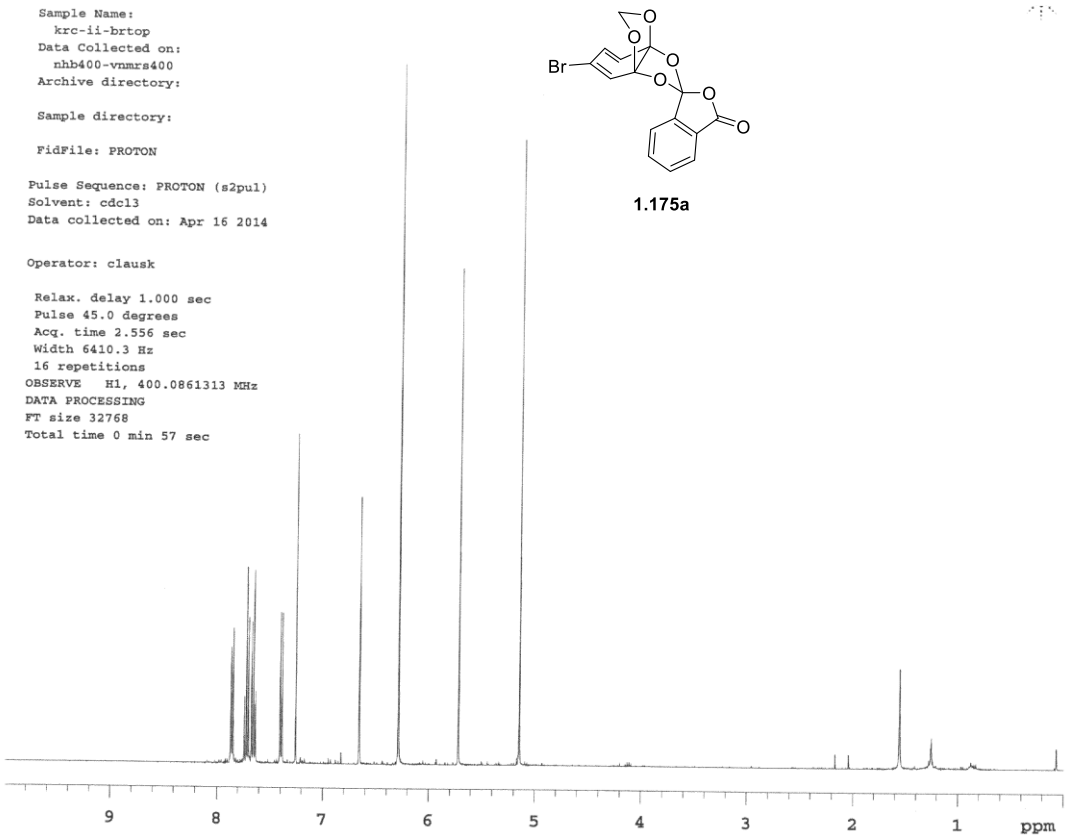
Sample Name:
krc-ii-brtop
Data Collected on:
nhb400-vnmrs400
Archive directory:
Sample directory:
FidFile: PROTON
Pulse Sequence: PROTON (s2pul)
Solvent: cdcl3
Data collected on: Apr 16 2014
Operator: clausk
Relax. delay 1.000 sec
Pulse 45.0 degrees
Acq. time 2.556 sec
Width 6410.3 Hz
16 repetitions
OBSERVE H1, 400.0861313 MHz
DATA PROCESSING
FT size 32768
Total time 0 min 57 sec
Br
O
1.175a
9
8
7
6
5
4
3
2
1
ppm

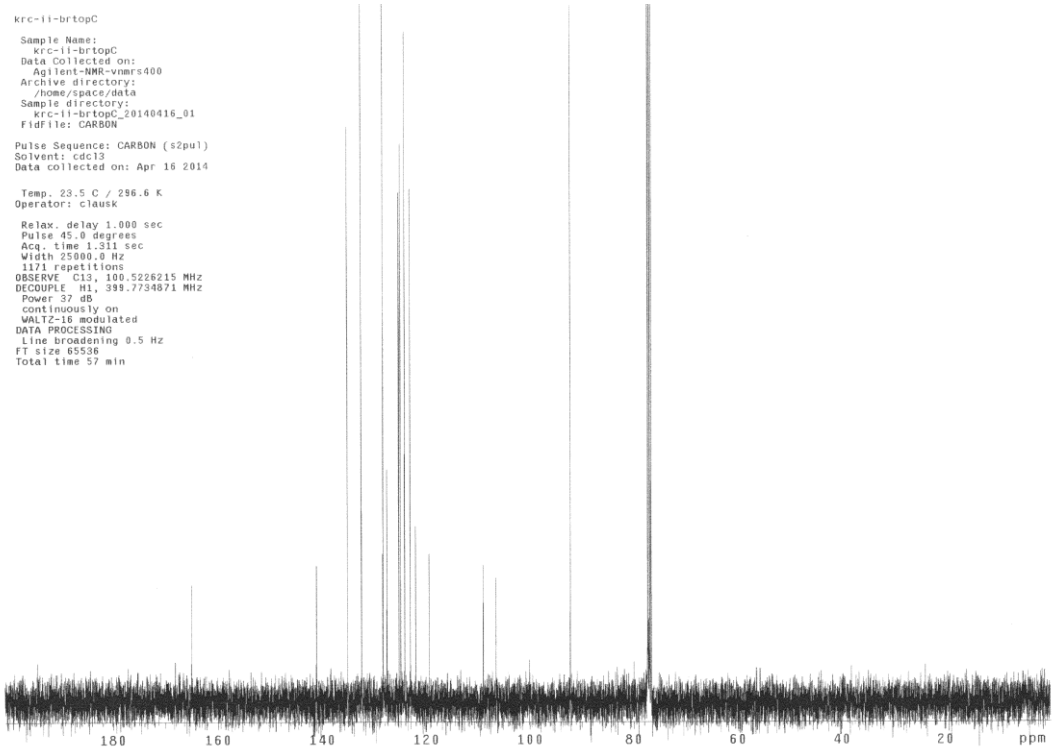
krc-ii-brtopC
Sample Name:
krc-ii-brtopC
Data Collected on:
Agilent-NMR-vnmrs400
Archive directory:
./home/space/data
Sample directory:
krc-ii-brtopC_20140416_01
FidFile: CARBON
Pulse Sequence: CARBON (s2pul)
Solvent: cdcl3
Data collected on: Apr 16 2014
Temp. 23.5 C / 296.6 K
Operator: clausk
Relax. delay 1.000 sec
Pulse 45.0 degrees
Acq. time 1.311 sec
Width 25000.0 Hz
1171 repetitions
OBSERVE C13, 100.5226215 MHz
DECOUPLE H1, 399.7734871 MHz
Power 37 dB
continuously on
WALTZ-16 modulated
DATA PROCESSING
Line broadening 0.5 Hz
FT size 65536
Total time 57 min
180
160
140
120
100
80
60
40
20
ppm

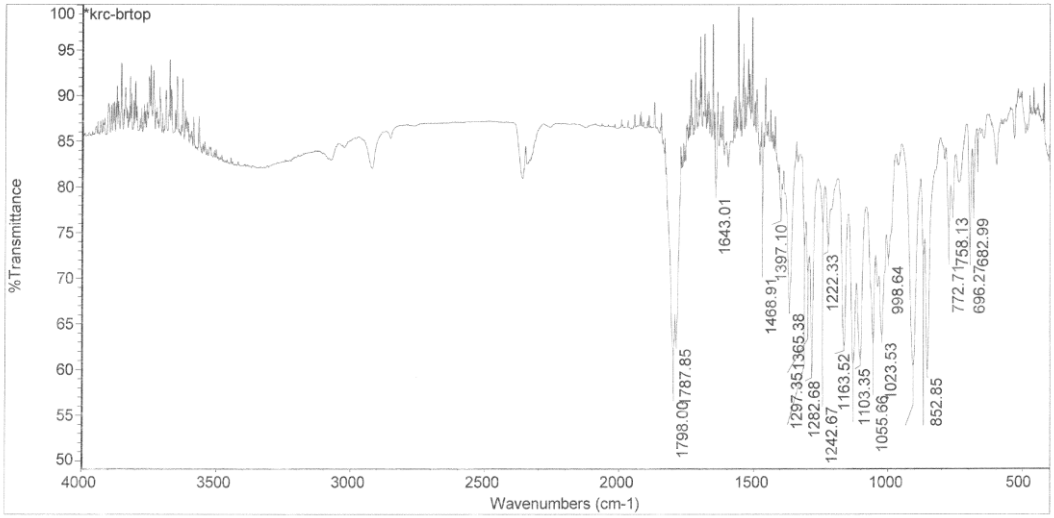

Tue Apr 15 15:52:10 2014 (GMT-05:00)
FIND PEAKS:

Spectrum:	*krc-brtop	
Region:	4000.00	400.00
Absolute threshold:	80.322	
Sensitivity:	50	
Peak list:		

Position:	682.99	Intensity:	77.368
Position:	696.27	Intensity:	72.998
Position:	758.13	Intensity:	77.480
Position:	772.71	Intensity:	75.337
Position:	852.85	Intensity:	59.872
Position:	867.36	Intensity:	72.508
Position:	906.02	Intensity:	60.430
Position:	998.64	Intensity:	72.152

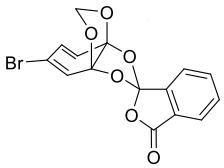
Br
O
O
O
O
O
O

1.175b

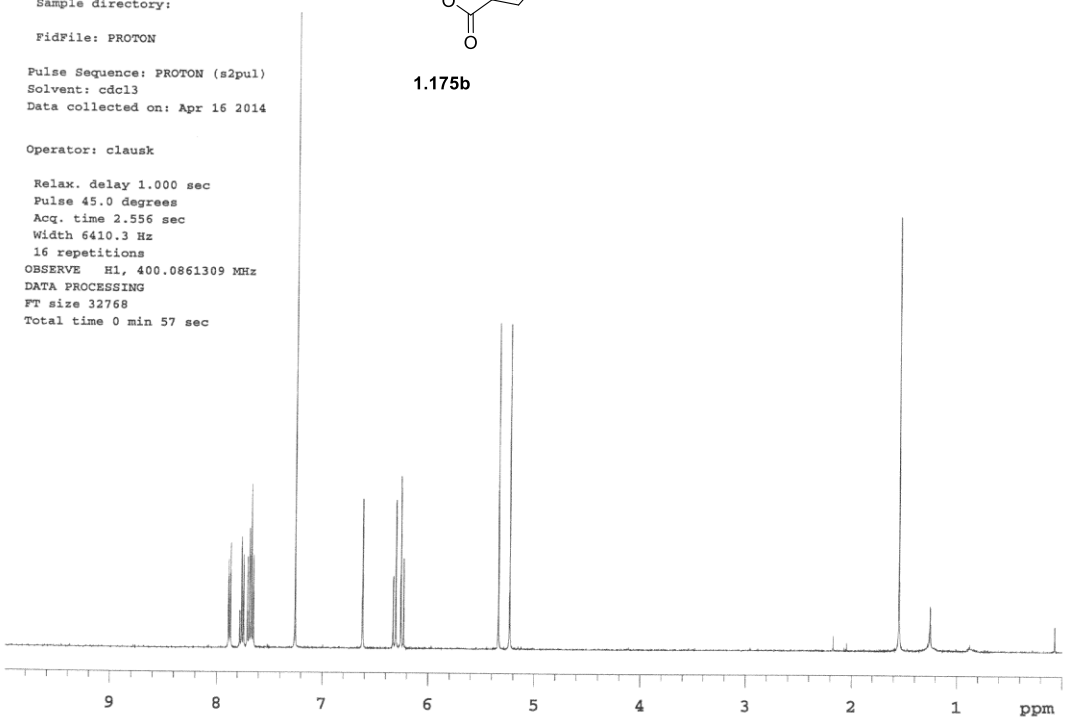
Sample Name:
krc-ii-brbottom
Data Collected on:
nhb400-vnmrs400
Archive directory:
Sample directory:
FidFile: PROTON
Pulse Sequence: PROTON (s2pul)
Solvent: cdcl3
Data collected on: Apr 16 2014
Operator: clausk
Relax. delay 1.000 sec
Pulse 45.0 degrees
Acq. time 2.556 sec
Width 6410.3 Hz
16 repetitions
OBSERVE H1, 400.0861309 MHz
DATA PROCESSING
FT size 32768
Total time 0 min 57 sec
9
8
7
6
5
4
3
2
1
ppm

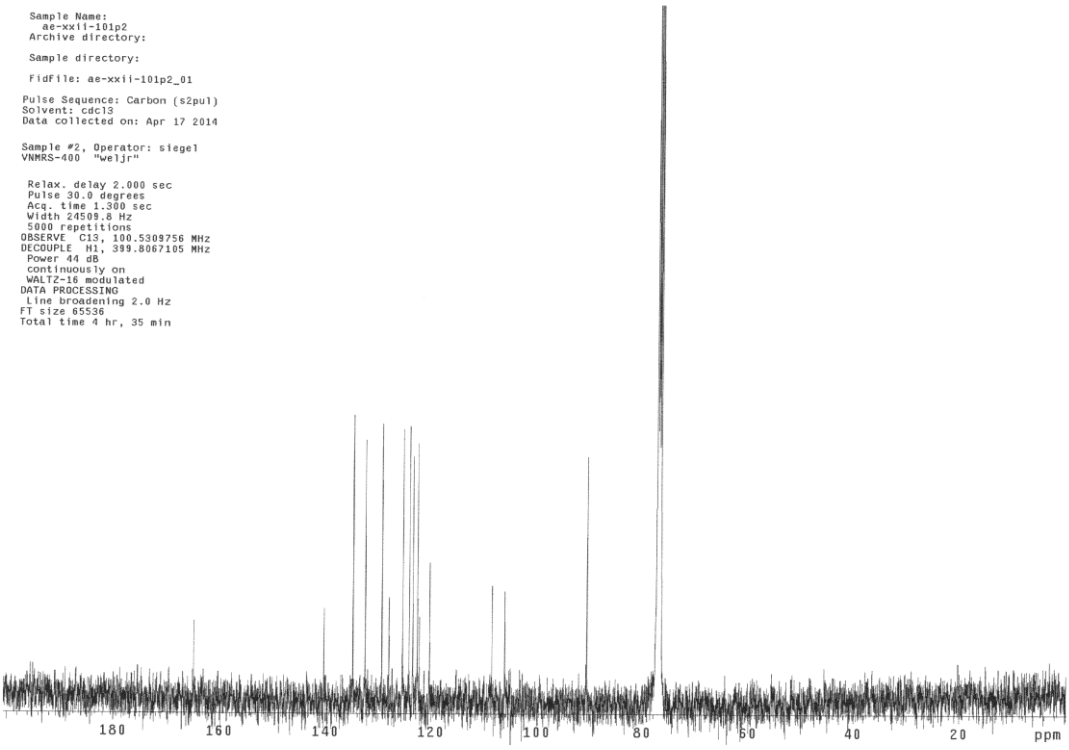
Sample Name:
ae-xxii-101p2
Archive directory:
Sample directory:
FidFile: ae-xxii-101p2_01
Pulse Sequence: Carbon (s2pul)
Solvent: cdcl3
Data collected on: Apr 17 2014
Sample #2, Operator: siegel
VNMRS-400 "weljr"
Relax. delay 2.000 sec
Pulse 30.0 degrees
Acq. time 1.300 sec
Width 24509.8 Hz
5000 repetitions
OBSERVE C13, 100.5309756 MHz
DECOUPLE H1, 399.8067105 MHz
Power 44 dB
continuously on
WALTZ-16 modulated
DATA PROCESSING
Line broadening 2.0 Hz
FT size 65536
Total time 4 hr, 35 min
180
160
140
120
100
80
60
40
20
ppm

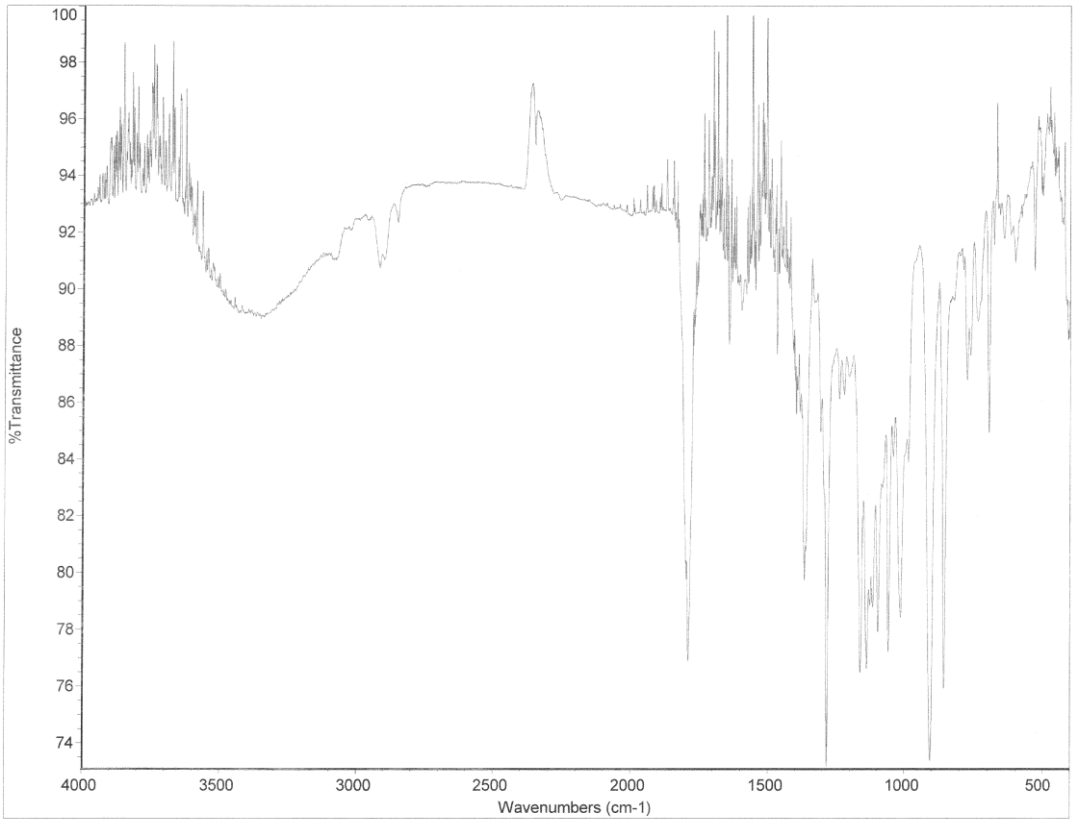
100
98
96
94
92
90
88
86
84
82
80
78
76
74
%Transmittance
4000
3500
3000
2500
2000
1500
1000
500
Wavenumbers (cm-1)

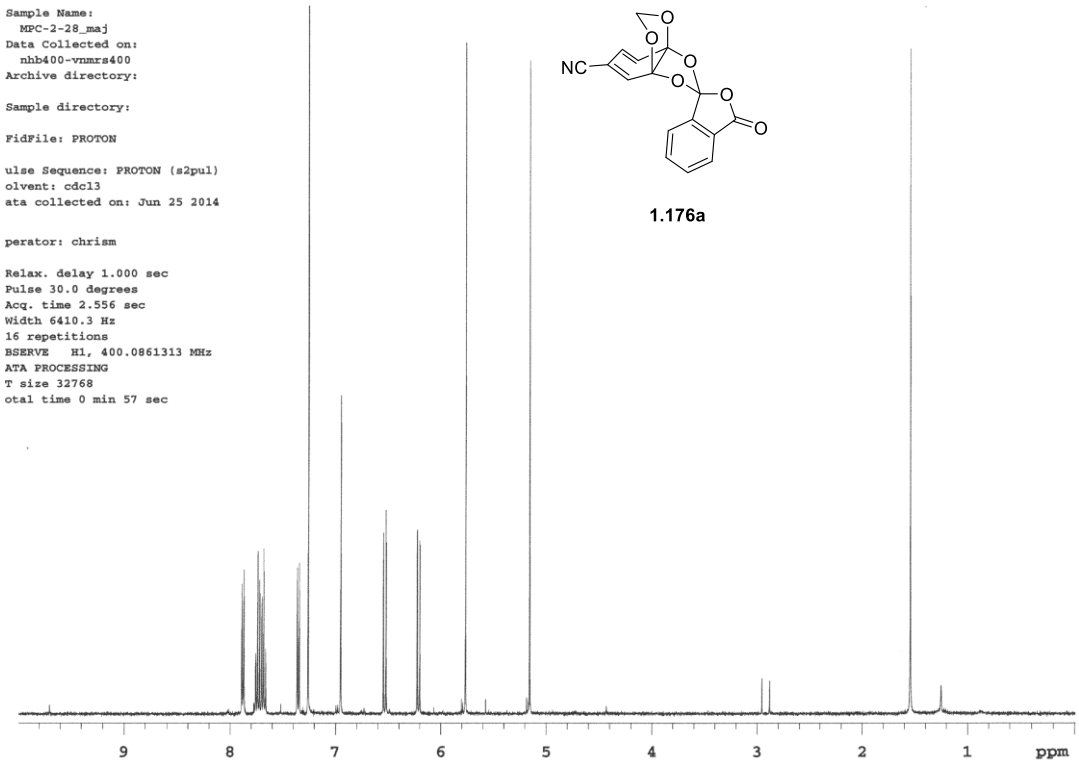
Sample Name:
MPC-2-28_maj
Data Collected on:
nhb400-vnmrs400
Archive directory:
Sample directory:
FidFile: PROTON
ulse Sequence: PROTON (s2pul)
olvent: cdcl3
ata collected on: Jun 25 2014
perator: chrism
Relax. delay 1.000 sec
Pulse 30.0 degrees
Acq. time 2.556 sec
Width 6410.3 Hz
16 repetitions
BSERVE H1, 400.0861313 MHz
ATA PROCESSING
T size 32768
otal time 0 min 57 sec
NC
O
1.176a
9
8
7
6
5
4
3
2
1
ppm

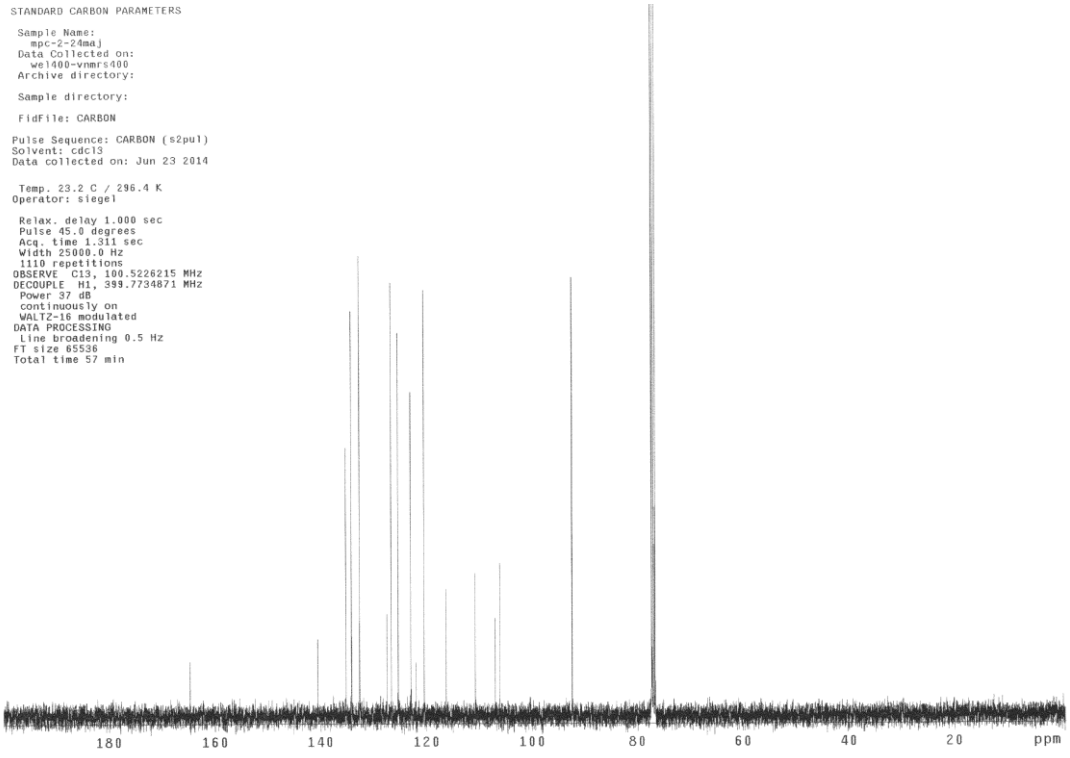
STANDARD CARBON PARAMETERS
Sample Name:
mpc-2-24maj
Data Collected on:
wel400-vnmrs400
Archive directory:
Sample directory:
FidFile: CARBON
Pulse Sequence: CARBON (s2pul)
Solvent: cdcl3
Data collected on: Jun 23 2014
Temp. 23.2 C / 296.4 K
Operator: siegel
Relax. delay 1.000 sec
Pulse 45.0 degrees
Acq. time 1.311 sec
Width 25000.0 Hz
1110 repetitions
OBSERVE C13, 100.5226215 MHz
DECOUPLE H1, 399.7734871 MHz
Power 37 dB
continuously on
WALTZ-16 modulated
DATA PROCESSING
Line broadening 0.5 Hz
FT size 65536
Total time 57 min
180
160
140
120
100
80
60
40
20
ppm

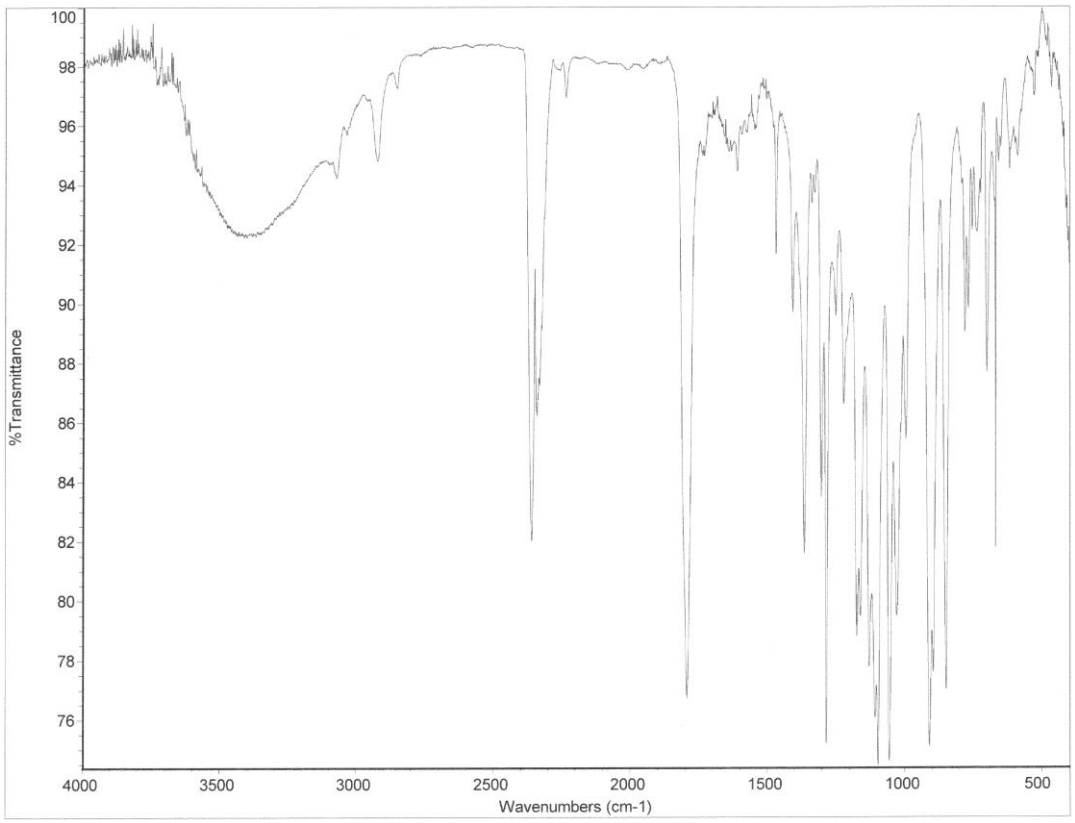
100
98
96
94
92
90
88
86
84
82
80
78
76
%Transmittance
4000
3500
3000
2500
2000
1500
1000
500
Wavenumbers (cm-1)

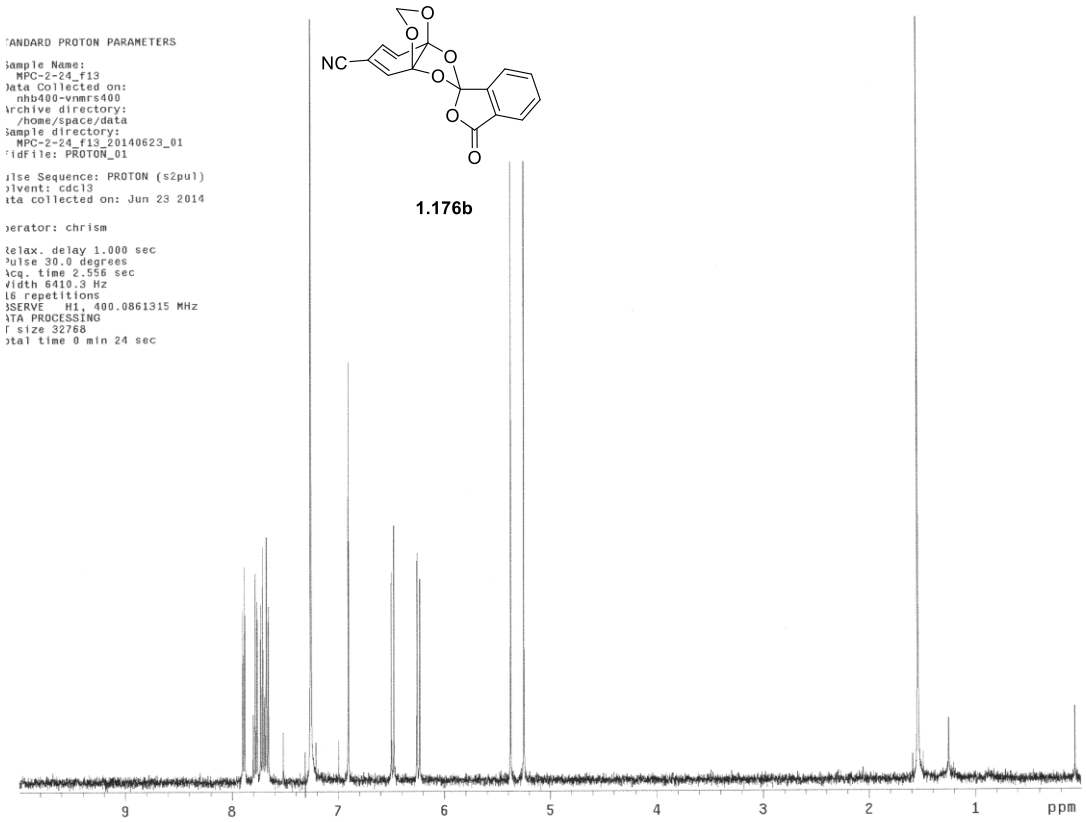
'ANDARD PROTON PARAMETERS
ample Name:
MPC-2-24_f13
ata Collected on:
nhb400-vnmrs400
rchive directory:
/home/space/data
ample directory:
MPC-2-24_f13_20140623_01
idFile: PROTON_01
lse Sequence: PROTON (s2pul)
lvent: cdcl3
ta collected on: Jun 23 2014
erator: chrism
elax. delay 1.000 sec
ulse 30.0 degrees
cq. time 2.556 sec
idth 6410.3 Hz
6 repetitions
SERVE H1, 400.0861315 MHz
TA PROCESSING
f size 32768
tal time 0 min 24 sec
NC
O
1.176b
9
8
7
6
5
4
3
2
1
ppm

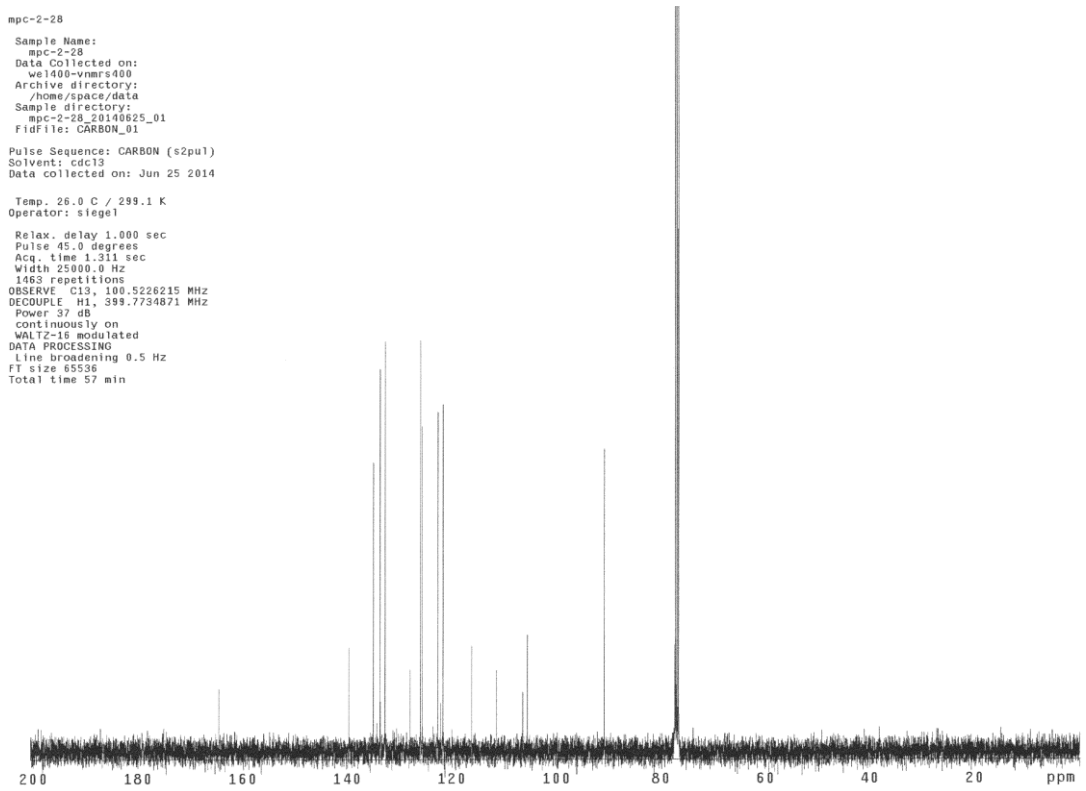
mpc-2-28
Sample Name:
mpc-2-28
Data Collected on:
we1400-vnmrs400
Archive directory:
/home/space/data
Sample directory:
mpc-2-28_20140625_01
FidFile: CARBON_01
Pulse Sequence: CARBON (s2pul)
Solvent: cdcl3
Data collected on: Jun 25 2014
Temp. 26.0 C / 299.1 K
Operator: siegel
Relax. delay 1.000 sec
Pulse 45.0 degrees
Acq. time 1.311 sec
Width 25000.0 Hz
1463 repetitions
OBSERVE C13, 100.5226215 MHz
DECOUPLE H1, 399.7734871 MHz
Power 37 dB
continuously on
WALTZ-16 modulated
DATA PROCESSING
Line broadening 0.5 Hz
FT size 65536
Total time 57 min
200
180
160
140
120
100
80
60
40
20
ppm

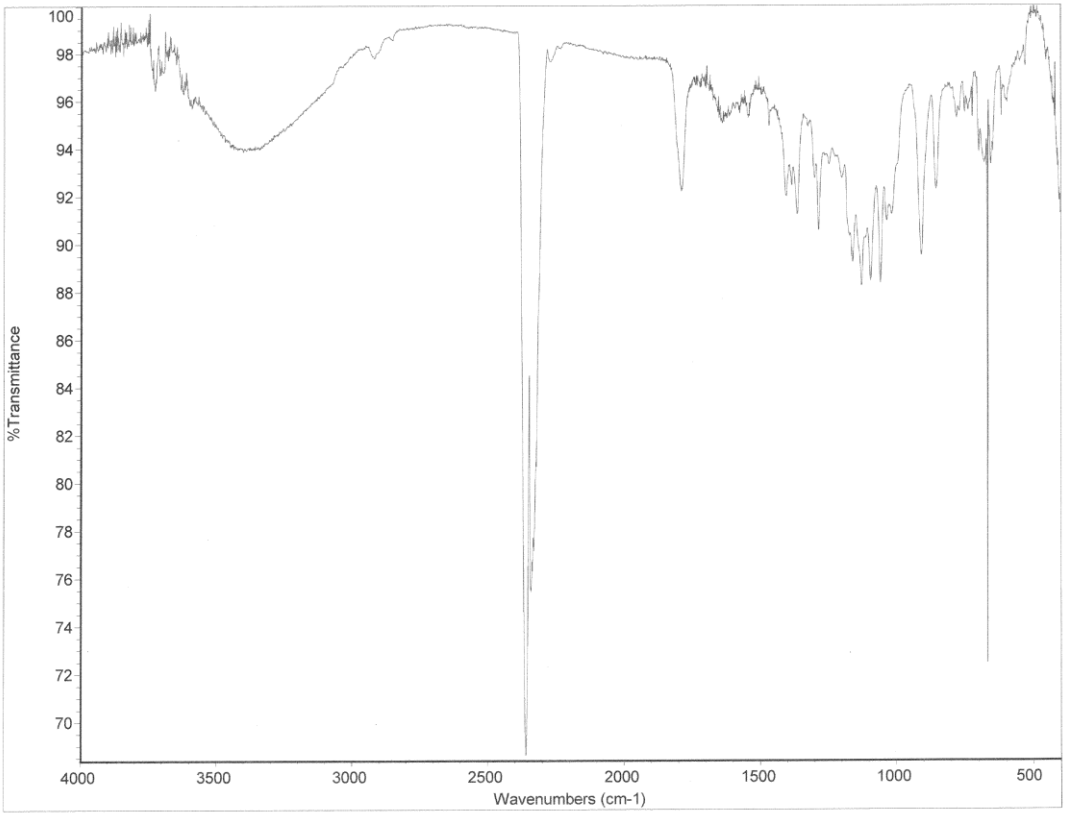
%Transmittance
100
98
96
94
92
90
88
86
84
82
80
78
76
74
72
70
4000
3500
3000
2500
2000
1500
1000
500
Wavenumbers (cm-1)

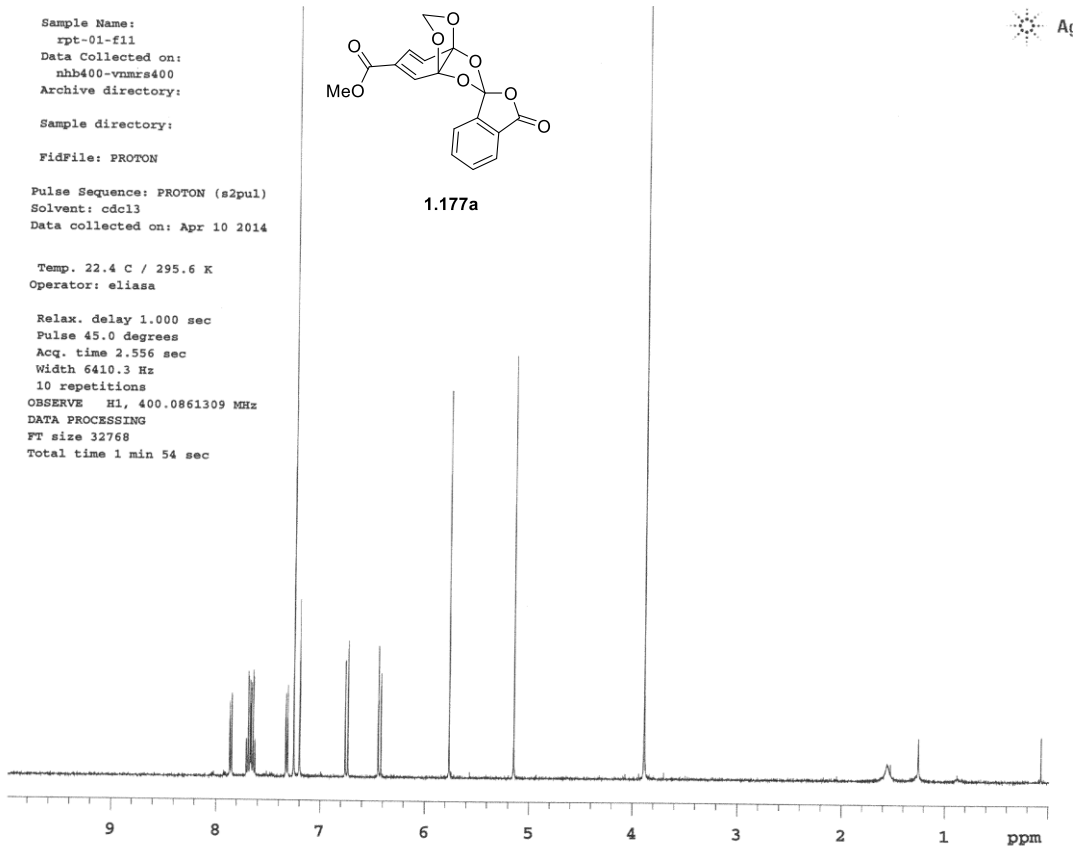
Sample Name:
rpt-01-f11
Data Collected on:
nhb400-vnmrs400
Archive directory:
Sample directory:
FidFile: PROTON
Pulse Sequence: PROTON (s2pul)
Solvent: cdcl3
Data collected on: Apr 10 2014
Temp. 22.4 C / 295.6 K
Operator: eliasa
Relax. delay 1.000 sec
Pulse 45.0 degrees
Acq. time 2.556 sec
Width 6410.3 Hz
10 repetitions
OBSERVE H1, 400.0861309 MHz
DATA PROCESSING
FT size 32768
Total time 1 min 54 sec
MeO
O
1.177a
9
8
7
6
5
4
3
2
1
ppm

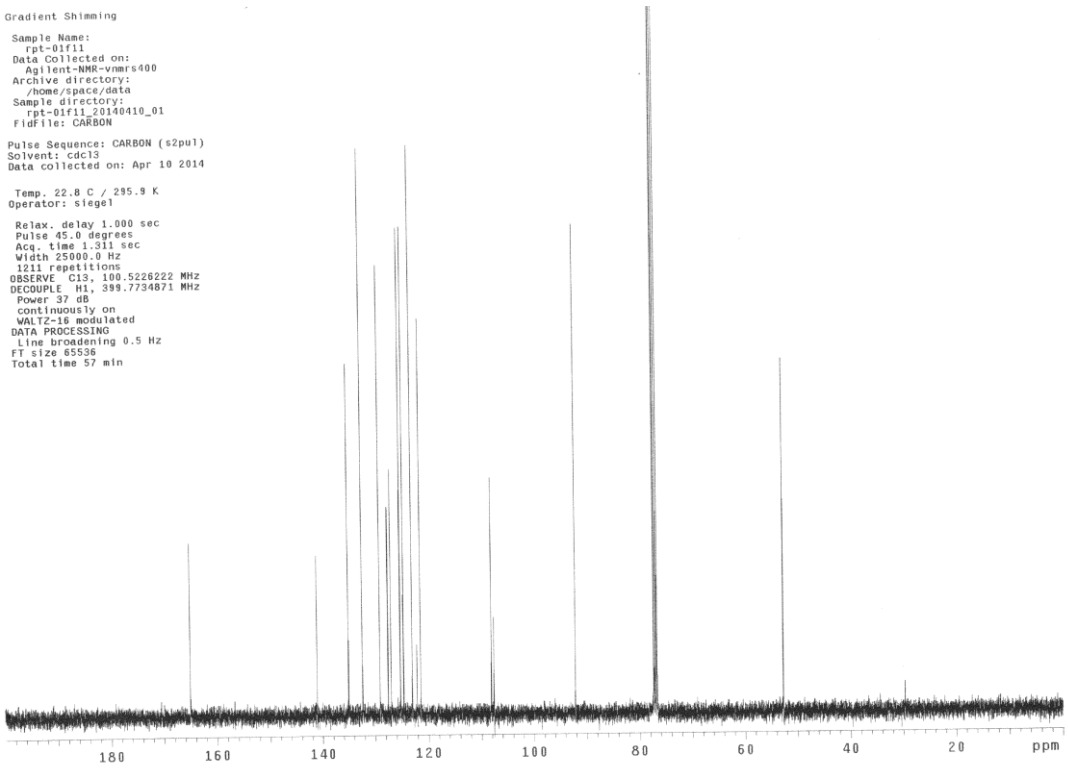
Gradient Shimming
Sample Name:
rpt-01f11
Data Collected on:
Agilent-NMR-vnmrs400
Archive directory:
/home/space/data
Sample directory:
rpt-01f11_20140410_01
FidFile: CARBON
Pulse Sequence: CARBON (s2pul)
Solvent: cdcl3
Data collected on: Apr 10 2014
Temp. 22.8 C / 295.9 K
Operator: siegel
Relax. delay 1.000 sec
Pulse 45.0 degrees
Acq. time 1.311 sec
Width 25000.0 Hz
1211 repetitions
OBSERVE C13, 100.5226222 MHz
DECOUPLE H1, 399.7734871 MHz
Power 37 dB
continuously on
WALTZ-16 modulated
DATA PROCESSING
Line broadening 0.5 Hz
FT size 65536
Total time 57 min
180
160
140
120
100
80
60
40
20
ppm

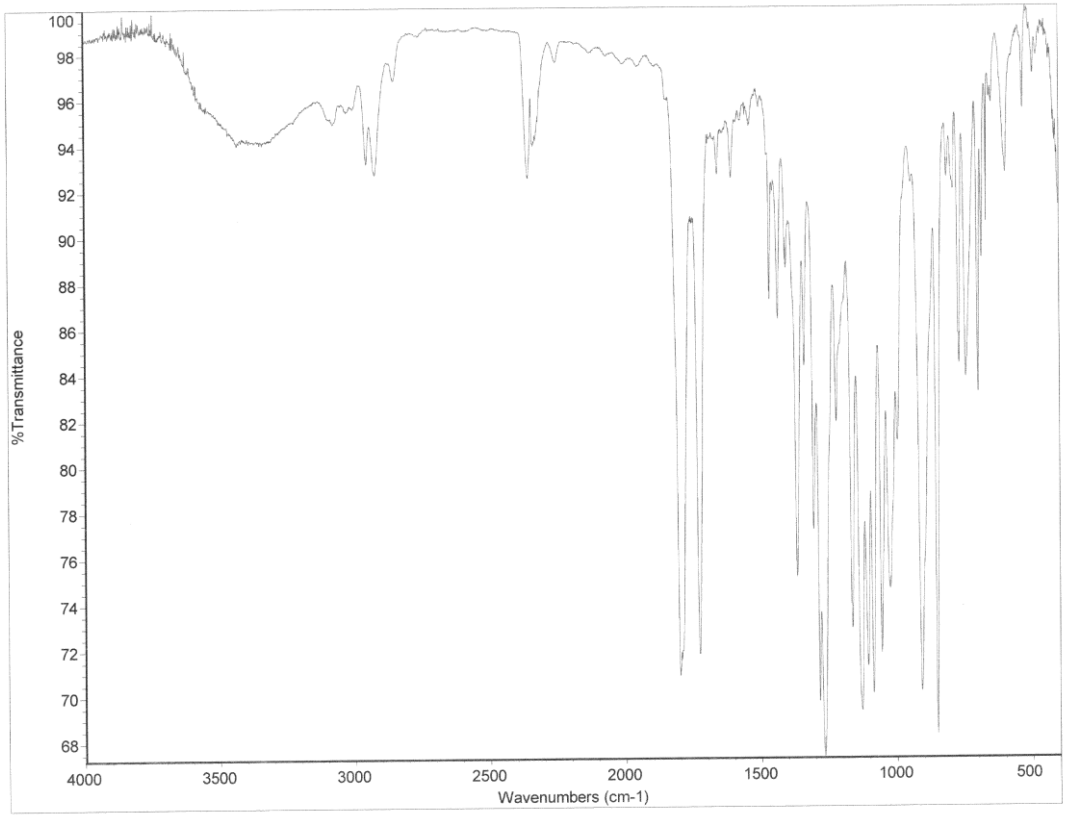
%Transmittance
100
98
96
94
92
90
88
86
84
82
80
78
76
74
72
70
68
4000
3500
3000
2500
2000
1500
1000
500
Wavenumbers (cm-1)

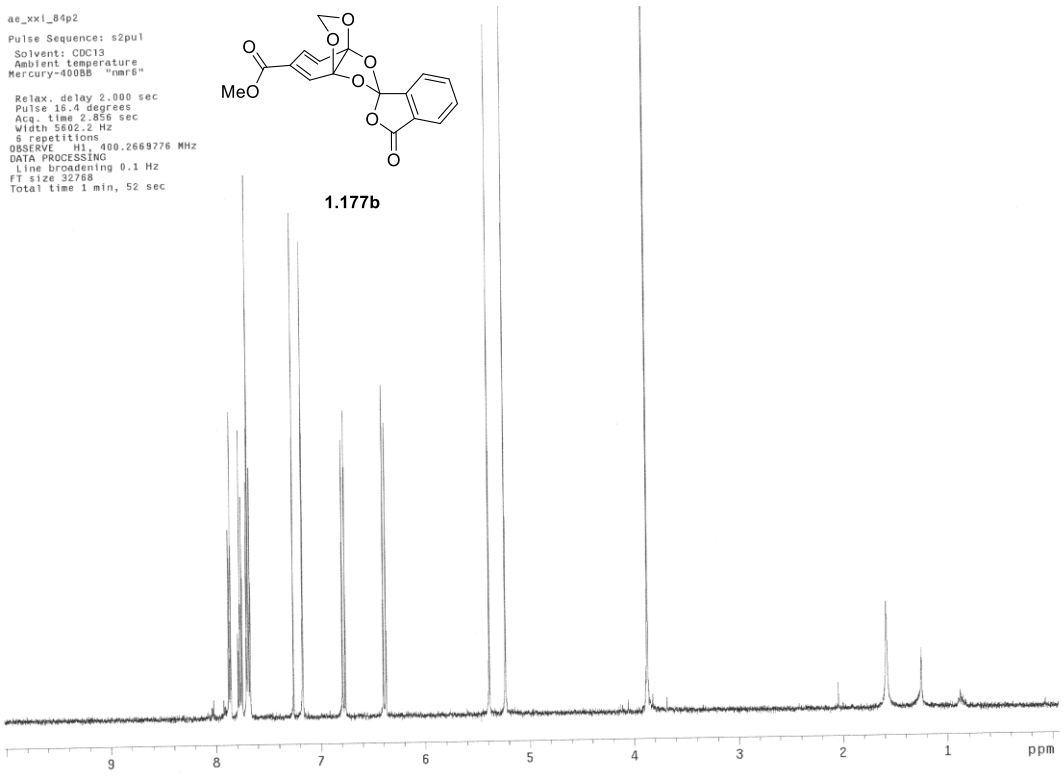
ae_xxi_84p2
Pulse Sequence: s2pul
Solvent: CDCl3
Ambient temperature
Mercury-400BB "nmr6"
Relax. delay 2.000 sec
Pulse 16.4 degrees
Acq. time 2.856 sec
Width 5602.2 Hz
6 repetitions
OBSERVE H1, 400.2669776 MHz
DATA PROCESSING
Line broadening 0.1 Hz
FT size 32768
Total time 1 min, 52 sec
MeO
O
1.177b
9
8
7
6
5
4
3
2
1
ppm

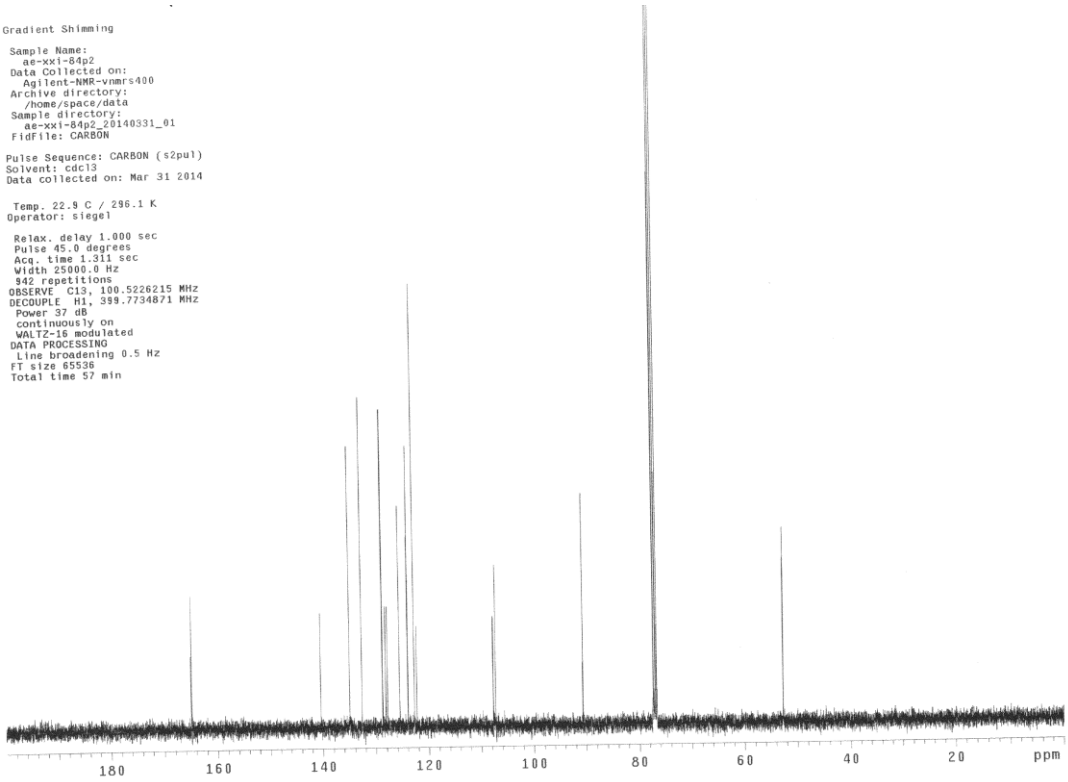
Gradient Shimming
Sample Name:
ae-xxi-84p2
Data Collected on:
Agilent-NMR-vnmrs400
Archive directory:
/home/space/data
Sample directory:
ae-xxi-84p2_20140331_01
FidFile: CARBON
Pulse Sequence: CARBON (s2pul)
Solvent: cdcl3
Data collected on: Mar 31 2014
Temp. 22.9 C / 296.1 K
Operator: siegel
Relax. delay 1.000 sec
Pulse 45.0 degrees
Acq. time 1.311 sec
Width 25000.0 Hz
942 repetitions
OBSERVE C13, 100.5226215 MHz
DECOUPLE H1, 399.7734871 MHz
Power 37 dB
continuously on
WALTZ-16 modulated
DATA PROCESSING
Line broadening 0.5 Hz
FT size 65536
Total time 57 min
180
160
140
120
100
80
60
40
20
ppm

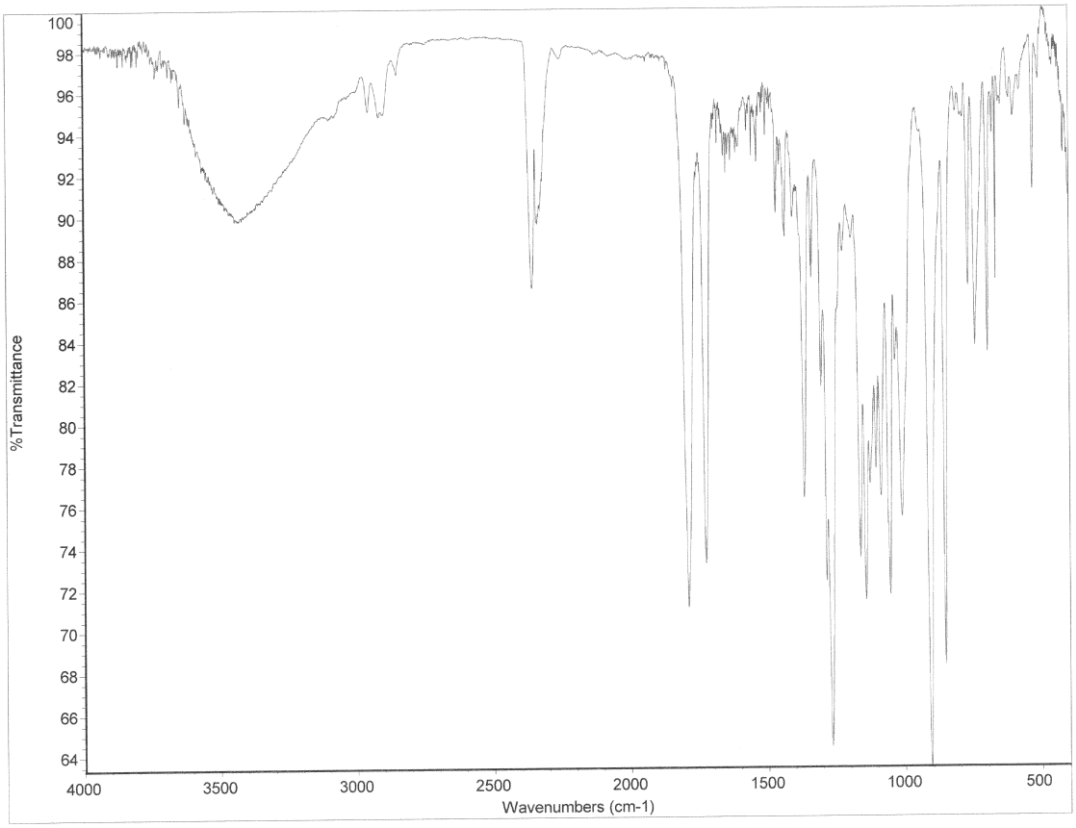
%Transmittance
100
98
96
94
92
90
88
86
84
82
80
78
76
74
72
70
68
66
64
4000
3500
3000
2500
2000
1500
1000
500
Wavenumbers (cm-1)

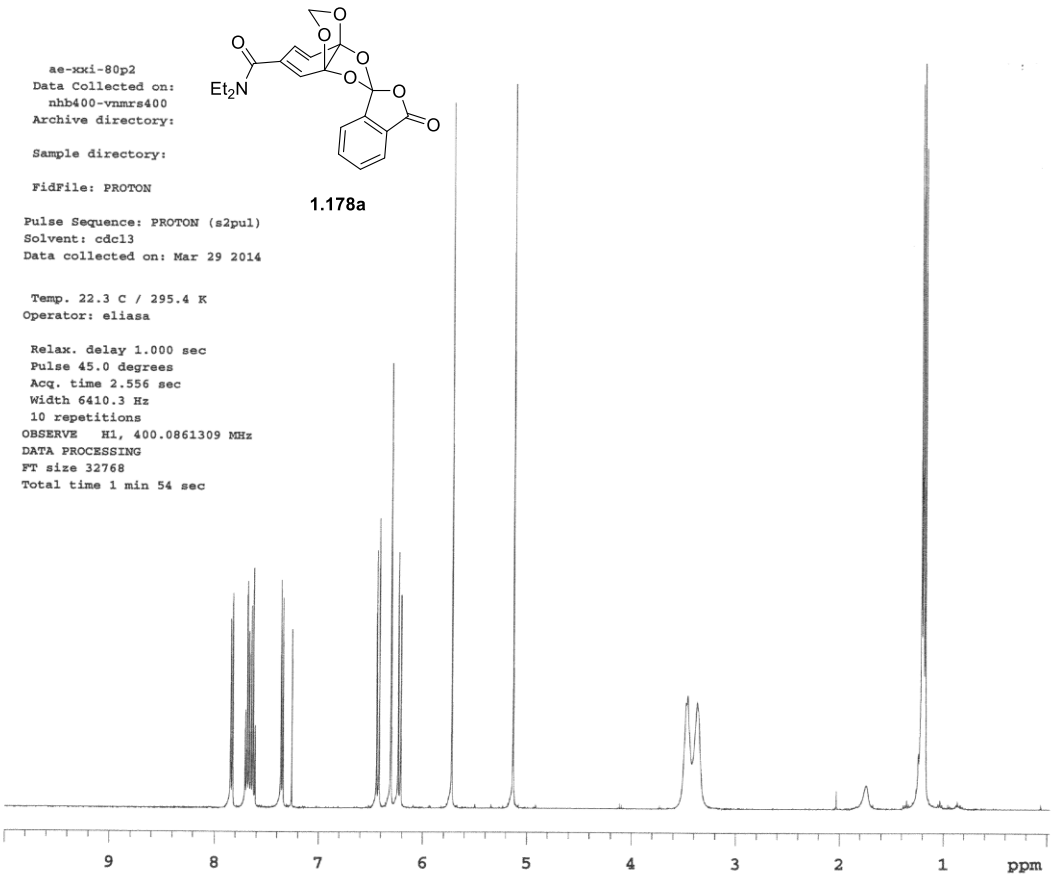
ae-xxi-80p2
Data Collected on:
nhb400-vnmrs400
Archive directory:
Sample directory:
FidFile: PROTON
Pulse Sequence: PROTON (s2pul)
Solvent: cdcl3
Data collected on: Mar 29 2014
Temp. 22.3 C / 295.4 K
Operator: eliasa
Relax. delay 1.000 sec
Pulse 45.0 degrees
Acq. time 2.556 sec
Width 6410.3 Hz
10 repetitions
OBSERVE H1, 400.0861309 MHz
DATA PROCESSING
FT size 32768
Total time 1 min 54 sec
Et2N
1.178a
9
8
7
6
5
4
3
2
1
ppm

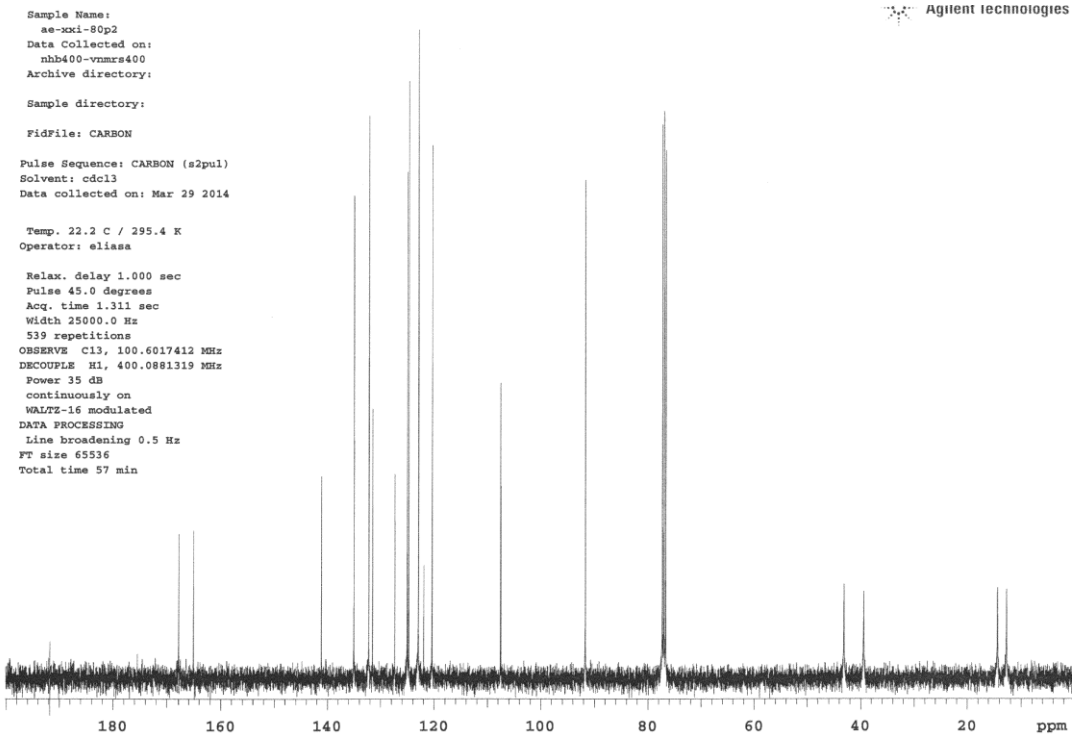
Agilent Technologies
Sample Name:
ae-xxi-80p2
Data Collected on:
nhb400-vnmrs400
Archive directory:
Sample directory:
FidFile: CARBON
Pulse Sequence: CARBON (s2pul)
Solvent: cdcl3
Data collected on: Mar 29 2014
Temp. 22.2 C / 295.4 K
Operator: eliasa
Relax. delay 1.000 sec
Pulse 45.0 degrees
Acq. time 1.311 sec
Width 25000.0 Hz
539 repetitions
OBSERVE C13, 100.6017412 MHz
DECOUPLE H1, 400.0881319 MHz
Power 35 dB
continuously on
WALTZ-16 modulated
DATA PROCESSING
Line broadening 0.5 Hz
FT size 65536
Total time 57 min
180
160
140
120
100
80
60
40
20
ppm

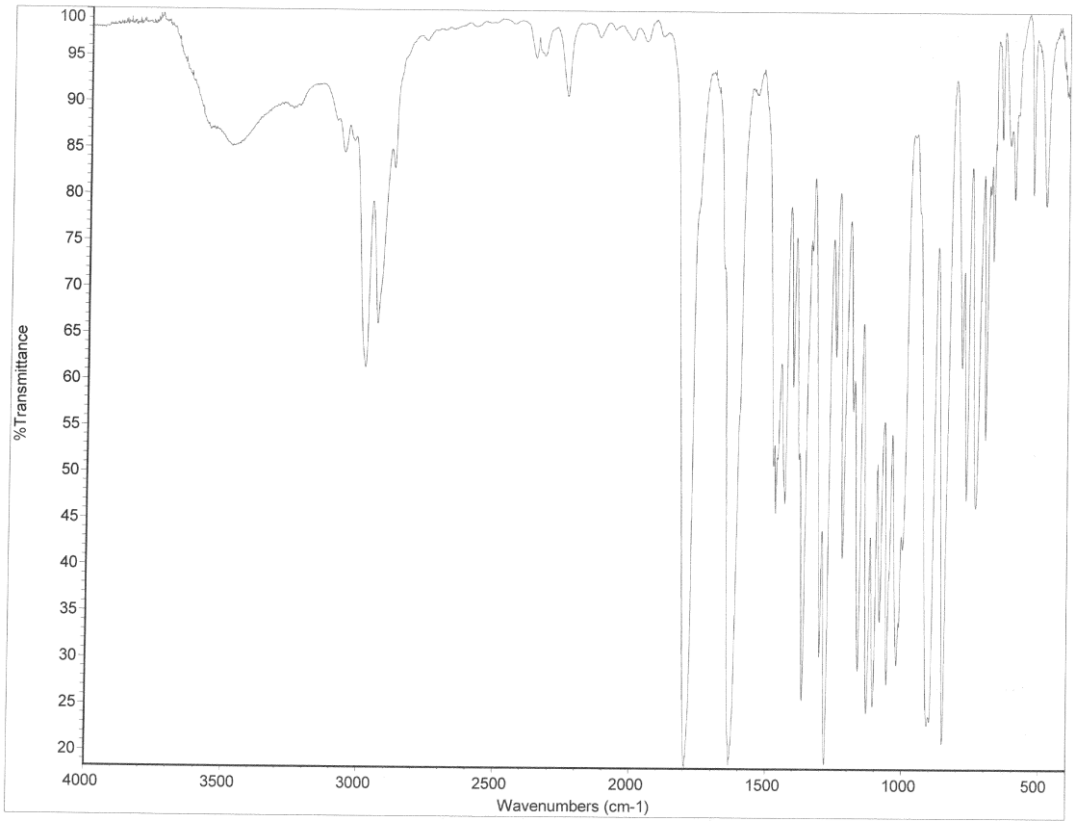
%Transmittance
100
95
90
85
80
75
70
65
60
55
50
45
40
35
30
25
20
4000
3500
3000
2500
2000
1500
1000
500
Wavenumbers (cm-1)

ae-xxi-80p1
Data Collected on:
nhb400-vnmrs400
Archive directory:

Sample directory:

FidFile: PROTON

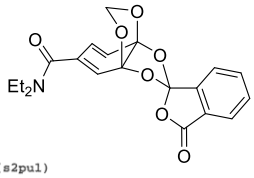

1.178b

Pulse Sequence: PROTON (s2pul)
Solvent: cdcl3
Data collected on: Mar 29 2014

Operator: eliasa

Relax. delay 1.000 sec
Pulse 45.0 degrees
Acq. time 2.556 sec
Width 6410.3 Hz
8 repetitions
OBSERVE H1, 400.0861309 MHz
DATA PROCESSING
FT size 32768
Total time 0 min 28 sec

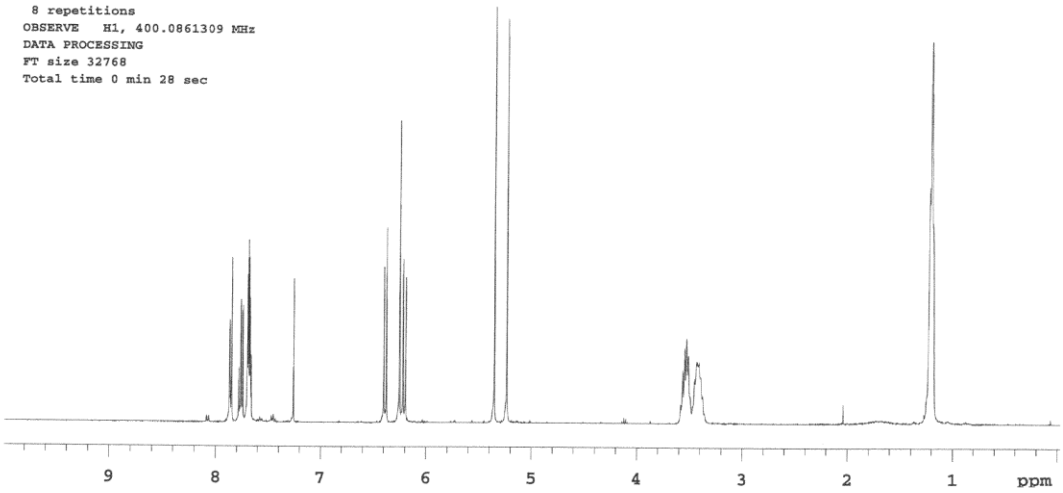

Agilent Technologies

Sample Name:
ae-xxi-80p1
Data Collected on:
nhb400-vnmrs400
Archive directory:

Sample directory:

FidFile: CARBON

Pulse Sequence: CARBON (s2pul)
Solvent: cdcl3
Data collected on: Mar 29 2014

Temp. 22.3 C / 295.4 K
Operator: eliasa

Relax. delay 1.000 sec
Pulse 45.0 degrees
Acq. time 1.311 sec
Width 25000.0 Hz
886 repetitions
OBSERVE C13, 100.6017396 MHz
DECOUPLE H1, 400.0881319 MHz
Power 35 dB
continuously on
WALTZ-16 modulated
DATA PROCESSING
Line broadening 0.5 Hz
FT size 65536
Total time 57 min

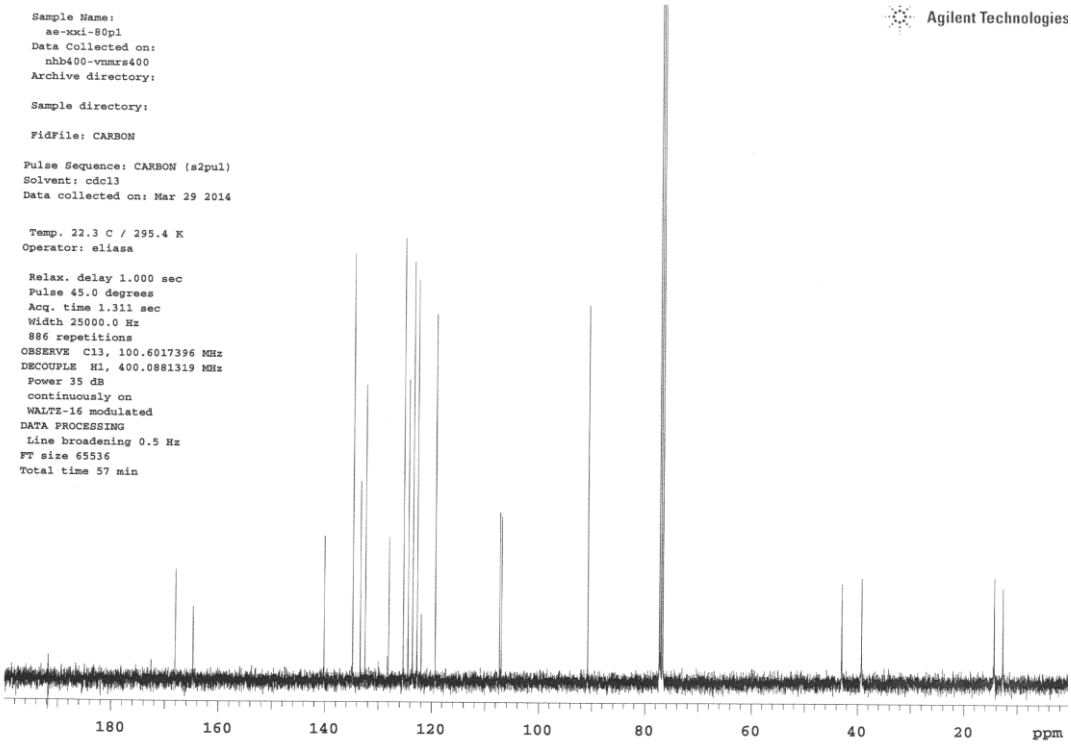

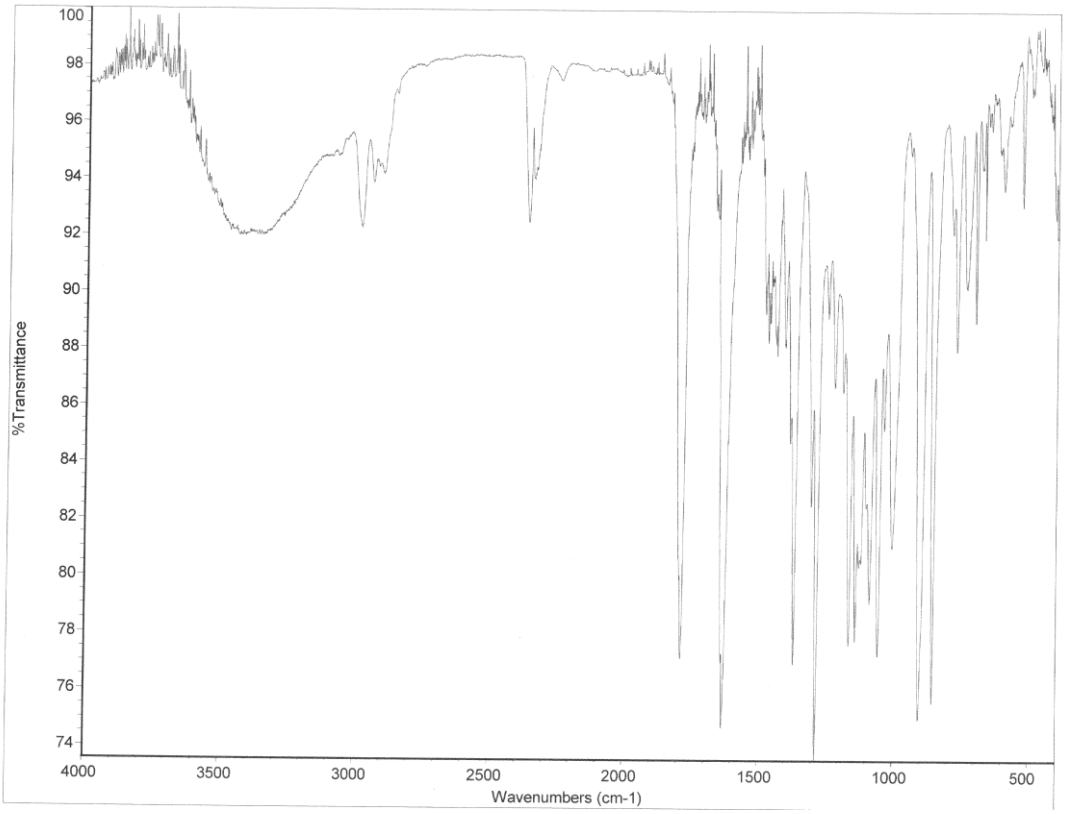
%Transmittance
100
98
96
94
92
90
88
86
84
82
80
78
76
74
4000
3500
3000
2500
2000
1500
1000
500
Wavenumbers (cm-1)

Sample Name:
ae-xx-83p3
Data Collected on:
nhb400-vnmrs400
Archive directory:

Sample directory:

FidFile: PROTON

Pulse Sequence: PROTON (s2pul)
Solvent: cdcl3
Data collected on: Mar 10 2014

1.179a

Temp. 22.1 C / 295.2 K
Operator: eliasa

Relax. delay 1.000 sec
Pulse 45.0 degrees
Acq. time 2.556 sec
Width 6410.3 Hz
11 repetitions
OBSERVE H1, 400.0861293 MHz
DATA PROCESSING
FT size 32768
Total time 1 min 54 sec

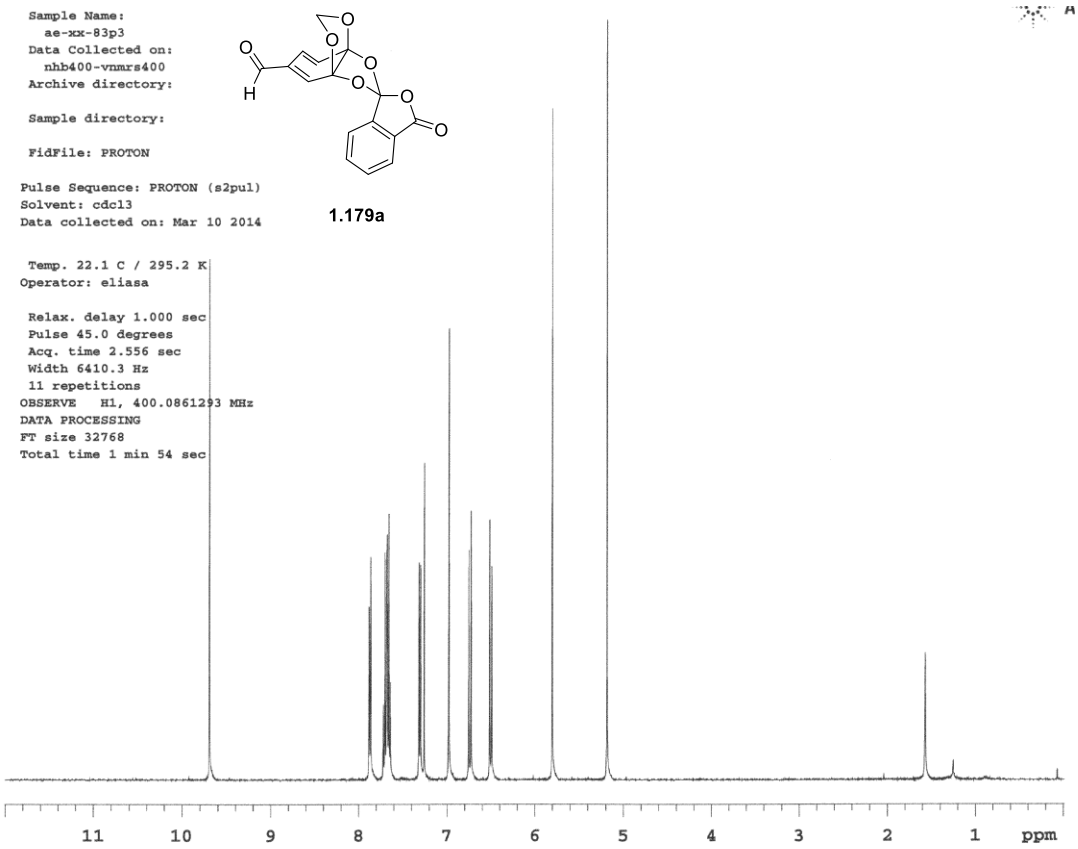

SAMPLE		SPECIAL	
date	Mar 11 2014	temp	27.0
solvent	cdcl3	gain	50
file	exp	spin	20
ACQUISITION		hst	0.008
sw	30165.9	pw90	11.600
at	1.958	alfa	10.000
np	118154	FLAGS	
fb	17000	il	n
bs	1	in	n
di	2.000	dp	y
nt	2000	hs	nn
ct	2000	PROCESSING	
TRANSMITTER		lb	1.00
tn	C13	fn	not used
sfrq	125.701	DISPLAY	
tof	1255.4	sp	-628.5
tpwr	55	wp	28279.6
pw	1.933	rfl	11596.2
DECOUPLER		rfp	9678.0
dn	H1	rp	163.6
dof	0	lp	-217.2
dm	yyy	PLOT	
dmm	w	wc	250
dpwr	38	sc	0
dmf	11800	vs	55569
		th	8
		al	ph

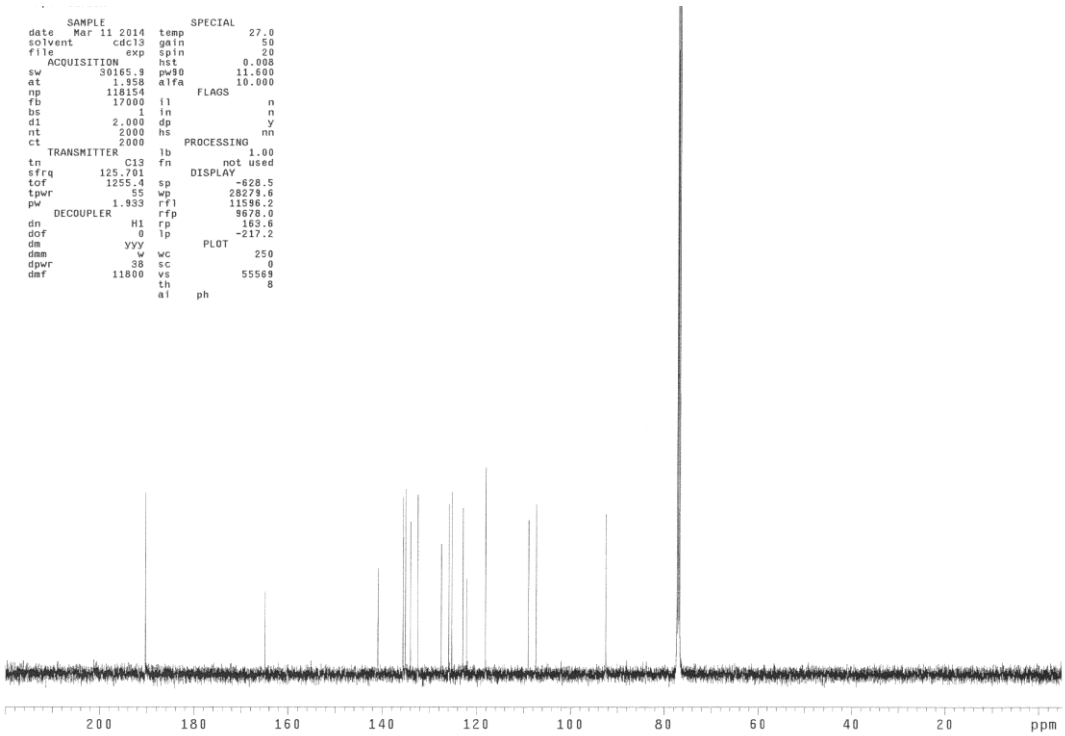

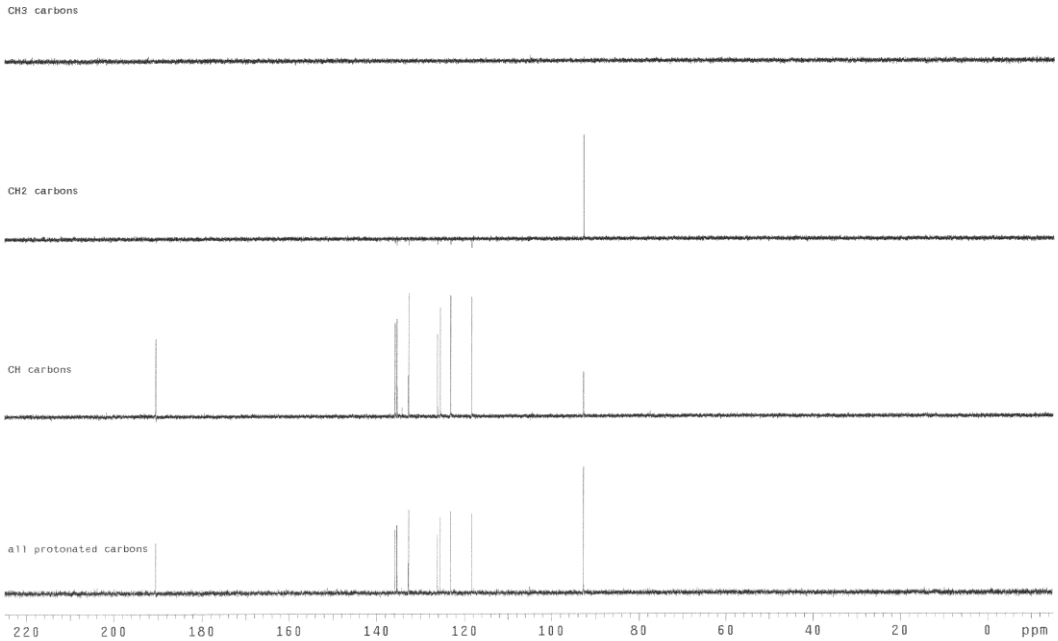
CH3 carbons
CH2 carbons
CH carbons
all protonated carbons
220
200
180
160
140
120
100
80
60
40
20
0
ppm

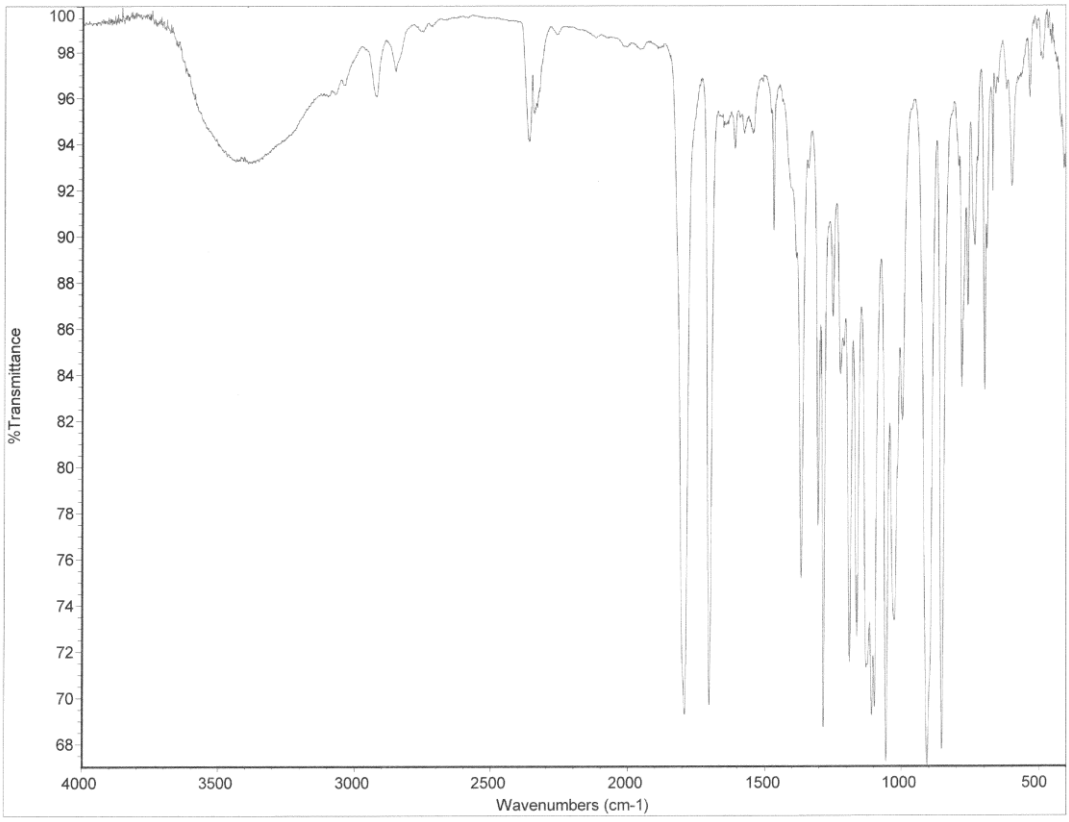
%Transmittance
100
98
96
94
92
90
88
86
84
82
80
78
76
74
72
70
68
4000
3500
3000
2500
2000
1500
1000
500
Wavenumbers (cm-1)

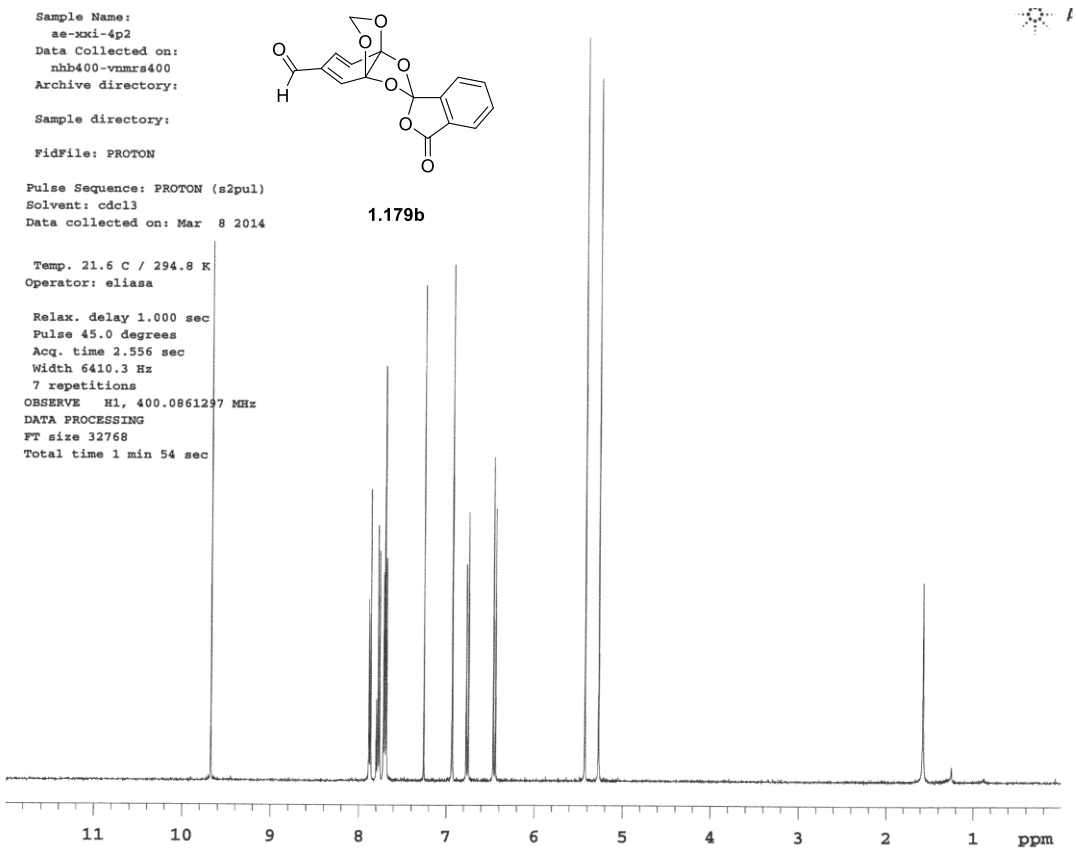
Sample Name:
ae-xxi-4p2
Data Collected on:
nhb400-vnmrs400
Archive directory:
Sample directory:
FidFile: PROTON
Pulse Sequence: PROTON (s2pul)
Solvent: cdcl3
Data collected on: Mar 8 2014
Temp. 21.6 C / 294.8 K
Operator: eliasa
Relax. delay 1.000 sec
Pulse 45.0 degrees
Acq. time 2.556 sec
Width 6410.3 Hz
7 repetitions
OBSERVE H1, 400.0861297 MHz
DATA PROCESSING
FT size 32768
Total time 1 min 54 sec
1.179b
11
10
9
8
7
6
5
4
3
2
1
ppm

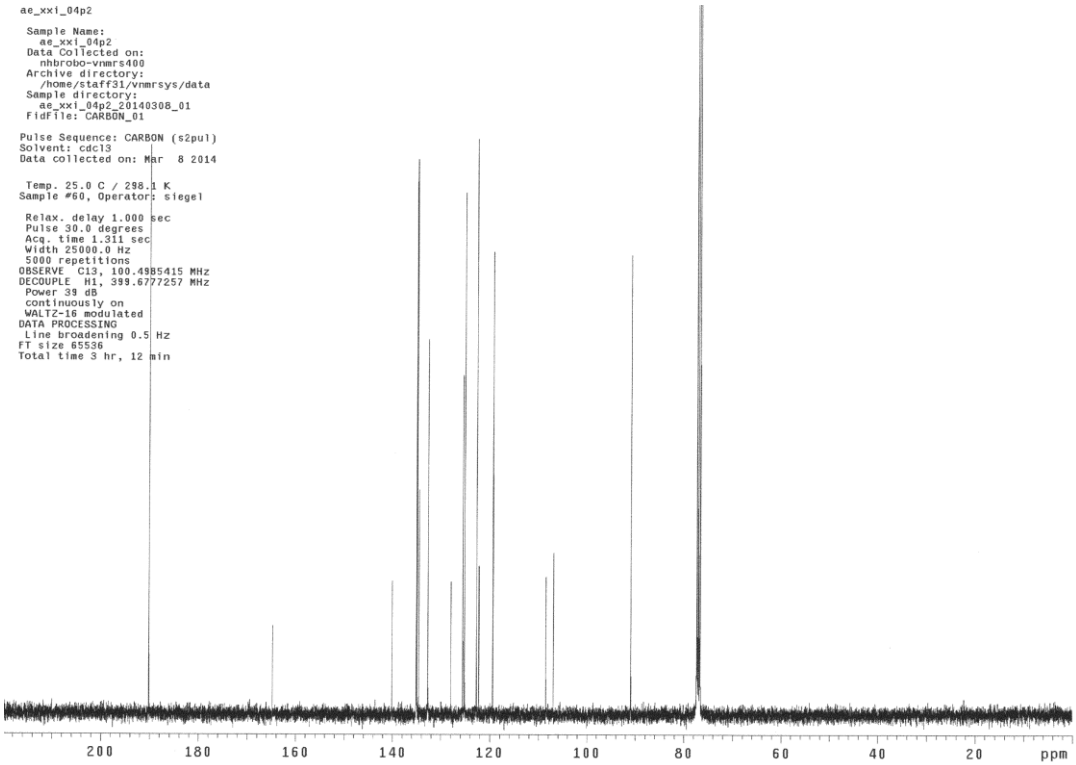
ae_xxi_04p2
Sample Name:
ae_xxi_04p2
Data Collected on:
nhbrobo-vnmrs400
Archive directory:
/home/staff31/vnmrsys/data
Sample directory:
ae_xxi_04p2_20140308_01
FidFile: CARBON_01
Pulse Sequence: CARBON (s2pul)
Solvent: cdcl3
Data collected on: Mar 8 2014
Temp. 25.0 C / 298.1 K
Sample #60, Operator: siegel
Relax. delay 1.000 sec
Pulse 30.0 degrees
Acq. time 1.311 sec
Width 25000.0 Hz
5000 repetitions
OBSERVE C13, 100.4985415 MHz
DECOUPLE H1, 399.6777257 MHz
Power 39 dB
continuously on
WALTZ-16 modulated
DATA PROCESSING
Line broadening 0.5 Hz
FT size 65536
Total time 3 hr, 12 min
200
180
160
140
120
100
80
60
40
20
ppm

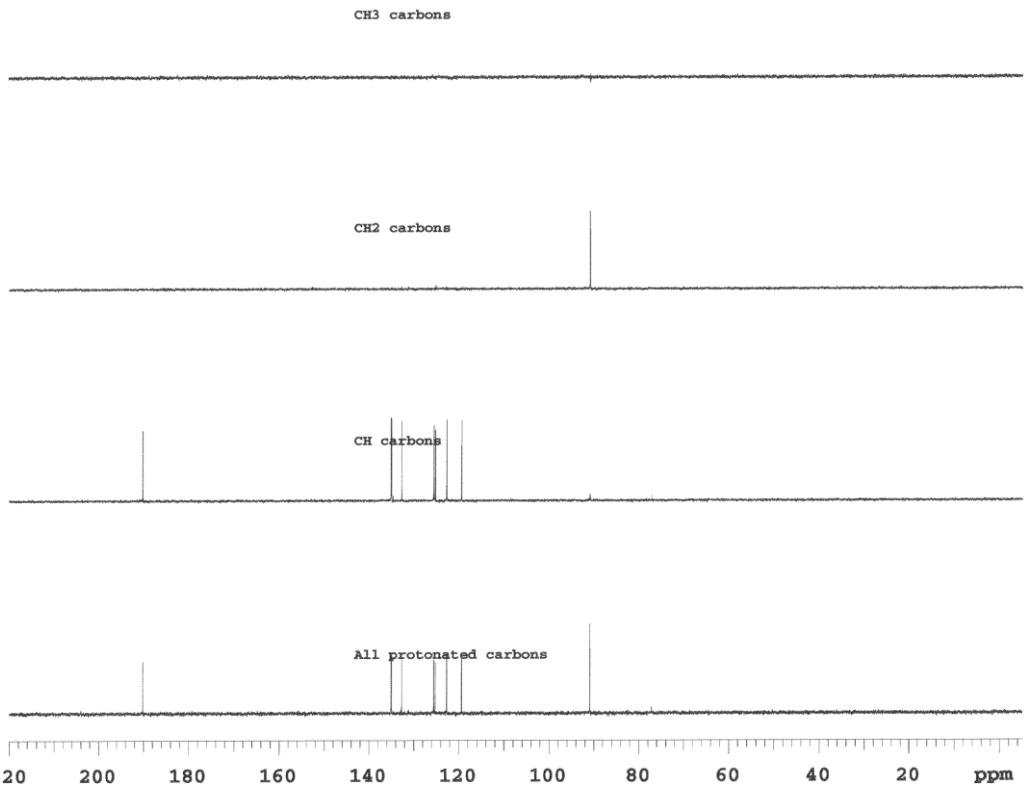
CH3 carbons
CH2 carbons
CH carbons
All protonated carbons
220 200 180 160 140 120 100 80 60 40 20 ppm

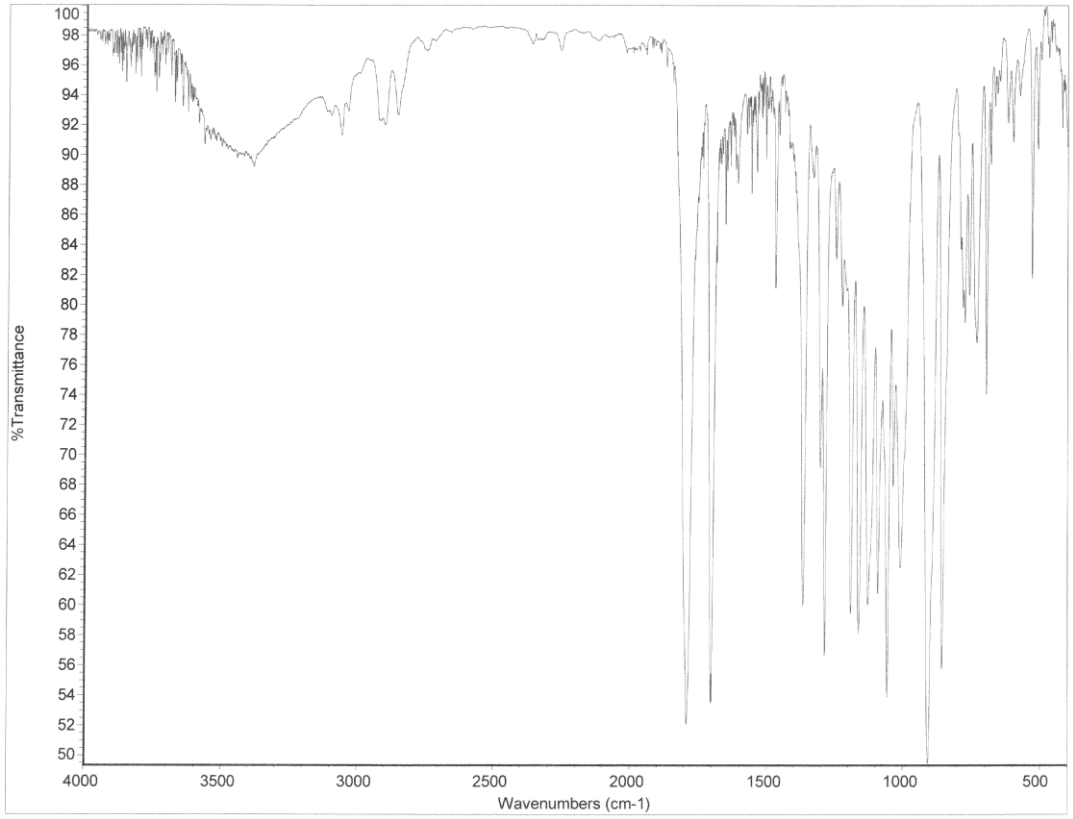
%Transmittance
100 98 96 94 92 90 88 86 84 82 80 78 76 74 72 70 68 66 64 62 60 58 56 54 52 50
4000 3500 3000 2500 2000 1500 1000 500
Wavenumbers (cm-1)

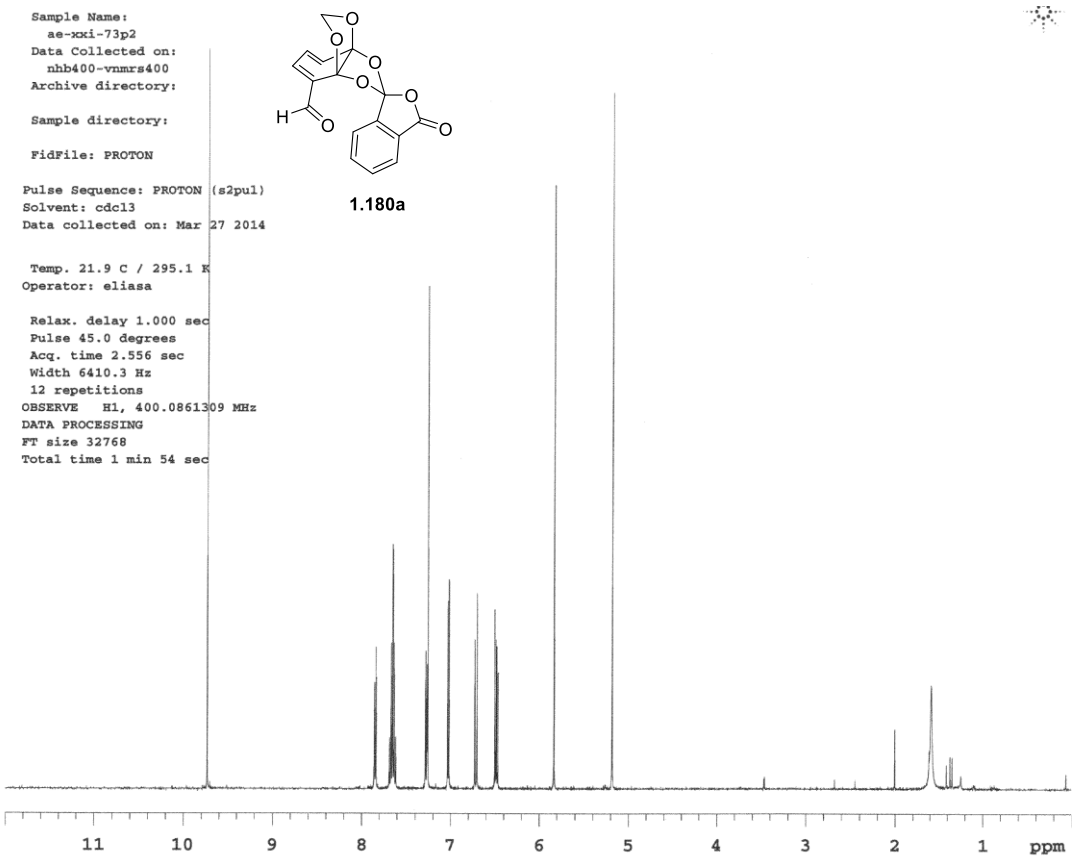
Sample Name:
ae-xxi-73p2
Data Collected on:
nhb400-vnmrs400
Archive directory:
Sample directory:
FidFile: PROTON
Pulse Sequence: PROTON (s2pul)
Solvent: cdcl3
Data collected on: Mar 27 2014
Temp. 21.9 C / 295.1 K
Operator: eliasa
Relax. delay 1.000 sec
Pulse 45.0 degrees
Acq. time 2.556 sec
Width 6410.3 Hz
12 repetitions
OBSERVE H1, 400.0861309 MHz
DATA PROCESSING
FT size 32768
Total time 1 min 54 sec
1.180a
11
10
9
8
7
6
5
4
3
2
1
ppm

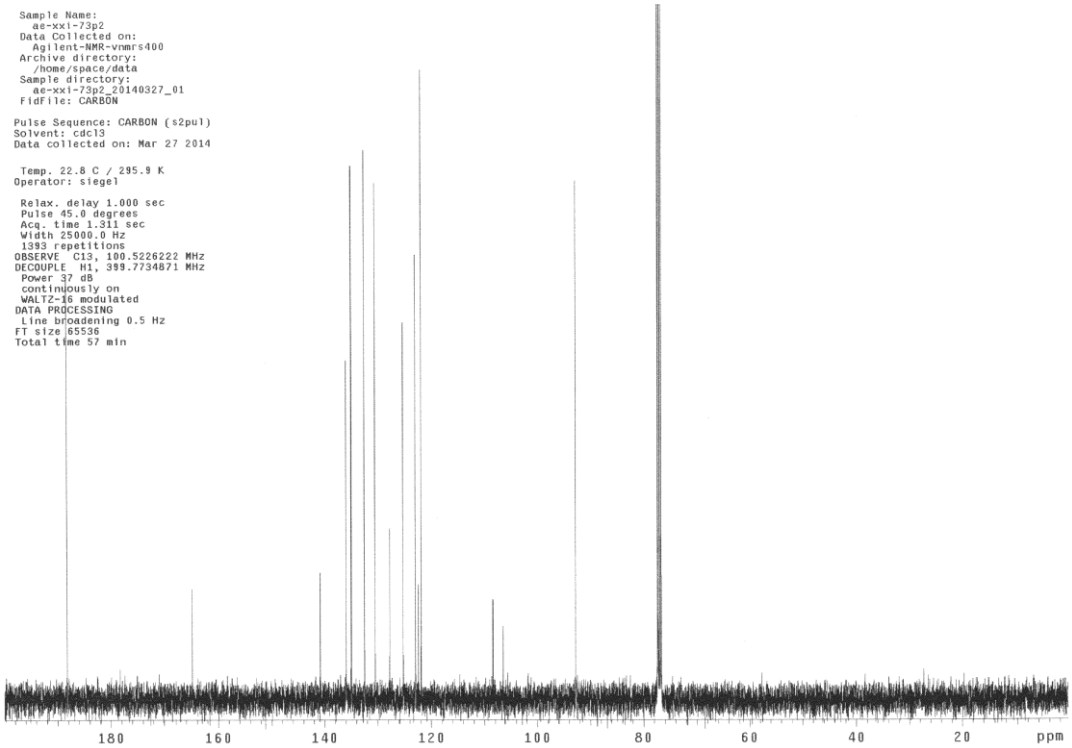
Sample Name:
ae-xxi-73p2
Data Collected on:
Agilent-NMR-vnmrs400
Archive directory:
/home/space/data
Sample directory:
ae-xxi-73p2_20140327_01
FidFile: CARBON
Pulse Sequence: CARBON (s2pul)
Solvent: cdcl3
Data collected on: Mar 27 2014
Temp. 22.8 C / 295.9 K
Operator: siegel
Relax. delay 1.000 sec
Pulse 45.0 degrees
Acq. time 1.311 sec
Width 25000.0 Hz
1393 repetitions
OBSERVE C13, 100.5226222 MHz
DECOUPLE H1, 399.7734871 MHz
Power 37 dB
continuously on
WALTZ-16 modulated
DATA PROCESSING
Line broadening 0.5 Hz
FT size 65536
Total time 57 min
180
160
140
120
100
80
60
40
20
ppm

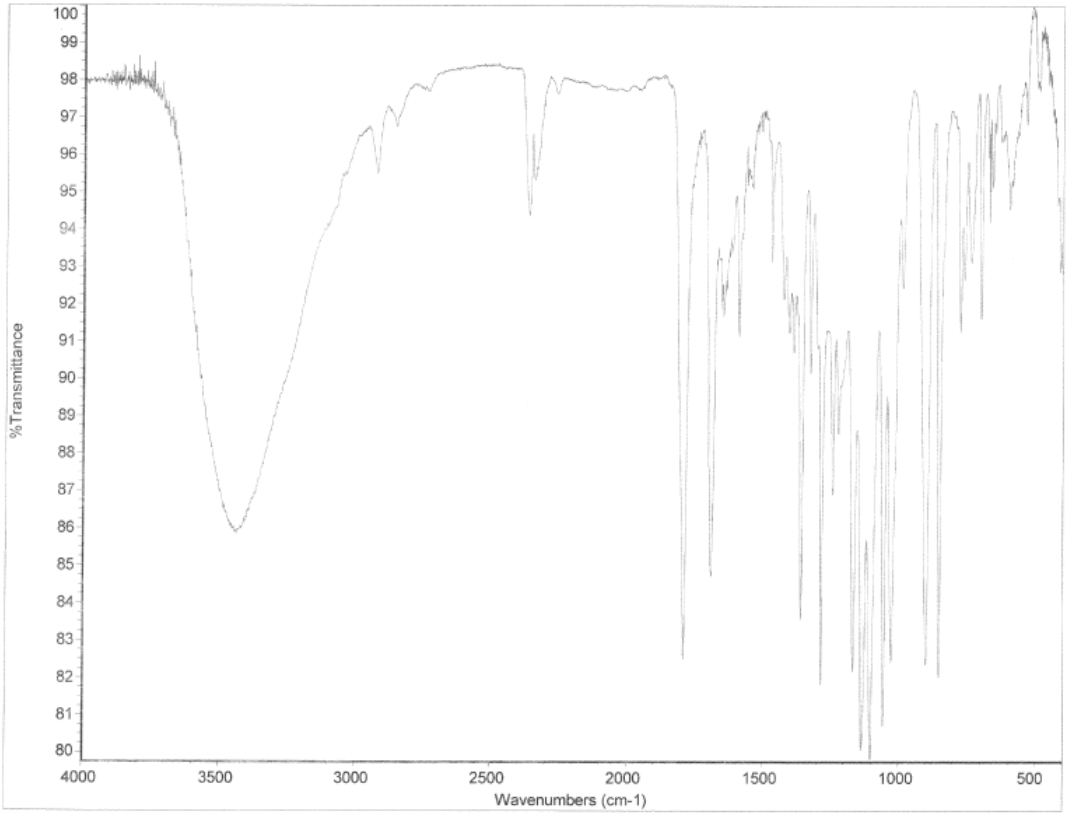
%Transmittance
100
99
98
97
96
95
94
93
92
91
90
89
88
87
86
85
84
83
82
81
80
4000
3500
3000
2500
2000
1500
1000
500
Wavenumbers (cm-1)

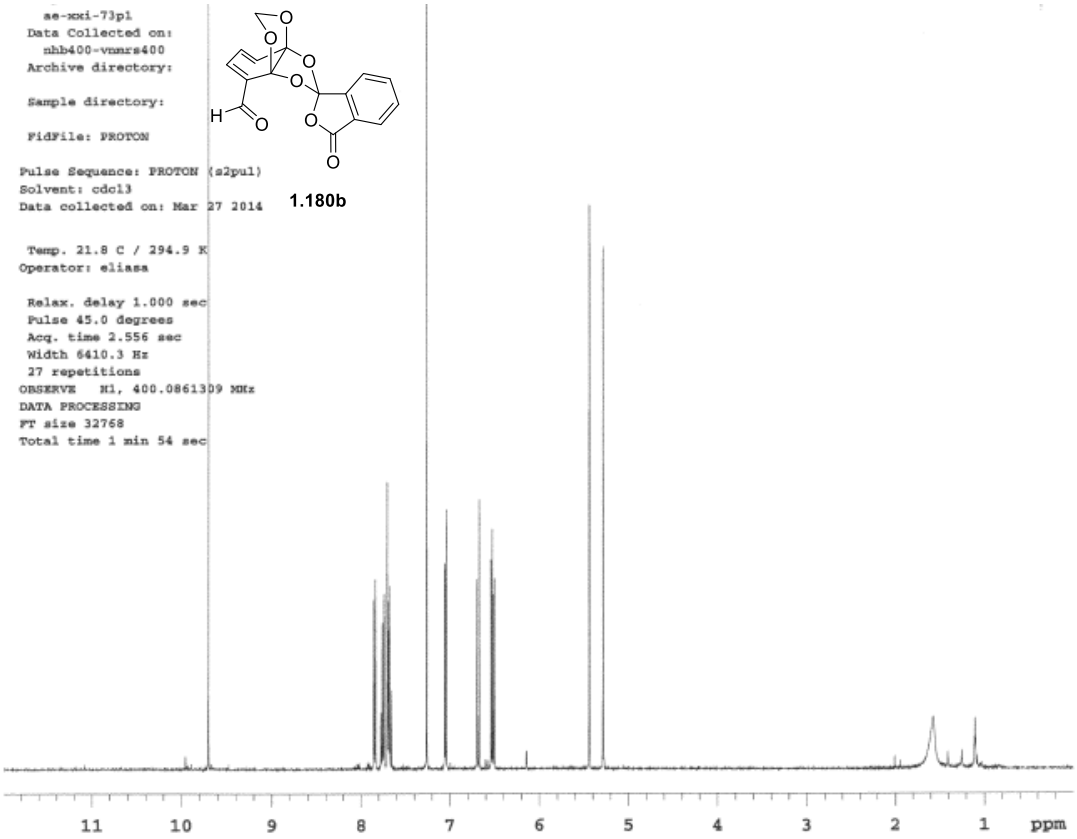
ae-xxi-73p1
Data Collected on:
nhb400-vnmrs400
Archive directory:
Sample directory:
FidFile: PROTON
Pulse Sequence: PROTON (s2pul)
Solvent: cdcl3
Data collected on: Mar 27 2014
Temp. 21.8 C / 294.9 K
Operator: eliasa
Relax. delay 1.000 sec
Pulse 45.0 degrees
Acq. time 2.556 sec
Width 6410.3 Hz
27 repetitions
OBSERVE H1, 400.0861309 MHz
DATA PROCESSING
FT size 32768
Total time 1 min 54 sec
1.180b
11
10
9
8
7
6
5
4
3
2
1
ppm

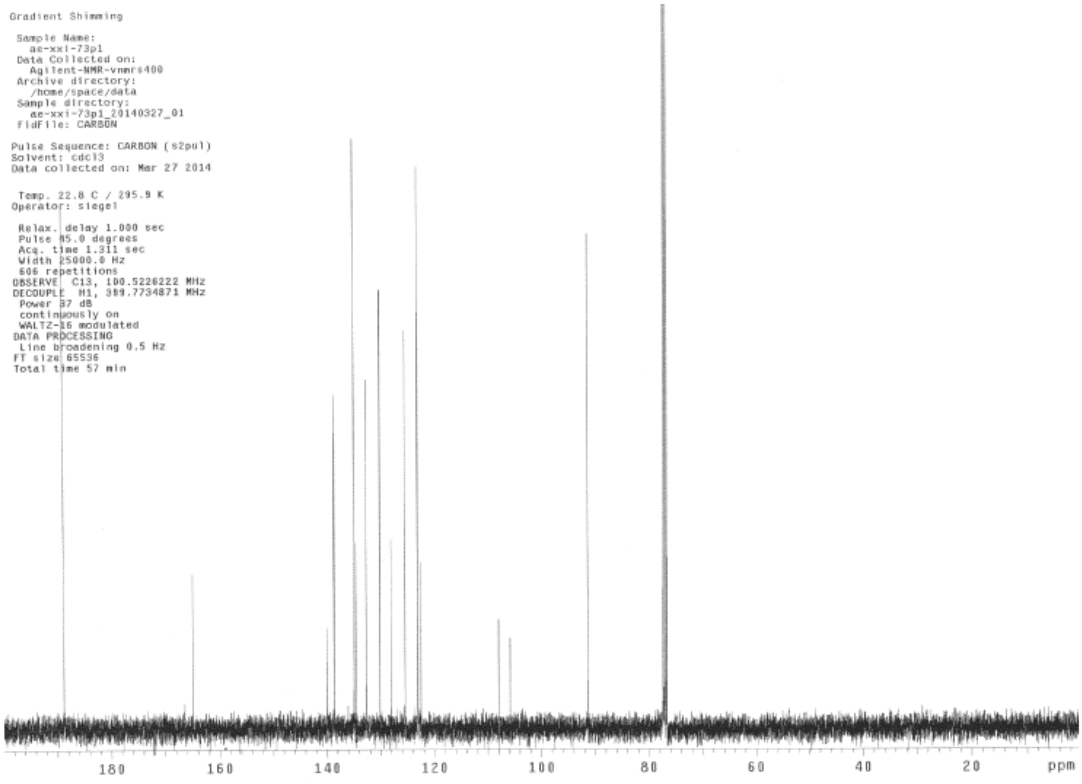
Gradient Shimming
Sample Name:
ae-xxi-73p1
Data Collected on:
Agilent-NMR-vnmrs400
Archive directory:
/home/space/data
Sample directory:
ae-xxi-73p1_20140327_01
FidFile: CARBON
Pulse Sequence: CARBON (s2pul)
Solvent: cdcl3
Data collected on: Mar 27 2014
Temp. 22.8 C / 295.9 K
Operator: siegel
Relax. delay 1.000 sec
Pulse 85.0 degrees
Acq. time 1.311 sec
Width 25000.0 Hz
606 repetitions
OBSERVE C13, 100.5226222 MHz
DECOUPLE H1, 389.7734871 MHz
Power 37 dB
continuously on
WALTZ-16 modulated
DATA PROCESSING
Line broadening 0.5 Hz
FT size 65536
Total time 57 min
180
160
140
120
100
80
60
40
20
ppm

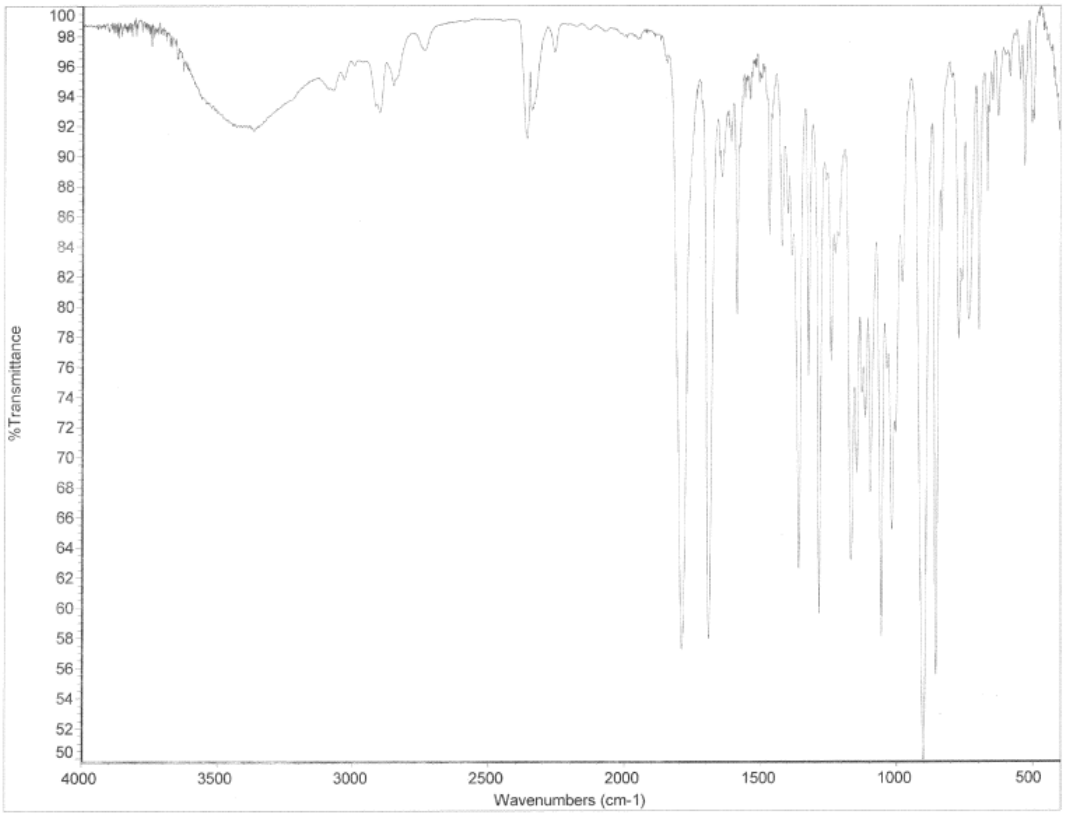
%Transmittance
100
98
96
94
92
90
88
86
84
82
80
78
76
74
72
70
68
66
64
62
60
58
56
54
52
50
4000
3500
3000
2500
2000
1500
1000
500
Wavenumbers (cm-1)

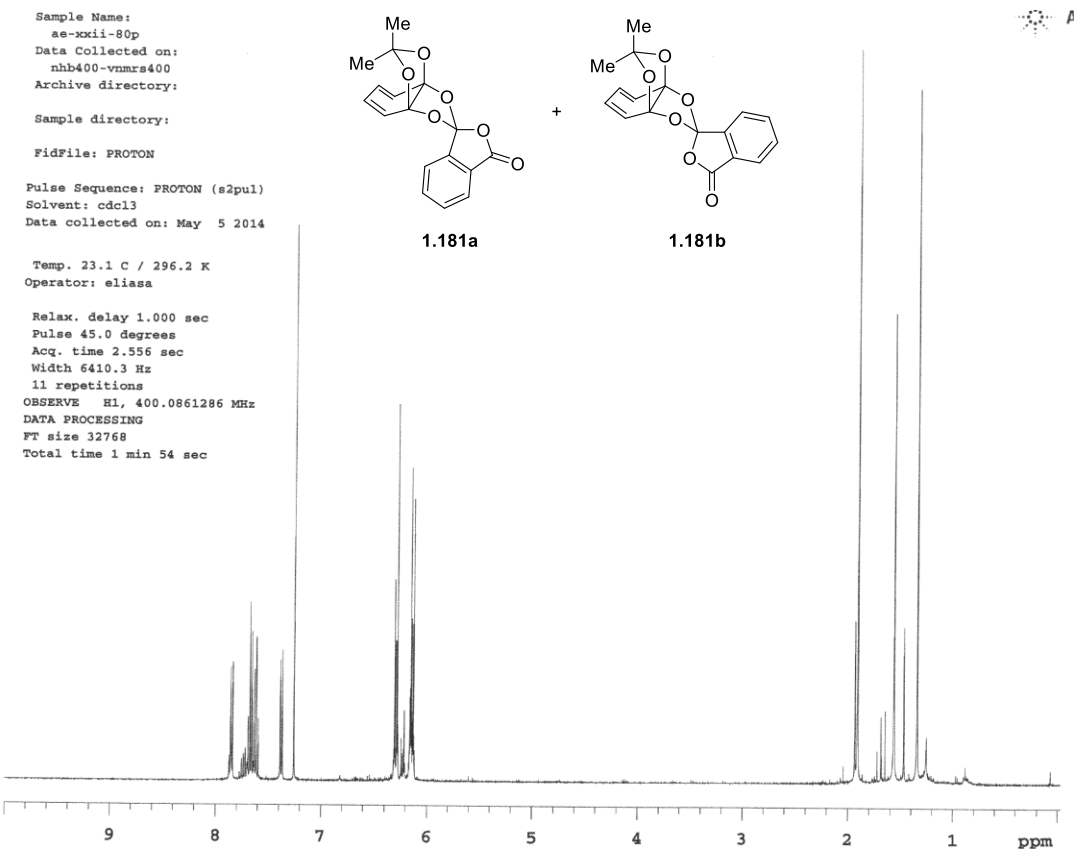
Sample Name:
ae-xxii-80p
Data Collected on:
nhb400-vnmrs400
Archive directory:
Sample directory:
FidFile: PROTON
Pulse Sequence: PROTON (s2pul)
Solvent: cdcl3
Data collected on: May 5 2014
Temp. 23.1 C / 296.2 K
Operator: eliasa
Relax. delay 1.000 sec
Pulse 45.0 degrees
Acq. time 2.556 sec
Width 6410.3 Hz
11 repetitions
OBSERVE H1, 400.0861286 MHz
DATA PROCESSING
FT size 32768
Total time 1 min 54 sec
Me
O
1.181a
+
1.181b
9
8
7
6
5
4
3
2
1
ppm

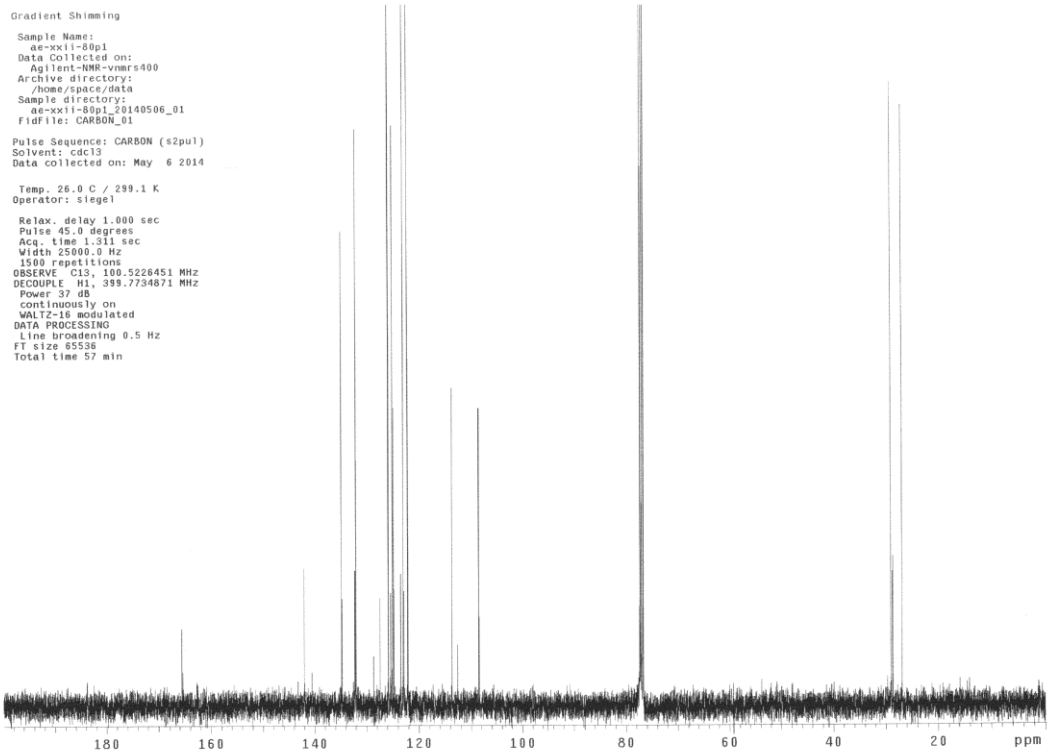
Gradient Shimming
Sample Name:
ae-xxii-80p1
Data Collected on:
Agilent-NMR-vnmrs400
Archive directory:
/home/space/data
Sample directory:
ae-xxii-80p1_20140506_01
FidFile: CARBON_01
Pulse Sequence: CARBON (s2pul)
Solvent: cdcl3
Data collected on: May 6 2014
Temp. 26.0 C / 299.1 K
Operator: siegel
Relax. delay 1.000 sec
Pulse 45.0 degrees
Acq. time 1.311 sec
Width 25000.0 Hz
1500 repetitions
OBSERVE C13, 100.5226451 MHz
DECOUPLE H1, 399.7734871 MHz
Power 37 dB
continuously on
WALTZ-16 modulated
DATA PROCESSING
Line broadening 0.5 Hz
FT size 65536
Total time 57 min
180
160
140
120
100
80
60
40
20
ppm

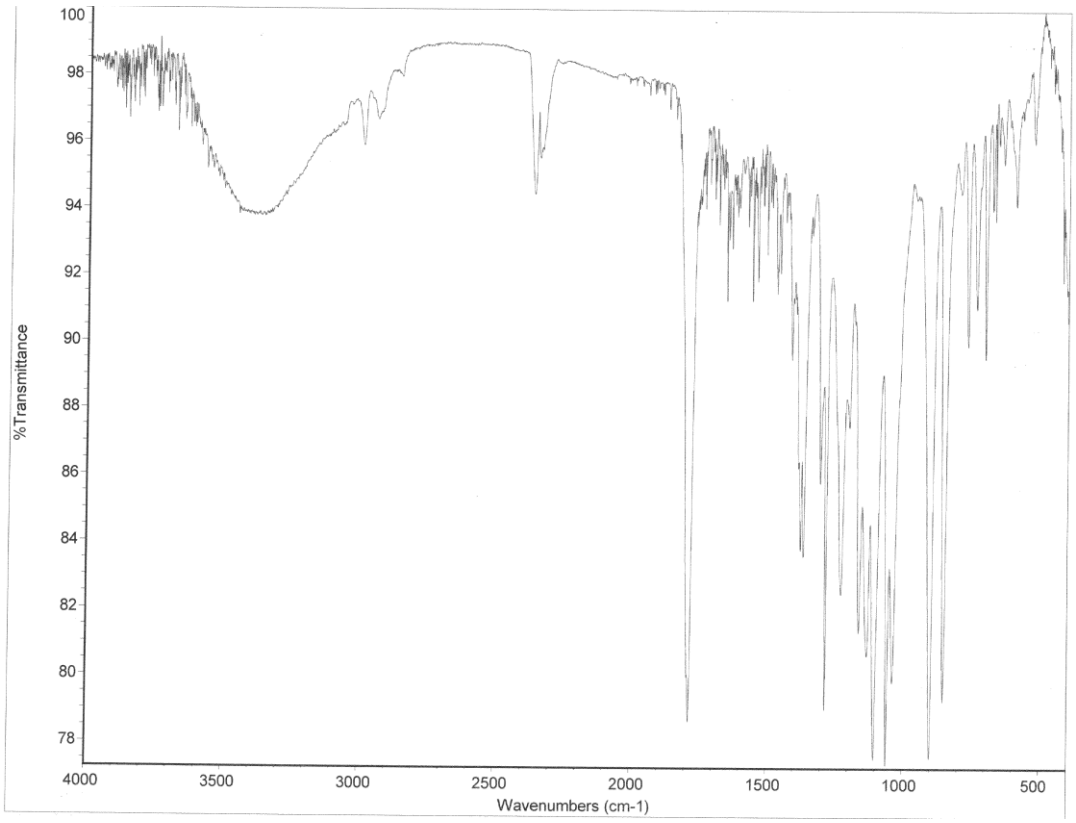
100
98
96
94
92
90
88
86
84
82
80
78
%Transmittance
4000
3500
3000
2500
2000
1500
1000
500
Wavenumbers (cm-1)

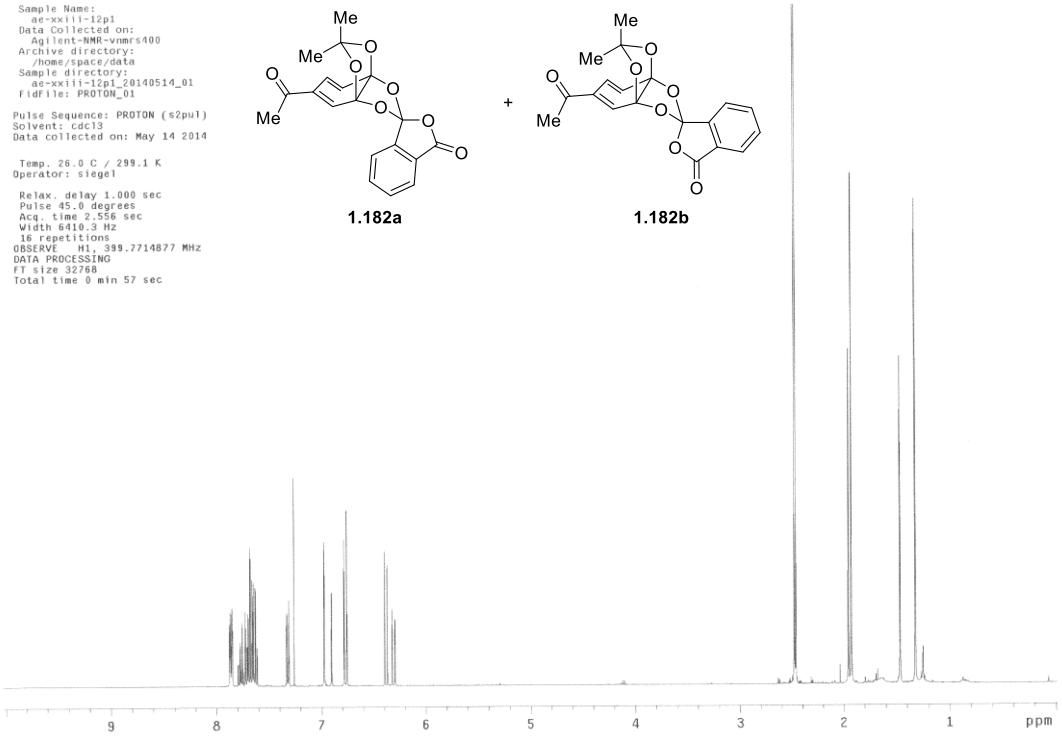
Sample Name:
ae-xxiii-12p1
Data Collected on:
Agilent-NMR-vnmrs400
Archive directory:
/home/space/data
Sample directory:
ae-xxiii-12p1_20140514_01
FidFile: PROTON_01
Pulse Sequence: PROTON (s2pul)
Solvent: cdcl3
Data collected on: May 14 2014
Temp. 26.0 C / 299.1 K
Operator: siegel
Relax. delay 1.000 sec
Pulse 45.0 degrees
Acq. time 2.556 sec
Width 6410.3 Hz
16 repetitions
OBSERVE H1, 399.7714877 MHz
DATA PROCESSING
FT size 32768
Total time 0 min 57 sec
Me
Me
O
O
O
O
O
O
Me
1.182a
+
Me
Me
O
O
O
O
O
O
Me
1.182b
9
8
7
6
5
4
3
2
1
ppm

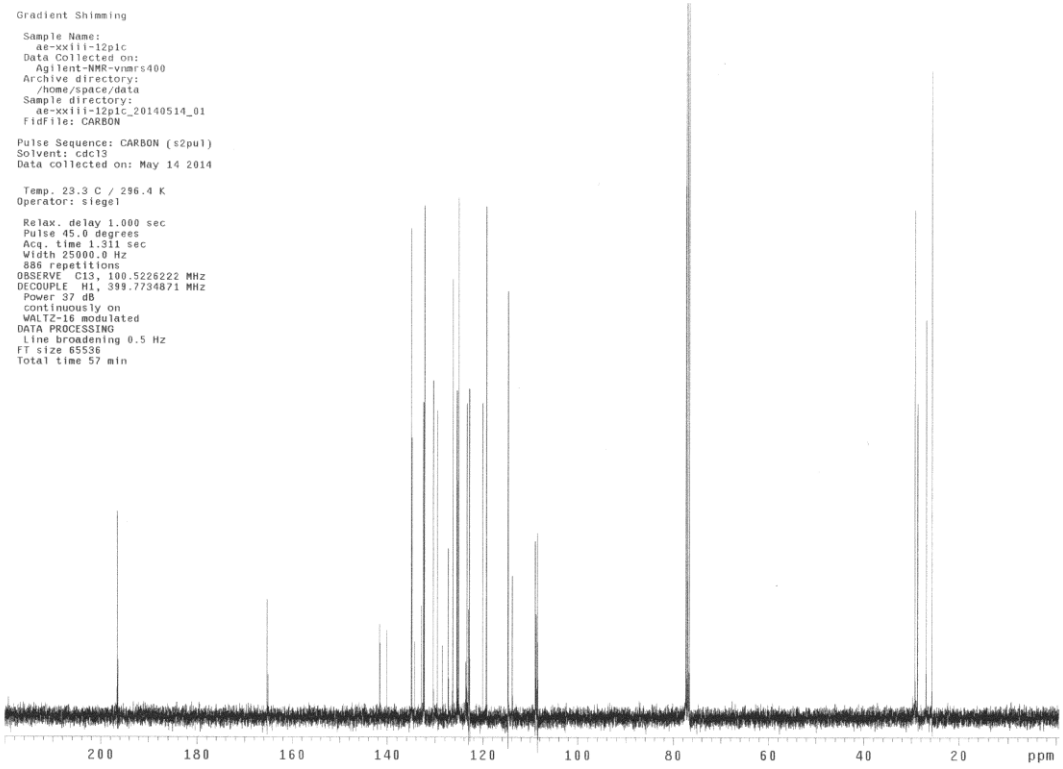
Gradient Shimming
Sample Name:
ae-xxiii-12p1c
Data Collected on:
Agilent-NMR-vnmrs400
Archive directory:
/home/space/data
Sample directory:
ae-xxiii-12p1c_20140514_01
FidFile: CARBON
Pulse Sequence: CARBON (s2pul)
Solvent: cdcl3
Data collected on: May 14 2014
Temp. 23.3 C / 296.4 K
Operator: siegel
Relax. delay 1.000 sec
Pulse 45.0 degrees
Acq. time 1.311 sec
Width 25000.0 Hz
886 repetitions
OBSERVE C13, 100.5226222 MHz
DECOUPLE H1, 399.7734871 MHz
Power 37 dB
continuously on
WALTZ-16 modulated
DATA PROCESSING
Line broadening 0.5 Hz
FT size 65536
Total time 57 min
200
180
160
140
120
100
80
60
40
20
ppm

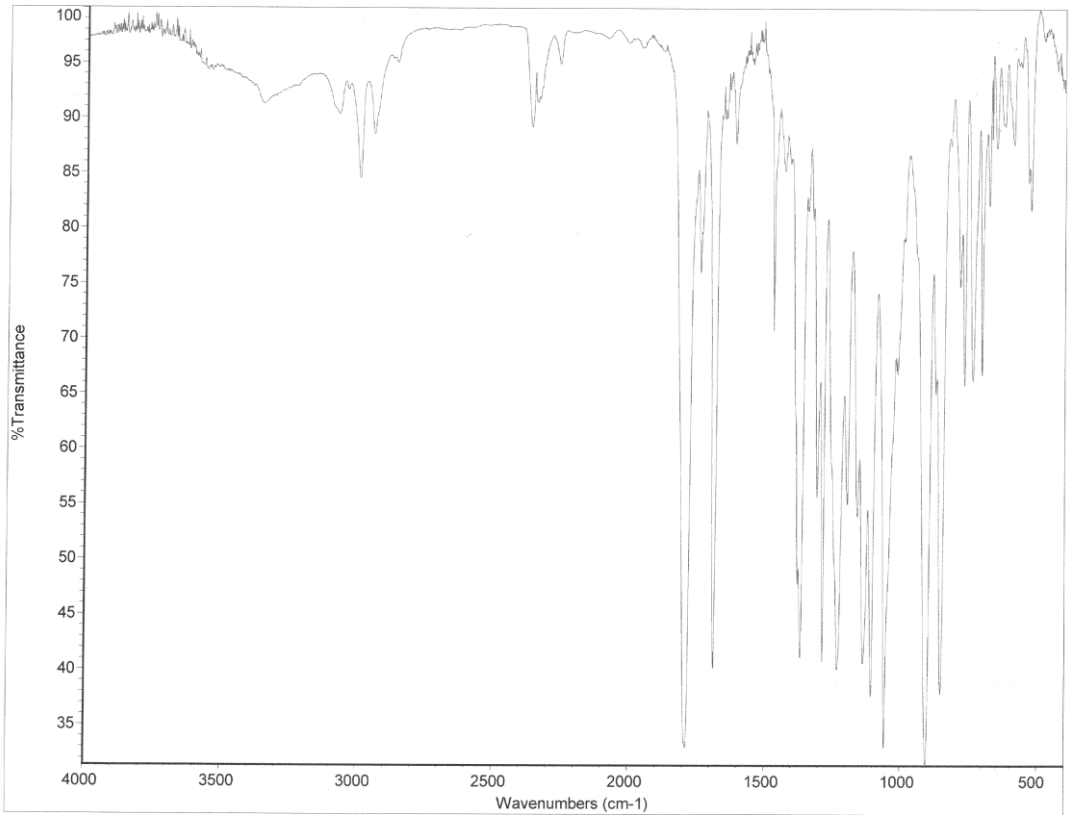
%Transmittance
100
95
90
85
80
75
70
65
60
55
50
45
40
35
4000
3500
3000
2500
2000
1500
1000
500
Wavenumbers (cm-1)

STANDARD PROTON PARAMETERS

Sample Name:
ae-xxiii-60p1
Data Collected on:
nhb400-vnmrs400
Archive directory:

Sample directory:

FidFile: PROTON

Pulse Sequence: PROTON (s2pul)
Solvent: cdcl3
Data collected on: Jun 14 2014

Temp. 22.8 C / 295.9 K
Operator: eliasa

Relax. delay 1.000 sec
Pulse 45.0 degrees
Acq. time 2.556 sec
Width 6410.3 Hz
11 repetitions
OBSERVE H1, 400.0861309 MHz
DATA PROCESSING
FT size 32768
Total time 1 min 54 sec

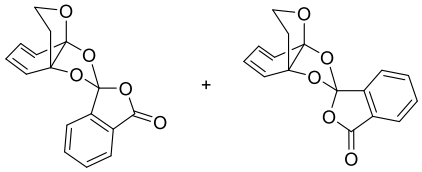

1.183a + **1.183b**

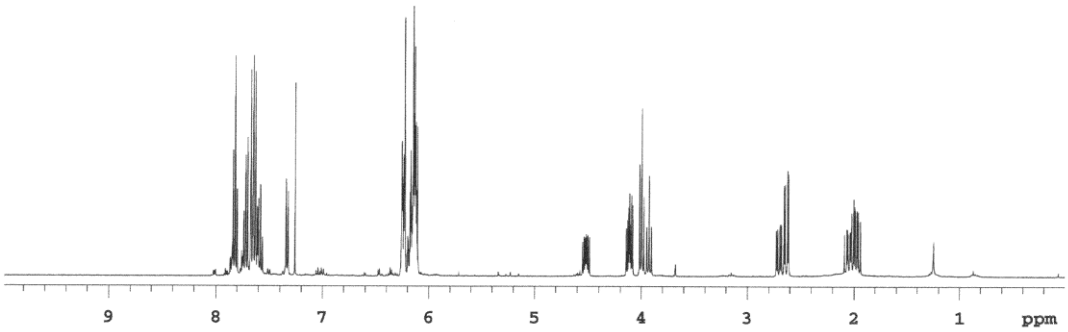

Sample Name:
ae-xxiii-60p1
Data Collected on:
we1400-vnmrs400
Archive directory:
/home/space/data
Sample directory:
ae-xxiii-60p1_20140614_01
FidFile: CARBON

Pulse Sequence: CARBON (s2pul)
Solvent: cdcl3
Data collected on: Jun 14 2014

Temp. 23.0 C / 296.1 K
Operator: siegel

Relax. delay 1.000 sec
Pulse 45.0 degrees
Acq. time 1.311 sec
Width 25000.0 Hz
579 repetitions
OBSERVE C13, 100.5226245 MHz
DECOUPLE H1, 399.7734871 MHz
Power 37 dB
continuously on
WALTZ-16 modulated
DATA PROCESSING
Line broadening 0.5 Hz
FT size 65536
Total time 57 min

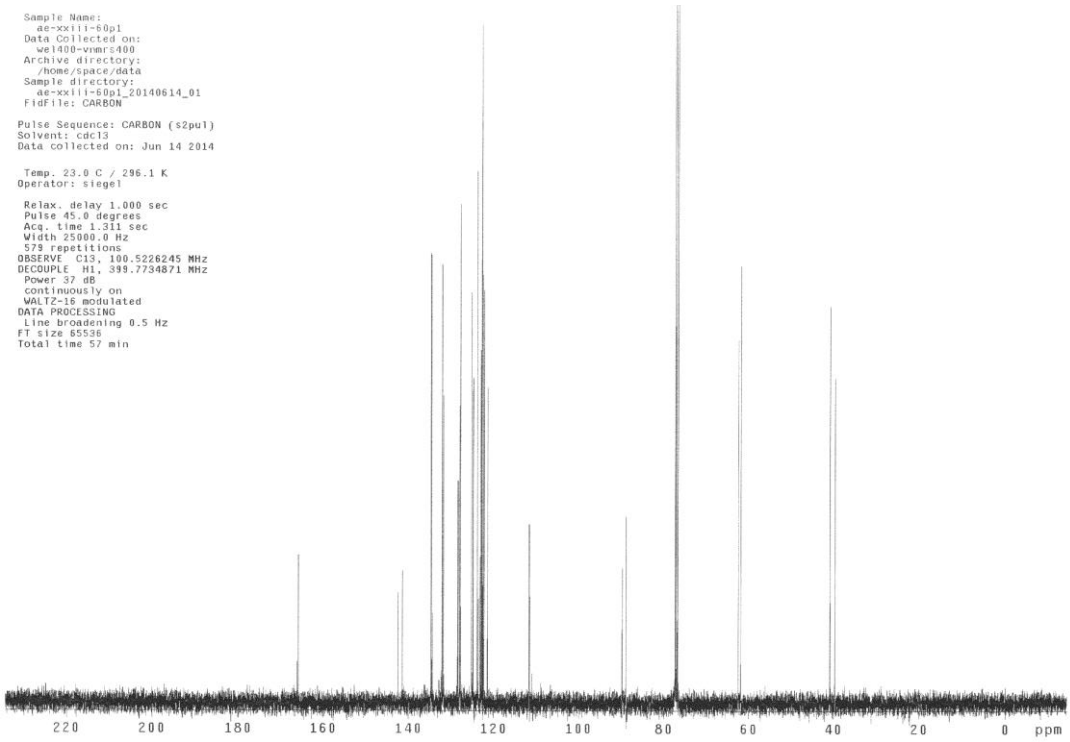

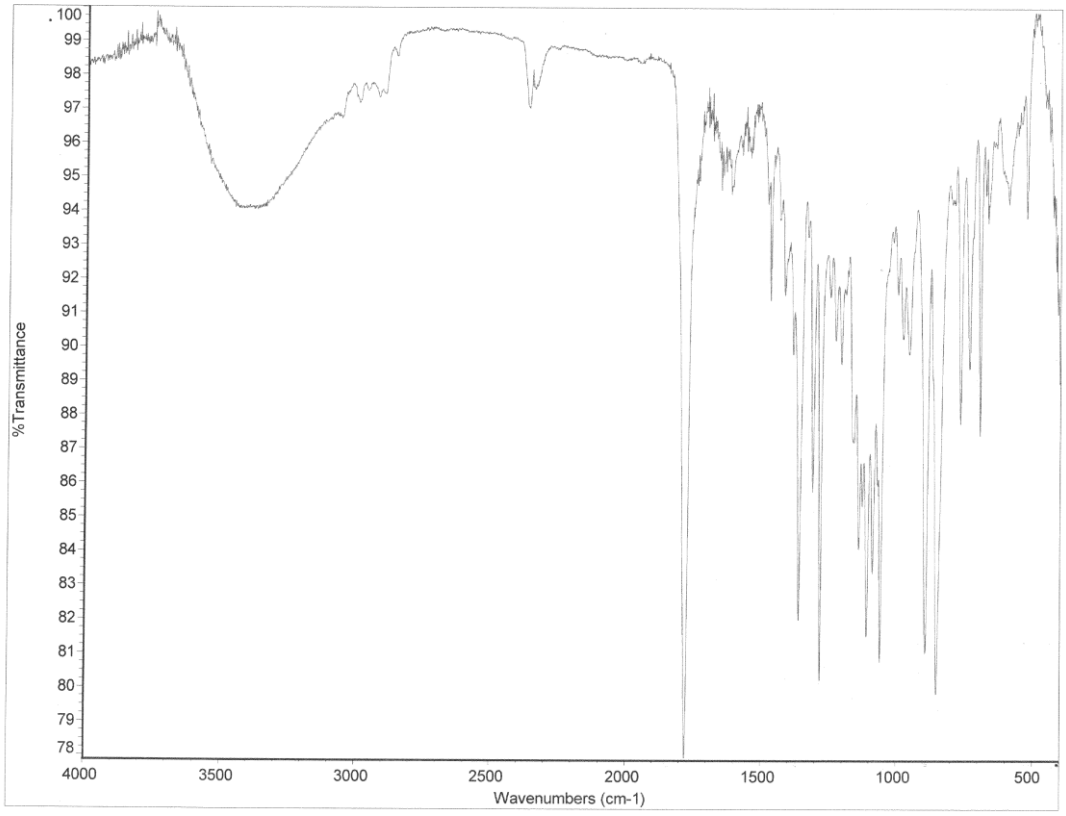
%Transmittance
100
99
98
97
96
95
94
93
92
91
90
89
88
87
86
85
84
83
82
81
80
79
78
4000
3500
3000
2500
2000
1500
1000
500
Wavenumbers (cm-1)

mple Name:
ae-xxiv-06p2
ta Collected on:
nhb400-vnmrs400
chive directory:
/home/space/data
mple directory:
ae-xxiv-06p2_20140711_01
dFile: PROTON_01

lse Sequence: PROTON (s2pul)
lvent: cdcl3
a collected on: Jul 11 2014

rator: eliasa

lax. delay 1.000 sec
lse 45.0 degrees
q. time 2.556 sec
dth 6410.3 Hz
repetitions
ERVE H1, 400.0861305 MHz
A PROCESSING
size 32768
al time 0 min 28 sec

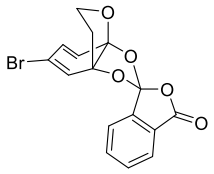

1.184a

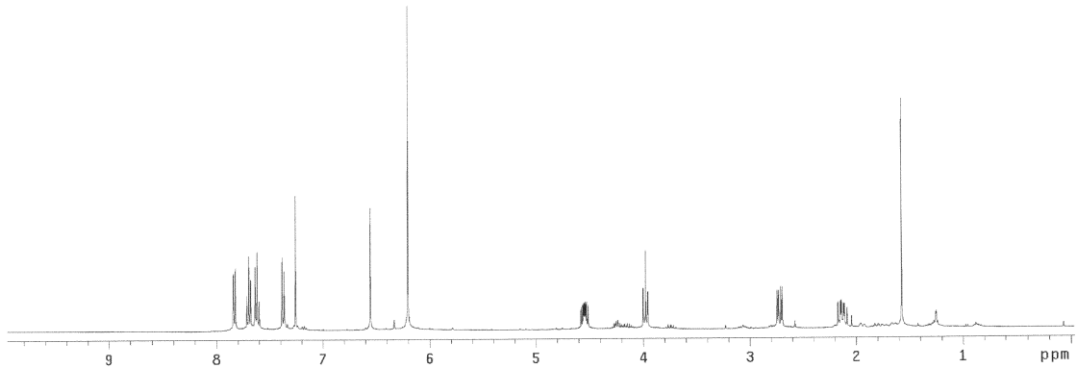

Sample Name:
ae-xxiv-06p2
Data Collected on:
nhb400-vnmrs400
Archive directory:

Sample directory:

FidFile: CARBON

Pulse Sequence: CARBON (s2pul)
Solvent: cdcl3
Data collected on: Jul 11 2014

Temp. 22.1 C / 295.2 K
Operator: eliasa

Relax. delay 1.000 sec
Pulse 45.0 degrees
Acq. time 1.311 sec
Width 25000.0 Hz
1444 repetitions
OBSERVE C13, 100.6017381 MHz
DECOUPLE H1, 400.0881319 MHz
Power 35 dB
continuously on
WALTZ-16 modulated
DATA PROCESSING
Line broadening 0.5 Hz
FT size 65536
Total time 1 hr, 17 min

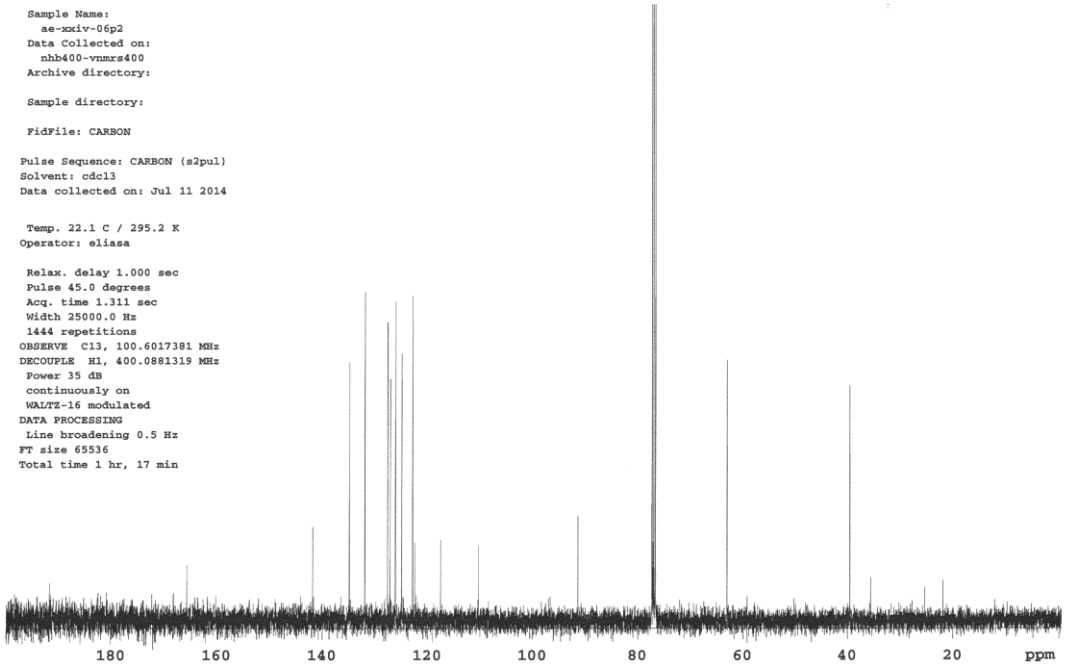

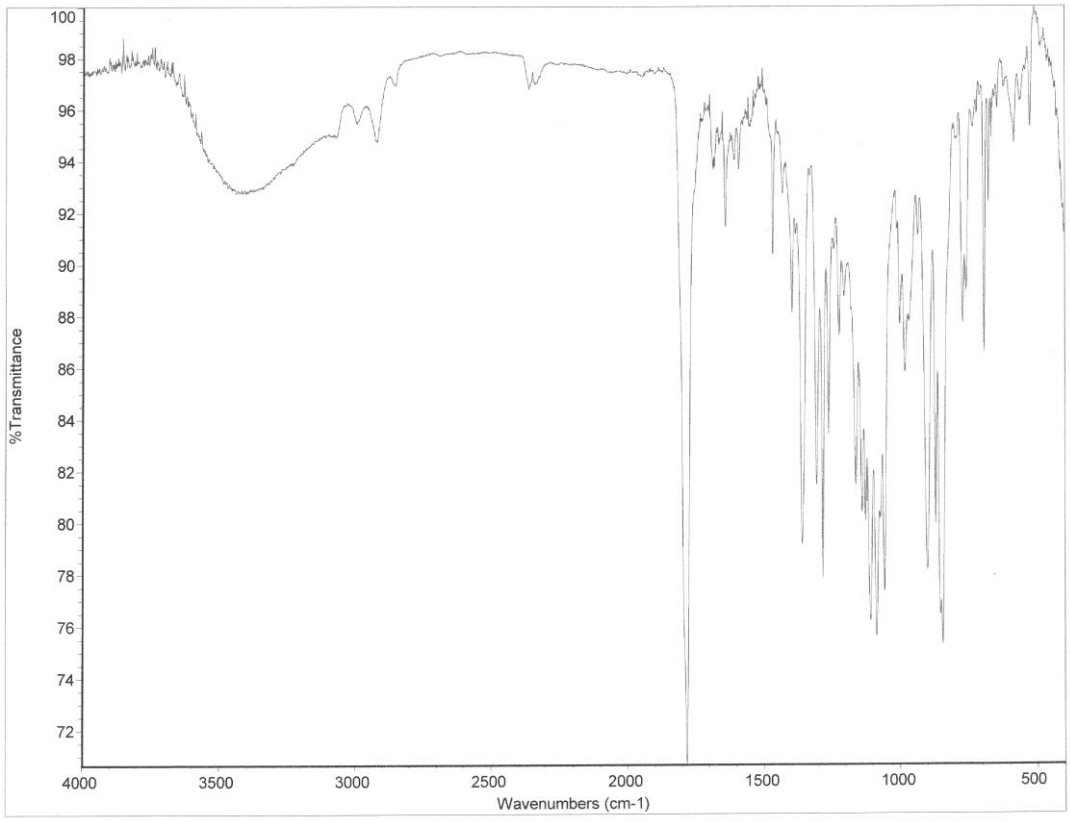
%Transmittance
100
98
96
94
92
90
88
86
84
82
80
78
76
74
72
4000
3500
3000
2500
2000
1500
1000
500
Wavenumbers (cm-1)

Sample Name:
ae-xxiv-06p1
Data Collected on:
nhb400-vnmrs400
Archive directory:

Sample directory:

FidFile: PROTON

Pulse Sequence: PROTON (s2pul)
Solvent: cdcl3
Data collected on: Jul 11 2014

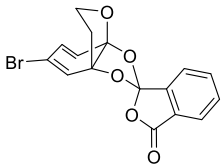

1.184b

Temp. 21.8 C / 294.9 K
Operator: eliasa

Relax. delay 1.000 sec
Pulse 45.0 degrees
Acq. time 2.556 sec
Width 6410.3 Hz
25 repetitions
OBSERVE H1, 400.0861305 MHz
DATA PROCESSING
FT size 32768
Total time 1 min 54 sec

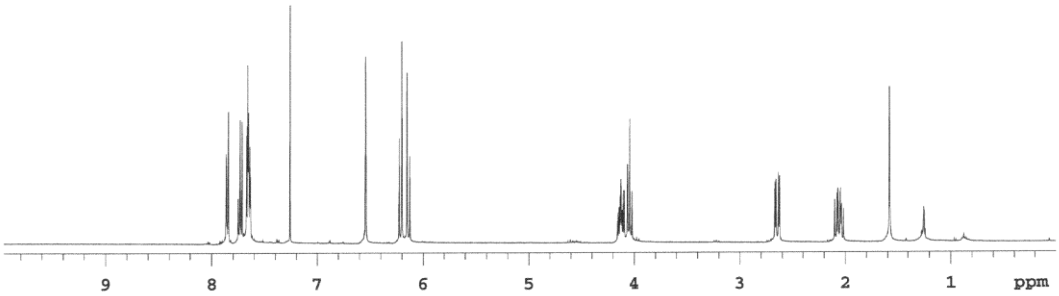

Sample Name:
ae-xxiv-06p1
Data Collected on:
wel400-vnmrs400
Archive directory:

Sample directory:

FidFile: CARBON

Pulse Sequence: CARBON (s2pul)
Solvent: cdcl3
Data collected on: Jul 11 2014

Temp. 23.2 C / 296.4 K
Operator: siegel

Relax. delay 1.000 sec
Pulse 45.0 degrees
Acq. time 1.311 sec
Width 25000.0 Hz
1308 repetitions
OBSERVE C13, 100.5226215 MHz
DECOUPLE H1, 399.7734871 MHz
Power 37 dB
continuously on
WALTZ-16 modulated
DATA PROCESSING
Line broadening 0.5 Hz
FT size 65536
Total time 57 min

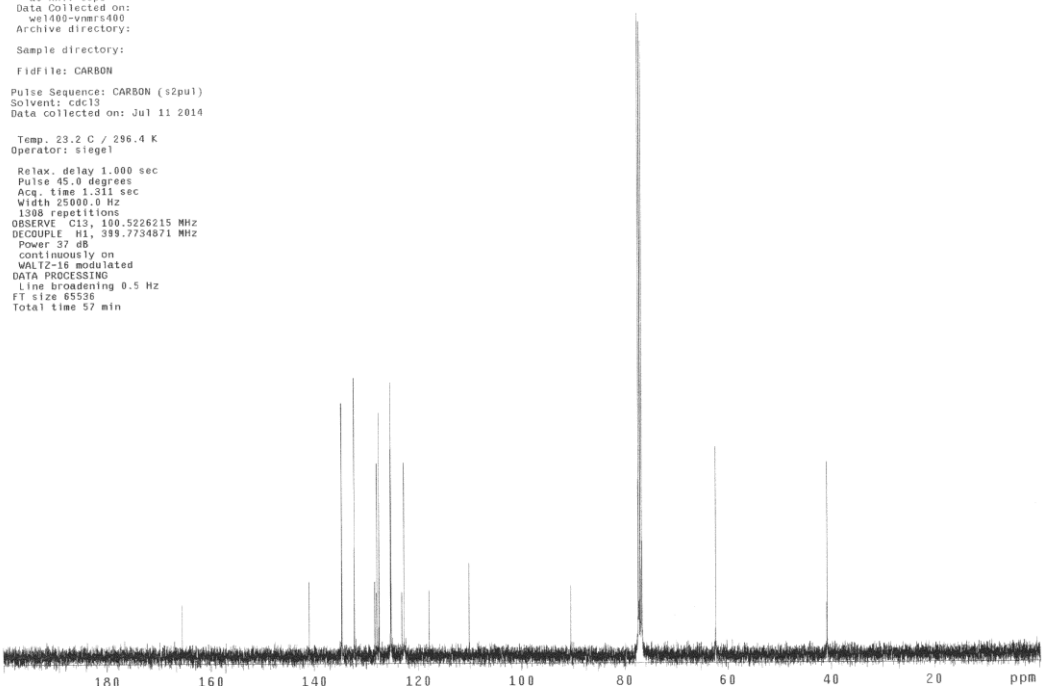

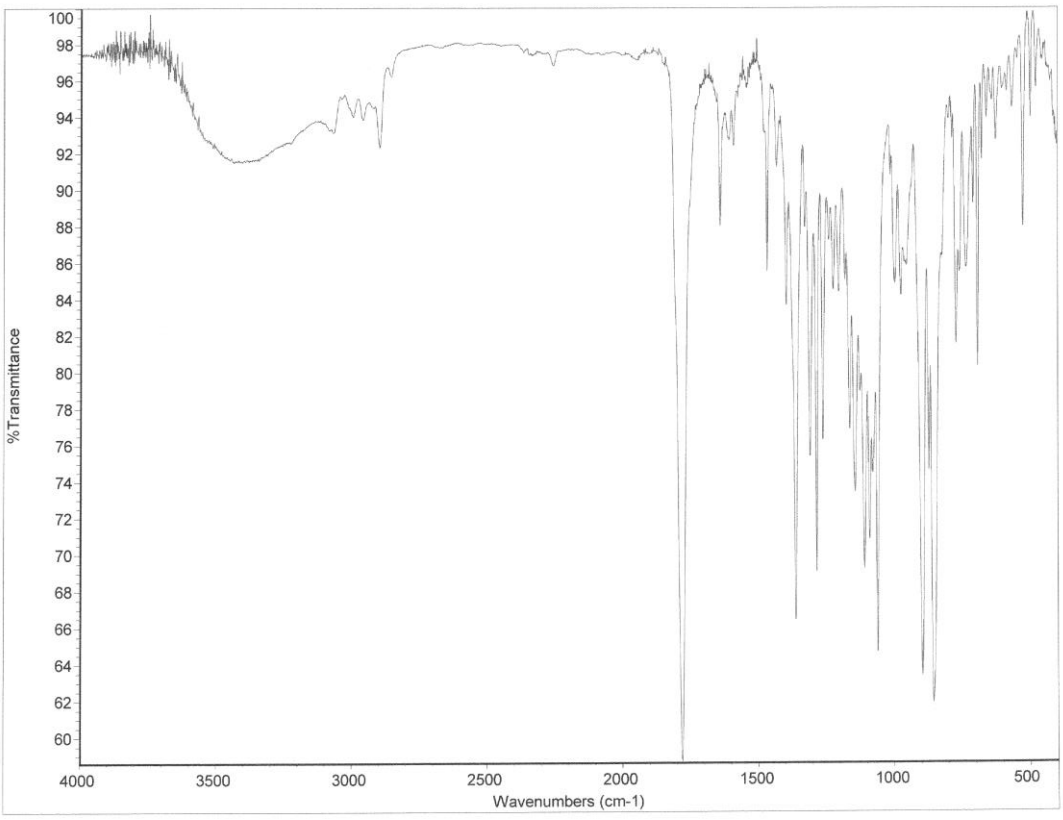
100
98
96
94
92
90
88
86
84
82
80
78
76
74
72
70
68
66
64
62
60
%Transmittance
4000
3500
3000
2500
2000
1500
1000
500
Wavenumbers (cm-1)

ae_ix_17c

Pulse Sequence: s2pul
Solvent: CDCl3
Ambient temperature
Mercury-400BB "nmr8"

Relax. delay 2.000 sec
Pulse 16.4 degrees
Acq. time 2.856 sec
Width 5602.2 Hz
16 repetitions
OBSERVE H1, 400.2668779 MHz
DATA PROCESSING
Line broadening 0.1 Hz
FT size 32768
Total time 1 min, 52 sec

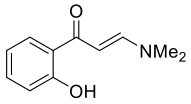

2.39

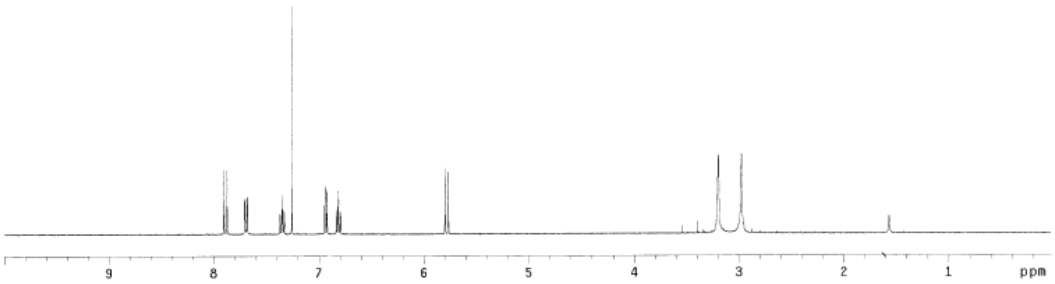

ae-ix-17c

Archive directory: /home/staff31/vnmrsys/data
Sample directory: ae_ix_17c_20120211_01

Pulse Sequence: s2pul
Solvent: cdcl3
Temp. 25.0 C / 298.1 K
User: 1-14-87
File: CARBON_01
INOVA-500 "nmrfred"

Relax. delay 2.000 sec
Pulse 30.0 degrees
Acq. time 1.285 sec
Width 25510.2 Hz
512 repetitions
OBSERVE C13, 100.4987162 MHz
DECOUPLE H1, 399.6783771 MHz
Power 39 dB
continuously on
WALTZ-16 modulated
DATA PROCESSING
Line broadening 0.5 Hz
FT size 65536
Total time 28 min, 6 sec

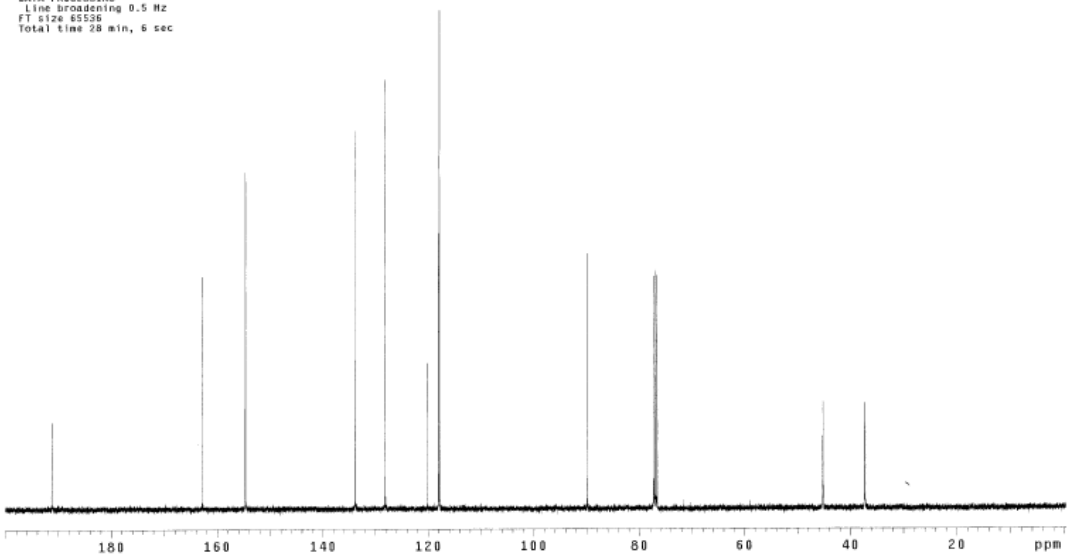

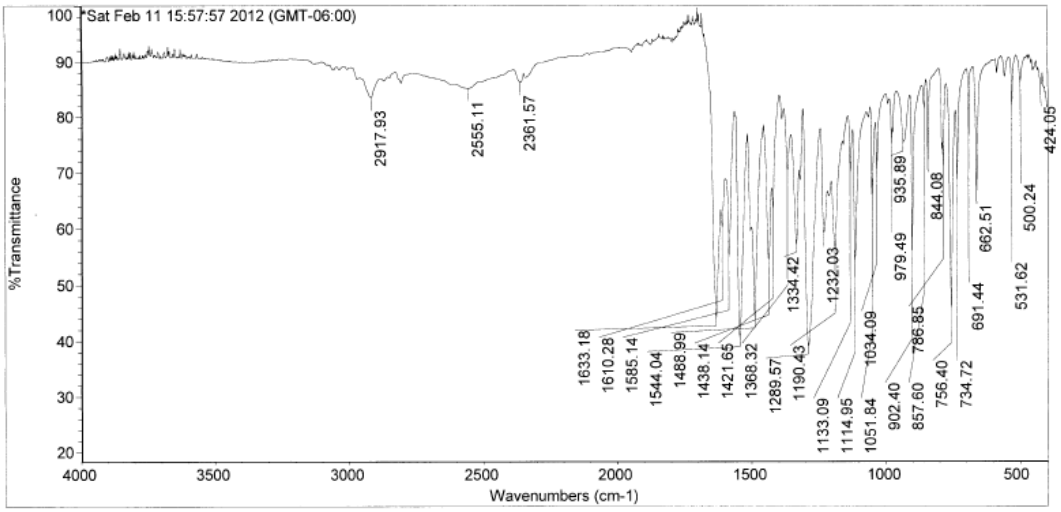

Sat Feb 11 16:04:04 2012 (GMT-06:00)
FIND PEAKS:

Spectrum:	*Sat Feb 11 15:57:57 2012 (GMT-06:00)			
Region:	4000.00	400.00		
Absolute threshold:	86.909			
Sensitivity:	50			
Peak list:				
	Position:	424.05	Intensity:	85.670
	Position:	500.24	Intensity:	86.463
	Position:	531.62	Intensity:	81.840
	Position:	662.51	Intensity:	66.688
	Position:	691.44	Intensity:	75.916
	Position:	734.72	Intensity:	68.433
	Position:	756.40	Intensity:	45.616
	Position:	786.85	Intensity:	71.327

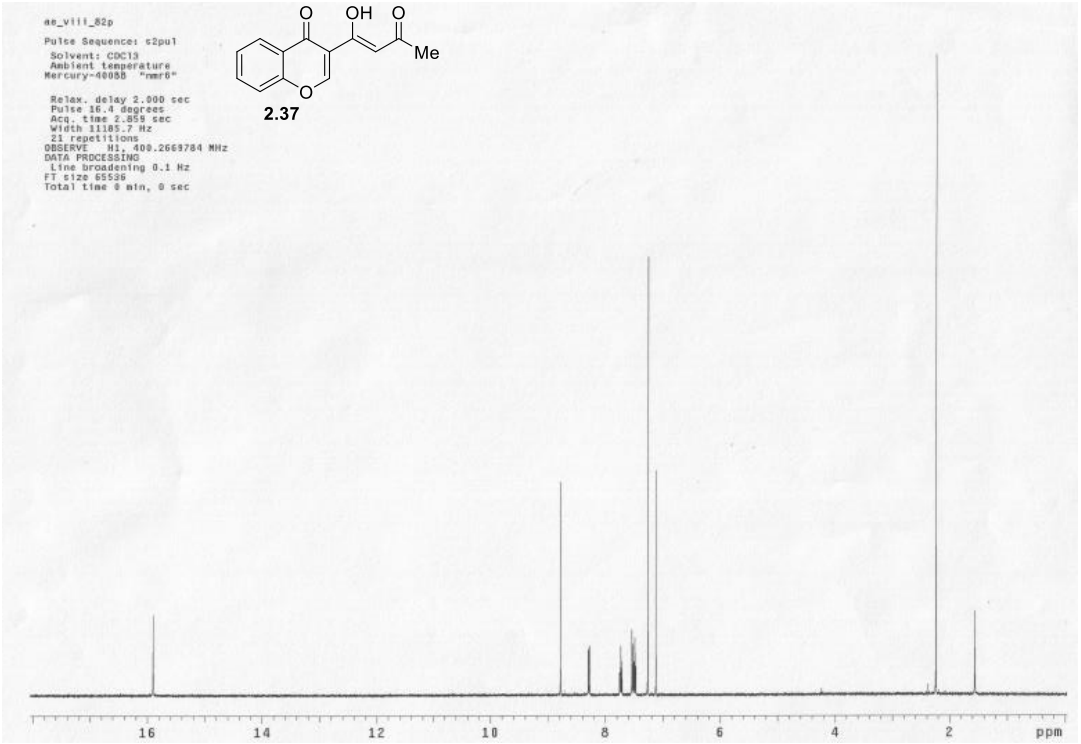
ae_viii_82p
Pulse Sequence: s2pul
Solvent: CDCl3
Ambient temperature
Mercury-400BB "nmr6"
Relax. delay 2.000 sec
Pulse 16.4 degrees
Acq. time 2.859 sec
Width 11185.7 Hz
21 repetitions
OBSERVE H1, 400.2669784 MHz
DATA PROCESSING
Line broadening 0.1 Hz
FT size 65536
Total time 0 min, 0 sec
O
OH
O
Me
O
2.37
16
14
12
10
8
6
4
2
ppm

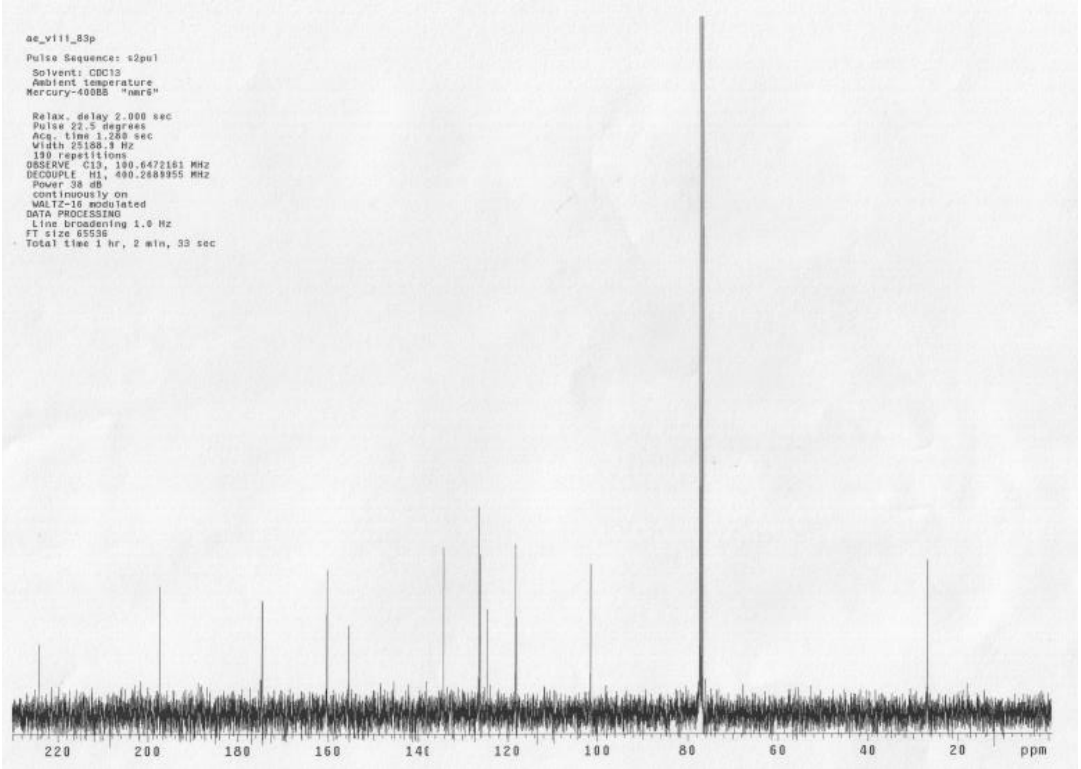
ae_viii_83p
Pulse Sequence: s2pul
Solvent: CDCl3
Ambient temperature
Mercury-400BB "nmr6"
Relax. delay 2.000 sec
Pulse 22.5 degrees
Acq. time 1.280 sec
Width 25188.9 Hz
190 repetitions
OBSERVE C13, 100.6472161 MHz
DECOUPLE H1, 400.2669955 MHz
Power 38 dB
continuously on
WALTZ-16 modulated
DATA PROCESSING
Line broadening 1.0 Hz
FT size 65536
Total time 1 hr, 2 min, 33 sec
220
200
180
160
140
120
100
80
60
40
20
ppm

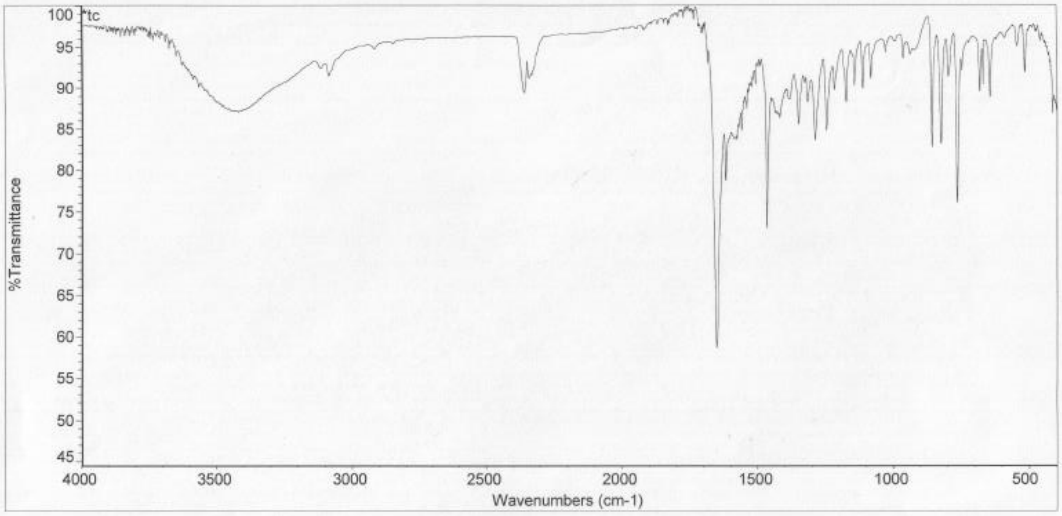

Mon Jan 16 09:00:34 2012 (GMT-06:00)
FIND PEAKS:

Spectrum:	*tc	
Region:	4000.00	400.00
Absolute threshold:	49.038	
Sensitivity:	50	
Peak list:		

No peaks were found.

ae_ix_18p2

Pulse Sequence: s2pul
Solvent: CDCl3
Ambient temperature
Mercury-400BB "nmr6"

Relax. delay 2.000 sec
Pulse 16.4 degrees
Acq. time 2.856 sec
Width 5602.2 Hz
4 repetitions
OBSERVE H1, 400.2669783 MHz
DATA PROCESSING
Line broadening 0.1 Hz
FT size 32768
Total time 0 min, 0 sec

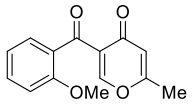

2.54

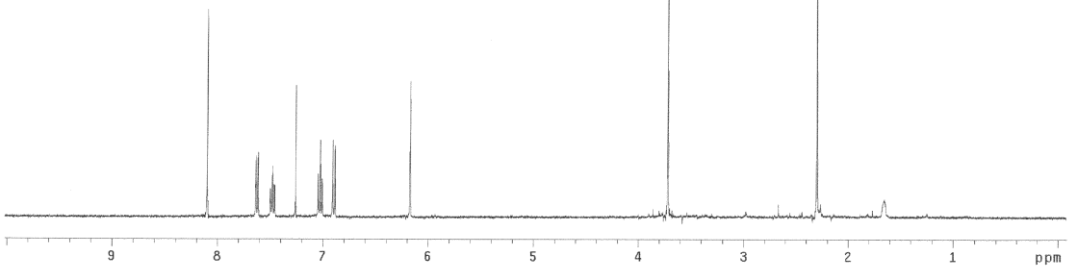

ae_ix_18p2

Archive directory: /home/staff31/vnmrsys/data
Sample directory: ae_ix_18p2_20120215_01

Pulse Sequence: s2pul
Solvent: cdcl3
Temp. 25.0 C / 298.1 K
User: 1-14-87
File: CARBON_01
INOVA-500 "nmrfred"

Relax. delay 2.000 sec
Pulse 30.0 degrees
Acq. time 1.285 sec
Width 25510.2 Hz
512 repetitions
OBSERVE C13, 100.4987077 MHz
DECOUPLE H1, 399.6783771 MHz
Power 39 dB
continuously on
WALTZ-16 modulated
DATA PROCESSING
Line broadening 0.5 Hz
FT size 65536
Total time 28 min, 6 sec

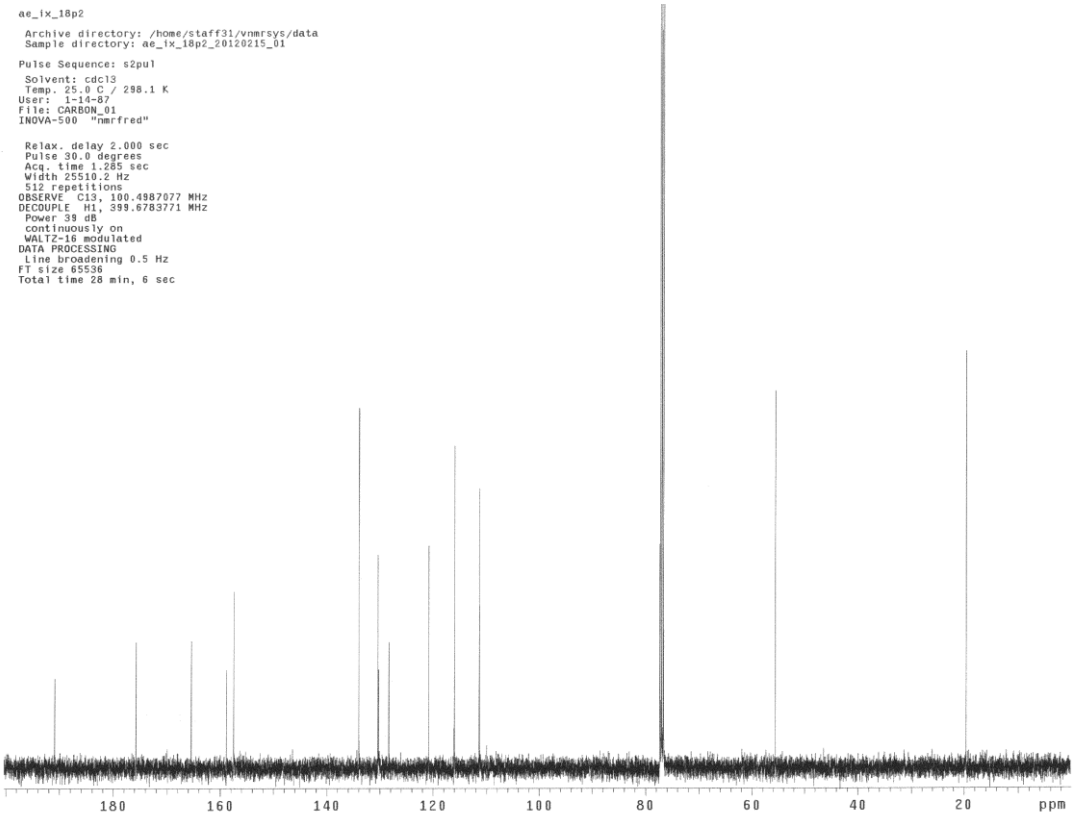

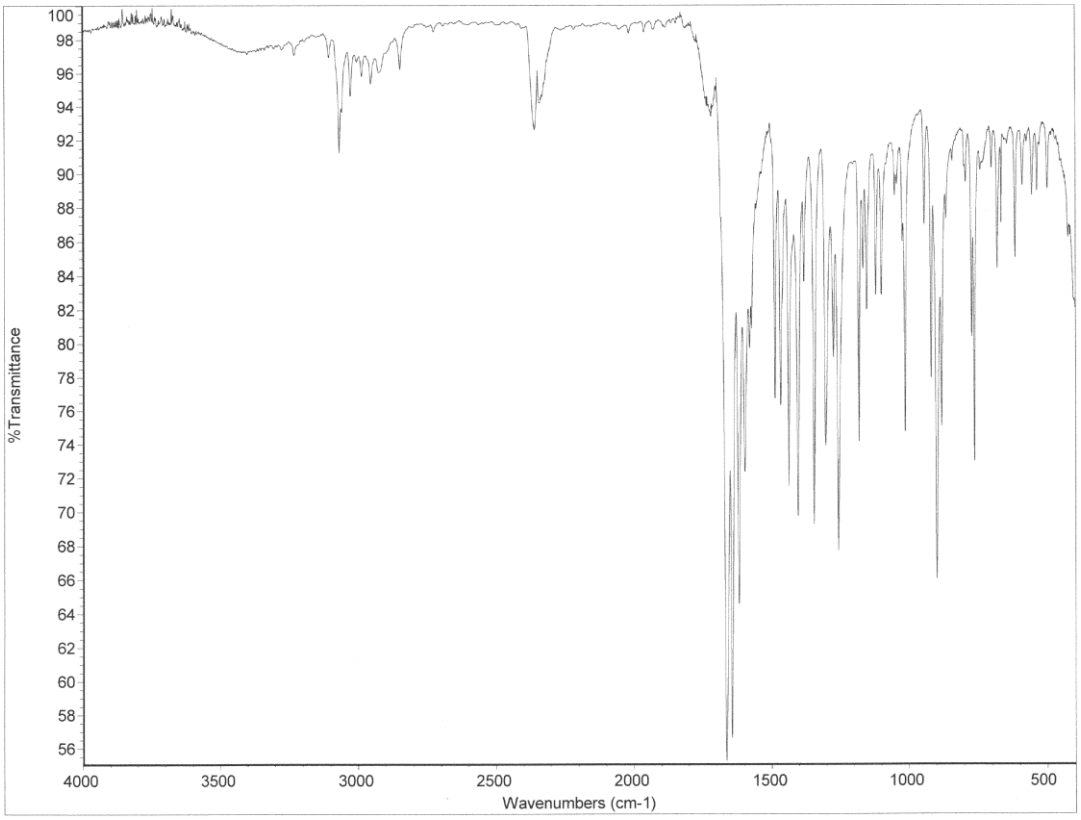
%Transmittance
100
98
96
94
92
90
88
86
84
82
80
78
76
74
72
70
68
66
64
62
60
58
56
4000
3500
3000
2500
2000
1500
1000
500
Wavenumbers (cm-1)

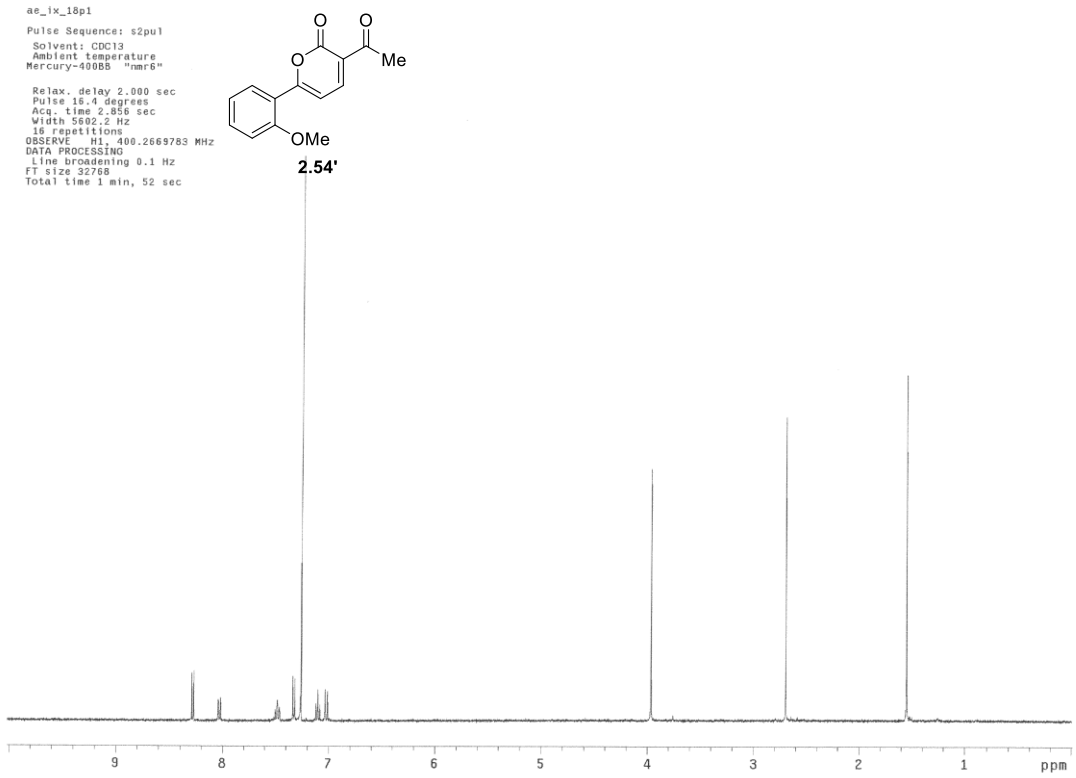
ae_ix_18p1
Pulse Sequence: s2pul
Solvent: CDCl3
Ambient temperature
Mercury-400BB "nmr6"
Relax. delay 2.000 sec
Pulse 16.4 degrees
Acq. time 2.856 sec
Width 5602.2 Hz
16 repetitions
OBSERVE H1, 400.2669783 MHz
DATA PROCESSING
Line broadening 0.1 Hz
FT size 32768
Total time 1 min, 52 sec
O
O
O
Me
OMe
2.54'
9
8
7
6
5
4
3
2
1
ppm

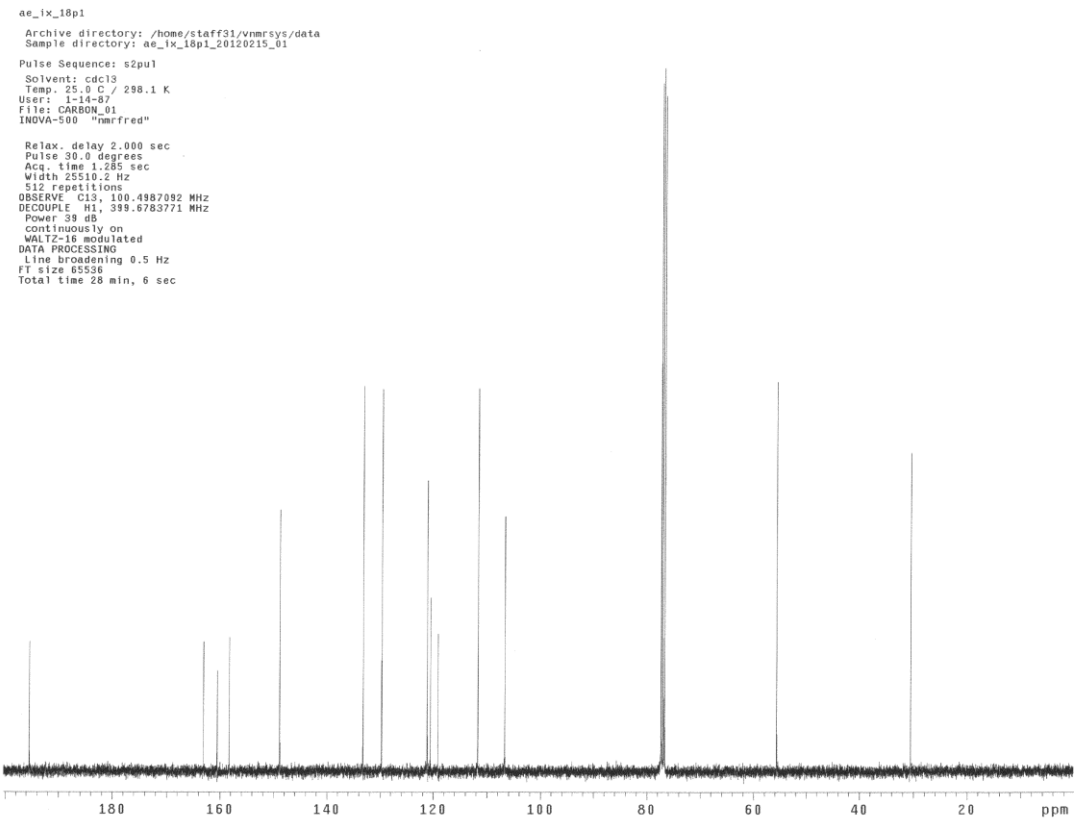
ae_ix_18p1
Archive directory: /home/staff31/vnmrsys/data
Sample directory: ae_ix_18p1_20120215_01
Pulse Sequence: s2pul
Solvent: cdcl3
Temp. 25.0 C / 298.1 K
User: 1-14-87
File: CARBON_01
INOVA-500 "nmrfred"
Relax. delay 2.000 sec
Pulse 30.0 degrees
Acq. time 1.285 sec
Width 25510.2 Hz
512 repetitions
OBSERVE C13, 100.4987092 MHz
DECOUPLE H1, 399.6783771 MHz
Power 39 dB
continuously on
WALTZ-16 modulated
DATA PROCESSING
Line broadening 0.5 Hz
FT size 65536
Total time 28 min, 6 sec
180
160
140
120
100
80
60
40
20
ppm

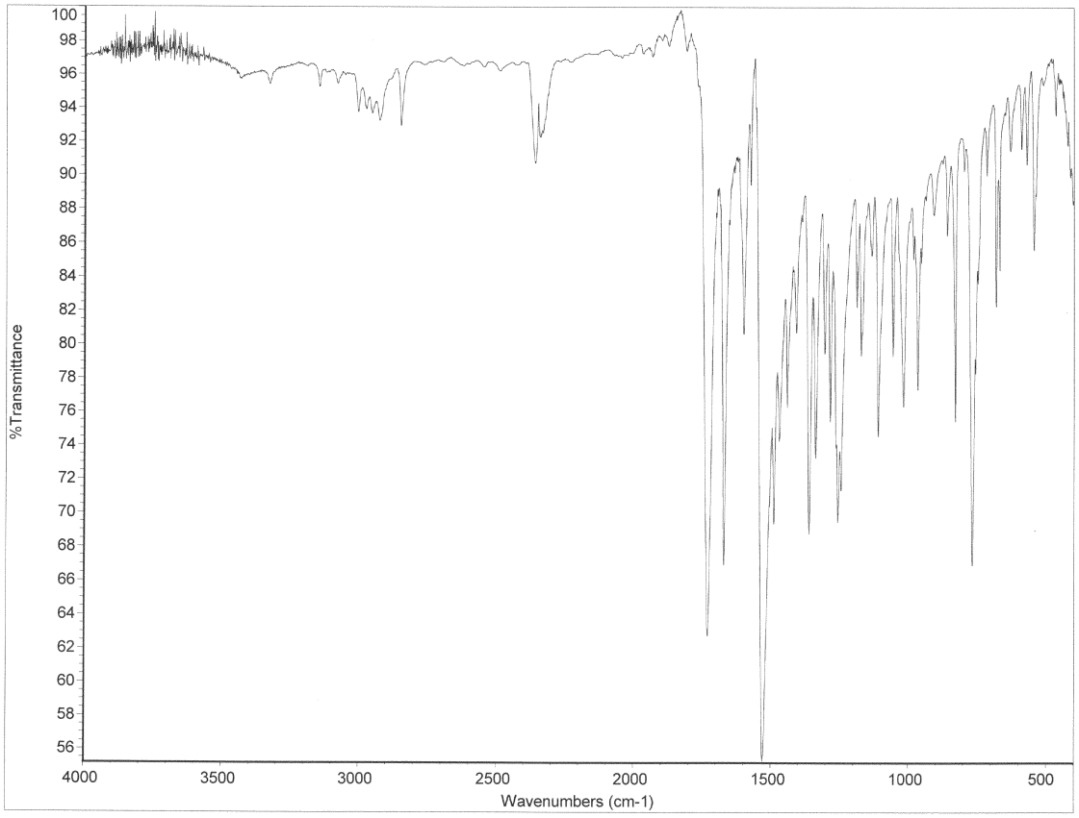
%Transmittance
100
98
96
94
92
90
88
86
84
82
80
78
76
74
72
70
68
66
64
62
60
58
56
4000
3500
3000
2500
2000
1500
1000
500
Wavenumbers (cm-1)

ae_ix_04p

Pulse Sequence: s2pul

Solvent: CDCl3
Ambient temperature
Mercury-400BB "nmr6"

Relax. delay 2.000 sec
Pulse 16.4 degrees
Acq. time 2.859 sec
Width 11185.7 Hz
15 repetitions
OBSERVE H1, 400.2669783 MHz
DATA PROCESSING
Line broadening 0.1 Hz
FT size 65536
Total time 0 min, 0 sec

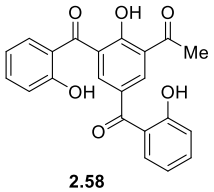

2.58

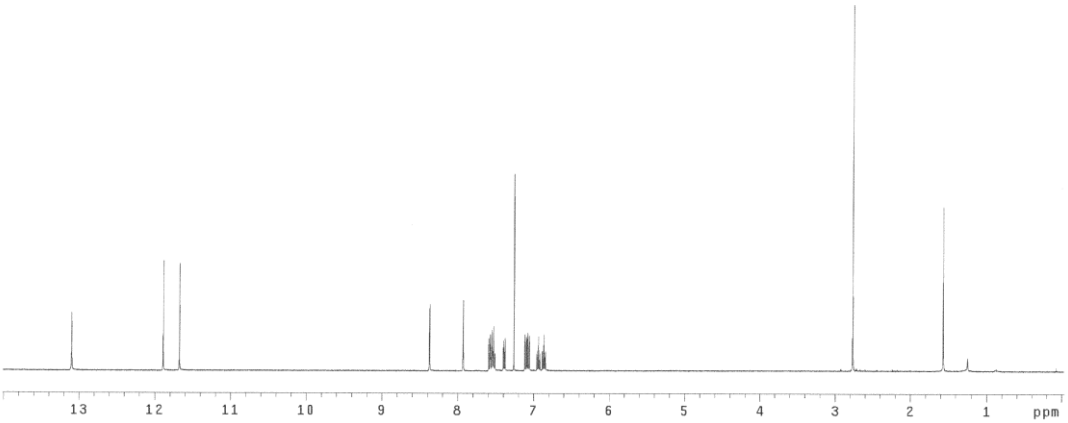

ae_ix_04

Archive directory:
Sample directory:

Pulse Sequence: s2pul

Solvent: cdcl3
Ambient temperature
User: 1-14-87
File: ae_ix_04_s2pul_C13
INOVA-500 "nmrastro"

Relax. delay 2.000 sec
Pulse 30.0 degrees
Acq. time 1.300 sec
Width 24509.8 Hz
5000 repetitions
OBSERVE C13, 100.5305749 MHz
DECOUPLE H1, 399.8067105 MHz
Power 44 dB
continuously on
WALTZ-16 modulated
DATA PROCESSING
Line broadening 2.0 Hz
FT size 65536
Total time 4 hr, 35 min, 47 sec

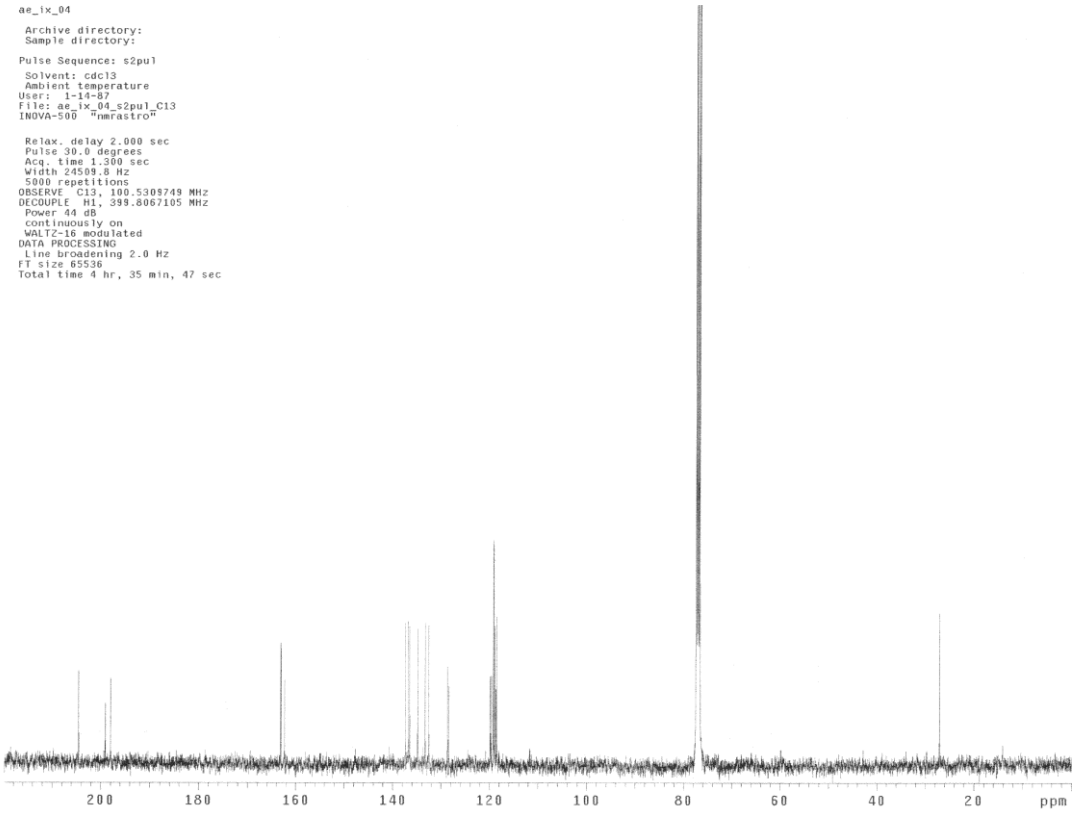

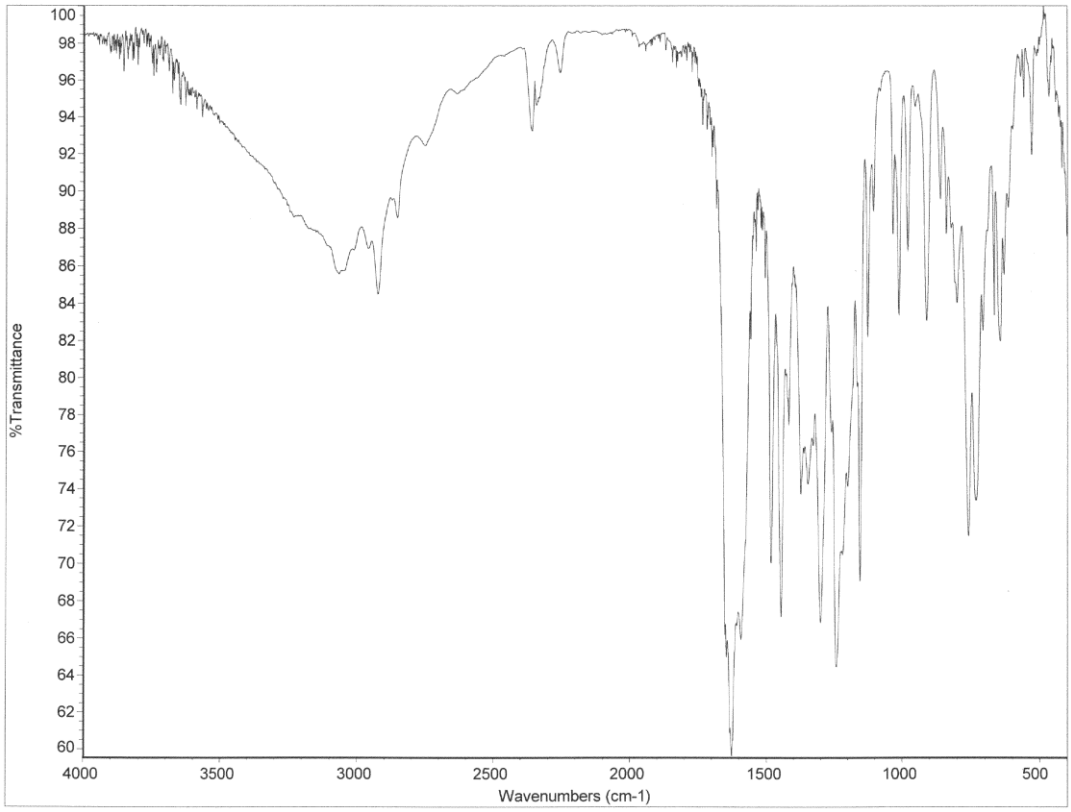
%Transmittance
100
98
96
94
92
90
88
86
84
82
80
78
76
74
72
70
68
66
64
62
60
4000
3500
3000
2500
2000
1500
1000
500
Wavenumbers (cm-1)

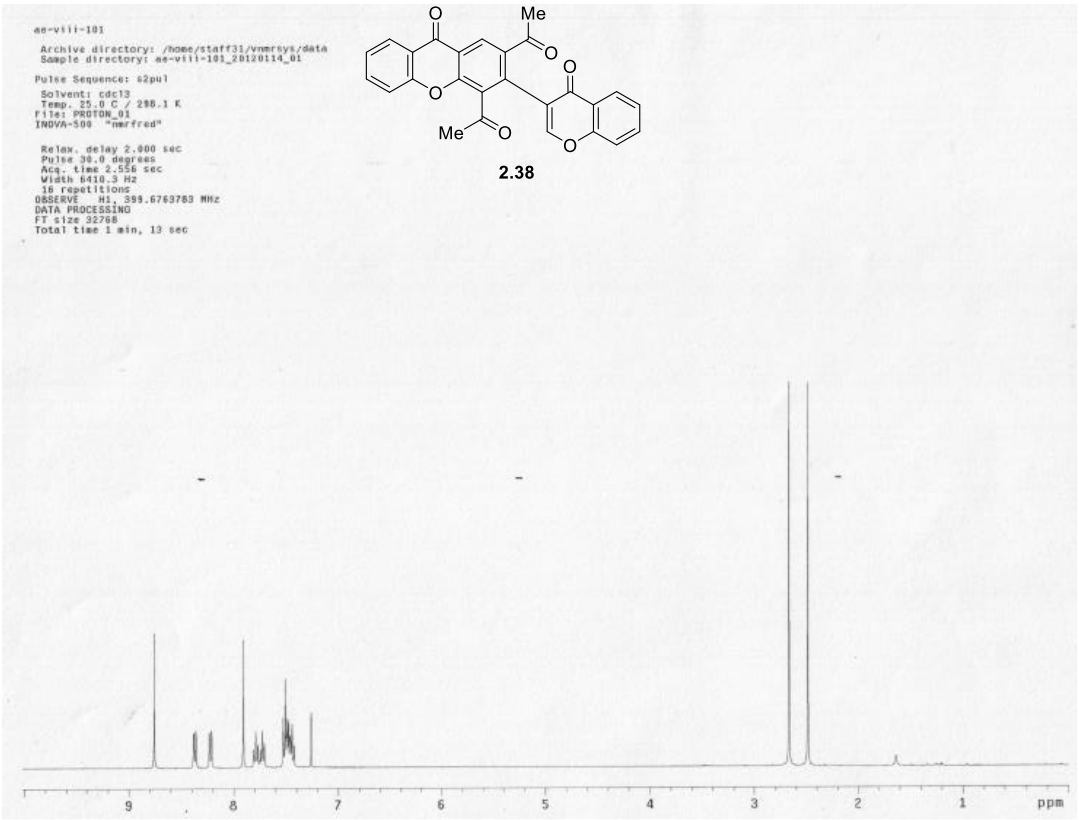
ae-viii-101
Archive directory: /home/staff31/vnmrsys/data
Sample directory: ae-viii-101_20120114_01
Pulse Sequence: s2pul
Solvent: cdcl3
Temp. 25.0 C / 298.1 K
File: PROTON_01
INOVA-500 "nmrfred"
Relax. delay 2.000 sec
Pulse 30.0 degrees
Acq. time 2.556 sec
Width 6410.3 Hz
16 repetitions
OBSERVE H1, 399.6763783 MHz
DATA PROCESSING
FT size 32768
Total time 1 min, 13 sec
Me
O
Me
O
O
O
O
2.38
9
8
7
6
5
4
3
2
1
ppm

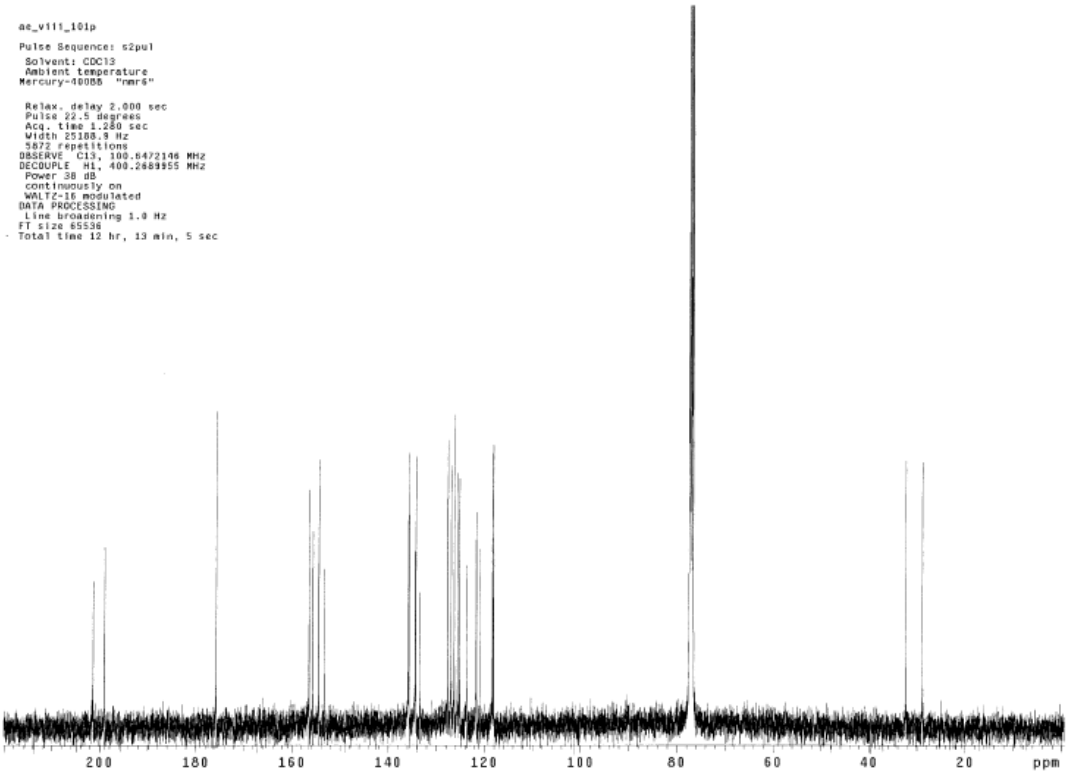
ae_viii_101p
Pulse Sequence: s2pul
Solvent: CDCl3
Ambient temperature
Mercury-400BB "nmr6"
Relax. delay 2.000 sec
Pulse 22.5 degrees
Acq. time 1.280 sec
Width 25188.9 Hz
5872 repetitions
OBSERVE C13, 100.6472146 MHz
DECOUPLE H1, 400.2689955 MHz
Power 38 dB
continuously on
WALTZ-16 modulated
DATA PROCESSING
Line broadening 1.0 Hz
FT size 65536
Total time 12 hr, 13 min, 5 sec
200
180
160
140
120
100
80
60
40
20
ppm

exp7 Ghmbc

SAMPLE	
date	Mar 10 2011
solvent	cdcl3
sample	
ACQUISITION	
sw	5282.6
at	0.128
np	1352
fb	3000
ss	32
d1	2.000
nt	16
2D ACQUISITION	
sw1	31421.8
ni	512
phase	0
PRESATURATION	
satmode	nnn
satdly	0
satfrq	499.8
satpwr	-13
TRANSMITTER	
tn	H1
sfrq	499.867
tof	-34.0
tpwr	57
pw	11.000
DECOUPLER	
dn	C13
dof	1883.9
dm	nnn
dmf	14285
dpwr	40
pwxlvl	56
pwx	9.500
HMBC	
j1xh	140.0
jnxh	8.0

FLAGS	
hs	n
sspul	n
PFGflg	y
hsglvl	4694
SPECIAL	
temp	27.0
gain	30
spin	0
GRADIENTS	
gzlvl1	4694
gt1	0.001000
gzlvl3	2355
gt3	0.001000
gstab	0.000500
F2 PROCESSING	
sb	0.064
sbs	not used
fn	2048
F1 PROCESSING	
sb1	0.017
sbs1	not used
proc1	lp
fn1	4096
DISPLAY	
sp	-178.6
wp	5277.5
sp1	-1887.7
wp1	31406.5
rf1	1414.6
rfp	1230.9
rfl1	27200.7
rfp1	25297.7
PLOT	
wc	116.0
sc	10.0
wc2	116.0
sc2	0
vs	328
th	2

ai cdc av

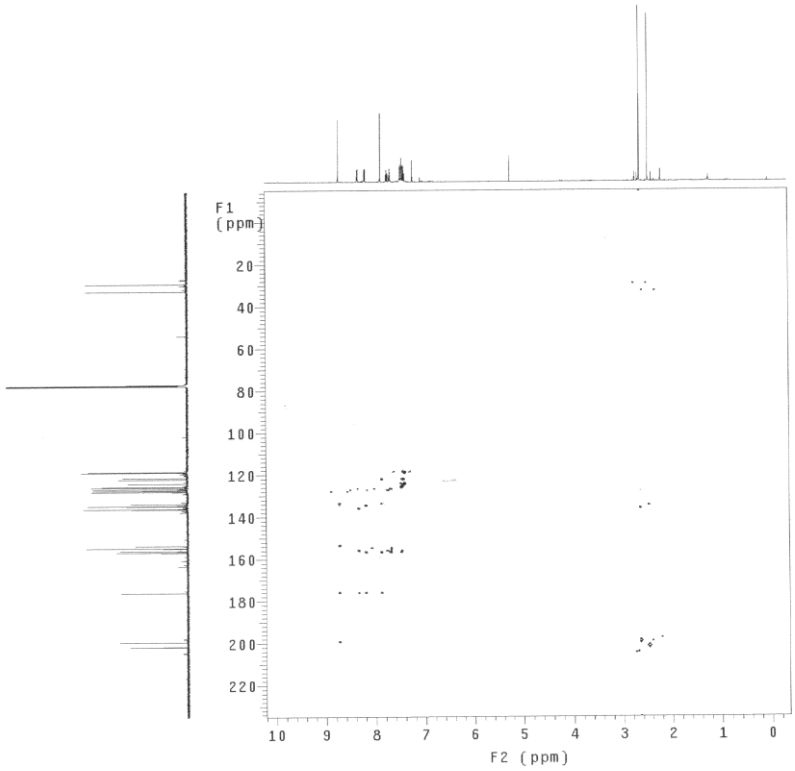

File: Ghmbc

Pulse Sequence: gHMBC

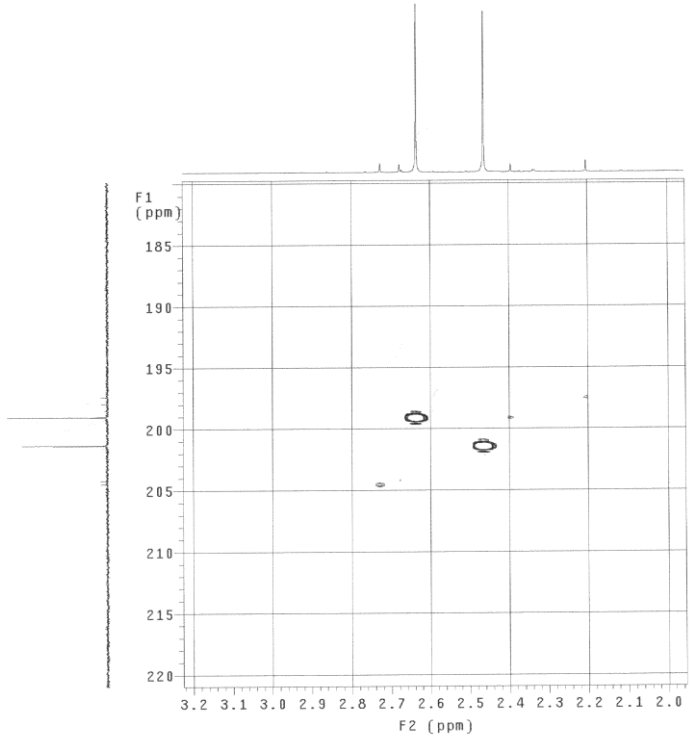

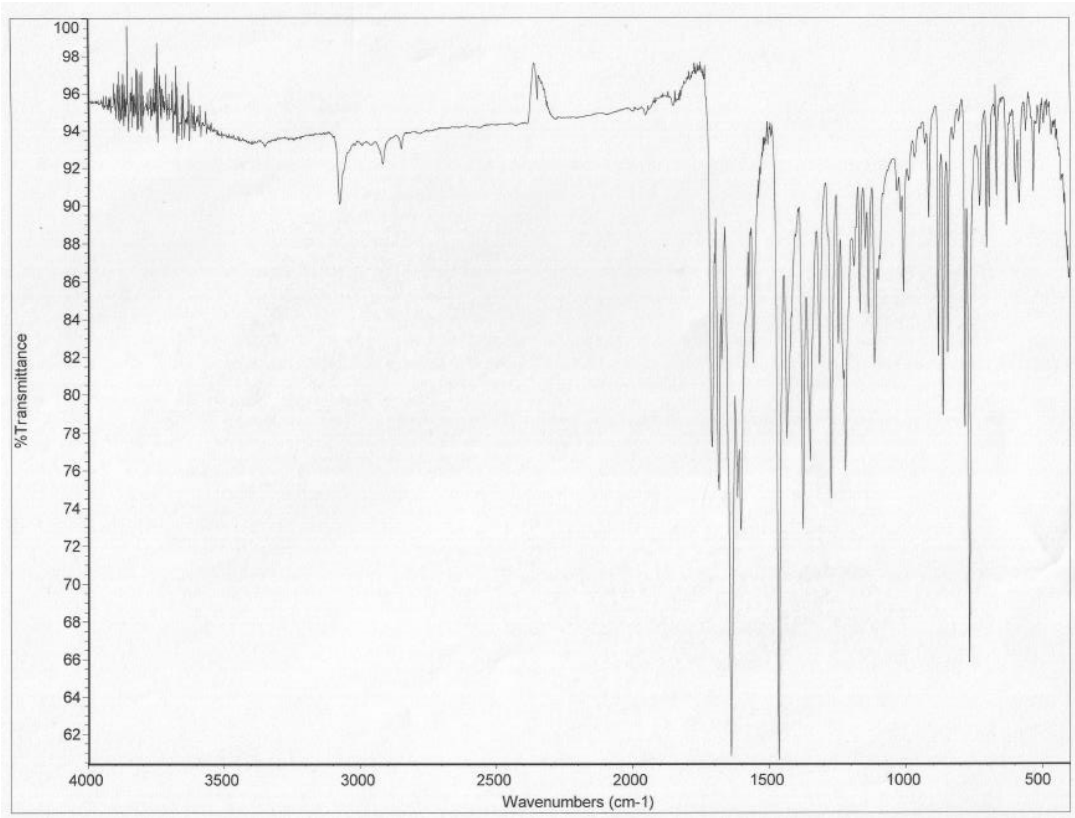
%Transmittance
100
98
96
94
92
90
88
86
84
82
80
78
76
74
72
70
68
66
64
62
4000
3500
3000
2500
2000
1500
1000
500
Wavenumbers (cm-1)

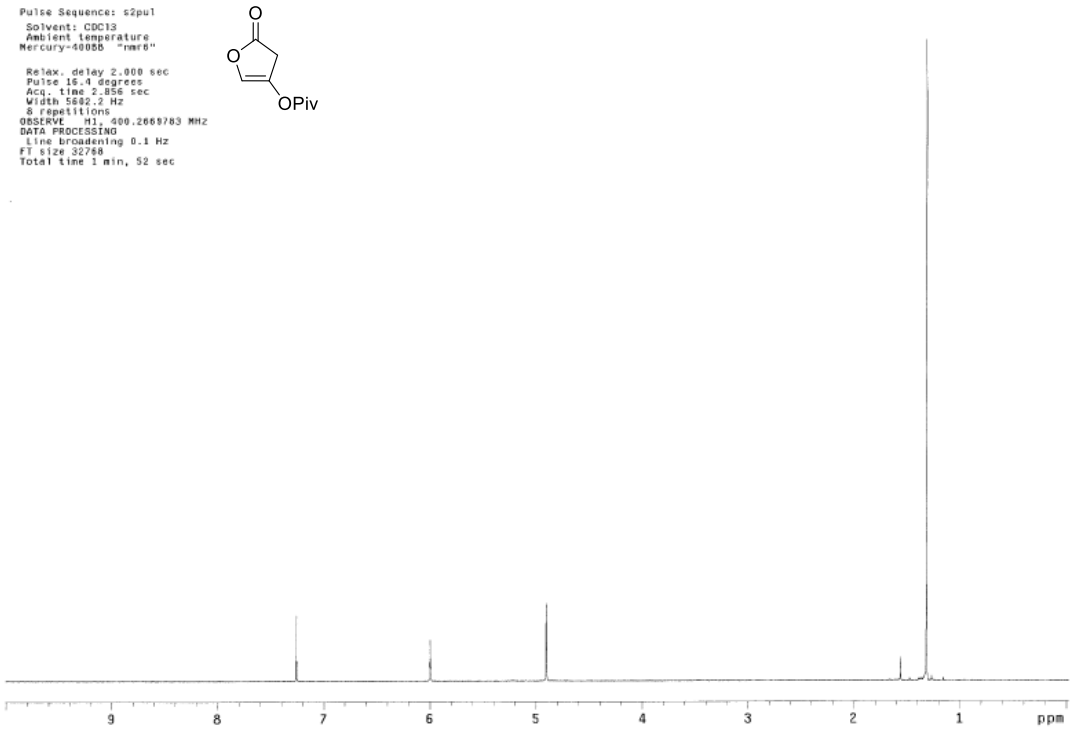
Pulse Sequence: s2pul
Solvent: CDCl3
Ambient temperature
Mercury-400BB "nmr6"
Relax. delay 2.000 sec
Pulse 16.4 degrees
Acq. time 2.856 sec
Width 5602.2 Hz
8 repetitions
OBSERVE H1, 400.2669783 MHz
DATA PROCESSING
Line broadening 0.1 Hz
FT size 32768
Total time 1 min, 52 sec
O
O
OPiv
9
8
7
6
5
4
3
2
1
ppm

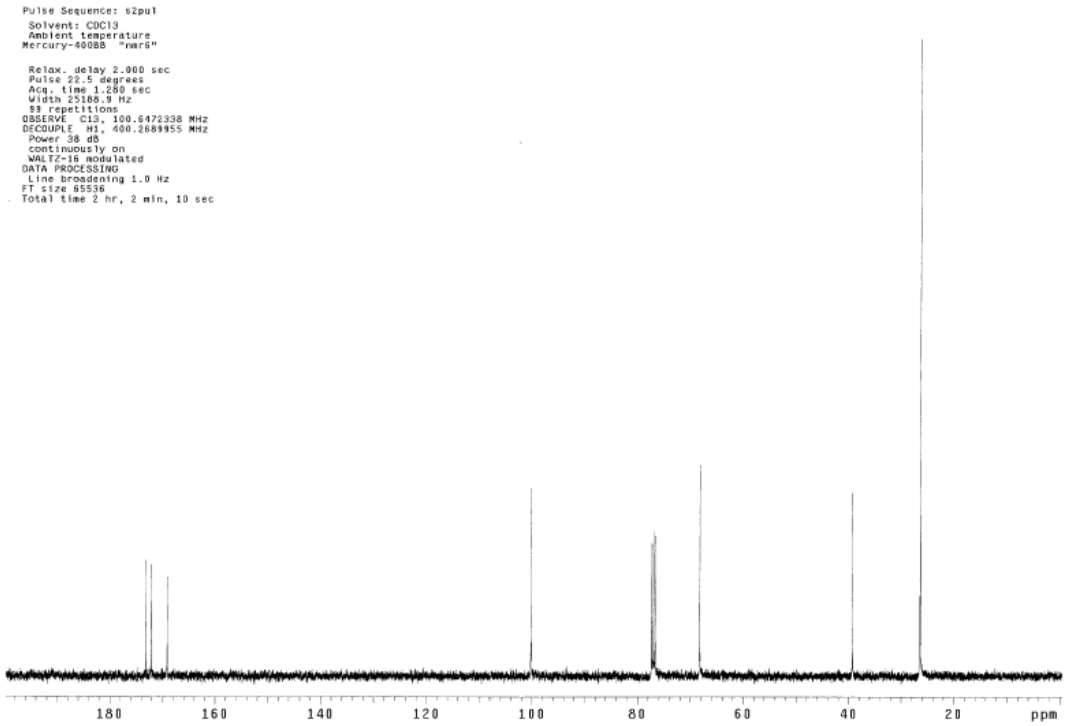
Pulse Sequence: s2pul
Solvent: CDCl3
Ambient temperature
Mercury-400BB "nmr6"
Relax. delay 2.000 sec
Pulse 22.5 degrees
Acq. time 1.280 sec
Width 25188.9 Hz
99 repetitions
OBSERVE C13, 100.6472338 MHz
DECOUPLE H1, 400.2689955 MHz
Power 38 dB
continuously on
WALTZ-16 modulated
DATA PROCESSING
Line broadening 1.0 Hz
FT size 65536
Total time 2 hr, 2 min, 10 sec
180
160
140
120
100
80
60
40
20
ppm

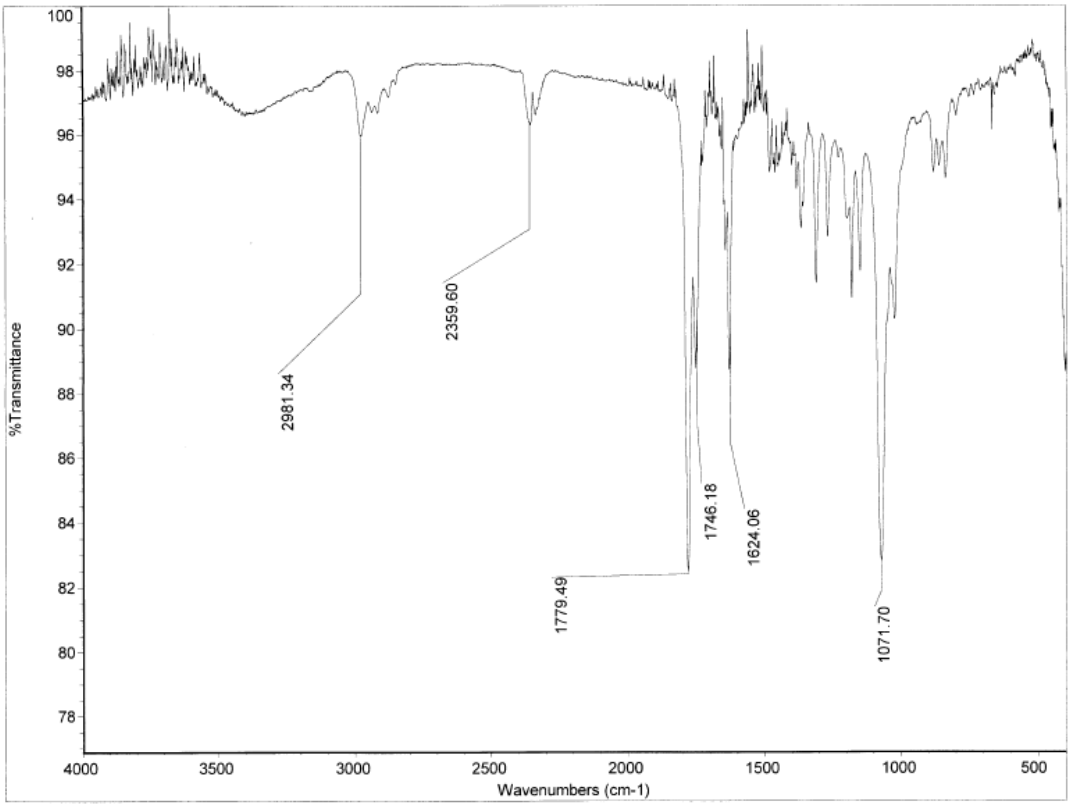
%Transmittance
100
98
96
94
92
90
88
86
84
82
80
78
2981.34
2359.60
1779.49
1746.18
1624.06
1071.70
4000
3500
3000
2500
2000
1500
1000
500
Wavenumbers (cm-1)

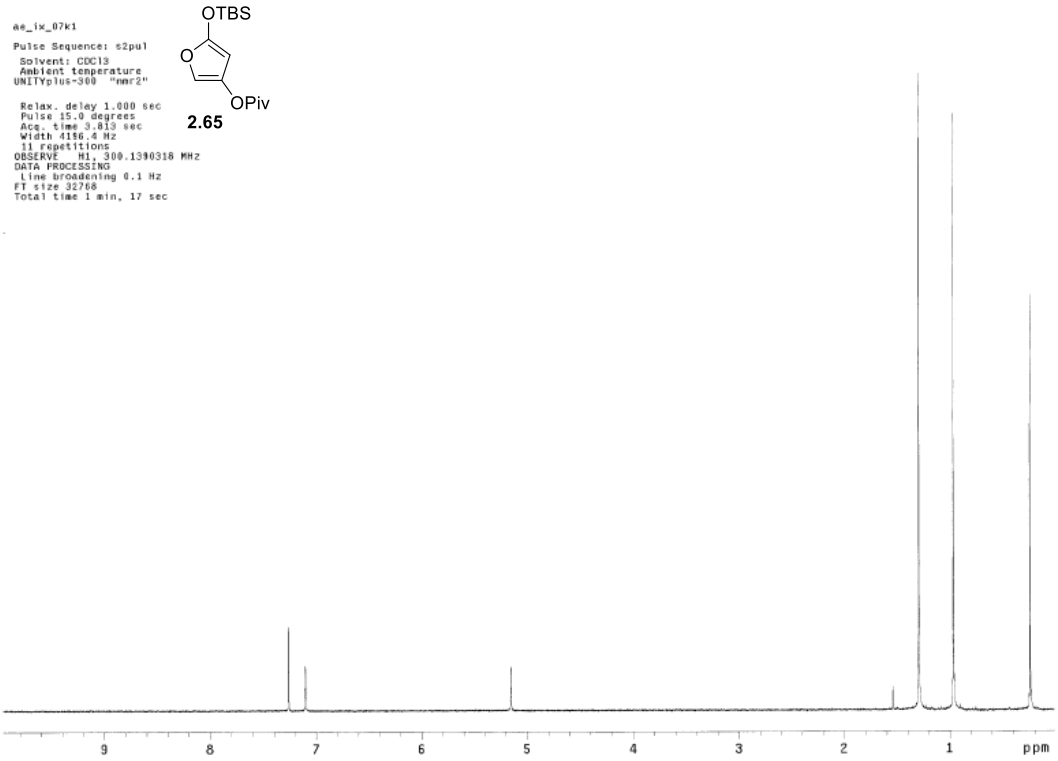
ae_ix_07k1
Pulse Sequence: s2pul
Solvent: CDCl3
Ambient temperature
UNITYplus-300 "nmr2"
Relax. delay 1.000 sec
Pulse 15.0 degrees
Acq. time 3.813 sec
Width 4156.4 Hz
11 repetitions
OBSERVE H1, 300.1390318 MHz
DATA PROCESSING
Line broadening 0.1 Hz
FT size 32768
Total time 1 min, 17 sec
OTBS
O
OPiv
2.65
9
8
7
6
5
4
3
2
1
ppm

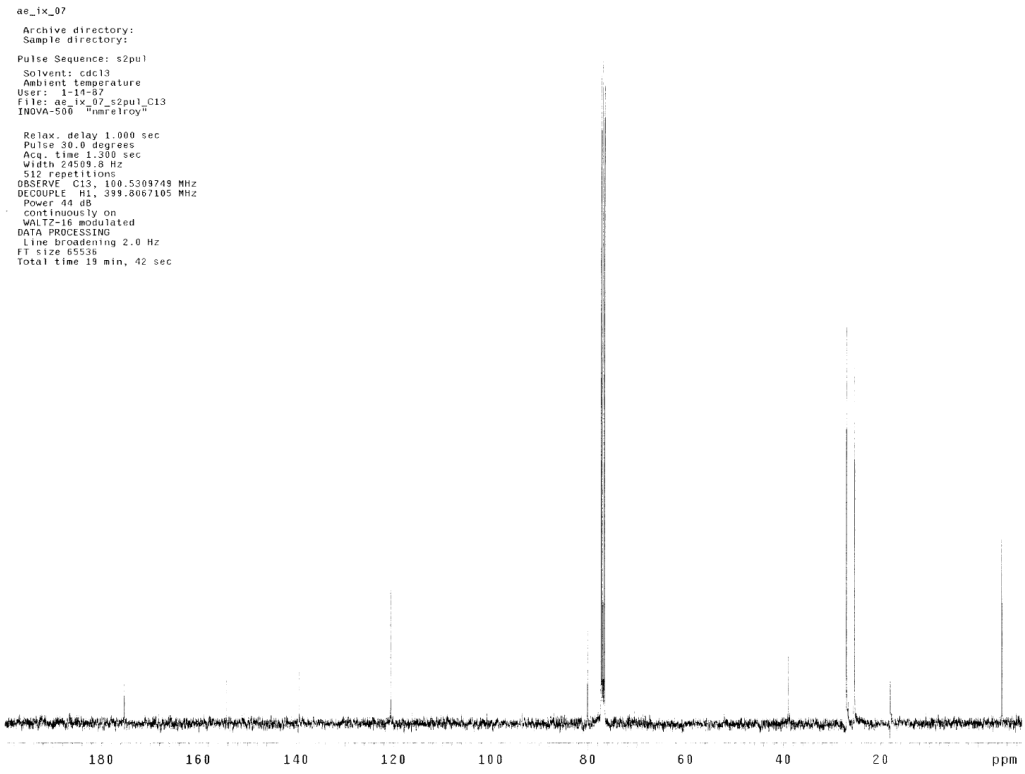
ae_ix_07
Archive directory:
Sample directory:
Pulse Sequence: s2pul
Solvent: cdcl3
Ambient temperature
User: 1-14-87
File: ae_ix_07_s2pul_C13
INOVA-500 "nmrelroy"
Relax. delay 1.000 sec
Pulse 30.0 degrees
Acq. time 1.300 sec
Width 24509.8 Hz
512 repetitions
OBSERVE C13, 100.5309749 MHz
DECOUPLE H1, 399.8067105 MHz
Power 44 dB
continuously on
WALTZ-16 modulated
DATA PROCESSING
Line broadening 2.0 Hz
FT size 65536
Total time 19 min, 42 sec
180
160
140
120
100
80
60
40
20
ppm

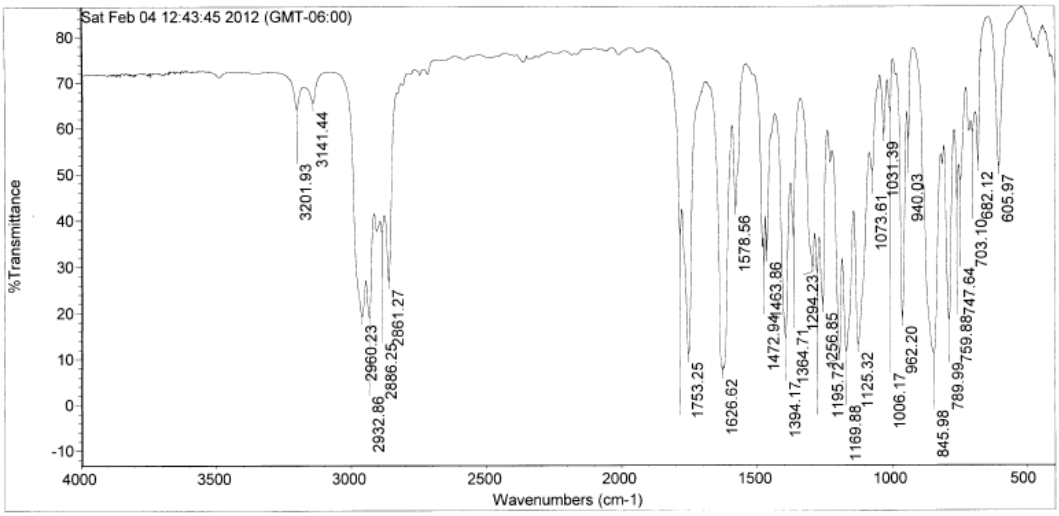

Sat Feb 04 12:46:46 2012 (GMT-06:00)
FIND PEAKS:

Spectrum:	Sat Feb 04 12:43:45 2012 (GMT-06:00)	
Region:	4000.00	400.00
Absolute threshold:	67.348	
Sensitivity:	50	
Peak list:		

Position:	605.97	Intensity:	51.457
Position:	682.12	Intensity:	52.099
Position:	703.10	Intensity:	59.048
Position:	747.64	Intensity:	48.561
Position:	759.88	Intensity:	44.164
Position:	789.99	Intensity:	18.408
Position:	845.98	Intensity:	11.187
Position:	940.03	Intensity:	57.167

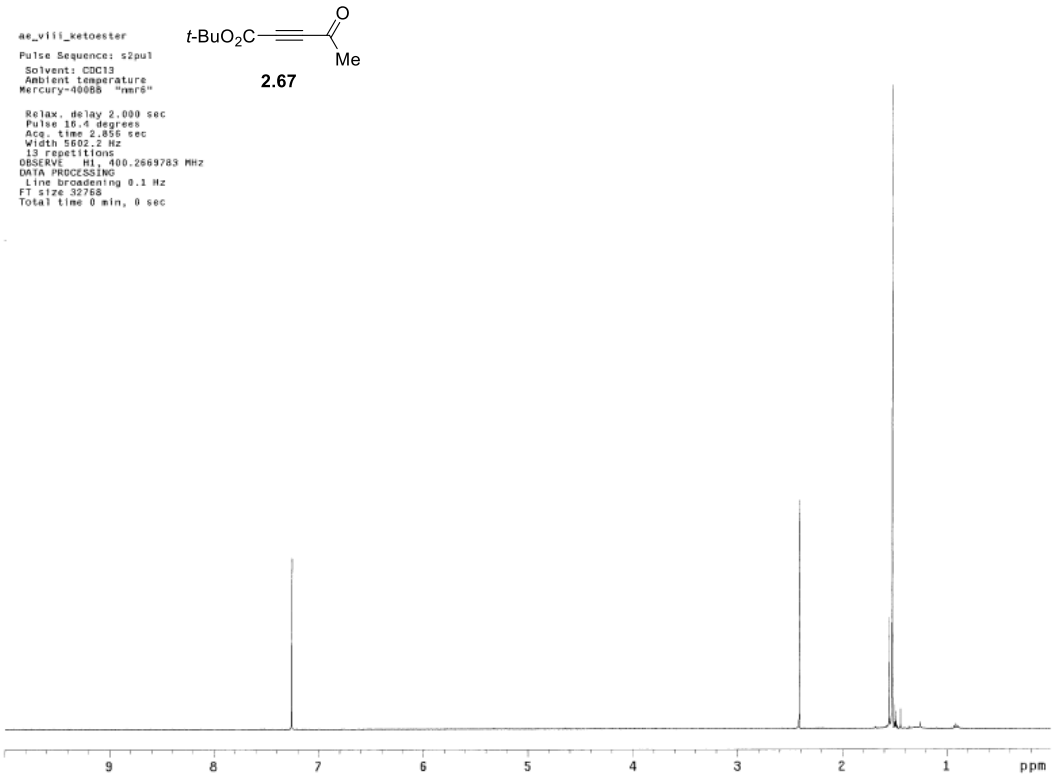
ae_viii_ketoester
Pulse Sequence: s2pul
Solvent: CDCl3
Ambient temperature
Mercury-400BB "nmr6"
Relax. delay 2.000 sec
Pulse 16.4 degrees
Acq. time 2.856 sec
Width 5602.2 Hz
13 repetitions
OBSERVE H1, 400.2669783 MHz
DATA PROCESSING
Line broadening 0.1 Hz
FT size 32768
Total time 0 min, 0 sec
t-BuO2C
O
Me
2.67
9
8
7
6
5
4
3
2
1
ppm

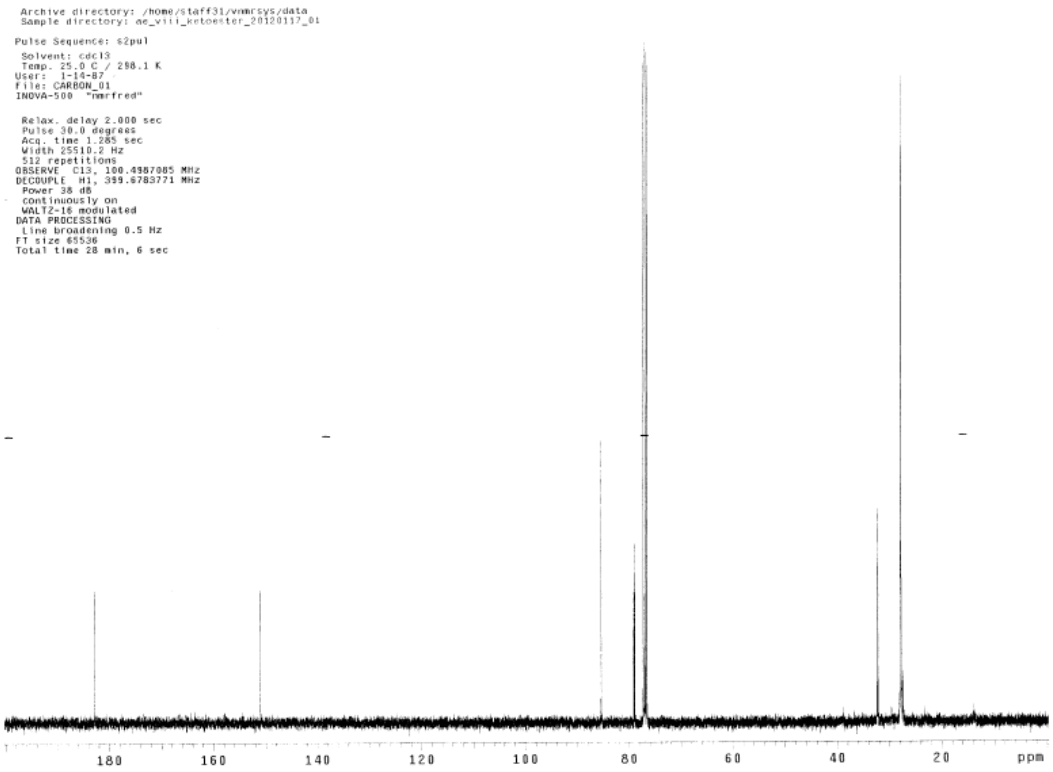
Archive directory: /home/staff31/vnmrsys/data
Sample directory: ae_viii_ketoester_20120117_01
Pulse Sequence: s2pul
Solvent: cdcl3
Temp. 25.0 C / 298.1 K
User: 1-14-87
File: CARBON_01
INOVA-500 "nmrfred"
Relax. delay 2.000 sec
Pulse 30.0 degrees
Acq. time 1.285 sec
Width 25510.2 Hz
512 repetitions
OBSERVE C13, 100.4987085 MHz
DECOUPLE H1, 399.6783771 MHz
Power 38 dB
continuously on
WALTZ-16 modulated
DATA PROCESSING
Line broadening 0.5 Hz
FT size 65536
Total time 28 min, 6 sec
180
160
140
120
100
80
60
40
20
ppm

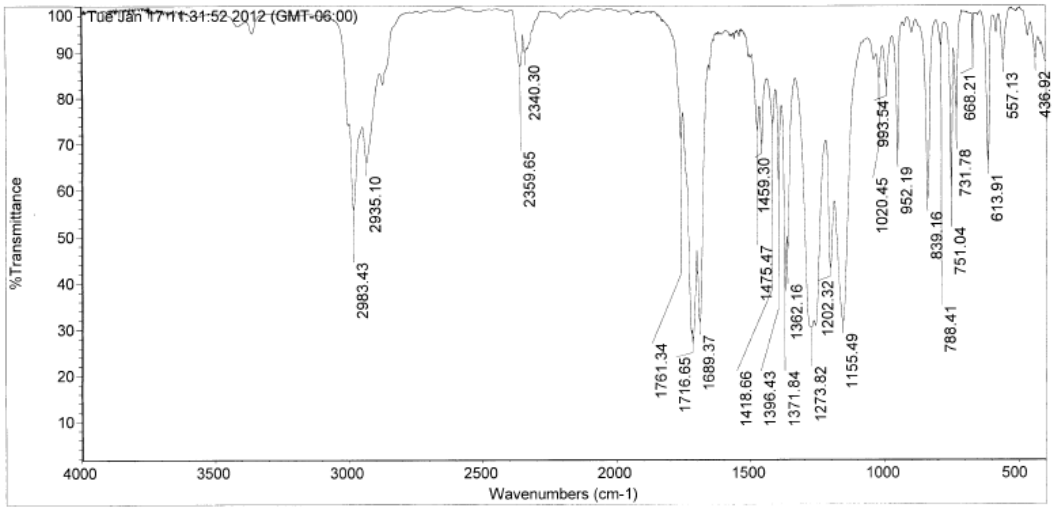

Tue Jan 17 11:34:27 2012 (GMT-06:00)
FIND PEAKS:

Spectrum: *Tue Jan 17 11:31:52 2012 (GMT-06:00)
Region: 4000.00 400.00
Absolute threshold: 92.120
Sensitivity: 50
Peak list:

Position:	436.92	Intensity:	88.647
Position:	557.13	Intensity:	88.308
Position:	613.91	Intensity:	66.064
Position:	668.21	Intensity:	88.066
Position:	731.78	Intensity:	77.586
Position:	751.04	Intensity:	60.575
Position:	788.41	Intensity:	91.346
Position:	839.16	Intensity:	58.011

ae_viii_ee

Archive directory: /home/staff31/vnmrsys/data
Sample directory: ae_viii_ee_20120125_01

Pulse Sequence: s2pul

Solvent: cdcl3
Temp. 25.0 C / 298.1 K
file: PROTON_01
INOVA-500 "nmrfred"

Relax. delay 2.000 sec
Pulse 30.0 degrees
Acq. time 2.556 sec
Width 6410.3 Hz
32 repetitions
OBSERVE H1, 399.6763783 MHz
DATA PROCESSING
FT size 32768
Total time 2 min, 26 sec

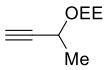

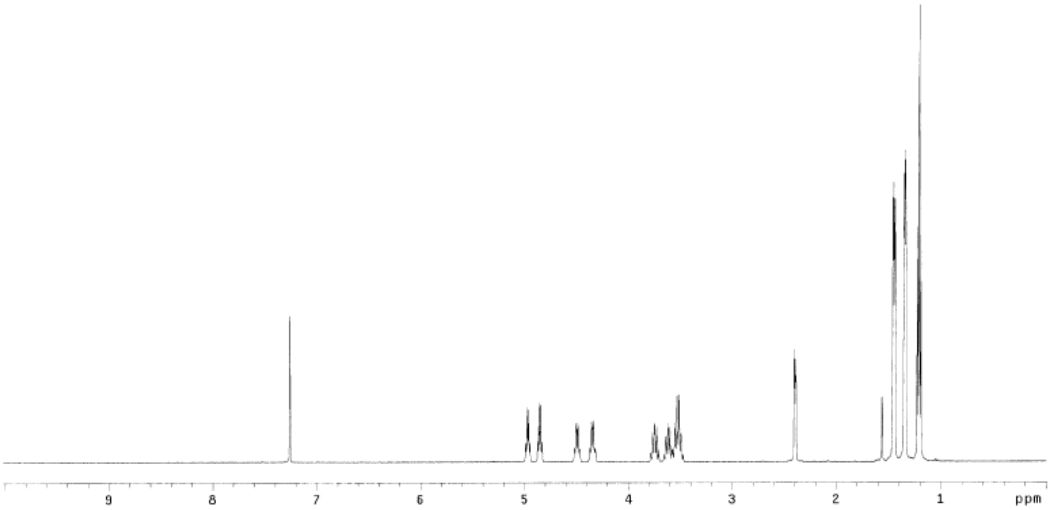

13C OBSERVE

Pulse Sequence: s2pul

Solvent: CDCl3
Ambient temperature
Mercury-400BB "nmr6"

Relax. delay 2.000 sec
Pulse 22.5 degrees
Acq. time 1.280 sec
Width 25188.9 Hz
67 repetitions
OBSERVE C13, 100.6472207 MHz
DECOUPLE H1, 400.2683955 MHz
Power 38 dB
continuously on
WALTZ-16 modulated
DATA PROCESSING
Line broadening 1.0 Hz
FT size 65536
Total time 15 min, 38 sec

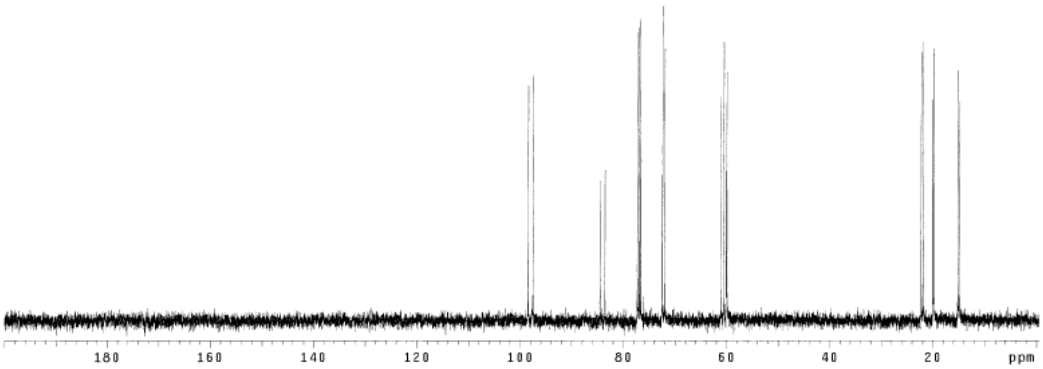

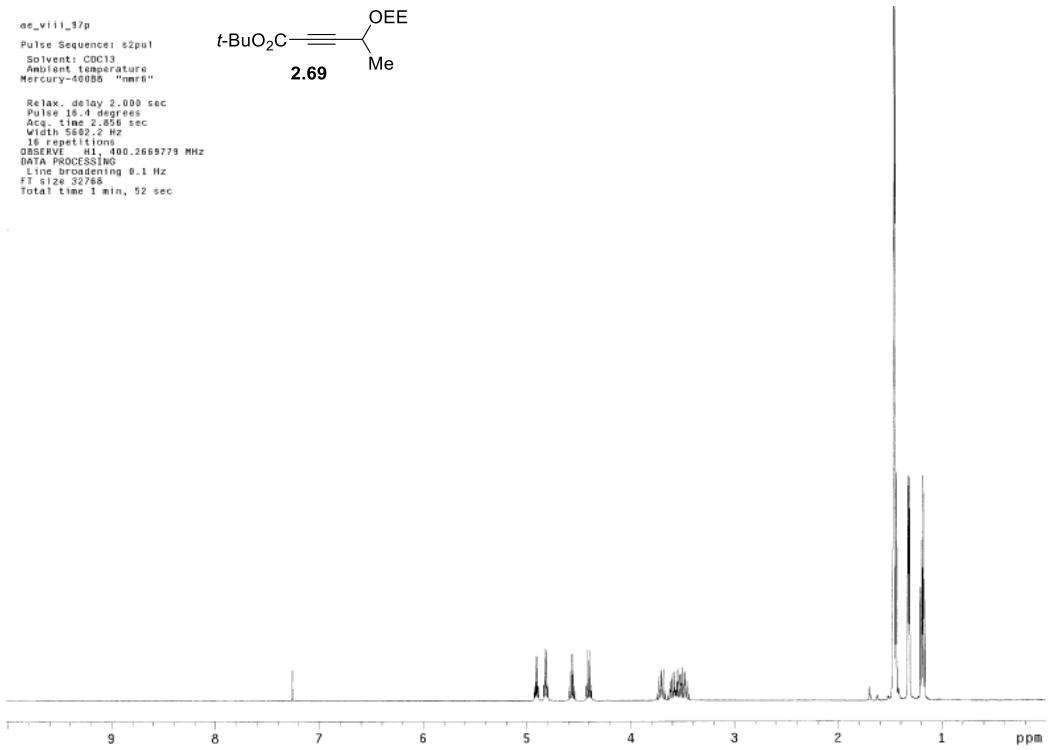
ae_viii_97p
Pulse Sequence: s2pul
Solvent: CDCl3
Ambient temperature
Mercury-400BB "nmr6"
Relax. delay 2.000 sec
Pulse 16.4 degrees
Acq. time 2.856 sec
Width 5602.2 Hz
16 repetitions
OBSERVE H1, 400.2669779 MHz
DATA PROCESSING
Line broadening 0.1 Hz
FT size 32768
Total time 1 min, 52 sec
t-BuO2C
OEE
Me
2.69
9
8
7
6
5
4
3
2
1
ppm

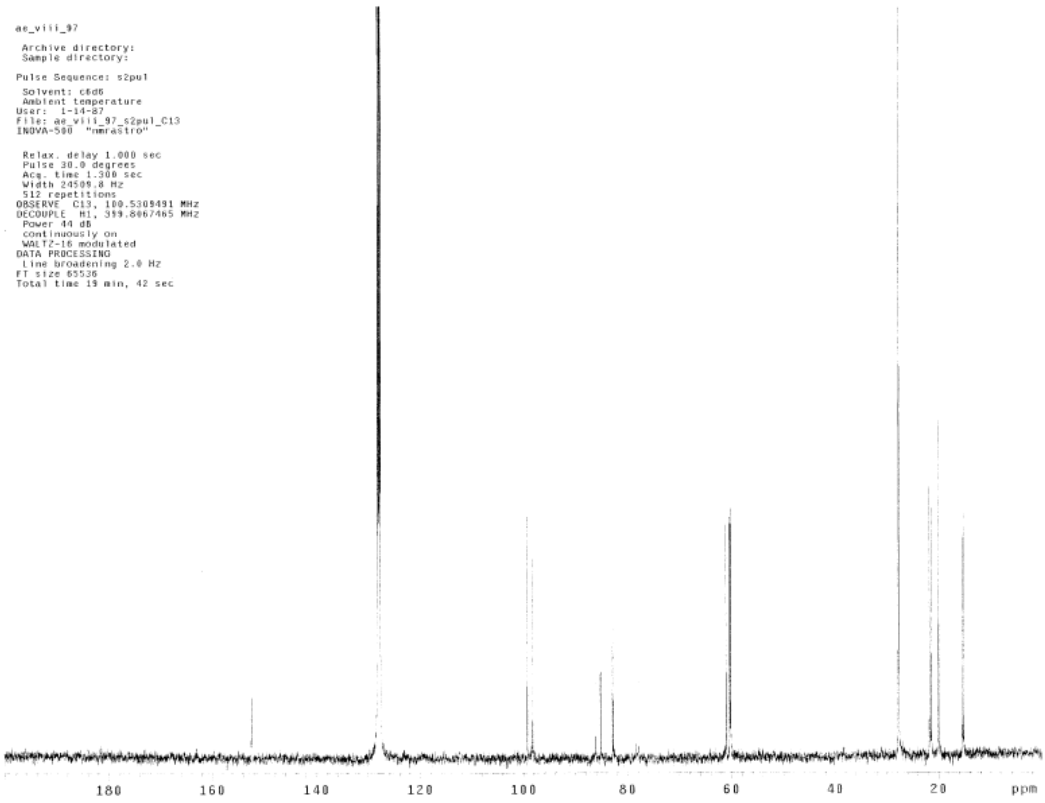
ae_viii_97
Archive directory:
Sample directory:
Pulse Sequence: s2pul
Solvent: c6d6
Ambient temperature
User: 1-14-87
File: ae_viii_97_s2pul_C13
INOVA-500 "nmrastro"
Relax. delay 1.000 sec
Pulse 30.0 degrees
Acq. time 1.300 sec
Width 24509.8 Hz
512 repetitions
OBSERVE C13, 100.5309491 MHz
DECOUPLE H1, 399.8067465 MHz
Power 44 dB
continuously On
WALTZ-16 modulated
DATA PROCESSING
Line broadening 2.0 Hz
FT size 65536
Total time 19 min, 42 sec
180
160
140
120
100
80
60
40
20
ppm

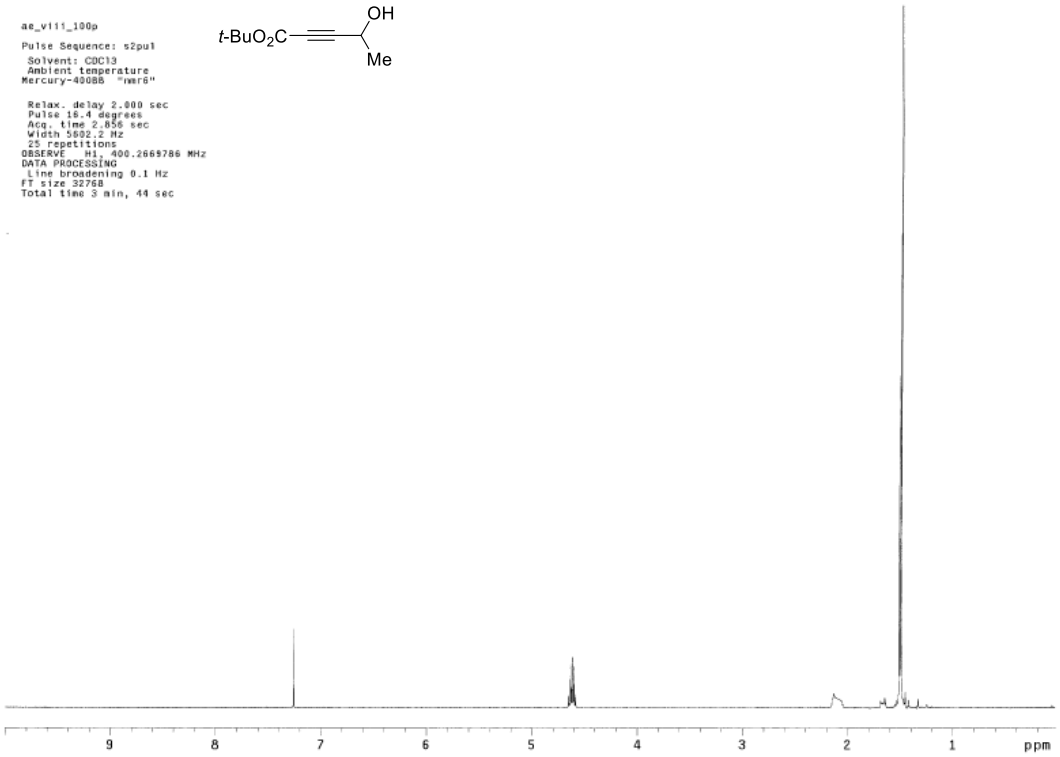
ae_viii_100p
Pulse Sequence: s2pul
Solvent: CDCl3
Ambient temperature
Mercury-400BB "nmr6"
Relax. delay 2.000 sec
Pulse 16.4 degrees
Acq. time 2.856 sec
Width 5602.2 Hz
25 repetitions
OBSERVE H1, 400.2669786 MHz
DATA PROCESSING
Line broadening 0.1 Hz
FT size 32768
Total time 3 min, 44 sec
t-BuO2C
OH
Me
9
8
7
6
5
4
3
2
1
ppm

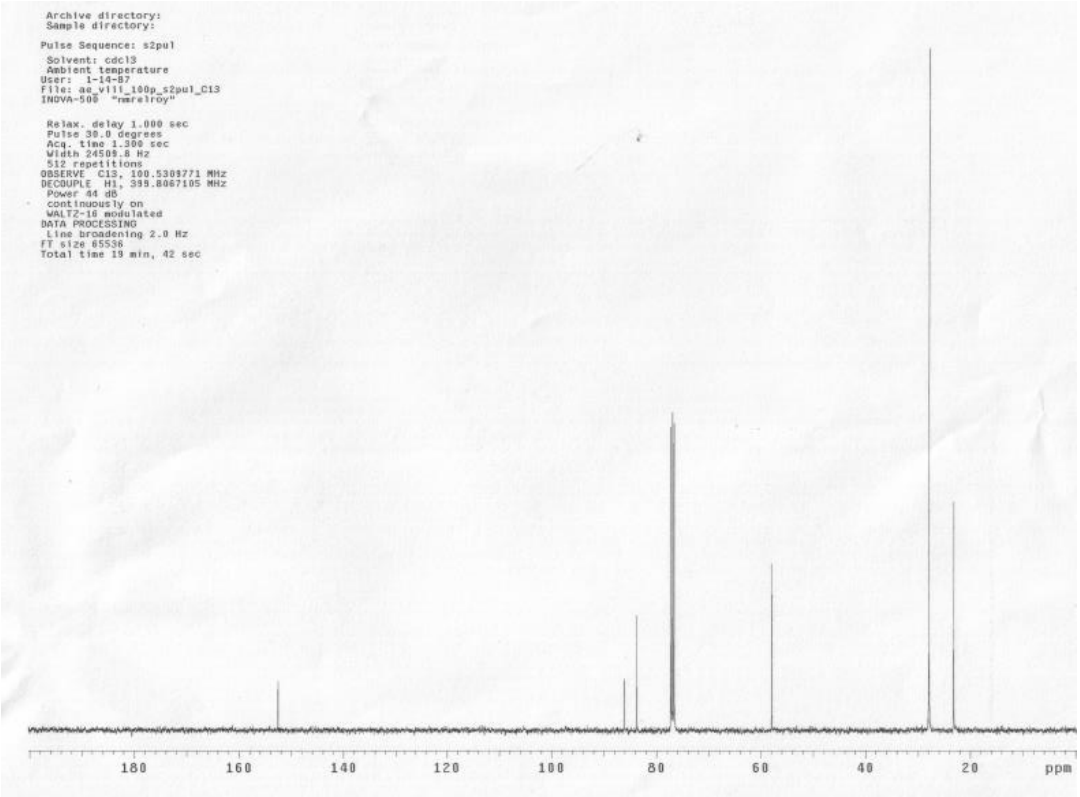
Archive directory:
Sample directory:
Pulse Sequence: s2pul
Solvent: cdcl3
Ambient temperature
User: 1-14-87
File: ae_viii_100p_s2pul_C13
INOVA-500 "nmrelroy"
Relax. delay 1.000 sec
Pulse 30.0 degrees
Acq. time 1.300 sec
Width 24509.8 Hz
512 repetitions
OBSERVE C13, 100.5309771 MHz
DECOUPLE H1, 399.8067105 MHz
Power 44 dB
continuously on
WALTZ-16 modulated
DATA PROCESSING
Line broadening 2.0 Hz
FT size 65536
Total time 19 min, 42 sec
180
160
140
120
100
80
60
40
20
ppm

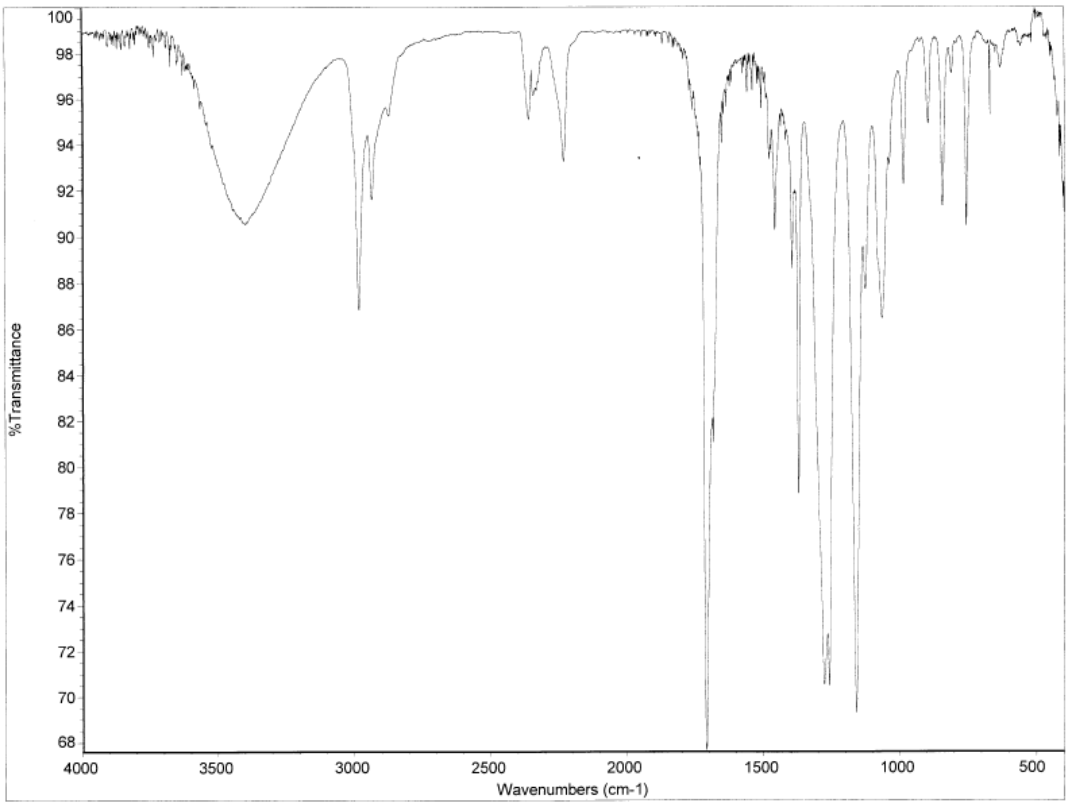
%Transmittance
100
98
96
94
92
90
88
86
84
82
80
78
76
74
72
70
68
4000
3500
3000
2500
2000
1500
1000
500
Wavenumbers (cm-1)

ae_ix_11

Pulse Sequence: s2pul

Solvent: CDCl3
Ambient temperature
Mercury-400BB "nmr6"

Relax. delay 2.000 sec
Pulse 16.4 degrees
Acq. time 2.856 sec
Width 5602.2 Hz
7 repetitions
OBSERVE H1, 400.2669786 MHz
DATA PROCESSING
Line broadening 0.1 Hz
FT size 32768
Total time 0 min, 0 sec

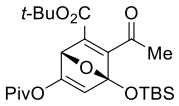

2.71

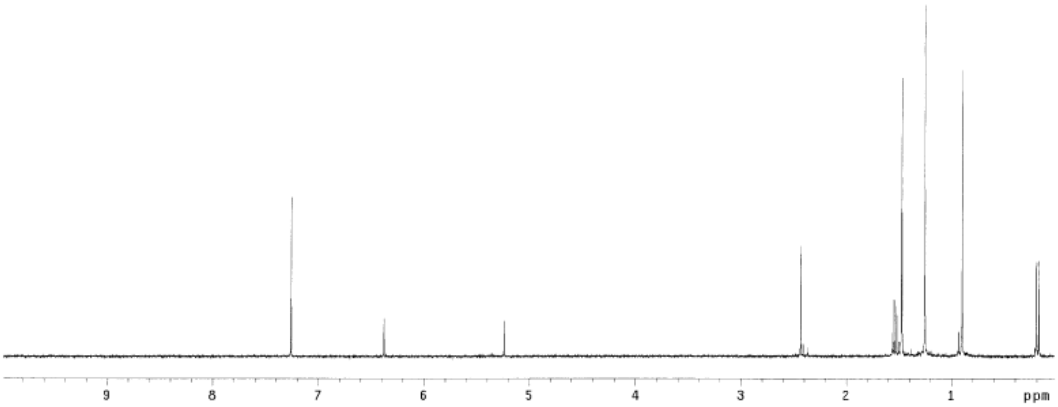

ae_ix_11

Archive directory:
Sample directory:

Pulse Sequence: s2pul

Solvent: cdcl3
Ambient temperature
User: 1-14-87
File: ae_ix_11_s2pul_C13
INOVA-500 "nmrelroy"

Relax. delay 1.000 sec
Pulse 30.0 degrees
Acq. time 1.300 sec
Width 24509.8 Hz
512 repetitions
OBSERVE C13, 100.5309756 MHz
DECOUPLE H1, 399.8867105 MHz
Power 44 dB
continuously on
WALTZ-16 modulated
DATA PROCESSING
Line broadening 2.0 Hz
FT size 65536
Total time 19 min, 42 sec

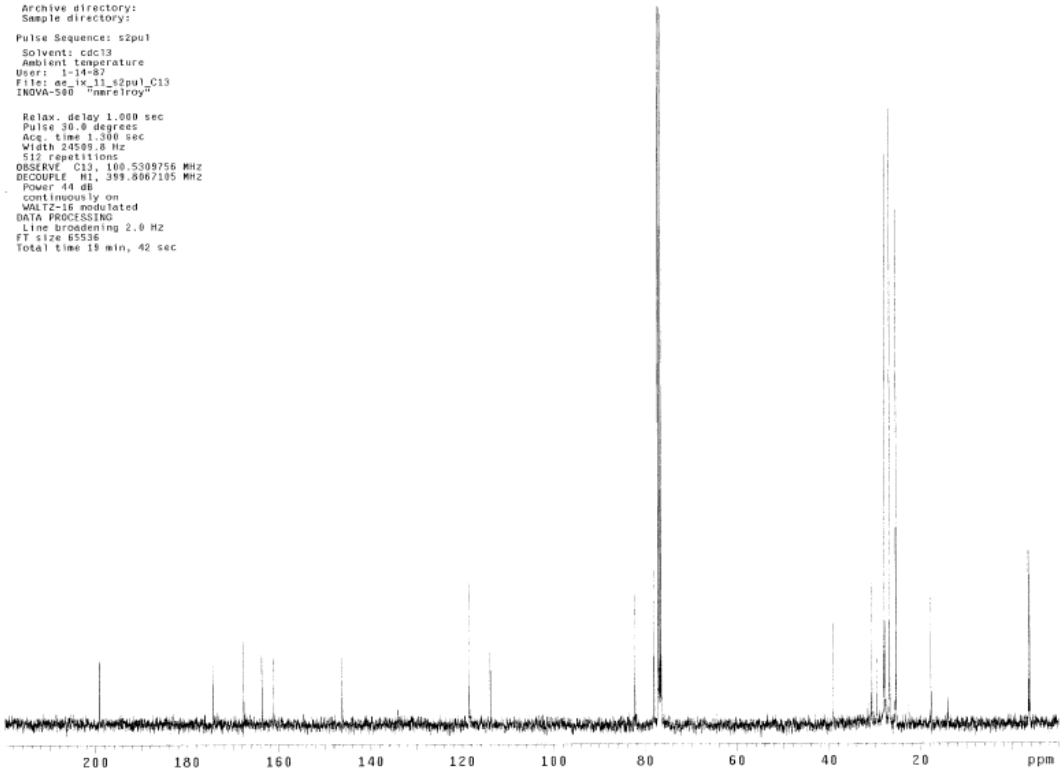

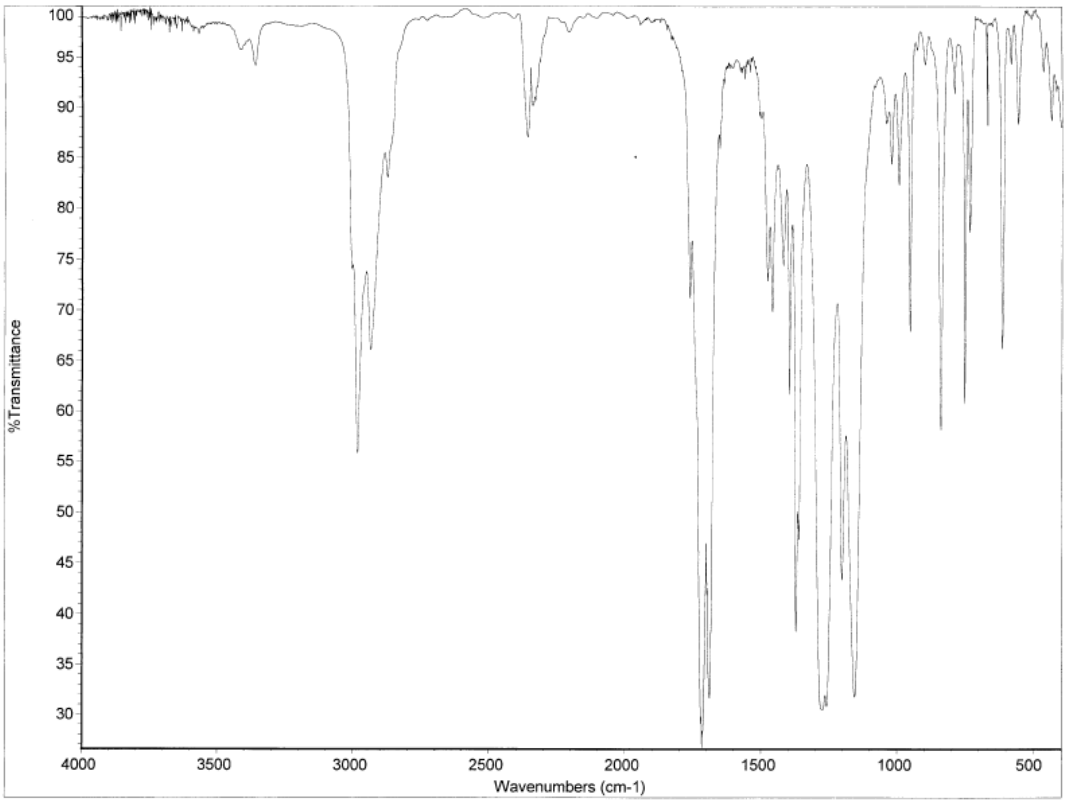
%Transmittance
100
95
90
85
80
75
70
65
60
55
50
45
40
35
30
4000
3500
3000
2500
2000
1500
1000
500
Wavenumbers (cm-1)

ae_ix_10p2

Pulse Sequence: s2pul
Solvent: CDCl3
Ambient temperature
Mercury-400BB "nmr6"

Relax. delay 2.000 sec
Pulse 16.4 degrees
Acq. time 2.856 sec
Width 5602.2 Hz
15 repetitions
OBSERVE H1, 400.2669783 MHz
DATA PROCESSING
Line broadening 0.1 Hz
FT size 32768
Total time 1 min, 52 sec

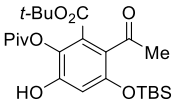

2.72

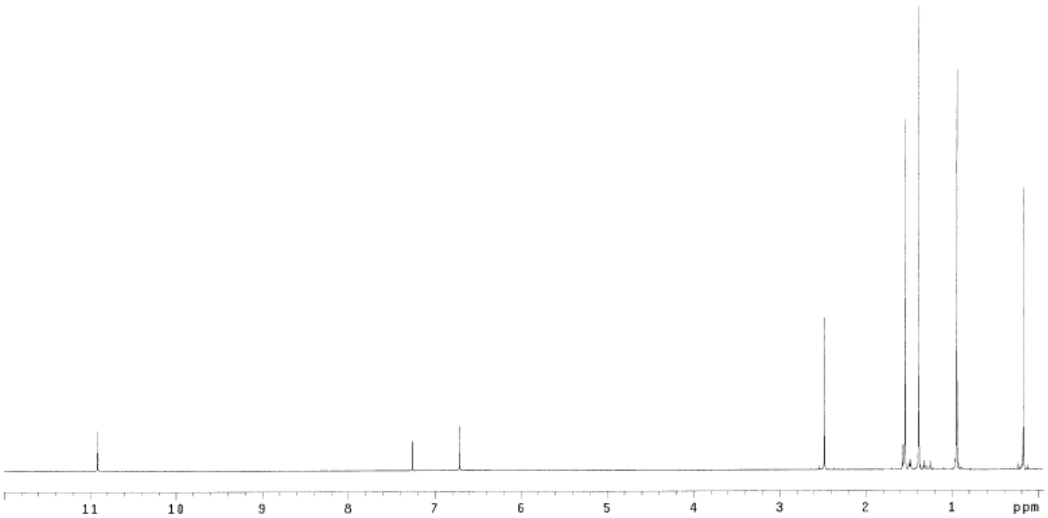

ae_ix_10

Archive directory:
Sample directory:

Pulse Sequence: s2pul
Solvent: cdcl3
Ambient temperature
User: 1-14-87
File: ae_ix_10_s2pul_C13
INOVA-500 "nmrelroy"

Relax. delay 1.000 sec
Pulse 30.0 degrees
Acq. time 1.300 sec
Width 24509.8 Hz
512 repetitions
OBSERVE C13, 100.5309756 MHz
DECOUPLE H1, 399.8067105 MHz
Power 44 dB
continuously on
WALTZ-16 modulated
DATA PROCESSING
Line broadening 2.0 Hz
FT size 65536
Total time 19 min, 42 sec

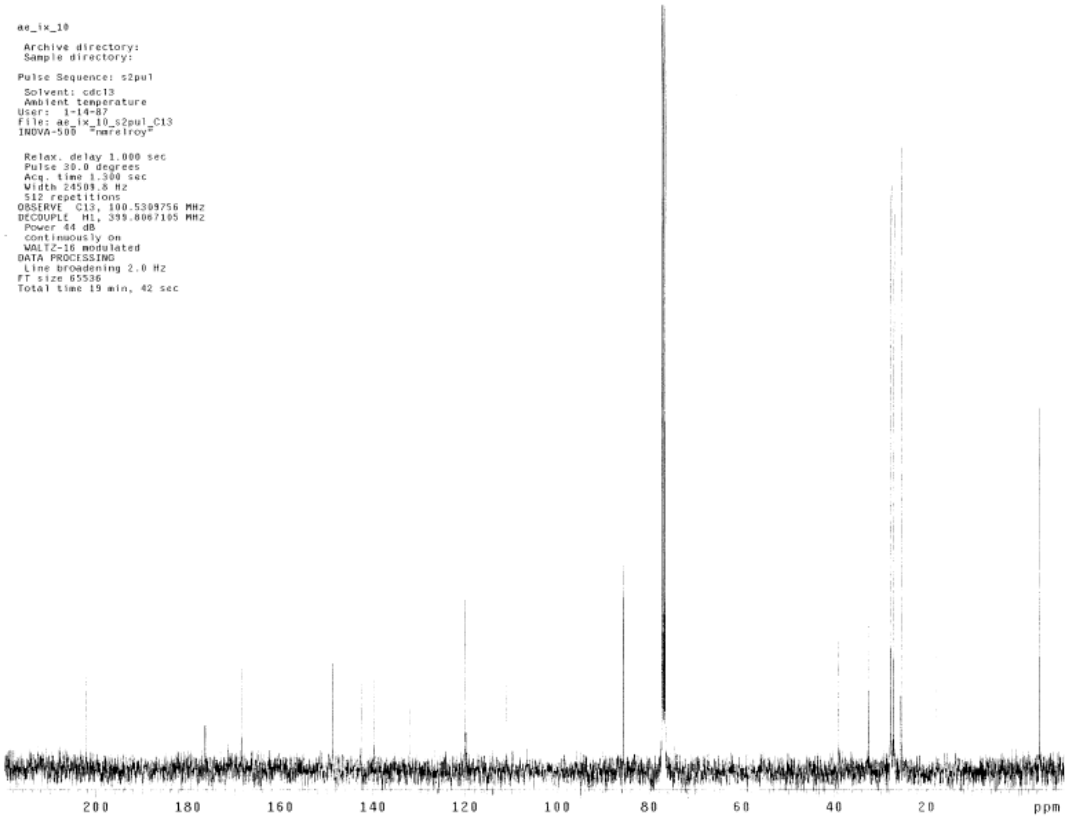

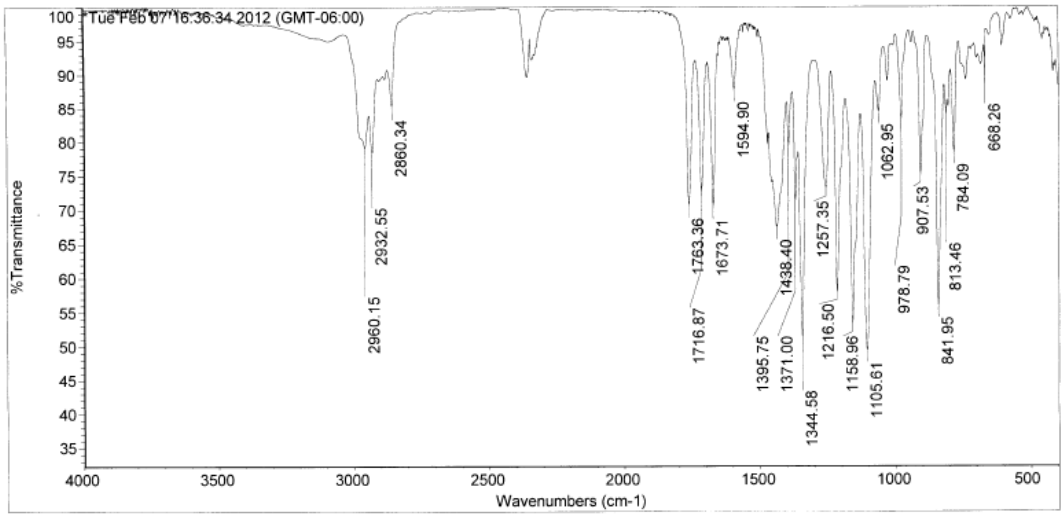

Tue Feb 07 16:39:52 2012 (GMT-06:00)
FIND PEAKS:

Spectrum: *Tue Feb 07 16:36:34 2012 (GMT-06:00)
Region: 4000.00 400.00
Absolute threshold: 88.265
Sensitivity: 50
Peak list:

Position:	668.26	Intensity:	87.548
Position:	784.09	Intensity:	78.591
Position:	813.46	Intensity:	84.057
Position:	841.95	Intensity:	56.166
Position:	907.53	Intensity:	75.255
Position:	978.79	Intensity:	83.479
Position:	1062.95	Intensity:	84.548
Position:	1105.61	Intensity:	49.433

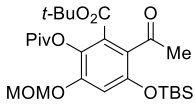
t-BuO2C
O
PivO
Me
MOMO
OTBS

2.73

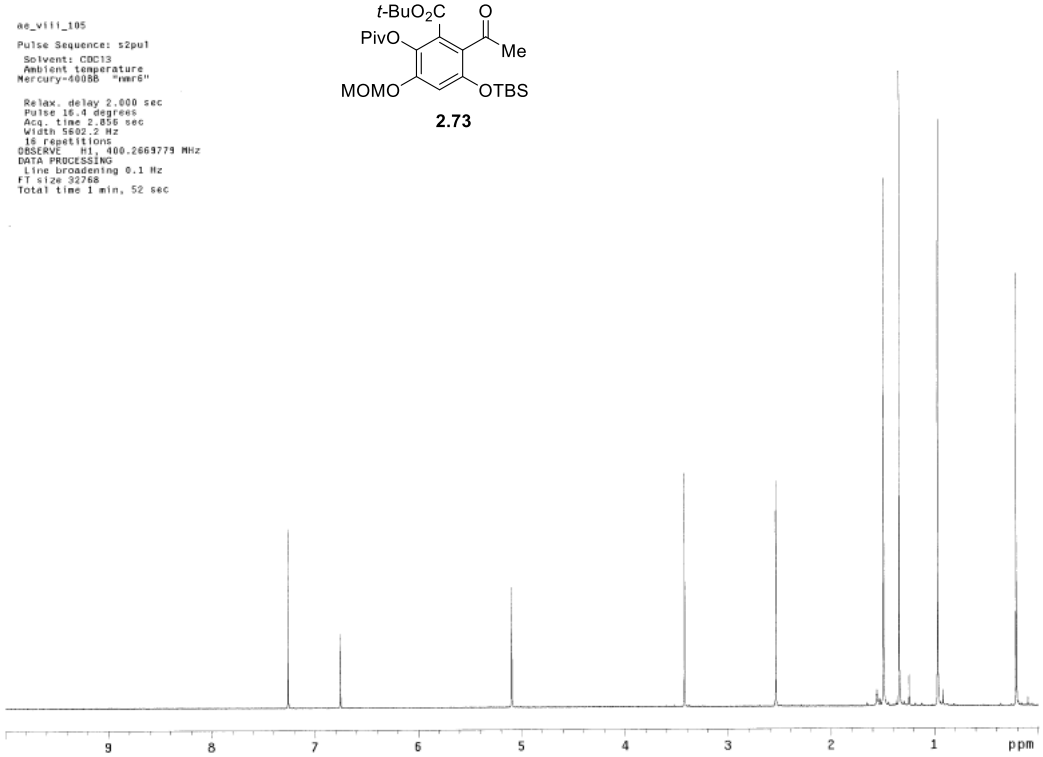
ae_viii_105
Pulse Sequence: s2pul
Solvent: CDCl3
Ambient temperature
Mercury-400BB "nmr6"
Relax. delay 2.000 sec
Pulse 16.4 degrees
Acq. time 2.856 sec
Width 5602.2 Hz
16 repetitions
OBSERVE H1, 400.2669779 MHz
DATA PROCESSING
Line broadening 0.1 Hz
FT size 32768
Total time 1 min, 52 sec
9
8
7
6
5
4
3
2
1
ppm

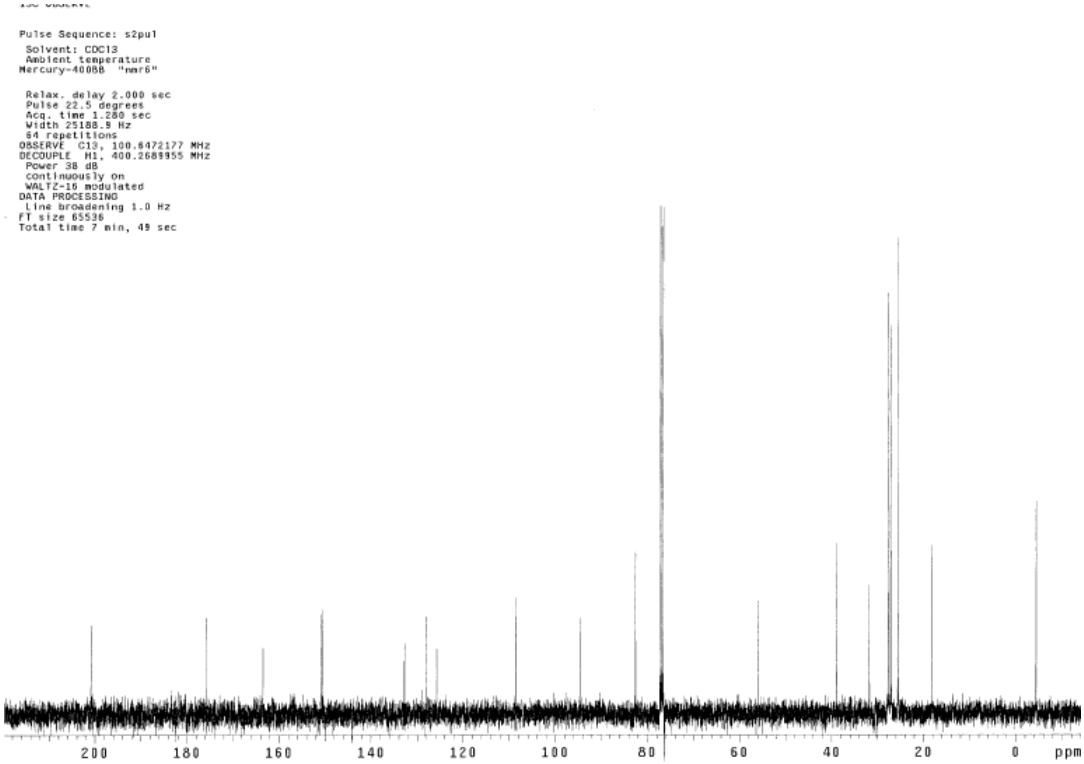
Pulse Sequence: s2pul
Solvent: CDCl3
Ambient temperature
Mercury-400BB "nmr6"
Relax. delay 2.000 sec
Pulse 22.5 degrees
Acq. time 1.280 sec
Width 25188.9 Hz
84 repetitions
OBSERVE C13, 100.6472177 MHz
DECOUPLE H1, 400.2689955 MHz
Power 38 dB
continuously on
WALTZ-16 modulated
DATA PROCESSING
Line broadening 1.0 Hz
FT size 65536
Total time 7 min, 49 sec
200
180
160
140
120
100
80
60
40
20
0
ppm

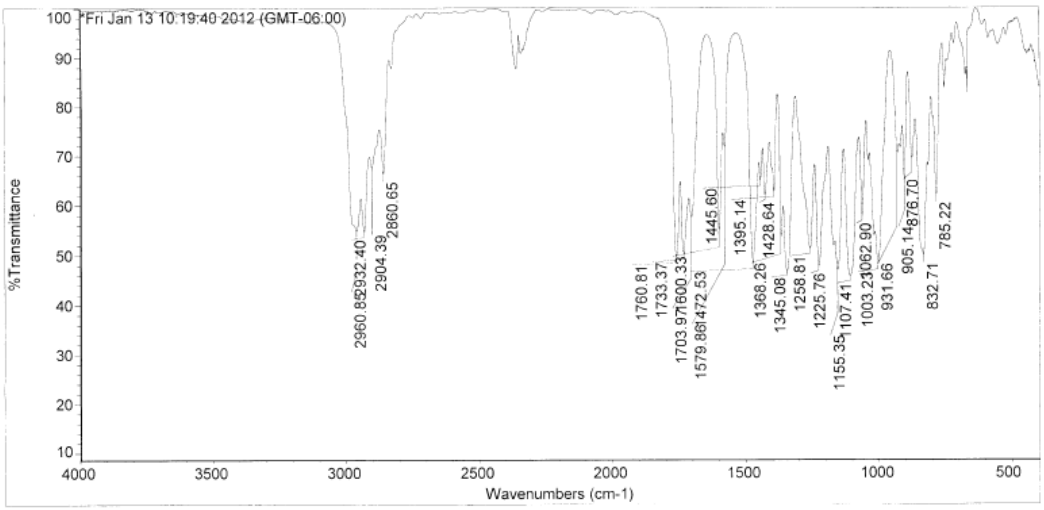

Fri Jan 13 10:24:19 2012 (GMT-06:00)
FIND PEAKS:

Spectrum:	*Fri Jan 13 10:19:40 2012 (GMT-06:00)
Region:	4000.00 400.00
Absolute threshold:	72.901
Sensitivity:	50
Peak list:	

Position:	785.22	Intensity:	62.100
Position:	832.71	Intensity:	50.042
Position:	876.70	Intensity:	69.451
Position:	905.14	Intensity:	64.933
Position:	931.66	Intensity:	70.488
Position:	1003.23	Intensity:	48.156
Position:	1062.90	Intensity:	57.936
Position:	1107.41	Intensity:	45.797

t-BuO2C
O
PivO
MOMO
OH
NMe2

2.74

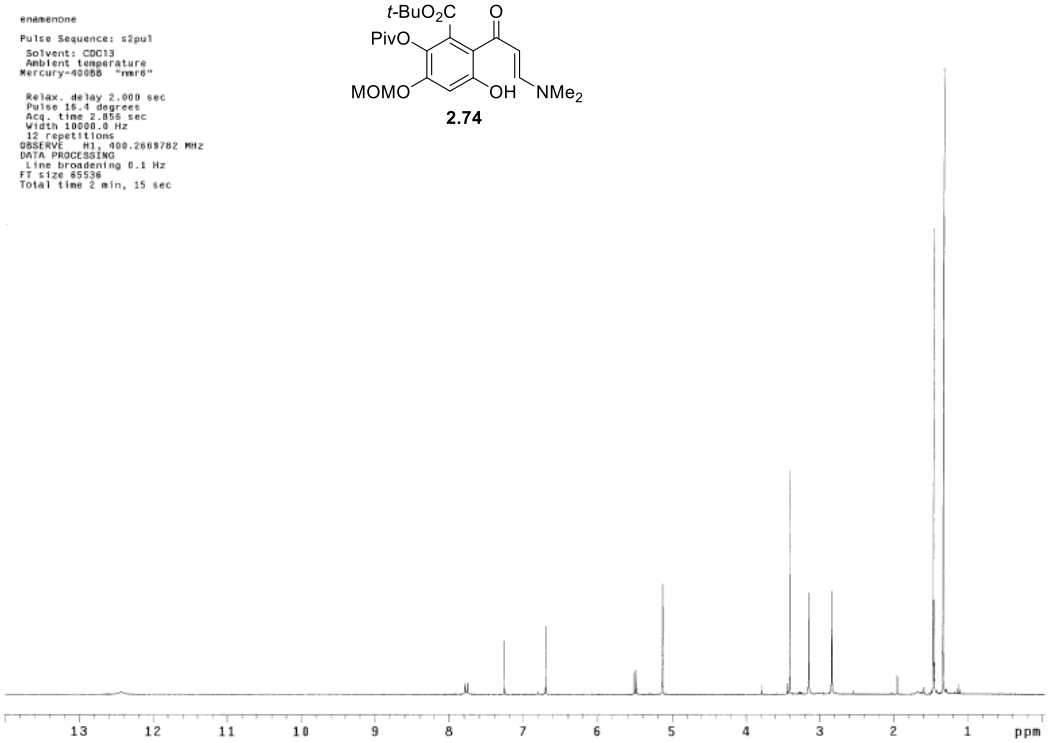
enamenone
Pulse Sequence: s2pul
Solvent: CDCl3
Ambient temperature
Mercury-400BB "nmr6"
Relax. delay 2.000 sec
Pulse 15.4 degrees
Acq. time 2.856 sec
Width 10000.0 Hz
12 repetitions
OBSERVE H1, 400.2669782 MHz
DATA PROCESSING
Line broadening 0.1 Hz
FT size 65536
Total time 2 min, 15 sec
13
12
11
10
9
8
7
6
5
4
3
2
1
ppm

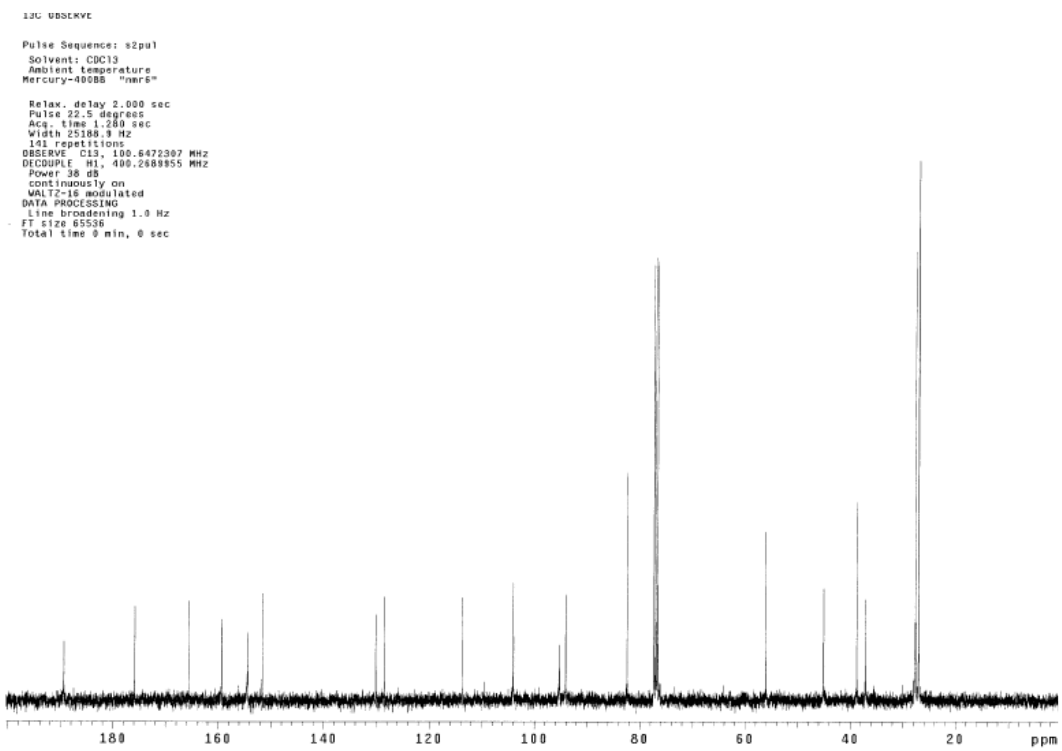
13C OBSERVE
Pulse Sequence: s2pul
Solvent: CDCl3
Ambient temperature
Mercury-400BB "nmr6"
Relax. delay 2.000 sec
Pulse 22.5 degrees
Acq. time 1.280 sec
Width 25188.9 Hz
141 repetitions
OBSERVE C13, 100.6472307 MHz
DECOUPLE H1, 400.2669855 MHz
Power 38 dB
continuously on
WALTZ-16 modulated
DATA PROCESSING
Line broadening 1.0 Hz
FT size 65536
Total time 0 min, 0 sec
180
160
140
120
100
80
60
40
20
ppm

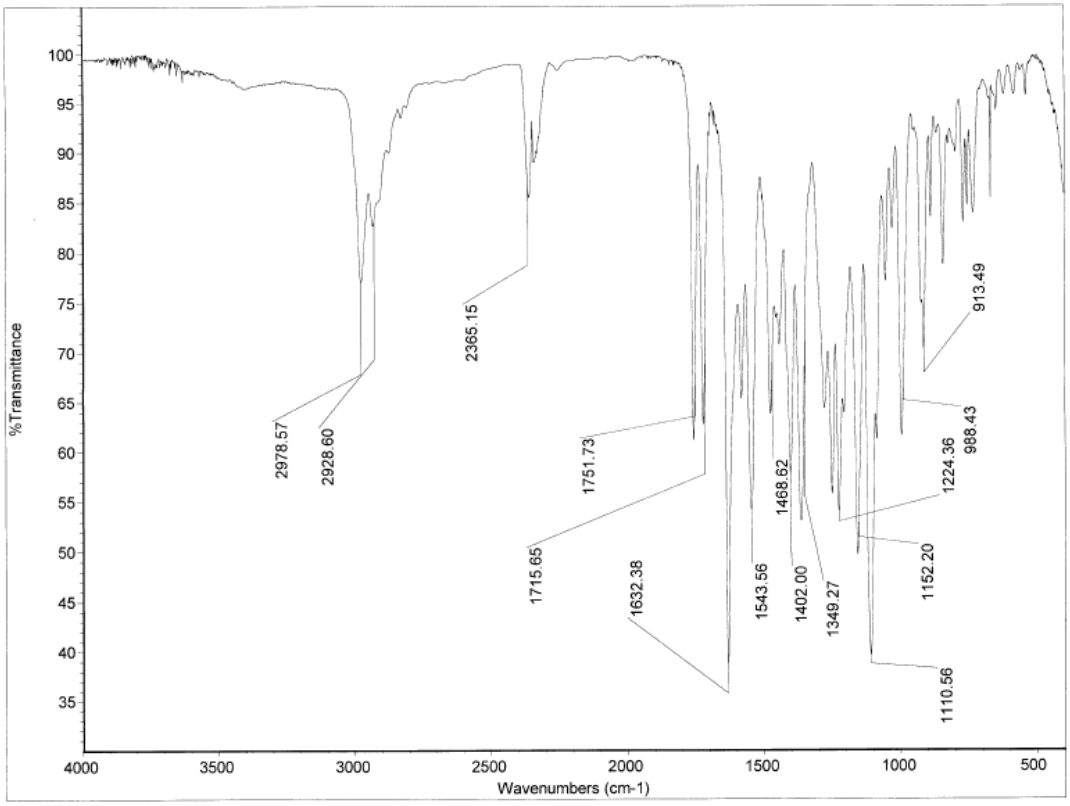
%Transmittance
100
95
90
85
80
75
70
65
60
55
50
45
40
35
4000
3500
3000
2500
2000
1500
1000
500
Wavenumbers (cm-1)
2978.57
2928.60
2365.15
1751.73
1715.65
1632.38
1543.56
1468.62
1402.00
1349.27
1224.36
1152.20
1110.56
988.43
913.49

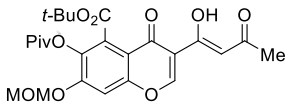
t-BuO2C
O
OH
O
PivO
Me
MOMO
O

2.75

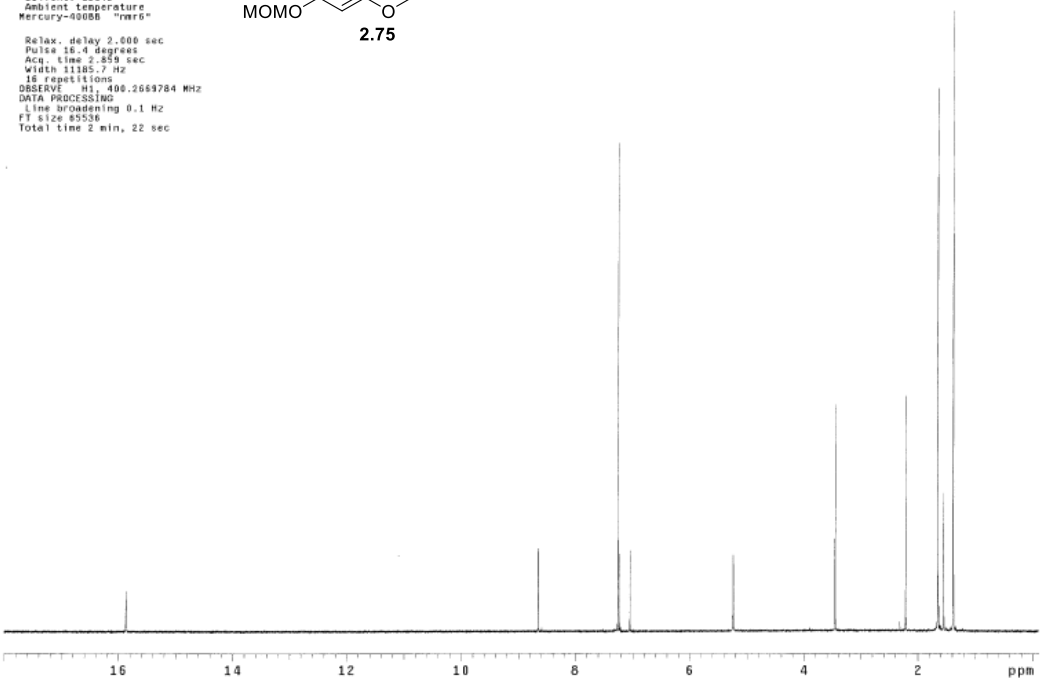
ae_viii_tc
Pulse Sequence: s2pul
Solvent: CDCl3
Ambient temperature
Mercury-400BB "rwr6"
Relax. delay 2.000 sec
Pulse 16.4 degrees
Acq. time 2.859 sec
Width 11185.7 Hz
16 repetitions
OBSERVE H1, 400.2669784 MHz
DATA PROCESSING
Line broadening 0.1 Hz
FT size 65536
Total time 2 min, 22 sec
16
14
12
10
8
6
4
2
ppm

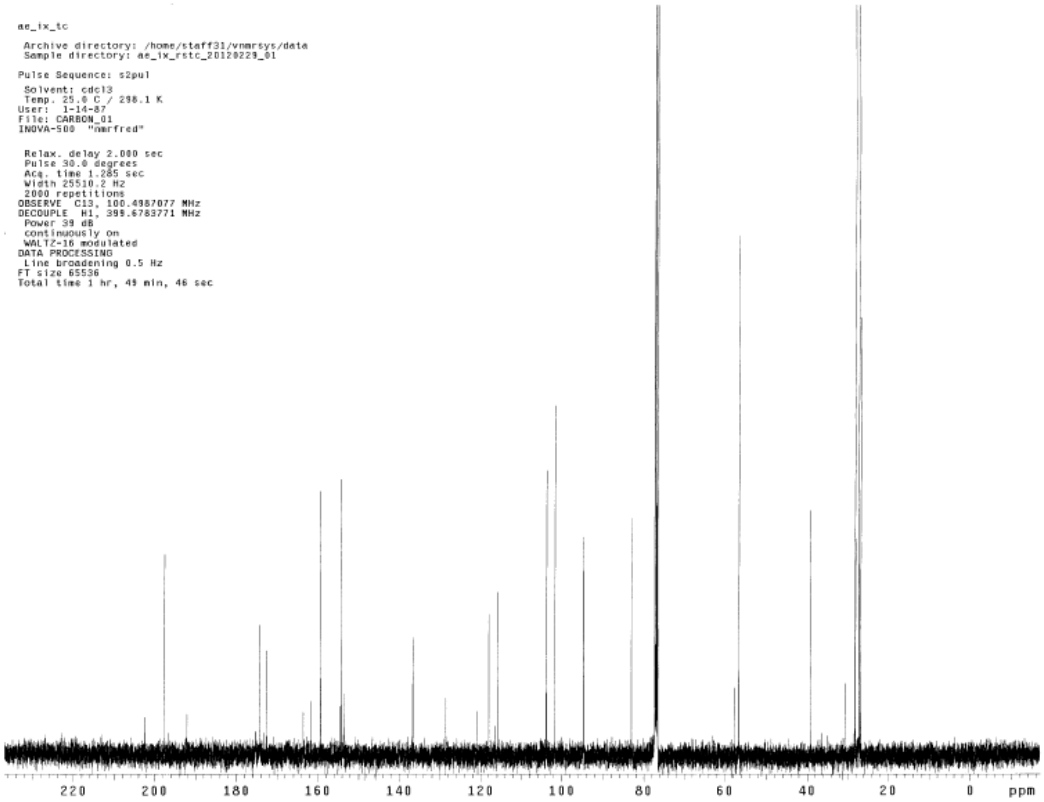
ae_ix_tc
Archive directory: /home/staff31/vnmrsys/data
Sample directory: ae_ix_rstc_20120229_01
Pulse Sequence: s2pul
Solvent: cdcl3
Temp. 25.0 C / 298.1 K
User: 1-14-87
File: CARBON_01
INOVA-500 "nmrfred"
Relax. delay 2.000 sec
Pulse 30.0 degrees
Acq. time 1.285 sec
Width 25510.2 Hz
2000 repetitions
OBSERVE C13, 100.4987077 MHz
DECOUPLE H1, 399.6783771 MHz
Power 39 dB
continuously on
WALTZ-16 modulated
DATA PROCESSING
Line broadening 0.5 Hz
FT size 65536
Total time 1 hr, 49 min, 46 sec
220
200
180
160
140
120
100
80
60
40
20
0
ppm

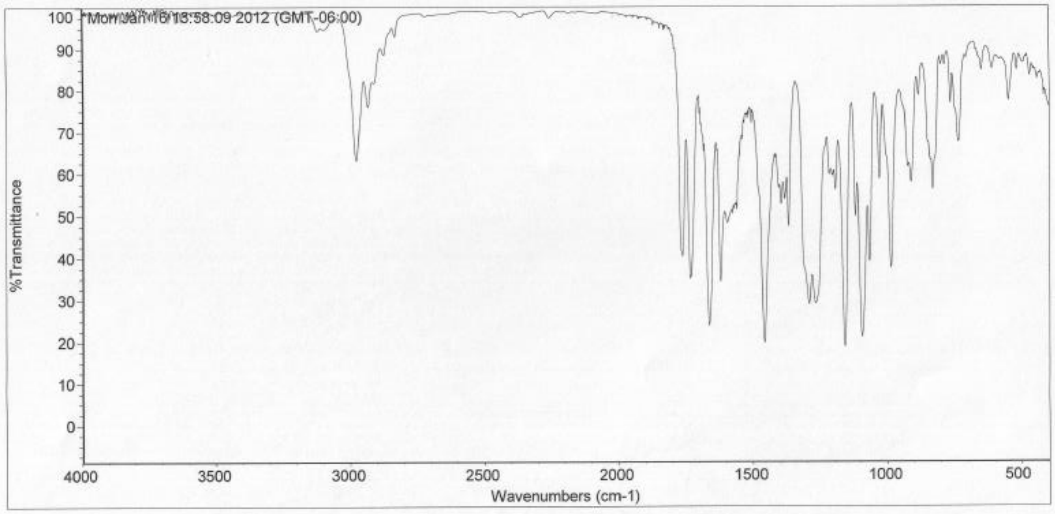

Mon Jan 16 14:02:19 2012 (GMT-06:00)
FIND PEAKS:

Spectrum:	*Mon Jan 16 13:58:09 2012 (GMT-06:00)	
Region:	4000.00	400.00
Absolute threshold:	15.889	
Sensitivity:	50	
Peak list:		

No peaks were found.

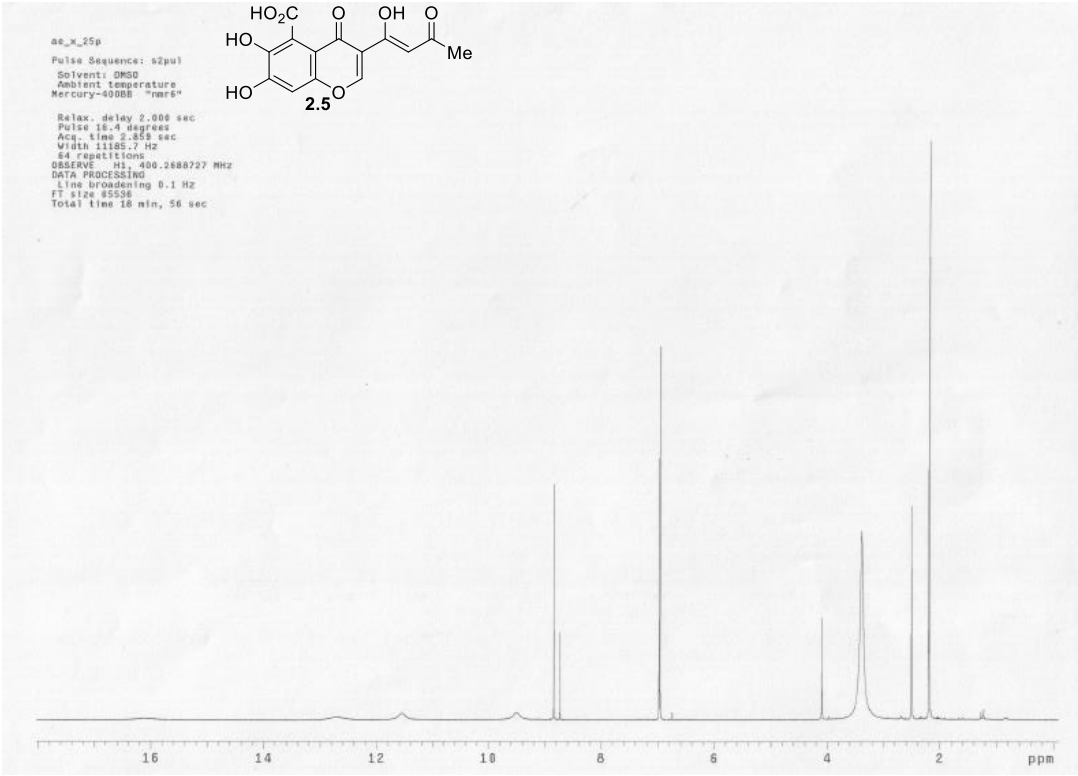
HO2C
O
OH
O
HO
Me
HO
O
2.5
ae_x_25p
Pulse Sequence: s2pul
Solvent: DMSO
Ambient temperature
Mercury-400BB "nmr5"
Relax. delay 2.000 sec
Pulse 16.4 degrees
Acq. time 2.859 sec
Width 11185.7 Hz
64 repetitions
OBSERVE H1, 400.2688727 MHz
DATA PROCESSING
Line broadening 0.1 Hz
FT size 65536
Total time 18 min, 56 sec
16
14
12
10
8
6
4
2
ppm

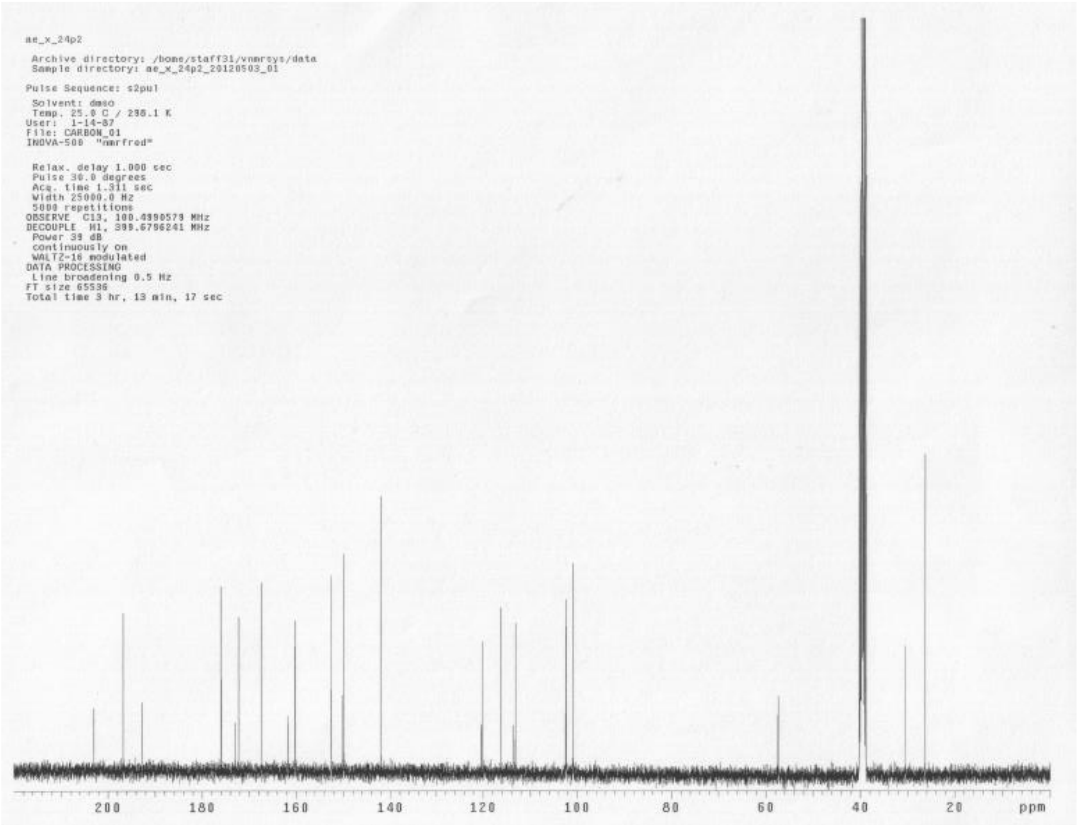
ae_x_24p2
Archive directory: /home/staff31/vnmrsys/data
Sample directory: ae_x_24p2_20120503_01
Pulse Sequence: s2pul
Solvent: dmso
Temp. 25.0 C / 298.1 K
User: 1-14-87
File: CARBON_01
INOVA-500 "nmrfred"
Relax. delay 1.000 sec
Pulse 30.0 degrees
Acq. time 1.311 sec
Width 25000.0 Hz
5000 repetitions
OBSERVE C13, 100.4990573 MHz
DECOUPLE H1, 399.6796241 MHz
Power 39 dB
continuously on
WALTZ-16 modulated
DATA PROCESSING
Line broadening 0.5 Hz
FT size 65536
Total time 3 hr, 13 min, 17 sec
200
180
160
140
120
100
80
60
40
20
ppm

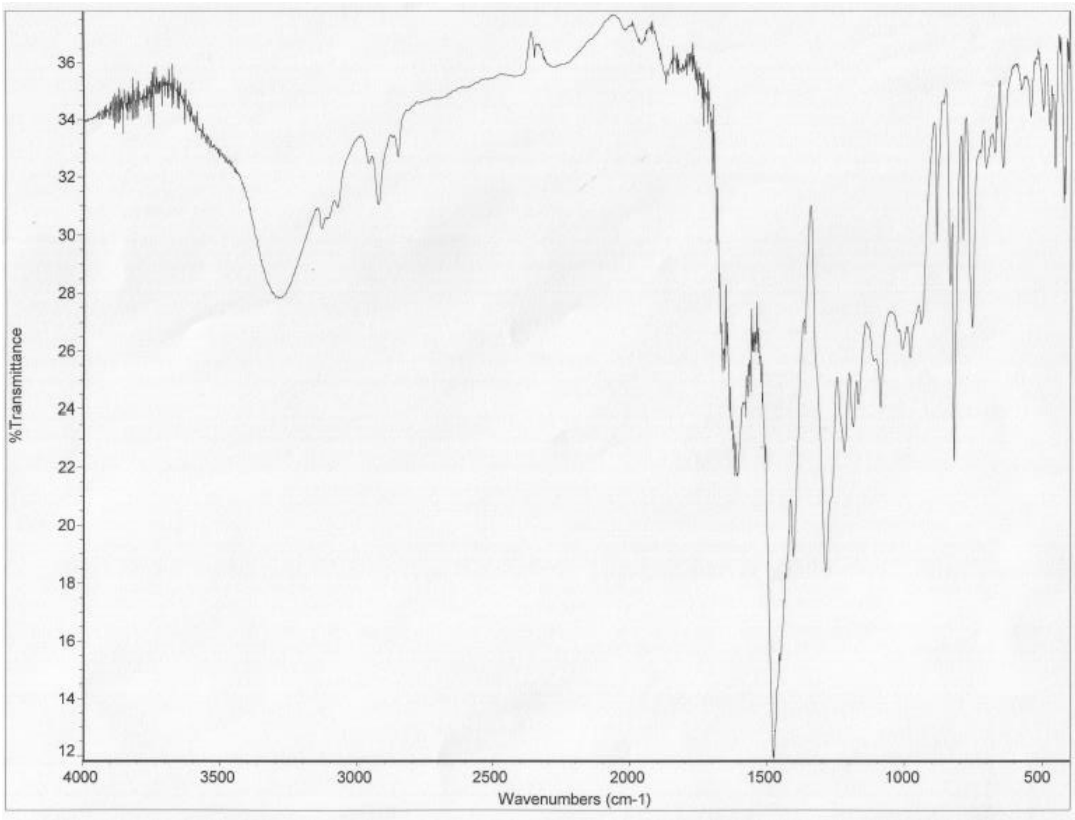
%Transmittance
36
34
32
30
28
26
24
22
20
18
16
14
12
4000
3500
3000
2500
2000
1500
1000
500
Wavenumbers (cm-1)

vinaxanthone (**2.1**)

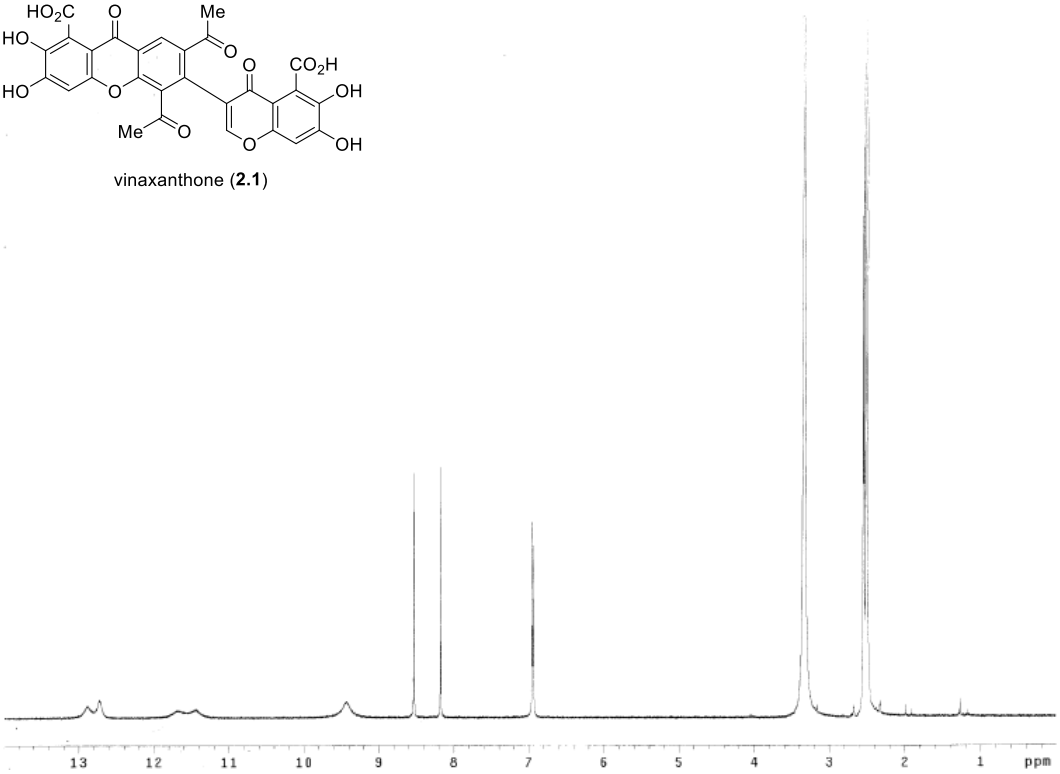

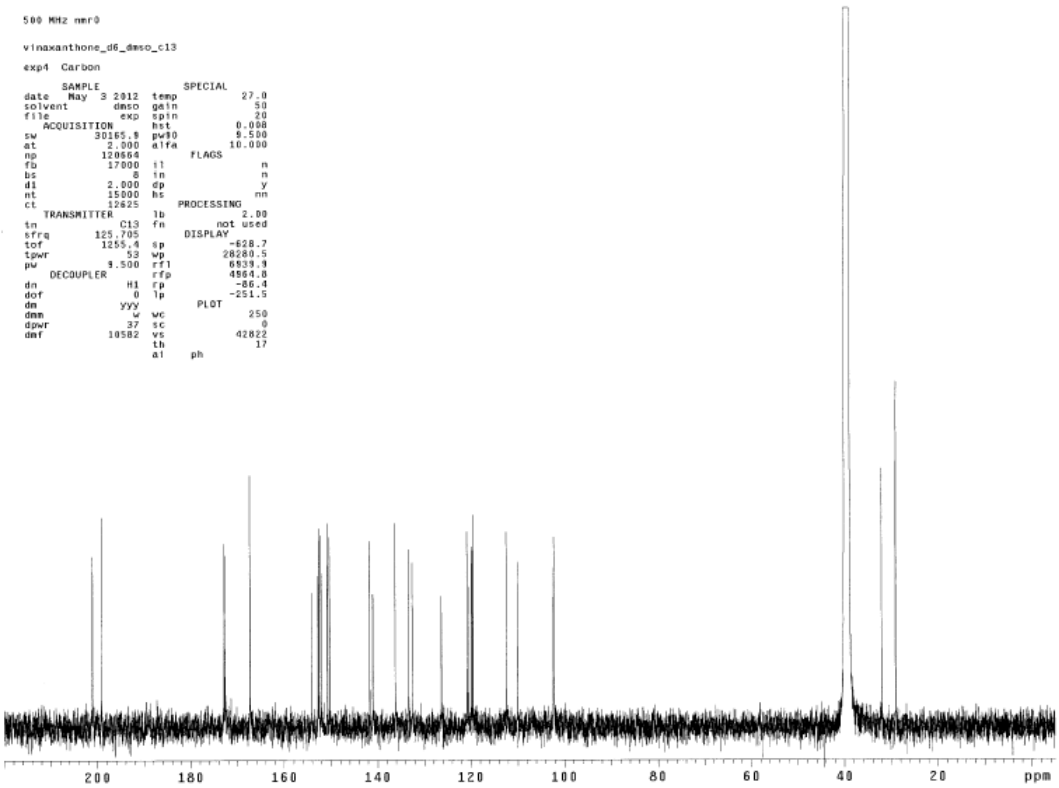

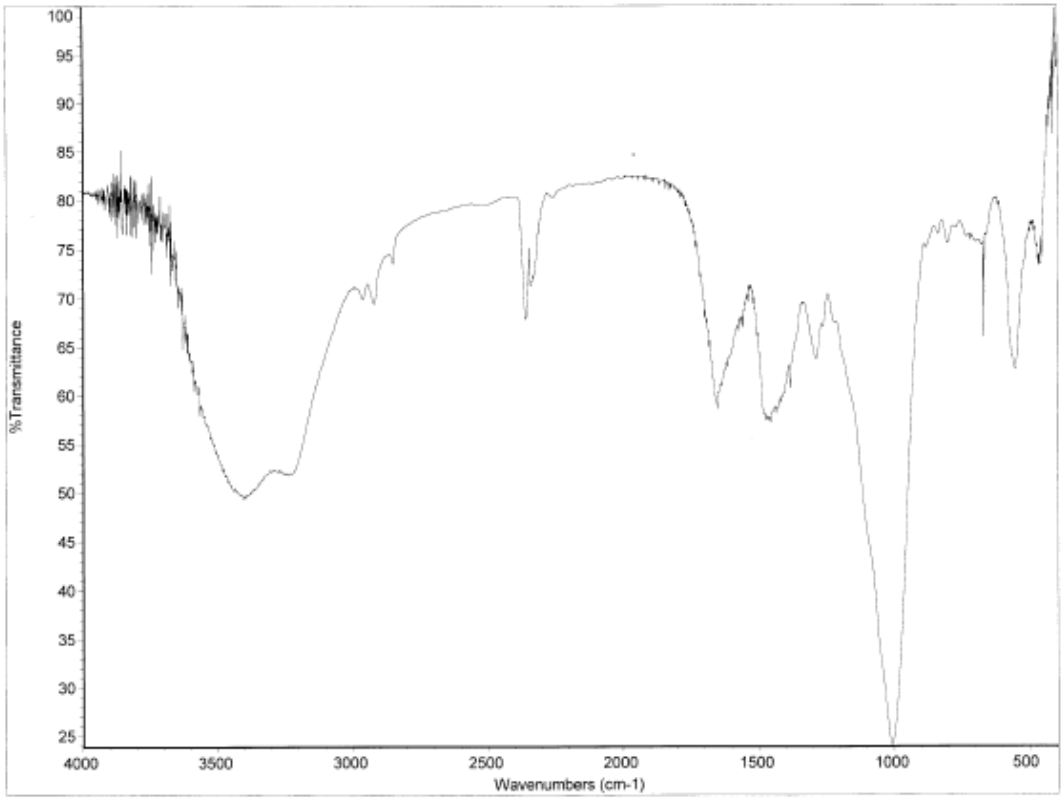
%Transmittance
100
95
90
85
80
75
70
65
60
55
50
45
40
35
30
25
4000
3500
3000
2500
2000
1500
1000
500
Wavenumbers (cm-1)

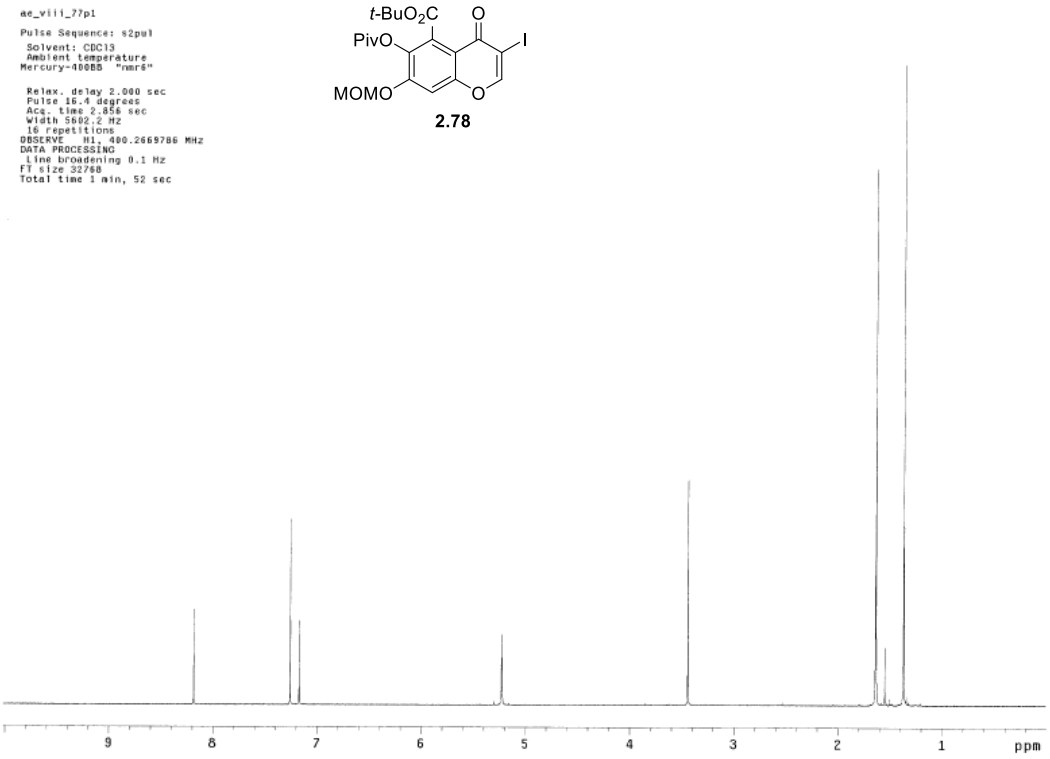
ae_viii_77p1
Pulse Sequence: s2pul
Solvent: CDCl3
Ambient temperature
Mercury-400BB "nmr6"
Relax. delay 2.000 sec
Pulse 16.4 degrees
Acq. time 2.856 sec
Width 5602.2 Hz
16 repetitions
OBSERVE H1, 400.2669786 MHz
DATA PROCESSING
Line broadening 0.1 Hz
FT size 32768
Total time 1 min, 52 sec
t-BuO2C
O
PivO
I
MOMO
O
2.78
9
8
7
6
5
4
3
2
1
ppm

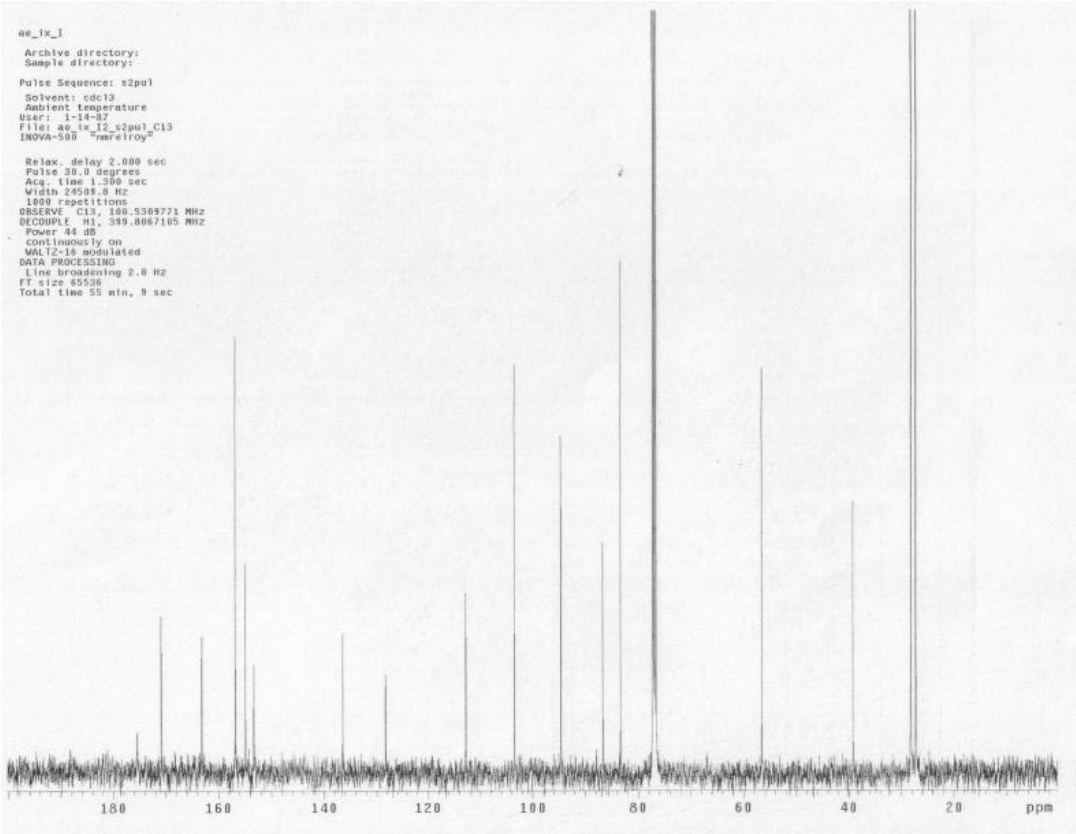
ae_ix_I
Archive directory:
Sample directory:
Pulse Sequence: s2pul
Solvent: cdcl3
Ambient temperature
User: 1-14-07
File: ae_ix_I2_s2pul_C13
INOVA-500 "nmrelroy"
Relax. delay 2.000 sec
Pulse 30.0 degrees
Acq. time 1.300 sec
Width 24509.8 Hz
1000 repetitions
OBSERVE C13, 100.5369771 MHz
DECOUPLE H1, 399.8067105 MHz
Power 44 dB
continuously on
WALTZ-16 modulated
DATA PROCESSING
Line broadening 2.0 Hz
FT size 65536
Total time 55 min, 9 sec
180
160
140
120
100
80
60
40
20
ppm

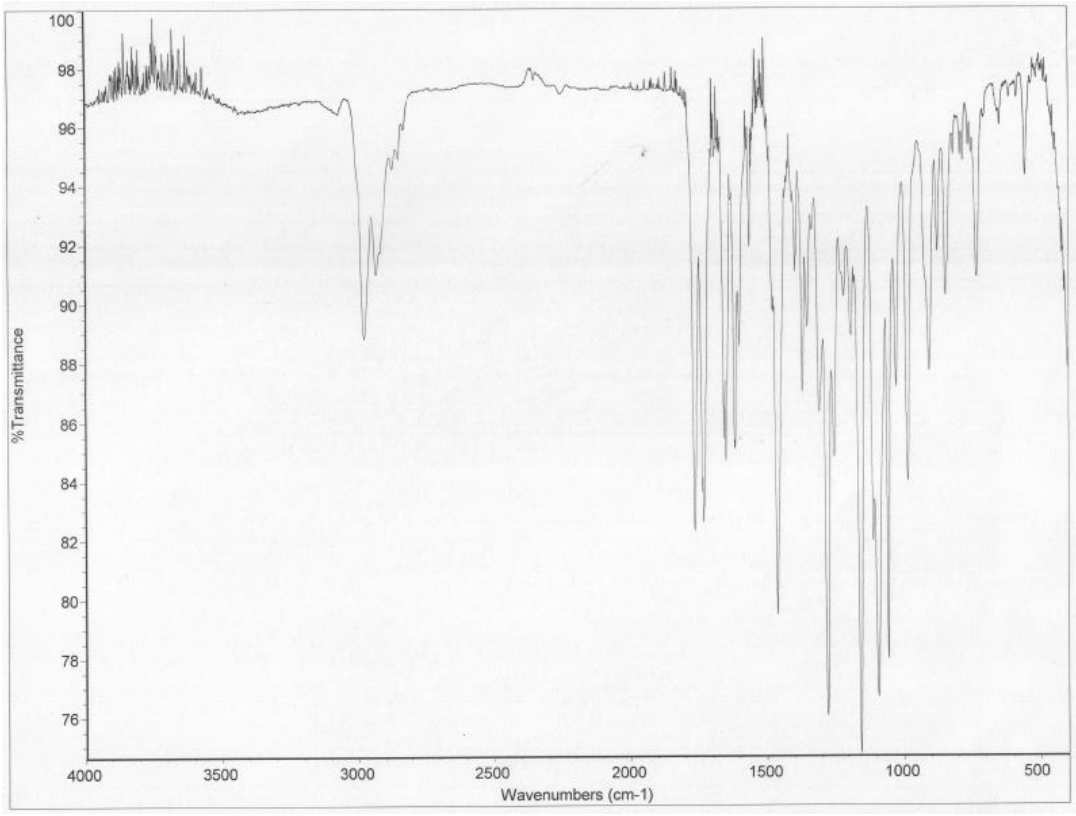
100
98
96
94
92
90
88
86
84
82
80
78
76
%Transmittance
4000
3500
3000
2500
2000
1500
1000
500
Wavenumbers (cm-1)

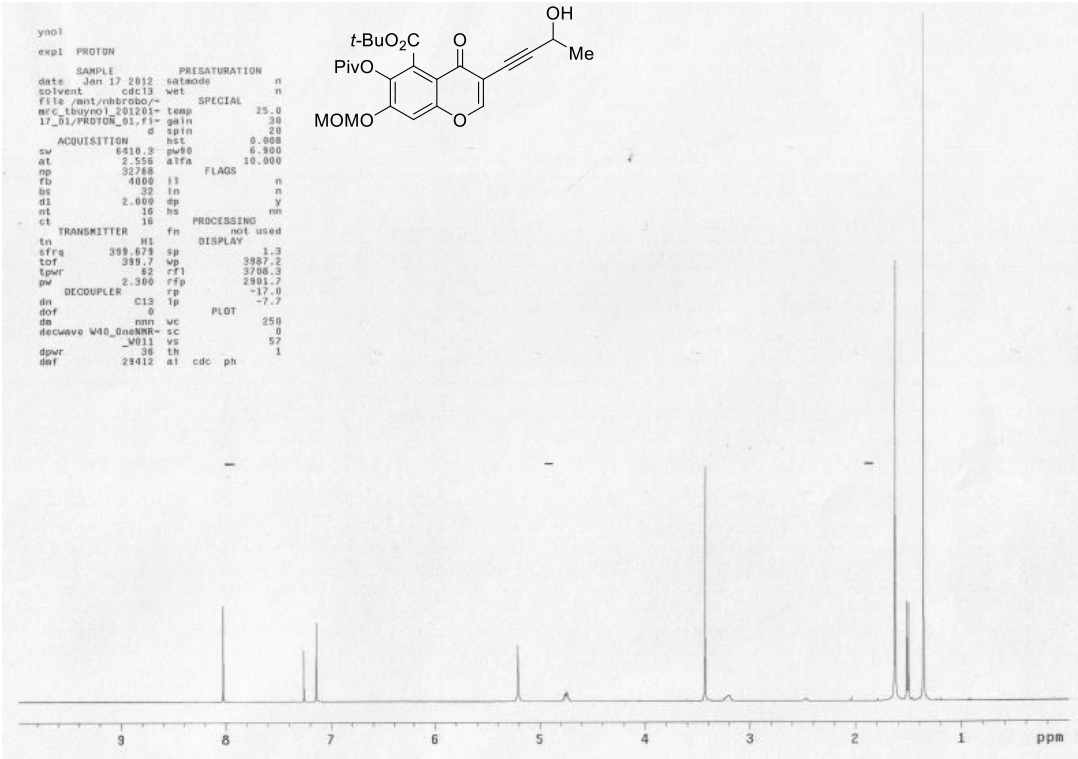
ynol
expl PROTON
SAMPLE
date Jan 17 2012
solvent cdcl3
file /mnt/nhbrobo/~
mrc_tbuynol_201201~
17_01/PROTON_01.fi~
d
ACQUISITION
sw 6410.3
at 2.556
np 32768
fb 4000
bs 32
d1 2.000
nt 16
ct 16
TRANSMITTER
tn H1
sfrq 399.679
tof 399.7
tpwr 62
pw 2.300
DECOUPLER
dn C13
dof 0
dm nnn
decwave W40_OneNMR~
_W011
dpwr 36
dmf 29412
PRESATURATION
satmode n
wet n
SPECIAL
temp 25.0
gain 30
spin 20
hst 0.008
pw90 6.300
alfa 10.000
FLAGS
il n
in n
dp y
hs nn
PROCESSING
fn not used
DISPLAY
sp 1.3
wp 3987.2
rf1 3708.3
rfp 2901.7
rp -17.0
lp -7.7
PLOT
wc 250
sc 0
vs 57
th 1
al cdc ph
t-BuO2C
O
OH
Me
PivO
MOMO
O
9
8
7
6
5
4
3
2
1
ppm

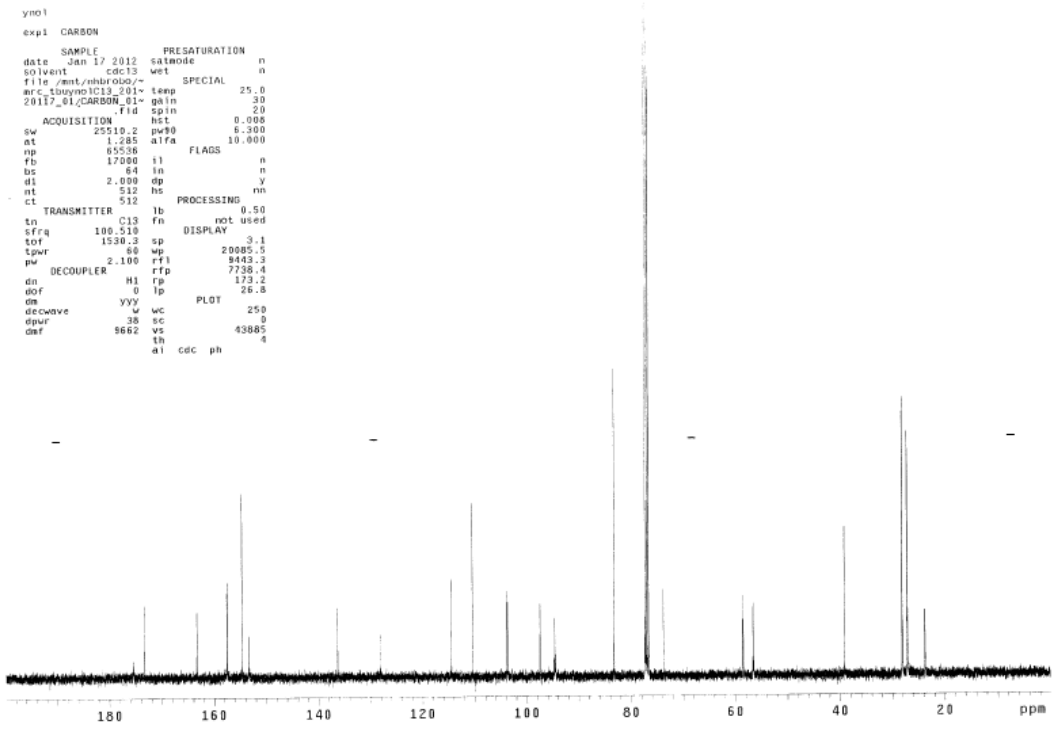
ynol
expl CARBON
SAMPLE
date Jan 17 2012
solvent cdcl3
file /mnt/nhbrobo/~
mrc_tbuynolC13_201~
20117_01/CARBON_01~
.fid
ACQUISITION
sw 25510.2
at 1.285
np 65536
fb 17000
bs 64
d1 2.000
nt 512
ct 512
TRANSMITTER
tn C13
sfrq 100.510
tof 1530.3
tpwr 60
pw 2.100
DECOUPLER
dn H1
dof 0
dm yyy
decwave w
dpwr 38
dmf 9662
PRESATURATION
satmode n
wet n
SPECIAL
temp 25.0
gain 30
spin 20
hst 0.008
pw90 6.300
alfa 10.000
FLAGS
il n
in n
dp y
hs nn
PROCESSING
lb 0.50
fn not used
DISPLAY
sp 3.1
wp 20085.5
rf1 9443.3
rfp 7738.4
rp 173.2
lp 26.8
PLOT
wc 250
sc 0
vs 43885
th 4
al cdc ph
180
160
140
120
100
80
60
40
20
ppm

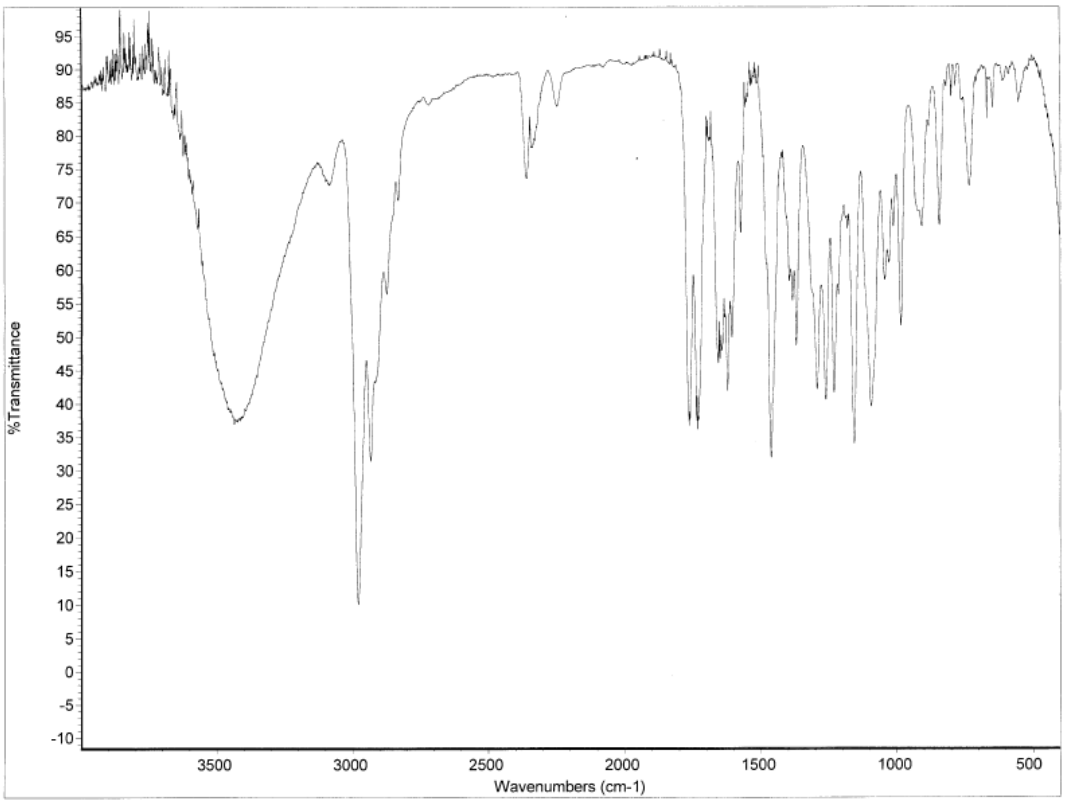
%Transmittance
95
90
85
80
75
70
65
60
55
50
45
40
35
30
25
20
15
10
5
0
-5
-10
3500
3000
2500
2000
1500
1000
500
Wavenumbers (cm-1)

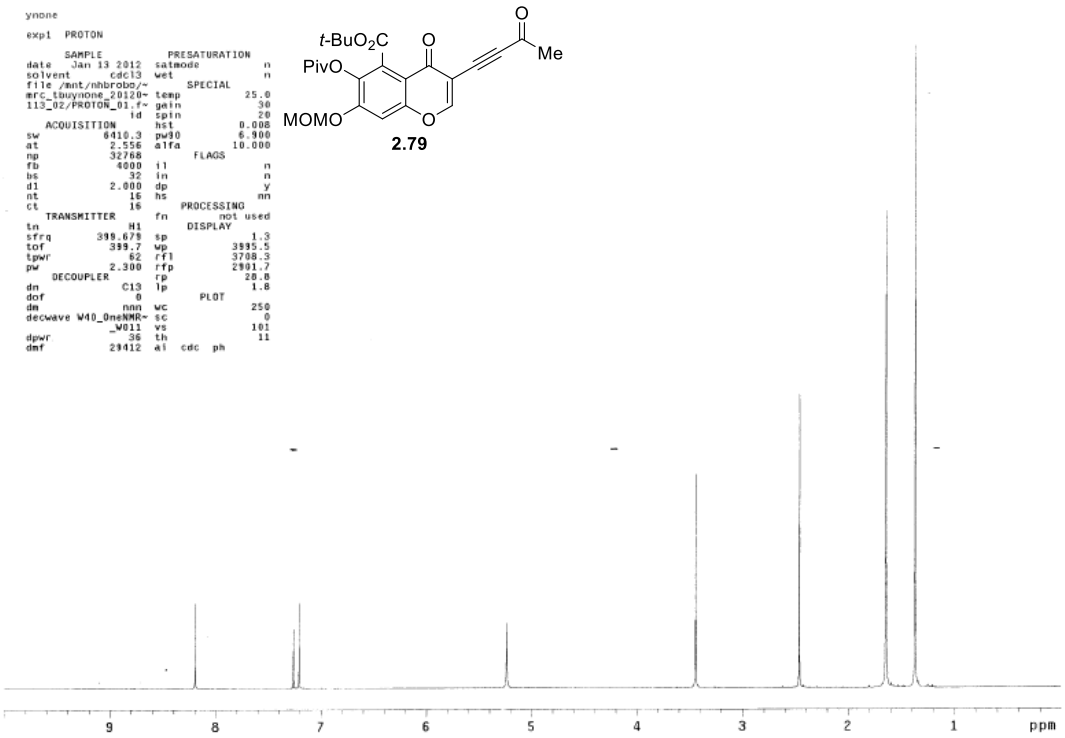
ynone
exp1 PROTON
SAMPLE
date Jan 13 2012
solvent cdcl3
file /mnt/nhbrobo/~
mrc_tbuynone_20120~
113_02/PROTON_01.f~
id
ACQUISITION
sw 6410.3
at 2.556
np 32768
fb 4000
bs 32
d1 2.000
nt 16
ct 16
TRANSMITTER
tn H1
sfrq 399.679
tof 399.7
tpwr 62
pw 2.300
DECOUPLER
dn C13
dof 0
dm nnn
decwave W40_OneNMR~
_W011
dpwr 36
dmf 29412
PRESATURATION
satmode n
wet n
SPECIAL
temp 25.0
gain 30
spin 20
hst 0.008
pw90 6.900
alfa 10.000
FLAGS
il n
in n
dp y
hs nn
PROCESSING
fn not used
DISPLAY
sp 1.3
wp 3995.5
rf1 3708.3
rfp 2901.7
rp 28.8
lp 1.8
PLOT
wc 250
sc 0
vs 101
th 11
al cdc ph
t-BuO2C
O
PivO
MOMO
O
O
Me
2.79
9
8
7
6
5
4
3
2
1
ppm

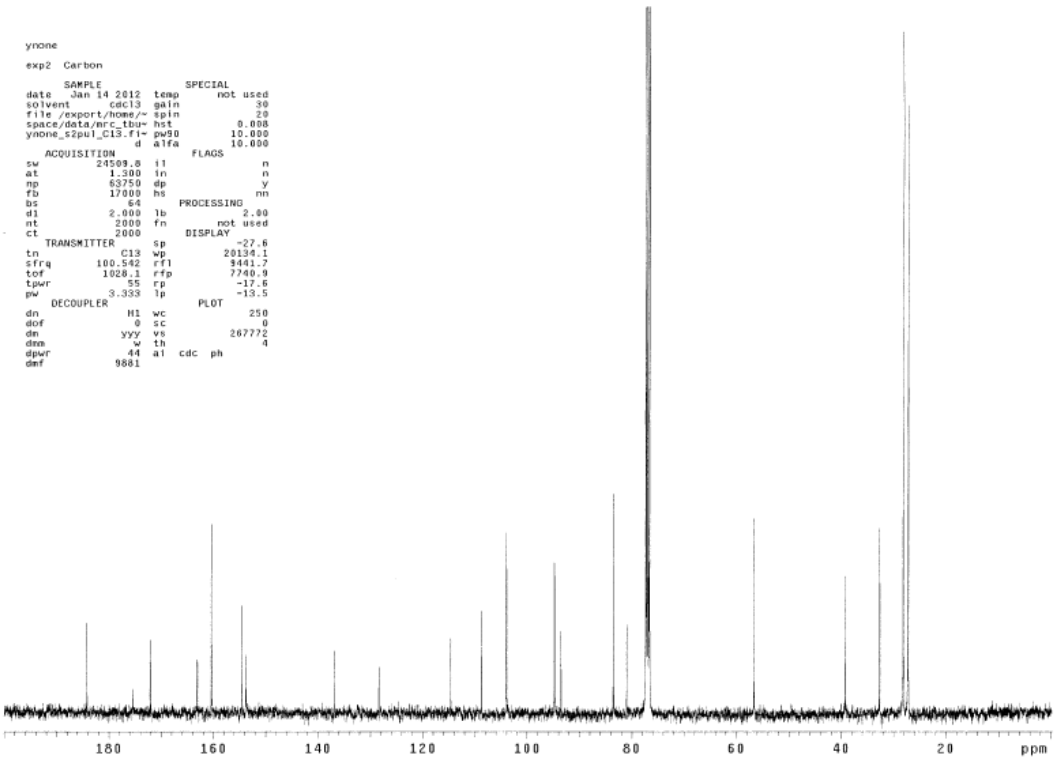
ynone
exp2 Carbon
SAMPLE
date Jan 14 2012
solvent cdcl3
file /export/home/~
space/data/mrc_tbu~
ynone_s2pul_C13.fi~
d
ACQUISITION
sw 24509.8
at 1.300
np 63750
fb 17000
bs 64
d1 2.000
nt 2000
ct 2000
TRANSMITTER
tn C13
sfrq 100.542
tof 1028.1
tpwr 55
pw 3.333
DECOUPLER
dn H1
dof 0
dm yyy
dmm w
dpwr 44
dmf 9881
SPECIAL
temp not used
gain 30
spin 20
hst 0.008
pw90 10.000
alfa 10.000
FLAGS
il n
in n
dp y
hs nn
PROCESSING
lb 2.00
fn not used
DISPLAY
sp -27.6
wp 20134.1
rf1 9441.7
rfp 7740.9
rp -17.6
lp -13.5
PLOT
wc 250
sc 0
vs 267772
th 4
al cdc ph
180
160
140
120
100
80
60
40
20
ppm

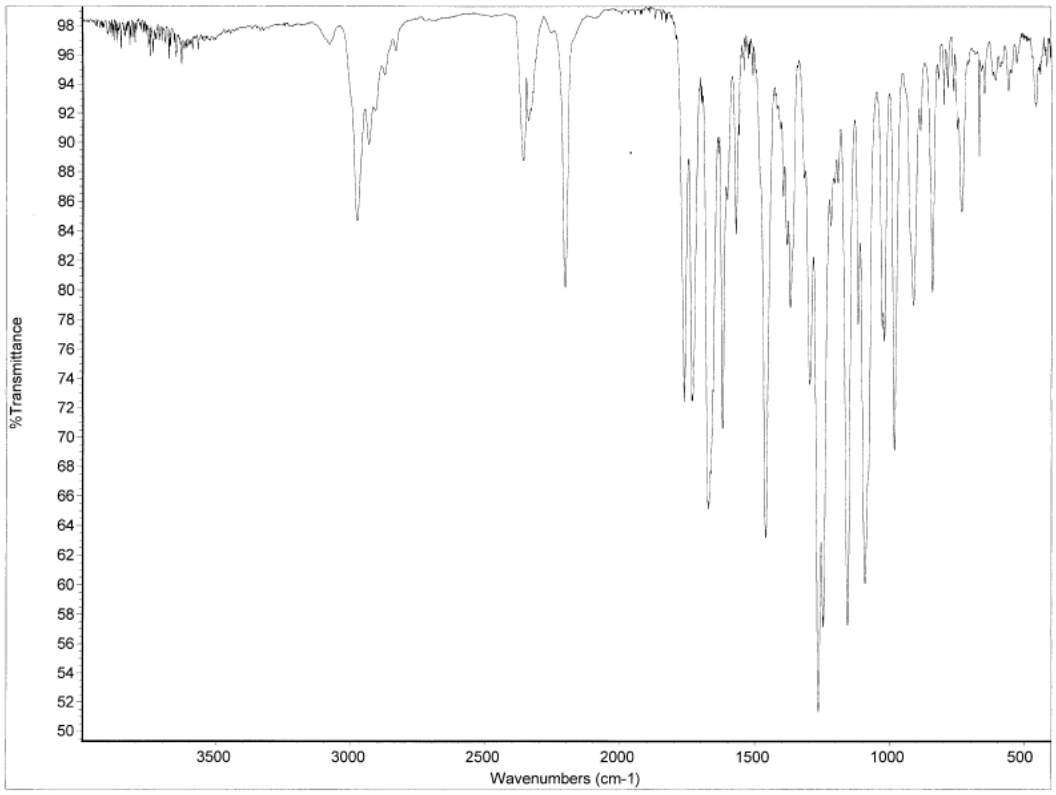
%Transmittance
98
96
94
92
90
88
86
84
82
80
78
76
74
72
70
68
66
64
62
60
58
56
54
52
50
3500
3000
2500
2000
1500
1000
500
Wavenumbers (cm-1)

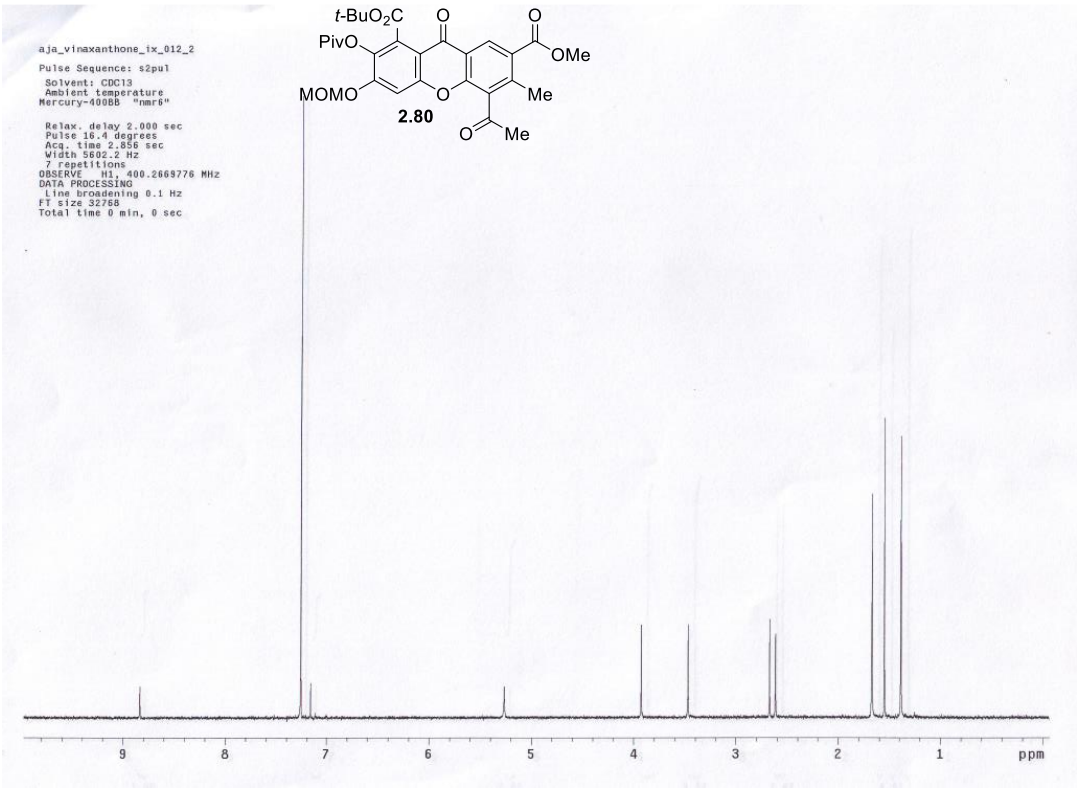
aja_vinaxanthone_ix_012_2
Pulse Sequence: s2pul
Solvent: CDCl3
Ambient temperature
Mercury-400BB "nmr6"
Relax. delay 2.000 sec
Pulse 16.4 degrees
Acq. time 2.856 sec
Width 5602.2 Hz
7 repetitions
OBSERVE H1, 400.2669776 MHz
DATA PROCESSING
Line broadening 0.1 Hz
FT size 32768
Total time 0 min, 0 sec
t-BuO2C
PivO
MOMO
OMe
Me
Me
2.80
9
8
7
6
5
4
3
2
1
ppm

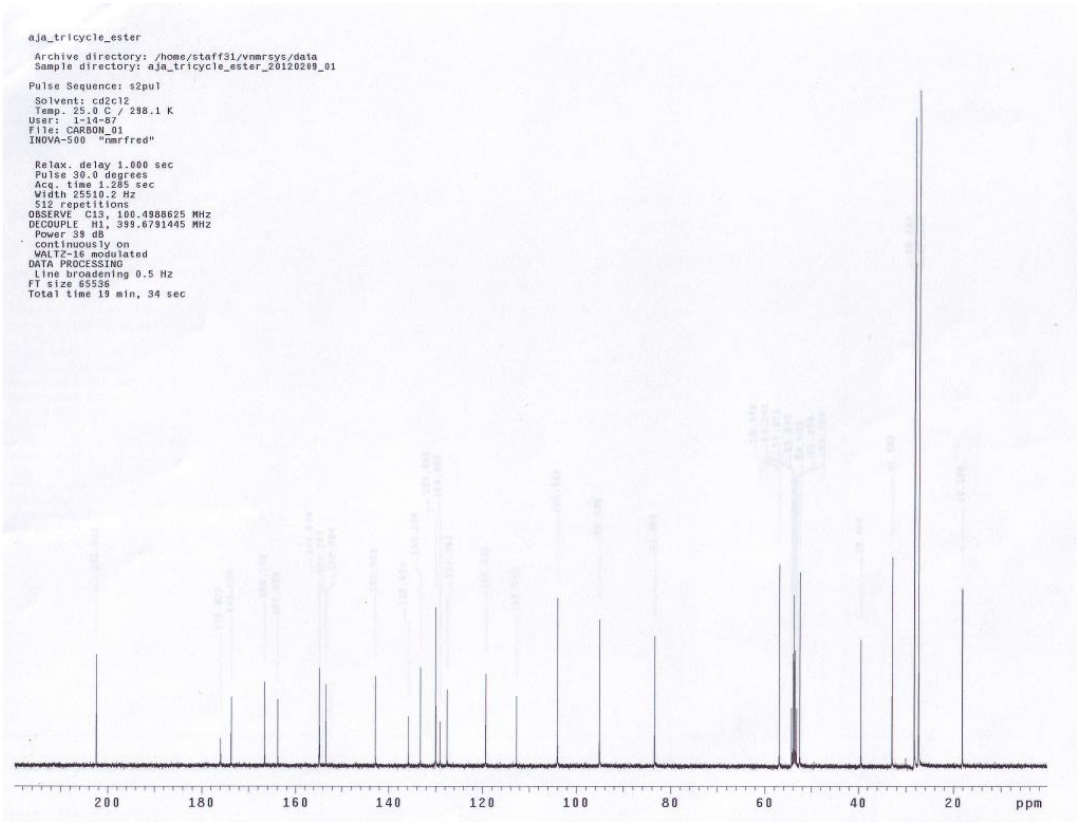
aja_tricycle_ester
Archive directory: /home/staff31/vnmrsys/data
Sample directory: aja_tricycle_ester_20120209_01
Pulse Sequence: s2pul
Solvent: cd2cl2
Temp. 25.0 C / 298.1 K
User: 1-14-87
File: CARBON_01
INOVA-500 "nmrfred"
Relax. delay 1.000 sec
Pulse 30.0 degrees
Acq. time 1.285 sec
Width 25510.2 Hz
512 repetitions
OBSERVE C13, 100.4988625 MHz
DECOUPLE H1, 399.6791445 MHz
Power 39 dB
continuously On
WALTZ-16 modulated
DATA PROCESSING
Line broadening 0.5 Hz
FT size 65536
Total time 19 min, 34 sec
200
180
160
140
120
100
80
60
40
20
ppm

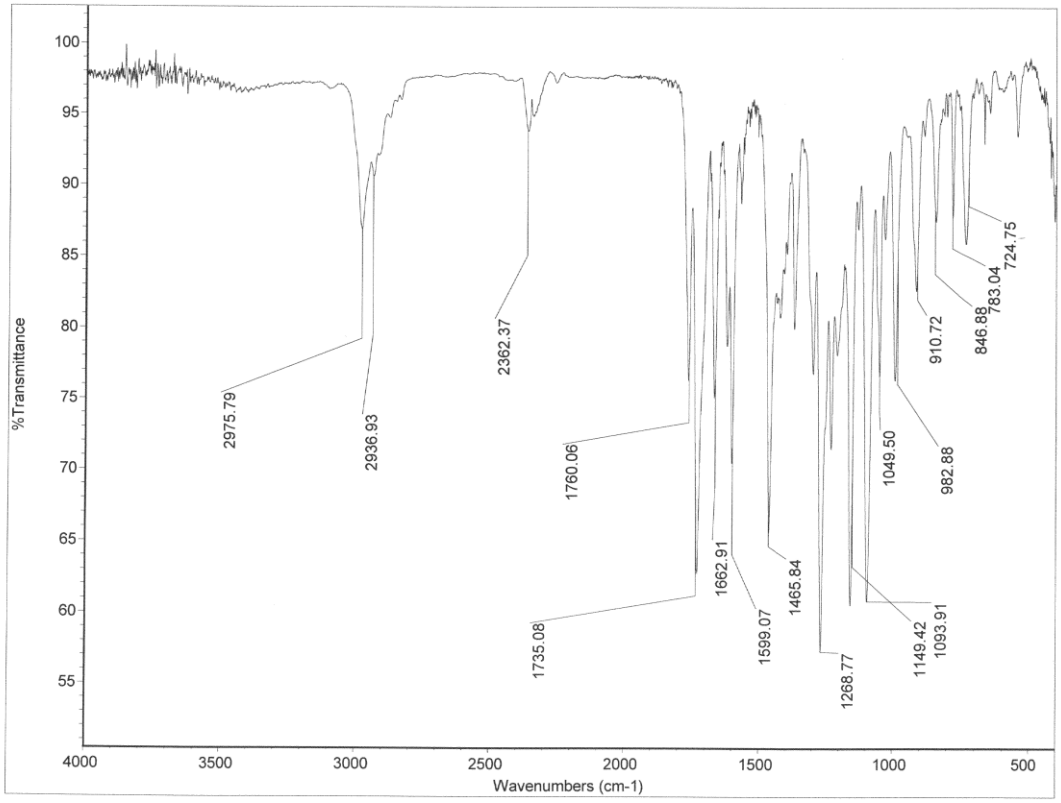
%Transmittance
100
95
90
85
80
75
70
65
60
55
2975.79
2936.93
2362.37
1760.06
1735.08
1662.91
1599.07
1465.84
1268.77
1149.42
1093.91
1049.50
982.88
910.72
846.88
783.04
724.75
4000
3500
3000
2500
2000
1500
1000
500
Wavenumbers (cm-1)

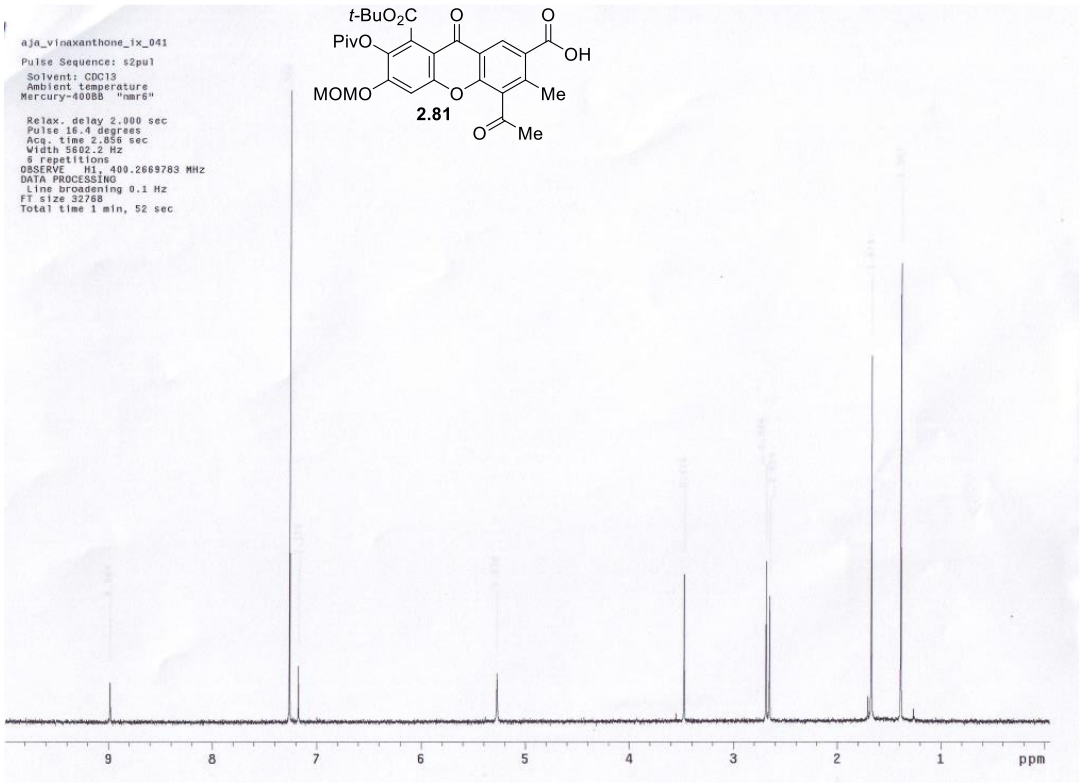
aja_vinaxanthone_ix_041
Pulse Sequence: s2pul
Solvent: CDCl3
Ambient temperature
Mercury-400BB "nmr6"
Relax. delay 2.000 sec
Pulse 16.4 degrees
Acq. time 2.856 sec
Width 5602.2 Hz
6 repetitions
OBSERVE H1, 400.2669783 MHz
DATA PROCESSING
Line broadening 0.1 Hz
FT size 32768
Total time 1 min, 52 sec
t-BuO2C
PivO
MOMO
O
OH
Me
Me
2.81
9
8
7
6
5
4
3
2
1
ppm

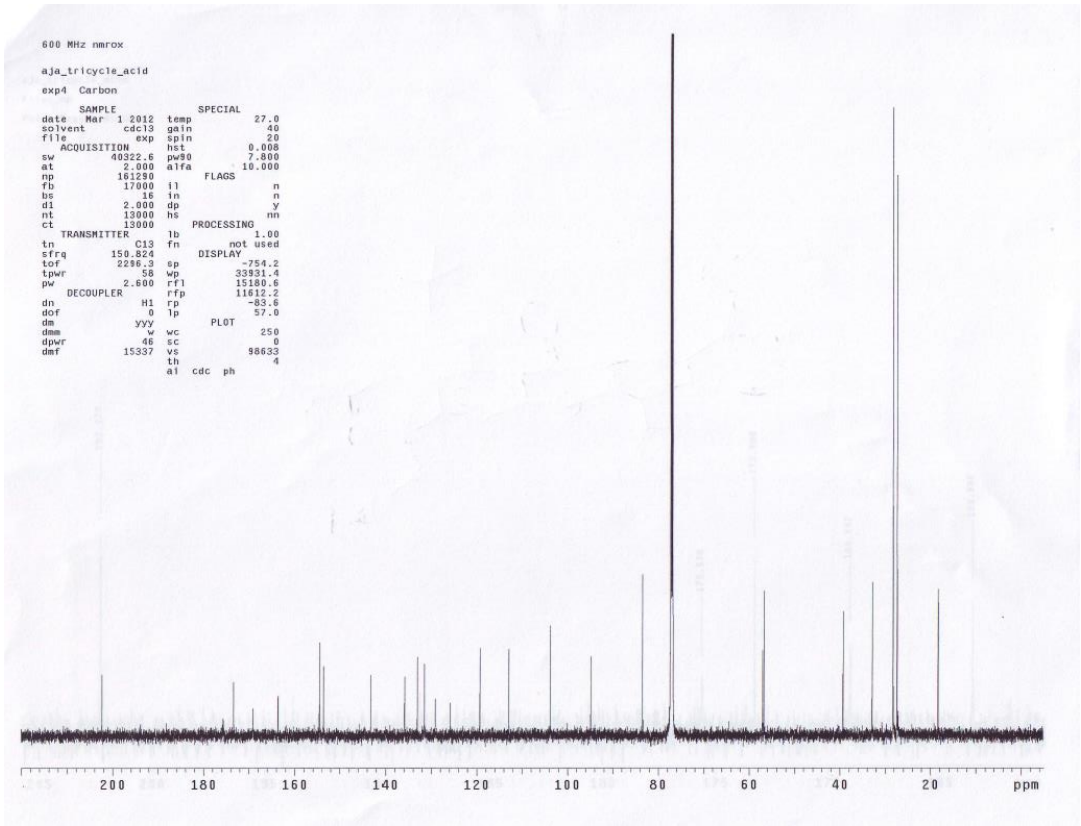
600 MHz nmrox
aja_tricycle_acid
exp4 Carbon
SAMPLE
date Mar 1 2012
solvent cdcl3
file exp
ACQUISITION
sw 40322.6
at 2.000
np 161290
fb 17000
bs 16
d1 2.000
nt 13000
ct 13000
TRANSMITTER
tn C13
sfrq 150.824
tof 2296.3
tpwr 58
pw 2.600
DECOUPLER
dn H1
dof 0
dm yyy
dmm w
dpwr 46
dmf 15337
SPECIAL
temp 27.0
gain 40
spin 20
hst 0.008
pw90 7.800
alfa 10.000
FLAGS
il n
in n
dp y
hs nn
PROCESSING
lb 1.00
fn not used
DISPLAY
sp -754.2
wp 33931.4
rf1 15180.6
rfp 11612.2
rp -83.6
lp 57.0
PLOT
wc 250
sc 0
vs 98633
th 4
al cdc ph
200
180
160
140
120
100
80
60
40
20
ppm

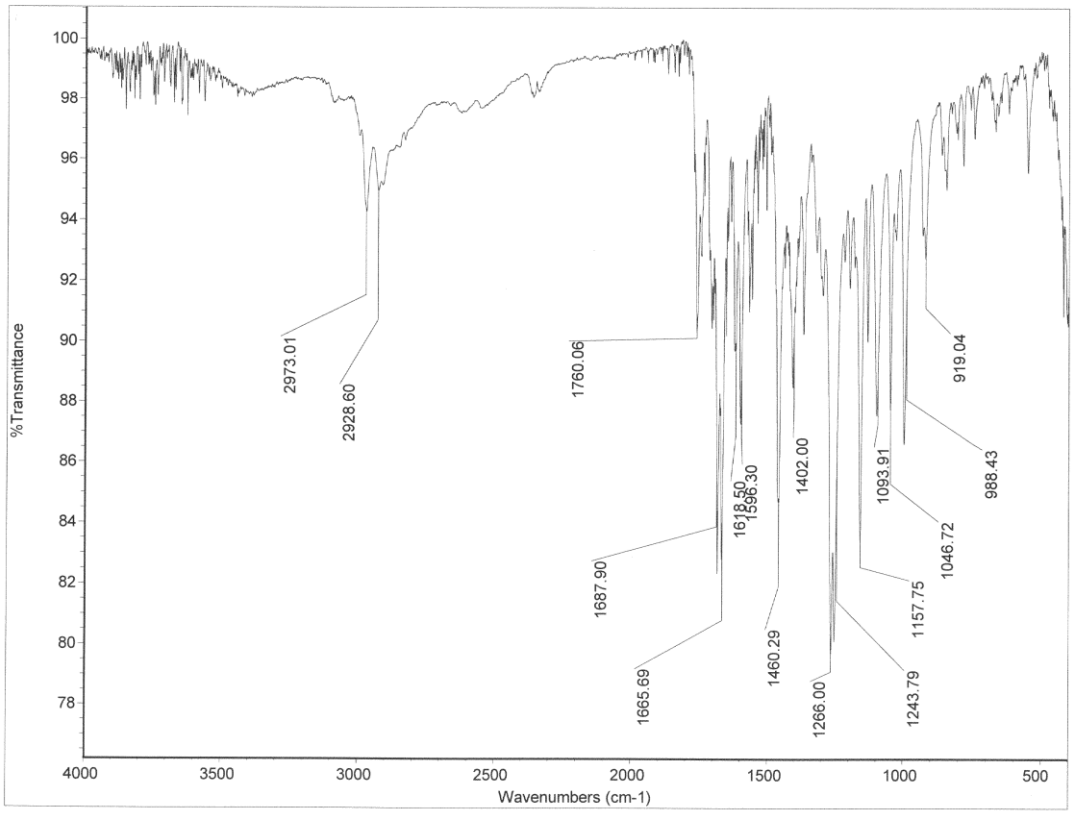
%Transmittance
100
98
96
94
92
90
88
86
84
82
80
78
4000
3500
3000
2500
2000
1500
1000
500
Wavenumbers (cm-1)
2973.01
2928.60
1760.06
1687.90
1665.69
1618.50
1596.30
1460.29
1402.00
1266.00
1243.79
1157.75
1093.91
1046.72
988.43
919.04

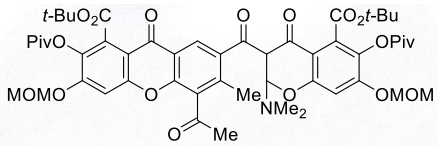

2.87

aja_aminal

Archive directory: /home/staff31/vnmrsys/data
Sample directory: aja_aminal_20120517_01

Pulse Sequence: s2pul

Solvent: acetone
Temp. 25.0 C / 298.1 K
File: PROTON_01
INOVA-500 "nmrfred"

Relax. delay 1.000 sec
Pulse 45.0 degrees
Acq. time 2.556 sec
Width 6410.3 Hz
16 repetitions
OBSERVE H1, 399.6777962 MHz
DATA PROCESSING
FT size 32768
Total time 0 min, 57 sec

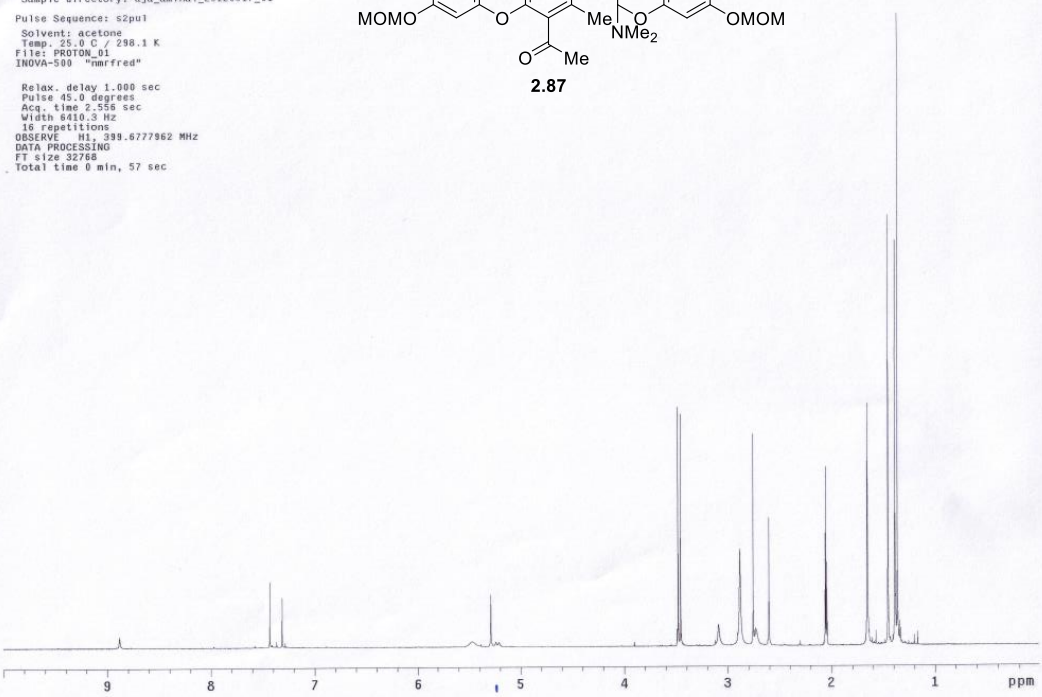

500 MHz nmr1

aja_vinaxanthone_aminal_c13

exp4 Carbon

SAMPLE		SPECIAL	
date	May 17 2012	temp	27.0
solvent	cdcl3	gain	40
file	exp	spin	20
ACQUISITION		hst	0.008
sw	30131.8	pw90	15.500
at	2.000	alfa	10.000
np	120528	FLAGS	
fb	17000	il	n
bs	8	in	n
d1	2.000	dp	y
nt	15000	hs	nn
ct	13622	PROCESSING	
TRANSMITTER		lb	1.00
tn	C13	fn	not used
sfrq	125.584	DISPLAY	
tof	1254.2	sp	-628.1
tpwr	51	wp	28253.2
pw	5.162	rf1	11584.5
DECOUPLER		rfp	9669.0
dn	H1	rp	159.2
dof	0	lp	-192.7
dm	yyy	PLOT	
dmm	w	wc	250
dpwr	39	sc	0
dmf	12600	vs	19289
		th	68
		al cdc ph	

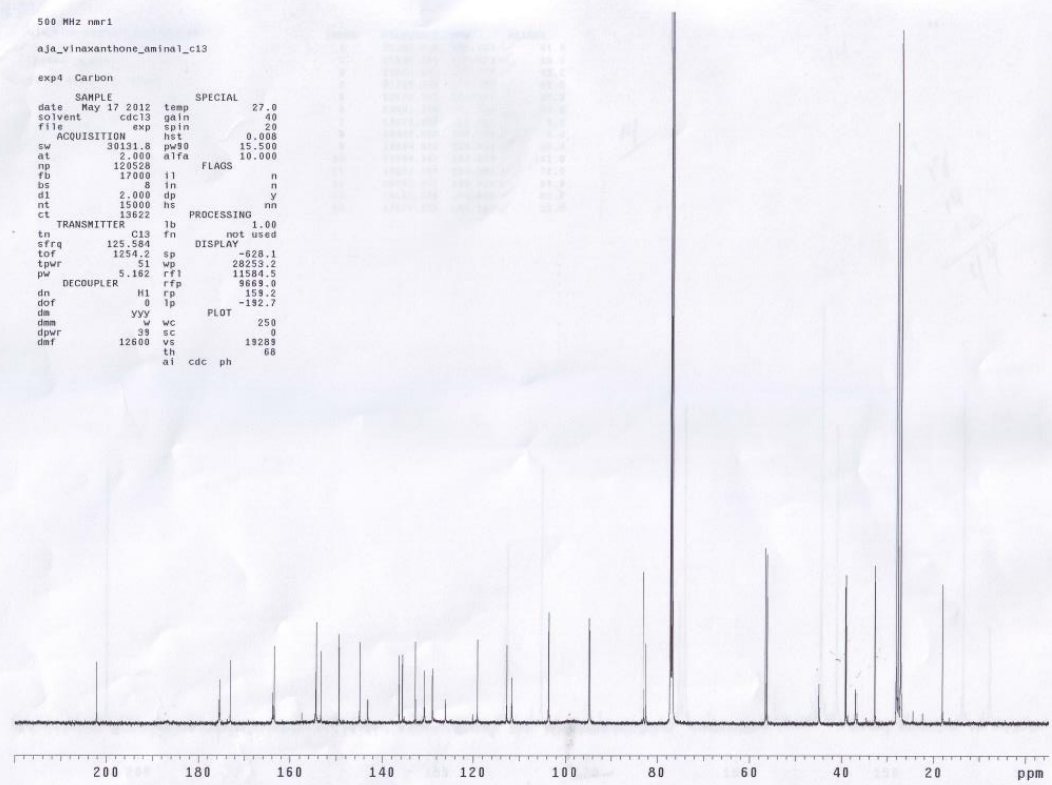

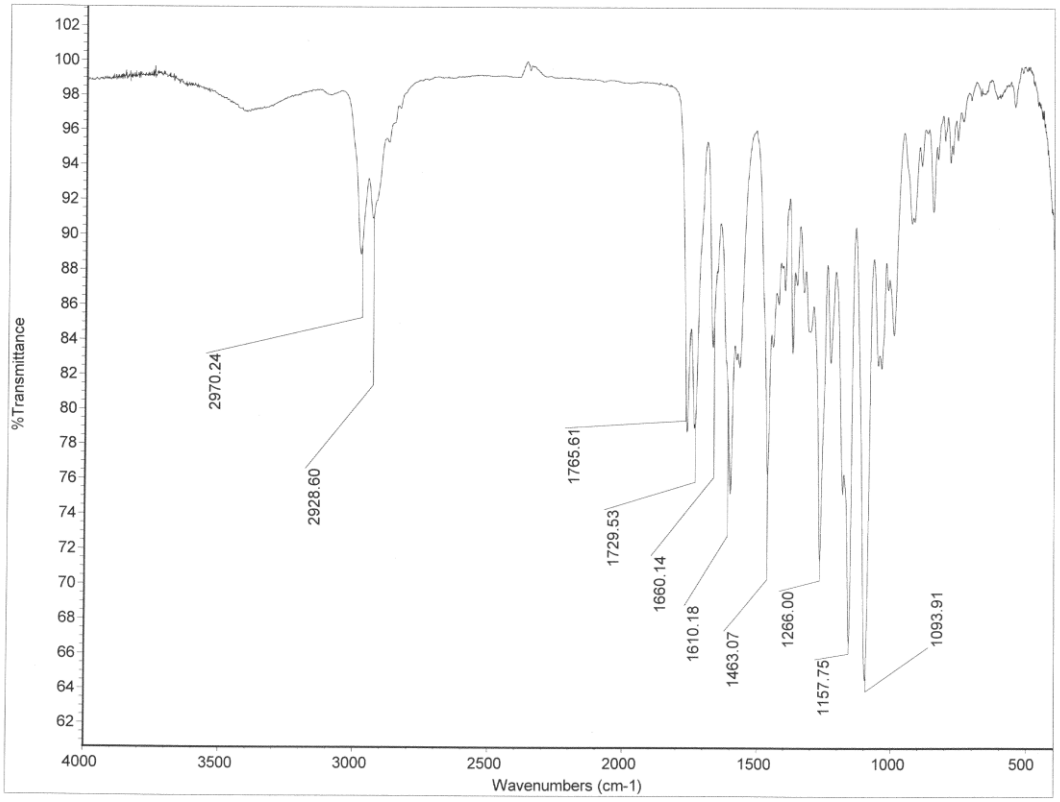
%Transmittance
102
100
98
96
94
92
90
88
86
84
82
80
78
76
74
72
70
68
66
64
62
2970.24
2928.60
1765.61
1729.53
1660.14
1610.18
1463.07
1266.00
1157.75
1093.91
4000
3500
3000
2500
2000
1500
1000
500
Wavenumbers (cm-1)

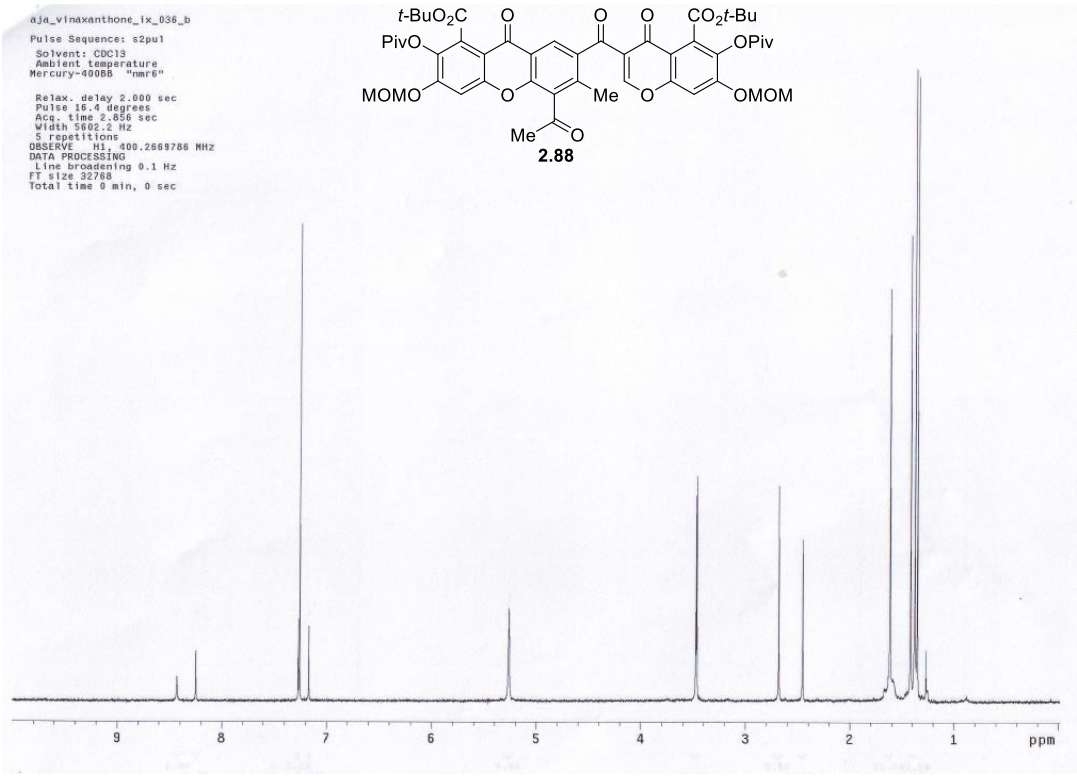
aja_vinaxanthone_ix_036_b
Pulse Sequence: s2pul
Solvent: CDCl3
Ambient temperature
Mercury-400BB "nmr6"
Relax. delay 2.000 sec
Pulse 16.4 degrees
Acq. time 2.856 sec
Width 5602.2 Hz
5 repetitions
OBSERVE H1, 400.2669786 MHz
DATA PROCESSING
Line broadening 0.1 Hz
FT size 32768
Total time 0 min, 0 sec
t-BuO2C
PivO
MOMO
Me
Me
CO2t-Bu
OPiv
OMOM
2.88
9
8
7
6
5
4
3
2
1
ppm

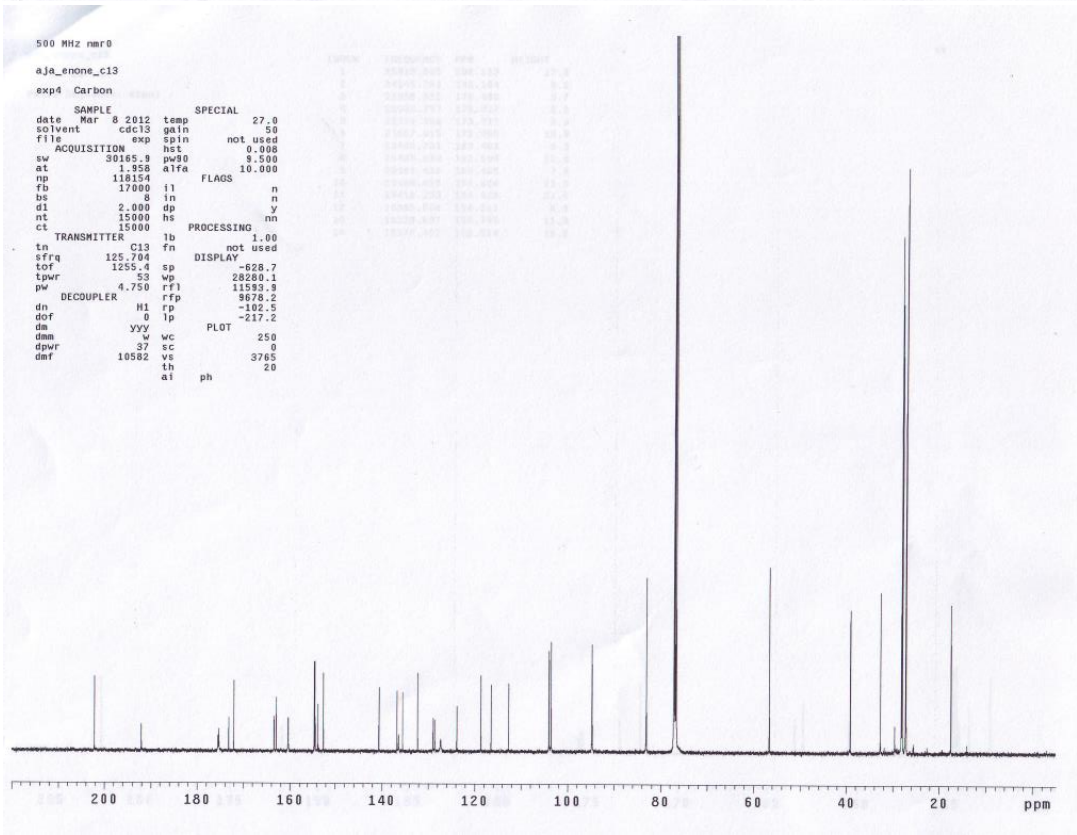
500 MHz nmr0
aja_enone_c13
exp4 Carbon
SAMPLE
date Mar 8 2012
solvent cdcl3
file exp
ACQUISITION
sw 30165.9
at 1.958
np 118154
fb 17000
bs 8
d1 2.000
nt 15000
ct 15000
TRANSMITTER
tn C13
sfrq 125.704
tof 1255.4
tpwr 53
pw 4.750
DECOUPLER
dn H1
dof 0
dm yyy
dmm w
dpwr 37
dmf 10582
SPECIAL
temp 27.0
gain 50
spin not used
hst 0.008
pw90 9.500
alfa 10.000
FLAGS
il n
in n
dp y
hs nn
PROCESSING
lb 1.00
fn not used
DISPLAY
sp -828.7
wp 28280.1
rf1 11593.9
rfp 9678.2
rp -102.5
lp -217.2
PLOT
wc 250
sc 0
vs 3765
th 20
ai ph
200
180
160
140
120
100
80
60
40
20
ppm

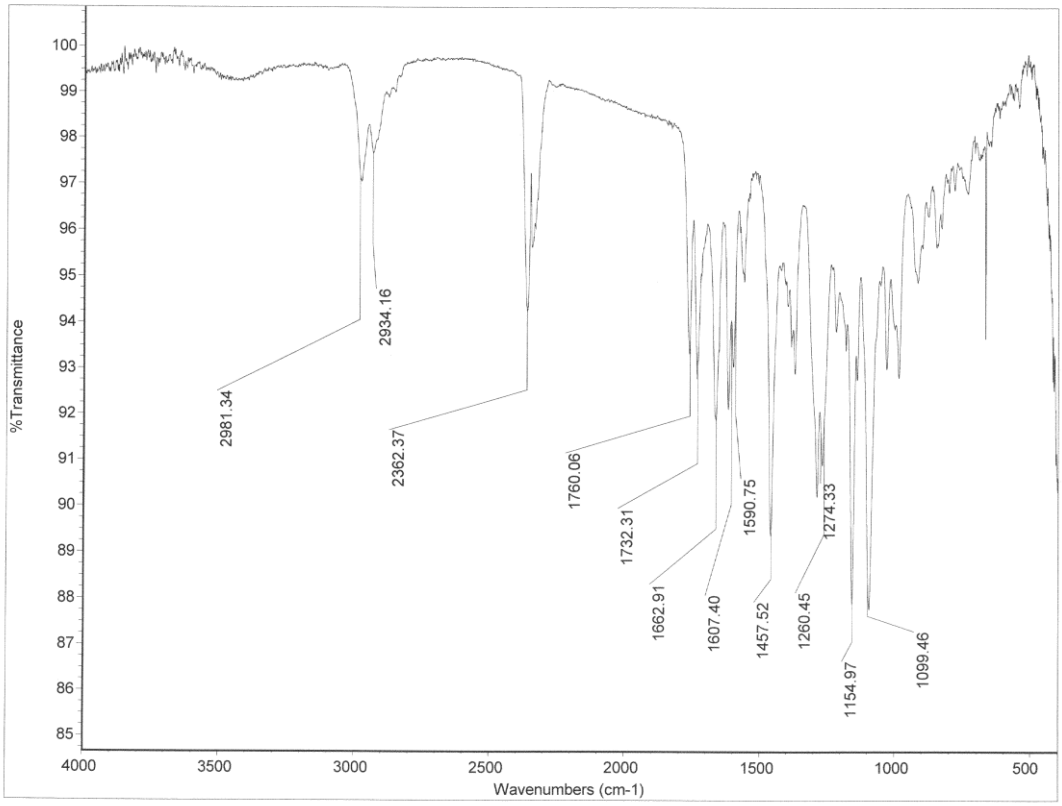
%Transmittance
100
99
98
97
96
95
94
93
92
91
90
89
88
87
86
85
4000
3500
3000
2500
2000
1500
1000
500
Wavenumbers (cm-1)
2981.34
2934.16
2362.37
1760.06
1732.31
1662.91
1607.40
1590.75
1457.52
1274.33
1260.45
1154.97
1099.46

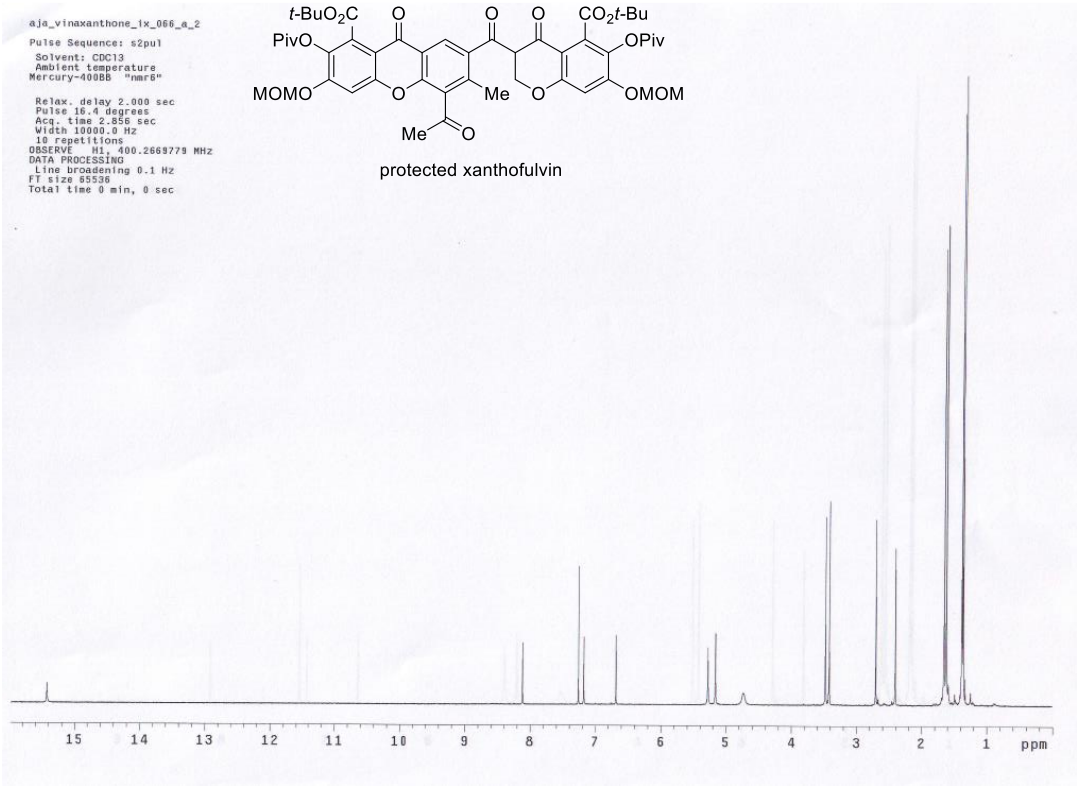
aja_vinaxanthone_ix_066_a_2
Pulse Sequence: s2pul
Solvent: CDCl3
Ambient temperature
Mercury-400BB "nmr6"
Relax. delay 2.000 sec
Pulse 16.4 degrees
Acq. time 2.856 sec
Width 10000.0 Hz
10 repetitions
OBSERVE H1, 400.2669779 MHz
DATA PROCESSING
Line broadening 0.1 Hz
FT size 65536
Total time 0 min, 0 sec
t-BuO2C
PivO
MOMO
Me
Me
CO2t-Bu
OPiv
OMOM
protected xanthofulvin
15
14
13
12
11
10
9
8
7
6
5
4
3
2
1
ppm

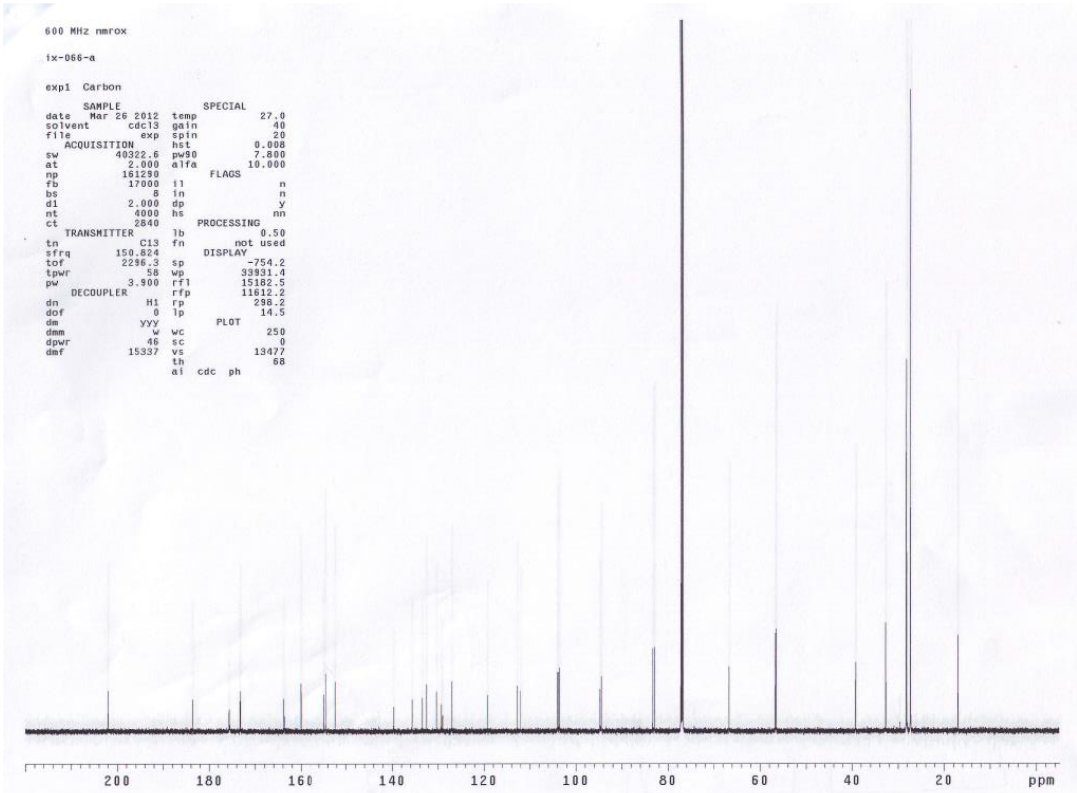
600 MHz nmrox
ix-066-a
exp1 Carbon
SAMPLE
date Mar 26 2012
solvent cdcl3
file exp
ACQUISITION
sw 40322.6
at 2.000
np 161290
fb 17000
bs 8
d1 2.000
nt 4000
ct 2840
TRANSMITTER
tn C13
sfrq 150.824
tof 2296.3
tpwr 58
pw 3.900
DECOUPLER
dn H1
dof 0
dm yyy
dmm w
dpwr 46
dmf 15337
SPECIAL
temp 27.0
gain 40
spin 20
hst 0.008
pw90 7.800
alfa 10.000
FLAGS
i1 n
in n
dp y
hs nn
PROCESSING
lb 0.50
fn not used
DISPLAY
sp -754.2
wp 33931.4
rf1 15182.5
rfp 11612.2
rp 298.2
lp 14.5
PLOT
wc 250
sc 0
vs 13477
th 68
ai cdc ph
200
180
160
140
120
100
80
60
40
20
ppm

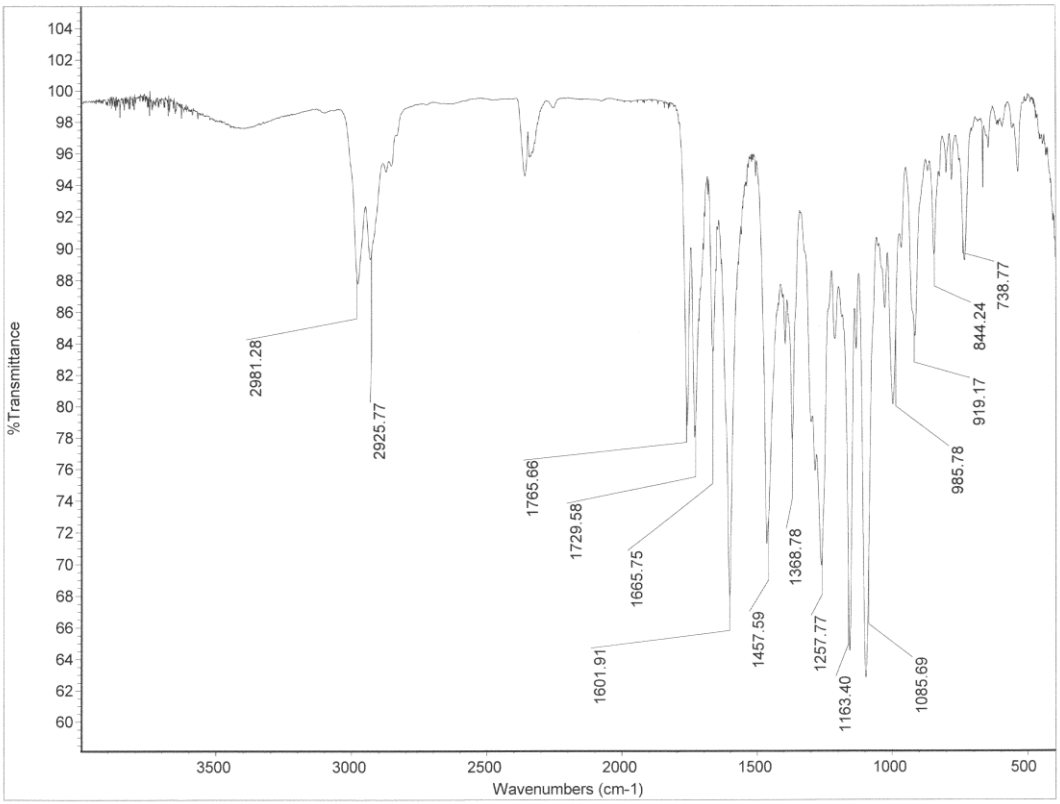
%Transmittance
104
102
100
98
96
94
92
90
88
86
84
82
80
78
76
74
72
70
68
66
64
62
60
3500
3000
2500
2000
1500
1000
500
Wavenumbers (cm-1)
2981.28
2925.77
1765.66
1729.58
1665.75
1601.91
1457.59
1368.78
1257.77
1163.40
1085.69
985.78
919.17
844.24
738.77

xanthofulvin (**2.2**)

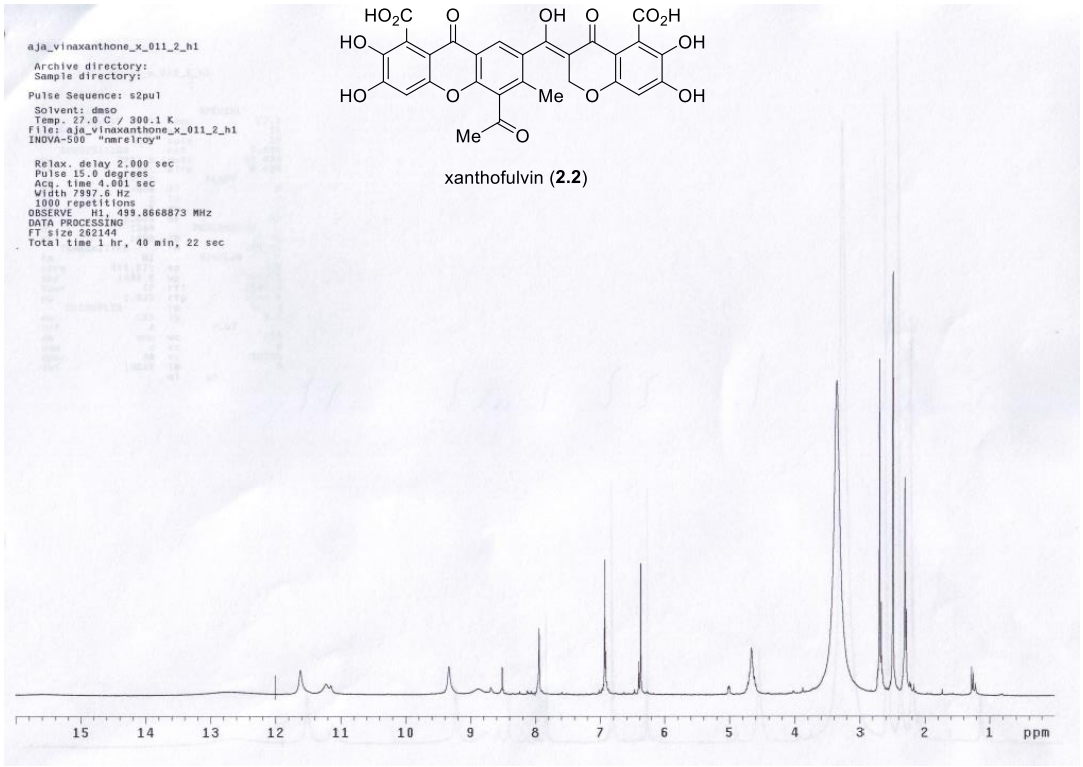

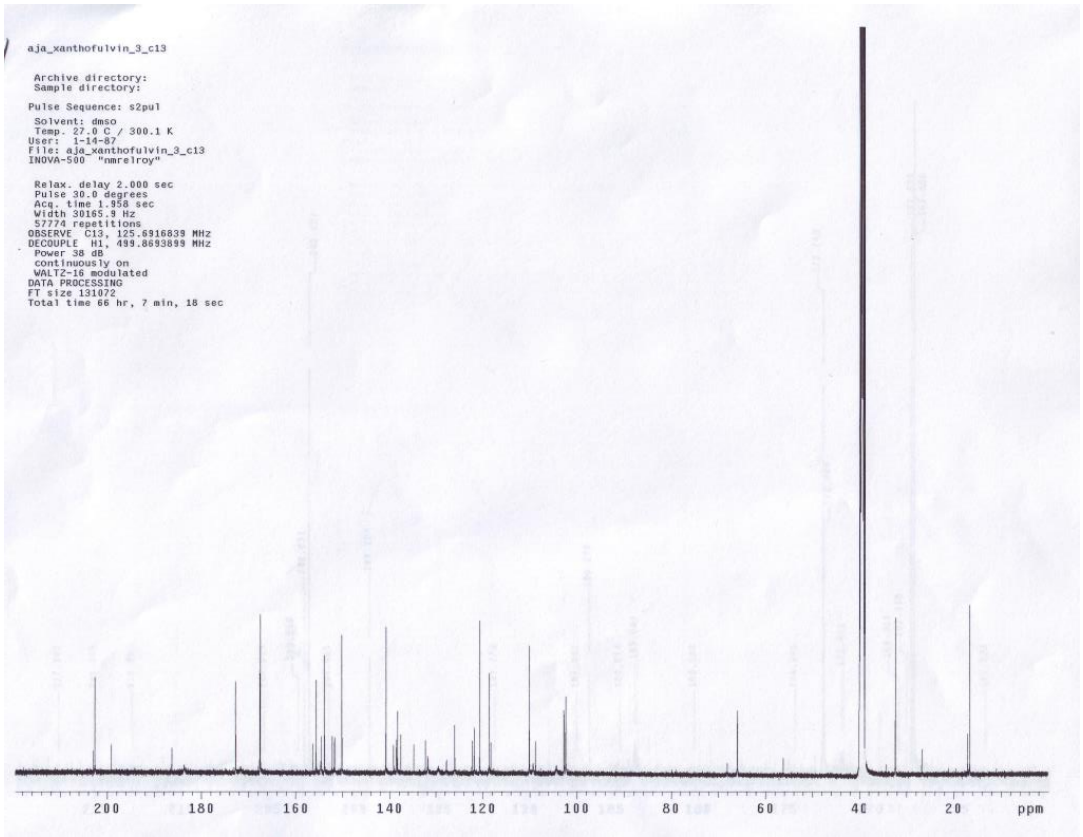

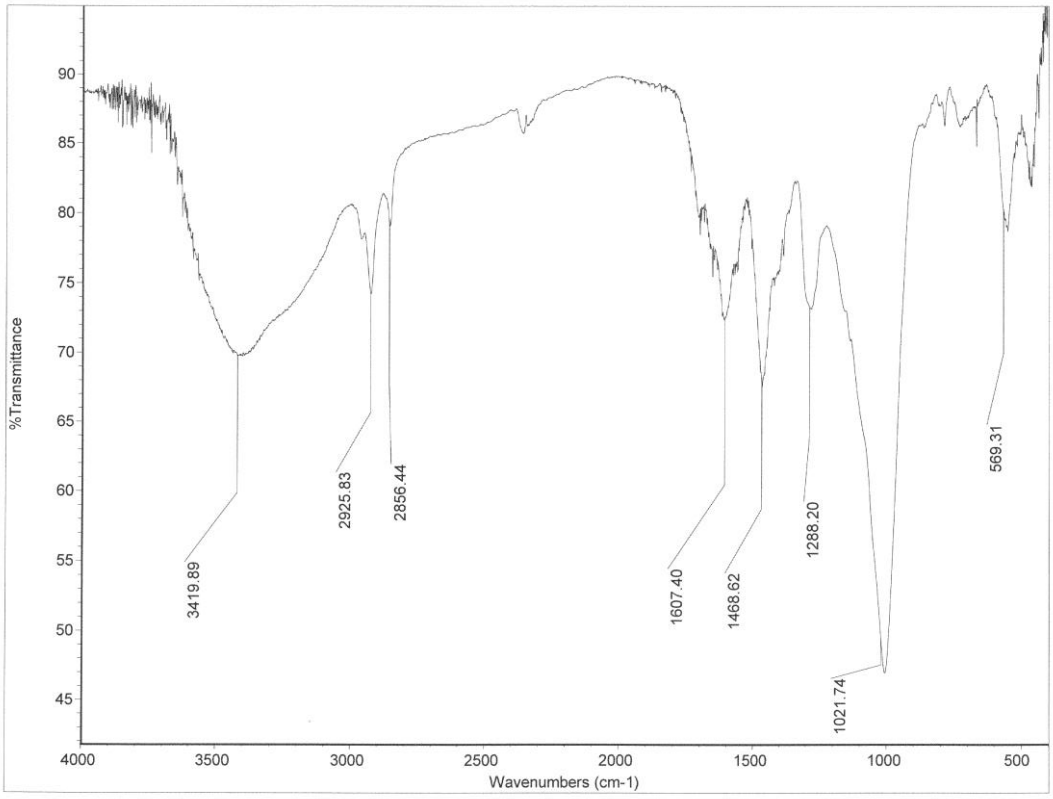
%Transmittance
90
85
80
75
70
65
60
55
50
45
3419.89
2925.83
2856.44
1607.40
1468.62
1288.20
1021.74
569.31
4000
3500
3000
2500
2000
1500
1000
500
Wavenumbers (cm-1)

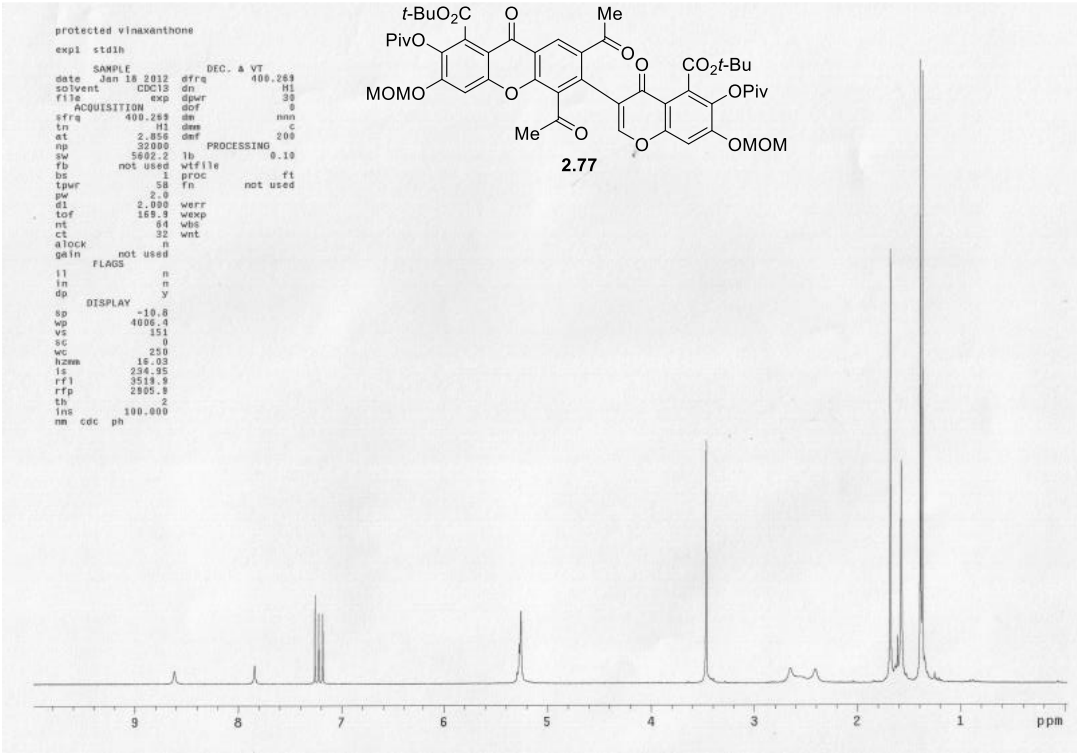
protected vinaxanthone
exp1 std1h
SAMPLE
date Jan 18 2012
solvent CDCl3
file exp
ACQUISITION
sfrq 400.269
tn H1
at 2.856
np 32000
sw 5602.2
fb not used
bs 1
tpwr 58
pw 2.0
d1 2.000
tof 169.9
nt 64
ct 32
alock n
gain not used
FLAGS
DISPLAY
sp -10.8
wp 4006.4
vs 151
sc 0
wc 250
hzmm 16.03
is 234.95
rf1 3519.9
rfp 2905.8
th 2
ins 100.000
nm cdc ph
DEC. & VT
dfrq 400.269
dn H1
dpwr 38
dof 0
dm nnn
dmm c
dmf 200
PROCESSING
lb 0.10
wtfile
proc ft
fn not used
werr
wexp
wbs
wnt
t-BuO2C
PivO
MOMO
Me
CO2t-Bu
OPiv
OMOM
2.77
9
8
7
6
5
4
3
2
1
ppm

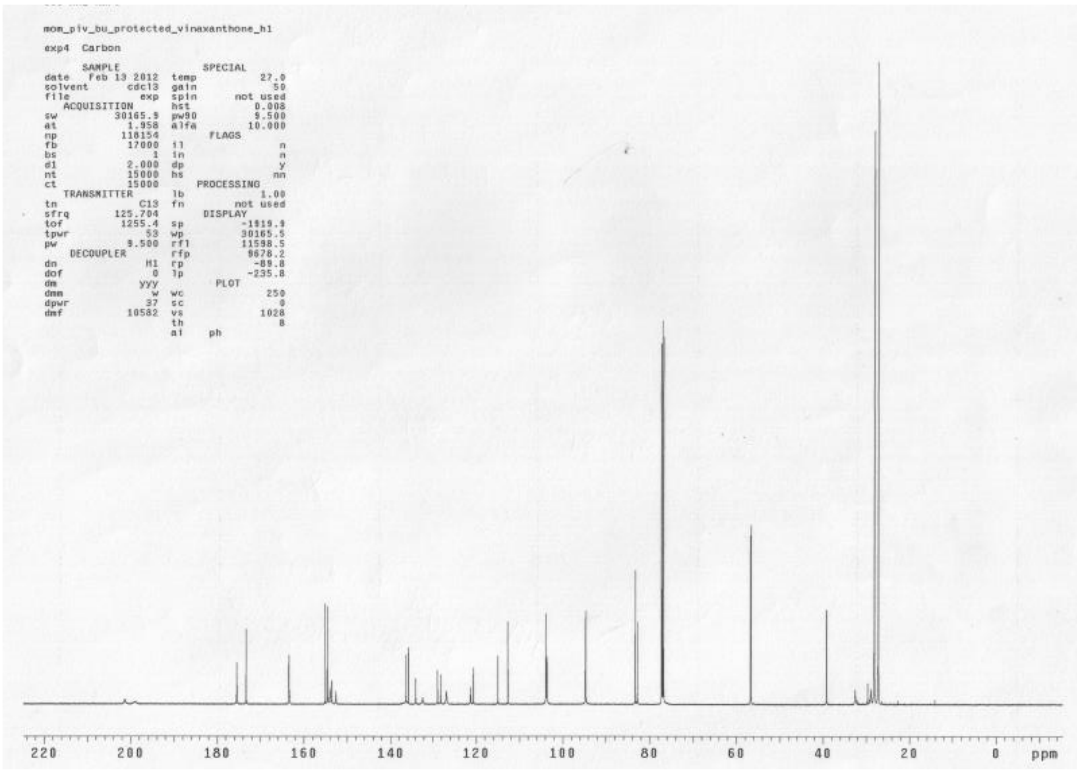
mom_piv_bu_protected_vinaxanthone_h1
exp4 Carbon
SAMPLE
date Feb 13 2012
solvent cdcl3
file exp
ACQUISITION
sw 30165.9
at 1.958
np 118154
fb 17000
bs 1
d1 2.000
nt 15000
ct 15000
TRANSMITTER
tn C13
sfrq 125.704
tof 1255.4
tpwr 53
pw 9.500
DECOUPLER
dn H1
dof 0
dm yyy
dmm w
dpwr 37
dmf 10582
SPECIAL
temp 27.0
gain 50
spin not used
hst 0.008
pw90 9.500
alfa 10.000
FLAGS
il n
in n
dp y
hs nn
PROCESSING
lb 1.00
fn not used
DISPLAY
sp -1819.9
wp 30165.5
rf1 11598.5
rfp 8676.2
rp -89.8
lp -235.8
PLOT
wc 250
sc 0
vs 1028
th 8
al ph
220
200
180
160
140
120
100
80
60
40
20
0
ppm

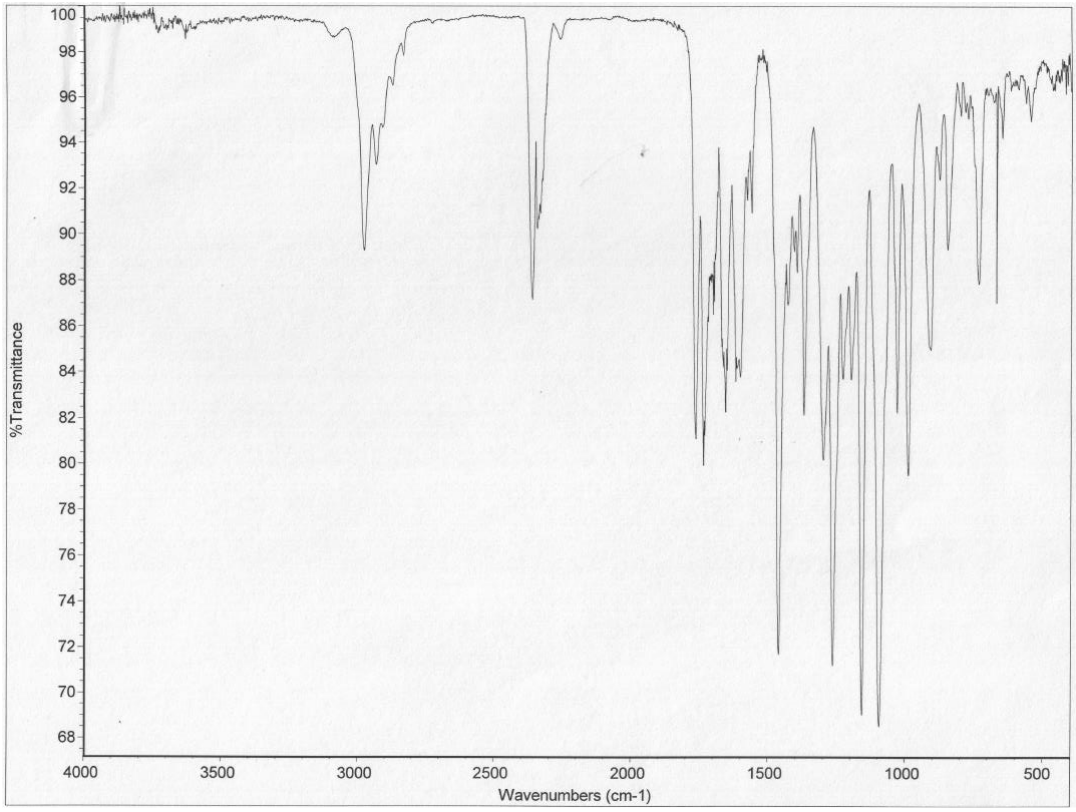
%Transmittance
100
98
96
94
92
90
88
86
84
82
80
78
76
74
72
70
68
4000
3500
3000
2500
2000
1500
1000
500
Wavenumbers (cm-1)

References

1 Pechmann, H. v. & Vanino, L. Preparation of acyl superoxides. *Berichte der Deutschen Chemischen Gesellschaft* **27**, 3 (1894).

2 Shah, H. A., Leonard, F. & Tobolsky, A. V. Phthaloyl peroxide as a polymerization initiator. *Journal of Polymer Science* **7**, 537-541, doi:10.1002/pol.1951.120070508 (1951).

3 Baeyer, A. & Villiger, V. On peracids and peroxide acids of dibasic organic acids. *Ber. Dtsch. Chem. Ges.* **34**, 762-767, doi:10.1002/cber.190103401128 (1901).

4 Kleinfeller, H. & Rastadter, K. Cycloperoxyde von dicarbonsauren. *Angew. Chem.* **65**, 543-543 (1953).

5 Russell, K. E. The preparation of phthaloyl peroxide and its decomposition in solution. *J. Am. Chem. Soc* **77**, 4814-4815, doi:10.1021/ja01623a037 (1955).

6 Nozaki, K. & Bartlett, P. D. The kinetics of decomposition of benzoyl peroxide in solvents. *J. Am. Chem. Soc* **68**, 1686-1692, doi:10.1021/ja01213a002 (1946).

7 Greene, F. D. Cyclic diacyl peroxides 1 monomeric phthaloyl peroxide. *J. Am. Chem. Soc* **78**, 2246-2250, doi:10.1021/ja01591a060 (1956).

8 Kikuchi, O., Hiyama, A., Yoshida, H. & Suzuki, K. Electronic-structure and homolytic dissociation of dibenzoyl peroxide. *Bull. Chem. Soc. Jpn.* **51**, 11-15, doi:10.1246/bcsj.51.11 (1978).

9 Patai, S. *The chemistry of peroxides*. (John Wiley and Sons, ltd., 1983).

10 Fujimori, K., Hirose, Y. & Oae, S. Thermal decomposition of diacyl peroxide .10. Evidence for acyloxyl radical pair mechanism for o-18-scrambling of o-18-labelled cyclopropanecarbonyl peroxide. *Journal of the Chemical Society-Perkin Transactions 2*, 405-412, doi:10.1039/p29960000405 (1996).

11 Greene, F. D. Cyclic diacyl peroxides 2 reaction of phthaloyl peroxide with cis-stilbene and trans-stilbene. *J. Am. Chem. Soc* **78**, 2250-2254, doi:10.1021/ja01591a061 (1956).

12 Greene, F. D. & Rees, W. W. Cyclic diacyl peroxides 5. Reaction of phthaloyl peroxide with norbornylene. *J. Am. Chem. Soc* **82**, 890-893, doi:10.1021/ja01489a031 (1960).

13 Gundermann, K. D. & Steinfatt, M. Phthaloyl peroxide as an efficient source of singlet oxygen. *Angew. Chem. Int. Ed.* **14**, 560-560, doi:10.1002/anie.197505601 (1975).

14 Zupancic, J. J., Horn, K. A. & Schuster, G. B. Electron-transfer-initiated reactions of organic peroxides - reaction of phthaloyl peroxide with olefins and other electron-donors. *J. Am. Chem. Soc* **102**, 5279-5285, doi:10.1021/ja00536a027 (1980).

15 Pellarin, K. R., McCready, M. S., Sutherland, T. I. & Puddephatt, R. J. Oxidative addition of phthaloyl peroxide to dmethylplatinum(ii) complexes. *Organometallics* **31**, 8291-8300, doi:10.1021/om3009074 (2012).
16 Greene, F. D. & Rees, W. W. Cyclic diacyl peroxides 3 the reaction of phthaloyl peroxide with olefins. *J. Am. Chem. Soc* **80**, 3432-3437, doi:10.1021/ja01546a058 (1958).
17 Fujimori, K., Hirose, Y. & Oae, S. Thermal decomposition of diacyl peroxide .10. Evidence for acyloxyl radical pair mechanism for o-18-scrambling of o-18-labelled cyclopropanecarbonyl peroxide. *J. Chem. Soc., Perkin Trans. 1*, 405-412, doi:10.1039/p29960000405 (1996).
18 Yuan, C. X., Eliasen, A. M., Camelio, A. M. & Siegel, D. Preparation of phenols by phthaloyl peroxide-mediated oxidation of arenes. *Nature Protocols* **9**, 2624-2629, doi:10.1038/nprot.2014.175 (2014).
19 McKillop, A. & Sanderson, W. R. Sodium perborate and sodium percarbonate - cheap, safe and versatile oxidizing-agents for organic synthesis. *Tetrahedron* **51**, 6145-6166, doi:10.1016/0040-4020(95)00304-q (1995).
20 Muzart, J. Sodium perborate and sodium percarbonate in organic-synthesis. *Synthesis*, 1325-1347 (1995).
21 Yuan, C. X., Axelrod, A., Varela, M., Danysh, L. & Siegel, D. Synthesis and reaction of phthaloyl peroxide derivatives, potential organocatalysts for the stereospecific dihydroxylation of alkenes. *Tetrahedron Lett.* **52**, 2540-2542, doi:10.1016/j.tetlet.2011.03.005 (2011).
22 Bevington, J. C., Breuer, S. W., Huckerby, T. N., Hunt, B. J. & Jones, R. Fluorinated derivatives of benzoyl peroxide as initiators of radical polymerizations: Study of the end-groups derived from the initiator. *Eur. Polym. J.* **33**, 1225-1229, doi:10.1016/s0014-3057(96)00253-4 (1997).
23 Yuan, C. X. *et al.* Metal-free oxidation of aromatic carbon-hydrogen bonds through a reverse-rebound mechanism. *Nature* **499**, 192-196, doi:10.1038/nature12284 (2013).
24 Neufeldt, S. R. & Sanford, M. S. Controlling site selectivity in palladium-catalyzed c-h bond functionalization. *Acc. Chem. Res.* **45**, 936-946, doi:10.1021/ar300014f (2012).
25 Emmert, M. H., Cook, A. K., Xie, Y. J. & Sanford, M. Remarkably high reactivity of pd(oac)(2)/pyridine catalysts: Nondirected c-h oxygenation of arenes. *Angew. Chem., Int. Ed.* **50**, 9409-9412, doi:10.1002/anie.201103327 (2011).
26 Zhang, Y. H. & Yu, J. Q. Pd(ii)-catalyzed hydroxylation of arenes with 1 atm of o-2 or air. *J. Am. Chem. Soc* **131**, 14654-+, doi:10.1021/ja907198n (2009).
27 Huang, C. H., Ghavtadze, N., Chattopadhyay, B. & Gevorgyan, V. Synthesis of catechols from phenols via pd-catalyzed silanol-directed c-h oxygenation. *J. Am. Chem. Soc* **133**, 17630-17633, doi:10.1021/ja208572v (2011).
28 Bartlett, P. D. & Hiatt, R. R. A series of tertiary butyl peresters showing concerted decomposition. *J. Am. Chem. Soc* **80**, 1398-1405, doi:10.1021/ja01539a031 (1958).

29 Daublain, P., Horner, J. H., Kuznetsov, A. & Newcomb, M. Solvent polarity effects and limited acid catalysis in rearrangements of model radicals for the methylmalonyl-coa mutase- and isobutyryl-coa mutase-catalyzed isomerization reactions. *J. Am. Chem. Soc* **126**, 5368-5369, doi:10.1021/ja049913+ (2004).
30 Smith, D. M., Golding, B. T. & Radom, L. Understanding the mechanism of b-12-dependent methylmalonyl-coa mutase: Partial proton transfer in action. *J. Am. Chem. Soc* **121**, 9388-9399, doi:10.1021/ja991649a (1999).
31 Smith, D. M., Golding, B. T. & Radom, L. Facilitation of enzyme-catalyzed reactions by partial proton transfer: Application to coenzyme-b-12-dependent methylmalonyl-coa mutase. *J. Am. Chem. Soc* **121**, 1383-1384, doi:10.1021/ja983512a (1999).
32 Adams, A. M. & Du Bois, J. Organocatalytic c-h hydroxylation with oxone (r) enabled by an aqueous fluoroalcohol solvent system. *Chem. Sci.* **5**, 656-659, doi:10.1039/c3sc52649f (2014).
33 Stratt, R. M. & Desjardins, S. G. Solvation of the methyl radical and its implications. *J. Am. Chem. Soc* **106**, 256-257, doi:10.1021/ja00313a053 (1984).
34 Groves, J. T. The bioinorganic chemistry of iron in oxygenases and supramolecular assemblies. *Proceedings of the National Academy of Sciences of the United States of America* **100**, 3569-3574, doi:10.1073/pnas.0830019100 (2003).
35 de Visser, S. P., Ogliaro, F., Sharma, P. K. & Shaik, S. What factors affect the regioselectivity of oxidation by cytochrome p450? A dft study of allylic hydroxylation and double bond epoxidation in a model reaction. *J. Am. Chem. Soc* **124**, 11809-11826, doi:10.1021/ja026872d (2002).
36 Groves, J. T. Key elements of the chemistry of cytochrome p450 - the oxygen rebound mechanism. *J. Chem. Educ.* **62**, 928-931 (1985).
37 Jursic, B. S. & Martin, R. M. Calculation of bond dissociation energies for oxygen containing molecules by ab initio and density functional theory methods. *Int. J. Quantum Chem.* **59**, 495-501, doi:10.1002/(sici)1097-461x(1996)59:6<495::aid-qua7>3.0.co;2-t (1996).
38 Chateauneuf, J., Lusztyk, J. & Ingold, K. U. Spectroscopic and kinetic characteristics of aroyloxyl radicals .1. The 4-methoxybenzoyloxyl radical. *J. Am. Chem. Soc* **110**, 2877-2885, doi:10.1021/ja00217a031 (1988).
39 Risdall, P. C., Adams, S. S., Crampton, E. L. & Marchant, B. Disposition and metabolism of flurbiprofen in several species including man. *Xenobiotica* **8**, 691-703 (1978).
40 Severini, F. & Gallo, R. Differential scanning calorimetry study of thermal-decomposition of benzoyl peroxide and 2,2'-azobisisobutyronitrile mixtures. *J. Therm. Anal.* **29**, 561-566, doi:10.1007/bf01913464 (1984).
41 Pastre, J. C., Browne, D. L. & Ley, S. V. Flow chemistry syntheses of natural products. *Chem. Soc. Rev.* **42**, 8849-8869, doi:10.1039/c3cs60246j (2013).

42 Hartman, R. L., McMullen, J. P. & Jensen, K. F. Deciding whether to go with the flow: Evaluating the merits of flow reactors for synthesis. *Angew. Chem., Int. Ed.* **50**, 7502-7519, doi:10.1002/anie.201004637 (2011).
43 Wiles, C. & Watts, P. Recent advances in micro reaction technology. *Chem. Commun.* **47**, 6512-6535, doi:10.1039/c1cc00089f (2011).
44 Wiles, C. & Watts, P. Continuous flow reactors: A perspective. *Green Chem.* **14**, 38-54, doi:10.1039/c1gc16022b (2012).
45 Wiles, C. & Watts, P. Continuous process technology: A tool for sustainable production. *Green Chem.* **16**, 55-62, doi:10.1039/c3gc41797b (2014).
46 Styring, P. & Parracho, A. I. R. From discovery to production: Scale-out of continuous flow meso reactors. *Beilstein J. Org. Chem.* **5**, 10, doi:10.3762/bjoc.5.29 (2009).
47 Nagy, K. D., Shen, B., Jamison, T. F. & Jensen, K. F. Mixing and dispersion in small-scale flow systems. *Org. Process Res. Dev.* **16**, 976-981, doi:10.1021/op200349f (2012).
48 Roydhouse, M. D. *et al.* Ozonolysis in flow using capillary reactors. *Org. Process Res. Dev.* **15**, 989-996, doi:10.1021/op200036d (2011).
49 Bedore, M. W., Zaborenko, N., Jensen, K. F. & Jamison, T. F. Aminolysis of epoxides in a microreactor system: A continuous flow approach to beta-amino alcohols. *Org. Process Res. Dev.* **14**, 432-440, doi:10.1021/op9003136 (2010).
50 Razzaq, T., Glasnov, T. N. & Kappe, C. O. Continuous-flow microreactor chemistry under high-temperature/pressure conditions. *Eur. J. Org. Chem.*, 1321-1325, doi:10.1002/ejoc.200900077 (2009).
51 Marre, S., Adamo, A., Basak, S., Aymonier, C. & Jensen, K. F. Design and packaging of microreactors for high pressure and high temperature applications. *Ind. Eng. Chem.* **49**, 11310-11320, doi:10.1021/ie101346u (2010).
52 Benito-Lopez, F. *et al.* Substantial rate enhancements of the esterification reaction of phthalic anhydride with methanol at high pressure and using supercritical co2 as a co-solvent in a glass microreactor. *Lab on a Chip* **7**, 1345-1351, doi:10.1039/b703394j (2007).
53 Tiggelaar, R. M. *et al.* Fabrication, mechanical testing and application of high-pressure glass microreactor chips. *Chem. Eng. J.* **131**, 163-170, doi:10.1016/j.cej.2006.12.036 (2007).
54 Ajmera, S. K., Losey, M. W., Jensen, K. F. & Schmidt, M. A. Microfabricated packed-bed reactor for phosgene synthesis. *Aiche Journal* **47**, 1639-1647, doi:10.1002/aic.690470716 (2001).
55 Pellegatti, L. & Buchwald, S. L. Continuous-flow preparation and use of beta-chloro enals using the vilsmeier reagent. *Org. Process Res. Dev.* **16**, 1442-1448, doi:10.1021/op300168z (2012).

56 Proctor, L. D. & Warr, A. J. Development of a continuous process for the industrial generation of diazomethane. *Org. Process Res. Dev.* **6**, 884-892, doi:10.1021/op020049k (2002).
57 Mastronardi, F., Gutmann, B. & Kappe, C. O. Continuous flow generation and reactions of anhydrous diazomethane using a teflon af-2400 tube-in-tube reactor. *Org. Lett.* **15**, 5590-5593, doi:10.1021/ol4027914 (2013).
58 Bartrum, H. E., Blakemore, D. C., Moody, C. J. & Hayes, C. J. Rapid access to alpha-alkoxy and alpha-amino acid derivatives through safe continuous-flow generation of diazoesters. *Chem.-Eur. J.* **17**, 9586-9589, doi:10.1002/chem.201101590 (2011).
59 Basavaraju, K. C., Sharma, S., Maurya, R. A. & Kim, D. P. Safe use of a toxic compound: Heterogeneous oso4 catalysis in a nanobrush polymer microreactor. *Angewandte Chemie-International Edition* **52**, 6735-6738, doi:10.1002/anie.201301124 (2013).
60 Ambreen, N., Kumar, R. & Wirth, T. Hypervalent iodine/tempo-mediated oxidation in flow systems: A fast and efficient protocol for alcohol oxidation. *Beilstein J. Org. Chem.* **9**, 1437-1442, doi:10.3762/bjoc.9.162 (2013).
61 Ye, X. A., Johnson, M. D., Diao, T. N., Yates, M. H. & Stahl, S. S. Development of safe and scalable continuous-flow methods for palladium-catalyzed aerobic oxidation reactions. *Green Chem.* **12**, 1180-1186, doi:10.1039/c0gc00106f (2010).
62 Kumar, G. S., Pieber, B., Reddy, K. R. & Kappe, C. O. Copper-catalyzed formation of c-o bonds by direct alpha-c-h bond activation of ethers using stoichiometric amounts of peroxide in batch and continuous-flow formats. *Chem.-Eur. J.* **18**, 6124-6128, doi:10.1002/chem.201200815 (2012).
63 Pieber, B. & Kappe, C. O. Direct aerobic oxidation of 2-benzylpyridines in a gas-liquid continuous-flow regime using propylene carbonate as a solvent. *Green Chem.* **15**, 320-324, doi:10.1039/c2gc36896j (2013).
64 Lange, H. *et al.* Oxidation reactions in segmented and continuous flow chemical processing using an n-(tert-butyl)phenylsulfinimidoyl chloride monolith. *Synlett*, 869-873, doi:10.1055/s-0030-1259923 (2011).
65 Levesque, F. & Seeberger, P. H. Highly efficient continuous flow reactions using singlet oxygen as a "green" reagent. *Org. Lett.* **13**, 5008-5011, doi:10.1021/ol2017643 (2011).
66 Bourne, S. L. & Ley, S. V. A continuous flow solution to achieving efficient aerobic anti-markovnikov wacker oxidation. *Adv. Synth. Catal.* **355**, 1905-1910, doi:10.1002/adsc.201300278 (2013).
67 Greene, J. F., Hoover, J. M., Mannel, D. S., Root, T. W. & Stahl, S. S. Continuous-flow aerobic oxidation of primary alcohols with a copper(i)/tempo catalyst. *Org. Process Res. Dev.* **17**, 1247-1251, doi:10.1021/op400207f (2013).
68 Battilocchio, C., Hawkins, J. M. & Ley, S. V. Mild and selective heterogeneous catalytic hydration of nitriles to amides by flowing through manganese dioxide. *Org. Lett.* **16**, 1060-1063, doi:10.1021/ol403591c (2014).

69 He, Z. & Jamison, T. F. Continuous-flow synthesis of functionalized phenols by aerobic oxidation of grignard reagents. *Angew. Chem., Int. Ed.* **53**, 3353-3357, doi:10.1002/anie.201310572 (2014).
70 Naber, J. R. & Buchwald, S. L. Packed-bed reactors for continuous-flow c-n cross-coupling. *Angew. Chem., Int. Ed.* **49**, 9469-9474, doi:10.1002/anie.201004425 (2010).
71 Noel, T., Maimone, T. J. & Buchwald, S. L. Accelerating palladium-catalyzed c-f bond formation: Use of a microflow packed-bed reactor. *Angew. Chem., Int. Ed.* **50**, 8900-8903, doi:10.1002/anie.201104652 (2011).
72 Deadman, B. J., Battilocchio, C., Sliwinski, E. & Ley, S. V. A prototype device for evaporation in batch and flow chemical processes. *Green Chem.* **15**, 2050-2055, doi:10.1039/c3gc40967h (2013).
73 Sono, M., Roach, M. P., Coulter, E. D. & Dawson, J. H. Heme-containing oxygenases. *Chem. Rev.* **96**, 2841-2887, doi:10.1021/cr9500500 (1996).
74 Gibson, D. T., Koch, J. R. & Kallio, R. E. Oxidative degradation of aromatic hydrocarbons by microorganisms 1: Formation of catechol from benzene. *Biochemistry* **7**, 2653-&, doi:10.1021/bi00847a031 (1968).
75 Smith, M. R. & Ratledge, C. Catabolism of alkylbenzenes by pseudomonas sp ncib-10643. *Applied Microbiology and Biotechnology* **32**, 68-75 (1989).
76 Solomon, E. I., Wong, S. D., Liu, L. V., Decker, A. & Chow, M. S. Peroxo and oxo intermediates in mononuclear nonheme iron enzymes and related active sites. *Curr. Opin. Chem. Biol.* **13**, 99-113, doi:10.1016/j.cbpa.2009.02.011 (2009).
77 Adler, E., Dahlen, J. & Westin, G. Perjodatoxydation von phenolen .7. 2,6-dimethylphenol sowie 2,4,6-trimethylphenol und 2,3,5-trimethylphenol. *Acta Chem. Scand.* **14**, 1580-1596, doi:10.3891/acta.chem.scand.14-1580 (1960).
78 Wessely, F., Lauterbachkeil, G. & Sinwel, F. Uber die einwirkung von bleitetraacetat auf phenole .1. *Monatsh. Chem.* **81**, 811-818, doi:10.1007/bf00899320 (1950).
79 Dong, S. W., Zhu, J. L. & Porco, J. A. Enantioselective synthesis of bicyclo 2.2.2 octenones using a copper-mediated oxidative dearomatization/ 4+2 dimerization cascade. *J. Am. Chem. Soc* **130**, 2738-+, doi:10.1021/ja711018z (2008).
80 Scott, A. I., McCapra, F., Dodson, P. A. & Meyers, M. B. Electrooxidaion of tyrosyl derivatives - a model for coumarin biosynthesis. *J. Am. Chem. Soc* **85**, 3702-&, doi:10.1021/ja00905a040 (1963).
81 Quideau, S., Fabre, I. & Deffieux, D. First asymmetric synthesis of orthoquinone monoketal enantiomers via anodic oxidation. *Org. Lett.* **6**, 4571-4573, doi:10.1021/ol048030k (2004).
82 Deffieux, D., Fabre, I., Titz, A., Leger, J. M. & Quideau, S. Electrochemical synthesis of dimerizing and nondimerizing orthoquinone monoketals. *J. Org. Chem.* **69**, 8731-8738, doi:10.1021/jo048677i (2004).

83 Deffieux, D., Fabre, I., Courseille, C. & Quideau, S. Electrochemically-induced spirolactonization of alpha-(methoxyphenoxy)alkanoic acids into quinone ketals. *J. Org. Chem.* **67**, 4458-4465, doi:10.1021/jo020023r (2002).
84 McKillop, A. *et al.* Thallium in organic synthesis .4. Direct oxidation of 4-substituted phenols to 4,4-disubstituted cyclohexa-2,5-dienones using thaillium(iii) nitrate. *J. Org. Chem.* **41**, 282-287, doi:10.1021/jo00864a020 (1976).
85 Rebelo, S. L. H., Simoes, M. M. Q., Neves, M., Silva, A. M. S. & Cavaleiro, J. A. S. An efficient approach for aromatic epoxidation using hydrogen peroxide and mn(iii) porphyrins. *Chem. Commun.*, 608-609, doi:10.1039/b313683c (2004).
86 Esguerra, K. V. N., Fall, Y., Petitjean, L. & Lumb, J.-P. Controlling the catalytic aerobic oxidation of phenols. *J. Am. Chem. Soc* **136**, 7662-7668, doi:10.1021/ja501789x (2014).
87 Hirokane, T., Hirata, Y., Ishimoto, T., Nishii, K. & Yamada, H. A unified strategy for the synthesis of highly oxygenated diaryl ethers featured in ellagitannins. *Nature Communications* **5**, 10, doi:10.1038/ncomms4478 (2014).
88 Ishikawa, K. & Griffin, G. W. Complementary route to anti-1,2,3,4-naphthalene dioxide- direct oxidation of arenes with m-chloroperbenzoic acid. *Angew. Chem., Int. Ed.* **16**, 171-172, doi:10.1002/anie.197701711 (1977).
89 Jeyaraman, R. & Murray, R. W. Production of arene oxides by the caroate acetone system (dimethyldioxirane). *J. Am. Chem. Soc* **106**, 2462-2463, doi:10.1021/ja00320a055 (1984).
90 Jerina, D. M. & Daly, J. W. Arene oxides - new aspect of drug-metabolism. *Science* **185**, 573-582, doi:10.1126/science.185.4151.573 (1974).
91 Boyd, D. R. *et al.* A h-1-nmr method for the determination of enantiomeric excess and absolute-configuration of cis-dihydrodiol metabolites of polycyclic arenes and heteroarenes. *Tetrahedron Lett.* **33**, 1241-1244, doi:10.1016/s0040-4039(00)91907-5 (1992).
92 Boyd, D. R. *et al.* Structures and stereochemical assignments of some novel chiral synthons derived from the biotransformation of 2,3-dihydrobenzofuran and benzofuran by pseudomonas putida. *Tetrahedron: Asymmetry* **4**, 1307-1324, doi:10.1016/s0957-4166(00)80242-6 (1993).
93 Myers, A. G., Siegel, D. R., Buzard, D. J. & Charest, M. G. Synthesis of a broad array of highly functionalized, enantiomerically pure cyclohexanecarboxylic acid derivatives by microbial dihydroxylation of benzoic acid and subsequent oxidative and rearrangement reactions. *Org. Lett.* **3**, 2923-2926, doi:10.1021/ol010151m (2001).
94 Ouyang, S. P., Liu, Q., Sun, S. Y., Chen, J. C. & Chen, G. Q. Genetic engineering of pseudomonas putida kt2442 for biotransformation of aromatic compounds to chiral cis-diols. *J. Biotechnol.* **132**, 246-250, doi:10.1016/j.jbiotec.2007.08.001 (2007).

95 Magdziak, D., Meek, S. J. & Pettus, T. R. R. Cyclohexadienone ketals and quinols: Four building blocks potentially useful for enantioselective synthesis. *Chem. Rev.* **104**, 1383-1429, doi:10.1021/cr0306900 (2004).
96 Roche, S. P. & Porco, J. A. Dearomatization strategies in the synthesis of complex natural products. *Angew. Chem., Int. Ed.* **50**, 4068-4093, doi:10.1002/anie.201006017 (2011).
97 Yang, Q. L., Njardarson, J. T., Draghici, C. & Li, F. Total synthesis of vinigrol. *Angew. Chem., Int. Ed.* **52**, 8648-8651, doi:10.1002/anie.201304624 (2013).
98 Yang, Q. L. *et al.* Evolution of an oxidative dearomatization enabled total synthesis of vinigrol. *Org. Biomol. Chem.* **12**, 330-344, doi:10.1039/c3ob42191k (2014).
99 Feng, Z. G., Bai, W. J. & Pettus, T. R. R. Unified total syntheses of (−)-medicarpin, (−)-sophoracarpan a, and (±)-kushecarpin a with some structural revisions. *Angew. Chem. Int. Ed. Engl.*, doi:10.1002/anie.201408910 (2014).
100 Xu, X. F., Zavalij, P. Y. & Doyle, M. P. Highly enantioselective dearomatizing formal 3+3 cycloaddition reactions of n-acyliminopyridinium ylides with electrophilic enol carbene intermediates. *Angew. Chem., Int. Ed.* **52**, 12664-12668, doi:10.1002/anie.201305539 (2013).
101 Bauer, R. A., Wenderski, T. A. & Tan, D. S. Biomimetic diversity-oriented synthesis of benzannulated medium rings via ring expansion. *Nature Chemical Biology* **9**, 21-+, doi:10.1038/nchembio.1130 (2013).
102 Huigens, R. W. *et al.* A ring-distortion strategy to construct stereochemically complex and structurally diverse compounds from natural products. *Nature Chemistry* **5**, 195-202, doi:10.1038/nchem.1549 (2013).
103 Grenning, A. J., Boyce, J. H. & Porco, J. A. Rapid synthesis of polyprenylated acylphloroglucinol analogs via dearomative conjunctive allylic annulation. *J. Am. Chem. Soc* **136**, 11799-11804, doi:10.1021/ja5060302 (2014).
104 Endo, S. *et al.* Rabbit 3-hydroxyhexobarbital dehydrogenase is a nadph-preferring reductase with broad substrate specificity for ketosteroids, prostaglandin d-2, and other endogenous and xenobiotic carbonyl compounds. *Biochem. Pharmacol.* **86**, 1366-1375, doi:10.1016/j.bcp.2013.08.024 (2013).
105 Noh, T., Gan, H., Halfon, S., Hrnjez, B. J. & Yang, N. C. C. Chemistry of anti-o,o'-dibenzene. *J. Am. Chem. Soc* **119**, 7470-7482, doi:10.1021/ja970199o (1997).
106 Berberian, V., Allen, C. C. R., Sharma, N. D., Boyd, D. R. & Hardacre, C. A comparative study of the synthesis of 3-substituted catechols using an enzymatic and a chemoenzymatic method. *Adv. Synth. Catal.* **349**, 727-739, doi:10.1002/adsc.200600437 (2007).
107 Carless, H. A. J., Busia, K., Dove, Y. & Malik, S. S. Syntheses of conduritol-d derivatives from aromatic compounds. *J. Chem. Soc., Perkin Trans. 1*, 2505-2506, doi:10.1039/p19930002505 (1993).

108 Carless, H. A. J. & Oak, O. Z. Short syntheses of conduritol-a and conduritol-d, and dehydroconduritols, from benzene- the photo-oxidation of cis-cyclohexa-3,5-diene-1,2-diol. *Tetrahedron Lett.* **30**, 1719-1720, doi:10.1016/s0040-4039(00)99564-9 (1989).
109 Golding, B. T., Kennedy, G. & Watson, W. P. Simple syntheses of isomers of muconaldehyde and 2-methylmuconaldehyde. *Tetrahedron Lett.* **29**, 5991-5994, doi:10.1016/s0040-4039(00)82248-0 (1988).
110 Aleksejczyk, R. A., Berchtold, G. A. & Braun, A. G. Benzene diol epoxides. *J. Am. Chem. Soc* **107**, 2554-2555, doi:10.1021/ja00294a061 (1985).
111 Mahon, M. F. *et al.* The chemistry of compounds derived by microbial oxidation of benzene and derivatives- cycloadditions involving 1,2-isopropylidenedioxycyclohexadienes. *J. Chem. Soc., Perkin Trans. 1*, 1255-1263, doi:10.1039/p19910001255 (1991).
112 Schleyer, P. V. & Jiao, H. J. What is aromaticity? *Pure Appl. Chem.* **68**, 209-218 (1996).
113 Begue, J. P., Bonnet-Delpon, D. & Crousse, B. Fluorinated alcohols: A new medium for selective and clean reaction. *Synlett*, 18-29, doi:10.1055/s-2003-44973 (2004).
114 Benson, S. W. & Buss, J. H. Additivity rules for the estimation of molecular properties - thermodynamic properties. *J. Chem. Phys.* **29**, 546-572, doi:10.1063/1.1744539 (1958).
115 Cohen, N. Revised group additivity values for enthalpies of formation (at 298 k) of carbon-hydrogen and carbon-hydrogen-oxygen compounds. *J. Phys. Chem. Ref. Data* **25**, 1411-1481 (1996).
116 Hansch, C., Leo, A. & Taft, R. W. A survey of hammett substituent constants and resonance field parameters. *Chem. Rev.* **91**, 165-195, doi:10.1021/cr00002a004 (1991).
117 Rys, P., Skrabal, P. & Zollinge.H. Structure and stereochemistry of transition-states and intermediates of heterolytic aromatic substitutions. *Angew. Chem., Int. Ed.* **11**, 874-&, doi:10.1002/anie.197208741 (1972).
118 Szostak, M., Spain, M. & Procter, D. J. Electron transfer reduction of carboxylic acids using smi2-h2o-et3n. *Org. Lett.* **14**, 840-843, doi:10.1021/ol203361k (2012).
119 Szostak, M., Spain, M. & Procter, D. J. Preparation of samarium(ii) iodide: Quantitative evaluation of the effect of water, oxygen, and peroxide content, preparative methods, and the activation of samarium metal. *J. Org. Chem.* **77**, 3049-3059, doi:10.1021/jo300135v (2012).
120 Yuasa, Y. & Shibuya, S. Resolution of racemic rhododendrol by lipase-catalyzed enantioselective acetylation. *Synthetic Commun.* **33**, 1469-1475, doi:10.1081/scc-120018756 (2003).
121 Kelly, B. D. & Lambert, T. H. Cyclopropenium-activated cyclodehydration of diols. *Org. Lett.* **13**, 740-743, doi:10.1021/ol102980t (2011).

122 Schmidt, B., Holter, F., Kelling, A. & Schilde, U. Pd-catalyzed arylation reactions with phenol diazonium salts: Application in the synthesis of diarylheptanoids. *J. Org. Chem.* **76**, 3357-3365, doi:10.1021/jo2002787 (2011).
123 Peters, M., Trobe, M., Tan, H., Kleineweischede, R. & Breinbauer, R. A modular synthesis of teraryl-based -helix mimetics, part1: Synthesis of core fragments with two electronically differentiated leaving groups. *Chem.-Eur. J.* **19**, 2442-2449, doi:10.1002/chem.201203005 (2013).
124 Maiti, G., Kayal, U., Karmakar, R. & Bhattacharya, R. N. An unexpected rearrangement-hydration reaction sequence of 2h-chromenes to dihydrochalcones under catalysis of haucl4. *Tetrahedron Lett.* **53**, 6321-6325, doi:10.1016/j.tetlet.2012.08.117 (2012).
125 Alcaide, B. *et al.* Unveiling the reactivity of propargylic hydroperoxides under gold catalysis. *J. Am. Chem. Soc* **135**, 898-905, doi:10.1021/ja3108966 (2013).
126 Rauniyar, V. & Hall, D. G. Rationally improved chiral bronsted acid for catalytic enantioselective allylboration of aldehydes with an expanded reagent scope. *J. Org. Chem.* **74**, 4236-4241, doi:10.1021/jo900553f (2009).
127 Marumoto, S. & Miyazawa, M. Microbial reduction of coumarin, psoralen, and xanthyletin by glomerella cingulata. *Tetrahedron* **67**, 495-500, doi:10.1016/j.tet.2010.10.089 (2011).
128 Chen, H., Wang, J. M., Hong, X. C., Zhou, H. B. & Dong, C. N. A simple and straightforward approach toward selective c = c bond reduction by hydrazine. *Can. J. Chem.* **90**, 758-761, doi:10.1139/v2012-057 (2012).
129 Rao, G. K., Gowda, N. B. & Ramakrishna, R. A. Raney nicel-catalyzed hydrogenation of unsaturated carboxylic acids with sodium borohydride in water. *Synthetic Commun.* **42**, 893-904, doi:10.1080/00397911.2010.533239 (2012).
130 Dong, C. Z. *et al.* Inhibition of secretory phospholipase a(2)center dot 2-synthesis and structure-activity relationship studies of 4,5-dihydro-3-(4-tetradecyloxybenzyl)-1,2,4-4h-oxadiazol-5-one (pms1062) derivatives specific for group ii enzyme. *Bioorgan. Med. Chem.* **13**, 1989-2007, doi:10.1016/j.bmc.2005.01.016 (2005).
131 Fleming, P. & O'Shea, D. F. Controlled anion migrations with a mixed metal li/k-tmp amide: General application to benzylic metalations. *J. Am. Chem. Soc* **133**, 1698-1701, doi:10.1021/ja110234v (2011).
132 Desage-El Murr, M., Nowaczyk, S., Le Gall, T. & Mioskowski, C. Synthesis of pulvinic acid and norbadione a analogues by suzuki-miyaura cross-coupling of benzylated intermediates. *Eur. J. Org. Chem.*, 1489-1498, doi:10.1002/ejoc.200500837 (2006).
133 Payne, R. J., Toscano, M. D., Bulloch, E. M. M., Abell, A. D. & Abell, C. Design and synthesis of aromatic inhibitors of anthranilate synthase. *Org. Biomol. Chem.* **3**, 2271-2281, doi:10.1039/b503802b (2005).

134 Churcher, I., Hallett, D. & Magnus, P. Dimerization of o-hydroxycyclohexadienones related to calicheamicinone: S(n)2 displacement of the 12 alpha-hydroxyl group. *Tetrahedron* **55**, 1597-1606, doi:10.1016/s0040-4020(98)01204-6 (1999).
135 Legrand, S., Nordlander, G., Nordenhem, H., Borg-Karlson, A. K. & Unelius, C. R. Hydroxy-methoxybenzoic methyl esters: Synthesis and antifeedant activity on the pine weevil, hylobius abietis. *Zeitschrift Fur Naturforschung Section B-a Journal of Chemical Sciences* **59**, 829-835 (2004).
136 Petrovic, D. & Bruckner, R. Deslongchamps annulations with benzoquinone monoketals. *Org. Lett.* **13**, 6524-6527, doi:10.1021/ol202809y (2011).
137 Sher, M. *et al.* Efficient synthesis of salicylates by catalytic 3+3 cyclizations of 1,3-bis(silyl enol ethers) with 1,1,3,3-tetramethoxypropane. *J. Org. Chem.* **72**, 6284-6286, doi:10.1021/jo070974a (2007).
138 Rosiak, A., Frey, W. & Christoffers, J. Synthesis of tetrahydropyran-4-ones and thiopyran-4-ones from donor-substituted alpha-bromostyrene derivatives. *Eur. J. Org. Chem.*, 4044-4054, doi:10.1002/ejoc.200600372 (2006).
139 *Sigma aldrich*, <www.sigmaaldrich.com/united-states.html> (
140 *Spectral database of organic compounds*, <http://sdbs.db.aist.go.jp/sdbs/cgi-bin/direct_frame_top.cgi> (2015).
141 Wilson, K. A. & Beck, J. J. The complete proton and carbon assignment of triclosan via one and two-dimensional nuclear magnetic resonance analysis. *Chemical Educator* **12**, 338-342 (2007).
142 Claudi, F. *et al.* Synthesis and dopamine receptor affinities of 2-(4-fluoro-3-hydroxyphenyl)ethylamine and n-substituted derivatives. *J. Med. Chem.* **33**, 2408-2412, doi:10.1021/jm00171a014 (1990).
143 Negoro, N. *et al.* Optimization of (2,3-dihydro-1-benzofuran-3-yl)acetic acids: Discovery of a non-free fatty acid-like, highly bioavailable g protein-coupled receptor 40/free fatty acid receptor 1 agonist as a glucose-dependent insulinotropic agent. *J. Med. Chem.* **55**, 3960-3974, doi:10.1021/jm300170m (2012).
144 Nagel, M. & Hansen, H. J. Synthesis of polyalkylphenyl prop-2-ynoates and their flash vacuum pyrolysis to polyalkylcyclohepta b furan-2(2h)-ones. *Helvetica Chimica Acta* **83**, 1022-1048, doi:10.1002/(sici)1522-2675(20000510)83:5<1022::aid-hlca1022>3.0.co;2-y (2000).
145 Bradbury, E. J. & McMahon, S. B. Opinion - spinal cord repair strategies: Why do they work? *Nature Reviews Neuroscience* **7**, 644-653, doi:10.1038/nrn1964 (2006).
146 Becerra, J. L. *et al.* Mr-pathological comparisons of wallerian degeneration in spinal-cord injury. *American Journal of Neuroradiology* **16**, 125-133 (1995).
147 Weiss, S. *et al.* Multipotent cns stem cells are present in the adult mammalian spinal cord and ventricular neuroaxis. *J. Neurosci.* **16**, 7599-7609 (1996).
148 Ramón y Cajal, S. *Degeneration and regeneration of the nervous system*. (Oxford Univ. Press, 1928).

149 Tom, V. J., Steinmetz, M. P., Miller, J. H., Doller, C. M. & Silver, J. Studies on the development and behavior of the dystrophic growth cone, the hallmark of regeneration failure, in an in vitro model of the glial scar and after spinal cord injury. *J. Neurosci.* **24**, 6531-6539, doi:10.1523/jneurosci.0994-04.2004 (2004).
150 Liuzzi, F. J. & Tedeschi, B. Peripheral nerve regeneration. *Neurosurgery clinics of North America* **2**, 31-42 (1991).
151 Aguayo, A. J. *et al.* Ensheathment and myelination of regenerating pns fibers by transplanted optic-nerve glia. *Neurosci. Lett.* **9**, 97-104, doi:10.1016/0304-3940(78)90055-1 (1978).
152 Moreau-Fauvarque, C. *et al.* The transmembrane semaphorin sema4d/cd100, an inhibitor of axonal growth, is expressed on oligodendrocytes and upregulated after cns lesion. *J. Neurosci.* **23**, 9229-9239 (2003).
153 Pasterkamp, R. J. *et al.* Expression of the gene encoding the chemorepellent semaphorin iii is induced in the fibroblast component of neural scar tissue formed following injuries of adult but not neonatal cns. *Molecular and Cellular Neuroscience* **13**, 143-166, doi:10.1006/mcne.1999.0738 (1999).
154 Koeberle, P. D. & Bahr, M. Growth and guidance cues for regenerating axons: Where have they gone? *J. Neurobiol.* **59**, 162-180, doi:10.1002/neu.10345 (2004).
155 Rudge, J. S. & Silver, J. Inhibition of neurite outgrowth on astroglial scars invitro. *J. Neurosci.* **10**, 3594-3603 (1990).
156 McKeon, R. J., Schreiber, R. C., Rudge, J. S. & Silver, J. Reduction of neurite outgrowth in a model of glial scarring following cns injury is corelated with the expression of inhibitory molecules on reactive astrocytes. *J. Neurosci.* **11**, 3398-3411 (1991).
157 Bovolenta, P. & Fernaud-Espinosa, I. Nervous system proteoglycans as modulators of neurite outgrowth. *Prog. Neurobiol.* **61**, 113-132, doi:10.1016/s0301-0082(99)00044-1 (2000).
158 Yu, T. W. & Bargmann, C. I. Dynamic regulation of axon guidance. *Nature Neuroscience* **4**, 1169-1176, doi:10.1038/nn748 (2001).
159 TessierLavigne, M. & Goodman, C. S. The molecular biology of axon guidance. *Science* **274**, 1123-1133, doi:10.1126/science.274.5290.1123 (1996).
160 David, S. & Aguayo, A. J. Axonal elongation into peripheral nervous-system bridges after central nervous-system injury in adult-rats. *Science* **214**, 931-933, doi:10.1126/science.6171034 (1981).
161 Meyer, M., Matsuoka, I., Wetmore, C., Olson, L. & Thoenen, H. Enhanced synthesis of brain-derived neurotrophic factor in the lesioned peripheral-nerve- different mechanisms are responsible for the regulation of bdnf and ngf messenger rna. *J. Cell Biol.* **119**, 45-54, doi:10.1083/jcb.119.1.45 (1992).
162 Kaneko, S. *et al.* A selective sema3a inhibitor enhances regenerative responses and functional recovery of the injured spinal cord. *Nat. Med.* **12**, 1380-1389, doi:10.1038/nm1505 (2006).

163 Zhang, L. *et al.* Rewiring of regenerated axons by combining treadmill training with semaphorin3a inhibition. *Mol. Brain* **7**, 17, doi:10.1186/1756-6606-7-14 (2014).
164 Pasterkamp, R. J., Anderson, P. N. & Verhaagen, J. Peripheral nerve injury fails to induce growth of lesioned ascending dorsal column axons into spinal cord scar tissue expressing the axon repellent semaphorin3a. *European Journal of Neuroscience* **13**, 457-471, doi:10.1046/j.0953-816X.2000.01398.x (2001).
165 De Winter, F. *et al.* Injury-induced class 3 semaphorin expression in the rat spinal cord. *Exp. Neurol.* **175**, 61-75, doi:10.1006/exnr.2002.7884 (2002).
166 Kumagai, K., Hosotani, N., Kikuchi, K., Kimura, T. & Saji, I. Xanthofulvin, a novel semaphorin inhibitor produced by a strain of penicillium. *J. Antibiot.* **56**, 610-616 (2003).
167 Pasterkarnp, R. J. & Verhaagen, J. Semaphorins in axon regeneration: Developmental guidance molecules gone wrong? *Philosophical Transactions of the Royal Society B-Biological Sciences* **361**, 1499-1511, doi:10.1098/rstb.2006.1892 (2006).
168 Moret, F., Renaudot, C., Bozon, M. & Castellani, V. Semaphorin and neuropilin co-expression in motoneurons sets axon sensitivity to environmental semaphorin sources during motor axon pathfinding. *Development* **134**, 4491-4501, doi:10.1242/dev.011452 (2007).
169 Chedotal, A. *et al.* Semaphorins iii and iv repel hippocampal axons via two distinct receptors. *Development* **125**, 4313-4323 (1998).
170 Pasterkamp, R. J., Giger, R. J. & Verhaagen, J. Regulation of semaphorin iii collapsin-1 gene expression during peripheral nerve regeneration. *Exp. Neurol.* **153**, 313-327, doi:10.1006/exnr.1998.6886 (1998).
171 Good, P. F. *et al.* A role for semaphorin 3a signaling in the degeneration of hippocampal neurons during alzheimer's disease. *Journal of Neurochemistry* **91**, 716-736, doi:10.1111/j.1471-4159.2004.02766.x (2004).
172 Chen, H., Chedotal, A., He, Z. G., Goodman, C. S. & TessierLavigne, M. Neuropilin-2, a novel member of the neuropilin family, is a high affinity receptor for the semaphorins sema e and sema iv but not sema iii. *Neuron* **19**, 547-559, doi:10.1016/s0896-6273(00)80371-2 (1997).
173 Takahashi, T. *et al.* Plexin-neuropilin-1 complexes form functional semaphorin-3a receptors. *Cell* **99**, 59-69, doi:10.1016/s0092-8674(00)80062-8 (1999).
174 Kolodkin, A. L., Matthes, D. J. & Goodman, C. S. The semaphorin genes encode a family of transmembrane and secreted growth cone guidance molecules. *Cell* **75**, 1389-1399, doi:10.1016/0092-8674(93)90625-z (1993).
175 Mamluk, R. *et al.* Neuropilin-1 binds vascular endothelial growth factor 165, placenta growth factor-2, and heparin via its b1b2 domain. *J. Biol. Chem.* **277**, 24818-24825, doi:10.1074/jbc.M200730200 (2002).
176 Gorgues, A., Simon, A., Lecoq, A., Hercouet, A. & Corre, F. Versatility of the reactivity of dicarbaldehyde acetylene and alpha-acetylenic aldehydes

concerning cyclic and heterocyclic conjugated dienes in acidic media. *Tetrahedron* **42**, 351-370, doi:10.1016/s0040-4020(01)87436-6 (1986).
177 Kikuchi, K. *et al.* In vitro and in vivo characterization of a novel semaphorin 3a inhibitor, sm-216289 or xanthofulvin. *J. Biol. Chem.* **278**, 42985-42991, doi:10.1074/jbc.M302395200 (2003).
178 Luo, Y. L., Raible, D. & Raper, J. A. Collapsin - a protein in brain that induces the collapse and paralysis of neuronal growth cones. *Cell* **75**, 217-227, doi:10.1016/0092-8674(93)80064-l (1993).
179 Aoki, M. *et al.* Structure of a novel phospholipase-c inhibitor, vinaxanthone (ro-09-1450), produced by penicillium vinaceum. *Tetrahedron Lett.* **32**, 4737-4740, doi:10.1016/s0040-4039(00)92295-0 (1991).
180 Wrigley, S. K., Latif, M. A., Gibson, T. M., Chicarellirobinson, M. I. & Williams, D. H. Structure elucidation of xanthone derivatives with cd4-binding activity from penicillium glabrum. *Pure Appl. Chem.* **66**, 2383-2386, doi:10.1351/pac199466102383 (1994).
181 Tatsuta, K. *et al.* The first total synthesis of vinaxanthone, a fungus metabolite possessing multiple bioactivities. *Chem. Lett.* **36**, 10-11, doi:10.1246/cl.2007.10 (2007).
182 Losgen, S., Schlorke, O., Meindl, K., Herbst-Irmer, R. & Zeeck, A. Structure and biosynthesis of chaetocyclinones, new polyketides produced by an endosymbiotic fungus. *Eur. J. Org. Chem.*, 2191-2196, doi:10.1002/ejoc.200601020 (2007).
183 Leroux, F. Atropisomerism, biphenyls, and fluorine: A comparison of rotational barriers and twist angles. *ChemBioChem* **5**, 644-649, doi:10.1002/cbic.200300906 (2004).
184 Cook, C. D. Oxidation of hindered phenols 1 oxidation of and oxidation inhibition by 2,6-di-tert-butyl-4-methylphenol. *J. Org. Chem.* **18**, 261-266, doi:10.1021/jo01131a005 (1953).
185 Stocking, E. M. & Williams, R. M. Chemistry and biology of biosynthetic diels-alder reactions. *Angew. Chem., Int. Ed.* **42**, 3078-3115, doi:10.1002/anie.200200534 (2003).
186 Gammill, R. B. New and efficient synthesis of 3-halogenated 4h-1-benzopyran-4-ones. *Synthesis-Stuttgart*, 901-903 (1979).
187 Ghosh, C. K., Bandyopadhyay, C. & Tewari, N. Benzopyrans .17. Triethylamine-mediated transformation of 4-oxo-4h-1-benzopyran-3-carboxaldehyde. *J. Org. Chem.* **49**, 2812-2815, doi:10.1021/jo00189a034 (1984).
188 Yokoe, I., Maruyama, K., Sugita, Y., Harashida, T. & Shirataki, Y. Facile syntehsis of 3-substituted chromones from an enaminoketone. *Chemical & Pharmaceutical Bulletin* **42**, 1697-1699 (1994).
189 Hopwood, D. A. Genetic contributions to understanding polyketide synthases. *Chem. Rev.* **97**, 2465-2497, doi:10.1021/cr960034i (1997).

190 Lacey, R. N. Derivatives of acetoacetic acid .1. The reaction of diketen with 1-2-ketols and 1-3-ketols to give gamma-lactones. *J. Chem. Soc.*, 816-822, doi:10.1039/jr9540000816 (1954).
191 Reber, K. P., Tilley, S. D. & Sorensen, E. J. Bond formations by intermolecular and intramolecular trappings of acylketenes and their applications in natural product synthesis. *Chem. Soc. Rev.* **38**, 3022-3034, doi:10.1039/b912599j (2009).
192 Wentrup, C., Heilmayer, W. & Kollenz, G. Alpha-oxoketenes- preparation and chemistry. *Synthesis-Stuttgart*, 1219-1248, doi:10.1055/s-1994-25673 (1994).
193 Freiermuth, B. & Wentrup, C. Direct observation of alpha-oxo ketenes formed from 1,3-dioxin-4-ones and the enols of beta-keto-esters. *J. Org. Chem.* **56**, 2286-2289, doi:10.1021/jo00007a008 (1991).
194 Bell, K., Sadasivam, D. V., Gudipati, I. R., Ji, H. & Birney, D. Sodium carbonate as a solid-phase reagent for the generation of acetylketene. *Tetrahedron Lett.* **50**, 1295-1297, doi:10.1016/j.tetlet.2009.01.008 (2009).
195 Rybalova, T. V., Gatilov, Y. V., Nekrasov, D. D., Rubtsov, A. E. & Tolstikovz, A. G. Synthesis of spiro (6-phenyl-3,4-dihydro-2h-1,3-dioxine)-2r(s), 3 '-(19 ',28 '-oxidooleanan) -4-ones and x-ray diffraction analysis of their configuration. *Journal of Structural Chemistry* **46**, 1126-1130, doi:10.1007/s10947-006-0256-1 (2005).
196 Hyatt, J. A., Feldman, P. L. & Clemens, R. J. Thermal-decomposition of 2'2,6-trimethyl-4h-1,3-dioxin-4-one and 1-ethoxybutyn-3-one acetylketene. *J. Org. Chem.* **49**, 5105-5108, doi:10.1021/jo00200a018 (1984).
197 Clemens, R. J. & Hyatt, J. A. Acetoacetylation with 2',2,6-trimethyl-4h-1,3-dioxin-4-one- a convenient alternative to diketene. *J. Org. Chem.* **50**, 2431-2435, doi:10.1021/jo00214a006 (1985).
198 Xu, F. *et al.* Mechanistic evidence for an alpha-oxoketene pathway in the formation of beta-ketoamides/esters via meldrum's acid adducts. *J. Am. Chem. Soc* **126**, 13002-13009, doi:10.1021/ja046488b (2004).
199 Oikawa, Y., Sugano, K. & Yonemitsu, O. Meldrums acid in organic-synthesis .2. General and versatile synthesis of beta-keto-esters. *J. Org. Chem.* **43**, 2087-2088, doi:10.1021/jo00404a066 (1978).
200 Kappe, C. O., Kollenz, G. & Wentrup, C. An improved synthesis of 5-alkyl-2,3-dihydro-furan-2,3-diones. *Heterocycles* **38**, 779-784 (1994).
201 Park, P., Broka, C. A., Johnson, B. F. & Kishi, Y. Total synthesis of debromoaplysiatoxin and aplysiatoxin. *J. Am. Chem. Soc* **109**, 6205-6207, doi:10.1021/ja00254a062 (1987).
202 May, A. E. & Hoye, T. R. Room temperature acylketene formation? 1,3-dioxin-4-ones via silver(i) activation of phenylthioacetoacetate in the presence of ketones. *J. Org. Chem.* **75**, 6054-6056, doi:10.1021/jo101372v (2010).

203 Frey, H. M. & Isaacs, N. S. Stereochemistry of cycloaddition of dimethylketen to cis-but-2-ene and trans-but-2-ene. *Journal of the Chemical Society B-Physical Organic*, 830-&, doi:10.1039/j29700000830 (1970).
204 Arnold, B. R., Brown, C. E. & Lusztyk, J. Solution photochemistry of 2h-pyran-2-one - laser flash-photolysis with infrared detection of transients. *J. Am. Chem. Soc* **115**, 1576-1577, doi:10.1021/ja00057a053 (1993).
205 Emtenas, H., Soto, G., Hultgren, S. J., Marshall, G. R. & Almqvist, F. Stereoselective synthesis of optically active beta-lactams, potential inhibitors of pilus assembly in pathogenic bacteria. *Org. Lett.* **2**, 2065-2067, doi:10.1021/ol0059899 (2000).
206 Yamamoto, Y., Watanabe, Y. & Ohnishi, S. 1,3-oxazines and related compounds .13. Reaction of acyl meldrum acids with schiff-bases giving 2,3-disubstituted 5-acyl-3,4,5,6-tetrahydro-2h-1,3-oxazine-4,6-diones and 2,3,6-trisubstituted 2,3-dihydro-1,3-oxazin-4-ones. *Chemical & Pharmaceutical Bulletin* **35**, 1860-1870 (1987).
207 Crimmins, M. T. & Smith, A. C. A hetero-diels-alder approach to complex pyrones: An improved synthesis of the spongistatin ab spiroketal. *Org. Lett.* **8**, 1003-1006, doi:10.1021/ol0601601 (2006).
208 Birney, D. M., Xu, X. L., Ham, S. & Huang, X. M. Chemoselectivity in the reactions of acetylketene and acetimidoylketene: Confirmation of theoretical predictions. *J. Org. Chem.* **62**, 7114-7120, doi:10.1021/jo971083d (1997).
209 Kelly, T. R., Bell, S. H., Ohashi, N. & Armstrongchong, R. J. Synthesis of (+/-)-fredericamycin-a. *J. Am. Chem. Soc* **110**, 6471-6480, doi:10.1021/ja00227a030 (1988).
210 Corey, E. J., Cho, H., Rucker, C. & Hua, D. H. Studies with trialkylsilyltriflates-new syntheses and applications. *Tetrahedron Lett.* **22**, 3455-3458, doi:10.1016/s0040-4039(01)81930-4 (1981).
211 Rassu, G., Zanardi, F., Battistini, L., Gaetani, E. & Casiraghi, G. Expeditious syntheses of sugar-modified nucleosides and collections thereof exploiting furan-, pyrrole-, and thiophene-based siloxy dienes. *J. Med. Chem.* **40**, 168-180, doi:10.1021/jm960400q (1997).
212 Cornelius, L. A. M. *et al.* Synthesis of 2-acetylbicyclo 2.2.1 hept-2-ene. *J. Org. Chem.* **58**, 3188-3190, doi:10.1021/jo00063a050 (1993).
213 Yerino, L. V., Osborn, M. E. & Mariano, P. S. The hydroazocine route to highly functionaalized pyrrolizidines. *Tetrahedron* **38**, 1579-1591, doi:10.1016/0040-4020(82)80133-6 (1982).
214 Davis, R. B. & Scheiber, D. H. The preparation of acetylenic ketones using soluble silver acetylides. *J. Am. Chem. Soc* **78**, 1675-1678, doi:10.1021/ja01589a050 (1956).
215 Nibbs, A. E. & Scheidt, K. A. Asymmetric methods for the synthesis of flavanones, chromanones, and azaflavanones. *Eur. J. Org. Chem.*, 449-462, doi:10.1002/ejoc.201101228 (2012).

216 Eilingsfeld, H., Weidinger, H. & Seefelder, M. Readtionen an der alpha-methylengruppe aliphatischer n,n-disubstituierter carbonsaureamidchloride. *Chemische Berichte-Recueil* **96**, 2899-&, doi:10.1002/cber.19630961111 (1963).
217 Eilingsfeld, H., Seefelder, M. & Weidinger, H. Synthesen mit amidchloriden 1. Reaktionen an der funktionellen gruppe n,n-disubstituierter carbonsaureamidchloride. *Chemische Berichte-Recueil* **96**, 2671-&, doi:10.1002/cber.19630961023 (1963).
218 Seefelder, M. & Eilingsfeld, H. Kupplung von diazoniumsalzen mit enolathern. *Angew. Chem., Int. Ed.* **75**, 724-&, doi:10.1002/ange.19630751511 (1963).
219 Zubatyuk, R. I., Volovenko, Y. M., Shishkin, O. V., Gorb, L. & Leszczynski, J. Aromaticity-controlled tautomerism and resonance-assisted hydrogen bonding in heterocyclic enaminone-iminoenol systems. *J. Org. Chem.* **72**, 725-735, doi:10.1021/jo0616411 (2007).
220 Kleinpeter, E., Bolke, U. & Koch, A. Subtle trade-off existing between (anti)aromaticity, push-pull interaction, keto-enol tautomerism, and steric hindrance when defining the electronic properties of conjugated structures. *Journal of Physical Chemistry A* **114**, 7616-7623, doi:10.1021/jp103353y (2010).
221 Rybarczyk-Pirek, A. J., Malecka, M., Grabowski, S. J. & Nawrot-Modranka, J. A benzopyran derivative substituted at position 3. *Acta Crystallographica Section C-Crystal Structure Communications* **58**, o405-o406, doi:10.1107/s0108270102008508 (2002).
222 Krygowski, T. M., Zachara-Horeglad, J. E., Palusiak, M., Pelloni, S. & Lazzeretti, P. Relation between pi-electron localization/delocalization and h-bond strength in derivatives of o-hydroxy-schiff bases. *J. Org. Chem.* **73**, 2138-2145, doi:10.1021/jo7023174 (2008).
223 Vasselin, D. A., Westwell, A. D., Matthews, C. S., Bradshaw, T. D. & Stevens, M. F. G. Structural studies on bioactive compounds. 40. Synthesis and biological properties of fluoro-, methoxyl-, and amino-substituted 3-phenyl-4h-1-benzopyran-4-ones and a comparison of their antitumor activities with the activities of related 2-phenylbenzothiazoles. *J. Med. Chem.* **49**, 3973-3981, doi:10.1021/jm060359j (2006).
224 Sonogashira, K., Tohda, Y. & Hagihara, N. Convenient synthesis of acetylenes-catalytic substitutions of acetylenic hydrogen with bromoalkenes, iodoarenes, and bromopyridines. *Tetrahedron Lett.*, 4467-4470 (1975).
225 Swamy, N. K., Tatini, L. K., Babu, J. M., Annamalai, P. & Pal, M. Pd-mediated synthesis of substituted benzenes fused with carbocycle/heterocycle. *Chem. Commun.*, 1035-1037, doi:10.1039/b612770c (2007).
226 Cornforth, R. H., Popjak, G. & Cornforth, J. W. Preparation of r- and s-mevalonolactones. *Tetrahedron* **18**, 1351-&, doi:10.1016/s0040-4020(01)99289-0 (1962).

227 Anastasia, L. & Negishi, E. Highly satisfactory procedures for the pd-catalyzed cross coupling of aryl electrophiles with in situ generated alkynylzinc derivatives. *Org. Lett.* **3**, 3111-3113, doi:10.1021/ol010145q (2001).
228 Negishi, E. I., Qian, M. X., Zeng, F. X., Anastasia, L. & Babinski, D. Highly satisfactory alkynylation of alkenyl halides via pd-catalyzed cross-coupling with alkynylzincs and its critical comparison with the sonogashira alkynylation. *Org. Lett.* **5**, 1597-1600, doi:10.1021/ol030010F (2003).
229 Zhao, L. Z., Xie, F. C., Cheng, G. & Hu, Y. H. A base-promoted tandem reaction of 3-(1-alkynyl)chromones with 1,3-dicarbonyl compounds: An efficient approach to functional xanthones. *Angew. Chem., Int. Ed.* **48**, 6520-6523, doi:10.1002/anie.200902618 (2009).
230 Liu, Y., Huang, L. P., Xie, F. C. & Hu, Y. H. Base-promoted one-pot tandem reaction of 3-(1-alkynyl)chromones under microwave irradiation to functionalized amino-substituted xanthones. *J. Org. Chem.* **75**, 6304-6307, doi:10.1021/jo1013614 (2010).
231 Liu, Y., Huang, L. P., Xie, F. C., Chen, X. X. & Hu, Y. H. Synthesis of novel functional polycyclic chromones through michael addition and double cyclizations. *Org. Biomol. Chem.* **9**, 2680-2684, doi:10.1039/c0ob01000f (2011).
232 Zlotkowski, K., Pierce-Shimomura, J. & Siegel, D. Small-molecule-mediated axonal branching in caenorhabditis elegans. *ChemBioChem* **14**, 307-310, doi:10.1002/cbic.201200712 (2013).
233 Rydel, R. E. & Greene, L. A. Camp analogs promote survival and neurite outgrowth in cultures of rat sympathetic and sensory neurons independently of nerve growth-factor. *Proceedings of the National Academy of Sciences of the United States of America* **85**, 1257-1261, doi:10.1073/pnas.85.4.1257 (1988).
234 Lee, J. K. *et al.* Combined genetic attenuation of myelin and semaphorin-mediated growth inhibition is insufficient to promote serotonergic axon regeneration. *J. Neurosci.* **30**, 10899-10904, doi:10.1523/jneurosci.2269-10.2010 (2010).
235 Sasaki, Y. *et al.* Fyn and cdk5 mediate semaphorin-3a signaling, which is involved in regulation of dendrite orientation in cerebral cortex. *Neuron* **35**, 907-920, doi:10.1016/s0896-6273(02)00857-7 (2002).
236 King, N., Hittinger, C. T. & Carroll, S. B. Evolution of key cell signaling and adhesion protein families predates animal origins. *Science* **301**, 361-363, doi:10.1126/science.1083853 (2003).
237 Overington, J. P., Al-Lazikani, B. & Hopkins, A. L. Opinion - how many drug targets are there? *Nature Reviews Drug Discovery* **5**, 993-996, doi:10.1038/nrd2199 (2006).
238 Pierce, K. L., Premont, R. T. & Lefkowitz, R. J. Seven-transmembrane receptors. *Nature Reviews Molecular Cell Biology* **3**, 639-650, doi:10.1038/nrm908 (2002).

239 May, L. T., Leach, K., Sexton, P. M. & Christopoulos, A. in *Annu. Rev. Pharmacol. Toxicol.* Vol. 47 *Annual review of pharmacology and toxicology* 1-51 (Annual Reviews, 2007).
240 Monod, J., Wyman, J. & Changeux, J. P. On nature of allosteric transitions - a plausible model. *Journal of Molecular Biology* **12**, 88-& (1965).
241 Christopoulos, A., May, L. T., Avlani, V. A. & Sexton, P. M. G-protein-coupled receptor allosterism: The promise and the problem(s). *Biochemical Society Transactions* **32**, 873-877 (2004).
242 He, W. H. *et al.* Citric acid cycle intermediates as ligands for orphan g-protein-coupled receptors. *Nature* **429**, 188-193, doi:10.1038/nature02488 (2004).
243 Joyal, J. S. *et al.* Neovascularization in retinopathy of prematurity: Opposing actions of neuronal factors gpr91 and semaphorins 3a. *Acta Paediatr.* **101**, 819-826, doi:10.1111/j.1651-2227.2012.02692.x (2012).